**Non-Native Small Molecules that Modulate Quorum Sensing in Gram-Negative Bacteria**

by

Daniel Evan Manson

A dissertation submitted in partial fulfillment of

The requirements for the degree of

Doctor of Philosophy

(Chemistry)

at the

UNIVERSITY OF WISCONSIN-MADISON

2020

Date of final oral examination: July 23, 2020

The dissertation is approved by the following members of the Final Oral Committee:
Helen E. Blackwell, Norman C. Craig Professor, Department of Chemistry
Samuel H. Gellman, Professor, Chemistry and Biochemistry
Judith Burstyn, Professor, Chemistry
Jeff Martell, Assistant Professor, Chemistry
.

**Abstract**

# Non-Native Small Molecules that Modulate Quorum Sensing in Gram-Negative Bacteria

Daniel E. Manson

Under the supervision of Professor Helen E. Blackwell

At The University of Wisconsin–Madison

## ABSTRACT

Research in the burgeoning field of chemical ecology has made it clear that chemically-mediated communication is common in Nature. This Ph.D. thesis examines bacterial quorum sensing (QS), a signaling process that involves the production and sensing of discrete signaling molecules, termed "autoinducers." Autoinducers are produced in proportion to bacterial growth, so at a certain stage of population density (i.e., a quorum) productive binding will occur between an autoinducer molecule and a target receptor protein. Receptor binding leads to changes in gene expression and, ultimately, bacterial phenotypes, which include behaviors that impact the environment, industry, agriculture, and human health.

Gram negative bacteria primarily utilize *N*-acylated L-homoserine lactones (AHLs) as their QS signals. These small molecules are recognized by cytoplasmic LuxR-type receptors. AHL-mediated QS is widespread; over 200 LuxR type receptors have been identified thus far. Multiple common human pathogens, including *Pseudomonas aeruginosa,* and enterohemorrhagic *Escherichia coli,* regulate their virulence (i.e., ability to initiate infection) via QS. Small molecules that can strongly block QS in these pathogens would be extremely valuable, especially as the antibiotic resistance crisis intensifies.

The majority of compounds designed to block QS in Gram-negative pathogens are based on the AHL scaffold. This scaffold has several inherent chemical liabilities that limit its usefulness as a chemical probe, chiefly its hydrolytic instability and high lipophilicity. This Ph.D. thesis focuses primarily on *non-AHL* scaffolds that could be useful as chemical probes of QS in Gram-negative bacteria, with an emphasis on *P. aeruginosa*.

Studies in this thesis include (1) the rational design of the most potent known antagonists of LasR, an important LuxR-type protein in *P. aeruginosa*; (2) the discovery of structurally distinct and potent LasR modulators via high throughput screening; (3) structural studies of LasR in complex with non-native ligands; (4) a survey of the AHL-binding 'preferences' of a group of LuxR-type proteins; and (5) a study of the molecular features that drive ligand specificity between LasR and its homologue QscR. Collectively, these studies provide several new paths forward for the development of non-AHL ligands that can strongly modulate LuxR-type receptors.

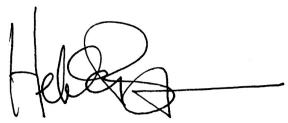

Helen E. Blackwell, Ph.D.

**Acknowledgements**

Where to begin? I would not be graduating with my PhD without the support of a wide network of mentors, family, and friends. I can't name all of you without further inflating the length of this (already way too long) document, but thank you all!

Helen, the thank you I owe you cannot be adequately expressed here, but briefly, let me say thank you for investing your time in mentoring me, for your empathy, and for your guidance. Thank you for taking me into your research group. I am leaving your group a smarter, better person than I was when I entered it. The ethos you instill in your group will help and guide me for the rest of my life: just try the experiment!

Thank you to my committee. When I joined this program in August of 2015, I did not appreciate how important it would be for my mental health to spend the next 5 years in a place where 'alternative facts' were never going to fly. Sam and Judith – I am extremely grateful to have had you as part of my mentoring team from my second-year exam all the way through my defense. The tough questions only made me a better scientist and critical thinker. To Andy Buller, who helped evaluate my RP, and Jeff Martell, who will be on my final committee, thank you for taking your time and mental energy to think about my science and contribute to my education.

Thank you to my colleagues in the Blackwell lab, who have been a pleasure to work with. I have had a great time at our happy hours, lunches, trips to the terrace, and just talking around the lab. You all have been great labmates, and I've enjoyed learning about science alongside all of you. I'll especially call out Drs. Matt O'Reilly and Michelle Boursier, who, as a postdoc and senior student, were extremely generous to me with their time when I was a junior student. To all the current students, especially the young ones: keep your heads up during COVID-19, and, as much as possible, don't let bad results in the lab get to you.

I absolutely would not have gotten through this program without my friends. To everyone in Madison, thank you for the nights out, for the backyard campfires, for the afternoons and evening on the terrace. Thank you for the camping trips and (Andrew and Megan) for being so into the Ice Age Trail, and helping me learn about backpacking! To all my friends from college, and the Katonah crew, you guys made visits back home special, and I loved our two long weekend trips. I look forward to seeing a lot more of you when I move back to the east coast!

To my family – thank you for the endless love and support. Donna and Rich – our weekly phone calls have kept me connected and grounded. While living in the Midwest, I have especially enjoyed reconnecting and seeing more of my Mom's family, who I didn't see enough growing up on the East Coast.

To Shannon – thank you for loving me as much as I love you. Thinking about starting the next chapter of our lives together in RI makes me feel like the luckiest person in the world. Getting this degree is great, but in terms of things I'm happy I did while living in Wisconsin, it doesn't really rate compared to meeting you.

Lastly, I will thank my parents. They are not alive to see me graduate – Mitch, dad, passed in 2016, at the very beginning of my second year of graduate school, and Ann, mom, passed in 2006, when I was only twelve years old. To say that I would not be here without them is not only true in the biological sense, also in that they instilled in me a bone-deep appreciation for the importance of becoming an educated person. They were smart people and deep thinkers and showed me how to have a loving family. Mom and Dad, this is for you.

## Table of Contents

## List of Figures, Tables, and Schemes

**CHAPTER 1**



**CHAPTER 2**

**CHAPTER 3**



**CHAPTER 4**

**CHAPTER 5**



**CHAPTER 6**

**CHAPTER 7**

## List of Abbreviations

| | |
|---|---|
| % | percent |
| (-) | negative |
| (+) | positive |
| $[M+H]^+$ | molecular ion + proton |
| $[M+Na]^+$ | molecular ion + sodium |
| ºC | degrees Celsius |
| α | alpha |
| δ | chemical shift of nuclear magnetic resonance |
| µL | microliter |
| µM | micromolar |
| µm | micrometer |
| A, abs | absorbance |
| Å | angstrom |
| AHL | *N*-acylated homoserine lactone |
| Aq. | Aqueous |
| Ac | acetyl |
| BHL | *N*-butyryl homoserine lactone |
| BME | β-mercaptoethanol |
| Bn | benzyl |
| Br | bromine |
| Cb | carbenicillin |
| CI | Confidence interval |

| | |
|---|---|
| CPRG | chlorophenol red-β-D-galactopyranoside |
| *C. violaceum* | *Chromobacterium violaceum* |
| d | doublet |
| dd/ddd | doublet of doublets, etc. |
| *d* | deuterated |
| DBD | DNA-binding domain |
| DCM | dichloromethane |
| DMAP | 4-(dimethylamino)pyridine |
| DMF | *N,N*-dimethyl formamide |
| DMSO | dimethyl sulfoxide |
| DNA | deoxyribonucleic acid |
| E | cis alkene isomer |
| *E. coli* | *Escherichia coli* |
| $EC_{50}$ | half-maximal effective concentration |
| EDC-HCl | *N*-(3-Dimethylaminopropyl)-*N*′-ethylcarbodiimide hydrochloride |
| ESI | electrospray ionization |
| Et | ethyl |
| Etc. | *et cetera* |
| $Et_2O$ | diethyl ether |
| $Et_3N$ | triethylamine |
| EtOAc | ethyl acetate |
| g | gram |
| gfp | green fluorescent protein |

| | |
|---|---|
| Gm | gentamicin |
| h | hours |
| $H_2O$ | water |
| Hex | hexanes |
| HSL | homoserine lactine |
| HPLC | high performance liquid chromatography |
| Hz | hertz |
| *i.e.* | *id est* |
| $IC_{50}$ | half maximal inhibitory concentration |
| IPTG | isopropyl β-D-1-thiogalactopyranoside |
| *J* | J-coupling constant |
| kD | kilodaltons |
| Km | kanamycin |
| L | liter |
| LacZ | β-galactosidase |
| LB | Luria Bertani |
| LBD | ligand binding domain |
| LiOH | lithium hydroxide |
| LVA*gfp* | unstable variant of green fluorescent protein |
| M | molar |
| MALDI | matrix assisted laser desorption ionization |
| m | multiplet |
| m/z | mass-to-charge ratio |

| | |
|---|---|
| Me | methyl |
| MeOH | methanol |
| mg | milligram |
| mL | milliliter |
| mM | millimolar |
| mmol | millimole |
| MW | molecular weight |
| MΩ | megaohm |
| NaH | sodium hydride |
| $Na_2CO_3$ | sodium carbonate |
| $NaHCO_3$ | sodium bicarbonate |
| nm | nanometer |
| nM | nanomolar |
| NMR | nuclear magnetic resonance |
| o/n | overnight |
| $OD_{600}$ | optical density (absorbance) at 600 nanometers |
| OdDHL | *N*-3-oxo-dodecanoyl-L-homoserine lactone |
| p | plasmid |
| *P. aeruginosa* | *Pseudomonas aeruginosa* |
| p-TsOH | p-toluene sulfonic acid |
| PAGE | polyacrylamide gel electrophoresis |
| PBS | phosphate buffered saline |
| PEG | poly(ethylene glycol) |

| | |
|---|---|
| pH | negative log of hydrogen ion concentration |
| PHL | phenylacetyl-L-homoserine lactone |
| PQS | *Pseudomonas* quinolone signal, (2-heptyl—hydroxy-4(*1H*-quinolone) |
| pyAOP | (7-Azabenzotriazol-1-yloxy)tripyrrolidinophosphonium hexafluorophosphate |
| q | quartet |
| QS | quorum sensing |
| RMSD | root mean square deviation |
| rpm | revolutions per minute |
| rt | room temperature |
| s | singlet |
| SAR | structure-activity relationship |
| SD | standard deviation |
| SDS | sodium dodecyl sulfate |
| t | triplet |
| TLC | thin layer chromatography |
| TMS | tetramethylsilane |
| TP | triphenyl |
| UV | ultraviolet light |
| vs. | versus |
| w/v | weight per volume |
| wt | wildtype |
| *Z* | trans alkene isomer |

# Chapter 1: Introduction

Daniel E. Manson and Helen E. Blackwell

D.E. Manson and H.E. Blackwell wrote the chapter.

### 1.1.1 Some consequences of living in a microbial world

The number of different of microbial *species* on earth is estimated to be larger than the total number of human beings by a factor of $10^3$.[1] Microbes live in essentially all environments, including within and on the bodies of all human beings (and all other animals). We are only beginning to appreciate the health implications of our microbiomes.[2]

One consequence of the omnipresence of bacteria—i.e., infection—has been known since the middle of the nineteenth century. Despite the advent and distribution of antibiotics in the twentieth century, infection remains a major cause of death globally.[3] As the antibiotic resistance crisis intensifies,[4] alternate strategies for managing infection must be explored.[5] The discovery that the ability of many common human pathogens to infect their hosts is dependent on their ability to communicate, made at the very end of the twentieth century, offers one potential "alternative" avenue forward to mitigate bacterial infection.

### 1.1.2 Quorum sensing: chemical communication between bacteria

Bacteria use chemical signals to communicate with each other in a process now known as quorum sensing (QS). The dependence of bacterial phenotypes on the synthesis and exchange of an external signal—e.g., genetic competence in *Streptococcus pnemoniae*[6] and bioluminescence in *Vibrio* species[7]—was first noted in the 1960s and 1970s, respectively. The discovery of the genes responsible for signal generation and reception,[8] and the subsequent elucidation of signal, or autoinducer, structure[9] followed in the 1980s. Synthesizing these and other studies, the term "quorum sensing" was first coined in 1994 by E. Peter Greenberg, Clay Fuqua, and coworkers.[10]

In the past 25 years, the QS field has flourished, with the discovery of many new chemical "languages",[11-13] and the structural elucidation of the key biomolecules that mediate

this signaling process.[14-16] The discovery of the intimate link between QS and virulence in many pathogenic bacteria[17] has motivated the development of strategies to apply these discoveries with the eventual goal of blocking infection.[18, 19] This Ph.D. thesis, focusing on QS in Gram-negative pathogens and primarily in *Pseudomonas aeruginosa*, offers a chemist's description of and perspective on small molecules that are *not* produced by Nature but could be useful as tools to intercept QS.

### 1.1.3 LuxI/LuxR-type quorum sensing in Gram-negative bacteria

The prototypical QS system in Gram-negative bacteria is the LuxI/LuxR circuit. This system involves a LuxI-type enzyme, which catalyzes the formation of an *N*-acylated homoserine lactone (AHL) signal from *S*-adenosyl methionine and an acyl carrier protein (ACP)-conjugated fatty acid,[20] and an intracellular LuxR-type receptor. The LuxR-type receptor is a transcription factor, which binds to DNA in an AHL-dependent fashion (**Figure 1.1**). [21] The advent of modern genomic technologies has enabled the discovery of several hundred LuxR homologues.[22] Certain bacteria also have LuxR "solos" or "orphans" – LuxR-type receptors without a corresponding LuxI-type synthase. Bacteria harboring only "orphan" LuxRs produce no AHL signal of their own, raising the intriguing possibility that their function may be eavesdropping on AHL signaling by other species,[23] or that they recognize non-AHL type signals produced by themselves, other bacteria, or the host.

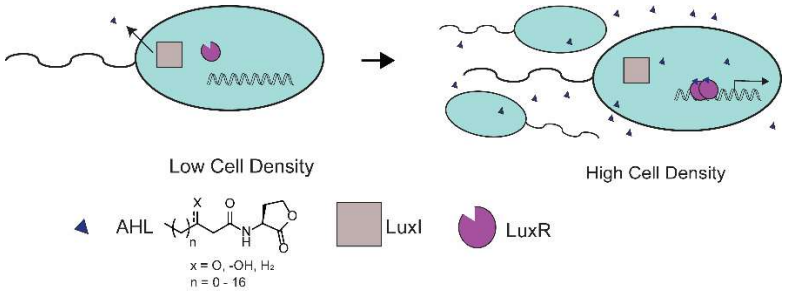


**Figure 1.1.** General schematic depicting LuxI/LuxR-type quorum sensing in Gram-negative bacteria. AHLs are synthesized by LuxI-type enzymes at a basal rate. At sufficiently high cell density (a "quorum"), AHLs bind to LuxR-type receptors, which are then activated and initiate gene transcription.

LuxR-type proteins contain two domains, an N-terminal ligand-binding domain and a C-terminal helix-turn-helix DNA binding domain (**Figure 1.2**). The ligand-binding domain is comprised of two three-α-helix bundles sandwiching a five-stranded anti-parallel α-sheet. AHL (and other) ligands bind in a pocket between the outermost β-helix bundle and the β-sheet. The DNA binding domain is smaller than the ligand binding domain, consisting almost entirely of a helix-turn-helix motif.

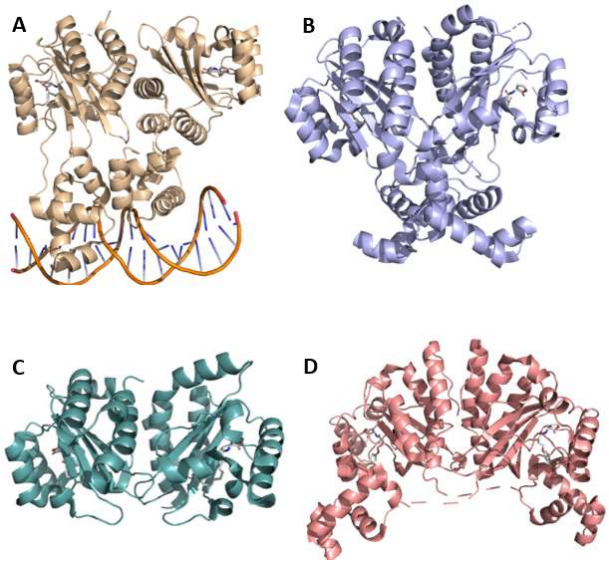


**Figure 1.2.** Representative X-ray crystal structures of LuxR-type QS receptors. (A) TraR, from *Agrobacterium tumefaciens*, bound to 3OC8 HSL and in complex with DNA (PDB ID 1H0M),[16] (B) QscR, from *P. aeruginosa*, bound to 3OC12 HSL (PDB ID 3SZT),[24] (C) the ligand binding domain of LasR, from *P. aeruginosa*, bound to 3OC12 HSL (PDB ID 2UV0),[14] and (D) CviR, from *Chromobacterium violaceum*, bound to synthetic antagonist chlorolactone (CL) (PDB ID 3QP5).[25]

LuxR-type proteins typically require a stabilizing ligand to be isolated *in vitro*.[26] As ligand binding typically promotes dimerization,[27] all X-ray crystal structures of LuxR-proteins (either full-length or just the ligand-binding domain) are of ligand-bound dimers.[28] Only one LuxR-type protein has been crystalized in complex with a small molecule antagonist (a chlorolactone AHL analog; CL): CviR from *Chromobacterium violaceum*.[25] In that structure, the CviR:CL dimer adopts a "crossed" conformation dissimilar to that of other LuxR-type receptors bound to agonists. This complex is presumably incapable of binding to DNA, as *in vitro* transcription experiments demonstrated that the CviR:CL complex is incapable of initiating transcription. The isolation and structural characterization of other LuxR-type proteins complexed with antagonists has been challenging; attempts to express LasR from *P. aeruginosa* along with non-native antagonists have yielded no soluble protein.[29] The possibility that certain antagonists function by causing the LuxR-type protein to misfold may explain this difficulty. Studies exploring whether the CviR:CL-type "crossed" conformation is unique to CviR or a more general mechanism of antagonism are ongoing, including work being pursued in our laboratory.

### 1.1.4 QS controls virulence in *Pseudomonas aeruginosa*

*P. aeruginosa* is a Gram-negative opportunistic pathogen that regulates much of its virulence via QS.[30] This bacterium's QS system involves two complete LuxI/LuxR circuits, a third orphan LuxR-type receptor, and a fourth QS receptor that utilizes a quinolone signal (Figure 1.3). Briefly, LasI synthesizes *N*-(3-oxo)-dodecanoyl L-homoserine lactone (OdDHL), which is recognized by both LasR and QscR (the Quorum Sensing Control Repressor), the orphan LuxR.[31] Intriguingly, LasR upregulates virulence phenotypes controlled by QS, while QscR represses them, yet they share a preferred native ligand.[32] RhlI synthesizes *N*-butyrl L-

homoserine lactone (BHL), which binds to RhlR. The Pseudomonas quinolone signal (PQS) is synthesized by a dedicated biosynthetic operon, and is sensed by the Pseudomonas quinolone signal receptor (PqsR).[33] These four receptors and three ligands work in an inter-regulated fashion to finely tune *P. aeruginosa* QS in response to its environment.[34]

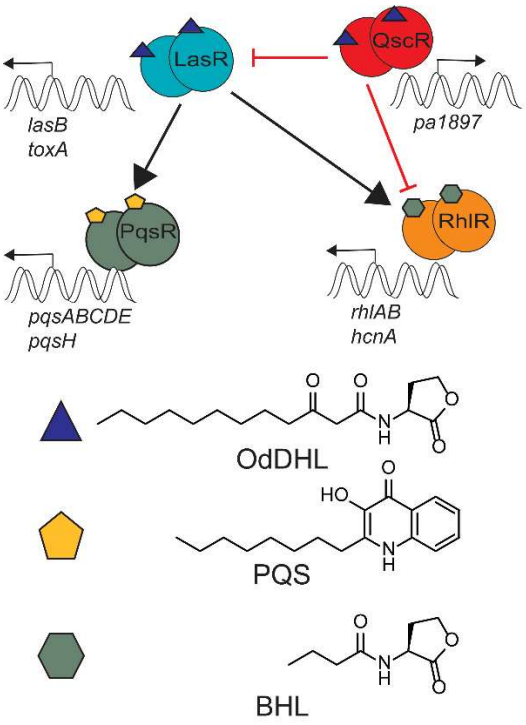


**Figure 1.3.** Simplified view of QS in *P. aeruginosa*. LasR, QscR, PqsR, and RhlR control transcription of distinct regulons in response to chemical signals.

Most likely to respond to rapidly changing environments, the QS system in *P. aeruginosa* is hierarchical. For example, under standard laboratory conditions, LasR expression is required to activate the Rhl and PQS systems.[35] Each of these receptors control its own regulon: among other products, LasR controls the production of elastase B and exotoxin A,[36] PqsR controls the production of pyocyanin and various phenazines,[37] and RhlR controls the production of

rhamnolipid and hydrogen cyanide.[38] Owing to its position at the top of the hierarchy, LasR has received significant attention as a target for antagonist development; indeed, that is the subject of two chapters of this thesis (Chapters 2 and 3). However, recent studies have demonstrated the importance of the RhlR,[39] particularly in chronic infections when LasR may be nonfunctional, [40] and a successful QS-based intervention will likely need to take RhlR into account as well.

### 1.2.1 Naturally-occurring small molecules that modulate LuxR type receptors

Naturally-occurring AHLs vary in the composition of their acyl tail (Figure 1.4).[41] Acyl tails vary in length from four to 20 carbons,[42] and in the oxidation state of the third carbon (methylene, hydroxyl, or ketone). AHLs may also contain one or more units of unsaturation. Typically, the acyl tail is derived from the pool of fatty acids available in the cell; however, in certain instances, the acid component can be derived from the environment. *Rhodopseudomonas palustris*, a photosynthetic bacterium, derives its "fatty" acid building block—*p*-coumaric acid—from its environment, rather than producing it itself.[43] In rarer cases, LuxR-type proteins may sense non-AHL ligands that are produced in their environment. *Pseudomonas* species GM79, a bacterium associated with the roots of the *Populus* plant, was recently shown to respond to a plant-produced ethanolamine derivative via its LuxR QS circuitry.[44] This is an intriguing example of cross-kingdom signaling mediated by LuxR-type QS machinery.

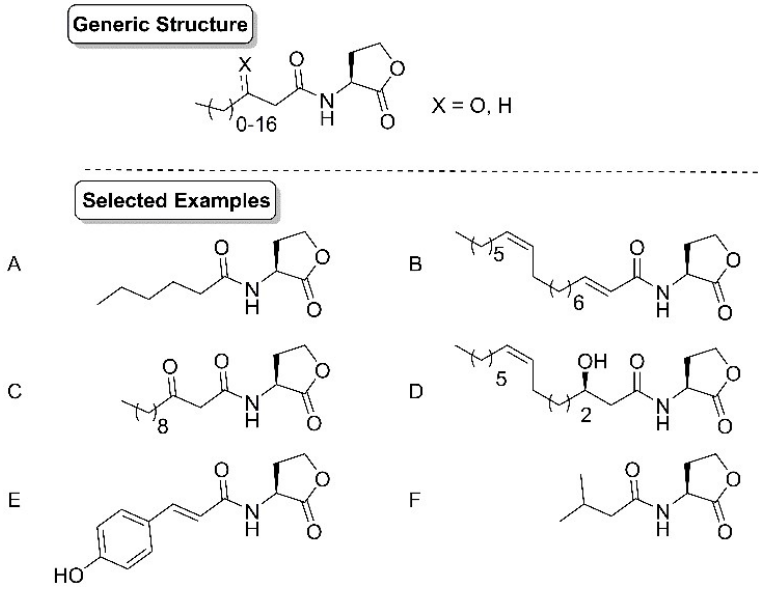


**Figure 1.4.** Selected naturally occurring N-acylated homoserine lactone QS signals. (A) *N*-Hexanoyl L-homoserine lactone (HHL), synthesized by CviI from *Chromobacterium violaceum*, native signal of CviR,[45] (B) *N*-(2*E*, 11*Z*)-2,11-octadecadienoyl L-homoserine lactone produced by a LuxI enzyme in *Dinoroseobacter shibae*,[46] (C) *N*-(3-oxo)-decanoyl L-homoserine lactone, synthesized by LasI from *Pseudomonas aeruginosa*, native ligand of LasR,[47] (D) *N*-(3*R*, 7*Z*)-3-hydroxy-7-tetradecenoyl homoserine lactone, synthesized by CinI from *Rhizobium leguminosarum*, native signal of CinR,[48, 49] (E) *p*-coumaroyl homoserine lactone, synthesized by RpaI from *Rhodopseudomonas palustris*, native ligand of RpaR [43] (F) Isovaleryl homoserine lactone, synthesized by BjaI from *Bradyrhizobium japonicum*, native ligand of BjaR.[50]

### 1.2.2 Chemical strategies for modulating LuxR type receptors with non-native ligands

Elucidation of the native AHL signal scaffold was closely followed by attempts to alter its structure through chemical synthesis to determine the features that are essential for its function.[47, 51, 52] These initial efforts in the 1990s produced molecules that largely resemble naturally occurring AHLs (i.e., analogues with conserved homoserine lactone "head groups" and unbranched acyl "tail groups" that varied in the length of their carbon chains). These studies clarified the optimal chain length for various receptors and demonstrated that synthetic, non-self AHLs could repress the activity of (i.e., antagonize) LuxR-type receptors. These past studies also showed that AHLs could activate LuxR-type receptors at low (nanomolar) concentrations, but only antagonize them at high concentrations (micromolar).

These synthetic studies required the concomitant development of screening assays for quantifying compound bioactivity. Researchers turned to reporter gene assays, in which a gene that can be easily measured (i.e., *gfp*) is placed under the control of a promoter recognized by the LuxR-type receptor of interest. Phenotypic assays, which measure the ability of chemical probes to modulate QS phenotypes of interest (commonly associated with virulence) were also developed. Together, these assay strategies allowed for the delineation of structure-activity relationship (SAR) trends and the development of compounds that can modulate QS in the wild-type organism.

Exploration of the structure-activity relationships (SARs) of AHLs for LuxR-type receptor modulation continued after this early work.[53-58] Given that potent activators already existed (the native signals), these studies were largely motivated by the need for compounds that could turn QS *off* (i.e., antagonists). Briefly, these studies involved (i) the replacement of the homoserine lactone head with a variety of lactones, thiolactones, and carbocycles, and (ii) the substitution of the unbranched acyl tail for diverse carboxylic acid coupling partners (Figure 1.5). These ligands were designed with the reasoning that they can bind competitively with native AHLs in the same site on the receptor. Efforts were also made to take advantage of nucleophilic residues in the AHL binding site (i.e., Cys 79 in LasR) by designing irreversible antagonists that incorporate electrophilic groups at the appropriate position to form a covalent bond with the protein.[59-61] These latter studies on irreversible ligands were met with mixed results—success depends heavily on *which* scaffold the researchers chose—but nonetheless represent intellectually novel approaches.

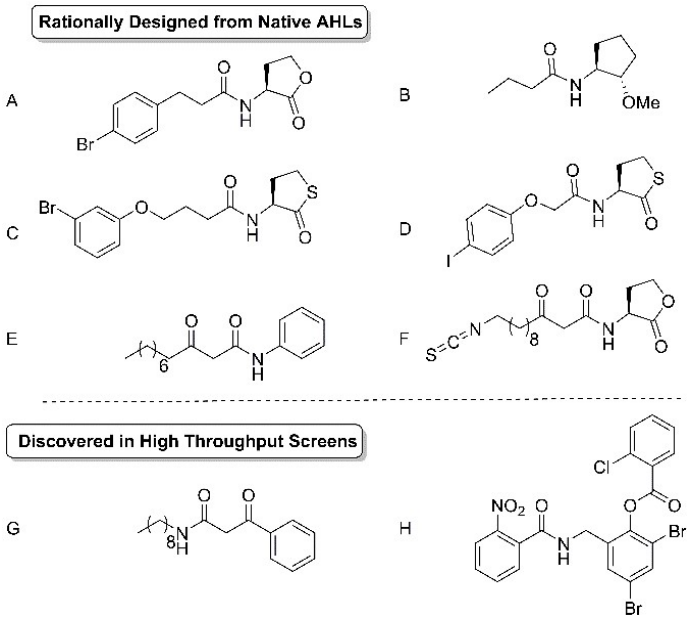


**Figure 1.5.** Selected non-native small molecules that modulate LuxR type proteins. (A) B7, a pan-active antagonist, designed by the Blackwell lab;[53] (B) BHL analogue with modified headgroup, designed by the Spring group, with activity in phenotypic assays in *P. aeruginosa*;[55] (C) mBTL, pan-active agonist, designed by the Bassler group;[58] (D) RN42, RhlR antagonist designed by the Blackwell group;[62] (E) 3-oxo-C12-aniline, LasR antagonist designed by the Blackwell group;[56] (F) ITC-12- covalent LasR partial agonist designed by the Meijler group;[59] (G) V-06-018, potent LasR antagonist discovered by the Greenberg group and Vertex Pharmaceuticals;[63] (H) TP1-R, discovered by the Greenberg group and Vertex Pharmaceuticals, structure revised by the Janda group.[64, 65]

These past efforts, focused primarily (but not exclusively) on LasR from *P. aeruginosa*, yielded a set of antagonists capable of modulating phenotypes in the wild-type organism, albeit at relatively high concentrations. In addition, the potency with which they antagonize (as measured in cell-based reporter assays in the wild-type organism) were modest (<10 μM, *vide infra*).

To accelerate the search for new scaffolds and compounds with higher efficacies/potencies, high throughput screening (HTS) campaigns have been conducted to identify LuxR-type receptor modulators in parallel with these rational design efforts. HTS is a proven strategy for discovering probe or drug-like molecules that are structurally unrelated to

known ligands.[66] As with the rational design projects, LasR became a prime target for screening campaigns.[67] Intelligent choice of libraries for screening can pay dividends; for example, the Meijler group discovered ligands that inhibit TraR from plant pathogen *Agrobacterium tumafaciens* after screening only 3,800 plant-produced natural products.[68] Additionally, ligands discovered in screens for one LuxR-type receptor may be useful in modulating another QS receptor. Chlorolactone (i.e., CL), best known for placing CviR in a non-DNA-binding, 'crossed' conformation (*vide supra)*,[25] is a minimally-modified analogue of a hit from a screen conducted by the Bassler group targeting LuxN, a membrane-bound, AHL-sensing, QS receptor from *Vibrio harveyi.*[57]

From the perspective of discovering ligands to modulate QS in *P. aeruginosa,* the most successful HTS studies were conducted collaboratively by the Greenberg lab and Vertex Pharmaceuticals. These studies identified V-06-018, a potent LasR antagonist, and the triphenyl (TP) family of LasR agonists (**Figure 1.4**).[63, 64] At the time of their discovery (2006), these scaffolds represented the most promising reported non-AHL LasR antagonists and agonists, respectively.

### 1.2.3. Challenges applying chemical strategies to block QS signaling in *P. aeruginosa*

Despite the advances described above, many challenges remain in developing "ideal" chemical probes of the LuxR-type proteins in *P. aeruginosa*. It is useful at this juncture to describe an ideal probe. This compound should be (1) highly potent and efficacious in both reporter gene assays conducted in a *P. aeruginosa* background and phenotypic assays in wild-type *P. aeruginosa*; (2) soluble in aqueous media; (3) non-toxic; (4) specific for its target receptor; (5) chemically stable (i.e.,. free of any labile bonds); and (6) composed of a structure

that is amenable to functional probe or translational applications (i.e., allowing for structural diversification and potentially not overly lipophilic, unlike OdDHL and V-06-018).

All existing AHL-based antagonists fail to satisfy these criteria. AHL-based antagonists are of low potency; none have an $IC_{50}$ in a *P. aeruginosa* based gene reporter experiment of < 10 μM. The lack of potent AHL-based antagonists is unlikely to be due to an insufficient exploration of the chemical space surrounding the scaffold; the Blackwell lab alone has synthesized and screened more than 200 synthetic AHLs. Instead, the scaffold itself suffers from inherent chemical and biological liabilities.

Lactones are hydrolytically unstable, particularly in *P. aeruginosa* culture, which becomes basic over time. The half-lives of AHLs are highly pH dependent; while at neutral conditions (pH = 7) their half-lives are on the order or days, in basic media (pH = 9.2) they are approximately one hour.[69] Additionally, both the lactone and amide bonds in AHLs are subject to enzymatic hydrolysis by acylases and amidases present in *P. aeruginosa* and other organisms.[70] Further limiting their utility is the fact that both native and synthetic AHLs are actively effluxed from *P. aeruginosa* by the MexAB-OprM multidrug efflux pump.[71] These factors mean that even a synthetic AHL that binds tightly to a LuxR-type receptor *and* interferes with its ability to initiate transcription, it will have limited effectiveness in the wild-type organism.

Structurally unrelated compounds found via HTS studies could have several advantages in *P. aeruginosa* relative to AHLs. First and foremost is the improvement in stability afforded by the removal of the lactone. Secondly, they may not be effluxed by the MexAB-OprM pump. The MexAB-OprM pump is not specific for AHLs; however, our lab has found that the non-AHL ligands V-06-018 and TP-1 are not subject to efflux.[71] Additionally, new antagonists discovered through screening may lack the long aliphatic tails that may reduce their *in vivo* utility. Lastly,

our group has found that V-06-018 and TP-1 are highly specific for LasR over QscR and RhlR (unpublished results), suggestive that non-AHL type compounds could exhibit higher receptor selectivities in *P. aeruginosa* relative to AHLs. All LuxR-type receptors can bind to the HSL head; selectivity is determined by the tail group. Screening a sufficient number of compounds from diversity libraries may allow for the discovery of ligands that are finely tuned to the subtle differences in each part of the LuxR-type receptor binding cavity, or potentially even target other sites on these receptors.

## 1.3 Dissertation Scope

### 1.3.1 Chapter 2: Design, synthesis, and biochemical characterization of non-native antagonists of the *Pseudomonas aeruginosa* quorum sensing receptor LasR with nanomolar $IC_{50}$ values

As indicated above, the QS field lacks highly potent inhibitors ($IC_{50}$ < 1 μM) of LasR. In Chapter 2, I describe my study of the SAR of V-06-018, the most potent LasR antagonist known at the outset of my Ph.D. research, for LasR antagonism. After developing an efficient synthetic route that enabled diversification of the V-06-018 scaffold, I systematically evaluated the effect of changes to the headgroup, linker, and tailgroup portions of the molecule. These experiments revealed strict SAR requirements for LasR activity, which I used to design antagonists that were found to be >10 fold more potent than V-06-018. Follow-up biochemical experiments indicate that these compounds function at least in part by allowing LasR to adopt a conformation that is unable to bind DNA. The lead compounds from this study represent, to our knowledge, the most potent known LasR antagonists to be reported.

### 1.3.2 Chapter 3: Abiotic antagonists of the *Pseudomonas aeruginosa* quorum sensing receptor LasR discovered from high-throughput screening

Only a limited number of chemical scaffolds are known to interact with LuxR-type proteins, and the most abundant class—AHLs—suffers from inherent chemical and biological liabilities (see above). This Chapter describes the implementation of a high-throughput screen to identify new LasR antagonist scaffolds. I screened a 25,000-compound library in a LasR gene reporter assay in *P. aeruginosa* and discovered four new LasR antagonist scaffolds. These compounds are potent ($IC_{50}$ values >1 μM for lead compounds), efficacious (>50% maximum inhibition), and may have significantly improved physicochemical properties as chemical probes relative to AHLs.

### 1.3.3 Chapter 4: Structural basis for partial agonism of the *Pseudomonas aeruginosa* quorum sensing receptor LasR

Limited 3D structural data (i.e., X-ray crystal s or NMR structures) are available for LuxR-type receptors, especially in complex with non-native ligands. This lack of data has hindered the development of mechanistic hypothesis for the both the agonism and antagonism of LuxR-type proteins by non-native molecules and represents one of the most significant challenges in the QS field. This Chapter describes a series of co-crystal structures of the LasR ligand binding domain complexed with non-native agonists and partial agonists discovered in a high throughput screen. These structures highlight the correlation between the position of the L3 loop—[72] a flexible portion of LasR flanking the ligand binding site hypothesized to transmit information between the ligand binding domain and DNA binding domain—and the activity of the ligand. As in previous studies, we observe that more-potent ligands cause the loop to pack closer to LasR,

sealing the ligand binding channel, while less-potent ligands position the loop away from LasR. These results serve to underscore the importance of the L3 loop for ligand activity in LasR.

### 1.3.4 Chapter 5: Profiling the specificity and promiscuity of LuxR-type receptors with a library of *N*-acylated homoserine lactones that vary in acyl tail length

Many species of bacteria that utilize LuxI/LuxR-type QS are known to coinhabit the same environments, raising the intriguing possibility of inter-species crosstalk via AHL signals. Such inter-species sensing requires the activity of LuxR-type receptors to be modulated by non-self AHLs. In this study, we systematically examined the ability of a family of AHLs with varying acyl tail lengths to activate and inhibit LuxR-type proteins from bacteria that are known to live together in the environment (e.g., soil, water, and plant and animal hosts). Our synthetic approach also allowed us to examine AHLs that are not found in Nature, and revealed ligands that could be useful in selectively manipulating QS in mixed cultures, including the two Gram-negative pathogens *P. aeruginosa* and *B. cepacia* that are known to coinfect humans.

### 1.3.5 Chapter 6: A comparative study of non-native *N*-acyl-L-homoserine lactone analogs in two *P. aeruginosa* QS receptors that share a common native ligand yet inversely regulate virulence

*P. aeruginosa* possess three LuxR-type proteins, two of which bind the same native ligand. Intriguingly, one of these proteins, LasR, promotes QS-associated virulence phenotypes, while the other, QscR, represses them. Identifying compounds that could selectively modulate each of these receptors would therefore be useful to interrogate their seemingly opposing roles in *P. aeruginosa* QS biology. In this study, we sought to examine the "preferences" of each receptor for a series of headgroup-modified OdDHL analogues. Our combined synthetic work and

reporter gene assays revealed structural features that bias ligands towards preferential activation of one receptor over the other.

### 1.3.6. Chapter 7: Future Directions

Various extensions of the work described in this thesis are proposed and their potential implications are expounded upon.

**References**


1. Locey, K. J.; Lennon, J. T., Scaling laws predict global microbial diversity. *Proc Natl Acad Sci U S A* **2016,** *113* (21), 5970-5.
2. Wilson, M. R.; Zha, L.; Balskus, E. P., Natural product discovery from the human microbiome. *J Biol Chem* **2017,** *292* (21), 8546-8552.
3. World Health Organization Global Health Observatory Data, Morbality and Global Health Esimates. https://www.who.int/gho/mortality_burden_disease/en/ (accessed May 22, 2020)
4. Brown, E. D.; Wright, G. D., Antibacterial drug discovery in the resistance era. *Nature* **2016,** *529* (7586), 336-43.
5. Clatworthy, A. E.; Pierson, E.; Hung, D. T., Targeting virulence: a new paradigm for antimicrobial therapy. *Nat Chem Biol* **2007,** *3* (9), 541-8.
6. Tomasz, A., Control of the Competent State in *Pneumoccoccus* by a Hormone-Like Cell Product: an Example for a New Type of Regulatory Mechanism in Bacteria *Nature* **1965,** *208*, 155-159.
7. Nealson, K. H. P., T.; Hastings, W.J., Cellular Control of the Synthesis and Activity of the Bacterial Luminescent System. *J. Bacteriol.* **1970,** *104* (1), 313-322.
8. Engebrecht, J. S., M., Identification of genes and gene products necessary for bacterial bioluminescence. *Proc. Natl. Acad. Sci. U. S. A.* **1984,** *81*, 4154-4158.
9. Eberhard, A. B., A.L.; Eberhard, C.; Kenyon, G.L.; Nealson, K.H.; Oppenheimer, N.J., Structural Identification of Autoinducer of Photobacterium fischeri Luciferase. *Biochemistry* **1981,** *20*, 2444-2449.
10. Fuqua, C. W., S.C.; Greenberg, E.P., Quorum Sensing in Bacteria: the LuxR-LuxI Family of Cell Density-Responsive Transcriptional Regulators. *J. Bacteriol.* **1994,** *176* (2), 269-275.
11. Erez, Z.; Steinberger-Levy, I.; Shamir, M.; Doron, S.; Stokar-Avihail, A.; Peleg, Y.; Melamed, S.; Leavitt, A.; Savidor, A.; Albeck, S.; Amitai, G.; Sorek, R., Communication between viruses guides lysis-lysogeny decisions. *Nature* **2017,** *541* (7638), 488-493.
12. Ji, G. B., R.C.; Novick, R.P., Cell density control of staphylococcal virulence mediated by an octapeptide pheromone. *Proc Natl Acad Sci U S A* **1995,** *92*, 12055 - 12059.
13. Chen, X. S., S.; Potier, N.; Dorsselaer, A.V.; Pelczer, I.; Bassler, B.L.; Hughson, F.M., Structural identification of a bacterial quorum-sensing signal containing boron. *Nature* **2002,** *415*, 545-549.
14. Bottomley, M. J.; Muraglia, E.; Bazzo, R.; Carfi, A., Molecular insights into quorum sensing in the human pathogen Pseudomonas aeruginosa from the structure of the virulence regulator LasR bound to its autoinducer. *J Biol Chem* **2007,** *282* (18), 13592-600.
15. Sidote, D. J.; Barbieri, C. M.; Wu, T.; Stock, A. M., Structure of the Staphylococcus aureus AgrA LytTR domain bound to DNA reveals a beta fold with an unusual mode of binding. *Structure* **2008,** *16* (5), 727-35.
16. Vannini, A. V., C.; Gargioli, C.; Muraglia, E.; Cortese, R.; Francesco, R.D.; Neddermann, P.; Marco, S.D., The crystal structure of the quorum sensing protein TraR bound to its autoinducer and target DNA. *EMBO Journal* **2002,** *21* (17), 4393-4401.
17. Rutherford, S. T.; Bassler, B. L., Bacterial quorum sensing: its role in virulence and possibilities for its control. *Cold Spring Harb Perspect Med* **2012,** *2* (11).
18. Ho, D. K.; Murgia, X.; De Rossi, C.; Christmann, R.; A, G. H. d. M. M.; Koch, M.; Andreas, A.; Herrmann, J.; Muller, R.; Empting, M.; R, W. H.; Desmaele, D.; Loretz, B.; Couvreru, P.; Lehr, C. M., Squalenyl Hydrogen Sulfate Nanoparticles for Simultaneous Delivery of Tobramycin and Alkylquinolone Quorum Sensing Inhibitor to Eradicate P. aeruginosa Biofilm Infections. *Angew Chem Int Ed Engl* **2020**.
19. Kratochvil, M. J.; Tal-Gan, Y.; Yang, T.; Blackwell, H. E.; Lynn, D. M., Nanoporous Superhydrophobic Coatings that Promote the Extended Release of Water-Labile Quorum Sensing Inhibitors and Enable Long-Term Modulation of Quorum Sensing in Staphylococcus aureus. *ACS Biomater Sci Eng* **2015,** *1* (10), 1039-1049.
20. Dong, S. F., N.D.; Christensen, Q.H.; Greenberg, E.P.; Nagarajan, R.; Nair, S.K., Molecular basis for the substrate specificity of quorum signal synthases. *Proc Natl Acad Sci U S A* **2017,** *114* (34), 9027-

9097.
21. Fuqua, C.; Greenberg, E. P., Listening in on bacteria: acyl-homoserine lactone signalling. *Nat Rev Mol Cell Biol* **2002,** *3* (9), 685-95.
22. Hudaiberdiev, S.; Choudhary, K. S.; Vera Alvarez, R.; Gelencser, Z.; Ligeti, B.; Lamba, D.; Pongor, S., Census of solo LuxR genes in prokaryotic genomes. *Front Cell Infect Microbiol* **2015,** *5*, 20.
23. Wellington, S. G., E.P., Quorum Sensing signal selectivity and the potential for interspecies cross talk. *mBio* **2019,** *10* (2), e00146-19.
24. Lintz, M. J.; Oinuma, K.; Wysoczynski, C. L.; Greenberg, E. P.; Churchill, M. E., Crystal structure of QscR, a Pseudomonas aeruginosa quorum sensing signal receptor. *Proc Natl Acad Sci U S A* **2011,** *108* (38), 15763-8.
25. Chen, G.; Swem, L. R.; Swem, D. L.; Stauff, D. L.; O'Loughlin, C. T.; Jeffrey, P. D.; Bassler, B. L.; Hughson, F. M., A strategy for antagonizing quorum sensing. *Mol Cell* **2011,** *42* (2), 199-209.
26. Schuster, M.; Urbanowski, M. L.; Greenberg, E. P., Promoter specificity in Pseudomonas aeruginosa quorum sensing revealed by DNA binding of purified LasR. *Proc Natl Acad Sci U S A* **2004,** *101* (45), 15833-9.
27. Wysoczynski-Horita, C. L.; Boursier, M. E.; Hill, R.; Hansen, K.; Blackwell, H. E.; Churchill, M. E. A., Mechanism of agonism and antagonism of the Pseudomonas aeruginosa quorum sensing regulator QscR with non-native ligands. *Mol Microbiol* **2018,** *108* (3), 240-257.
28. There is one excetption: SdiA from E. coli and S. enterica. SdiA is unique among LuxR type receptors in its stabliity and activity without a ligand, and a crystal structure has been captured of SdiA with a detergent molecule in its binding pocket rather than an AHL. Studies into the origin of SdiA's unique stability are ongoing in our laboratory. See Kim et al, Acta Cryst. (2014) D70, 694 - 707
29. Zou, Y.; Nair, S. K., Molecular basis for the recognition of structurally distinct autoinducer mimics by the Pseudomonas aeruginosa LasR quorum-sensing signaling receptor. *Chem Biol* **2009,** *16* (9), 961-70.
30. Schuster, M.; Greenberg, E. P., A network of networks: quorum-sensing gene regulation in Pseudomonas aeruginosa. *Int J Med Microbiol* **2006,** *296* (2-3), 73-81.
31. Chugani, S.; Greenberg, E. P., An evolving perspective on the Pseudomonas aeruginosa orphan quorum sensing regulator QscR. *Front Cell Infect Microbiol* **2014,** *4*, 152.
32. Boursier, M. E.; Manson, D. E.; Combs, J. B.; Blackwell, H. E., A comparative study of non-native N -acyl l -homoserine lactone analogs in two Pseudomonas aeruginosa quorum sensing receptors that share a common native ligand yet inversely regulate virulence. *Bioorganic & Medicinal Chemistry* **2018**.
33. Pesci, E. C. M., J.B.J.; Pearson, J.P.; McKnight, S.; Kende, A.S.; Greenberg, E.P.; Iglewski, B.H., Quinolone signaling in the cell-to-cell communication system of Pseudomonas aeruginosa. *Proc Natl Acad Sci U S A* **1999,** *96*, 11229-11234.
34. Welsh, M. A.; Blackwell, H. E., Chemical Genetics Reveals Environment-Specific Roles for Quorum Sensing Circuits in Pseudomonas aeruginosa. *Cell Chem Biol* **2016,** *23* (3), 361-9.
35. Lee, J.; Zhang, L., The hierarchy quorum sensing network in Pseudomonas aeruginosa. *Protein Cell* **2015,** *6* (1), 26-41.
36. Pearson, J. P. P., E.C.; Iglewski, B.H., Roles of *Pseudomonas aeruginosa las* and *rhl* Quorum-Sensing Systems in Control of Elastase and Rhamnolipid Biosynthesis Genes. *Journal of Bacteriology* **1997,** *179* (18), 5756-5767.
37. Maura, D.; Hazan, R.; Kitao, T.; Ballok, A. E.; Rahme, L. G., Evidence for Direct Control of Virulence and Defense Gene Circuits by the Pseudomonas aeruginosa Quorum Sensing Regulator, MvfR. *Sci Rep* **2016,** *6*, 34083.
38. Brint, J. M. O., D.E., Synthesis of Multiple Exoproducts in *Pseudomonas aeruginosa* Is under the Control of RhlR-RhlI, Another Set of Regulators in Strain PAO1 with Homology to the Autoinducer-Responsive LuxR-LuxI Family. *J Bacteriol* **1995,** *177* (24), 7155-7163.
39. Mukherjee, S.; Moustafa, D. A.; Stergioula, V.; Smith, C. D.; Goldberg, J. B.; Bassler, B. L., The PqsE and RhlR proteins are an autoinducer synthase-receptor pair that control virulence and biofilm

development in Pseudomonas aeruginosa. *Proc Natl Acad Sci U S A* **2018,** *115* (40), E9411-E9418.
40. Feltner, J. B.; Wolter, D. J.; Pope, C. E.; Groleau, M. C.; Smalley, N. E.; Greenberg, E. P.; Mayer-Hamblett, N.; Burns, J.; Deziel, E.; Hoffman, L. R.; Dandekar, A. A., LasR Variant Cystic Fibrosis Isolates Reveal an Adaptable Quorum-Sensing Hierarchy in Pseudomonas aeruginosa. *MBio* **2016,** *7* (5).
41. Galloway, R. J. D. H., J.T.; Bowden, S.D.; Welch, M.; Spring, D.R., Quorum Sensing in Gram-Negative Bacteria: Small-Molecule Modulation of AHL and AI-2 Quorum Sensing Pathways. *Chem Rev* **2011,** *111*, 28-67.
42. Arashida, N.; Shimbo, K.; Terada, T.; Okimi, T.; Kikuchi, Y.; Hashiro, S.; Umekage, S.; Yasueda, H., Identification of novel long chain N-acylhomoserine lactones of chain length C20 from the marine phototrophic bacterium Rhodovulum sulfidophilum. *Biosci Biotechnol Biochem* **2018,** *82* (10), 1683-1693.
43. Schaefer, A. L.; Greenberg, E. P.; Oliver, C. M.; Oda, Y.; Huang, J. J.; Bittan-Banin, G.; Peres, C. M.; Schmidt, S.; Juhaszova, K.; Sufrin, J. R.; Harwood, C. S., A new class of homoserine lactone quorum-sensing signals. *Nature* **2008,** *454* (7204), 595-9.
44. Coutinho, B. G.; Mevers, E.; Schaefer, A. L.; Pelletier, D. A.; Harwood, C. S.; Clardy, J.; Greenberg, E. P., A plant-responsive bacterial-signaling system senses an ethanolamine derivative. *Proc Natl Acad Sci U S A* **2018**.
45. McClean, K. M., K.H.; Fish, L.; Taylor, A.; Chhabra, S.R.; Camara, M.; Daykin, M.; Lamb, J.H.; Swift, S.; Bycroft, B.W.; Stewart, G.S.A.B.; Williams, P. , Quorum sensing and Chromobacterium violaceum: exploitation of violacein production and inhibition for the detection of N-acyl homoserine lactones. *Microbiology* **1997,** *143*, 3703-3711.
46. Neumann, A.; Patzelt, D.; Wagner-Dobler, I.; Schulz, S., Identification of new N-acylhomoserine lactone signalling compounds of Dinoroseobacter shibae DFL-12(T) by overexpression of luxI genes. *Chembiochem* **2013,** *14* (17), 2355-61.
47. Passador, L. T., K.D.; Buertin, K.R.; Journet, M.P.; Kende, A.S.; Iglewski, B.H., Functional Analysis of the *Pseuomonas aeruginosa* Autoinducer PAI. *J Bacteriol* **1996,** *178* (20), 5995-6000.
48. Yajima, A. V. B., A.A.N.; Schripsema, J.; Nukada, T.; Yabuta, G., Synthesis and Stereochemistry-Activity Relationship of small Bacteriocin, an Autoinducer of the Symbiotic Nitrogen-Fixing Bacterium Rhizobium leguminosarum. *Org Lett* **2008,** *10* (10), 2047 - 2050.
49. Hirsch, P. R., Plasmid-determined Bacteriocin Production by Rhizobium leguminosarum. *J. Gen. Microbiol.* **1979,** *113*, 219-228.
50. Lindemann, A.; Pessi, G.; Schaefer, A. L.; Mattmann, M. E.; Christensen, Q. H.; Kessler, A.; Hennecke, H.; Blackwell, H. E.; Greenberg, E. P.; Harwood, C. S., Isovaleryl-homoserine lactone, an unusual branched-chain quorum-sensing signal from the soybean symbiont Bradyrhizobium japonicum. *Proc Natl Acad Sci U S A* **2011,** *108* (40), 16765-70.
51. Zhu J, B. J., More MI, Fuqua C, Eberhard A, Winans SC, Analogs of the Autoinducer 3-Oxooctanoyl-Homoserine Lactone Strongly Inhibit Activity of the TraR Protein of *Agrobacterium tumefaciens*. *Journal of Bacteriology* **1998,** *180* (20), 5398-5405.
52. Schaefer, A., Hanzelka BL, Eberhard A, Greenberg EP, Quorum Sensing in *Vibrio fischeri*: Probing Autoinducer-LuxR Interactions with Autoinducer Analogs. *Journal of Bacteriology* **1996,** *178* (10), 2897-2901.
53. Geske, G. D. W., R.J.; Siegel, A.P.; Blackwell, H.E., Smal Molecule Inhibitors of Bacterial Quorum Sensing and Biofilm Formation. *J Am Chem Soc* **2005,** *127*, 12762-12763.
54. Glansdorp, F. G.; Thomas, G. L.; Lee, J. K.; Dutton, J. M.; Salmond, G. P.; Welch, M.; Spring, D. R., Synthesis and stability of small molecule probes for Pseudomonas aeruginosa quorum sensing modulation. *Org Biomol Chem* **2004,** *2* (22), 3329-36.
55. Lee, L. Y.; Hupfield, T.; Nicholson, R. L.; Hodgkinson, J. T.; Su, X.; Thomas, G. L.; Salmond, G. P.; Welch, M.; Spring, D. R., 2-Methoxycyclopentyl analogues of a Pseudomonas aeruginosa quorum sensing modulator. *Mol Biosyst* **2008,** *4* (6), 505-7.
56. McInnis, C. E.; Blackwell, H. E., Design, synthesis, and biological evaluation of abiotic, non-

lactone modulators of LuxR-type quorum sensing. *Bioorg Med Chem* **2011,** *19* (16), 4812-9.
57. Swem, L. R.; Swem, D. L.; O'Loughlin, C. T.; Gatmaitan, R.; Zhao, B.; Ulrich, S. M.; Bassler, B. L., A quorum-sensing antagonist targets both membrane-bound and cytoplasmic receptors and controls bacterial pathogenicity. *Mol Cell* **2009,** *35* (2), 143-53.
58. O'Loughlin, C. T.; Miller, L. C.; Siryaporn, A.; Drescher, K.; Semmelhack, M. F.; Bassler, B. L., A quorum-sensing inhibitor blocks Pseudomonas aeruginosa virulence and biofilm formation. *Proc Natl Acad Sci U S A* **2013,** *110* (44), 17981-6.
59. Amara, N. M., R.; Amar, D.; Krief, P.; Spieser, S.A.H.; Bottomley, M.J.; Aharoni, A.; and Meijler, M.M., Covalent Inhibition of Bacterial Quorum Sensing. *J Am Chem Soc* **2009**.
60. Amara, N.; Gregor, R.; Rayo, J.; Dandela, R.; Daniel, E.; Liubin, N.; Willems, H. M.; Ben-Zvi, A.; Krom, B. P.; Meijler, M. M., Fine-Tuning Covalent Inhibition of Bacterial Quorum Sensing. *Chembiochem* **2016,** *17* (9), 825-35.
61. O'Brien, K. T.; Noto, J. G.; Nichols-O'Neill, L.; Perez, L. J., Potent Irreversible Inhibitors of LasR Quorum Sensing in Pseudomonas aeruginosa. *ACS Med Chem Lett* **2015,** *6* (2), 162-7.
62. Boursier, M. E. C., J.B.; Blackwell, H.E., N-Acyl L-Homocysteine Thiolactones Are Potent and Stable Synthetic Modulators of the RhlR Quorum Sensing Receptor in Pseudomonas aeruginosa. *ACS Chem Biol* **2019,** *14*, 186-191.
63. Muh, U.; Schuster, M.; Heim, R.; Singh, A.; Olson, E. R.; Greenberg, E. P., Novel Pseudomonas aeruginosa quorum-sensing inhibitors identified in an ultra-high-throughput screen. *Antimicrob Agents Chemother* **2006,** *50* (11), 3674-9.
64. Muh, U.; Hare, B. J.; Duerkop, B. A.; Schuster, M.; Hanzelka, B. L.; Heim, R.; Olson, E. R.; Greenberg, E. P., A structurally unrelated mimic of a Pseudomonas aeruginosa acyl-homoserine lactone quorum-sensing signal. *Proc Natl Acad Sci U S A* **2006,** *103* (45), 16948-52.
65. Zakhari, J. S.; Kinoyama, I.; Struss, A. K.; Pullanikat, P.; Lowery, C. A.; Lardy, M.; Janda, K. D., Synthesis and molecular modeling provide insight into a Pseudomonas aeruginosa quorum sensing conundrum. *J Am Chem Soc* **2011,** *133* (11), 3840-2.
66. Macarron, R. H., R.P., Design and Implementation of High Throughput Screnning Assays. In *High Throughput Screening Methods and Protocols*, 2 ed.; Springer, Ed. Springer: 2009; pp 1-32.
67. Borlee, B. R.; Geske, G. D.; Blackwell, H. E.; Handelsman, J., Identification of synthetic inducers and inhibitors of the quorum-sensing regulator LasR in Pseudomonas aeruginosa by high-throughput screening. *Appl Environ Microbiol* **2010,** *76* (24), 8255-8.
68. David, S.; Mandabi, A.; Uzi, S.; Aharoni, A.; Meijler, M. M., Mining Plants for Bacterial Quorum Sensing Modulators. *ACS Chem Biol* **2017**.
69. Ziegler, E. W.; Brown, A. B.; Nesnas, N.; Palmer, A. G., Abiotic Hydrolysis Kinetics of N-Acyl-L-homoserine Lactones: Natural Silencing of Bacterial Quorum Sensing Signals. *European Journal of Organic Chemistry* **2019,** *2019* (17), 2850-2856.
70. Bokhove, M.; Nadal Jimenez, P.; Quax, W. J.; Dijkstra, B. W., The quorum-quenching N-acyl homoserine lactone acylase PvdQ is an Ntn-hydrolase with an unusual substrate-binding pocket. *Proc Natl Acad Sci U S A* **2010,** *107* (2), 686-91.
71. Moore, J. D.; Gerdt, J. P.; Eibergen, N. R.; Blackwell, H. E., Active efflux influences the potency of quorum sensing inhibitors in Pseudomonas aeruginosa. *Chembiochem* **2014,** *15* (3), 435-42.
72. O'Reilly, M. C.; Dong, S. H.; Rossi, F. M.; Karlen, K. M.; Kumar, R. S.; Nair, S. K.; Blackwell, H. E., Structural and Biochemical Studies of Non-native Agonists of the LasR Quorum-Sensing Receptor Reveal an L3 Loop "Out" Conformation for LasR. *Cell Chem Biol* **2018**, *25* 1128-1139

# CHAPTER TWO: Design, synthesis, and biochemical characterization of non-native antagonists of the *Pseudomonas aeruginosa* quorum sensing receptor LasR with nanomolar $IC_{50}$ values

Daniel E. Manson, Matthew C. O'Reilly, Kayleigh E. Nyffeler, Helen E. Blackwell

**This Chapter has been published under the same title.** Reference: Manson, D.E., O'Reilly, M.C., Nyffeler, K.E.; Blackwell, H.E. Blackwell. Design, Synthesis, and Biochemical Characterization of non-native antagonists of the *Pseudomonas aeruginosa* quorum sensing receptor LasR with nanomolar $IC_{50}$ values. *ACS Infect. Dis.* **2020** *6* (4) 649-661

D.E. Manson and H.E. Blackwell designed experiments. D.E. Manson and M.C. O'Reilly synthesized and characterized compounds. D.E. Manson and K.E. Nyffeler performed screening experiments. D.E. Manson performed biochemical experiments. D.E. Manson and H.E. Blackwell wrote the chapter.

## Abstract

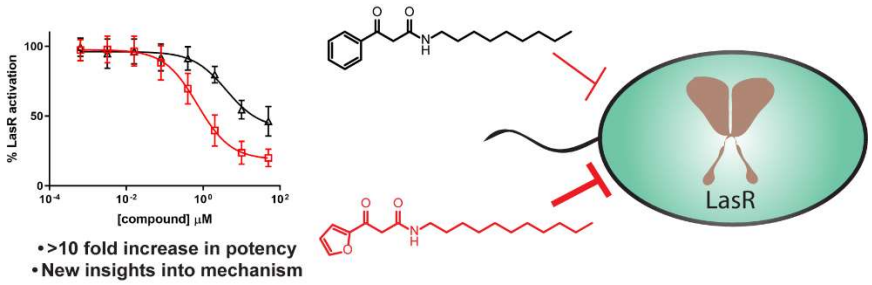


Quorum sensing (QS), a bacterial cell-to-cell communication system mediated by small molecules and peptides, has received significant interest as a potential target to block infection. The common pathogen *Pseudomonas aeruginosa* uses QS to regulate many of its virulence phenotypes at high cell densities, and the LasR QS receptor plays a critical role in this process. Small molecule tools that inhibit LasR activity would serve to illuminate its role in *P. aeruginosa* virulence, but we currently lack highly potent and selective LasR antagonists, despite considerable research in this area. V-06-018, an abiotic small molecule discovered in a high-throughput screen, represents one of the most potent known LasR antagonists, but has seen little study since its initial report. Herein, we report a systematic study of the structure-activity relationships (SARs) that govern LasR antagonism by V-06-018. We synthesized a focused library of V-06-018 derivatives and evaluated the library for bioactivity using a variety of cell-based LasR reporter systems. The SAR trends revealed by these experiments allowed us to design probes with 10-fold greater potency than V-06-018 and 100-fold greater potency than other commonly used *N*-acyl L-homoserine lactone (AHL)-based LasR antagonists, along with high selectivities for LasR. Biochemical experiments to probe the mechanism of antagonism by V-06-018 and its analogs support these compounds interacting with the native ligand-binding site in LasR and, at least in part, stabilizing an inactive form of the protein. The compounds described herein are the most potent and efficacious antagonists of LasR known and represent robust probes both for characterizing the mechanisms of LuxR-type QS and for chemical biology research in general in the growing QS field.

## Introduction

**Keywords:** *N*-acyl L-homoserine lactone; bacterial communication; intercellular signaling; LuxR-type receptor; small molecule probes; virulence

Quorum sensing (QS), a bacterial cell-to-cell communication system mediated by small molecules and peptides, has received significant interest as a potential target to block infection. The common pathogen *Pseudomonas aeruginosa* uses QS to regulate many of its virulence phenotypes at high cell densities, and the LasR QS receptor plays a critical role in this process. Small molecule tools that inhibit LasR activity would serve to illuminate its role in *P. aeruginosa* virulence, but we currently lack highly potent and selective LasR antagonists, despite considerable research in this area. V-06-018, an abiotic small molecule discovered in a high-throughput screen, represents one of the most potent known LasR antagonists, but has seen little study since its initial report. Herein, we report a systematic study of the structure-activity relationships (SARs) that govern LasR antagonism by V-06-018. We synthesized a focused library of V-06-018 derivatives and evaluated the library for bioactivity using a variety of cell-based LasR reporter systems. The SAR trends revealed by these experiments allowed us to design probes with 10-fold greater potency than V-06-018 and 100-fold greater potency than other commonly used *N*-acyl L-homoserine lactone (AHL)-based LasR antagonists, along with high selectivities for LasR. Biochemical experiments to probe the mechanism of antagonism by V-06-018 and its analogs support these compounds interacting with the native ligand-binding site in LasR and, at least in part, stabilizing an inactive form of the protein. The compounds described herein are the most potent and efficacious antagonists of LasR known and represent robust probes both for characterizing the mechanisms of LuxR-type QS and for chemical biology research in general in the growing QS field.

Microbial resistance to antibiotics is emerging faster than new treatments are being developed, setting the stage for a public health crisis.[1-2] As traditional antibiotics become less effective, interest has arisen in attenuating virulence via interference with nonessential pathways.[3] Inhibition of quorum sensing (QS), a mode of bacterial communication dependent on the exchange of chemical signals, has been shown to reduce virulence phenotypes in multiple human pathogens without affecting cell viability.[4-6] Accordingly, it has attracted significant interest as a potential anti-virulence strategy for combatting bacterial infections.[7-8] Our laboratory[9-11] and others[12-15] are interested in the development of small molecule and peptide probes to dissect the mechanisms of QS and their roles in infection.

The prototypical QS circuit in Gram-negative bacteria is the LuxI/LuxR synthase/receptor pair, first discovered in the marine symbiont *Vibrio fischeri*.[6] At low cell density, a LuxI-type enzyme synthesizes the QS signal, an *N*-acyl L-homoserine lactone (AHL), at a low basal rate. These low-molecular weight molecules can freely diffuse out of the cell, although in certain cases they are also actively exported.[16] The concentration of AHL signal is largely proportional to cell density (and this correlation is highly dependent on the environment), but as a bacterial community grows, the level of AHL signal in the local environment likewise increases (Figure 1A). At high cell densities, the intracellular AHL concentration is sufficient for productive binding of the AHL to its cognate LuxR-type receptor, a transcription factor. The activated receptor:ligand complex then typically dimerizes and binds to DNA, which subsequently alters gene expression levels to promote group-beneficial behaviors. In pathogenic bacteria, these behaviors can include the production of toxic virulence factors and biofilm. Typically, once a "quorum" is achieved, expression of the LuxI-type synthase is also increased, amplifying AHL production in a positive "autoinduction" feedback loop.[17]

*Pseudomonas aeruginosa* is an opportunistic pathogen that regulates many aspects of virulence using QS. This bacterium has a high rate of resistance to traditional antibiotics and causes infections that are especially dangerous for individuals with cystic fibrosis (CF), burn victims, and AIDS patients. The QS system in *P. aeruginosa* is relatively complex (Figure 1B),[18] consisting of two LuxI/LuxR pairs (LasI/LasR and RhlI/RhlR) along with an orphan LuxR-type receptor (QscR), which lacks a related synthase and native AHL signal. LasI synthesizes *N*-(3-oxo-dodecanoyl)-L-homoserine lactone (OdDHL), which targets LasR but also strongly activates QscR. RhlI synthesizes *N*-butyryl-L-homoserine lactone (BHL), which targets RhlR. Additionally, *P. aeruginosa* has a LysR-type receptor, PqsR, which is unrelated to LuxR-type receptors and uses 2-heptyl-3-hydroxy-4-(1*H*)-quinolone (i.e., the Pseudomonas quinolone signal (PQS)) as its ligand. These four QS systems are intimately linked and control different aspects of *P. aeruginosa* virulence that are highly dependent on the environment (Figure 1B).[9] LasR plays a central role in the QS hierarchy. For instance, LasR directly regulates the production of virulence factors such as elastase, alkaline protease, and exotoxin, and regulates rhamnolipid, HCN, and pyocyanin production via control of the *rhl* and *pqs* systems.[18] Biofilm, a major virulence phenotype in *P. aeruginosa*, is also regulated by LasR via the *rhl* and *pqs* systems.[19] In turn, LasR and RhlR are repressed by QscR, which again is strongly activated via LasR's native signal, OdDHL.

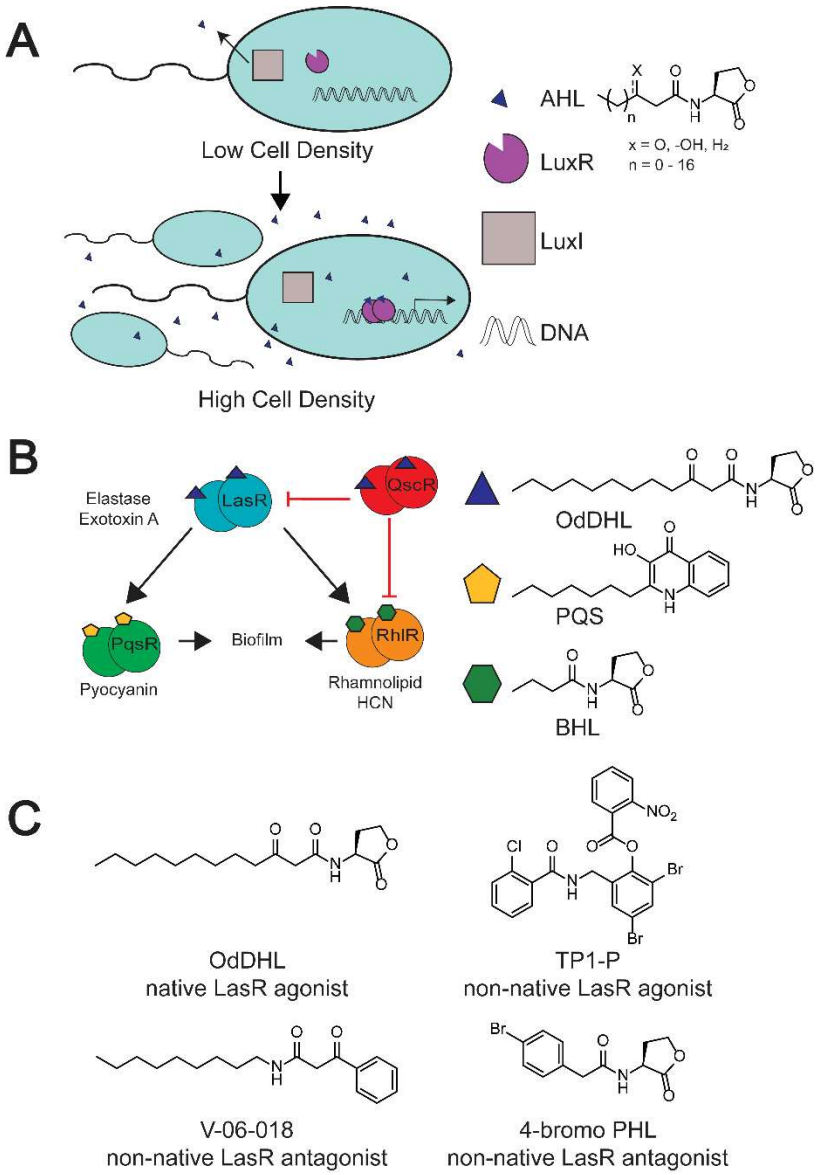


**Figure 2.1:** (A) General schematic of LuxI/LuxR-type quorum sensing (QS) in Gram-negative bacteria. (B) Simplified view of QS in *P. aeruginosa*. LasI/R and RhlI/R are LuxI/R homologues. QscR is an "orphan" LuxR-type receptor and responds to OdDHL. PqsR is a LysR-type receptor that responds to the Pseudomonas quinolone signal (PQS). AHL synthases are omitted for clarity. (C) Structures of native agonist OdDHL ($EC_{50}$ = 139 nM), non-AHL antagonist V-06-018 ($IC_{50}$ = 5.2 μM), non-AHL agonist TP1-P ($EC_{50}$ = 71 nM), and representative, synthetic AHL antagonist 4-bromo PHL ($IC_{50}$ = 116 μM); potency values all obtained in the same *P. aeruginosa* LasR reporter (from ref. 30).[20]

The connection between QS and virulence in *P. aeruginosa*, and in other Gram-negative bacterial pathogens, has motivated the development of small molecules and macromolecules

capable of inhibiting LuxI-type synthases,[21] destroying or sequestering AHL signals,[22] or blocking the binding of AHL signal to LuxR-type receptor.[23] The latter competitive inhibition strategy has seen the most study to date, with significant contributions by the Spring,[7] Bassler,[24] Greenberg,[25] and Meijler[15] labs, as well as our lab.[26] Due to its prominent position in the *P. aeruginosa* QS system (*vide supra*), much of the effort devoted to identifying small molecule modulators of QS in *P. aeruginosa* has focused on LasR. The majority of the known synthetic ligands that modulate LasR were identified by making systematic changes to the lactone "head group" and acyl "tail group" of OdDHL (e.g., 4-bromo PHL; Figure 1C).[27-28] However, these past efforts have failed to yield compounds that antagonize LasR with both high efficacies and potencies.[29] To our knowledge, none of these AHL analogs have lower than double-digit micromolar (□M) $IC_{50}$ values in reporter gene assays of LasR activity in *P. aeruginosa*.[30] These $IC_{50}$ values contrast with the nanomolar (nM) $EC_{50}$ value of LasR's native ligand, OdDHL, and those of other non-native agonists (e.g., the triphenyl derivative TP-1; Figure 1C).[25-26] The poor antagonism potencies for AHL analogs may be due, at least in part, to reliance on the AHL scaffold, which has several major liabilities for probe molecules. AHLs are susceptible to lactone hydrolysis, enzymatic degradation, and active efflux by *P. aeruginosa*.[16, 31-32] These drawbacks make the development of non-AHL antagonists of LasR, and other LuxR-type receptors, highly desirable.[30] That said, conversion of non-AHL scaffolds known to strongly agonize LasR (e.g., TP-1) into antagonists (i.e., "mode switching") has also not provided sub-□M LasR antagonists so far,[26] underscoring the challenges of this process.

High-throughput screens of small molecule libraries provide another pathway to identify non-AHL LasR antagonists.[33] One such screen by Greenberg and coworkers in 2006 revealed the compound V-06-018, a β-keto amide with a phenyl head group and a nine carbon tail (Figure

1C).[33] V-06-018 is a relatively potent LasR antagonist in both *E. coli* and *P. aeruginosa* LasR reporter strains (single digit micromolar $IC_{50}$) and has been shown to inhibit genes and phenotypes related to virulence in *P. aeruginosa*.[9, 33] The phenyl head group and aliphatic acyl tail of V-06-018 resemble that of the homoserine lactone head group and acyl tail of LasR's native ligand, OdDHL (Figure 1C). However, as V-06-018 lacks a lactone moiety, it is not susceptible to hydrolysis or enzymatic cleavage by AHL lactonases.[31-32] A prior study of ours also revealed that V-06-018 is not actively effluxed from *P. aeruginosa* by the promiscuous MexAB-OprM efflux pump, which is known to efflux both native and non-native AHLs with long acyl tails.[16] Despite these desirable qualities, V-06-018 has seen practically no scrutiny from a structure–function perspective and no substantive use as a chemical probe since its initial report over a decade ago.[30] We reasoned that the V-06-018 scaffold could provide entry into LasR antagonists with improved potencies along with robust physical properties, and in the current study we report our findings with regard to the first structure-function analysis of this scaffold. Our combined cell-based assays, synthesis, and iterative compound design revealed a set of new LasR antagonists based on V-06-018 with potencies, efficacies, and receptor selectivities in *P. aeruginosa* that, to our knowledge, surpass all known compounds reported to date. Follow on biochemical experiments on these compounds and V-06-018 support a mechanism of antagonism by which they interact with the OdDHL-binding site in LasR and, at least in part, stabilize an inactive form of the protein.

## RESULTS AND DISCUSSION

### V-06-018 is selective for LasR over RhlR and QscR in *P. aeruginosa*

We began our study by exploring the selectivity of V-06-018 for LasR over the other two LuxR-type receptors (RhlR and QscR) in *P. aeruginosa*, as other than its antagonistic activity in LasR,[30] this profile was unknown. In view of the overlapping activities of these three receptors in *P. aeruginosa* (see Figure 1B), small molecule tools that are selective for LasR (or indeed any of these receptors) are of significant interest for use as mechanistic probes in this pathogen. We submitted V-06-018 to reporter gene assays in *E. coli* to examine its antagonistic activity (in competition with the receptors' native or preferred ligand) and agonistic activity (alone) in LasR, RhlR, and QscR, using our previously reported methods (see Experimental Section). In these reporter assays in a heterologous background (i.e., *E. coli*), each of the receptors was examined in isolation from the others, allowing for clearer selectivity profiles to be defined relative to using analogous *P. aeruginosa* reporter systems. Receptor activity was monitored via □-galactosidase production. These experiments revealed V-06-018 was only an antagonist of LasR, displayed no activity (as either an antagonist or agonist) in RhlR, and was only a very weak antagonist QscR at the highest concentrations tested (see Figure S1). This high receptor selectivity profile rendered the V-06-018 scaffold even more compelling for new LasR antagonist development in *P. aeruginosa*.

### An efficient synthesis of V-06-018 and analogs

We next sought to devise a synthetic route to V-06-018 that was scalable and adaptable to analog synthesis. The only previously reported synthesis of V-06-018 gave the molecule in 5% yield, albeit in one step.[24] That synthesis involved refluxing ethyl benzoyl acetate and nonylamine in

ethanol. We reasoned the low yield for this reaction could be due to imine formation; therefore, we decided to protect the ketone in ethyl benzoyl acetate as a ketal (e.g., **2** → **3**; Scheme 1), and then saponified the ester to access the carboxylic acid (**4**). Standard carbodiimide-mediated amide bond coupling (via EDC) of the acid with nonylamine proceeded smoothly to yield amide **5**. Deprotection of the ketone furnished V-06-018 in 44% yield over four steps, in quantities typically greater than 100 mg. This synthetic route was advantageous as it could be easily modified to generate V-06-018 analogs with alternate tail groups (R' in Scheme 1) through the coupling of different amines. In turn, alternate head groups could be incorporated by coupling different carboxylic acid building blocks (**4**), many of which are readily accessible from acylation reactions of substituted acetophenones using diethyl carbonate as an electrophile (e.g., **1** → **2**; Scheme 1).[34] We introduced both modifications in our subsequent synthesis of a focused library of V-06-018 analogs

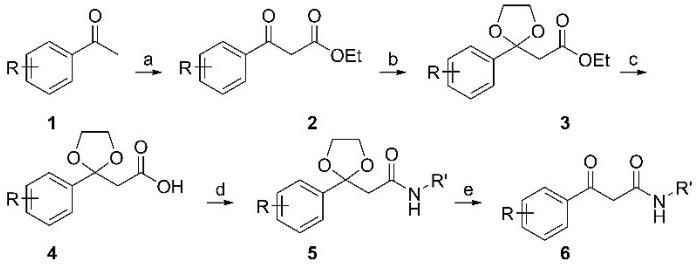


**Scheme 2.1:** Synthesis of V-06-018 and related analogs. Reagents over arrows: a = NaH, $(C_2H_5)_2CO_3$, THF, Δ; b = $C_2H_6O_2$, *p*-TsOH, benzene, Δ, Dean-Stark trap; c = 1:1 LiOH (1M, aq.), THF; d = EDC·HCl, DMAP, $H_2NR'$, $CH_2Cl_2$; e = *p*-TsOH, acetone. See Experimental Section and SI for additional details.

**Structure-informed design of a V-06-018 analog library**

We approached our design of V-06-018 analogs by first considering the binding mode of OdDHL to LasR (Figure 2). The reported X-ray structure of OdDHL bound to the LasR ligand-binding domain (LBD) indicates that the lactone, amide, and keto functionality in OdDHL can make several hydrogen bonds with residues in the LasR ligand-binding site (e.g., Tyr 56, Trp 60, Asp 73, and Ser 129).[35] In view of their structural similarity (see Figure 1C), it is not unreasonable to assume that V-06-018 could target the same binding site on LasR as OdDHL. We therefore were interested in synthesizing analogs that could either gain or lose the ability to make the same hydrogen bonding contacts as OdDHL, to examine their effects on V-06-018 activity. As the phenyl head group of V-06-018 cannot engage in a hydrogen bond with LasR, we synthesized a series of analogs via Scheme 1 with alternate head groups (**8**, **12**, **13**, and **17**–**21**; Figure 3) that either place a heteroatom in a position to potentially accept, or in the case of phenols **17** and **18**, accept and/or donate a hydrogen bond.

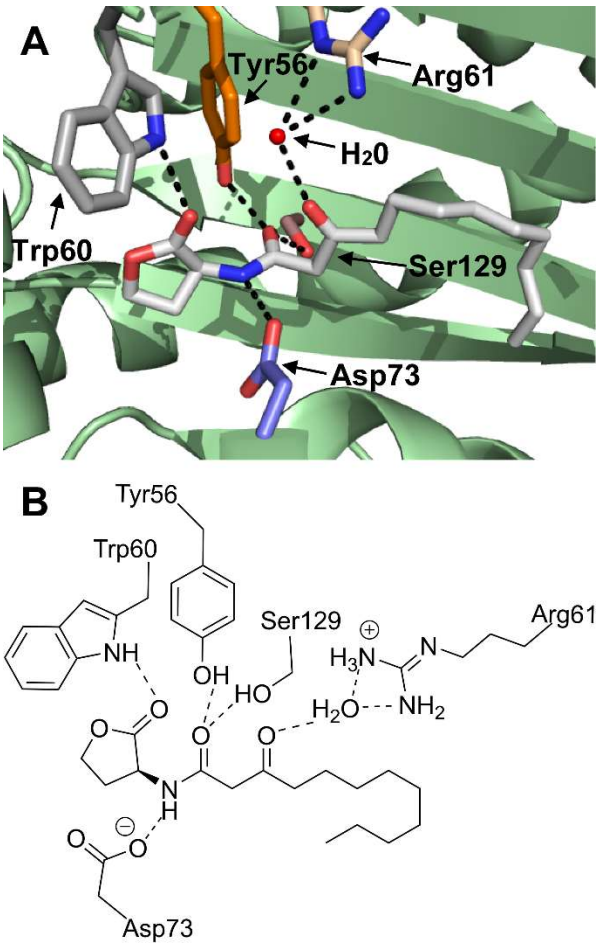


**Figure 2.2:** Three-dimensional (A) and two-dimensional (B) images of the OdDHL-binding site in the [LasR LBD:OdDHL]$_2$ co-crystal structure (PDB ID: 2UV0).[36] Dashed lines indicate putative hydrogen bonds between the labeled residues or water (shown as a red ball in part A) and OdDHL. OdDHL in part A is shown with carbon in grey, oxygen in red, and nitrogen in blue.

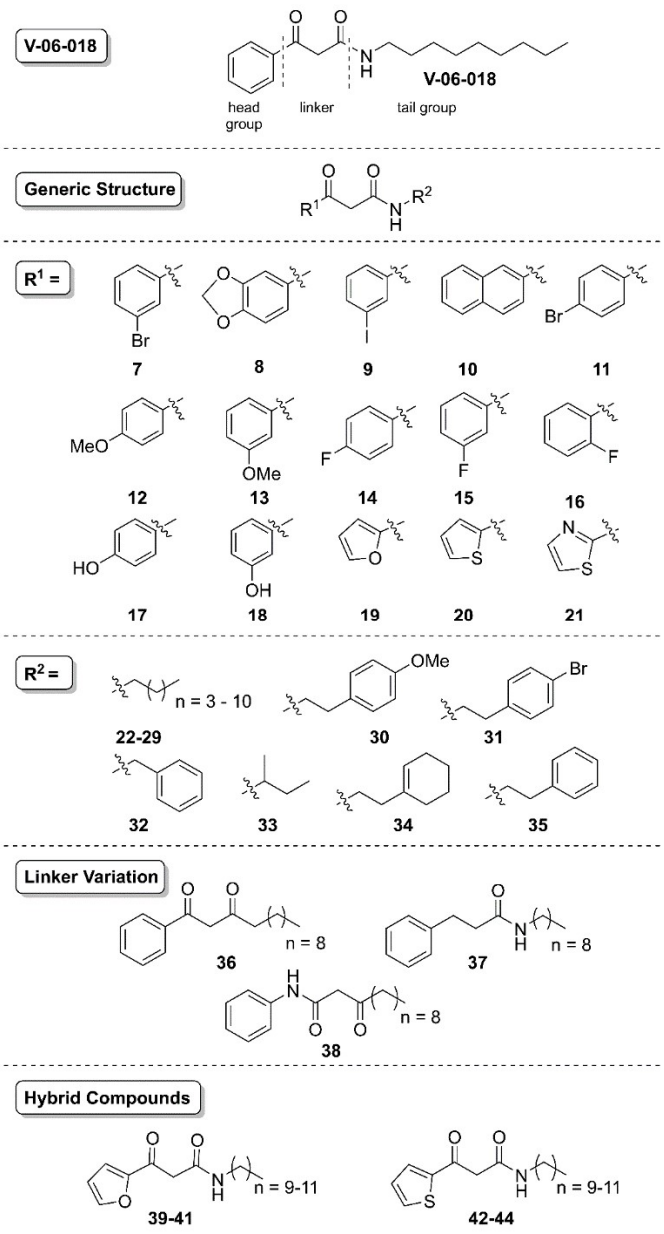


**Figure 2.3:** Library of V-06-018 analogs. Systematic changes were made to the head, tail, and linker regions of V-06-018 (see text). Compound **26** in this series, comprised of a phenyl head and nine carbon tail, is V-06-018.

To examine LasR's tolerance for increased steric bulk on V-06-018's headgroup, we synthesized napthyl derivative **10** (Figure 3). We also synthesized a variety of analogs with halogenated aryl headgroups (**7**, **9**, **11**, and **14**-**16**) to explore electronic effects on activity.

Within this set, compounds **9**, **12**, and **13** were also inspired by work reported by Spring and coworkers, who found that related molecules with these head groups were efficacious inhibitors of the production of QS-regulated virulence factors in *P. aeruginosa*.[14] To alter the electronics and hydrogen-bonding ability of the V-06-018 headgroup without significantly increasing its size, we constructed a set of analogs with heterocyclic, aromatic headgroups (**19**-**21**).

Turning to the tail group of V-06-018, we again looked to OdDHL for guidance. The importance of hydrophobic contacts between ligands and the OdDHL acyl tail binding pocket in LasR has been noted (i.e., at residues Ala 127 and Leu 130),[37-38] and AHL-based LasR agonists decrease in potency as their tails decrease from 12 carbons in length.[39] To examine the importance of tail length for V-06-018's antagonistic activity, we introduced five to twelve carbon tails via the amine coupling in Scheme 1, yielding compounds **22**-**29** (Figure 3; compound **26** is V-06-018). To mimic the molecular architecture of known AHL[30] and TP-type[26] antagonists of LasR, we included several derivatives with cyclic tail groups (**30**-**32**, **34** and **35** ). In addition, we examined an analog with a *sec*-butyl tail (**33**, racemic) to evaluate LasR's tolerance for bulk at the position vicinal to the V-06-018 amide nitrogen. Lastly, to evaluate the importance of the heteroatoms in the "linker" region between the headgroup and tail, we synthesized diketone **36** and amide **37**. Compound **38**, a constitutional isomer of V-06-018, was reported previously by our lab;[40] we included it here for comparison and to further expand our SAR analyses.

**Evaluation of the V-06-018 library for LasR antagonism**

We examined the activity of the V-06-018 library for LasR antagonism using a *P. aeruginosa* mutant strain (PAO-JP2, Δ*lasIrhlI*) that lacks the ability to synthesize OdDHL (or BHL) and contains a green fluorescent protein (GFP) reporter plasmid to examine LasR activity.[16, 41] We used a *P. aeruginosa* LasR reporter as opposed to the *E. coli* LasR reporter introduced above, as we were most interested in the activity of the compounds (and their eventual use as probes) in the native organism. Further, as we previously showed that V-06-018 is not subject to active efflux by the MexAB-OprM pump in *P. aeruginosa*,[16] we wanted to examine if these close analogs were also active in the presence of this pump. In this *P.* aeruginosa reporter system, compounds capable of LasR antagonism should reduce GFP production, and this loss can be quantitated by fluorescence (see Experimental Section). To start, we screened the library for LasR antagonism at a concentration of 10 □M in competition against 150 nM OdDHL. Analogs with substituents on the head group were found to be generally less efficacious as LasR antagonists relative to V-06-018 (compounds **7**–**18**, Figure 4A), suggestive that bulkier V-06-018 analogs may not be as well accommodated in the AHL binding site, regardless of their hydrogen bonding ability. Decreasing the size of the headgroup and including a polar atom was more fruitful. Two of the analogs based on five-membered heterocycles, furan **19** and thiophene **20**, had equivalent efficacy to V-06-018 (~90% LasR antagonism). Not all heterocycles were effective as headgroups, however; thiazole **21** lost efficacy relative to V-06-018.

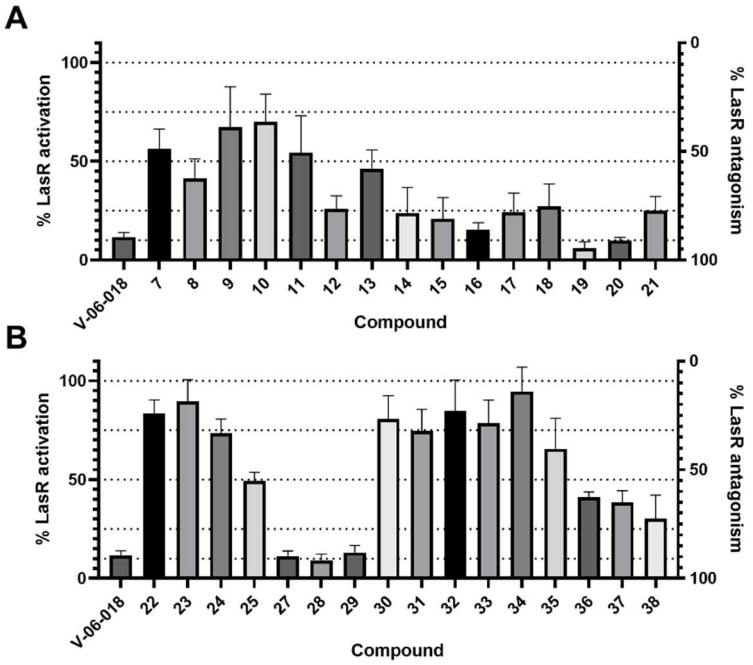


**Figure 2.4:** Primary LasR antagonism screening data in *P. aeruginosa* reporter PAO-JP2 for the (A) head group and (B) tail group and linker modified V-06-018 analogs. Compounds were screened at 10 □M in the presence of 150 nM OdDHL. Bacteria treated with 150 nM OdDHL only was defined as 100% LasR activity/0% LasR antagonism; conversely, bacteria treated with DMSO only (i.e., vehicle) was defined as 0% LasR activation/100% LasR antagonism. Error bars indicate SD of n ≥ 3 trials.

Turning to the tail group modified V-06-018 analogs, we found that only compounds with unbranched, acyclic alkyl tails were efficacious LasR antagonists (e.g., **27**–**29**, Figure 4B). No compounds with cyclic moieties or branching (i.e., **30**-**35**) in their tails were capable of antagonizing LasR by more than 50%. The length of the tail was also important; analogs **27**-**29**, with 10- to 12-carbon tails, were equally as efficacious as V-06-018. The shorter tail analogs **22**-**25**, however, antagonized LasR by less than 50%. These data suggest that binding interactions between LasR and these truncated V-06-018 analogs may have been reduced due to the lack of hydrophobic contacts (again, shown to be important for LasR:OdDHL binding).[37-38] Modifications to the linker region also resulted in less active analogs. All three linker-modified

compounds (**36**-**38**) lost efficacy relative to V-06-018, implicating the presence and position of the amide in V-06-018 as critical to LasR antagonism. Overall, these primary screening data indicated that only subtle alterations to the head and tail groups of V-06-018, and not the linker group, were tolerated for strong LasR antagonism.

**Dose-response antagonism analysis of primary screening hits**

To obtain a quantitative measure of compound potency, we performed dose-response analyses on the compounds that antagonized LasR ≥ 90% at 10 μM (**19**, **20**, and **27**-**29**) using the same *P. aeruginosa* LasR reporter strain and calculated their $IC_{50}$ values (Table 1). We were excited to observe that each of these analogs was more potent than V-06-018. Increasing the length of the V-06-018 tail from 10 to 12 carbons (i.e., as in **27**-**29**) led to a ~3-4-fold increase in potency. The heterocyclic analogs were also stronger LasR antagonists than V-06-018; furan **19** was approximately two-fold more potent than V-06-018, and thiophene **20** was closer to five-fold.

**Table 2.1.** Potency and maximum LasR inhibition (efficacy) data for selected compounds in *P. aeruginosa*

| compound | $IC_{50}$ (μM)[a] | 95% CI (μM)[b] | Maximum Inhibition (%)[c] |
|---|---|---|---|
| V-06-018 (**26**) | 2.3 | (1.7 – 3.1) | 89 |
| **19** | 1.2 | (0.8 – 1.8) | 96 |
| **20** | 0.5 | (0.3 – 0.6) | 84 |
| **27** | 0.7 | (0.5 – 0.9) | 93 |
| **28** | 0.5 | (0.4 – 0.7) | 92 |
| **29** | 0.7 | (0.5 – 1.0) | 91 |
| **39** | 0.2 | (0.2 – 0.3) | 83 |
| **40** | 0.2 | (0.2 – 0.3) | 85 |
| **41** | 3.8 | (2.0 – 7.1) | 89 |
| **42** | 0.2[d] | (0.1 – 0.2) | 91 |
| **43** | 0.2[d] | (0.1 – 0.2) | 93 |
| **44** | 0.6 | (0.5 – 0.8) | 84 |

[a]For details of PAO-JP2 reporter strain, see Experimental Section. [a]Antagonism experiments performed by competing the compounds against OdDHL (**1**) at its approximate $EC_{50}$ (150 nM for PAO-JP2) and inhibitory activity was measured relative to receptor activation at this $EC_{50}$. $IC_{50}$ values determined by testing compounds over a range of concentrations (0.64 nM – 50 □M). All assays performed in triplicate. [b]CI = confidence interval. 95% CIs calculated from the SEM of $n \geq 3$ trials. [c]Denotes the best-fit value for the bottom of the computed dose-response curve. [d]Compound exhibited non-monotonic dose-response behavior. Reported $IC_{50}$ corresponds to the antagonism portion of the curve. Full antagonism dose response curves are shown in Figure S2.

## Second-generation V-06-108 analogs and LasR agonism profiles

Encouraged by the antagonistic activity profiles of our initial set of compounds, we designed and synthesized a set of "hybrid" second-generation V-06-018 analogs that combined features of the most active compounds. These compounds were comprised of a furan or thiophene head group united with 10, 11, or 12 carbon tails (compounds **39-44**; see Figure 2), and were synthesized and evaluated for LasR antagonism in *P. aeruginosa* as described above. The second-generation compounds displayed a variety of activities in the LasR antagonism assay (listed in Table 1). Notably, furan derivatives **39** and **40**, containing 10 or 11 carbon tails, respectively, were more

potent than their parent compounds and were each 10-fold more potent than V-06-018. The 12-carbon furan analog **41**, however, lost activity relative to its parent compounds.

We note that the thiophene analogs of **39** and **40**, compounds **42** and **43**, displayed non-monotonic partial agonism behavior in the LasR dose-response assays; [30 30 2929] namely, at concentrations below 2 μM these compounds antagonized LasR, while at concentrations above 2 μM they agonized LasR. We have reported this activity profile for a series of ligands in reporter assays of LuxR-type proteins to date.[27-28, 30] The antagonist portions of their dose-response curves indicated that **42** and **43** were each highly potent at lower concentrations, with $IC_{50}$ values 10-fold lower than that of V-06-018. Interestingly, thiophene analog **44**, differing by only one methylene unit than **43**, lacked observable non-monotonic activity.

The discovery that two of the hybrid compounds were non-monotonic partial LasR agonists prompted us to measure dose-response *agonism* curves for all our most potent compounds (Figure S3). V-06-018 and compounds **27**-**29**, comprised of phenyl headgroups, did not activate LasR. We also screened our first-generation library for LasR agonism at a single concentration (100 □M) and found that none of the analogs with phenyl headgroups activated LasR; however, thiophene **20** weakly agonized LasR (to 20%; Figure S4). We found that furans **39** and **40** could very weakly agonize LasR (7% and 4%, respectively) at the highest concentration screened (50 μM). Relative to **39** and **40**, thiophenes **42** and **43** were stronger LasR agonists at 50 μM (30% and 22%, respectively), which matched their activity profile at this concentration in the dose-response *antagonism* analysis (as described above).

Activation in this cell-based reporter assay requires LasR to initiate transcription of *gfp*. This process requires LasR to adopt a conformation capable of homodimerization and productive DNA binding. Our results suggest that, at sufficiently high compound concentration, these furan

and thiophene ligands can make contacts with LasR (either directly or indirectly via some other target) that promotes this process. However, contacts with just the head groups of **39**, **40**, **42**, and **43** are presumably insufficient, as compounds **41** and **44**, comprised of the same furan and thiophene head groups, respectively, yet linked to a twelve-carbon tail, failed to activate LasR even at high concentrations. These results suggest that contacts with the tail—specifically, a tail of 9–11 carbons—along with the head group are necessary for LasR agonism by this ligand class at high concentrations. Whether these ligands target the OdDHL binding site or another site on LasR, or another factor altogether, to promote LasR activation at these concentrations remains to be determined.

### *E. coli* reporter assays indicate V-06-018 and analogs act directly via LasR

We next examined if our improved V-06-018 analogs elicit their antagonistic activity via acting directly on LasR using an *E. coli* LasR reporter system (see Experimental Section).[42-44] As highlighted above, LasR is directly and indirectly regulated by other QS systems in *P. aeruginosa*, and thus activity profiles in the *P. aeruginosa* LasR reporter are a measure of this inter-regulated network. To address this question, we obtained dose-response curves for all of the compounds in Table 1 in an *E. coli* LasR reporter strain, and found that their relative efficacies and potencies largely tracked between the *E. coli* and *P. aeruginosa* reporters (Figure S5, Table S2). This alignment between the *P. aeruginosa* and *E. coli* reporter data suggests that these compounds elicit their effects via direct interactions with LasR. We note that all of our antagonists were less efficacious and potent against LasR in the *E. coli* reporter relative to *P. aeruginosa*. For example, the lead compound **40** was only four-fold more potent than V-06-018 in *E. coli* vs. being 10-fold more potent in *P. aeruginosa*. This reduction in potency also

obscured the non-monotonic effects observed above for compounds **42** and **43**. We postulate that this reduction in potency in *E. coli* is an artifact of differences in LasR expression levels between the two reporter systems (non-native level in *E. coli* vs. native level in *P. aeruginosa*).[45] With more LasR present, higher concentrations of ligands are presumably required to inhibit LasR activity. Critically, the stronger efficacies and potencies of these V-06-018 derived antagonists in the native host background will increase their utility as probe molecules.

We were also curious to see if the new antagonists, like V-06-018, were selective for LasR over RhlR and QscR in *P. aeruginosa*. Screening representative compounds (**39** and **40**) in the *E. coli* RhlR and QscR reporter systems showed that **40** is highly LasR selective, with no observable activity in either RhlR or QscR (Figure S6). Compound **39** was found to be inactive in RhlR and, similar to V-06-018, only a weak QscR antagonist (~35% inhibition) at the very highest concentration tested. These results further underscore the receptor selectivity profile of the V-06-018 scaffold and the value of these compounds as chemical tools to study QS in *P. aeruginosa*.

### *P. aeruginosa* reporter data support a competitive mechanism of LasR antagonism for V-06-018 and related compounds

We were interested to determine if V-06-018 and our new lead antagonists were acting as competitive LasR antagonists, and examined this question by testing them against OdDHL at varying concentrations in the *P. aeruginosa* LasR reporter assay. The observed potency of a competitive LasR antagonist should vary with OdDHL concentration, as both molecules are competing for space in the same ligand-binding site. We obtained antagonism dose response curves for V-06-018 and one of our lead compounds (**40**, which did not display non-monotonic

behavior) in competition with OdDHL at 150 nM, 1 □M, and 10 □M (Figure 5). We observed an OdDHL-concentration-dependent decrease in the potency of both compounds. The relative potency trends for V-06-018 and **40** were also maintained, with compound **40** significantly more potent than V-06-018 at 150 nM and 1 µM. Unlike V-06-018, compound **40** was still capable of antagonizing LasR (to 55%) even in the presence of 10 µM OdDHL. These results are supportive of the ability of V-06-018 and its close analogs to act as competitive antagonists of LasR.

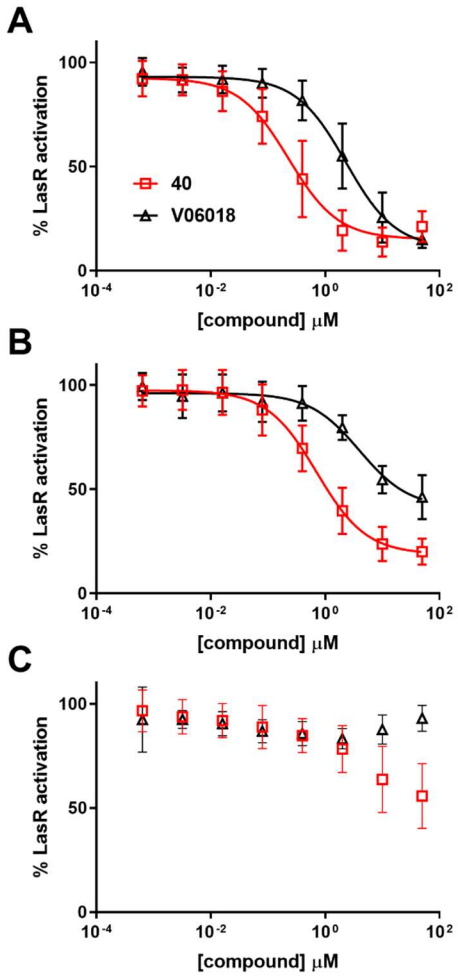


**Figure 2.5:** Dose-response LasR antagonism curves for V-06-018 and analog **40** in *P. aeruginosa* PAO-JP2. Dose-response curves of V-06-018 (black triangles) and **40** (red squares) in competition with (A) 150 nM, (B) 1 □M, and (C) 10 □M OdDHL. V-06-018 has $IC_{50}$ values of 2.3 and 3.9 µM vs. 0.15 and 1 µM OdDHL, respectively; **40** has $IC_{50}$ values of 0.2 and 0.7 µM vs. 0.15 and 1 µM OdDHL, respectively. $IC_{50}$ values could not be calculated for these compounds in competition with 10 □M OdDHL (curves in part C).

**Antagonists and non-classical partial agonist 42 solubilize LasR**

We sought to further characterize the interactions between V-06-018 and related analogs with LasR, to understand how they engender receptor antagonism. Very little is known about the molecular mechanisms that lead to antagonism of LuxR-type receptors by small molecules, largely due to the instability of these proteins *in vitro* even in the presence of their native AHL ligand.[46] LasR requires OdDHL throughout the production and purification process to be isolated, and has proven intractable to structural studies in full length form.[36, 47-48] In principle, antagonists of LuxR-type proteins can operate by binding either in place of an AHL signal, or to a hypothetical, allosteric binding site. Once bound, antagonists can then cause antagonism by further destabilizing the protein (as has been shown for QscR and LasR)[38, 47, 49] or by forming soluble complexes that are either incapable of dimerization or binding to DNA (as has been shown for CviR and LasR),[50,51-52] or presumably combinations of these mechanisms (and potentially others). We were curious to investigate whether soluble LasR could be isolated when it was produced in the presence of V-06-018 or our new antagonists, or if it was destabilized in their presence relative to OdDHL. To test these questions, we produced LasR in *E. coli* grown in the presence of no compound (DMSO control) or 50 μM OdDHL, V-06-018, **40**, or **42** (see Experimental Methods). After 16 h of protein production, we lysed the *E. coli* cells and separated the whole cell (WC) and soluble (S) lysate on an SDS-PAGE gel (Figure 6; quantitative analysis of the bands in the gel is provided in Table S3).

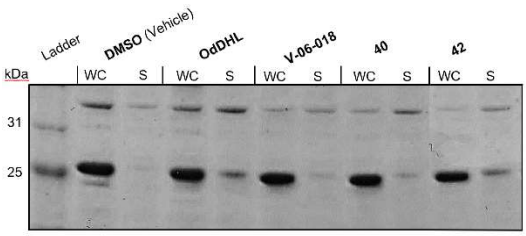


**Figure 2.6.** Characterization of LasR via SDS-PAGE gel in the presence of different ligands. Whole Cell (WC) and soluble (S) portions of *E. coli* cell lysates with LasR overexpressed in the presence of DMSO or 50 μM of OdDHL, V-06-018, **40**, or **42**. LasR has a mol. wt. of 27.9 kD.

As expected, we did not obtain any LasR in the soluble fraction of cells grown without exogenous compound (DMSO), while we obtained soluble LasR in the culture grown with exogenous OdDHL (S band ~30% as intense as WC band; Figure 6). These data recapitulate the finding that LasR requires a ligand to be soluble *in vitro*.[53] We detected soluble bands for LasR produced in the presence of V-06-018 and furan **40**. The bands were four-fold smaller than that of OdDHL (~7% as intense as WC band, vs. ~30% for OdDHL, Table S3), suggesting that these ligands do not solubilize LasR to the same extent as OdDHL. This result correlates with the previous report of Schneider and co-workers demonstrating that certain synthetic AHL-type antagonists (along with the close V-06-018 analog **38**) form soluble complexes with LasR, albeit in less amounts than OdDHL.[51] Schneider went on to show that these complexes were unable to bind to LasR's target DNA using electrophoretic mobility shift assays (EMSAs), which allows for the interpretation that these ligands can stabilize an inactive LasR complex (e.g., incapable of dimerization or DNA binding). We also observed thiophene **42** solubilize LasR. The soluble band for **42** was more intense than those observed for V-06-018 and **40**, and comparable to OdDHL (~30%). We note that **42** has a non-monotonic activity profile in the *P. aeruginosa* reporter assay and is capable of weak LasR agonism at higher concentrations; the larger quantity of LasR isolated in this experiment relative to V-06-018 and **40** (at 50 □M concentration) is

therefore interesting and could arise due to this agonistic activity profile. Collectively, these SDS-PAGE data support the hypothesis that V-06-018 and related analogs act at LasR antagonists, at least in part, via inducing a soluble but inactive conformation of LasR. The reduced amount of protein in these soluble fractions relative to OdDHL suggests that V-06-018 and **40** may also cause antagonism by promoting LasR unfolding (i.e., destabilizing the receptor); thus, more than one mechanism of antagonism is likely operative. Further biochemical (e.g., EMSAs) and structural experiments are required to test these mechanistic hypotheses and are ongoing in our laboratory.

**LasR mutants reveal residues critical for activation and inhibition by synthetic ligands**

The results of the competitive LasR antagonism dose response assays, *E. coli* reporter assays, and protein production experiments outlined above suggest that V-06-018 and the lead analogs target LasR and interact with the OdDHL binding site to cause antagonism. In view of our original compound design, we were curious as to whether the residues in LasR that are known to govern LasR:OdDHL interactions (Figure 2) were also important to LasR antagonism by the V-06-018 ligand class, and applied a method utilized previously in our laboratory involving LasR mutants with modifications to the OdDHL binding site.[35-36, 54] In this past work, a set of LasR single-point mutants were generated in which residues implicated in hydrogen bonding interactions with OdDHL were converted to residues incapable of hydrogen bonding but approximately the same steric size (e.g., Tyr → Phe). The mutant LasR proteins were then tested for activity using a LasR reporter plasmid in an *E. coli* host background (analogous to the *E. coli* LasR reporter assay system above). Compounds showing reduced activity in these mutants relative to wild-type LasR then can be postulated to make a contact with LasR that depends on

the mutated residue. We tested V-06-018 and furan **39** at 100 μM in three LasR mutants with modifications to residues that make hydrogen-bonds to OdDHL (Tyr 56, Trp 60, and Ser 129; see Figure 3).[54] Notably, all of these single-point LasR mutants (Y56F, W60F, and S129A) are still functional in the reporter assay, but are less active than wild-type LasR (as measured via reduced OdDHL potencies; Figure S7), reflective of the importance of these LasR:OdDHL interactions for activation. (As noted above, antagonists display reduced efficacy in general in this heterologous background relative to the native (*P. aeruginosa*) reporter system.)

V-06-018 was found to antagonize all three LasR mutants to a significantly lesser extent than wild-type LasR (Figure 7A). The same trend was true for furan **39**. Tyr 56 and Ser 129 are believed to form hydrogen bonds with the amide carbonyl of OdDHL (Figure 2), and potentially could bind to one of the two linker carbonyl oxygens in V-06-018 and its analogs.[36] Trp 60 hydrogen bonds with the lactone carbonyl oxygen of OdDHL, and it may be capable of hydrogen bonding with the furan oxygen of **39**. An analogous hydrogen-bond to the head-group of V-06-018 is not possible, but the lower activity of V-06-018 in the W60F LasR mutant suggests that Trp 60 interacts in some other manner with V-06-018 to enforce antagonism. Further studies are necessary to pinpoint the specific molecular interactions that govern LasR antagonism by these two ligands. Nevertheless, these experiments with LasR mutants support V-06-018 and new antagonist **39** interacting with the OdDHL binding site in LasR.

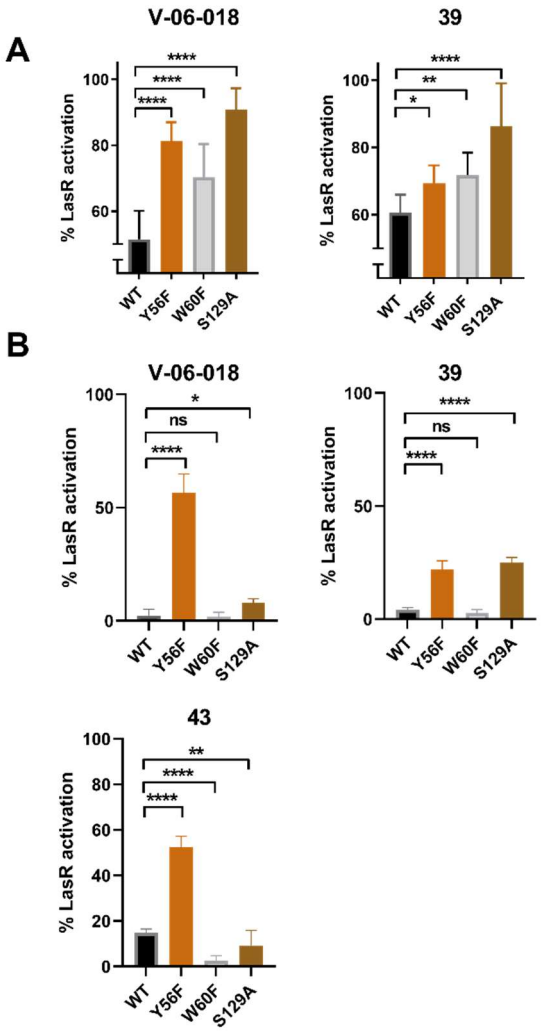


**Figure 2.7:** (A) LasR mutant antagonism data for V-06-018 and lead compound **39**. Compounds tested at 100 □M against OdDHL at its approximate $EC_{50}$ value in the specific *E. coli* LasR reporter strain (as indicated on the X-axis). (B) LasR mutant agonism data for V-06-018, **39**, and **43**. Compounds tested at 100 □M. For antagonism experiments, 100% is defined as the $EC_{50}$ concentration of OdDHL in that specific LasR reporter strain (see Figure S6); for agonism experiments, 100% is defined as the activity of 100 □M OdDHL in that specific LasR reporter strain. Significance was assessed via a one-way ANOVA: **** = $p < 0.0001$; *** = $p < 0.001$; ** = $p < 0.01$; * = < 0.05. ns = no significant difference.

We also were curious to learn whether alternations to these LasR residues could impact the ability of our compounds to *agonize* LasR. Therefore, we examined the agonistic activities V-06-018, furan **39**, and thiophene **43** in the three LasR mutant reporter strains at 100 □M; thiophene **43** was included in these agonism assays due to its non-monotonic agonism profile

(see above). We were surprised to find that all three compounds agonized the LasR Y56F mutant to a significantly greater extent than wild-type LasR. For example, V-06-018, which does not agonize wild-type LasR, activated LasR Y56F to ~60% (relative to OdDHL) at 100 □M. In view of this unexpected result, we screened the remainder of our lead compounds in this LasR mutant reporter and found that they all were capable of activating the LasR Y56F mutant to some extent (from 9–56% at 100 □M; Figure S8). V-06-018 and **39** also agonized the LasR S129A mutant significantly more than wild-type LasR. These results suggest that removing the hydrogen bonds donated by Tyr 56 or Ser 129, or reducing sterics at these positions, may allow these V-06-018 type ligands more freedom to adjust their position in the LasR OdDHL binding pocket and adopt new contacts that engender LasR agonism as opposed to antagonism. None of our compounds were found to agonize the LasR W60F mutant; in fact, **43** lost agonistic activity in that mutant relative to wild-type LasR.

In our laboratory's prior mutational studies of LasR, we observed compound **38** (Figure 3), a LasR antagonist and constitutional isomer of V-06-018, could agonize both the LasR Y56F and W60F mutants. We termed this transition from antagonist to agonist "Janus" behavior (after the two-faced Roman god).[35] Here, we observed V-06-018 and compound **39** exhibit analogous "Janus" behavior in Y56F and S129A, but not in W60F (like **38**). These results suggest that chemical modification of either the ligand (via chemical synthesis; i.e., V-06-018 → **38** or **39**) or LasR (via mutagenesis of at least these three residues) is sufficient to alter contacts between the ligand and receptor to allow for either agonism or antagonism, or the degree thereof, and that these changes to molecular contacts are likely very subtle. The implications of these findings—specifically, that single point mutations can convert potent LasR antagonists into agonists—on the propensity for resistance to arise in *P. aeruginosa* to LasR antagonists did not escape our

attention. We do note that the agonistic activity of these compounds is quite low (relative to OdDHL in wild type LasR). Additional experiments are required to explore the possibility of LasR mutants to arise naturally upon sustained treatment with V-06-018 or related analogs. However, our lab and others has shown previously that resistance to QS inhibitors, even if it was to develop, should be slow to spread through and not overtake a population of bacteria,[55-56] supporting the continued search for such compounds. Moreover, the ability of V-06-018, **38**, **39**, and **43** to agonize the LasR mutants suggests that structural studies of these LasR mutant:ligand complexes could be particularly noteworthy, as they could illuminate the mechanisms by which these ligands both agonize LasR mutants and antagonize wild-type LasR. The heightened stability of LasR:agonist complexes relative to LasR:antagonist complexes could significantly enable such structural studies.

## SUMMARY AND CONCLUSIONS

The work reported herein was motivated by the need for chemical probes of a key QS receptor, LasR, in the opportunistic pathogen *P. aeruginosa*. Despite considerable research to date, antagonists with sub-micromolar potencies, high efficacies, and selectivities for LasR over the other QS circuits in *P. aeruginosa* have been elusive. We performed the first structure-function analysis of the small molecule V-06-018, a promising yet unstudied LasR antagonist emerging from a high-throughput screen reported over 10 years ago.[33] We developed a versatile and efficient synthetic route to V-06-018, produced a focused library of analogs using this route to explore the headgroup, linker, and tail portions of V-06-018, and evaluated the library for LasR modulatory ability using cell-based reporter systems. These screening data revealed stringent SARs for LasR antagonism by this ligand scaffold, including the requirement for a linear, alkyl

tail group between nine to 12 carbons in length, an amide in the linker, an intolerance for substitution on the aryl head group, and a tolerance of certain 5-membered heterocyclic head groups. These SARs allowed us to design and synthesize second-generation LasR antagonists with nanomolar $IC_{50}$ values in *P. aeruginosa* (*e.g.*, **39** and **40**). These compounds represent, to our knowledge, the most potent and efficacious synthetic antagonists of LasR to be reported, with $IC_{50}$ values in *P. aeruginosa* 10-fold lower than V-06-018 and at least 100-fold lower than other AHL-based ligands.[48] We note that we discovered these analogs after synthesizing fewer than 40 compounds; further development of the V-06-018 scaffold would likely yield even more potent compounds.

Our results indicate that the V-06-018 scaffold is quite selective for LasR over the other two LuxR-type receptors in *P. aeruginosa*, with **39**, **40**, and V-06-018 showing neither antagonistic nor agonistic activity in RhlR, **40** being inactive in QscR, and **39** and V-06-018 showing only modest antagonistic activity in QscR at the very highest concentrations tested. This activity profile is significant because the ability to selectively attenuate LasR activity in the midst of the highly inter-regulated QS system of this pathogen will facilitate mechanistic studies, and highlights the value of these V-06-018 analogs as chemical tools to study QS in *P. aeruginosa*.

We also report herein our investigations into the mechanism by which V-06-018 and related compounds modulate LasR activity. In the course of these studies, certain analogs were found to display interesting dual activity profiles—capable of strong LasR antagonism at nanomolar levels, yet LasR agonism at micromolar levels (i.e., non-monotonic partial agonists)—and we were intrigued by their mechanisms of action as well. Examination of the lead compounds against OdDHL at various concentrations and in an *E. coli* LasR reporter support a mechanism by which they bind competitively with OdDHL and interact directly with LasR. V-

06-018 and furan antagonist **39** were found to be significantly less efficacious in LasR mutants that lack key residues in the ligand-binding site shown to make hydrogen-bonding contacts with OdDHL. This result is congruent with these compounds binding in the same site on LasR as or near to OdDHL. Protein production studies of LasR in the presence of V-06-018, furan-based antagonist **40**, and thiophene-based antagonist **42** demonstrated that these compounds support folding of the protein into a soluble form, suggestive that they may stabilize an inactive form of the protein, analogous to the mechanism of CviR antagonism by the chlorolactone AHL analog (CL).[50] V-06-018 and **40** also appear to reduce the amount of soluble LasR relative to **42** or the native agonist OdDHL, indicating that receptor destabilization could also contribute to the mechanism of inactivation by certain of these compounds. Finally, study of V-06-018 and furan-based antagonist **39** revealed that they were each capable of shifting from LasR antagonists to agonists in a LasR mutant lacking a single hydrogen-bonding motif in the ligand-binding site (e.g., Tyr 56→ Phe 56; removal of the Tyr hydroxyl). This finding indicates that subtle interactions of these ligands with LasR can have dramatic effects on receptor activity and suggests a novel route for exploring the mechanisms of this ligand class via structural studies of LasR mutant:ligand complexes. Overall, this study has provided a set of highly potent LasR antagonists that should find broad use as chemical probes of QS in *P. aeruginosa*, a robust chemical route to generate these compounds, and new insights into the mechanisms of LasR antagonism. These compounds and insights expand the understanding of LuxR-type QS in this important opportunistic pathogen.

**ACKNOWLEDGEMENTS**

Financial support for this work was provided by the NIH (R01 GM109403 and R35 GM131817). M.C.O. acknowledges support from the Arnold and Mabel Beckman Foundation through an Arnold O. Beckman Postdoctoral Fellowship. K.E.N. was supported in part by the UW−Madison NIH Chemistry−Biology Interface Training Program (T32 GM008505). NMR facilities in the UW–Madison Department of Chemistry were supported by the NSF (CHE-0342998) and a gift from Paul J. Bender. MS facilities in the UW–Madison Department of Chemistry were supported by the NSF (CHE-9974839).

## Materials and Methods

### Chemistry

All chemicals were obtained from Sigma-Aldrich, Agros Organics, or TCI America. All reagents and solvents were used without further purification except for hexane, ethyl acetate, and dichloromethane, which were distilled prior to use. Analytical thin-layer chromatography (TLC) was performed on 250 μm glass backed silica plates with F-254 fluorescent indicator from Silicycle. Visualization was performed using UV light and iodine. All new compounds were fully characterized for purity and identity; see SI for characterization data. Compound stock solutions were prepared in DMSO at appropriate concentrations and stored at -4 °C prior to use.

### Representative procedures for the synthesis of V-06-018

*Synthesis of ethyl 2-(2-phenyl-1,3-dioxolan-2-yl)acetate* (**3**; R = H): Ethyl benzoyl acetate (1.92 mL, 10 mmol, 1 equiv.), ethylene glycol (3.35 mL, 60 mmol, 6 equiv.), and *p*-toluene sulfonic acid (192 mg, 1 mmol, 0.1 equiv.) was added to a 250 mL round-bottom flask equipped with a Dean-Stark trap. The mixture was heated to reflux for approximately 24 h. The mixture was

washed with saturated sodium bicarbonate (1 x 100 mL), water (1 x100 mL), and saturated brine (1 x 100 mL). The organic portion was dried over magnesium sulfate and concentrated under reduced pressure. The crude material was purified by flash silica gel chromatography (20% ethyl acetate in hexane), and **3** was isolated as a colorless oil (1.87 g, 79% isolated yield).

*Synthesis of 2-(2-phenyl-1,3-dioxolan-2-yl)acetic acid* (**4**; R = H): Compound **3** (287 mg, 1.2 mmol, 1 equiv.) was dissolved in THF (12 mL, 0.1 M) in a 100 mL round-bottom flask, after which aqueous 1M lithium hydroxide (12 mL, 12 mmol, 10 equiv.) was added. The reaction mixture was heated to 70 °C, and reaction progress was monitored by TLC. Upon consumption of the starting material, the organic layer was washed with saturated sodium bicarbonate (20 mL). The combined aqueous layers were extracted with ethyl acetate (20 mL). The pH of the combined aqueous layers was acidified with 10% aq. citric acid, and then extracted with ethyl acetate (3 x 20 mL). These organic portions were combined, dried over magnesium sulfate, and concentrated under reduced pressure to yield **4** as a colorless, crystalline solid that was >95% pure by $^{1}$H NMR and used without further purification (226 mg, 90% crude yield).

*Synthesis of N-nonyl-2-(2-phenyl-1,3-dioxolan-2-yl)acetamide* (**5**; R = H, R'= nonyl): Acid **4** (226 mg, 1.08 mmol, 1 equiv.), *N*-(3-dimethylaminopropyl)-*N'*-ethylcarbodiimide hydrochloride (EDC-HCl; 207 mg, 1.62 mmol, 1.5 equiv.), 4-dimethylaminopyridine (DMAP; 20 mg, 0.162 mmol, 0.15 equiv.), and nonylamine (238 □L, 1.3 mmol, 1.2 equiv.) were dissolved in $CH_2Cl_2$ (10.8 mL, 0.1M), and the reaction mixture was stirred for ~15 h at room temperature. The reaction mixture was diluted into diethyl ether and washed with 1M HCl (2 x 30 mL), saturated sodium bicarbonate (2 x 30 mL), water (1 x 30 mL), and brine (1 x 30 mL). The organic portion

was dried over magnesium sulfate and concentrated under reduced pressure to yield **5** as a colorless, crystalline solid that was >95% pure by $^{1}$H NMR and used without further purification (303 mg, 85% crude yield).

*N-nonyl-3-oxo-3-phenylpropanamide* (V-06-018, **26**): Compound **5** (303 mg, 0.92 mmol, 1 equiv.) and *p*-toluene sulfonic acid (175 mg, 0.92 mmol, 1 equiv.) were dissolved in acetone (9.2 mL, 0.1 M) in a 25 mL round-bottom flask. The reaction mixture was stirred at room temperature for 24 h. The mixture was diluted in diethyl ether (20 mL) and washed with saturated sodium bicarbonate (1 x 30 mL), water (1 x 30 mL), and brine (1 x 30 mL), then dried over magnesium sulfate and concentrated under reduced pressure. The resulting solid was purified by flash silica gel chromatography (20% ethyl acetate in hexanes) to give a V-06-018 (**26**) as a white solid (170 mg, 64% isolated yield).

**Biology**

A listing of all of the bacterial strains and plasmids used in this study is provided in Table S1. Bacteria were cultured in Luria-Bertani medium (LB) and grown at 37 °C. Growth was quantified by absorbance at 600 nm ($OD_{600}$). Absorbance and fluorescence measurements were made on a Biotek Synergy 2 plate reader running Gen 5 software (version 1.05). Buffers used in biological experiments included: Z buffer (60 mM $Na_2HPO_4$, 40 mM $NaH_2PO_4$, 10 mM KCl, 1 mM $H_2O$), phosphate buffer (60 mM $Na_2HPO_4$, 40 mM $NaH_2PO_4$), and phosphate buffered saline (137 mM NaCl, 2.68 mmol KCl, 10 mM $Na_2HPO_4$, 1.8 mM $KH_2PO_4$). Dose-response curves were generated using GraphPad Prism software (version 8). Detailed descriptions of all biological experiments are provided in the SI.

### *P. aeruginosa* reporter assay protocol

LasR reporter experiments in *P. aeruginosa* were performed as reported previously.[30] Briefly, a single colony of *P. aeruginosa* PAO-JP2[41] was grown overnight in LB medium containing 300 □g/mL carbenicillin. Culture was diluted 1:100 in fresh LB medium without antibiotic. Subculture was grown to $OD_{600}$ = 0.25–0.3. A 2-□L aliquot of compound stock solution (in DMSO) was added to the interior wells of black, clear-bottom 96-well plate. A 198-µL aliquot of bacterial culture was added to all compound containing wells. For antagonism experiments, at least three wells were filled with 198 µL of grown subculture (i.e., untreated subculture); the remainder of the subculture was treated with exogenous OdDHL (i.e., treated subculture) at various concentrations (150 nM, 1 µM, or 10 µM) prior to dispensing. Plates were incubated without shaking (static) for 6 h, after which GFP production was read for each well using a plate reader (excitation at 500 nM, emission at 540 nM) and normalized to cell growth. Activity was reported relative to cells containing only OdDHL.

### *E.* coli reporter assay protocol

LasR, RhlR, and QscR assays in *E. coli* JLD271 (△*sdiA*) or DH5α utilized a □-galactosidase reporter and were conducted as previously reported.[26] A representative protocol for the LasR assay is provided here. Briefly, a single colony of *E. coli* strain JLD271 bearing plasmids pJN105-L[44] and pSC11-L[42] was grown in LB medium. Overnight culture was diluted 1:10 in fresh LB medium with 100 µg/mL ampicillin and 10 µg/mL gentamicin and grown to an $OD_{600}$ = 0.23–0.27. Once grown, arabinose was added to a final concentration of 4 mg/mL. A 2-µL aliquot of compound stock solution (in DMSO) or only DMSO (vehicle control) was added to the interior wells of a

clear 96-well microtiter plate. For agonism assays, 198 μL aliquots of the subculture was dispensed into all internal wells. For antagonism assays, subculture was dispensed into at least three wells containing only DMSO; the remainder of the subculture was treated with the appropriate concentration of OdDHL and dispensed into all remaining interior wells. Plates were incubated at 37 °C with shaking at 200 rpm for 4 h.

To measure resulting β-galactosidase production, each interior well of a chemical-resistant 96-well plate (Costar 3879) was filled with 200 □L Z buffer, 8 □L $CHCl_3$, and 4 □L 0.1% aqueous SDS. After the incubation period, the $OD_{600}$ of each well of the bacteria-containing plate was measured. A 50-□L aliquot of each well of the bacteria-containing plate was transferred to the lysis-buffer containing chemical resistant plate, and the cells were lysed. A 100-□L aliquot from each well was transferred to a fresh clear-bottom 96-well plate. The Miller assay was started by adding 20 □L of the substrate *ortho*-nitrophenyl-□-galactoside (ONPG, 4 mg/mL in phosphate buffer) to each well. The plates were then incubated at 30 °C for 30 min and absorbances at 420 and 550 nm were read. Miller units were calculated for each well (see SI for detailed description). Activity was reported relative to wells containing only OdDHL.

**LasR overexpression and SDS-PAGE protocols**

*E. coli* BL21-DE3 harboring the pET17b (LasR) plasmid was grown overnight in LB medium from a single colony. The overnight culture was diluted 1:80 into fresh LB medium buffered with 100 mM MOPS, adjusted to pH 7, and grown to an $OD_{600}$ = 0.5. Protein expression was induced by the addition of 0.4 M isopropyl β-D-1-thiogalactopyranoside (IPTG), and the culture was grown overnight at 17 °C. The next day, cells were pelleted by centrifugation. Whole cell and soluble portions of cell lysate were isolated and prepared via the Bacterial Protein Extraction

Reagent (B-PER, ThermoFisher Scientific) according to package instructions. Cell lysates were run on a Biorad 10% SDS gel and stained with Coomassie. Band intensities were quantified using ImageJ (see Table S3).

## General instrumentation information

NMR spectra were recorded in deuterated solvents at 400 MHz on a Bruker-Avance spectrometer equipped with a BFO probe, and at 500 MHz on a Bruker Avance spectrometer equipped with a DCH cryoprobe. Chemical shifts are reported in parts per million using residual solvent peaks or tetramethylsilane (TMS) as a reference. Couplings are reported in hertz (Hz). Electrospray ionization–exact mass measurement (ESI-EMM) mass spectrometry data were collected on a Waters LCT instrument. Absorbance and fluorescence measurements were obtained on a Biotek Synergy 2 plate reader using Gen5 analysis software.

## Synthetic protocols for representative compounds

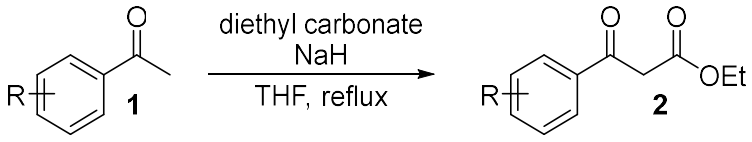


*Synthesis of β-ketoesters (**2**)*

To a solution of acetophenone (**1**, 1 equiv.) in THF (0.5 M), NaH (2 equiv.) was added at 75 °C. The solution was allowed to stir for 2.5 h at reflux, after which it was diluted with diethyl ether (30 mL). The mixture was washed with 1M HCl (2 x 25 mL), water (1 x 25 mL), and saturated brine (1 x 25 mL). The organic layer was separated, dried over magnesium sulfate, filtered, and concentrated under reduced pressure. Compounds (**2**) were purified via flash silica gel chromatography with hexanes and ethyl acetate as eluent (56–91% isolated yield).

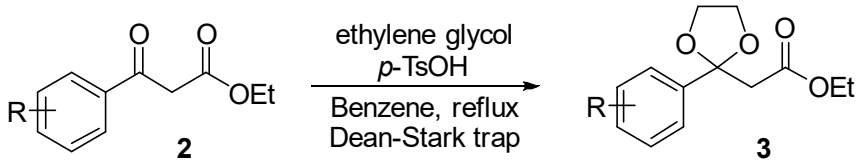


*Synthesis of β-ketal esters (**3**)*

To a solution of β-keto ester (**2**, 1 equiv.) in benzene (0.2 M) was added *p*-TsOH (0.1 equiv.) and ethylene glycol (6 equiv.) at 90 °C. A Dean-Stark trap was assembled, and the experimental apparatus was heavily insulated with glass wool and tin foil. The mixture was allowed to reflux overnight. The mixture was washed with saturated sodium carbonate (2 x 30 mL), water (1 x 30 mL), and saturated brine (1 x 30 mL). The organic layer was separated, dried over magnesium sulfate, filtered, and concentrated under reduced pressure. Compounds (**3**) were purified via flash silica gel chromatography with hexanes and ethyl acetate as eluent (38–83% isolated yield).

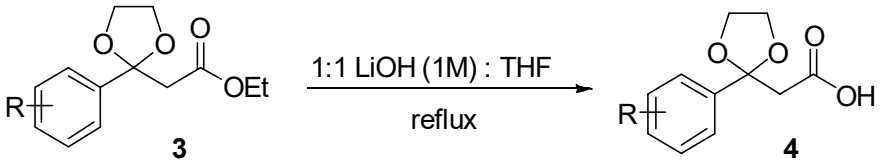


*Synthesis of β-ketal acids (**4**)*

To a solution of β-ketal ester (**3**, 1 equiv.) in MeOH (0.1 M) was added 1M LiOH (10 equiv.) at 75 °C. The mixture was allowed to stir at reflux for 2 h. The solution was then allowed to cool to rt. The aqueous layer was separated, and its pH was adjusted to 2–3 with citric acid (10% in water). The acidified aqueous layer was washed with ethyl acetate (3 x 20 mL). The ethyl acetate layer was separated, dried over magnesium sulfate, and concentrated under reduced pressure. Products (**4**) were used without further purification (42–100% crude yield).

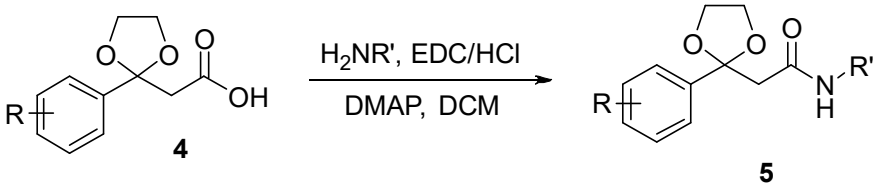


*Synthesis of β-ketal amides (**5**)*

To a solution of β-ketal acids (**4**, 1 equiv.) in dichloromethane (0.1 M) was added DMAP (0.15 equiv.) and EDC·HCl (1.5 equiv.). After 10 min of stirring at rt, the desired amine (1.2 equiv.) was added. The solution was stirred at rt overnight. The mixture was diluted with diethyl ether (15 mL) and washed with 1M HCl (1 x 15 mL), saturated sodium bicarbonate (1 x 15 mL), and saturated brine (1 x 15 mL). The organic layer was separated, dried over magnesium sulfate, and

concentrated under reduced pressure. Products (**5**) were used without further purification (64–94% crude yield).

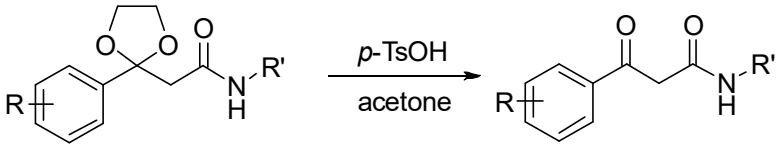


**5** **6**

S*ynthesis of β-keto amides (**6**)*

To a solution of β-ketal amides (**5**, 1 equiv.) in acetone (0.1 M) was added *p*-TsOH (0.1M) at rt. The mixture was allowed to stir overnight. The solution was diluted with diethyl ether (15 mL), washed with saturated sodium bicarbonate (2 x 15 mL), water (1 x 15 mL), and saturated brine (1 x 15 mL). The organic layer was separated, dried over magnesium sulfate, and concentrated under reduced pressure. Products (**6**) were purified via flash silica gel chromatography with hexanes and ethyl acetate as eluent (66–92% isolated yield).

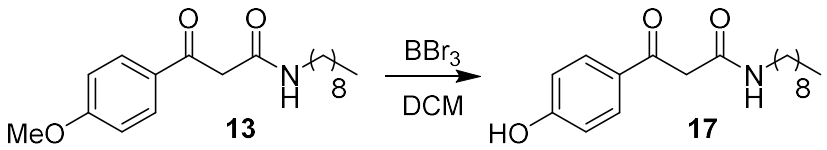


*Deprotection of **13** to provide analog **17***

To a flame dried round bottom flask was added **13** (1 equiv.) in dichloromethane (0.25 M). $BBr_3$ (3 equiv.) was added dropwise, and the reaction was monitored by TLC. Upon consumption of starting material, the reaction was quenched by addition of 2 mL of ice cold water. The reaction mixture was extracted with ethyl acetate (3 x 20 mL). The organic layer was washed with water (1 x 10 mL) and brine (1 x 10 mL), dried over magnesium sulfate, and concentrated under reduced pressure. Product (**17**) was purified via flash silica gel chromatography with hexanes and ethyl acetate as eluent (11% isolated yield).

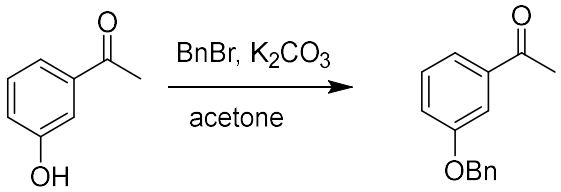


*Protection of phenol in acetophenone precursor to analog **18***

To a solution of 3-hydroxyacetophenone (1 equiv.) in DMF (0.1 M) was added benzyl bromide (2.5 equiv.) and potassium carbonate (2.5 equiv.). The reaction mixture was stirred overnight at rt. Solids were removed by filtration, the solution was diluted with ethyl acetate (75 mL), and the reaction mixture was washed with water (3 x 75 mL). The organic layer was separated and

concentrated under reduced pressure. Benzyl-protected product was purified via flash silica gel chromatography with hexanes and ethyl acetate as eluent (81% isolated yield).

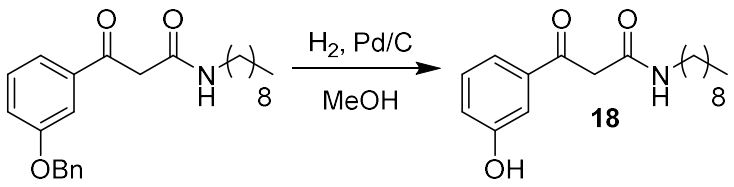


**18**

*Deprotection to provide analog **18***

To a flame dried round-bottom flask equipped with a stir bar was added Pd/C (10% mol equiv.). The flask was sealed and flushed with nitrogen. The β-keto amide starting material was dissolved in MeOH (0.1 M) and added via syringe. The reaction mixture was stirred overnight under $H_2$ (1 atm). The solution was diluted with ethyl acetate and filtered over celite. Product **18** was purified via flash silica gel chromatography with hexanes and ethyl acetate as eluent (67% isolated yield).

**Table S2.1:** Bacterial strains and plasmids used in this study[a]

| Strain or Plasmid | Description | Ref. |
|---|---|---|
| *E. coli* | | |
| JLD271 | K-12 Δ*lacX74 sdiA271*::CAM; $Cl^R$ | [1] |
| DH5α | F- , j80d*lac*ZDM15D(*lacZYA-argF*)U169 *deoR recA*1 *endA*1 *hsdR*17(rk- , mk+ ) *phoA supE*44 λ - *thi*-1 *gyrA*96 *relA*1 | Invitrogen |
| BL21(DE3) | Δ*lacZY* pLysS; $Cl^R$ | Novagen |
| *P. aeruginosa* | | |
| PAO-JP2 | PAO1 *lasI::Tet rhlI::Tn501-2;* $Hg^R$ $Tc^R$ | [2] |
| *Plasmids* | | |
| pSC11-L | Broad host range *lasI'-lacZ* reporter; $Ap^R$ | [3] |
| pSC11-Q | Broad host range *PA1897'-lacZ* reporter; $Ap^R$ | |
| pSC11-R | Broad host range *rhlI'-lacZ* reporter; $Ap^R$ | |
| pJN105L | Arabinose-inducible *lasR* expression vector; pBBRMCS backbone; $Gm^R$ | [4] |
| pJN105Q | Arabinose-inducible *qscR* expression vector; pBBRMCS backbone; $Gm^R$ | [4] |
| pJN105R | Arabinose-inducible *rhlR* expression vector; pBBRMCS backbone; $Gm^R$ | [5] |
| p*lasI*-LVAGFP | *lasI'-gfp* [LVA] transcriptional fusion; $Cb^R$ | [6] |
| pJG044 | Y56F mutant analog of pJN105L | [7] |
| pJG045 | W60F mutant analog of pJN105L | [7] |
| pJG051 | S129A mutant analog of pJN105L | [7] |
| pET17b.*lasR* | Full length LasR overexpression vector | [8] |

[a]Abbreviations: $Cl^R$ = Chloramphenicol resistance; $Hg^R$ = Mercury resistance; $Tc^R$ = tetracycline resistance; $Ap^R$ = Ampicillin resistance; $Gm^R$ = Gentamicin resistance; $Cb^R$ = Carbenicillin resistance

## Reporter assay protocols

### *E. coli* reporter assays (β-galactosidase)

The LasR, QscR, and RhlR assays in *E. coli* JLD271 or DH5α were each performed according to our previously reported protocols.[5, 9-11] Our method with *E. coli* JLD271 is provided here as a general example. A 5-mL sample of LB medium containing 100 μg/mL Ampicillin and 10 μg/mL Gentamicin was inoculated with a single colony of *E. coli* strain JLD271 transformed with pSC11 (*lacZ* reporter plasmid for LasR, QscR, or RhlR; see Table S1) and pJN105 (LasR, QscR, and RhlR production plasmid). The culture was grown overnight at 37 °C with shaking at 200 rpm. Overnight culture was diluted 1:10 in fresh LB medium with 100 μg/mL Ampicillin and 10 μg/mL Gentamicin and grown to an $OD_{600}$ = 0.23–0.27 with path length correction. Aliquots (2 μL) of test compound stock solution in DMSO were added to the interior wells of a clear 96-well microtiter plate (Costar 3370), with final DMSO concentrations <1%.

*For antagonism assays*, 12 wells on each microtiter plate were filled with 2 μL DMSO and no compound (for use as positive and negative controls). Once subculture reached the appropriate OD, arabinose was added to a final concentration of 4 mg/mL to induce expression of pJN105. Six DMSO containing wells were filled with 198 μL of this subculture as a negative control. The remainder of the culture was adjusted to a final concentration of 2 nM OdDHL (for LasR), 10 nM OdDHL (for QscR), or 10 □M BHL (for RhlR), and 198 μL aliquots of treated culture were added to all experimental wells and DMSO wells (the latter as a positive control). The outer wells of the plate were filled with 200 μL of water (to help maintain the plate humidity and slow

evaporation overall for the interior wells). Plates were incubated at 37 °C with shaking at 200 rpm for 4 h.

*For agonism assays,* 2 µL DMSO was added to six wells (negative control), and 2 µL of either 10 mM OdDHL in DMSO (for LasR and QscR) or 100 mM BHL (for RhlR) were added to another six wells (positive control). Once subculture reached the appropriate $OD_{600}$, arabinose was added to a final concentration of 4 mg/mL to induce expression of pJN105. Aliquots (198 µL) of this subculture were dispensed into all internal wells. The outer wells of the plate were filled with 200 µL of water (to help maintain the plate humidity/environment and slow evaporation overall for the interior wells). Plates were incubated at 37 °C with shaking at 200 rpm for 4 h.

After the incubation period, the $OD_{600}$ of each cell was measured. Thereafter, each interior well of a fresh, chemical-resistant 96 well plate (Costar 3879) was filled with 200 µL Z buffer, 8 µL $CHCl_3$, and 4 µL 0.1% aqueous SDS. A 50-µL aliquot of each well in the initial plate was transferred to the lysis-buffer containing chemical resistant plate and lysed by aspirating 20 times. Thereafter, the assays for the receptors differed, as described below.

*For LasR assays*, a 100-µL aliquot from each well was transferred to a fresh, clear-bottom 96-well plate. At t = 0 minutes, the Miller assay (measuring β-galactosidase enzyme activity)[12] was started by adding 20 µL of the substrate *ortho*-nitrophenyl-β-galactoside (ONPG, 4 mg/mL in phosphate buffer) to each well. The plates were then incubated without shaking at 30 °C for 30 minutes. The enzymatic reaction was quenched by the addition of 50 µL of sodium carbonate

(1M in water) to each well. Absorbances at 420 and 550 nm were measured for each well. Miller units were calculated according to the following formula:

$$Miller\ unit = \frac{1000 * \left(A420 - (1.75 * A550)\right)}{t * v * OD600}$$

*t* = time ONPG incubated with lysate in min (30)

*v* = volume of culture lysed in mL (0.05)

Miller units were reported as a percentage relative to the OdDHL-only containing wells (*i.e.*, wells containing only agonist = 100% activity). All assays were conducted as technical triplicates and performed at least three times (*i.e.*, biological replicates). Dose-response curves were generated as three-parameter fits to the data using Graphpad Prism software (version 8).

*For QscR and RhlR assays*, a 150 µL-aliquot from each well was transferred to a fresh, clear bottom 96-well plate. At t = 0 minutes, the Miller assay was started by adding 25 µL of substrate chlorophenol red-β-galactopyranoside (CPRG, 4 mg/mL in phosphate buffered saline) and incubated without shaking at 30 °C for 20 min (for RhlR) or 45 min (for QscR). Miller units were calculated according to the following formula:

$$Miller\ unit = \frac{1000 * (A570)}{t * v * OD600}$$

*t* = time CPRG incubated with lysate in min (20 or 45)

*v* = volume of culture lysed in mL (0.05)

Miller units were reported as a percentage relative to OdDHL-only (for QscR) or BHL-only (for RhlR) containing wells (i.e., wells containing only agonist = 100% activity). All assays were conducted as technical triplicates and performed at least three times (*i.e.*, biological replicates). Dose-response curves were generated as three-parameter fits for QscR and four-parameter fits for RhlR using Graphpad Prism software (version 8).

### ***P. aeruginosa*** **PAO-JP2 reporter assay (GFP*)***

The LasR assay in *P. aeruginosa* PAO-JP2 was performed as previously described.[13] A 2-mL sample of LB medium containing 300 µg/mL Carbenicillin was inoculated with a single colony of PAO-JP2 and grown overnight (~16 h). Overnight culture was diluted 1:100 in fresh LB medium without antibiotic and grown to an $OD_{600}$ = 0.3 with path length correction. Aliquots (2 µL) of test compound stock solution in DMSO were added to the interior wells of a black, clear-bottomed 96-well microtiter plate with final DMSO concentrations <1%. In at least six "control wells" on each plate, only DMSO was added.

*For LasR agonism assays,* 2 µL of a 10 mM OdDHL solution (in DMSO) was added to at least six interior wells on each plate (to give an 100 µM final concentration). All interior wells then were filled with 198 µL of untreated subculture.

*For LasR antagonism assays,* at least three interior wells were filled with 198 µL of untreated subculture; the remainder of the subculture was treated with OdDHL (to give 150 nM, 1 µM, or 10 µM final concentrations) and then dispensed into all remaining interior wells.

The outer wells of each plate were filled with 200 µL of water (to help maintain the plate humidity/environment and slow evaporation overall for the interior wells). Plates were then incubated at 37 °C without shaking for 6 h. After incubation, GFP levels (excitation at 500 nM, emission at 540 nM) and $OD_{600}$ were read using a plate reader. OD-normalized fluorescence data were reported relative to OdDHL-containing wells (i.e., wells containing only OdDHL = 100% activity). All assays were conducted as technical triplicates and performed at least three times (*i.e.*, biological replicates). Dose-response curves were generated as three-parameter fits to the data using Graphpad Prism software (version 8).

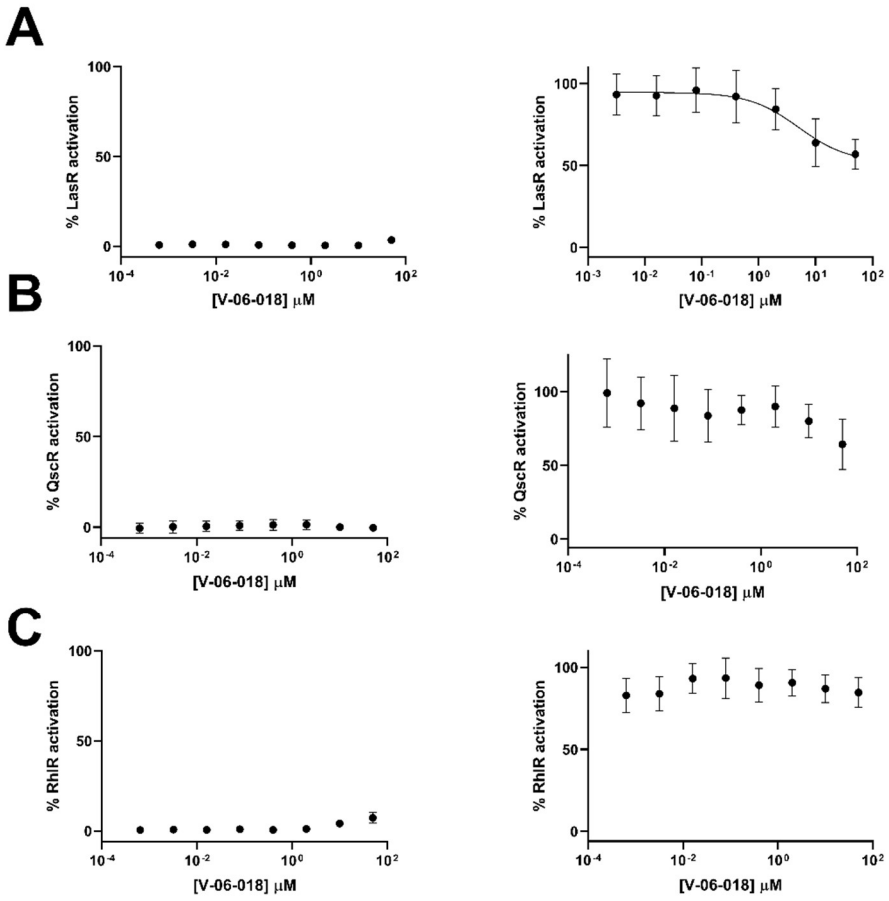


**Figure S2.1:** Dose response reporter assay data for V-06-018 in the *E. coli* LasR, QscR, and RhlR reporters.

V-06-018 agonism (*left*) and antagonism (*right*) profiles in the (A) *E. coli* LasR reporter *(*JLD271 + pJN105L + pSC11-L*)*, (B) *E. coli* QscR reporter *(*JLD271 + pJN105Q + pSC11-Q), and (C) *E. coli* RhlR reporter (JLD271 + pJN105R + pSC11-R). These data indicate that V-06-018 is an appreciably selective LasR antagonist; it only minimally modulates QscR and RhlR, the other two LuxR-type receptors in *P. aeruginosa*, and does so at only the highest concentrations tested (50 μM). At this concentration, V-06-018 very weakly agonizes RhlR and weakly antagonizes QscR. We note that the activity (i.e., efficacy) and potency of V-06-018 in the *E. coli* LasR reporter is markedly reduced relative to the *P.* aeruginosa LasR reporter, which may be an artifact of LasR overexpression in *E. coli* (see main text for a discussion of this phenomenon). Data is plotted for at least three biological replicates, each of which is composed of three technical replicates. Error bars indicate SD.

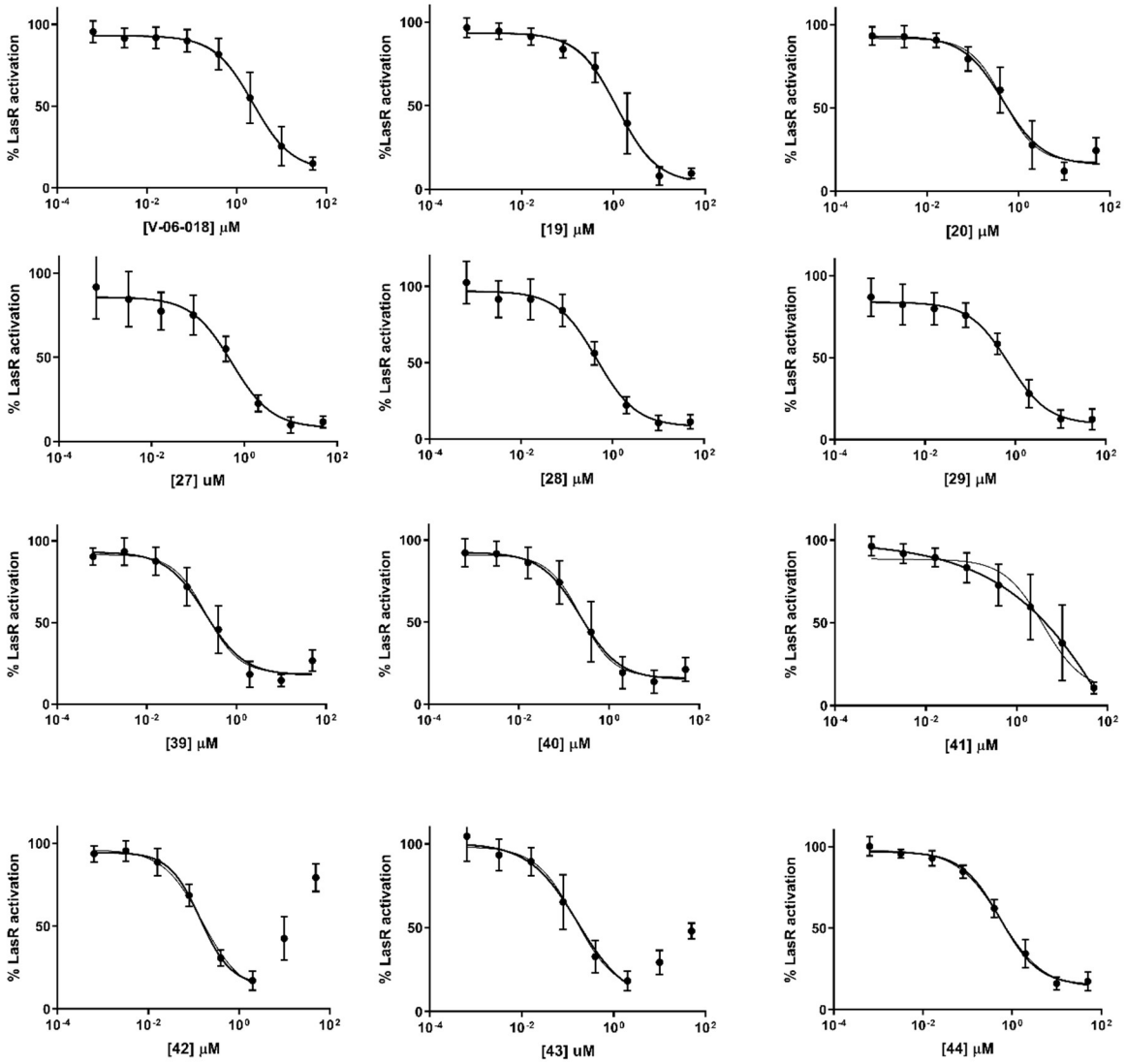


**Figure S2.2:** Dose-response antagonism assay data for selected compounds in the *P. aeruginosa* LasR reporter (PAO-JP2 + pLVA-GFP).

For compounds displaying appreciable non-monotonic partial agonism behavior (i.e., **42** and **43**, but not **20**), $IC_{50}$ values were calculated from the antagonism part of the curve. Three and four parameter fits were used to calculate $IC_{50}$ values. Both fits are included in each of the curves; $IC_{50}$ values from the three parameter fits are included in Table 1. Data plotted is for three biological replicates, each performed as three technical replicates. Error bars indicate SD.

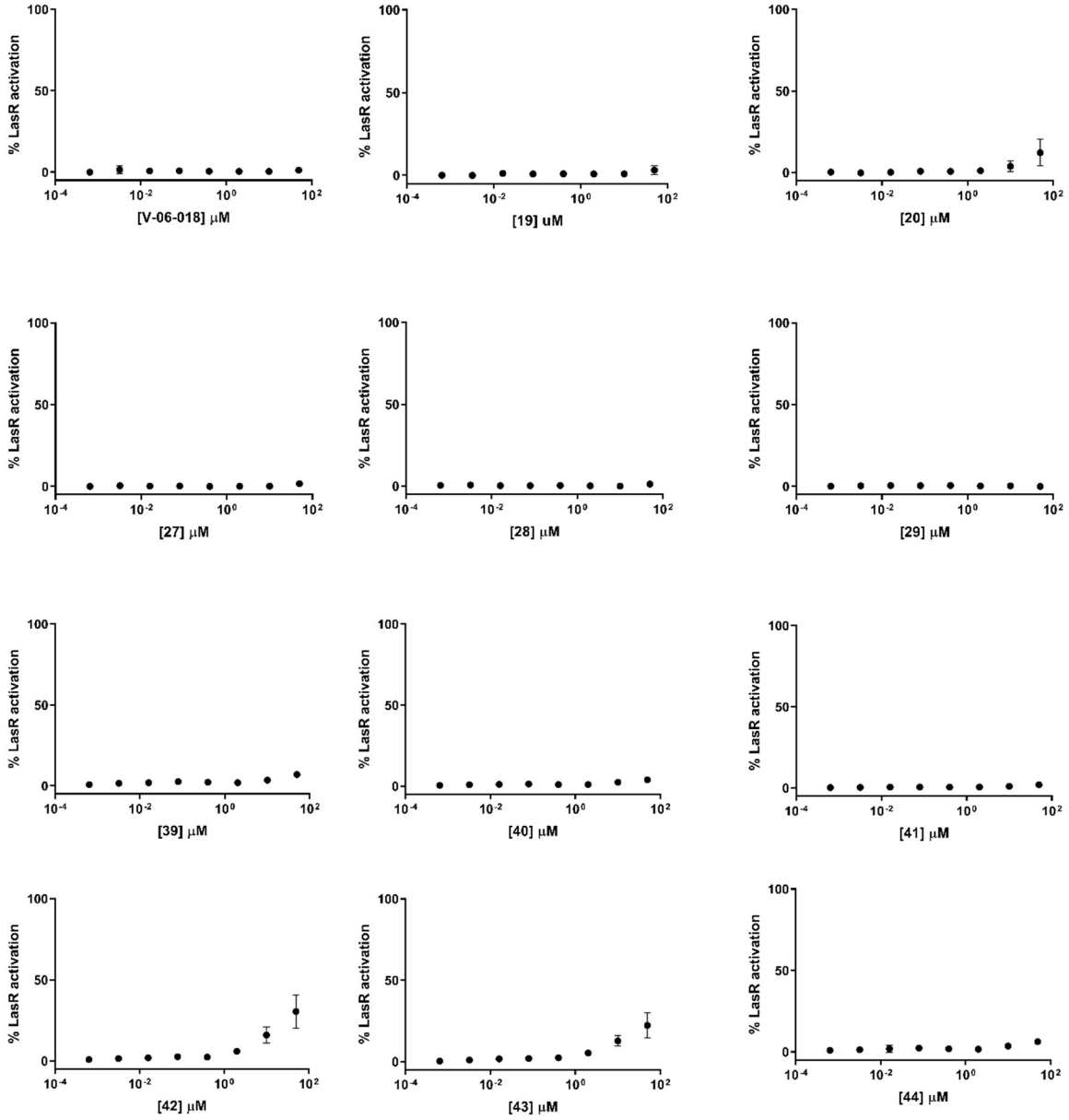


**Figure S2.3:** Dose-response agonism assay data for selected compounds in the *P. aeruginosa* LasR reporter (PAO-JP2 + pLVA-GFP).

Thiophene compounds **20**, **42** and **43**, each with non-monotonic partial agonism profiles (see Figure S2 above), display agonistic activity at the highest concentrations. Data plotted is for three biological replicates, each performed as three technical replicates. Error bars indicate SD.

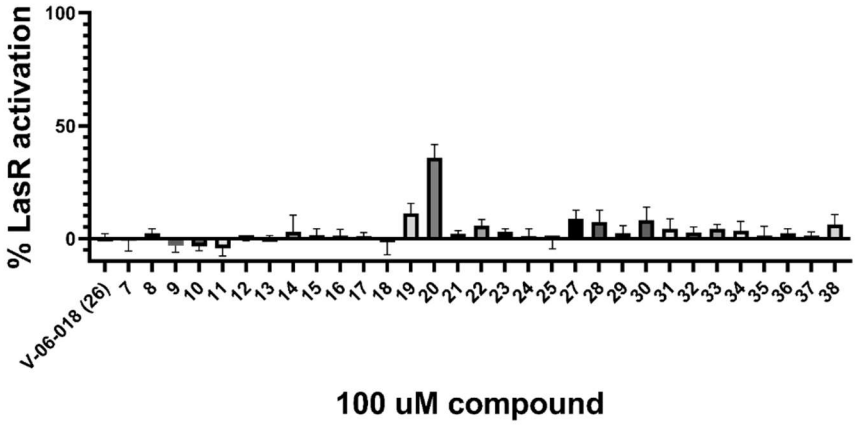


**Figure S2.4:** Primary agonism assay data for selected compounds in the *P. aeruginosa* LasR reporter (PAO-JP2 + pLVA-GFP).

Compounds tested at 100 μM. LasR agonism assay data for compounds not included on this plot can be found in Figure S3 above.

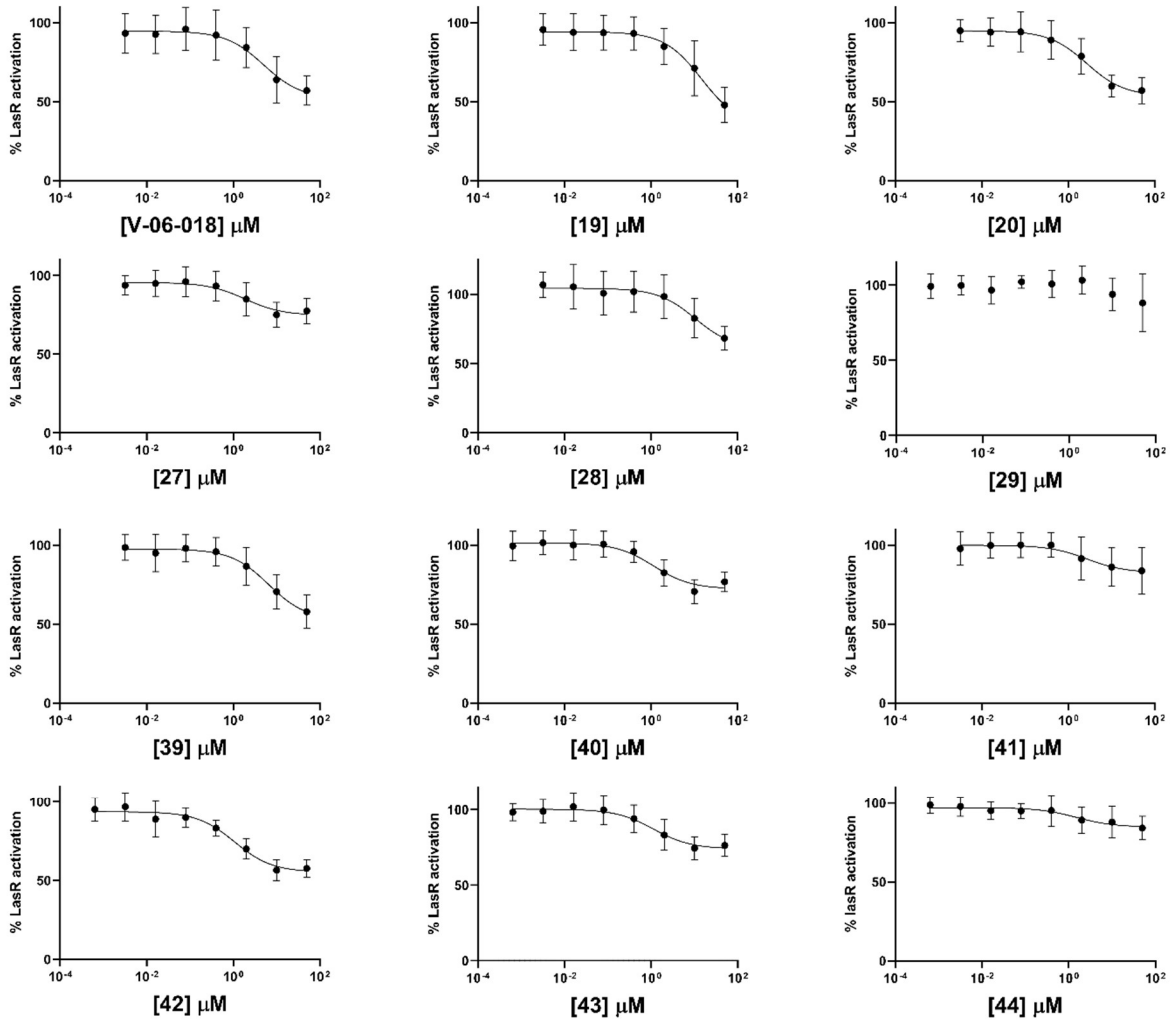


**Figure S2.5:** Dose-response antagonism curves for selected compounds in the *E. coli* LasR reporters.

Compounds **29** and **42**–**44** were evaluated in *E. coli* DH5α (pJN105L + pSC11-L); all other compounds were evaluated in *E. coli* JLD271 (pJN105L + pSC11-L). All of the compounds were active in these heterologous systems, suggesting that they elicit their inhibitory effects in the *P. aeruginosa* assay via direct interaction with LasR. We note that potency and efficacy were markedly decreased in all cases relative to in *P. aeruginosa* (see for comparison Figure S2), which may be an artifact of LasR overexpression in *E. coli* (see main text for a discussion of this phenomenon). We believe this phenomenon simply masks the activity of **29**, which only begins to display antagonistic activity at the highest concentration tested, preventing an accurate curve fit. See Table S2 for a listing of efficacy and potency data. Data plotted is for three biological replicates, each performed as three technical replicates. Error bars indicate SD.

**Table S2.2:** Potency and efficacy of selected compounds in the *E. coli* LasR reporters (from data in Figure S5)[a]

| Compound | $IC_{50}$ (μM) | 95% CI of $IC_{50}$ (μM)[b] | Maximum Inhibition (%)[c] |
|---|---|---|---|
| V-06-018 | 5.0 | 3.2 – 7.9 | 48 |
| **19** | 14 | 5.6 – 51 | 52 |
| **20** | 2.7 | 1.4 – 5.0 | 47 |
| **27** | 1.8 | 0.7 – 5.1 | 25 |
| **28** | 11 | 2.7 – 54 | 32 |
| **29** | -[d] | - | - |
| **39** | 6.6 | 3.1 – 14 | 42 |
| **40** | 1.1 | 0.5 – 2.4 | 29 |
| **41** | 2.7 | 0.4 – 24 | 18 |
| **42** | 1.1 | 0.6 – 1.7 | 45 |
| **43** | 1.1 | 0.5 – 2.6 | 26 |
| **44** | 1.5 | 0.2 - 14 | 15 |

[a]Antagonism experiments performed by competing the compounds against OdDHL at its $EC_{50}$ (2 nM for *E. coli* JLD271; 3.6 nM for *E. coli* DH5α); inhibitory activity was measured relative to receptor activation at this $EC_{50}$. $IC_{50}$ values determined by testing compounds over a range of concentrations (0.64 nM – 50 □M). All assays performed in triplicate. [b]CI = 95% confidence interval. [c]Denotes the best-fit value for the bottom of the computed dose-response curve. [d]Not calculated.

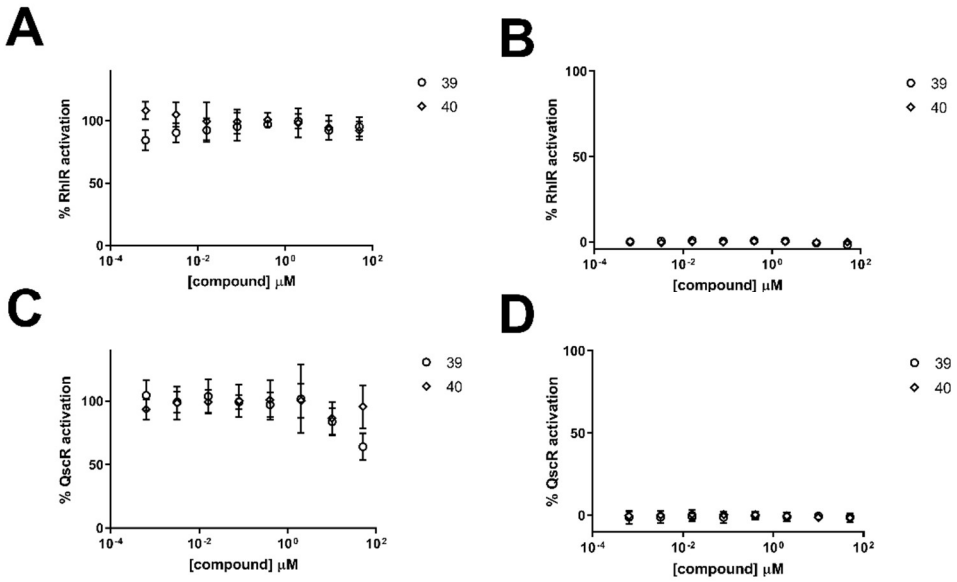


**Figure S2.6:** Activity profiles for lead LasR antagonists (**39** and **40**) in RhlR and QscR.

Profiles for (A) RhlR antagonism and (B) RhlR agonism in the *E. coli* reporter (JLD271 + pJN105R + pSC11-R), and (C) QscR antagonism and (D) QscR agonism in the *E. coli* reporter *(*JLD271 + pJN105Q + pSC11-Q). These data indicate that these V-06-018 analogs, like V-06-018, are selective for LasR. Analog **40** modulates neither RhlR nor QscR; **39** does not modulate RhlR and is a weak QscR antagonist. Data represent three biological triplicates, each of which is composed of three technical replicates. Error bars indicate SD.

**Protein expression and SDS PAGE gel methods**

A single colony of *E. coli* strain BL21(DE3) containing both pLysS and pET17b was inoculated into 5 mL of LB medium supplemented with Ampicillin (100 μg/mL) and Chloramphenicol (34 μg/mL) and grown overnight. Overnight culture was diluted 1:50 into fresh LB medium supplemented with 50 mM MOPS (pH adjusted to 7 after adding MOPS) and the appropriate amount of antibiotic. Compound was added to the appropriate concentration (50 μM) from DMSO stock solutions. Cultures were grown to an $OD_{600}$ = 0.5 with pathlength correction, and IPTG was added to a final concentration 0.4 mM to induce protein production. Cells were grown overnight at 15 °C with shaking at 200 RPM, before being pelleted.

Whole cell and soluble portions of cell lysate were isolated and prepared via the Bacterial Protein Extraction Reagent (B-PER, ThermoFisher Scientific) according to package instructions. Total protein quantities in each whole cell and soluble sample were quantified by Bradford assays.[14] Protein samples comprised of 15 □g total protein, 100 mM DTT, and 2.5 □L loading dye were boiled for 10 min prior to loading onto a Biorad 10% SDS gel. A MidSci bullseye protein ladder was run alongside samples. Gels were run in Tris-glycine SDS running buffer and stained overnight with Coomassie. After destaining and imaging, band intensities were quantified using ImageJ software (data listed in Table S3).

**Table S2.3.** Intensities of bands in Figure 5 (in the main text) as quantitated by ImageJ

| **Lane (WC = whole cell; S = soluble)** | **Calculated intensity of band (Arbitrary unit)** | **Ratio of WC/S band intensities (x 100%)** |
|---|---|---|
| DMSO WC | 13060.125 | 2.6% |
| DMSO S | 348.092 | |
| OdDHL WC | 10200.953 | 29% |
| OdDHL S | 2968.154 | |
| V-06-018 WC | 11341.024 | 7.3% |
| V-06-018 S | 828.527 | |
| **40** WC | 9102.539 | 7.5% |
| **40** S | 681.577 | |
| **42** WC | 10140.175 | 22% |
| **42** S | 2211.669 | |

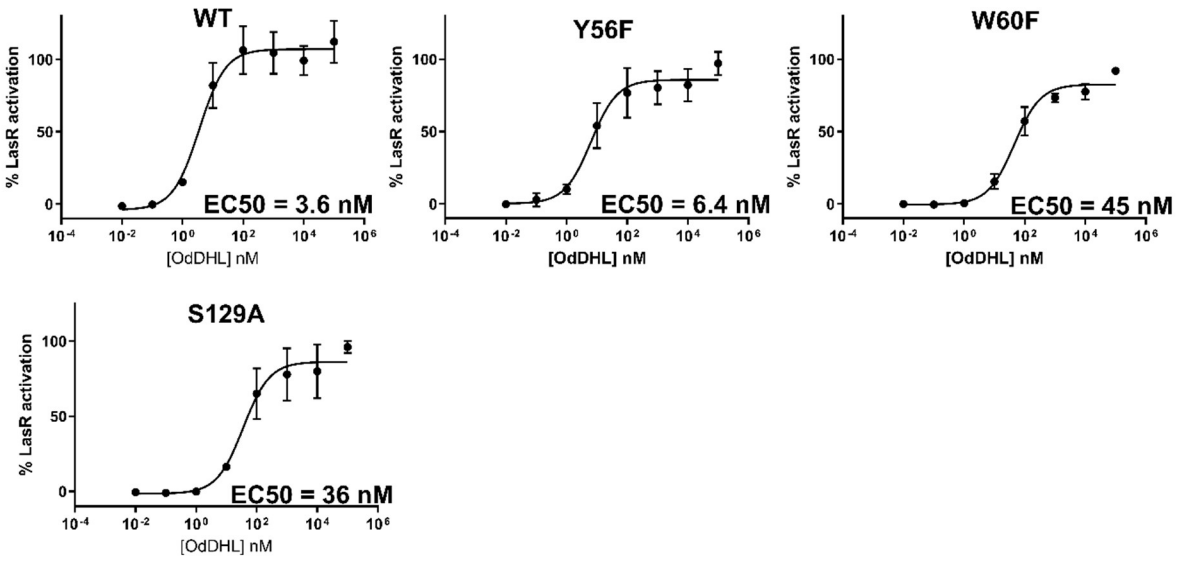


**Figure S2.7:** Dose-response agonism curves for OdDHL in selected *E. coli* LasR reporters (with wt and mutant LasR).

*E. coli* (DH5α+ pSC11 + wt or mutant LasR expression plasmid) strains were used for these reporter assays (see Table S1 for listing of plasmids). $EC_{50}$ values for OdDHL in each reporter are shown. OdDHL was found to be less potent in each mutant relative to wt LasR (i.e., 2–15-fold less potent), which is indicative of the deleterious effect of these mutations on the ability of LasR to be activated by OdDHL. Each curve represents three biological triplicates, each of which is composed of three technical replicates. Error bars represent SD.

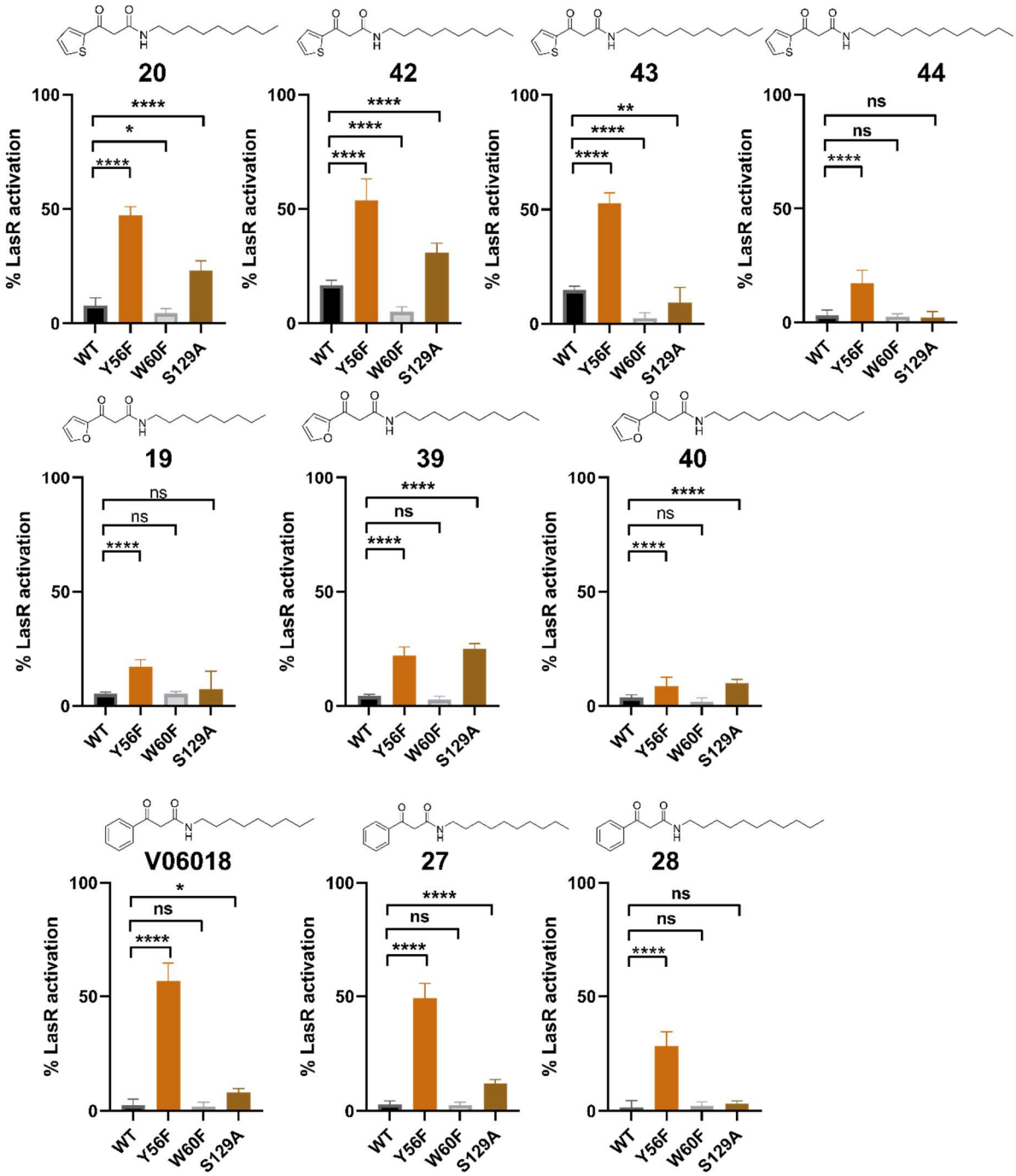


**Figure S2.8:** Single-concentration agonism assay data for various compounds in wt LasR and the three mutant LasR *E. coli* reporter systems.

All compounds tested at 100 □M. 100% LasR activation is defined as that caused by 100 □M OdDHL in that particular reporter strain. Significance was assessed via a one-way ANOVA: **** = $p < 0.0001$; *** = $p < 0.001$; ** = $p < 0.01$; * = $< 0.05$. ns = no significant difference.

**Compound characterization data for V-06-018 (26) and new compounds (7–37 and 39–44)**

*Note:* NMR peaks are reported for keto tautomers, although the minor enol tautomer was detected in all samples.

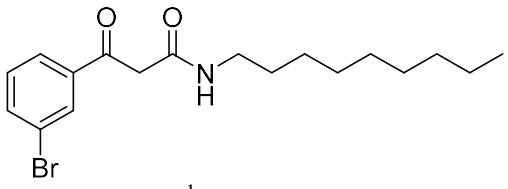

Compound **7**: $^{1}$H NMR (500 MHz, Chloroform-*d*) δ 8.14 (t, *J* = 1.8 Hz, 1H), 7.93 (d, *J* = 7.8 Hz, 1H), 7.77 – 7.70 (dt, J = 7.8 Hz, 1.8 Hz, 1H), 7.38 (t, *J* = 7.9 Hz, 1H), 6.92 (bs, 1H), 3.91 (s, 2H), 3.29 (apparent q, *J* = 6.7 Hz, 2H), 1.52 (p, *J* = 7.6, 7.2 Hz, 2H), 1.38 – 1.09 (m, 12H), 0.88 (t, *J* = 6.9 Hz, 3H). $^{13}$C NMR (126 MHz, $CDCl_3$) δ 194.86, 164.97, 137.86, 136.86, 131.55, 130.41, 127.23, 123.24, 77.27, 77.22, 77.02, 76.76, 45.69, 39.79, 31.85, 29.47, 29.38, 29.25, 29.23, 26.88, 22.66, 14.11. ESI-EMM: $[M+H]^+$ calculated 368.1220; measured 368.1219.

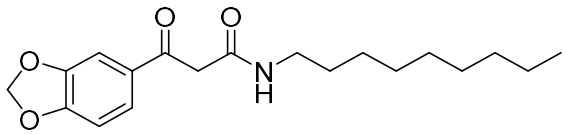

Compound **8**:$^{1}$H NMR (400 MHz, Chloroform-*d*) δ 7.63 (dd, *J* = 8.2, 1.8 Hz, 1H), 7.46 (d, *J* = 1.7 Hz, 1H), 7.05 (s, 1H), 6.87 (d, *J* = 8.2 Hz, 1H), 6.07 (s, 1H), 3.86 (s, 2H), 3.43 – 3.17 (apparent q, 2H), 1.51 (dd, *J* = 13.8, 6.8 Hz, 2H), 1.27 (d, *J* = 16.6 Hz, 12H), 0.88 (t, *J* = 6.6 Hz, 3H). $^{13}$C NMR (126 MHz, $CDCl_3$) δ 194.22, 165.61, 152.67, 148.46, 131.02, 125.57, 108.10, 108.06, 102.10, 45.38, 39.71, 31.86, 29.48, 29.40, 29.27, 29.24, 26.90, 22.67, 14.12. ESI-EMM: $[M+H]^+$ calculated 334.2013; measured 334.2009.

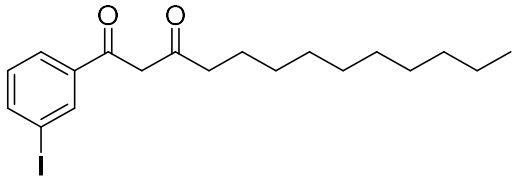

Compound **9**: $^{1}$H NMR (500 MHz, Chloroform-*d*) δ 8.33 (t, *J* = 1.6 Hz, 1H), 7.97 (dt, *J* = 8.0, 1.4 Hz, 1H), 7.94 (dt, *J* = 8.0, 1.3 Hz, 1H), 7.23 (d, *J* = 7.9 Hz, 1H), 6.92 (s, 1H), 3.90 (s, 2H), 3.29 (td, *J* = 7.2, 5.7 Hz, 2H), 1.52 (p, *J* = 7.2 Hz, 2H), 1.40 – 1.16 (m, 12H), 0.88 (t, *J* = 6.8 Hz, 3H). $^{13}$C NMR (126 MHz, $CDCl_3$) δ 194.85, 164.97, 142.74, 137.84, 137.46, 130.49, 127.80, 94.59, 45.55, 39.78, 31.85, 29.47, 29.38, 29.25, 29.23, 26.88, 22.66, 14.12. ESI-EMM: $[M+H]^+$ calculated 416.1081; measured 416.1076.

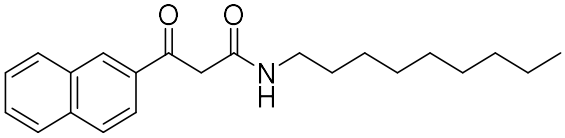

Compound **10**: $^{1}$H NMR (500 MHz, Chloroform-*d*) δ 8.68 – 8.42 (m, 1H), 8.03 (dd, *J* = 8.6, 1.8 Hz, 1H), 7.98 (dd, *J* = 8.2, 1.2 Hz, 1H), 7.91 (d, *J* = 8.7 Hz, 1H), 7.91 – 7.85 (d, J = 7.7 Hz, 1H), 7.63 (ddd, *J* = 8.2, 6.9, 1.3 Hz, 1H), 7.57 (ddd, *J* = 8.1, 6.8, 1.3 Hz, 1H), 7.14 (s, 1H), 4.08 (s, 2H), 3.31 (td, *J* = 7.2, 5.7 Hz, 2H), 1.65 – 1.47 (m, 2H), 1.41 – 1.16 (m, 12H), 0.96 – 0.79 (t, *J* = 7.1 Hz, 3H).$^{13}$C NMR (126 MHz, $CDCl_3$) δ 196.23, 165.59, 135.93, 133.51, 132.40, 131.04, 129.86, 129.09, 128.78, 127.77, 127.06, 123.61, 77.28, 77.03, 76.77, 45.54, 39.75, 31.84, 29.46, 29.41, 29.26, 29.22, 26.90, 22.65, 14.11. ESI-EMM: $[M+H]^+$ calculated 340.2271; measured 340.2267.

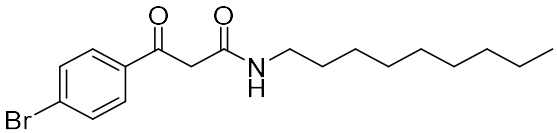

Compound **11**: $^{1}$H NMR (500 MHz, Chloroform-*d*) δ 7.93 – 7.84 (m, 2H), 7.71 – 7.62 (m, 2H), 6.92 (s, 1H), 3.90 (s, 2H), 3.42 – 3.14 (td, J = 7.2Hz, 5.7 Hz, 2H), 1.52 (p, *J* = 7.0 Hz, 2H), 1.43 – 1.16 (m, 12H), 0.88 (t, *J* = 6.9 Hz, 3H). $^{13}$C NMR (126 MHz, $CDCl_3$) δ 195.15, 165.12, 134.88, 132.21, 130.11, 129.49, 45.72, 39.78, 31.85, 29.47, 29.38, 29.24, 29.22, 26.87, 22.66, 14.11. ESI-EMM: $[M+Na]^+$ calculated 390.1039; measured 390.1034.

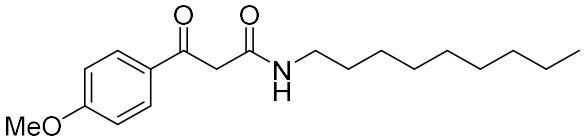

Compound **12**: $^{1}$H NMR (500 MHz, Chloroform-*d*) δ 8.12 – 7.91 (m, 2H), 7.16 (s, 1H), 7.01 – 6.88 (m, 2H), 3.89 (s, 3H), 3.88 (s, 3H), 3.28 (td, *J* = 7.2, 5.8 Hz, 2H), 1.52 (t, *J* = 7.2 Hz, 2H), 1.36 – 1.19 (m, 12H), 0.88 (t, *J* = 6.9 Hz, 3H). $^{13}$C NMR (126 MHz, $CDCl_3$) δ 194.80, 165.82, 164.32, 131.07, 129.25, 114.06, 55.59, 45.05, 39.68, 31.87, 29.49, 29.41, 29.28, 29.25, 26.91, 22.68, 14.13. ESI-EMM: $[M+H]^+$ calculated 320.220; measured 320.2224.

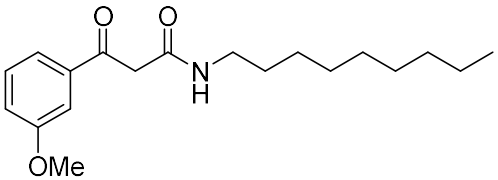

Compound **13**: $^{1}$H NMR (500 MHz, Chloroform-*d*) δ 7.58 (ddd, *J* = 7.7, 1.6, 0.9 Hz, 1H), 7.50 (dd, *J* = 2.7, 1.6 Hz, 1H), 7.39 (t, *J* = 8.0 Hz, 1H), 7.15 (ddd, *J* = 8.3, 2.6, 0.9 Hz, 1H), 6.21 (s, 1H), 3.93 (s, 2H), 3.86 (s, 3H), 3.29 (td, *J* = 7.2, 5.7 Hz, 2H), 1.52 (p, *J* = 7.2 Hz, 2H), 1.37 – 1.14 (m, 12H), 0.88 (t, *J* = 6.9 Hz, 3H). $^{13}$C NMR (126 MHz, $CDCl_3$) δ 196.11, 165.54, 159.94, 137.53, 129.86, 121.29, 120.69, 112.47, 55.47, 45.53, 39.72, 31.85, 29.48, 29.40, 29.27, 29.24, 26.90, 22.66, 14.11. ESI-EMM: $[M+Na]^+$ calculated 342.2040; measured 342.2036.

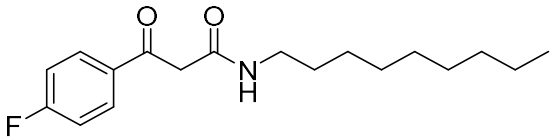

Compound **14**: $^{1}$H NMR (500 MHz, Chloroform-*d*) δ 8.09 – 8.01 (ddd, J = 2H), 7.16 (t, *J* = 8.6 Hz, 2H), 7.01 (s, 1H), 3.91 (s, 2H), 3.36 – 3.24 (m, 2H), 1.52 (t, *J* = 7.2 Hz, 2H), 1.34 – 1.20 (m, 12H), 0.88 (t, *J* = 6.9 Hz, 3H). $^{13}$C NMR (126 MHz, $CDCl_3$) δ 194.52, 167.32, 165.34, 165.27, 132.64, 132.62, 131.49, 131.41, 116.13, 115.96, 45.72, 39.77, 31.85, 29.48, 29.39, 29.26, 29.23, 26.89, 22.66, 14.11. ESI-EMM: $[M+H]^+$ calculated 308.2020; measured 308.2017.

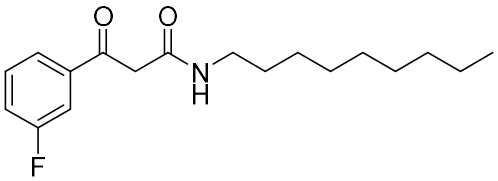

Compound **15**: $^{1}$H NMR (500 MHz, Chloroform-*d*) δ 7.80 (dt, *J* = 7.8, 1.2 Hz ($J_{H-F}$), 1H), 7.69 (dt, *J* = 9.3 ($J_{H-F}$), 2.1 Hz, 1H), 7.49 (td, *J* = 8.0, 5.4 Hz, 2H), 7.32 (td, *J* = 8.2, 2.3 Hz, 3H) 6.94 (s, 1H), 3.92 (s, 2H), 3.29 (td, *J* = 7.2, 5.7 Hz, 2H), 1.56 – 1.48 (p, *J* = 7.1 Hz, 2H), 1.32 – 1.17 (m, 10H), 0.88 (t, *J* = 6.9, 3H). $^{13}$C NMR (500 MHz, $CDCl_3$) δ 194.49 ($J_{CF}$ = 2.41 Hz) , 165.05, 162.89 (d, $J_{CF}$ = 248.8 Hz), 138.22 (d, $J_{CF}$ = 6.3 Hz), 130.59 (d, $J_{CF}$ = 7.6 Hz), 124.52 (d, $J_{CF}$ = 3.1 Hz), 121.14 (d, $J_{CF}$ = 21.5 Hz), 115.24 (d, $J_{CF}$ = 22.75 Hz), 45.76, 39.78, 31.85, 29.47, 29.38, 29.25, 29.23, 26.88, 22.66, 14.11. ESI-EMM: $[M+H]^+$ calculated 308.2020; measured 308.2017.

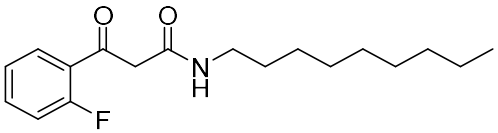

Compound **16**: $^{1}$H NMR (400 MHz, Chloroform-*d*) δ 7.88 (dtd, *J* = 11.5, 7.7, 1.9 Hz, 1H), 7.62 – 7.52 (m, 1H), 7.30 – 7.04 (m, 2H), 6.95 (s, 1H), 3.97 (d, *J* = 2.5 Hz, 1H), 3.39 – 3.26 (m, 2H), 1.58 – 1.50 (m, 2H), 1.39 – 1.19 (m, 12H), 0.88 (t, *J* = 6.7 Hz, 3H). $^{13}$C NMR (126 MHz, $CDCl_3$) δ 194.68, 165.61, 135.68, 135.61, 130.90, 124.81, 117.16, 116.97, 49.55, 39.84, 32.01, 29.64, 29.58, 29.43, 29.39, 27.06, 22.82, 14.26. ESI-EMM: $[M+H]^+$ calculated 308.2020; measured 208.2017

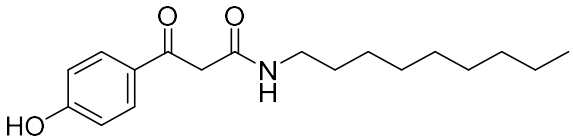

Compound **17**: $^{1}$H NMR (400 MHz, Chloroform-*d*) δ 7.93 – 7.84 (m, 2H), 7.68 (s, 1H), 7.08 (s, 1H), 6.89 – 6.83 (m, 2H), 3.87 (s, 2H), 3.28 (td, *J* = 7.2, 5.7 Hz, 2H), 1.51 (q, *J* = 7.1 Hz, 2H), 1.27 (d, *J* = 17.4 Hz, 12H), 0.92 – 0.83 (m, 3H). $^{13}$C NMR (126 MHz, $CDCl_3$) δ 194.30, 166.24,

161.35, 131.48, 129.11, 115.77, 45.30, 39.85, 31.86, 29.47, 29.34, 29.25, 29.23, 26.88, 22.67, 14.11. ESI-EMM: $[M-H]^-$ calculated 304.1918; measured 304.1918.

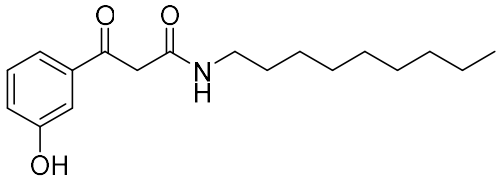

Compound **18**: $^1$H NMR (400 MHz, Chloroform-*d*) δ 7.98 (s, 1H), 7.56 (t, *J* = 2.1 Hz, 1H), 7.49 (dt, *J* = 8.0, 1.2 Hz, 1H), 7.49 – 7.41 (m, 2H), 7.32 (t, *J* = 7.9 Hz, 1H), 7.12 (ddd, *J* = 8.1, 2.5, 1.0 Hz, 1H), 3.96 (s, 2H), 3.32 (td, *J* = 7.2, 5.7 Hz, 2H), 1.54 (t, *J* = 7.0 Hz, 2H), 1.27 (d, *J* = 16.0 Hz, 12H), 0.87 (t, *J* = 6.8 Hz, 3H). $^{13}$C NMR (126 MHz, $CDCl_3$) δ 196.10, 166.49, 157.07, 137.30, 130.15, 121.79, 120.23, 115.40, 44.82, 39.95, 31.85, 29.47, 29.27, 29.25, 29.24, 26.90, 22.66, 14.10. ESI-EMM: $[M-H]^-$ calculated 306.2064; measured 306.2057.

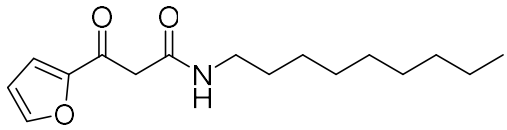

Compound **19**: $^1$H NMR (500 MHz, Chloroform-*d*) δ 7.66 (d, *J* = 1.6 Hz, 1H), 7.34 (d, *J* = 3.7 Hz, 1H), 6.59 (dd, *J* = 3.6, 1.7 Hz, 1H), 3.81 (s, 2H), 3.28 (td, *J* = 7.3, 5.7 Hz, 2H), 1.52 (-, *J* = 7.2 Hz, 2H), 1.36 – 1.21 (m, 12H), 0.88 (t, *J* = 6.9 Hz, 3H). $^{13}$C NMR (500 MHz, $CDCl_3$) δ 184.35, 164.95, 151.82, 147.81, 119.63, 112.84, 44.84, 39.73, 31.86, 29.48, 29.38, 29.27, 29.24, 26.90, 22.67, 14.12. ESI-EMM: $[M+H]^+$ calculated 280.1907; measured 280.1903.

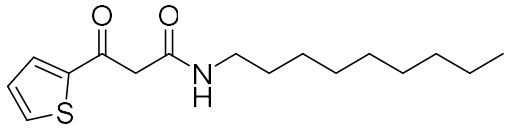

Compound **20**: $^1$H NMR (400 MHz, Chloroform-*d*) δ 7.83 (dd, *J* = 3.9, 1.2 Hz, 1H), 7.73 (dd, *J* = 4.9, 1.1 Hz, 1H), 7.16 (dd, *J* = 5.0, 3.9 Hz, 2H), 3.87 (s, 2H), 3.27 (td, *J* = 7.2, 5.7 Hz, 2H), 1.51 (p, *J* = 7.1 Hz, 2H), 1.34 – 1.19 (m, 13H), 0.91 – 0.82 (m, 3H). $^{13}$C NMR (126 MHz, $CDCl_3$) δ 188.79, 165.06, 143.43, 135.62, 133.91, 128.62, 45.89, 39.75, 31.86, 29.47, 29.38, 29.26, 29.23, 26.90, 22.66, 14.11. ESI-EMM: $[M+H]^+$ calculated 296.1679; measured 296.1674.

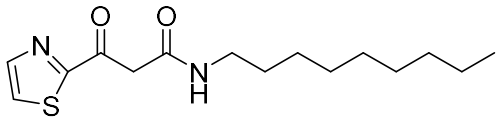

Compound **21**: $^1$H NMR (400 MHz, Chloroform-*d*) δ 8.05 (d, *J* = 3.0 Hz, 1H), 7.76 (d, *J* = 3.0 Hz, 1H), 4.16 (s, 2H), 3.38 – 3.25 (m, 2H), 1.53 (h, *J* = 7.0 Hz, 2H), 1.36 – 1.18 (m, 13H), 0.88 (t, *J* = 6.8 Hz, 3H). $^{13}$C NMR (101 MHz, $CDCl_3$) δ 188.57, 166.05, 164.71, 145.11, 127.48, 45.67, 39.83, 31.86, 29.49, 29.37, 29.27, 29.24, 26.88, 22.67, 14.12. ESI-EMM: $[M+H]^+$ calculated 297.1631; measured 297.1626.

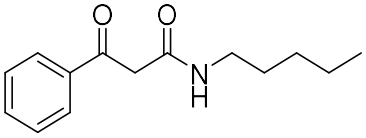

Compound **22**: $^{1}$H NMR (500 MHz, Chloroform-*d*) δ 8.01 (m, 2H), 7.62 (tt, *J* = 7.38, 1.32, 1H), 7.50 (m, 2H) 3.95 (s, 1H), 3.30 (td, *J* = 7.2, 5.7 Hz, 2H), 1.54 (p, *J* = 7.4 Hz, 1H), 1.39 – 1.27 (m, 4H), 0.89 (t, *J* = 6.9 Hz, 3H). $^{13}$C NMR (126 MHz, $CDCl_3$) δ 196.41, 165.51, 136.22, 134.08, 128.88, 128.59, 77.28, 77.23, 77.02, 76.77, 45.35, 39.68, 29.09, 29.05, 22.33, 13.97. ESI-EMM: $[M+H]^+$ calculated 234.1489; measured 234.1486.

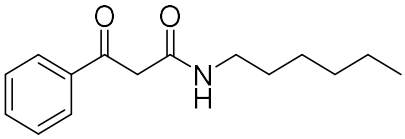

Compound **23**: $^{1}$H NMR (400 MHz, Chloroform-*d*) δ 8.05 – 7.95 (m, 2H), 7.66 – 7.58 (tt, *J* = 7.49, 1.39, 1H), 7.49 (m, 2H), 7.13 (s, 1H) 3.94 (s, 1H), 3.29 (td, *J* = 7.3, 5.7 Hz, 2H), 1.59 – 1.46 (m, 1H), 1.38 – 1.20 (m, 6H), 0.87 (t, *J* = 6.8 Hz, 3H). $^{13}$C NMR (101 MHz, $CDCl_3$) δ 196.28, 165.57, 136.21, 134.03, 45.44, 39.72, 31.44, 29.36, 26.56, 22.53, 14.01. ESI-EMM: $[M+H]^+$ calculated 248.1645; measured 248.1642.

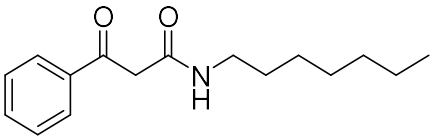

Compound **24**: $^{1}$H NMR (500 MHz, Chloroform-*d*) δ 8.05 – 7.98 (m, 2H), 7.61 (tt, *J* = 7.4, 1.36 Hz, 1H), 7.49 (m, 2H), 7.11 (s, 1H), 3.95 (s, 1H), 3.29 (td, *J* = 7.3, 5.8 Hz, 2H), 1.53 (t, *J* = 7.2 Hz, 2H), 1.43 – 1.20 (m, 8H), 0.87 (t, *J* = 6.8 Hz, 3H). $^{13}$C NMR (126 MHz, $CDCl_3$) δ 196.33, 165.52, 136.21, 134.04, 128.86, 128.57, 77.29, 77.04, 76.78, 45.41, 39.71, 31.71, 29.40, 28.92, 26.85, 22.57, 14.07. ESI-EMM: $[M+H]^+$ calculated 262.1802; measured 262.1798.

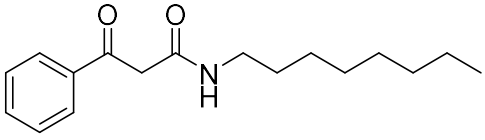

Compound **25**: $^{1}$H NMR (500 MHz, Chloroform-*d*) δ 8.17 – 7.93 (m, 2H), 7.68 – 7.57 (m, 1H), 7.49 (t, *J* = 7.8 Hz, 2H), 7.14 (s, 1), 3.94 (s, 1H), 3.29 (td, *J* = 7.2, 5.7 Hz, 2H), 1.52 (t, *J* = 7.0 Hz, 2H), 1.44 – 1.17 (m, 10H), 0.87 (t, *J* = 6.9 Hz, 3H). $^{13}$C NMR (126 MHz, $CDCl_3$) δ 196.29, 165.58, 136.20, 134.03, 128.85, 128.57, 45.43, 39.72, 31.77, 29.39, 29.22, 29.18, 26.90, 22.64, 14.09. ESI-EMM: $[M+H]^+$ calculated 276.1958; measured 276.1954.

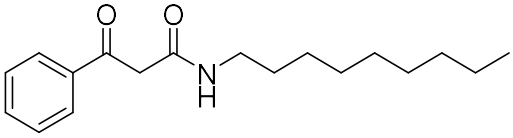

Compound **26** (V-06-018): $^{1}$H NMR (500 MHz, Chloroform-*d*) δ 8.04 – 7.96 (m, 2H), 7.67 – 7.57 (m, 1H), 7.49 (t, *J* = 7.8 Hz, 2H), 7.20 – 7.05 (s, 1H), 3.94 (s, 2H), 3.29 (td, *J* = 7.2, 5.7 Hz, 2H), 1.52 (p, *J* = 7.2 Hz, 2H), 1.44 – 1.15 (m, 12H), 0.88 (t, *J* = 6.9 Hz,3). $^{13}$C NMR (126 MHz, $CDCl_3$) δ 196.31, 165.57, 136.23, 134.05, 128.87, 128.59, 45.44, 39.73, 31.86, 29.48, 29.41, 29.27, 29.24, 26.91, 22.67, 14.12. ESI-EMM: $[M+H]^+$ calculated 290.115; measured 290.2114.

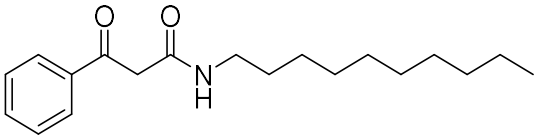

Compound **27**: $^{1}$H NMR (400 MHz, Chloroform-*d*) δ 8.08 – 7.94 (m, 2H), 7.67 – 7.57 (tt, *J* = 7.42, 1.32, 1H), 7.49 (m, 2H), 7.12 (s, 1H), 3.94 (s, 2H), 3.28 (td, *J* = 7.2, 5.7 Hz, 2H), 1.52 (p, *J* = 7.1 Hz, 2H), 1.37 – 1.17 (m, 14H), 0.87 (t, *J* = 6.8 Hz, 3H). $^{13}$C NMR (126 MHz, $CDCl_3$) δ 196.39, 165.46, 136.21, 134.07, 128.87, 128.57, 45.35, 39.71, 31.89, 29.53, 29.51, 29.39, 29.30, 29.26, 26.90, 22.68, 14.12. ESI-EMM: $[M+H]^+$ calculated 304.2271; measured 304.2265.

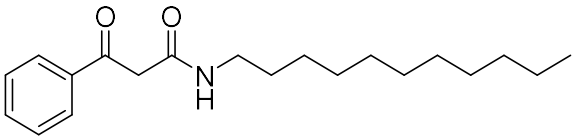

Compound **28**: $^{1}$H NMR (500 MHz, Chloroform-*d*) δ 8.10 – 7.89 (m, 2H), 7.68 – 7.58 (m, 1H), 7.55 – 7.45 (m, 2H), 7.10 (s, 1H), 3.95 (s, 1H), 3.29 (td, *J* = 7.2, 5.7 Hz, 2H), 1.59 – 1.46 (m, 2H), 1.27 (d, *J* = 17.4 Hz, 16H), 0.88 (t, *J* = 6.9 Hz, 3H). $^{13}$C NMR (126 MHz, $CDCl_3$) δ 196.39, 165.50, 136.22, 134.07, 128.88, 128.59, 77.28, 77.23, 77.02, 76.77, 45.37, 39.72, 31.91, 29.60, 29.58, 29.52, 29.40, 29.33, 29.27, 26.90, 22.69, 14.13. ESI-EMM: $[M+H]^+$ calculated 318.2428; measured 318.2425.

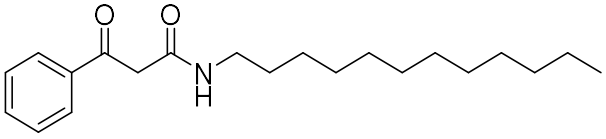

Compound **29**: $^{1}$H NMR (500 MHz, Chloroform-*d*) δ 8.17 – 7.92 (m, 2H), 7.61 (d, *J* = 7.5 Hz, 1H), 7.50 (t, *J* = 7.7 Hz, 2H), 7.13 (s, 1H), 3.95 (s, 2H), 3.37 – 3.19 (m, 2H), 1.53 (p, *J* = 7.2 Hz, 2H), 1.38 – 1.17 (m, 18H), 0.88 (t, *J* = 6.8 Hz, 3H). $^{13}$C NMR (126 MHz, $CDCl_3$) δ 196.36, 165.58, 136.19, 134.07, 128.87, 128.58, 45.34, 39.73, 31.92, 29.65, 29.63, 29.57, 29.52, 29.38, 29.35, 29.26, 26.90, 22.69, 14.13. ESI-EMM: $[M+H]^+$ calculated 332.2584; measured 332.2589.

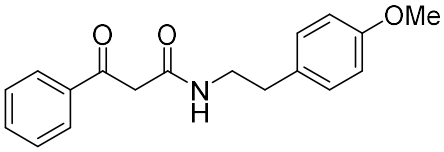


Compound **30**: $^{1}$H NMR (500 MHz, Chloroform-*d*) δ 8.01 – 7.93 (m, 2H), 7.66 – 7.57 (tt, *J* = 7.38, 1.69 Hz, 1H), 7.49 (m, 2H), 7.14 – 7.06 (m, 2H), 7.03 (s, 1H), 6.93 – 6.76 (2, 1H), 3.91 (s, 2H), 3.78 (s, 3H), 3.52 (td, *J* = 7.1, 5.7 Hz, 2H), 2.77 (t, *J* = 7.1 Hz, 2H). $^{13}$C NMR (126 MHz, $CDCl_3$) δ 194.96, 164.53, 157.19, 135.14, 133.01, 129.69, 128.65, 127.82, 127.57, 112.96, 54.21, 44.54, 40.10, 33.68. ESI-EMM: $[M+H]^+$ calculated 298.1438; measured 298.1434.

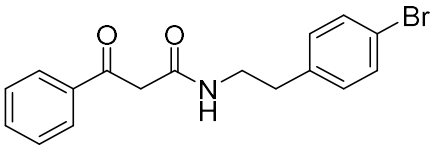


Compound **31**: $^{1}$H NMR (500 MHz, Chloroform-*d*) δ 8.01 – 7.93 (m, 2zH), 7.63 (tt, *J* = 7.31, 1.31, 1H), 7.52 – 7.47 (m, 2fH), 7.37 (m, 2fH), 7.14 – 7.08 (m, 1H), 7.04 (m, 2H), 3.91 (s, 1H), 3.57 – 3.50 (td, *J* = 7.1, 5.9, 2H), 2.79 (t, *J* = 7.1 Hz, 1H). $^{13}$C NMR (126 MHz, $CDCl_3$) δ 196.01, 165.67, 137.67, 136.07, 134.14, 131.62, 130.47, 128.89, 128.57, 120.34, 77.28, 77.02, 76.77, 45.40, 40.64, 35.04. ESI-EMM: $[M+H]^+$ calculated 346.0437; measured 346.0437.

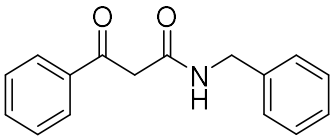


Compound **32**: $^{1}$H NMR (500 MHz, Chloroform-*d*) δ 8.06 – 7.95 (m, 2H), 7.68 – 7.58 (tt, *J* = 7.46, 1.27, 1H), 7.50 (m, 2H), 7.37 – 7.24 (m, 5H), 4.51 (d, *J* = 5.7 Hz, 2H), 4.01 (s, 2H). $^{13}$C NMR (126 MHz, $CDCl_3$) δ 196.06, 165.63, 137.86, 136.13, 134.13, 128.89, 128.71, 128.57, 127.69, 127.49, 45.21, 43.66. ESI-EMM: $[M+H]^+$ calculated 254.1176; measured 254.1174.

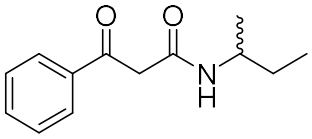


Compound **33**: $^{1}$H NMR (400 MHz, Chloroform-*d*) δ 7.98 – 7.89 (m, 2H), 7.58 – 7.48 (tt, *J* = 7.42, 1.29 H), 7.42 (m, 2H), 6.81 (s, 1H) 4.23 – 3.59 (m, 3H), 1.42 (p, *J* = 7.3 Hz, 2H), 1.21 – 1.00 (d, *J* = 6.6, 3H), 0.92 – 0.72 (t, , *J* = 6.7, 3H). $^{13}$C NMR (101 MHz, $CDCl_3$) δ 196.35, 164.93, 136.23, 134.02, 128.85, 128.57, 46.87, 45.62, 29.52, 20.31, 10.28. ESI-EMM: $[M+H]^+$ calculated 220.1332; measured 220.1331.

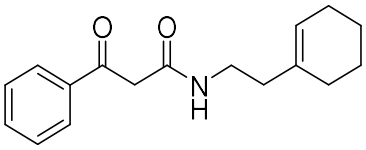

Compound **34**: $^{1}$H NMR (500 MHz, Chloroform-*d*) δ 8.01 (m, 3H), 7.66 – 7.58 (tt, *J* = 7.23, 1.37, 1H), 7.50 (m, 2fH), 6.96 (s, 1H), 5.45 (m, 1H), 3.93 (s, 2H), 3.37 (td, *J* = 6.8, 5.4 Hz, 2zH), 2.15 (t, *J* = 6.9 Hz, 1H), 2.00 – 1.81 (m, 4H), 1.60 (m, 3H), 1.56 – 1.50 (m, 2H). $^{13}$C NMR (126 MHz, $CDCl_3$) δ 196.09, 165.40, 136.25, 134.27, 134.01, 128.86, 128.62, 123.91, 45.66, 37.53, 37.41, 27.83, 25.22, 22.80, 22.32. ESI-EMM: $[M+H]^+$ calculated 272.1645; measured 272.1641.

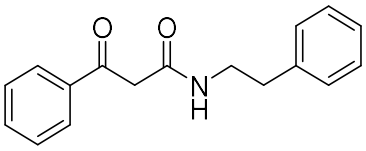

Compound **35**: $^{1}$H NMR (500 MHz, Chloroform-*d*) δ 7.98 (m, *J* = 2H), 7.62 (tt, *J* = 7.39, 1.3, 1H), 7.52 – 7.46 (m, 2H), 7.31 – 7.15 (m, 5H), 7.06 (s, 1H), 3.92 (s, 1H), 3.56 (td, *J* = 7.1, 5.9 Hz, 1H), 2.84 (t, *J* = 7.1 Hz, 1H). $^{13}$C NMR (126 MHz, $CDCl_3$) δ 195.99, 165.59, 138.71, 136.16, 134.05, 128.86, 128.80, 128.74, 128.59, 128.58, 126.49, 45.50, 40.94, 35.62. ESI-EMM: $[M+H]^+$ calculated 268.1332; measured 268.1330.

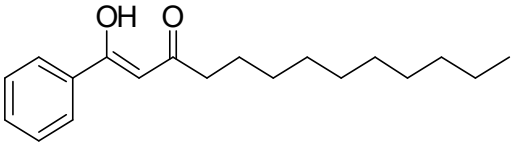

Compound **36**: $^{1}$H NMR (400 MHz, Chloroform-*d*) δ 7.94 – 7.79 (m, 2H), 7.55 – 7.50 (m, 1H), 7.48 – 7.42 (m, 2H), 6.17 (s, 1H), 2.52 – 2.32 (t, *J* = 7.51 2H), 1.68 (p, *J* = 7.6 Hz, 2H), 1.27 (m, *J* = 8.3 Hz, 14H), 0.95 – 0.83 (t, *J* = 7.0 , 3H). $^{13}$C NMR (101 MHz, $CDCl_3$) δ 197.03, 183.50, 135.11, 132.21, 128.60, 126.99, 96.08, 39.30, 31.91, 29.59, 29.49, 29.40, 29.32, 25.88, 22.70, 14.13. ESI-EMM: $[M+H]^+$ calculated 289.2162, measured 289.2161.

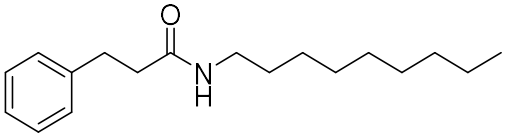

Compound **37**: $^{1}$H NMR (500 MHz, Chloroform-*d*) δ 7.26 (t, *J* = 7.5 Hz, 2H), 7.21 – 7.17 (m, 3H), 5.86 (s, 1H), 3.21 – 3.15 (td, *J* = 7.02, 5.29, 2H), 2.96 (t, *J* = 7.7 Hz, 2H), 2.48 (t, *J* = 7.62 Hz, 2H), 1.41 (p, *J* = 7.2 Hz, 2H), 1.24 (m, 12H), 0.88 (t, *J* = 7.0 Hz, 3H). $^{13}$C NMR (126 MHz, $CDCl_3$) δ 172.38, 140.88, 128.56, 128.42, 126.30, 77.41, 77.16, 76.90, 39.75, 38.46, 31.95, 29.58, 29.38, 29.34, 26.96, 22.75, 14.20. ESI-EMM: $[M+H]^+$ calculated 276.2322; measured 276.2317.

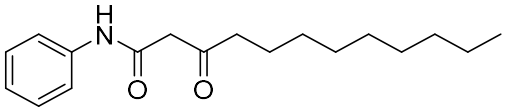

Compound **38** has been fully characterized and reported previously by our laboratory.[15] Spectra matched previously reported data.

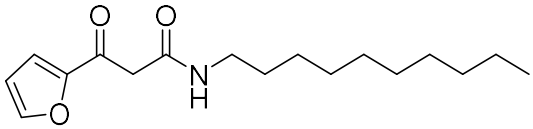

Compound **39**: $^{1}$H NMR (500 MHz, Chloroform-*d*) δ 7.66 (d, *J* = 1.6 Hz, 1H), 7.34 (d, *J* = 3.6 Hz, 1H), 7.06 (s, 1H), 6.59 (dd, *J* = 3.6, 1.7 Hz, 1H), 3.81 (s, 2H), 3.28 (td, *J* = 7.2, 5.7 Hz, 2H), 1.52 (p, *J* = 7.2 Hz, 2H), 1.28 (m, *J* = 22.2 Hz, 14H), 0.88 (t, *J* = 6.9 Hz, 3H). $^{13}$C NMR (126 MHz, $CDCl_3$) δ 184.32, 165.00, 151.83, 147.80, 119.63, 112.84, 44.88, 39.73, 31.88, 29.54, 29.52, 29.37, 29.30, 29.27, 26.90, 22.68, 14.12. ESI-EMM: $[M+H]^+$ calculated 294.2064; measured 294.2060.

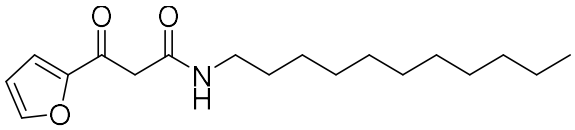

Compound **40**: $^{1}$H NMR (500 MHz, Chloroform-*d*) δ 7.66 (d, *J* = 1.6 Hz, 1H), 7.34 (d, *J* = 3.6 Hz, 1H), 7.06 (s, 1H), 6.59 (dd, *J* = 3.6, 1.7 Hz, 1H), 3.81 (s, 2H), 3.28 (td, *J* = 7.2, 5.7 Hz, 3H), 1.51 (q, *J* = 7.2 Hz, 3H), 1.27 (d, *J* = 20.5 Hz, 21H), 0.88 (t, *J* = 6.9 Hz, 3H). $^{13}$C NMR (126 MHz, $CDCl_3$) δ 184.33, 164.99, 151.83, 147.81, 119.63, 112.84, 44.87, 39.73, 31.91, 29.60, 29.59, 29.52, 29.37, 29.33, 29.28, 26.91, 22.69, 14.13. ESI-EMM: $[M+H]^+$ calculated 308.2220; measured 308.2218.

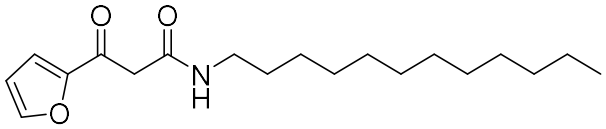

Compound **41**: $^{1}$H NMR (400 MHz, Chloroform-*d*) δ 7.66 (d, *J* = 1.6 Hz, 1H), 7.34 (d, *J* = 3.6 Hz, 1H), 7.06 (s, 1H), 6.59 (dd, *J* = 3.6, 1.7 Hz, 1H), 3.81 (s, 2H), 3.28 (td, *J* = 7.2, 5.7 Hz, 2H), 1.52 (p, *J* = 7.1 Hz, 2H), 1.36 – 1.17 (m, 18H), 0.88 (t, *J* = 6.8 Hz, 3H). $^{13}$C NMR (126 MHz, $CDCl_3$) δ 184.33, 164.97, 151.82, 147.80, 119.62, 112.84, 44.85, 39.73, 31.92, 29.65, 29.63, 29.59, 29.53, 29.37, 29.35, 29.28, 26.91, 22.70, 14.13. ESI-EMM: $[M+H]^+$ calculated 322.2377; measured 322.2372.

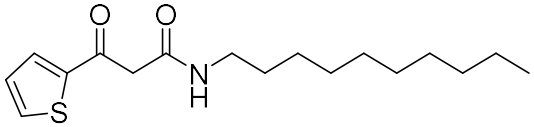

Compound **42**: $^{1}$H NMR (500 MHz, Chloroform-*d*) δ 7.84 (d, *J* = 3.8 Hz, 1H), 7.74 (d, *J* = 4.9 Hz, 1H), 7.17 (apparent t, *J* = 4.4 Hz, 1H), 7.15 (s, 1H), 3.89 (s, 2H), 3.28 (apparent q, *J* = 6.8 Hz, 2H), 1.52 (t, *J* = 7.2 Hz, 2H), 1.27 (d, *J* = 19.8 Hz, 17H), 0.88 (t, *J* = 6.8 Hz, 4H). $^{13}$C NMR (126 MHz, $CDCl_3$) δ 188.81, 165.05, 143.41, 135.65, 133.91, 128.63, 45.82, 39.74, 31.89, 29.53, 29.51, 29.36, 29.30, 29.26, 26.90, 22.68, 14.13. ESI-EMM: $[M+H]^+$ calculated 310.1835; measured 310.1836.

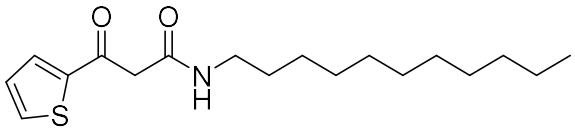

Compound **43**: $^{1}$H NMR (500 MHz, Chloroform-*d*) δ 7.84 (d, *J* = 3.8 Hz, 1H), 7.74 (d, *J* = 4.9 Hz, 1H), 7.19 – 7.16 (apparent t, *J* = 4.4 Hz, 1H), 7.15 (s, 1H), 3.89 (s, 1H), 3.28 (q, *J* = 6.8 Hz, 1H), 1.52 (p, *J* = 7.1 Hz, 1H), 1.27 (d, *J* = 18.2 Hz, 8H), 0.88 (t, *J* = 6.9 Hz, 2H). $^{13}$C NMR (126 MHz, $CDCl_3$) δ 188.81, 165.07, 143.41, 135.65, 133.92, 128.63, 77.30, 77.05, 76.79, 45.83, 39.75, 31.92, 29.61, 29.59, 29.52, 29.37, 29.34, 29.27, 26.91, 22.70, 14.14. ESI-EMM: $[M+H]^+$ calculated 324.1992; measured 324.1996.

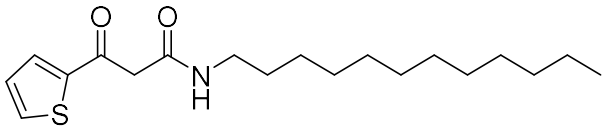

Compound **44**: $^{1}$H NMR (500 MHz, Chloroform-*d*) δ 7.84 (d, *J* = 3.8 Hz, 1H), 7.74 (d, *J* = 4.9 Hz, 1H), 7.17 (apparent t, *J* = 4.4 Hz, 1H), 7.14 (s, 1H), 3.89 (s, 2H), 3.28 (apparent q, *J* = 6.6 Hz, 2H), 1.52 (p, *J* = 7.1 Hz, 2H), 1.27 (d, *J* = 17.8 Hz, 18H), 0.88 (t, *J* = 6.8 Hz, 3H). $^{13}$C NMR (126 MHz, $CDCl_3$) δ 188.83, 165.05, 143.41, 135.67, 133.92, 128.64, 77.29, 77.24, 77.04, 76.78, 45.82, 39.75, 31.93, 29.66, 29.64, 29.59, 29.53, 29.38, 29.36, 29.28, 26.91, 22.71, 14.14. ESI-EMM: $[M+H]^+$ calculated 338.2148; measured 338.2144.

**References for materials and methods**


1. Lindsay, A.; Ahmer, B. M., Effect of sdiA on biosensors of *N*-acylhomoserine lactones. *J. Bacteriol.* **2005,** *187* (14), 5054-8.
2. Pearson, J. P.; Pesci, E. C.; Iglewski, B. H., Roles of *Pseudomonas aeruginosa las* and *rhl* Quorum-Sensing Systems in Control of Elastase and Rhamnolipid Biosynthesis Genes. *J. Bacteriol.* **1997,** *179* (18), 5756-5767.
3. Chugani, S. A.; Whiteley, M.; Lee, K. M.; D'Argenio, D.; Manoil, C.; Greenberg, E. P., QscR, a modulator of quorum-sensing signal synthesis and virulence in *Pseudomonas aeruginosa*. *Proc. Natl. Acad. Sci. U. S. A.* **2001,** *98* (5), 2752-7.
4. Lee, J. H.; Lequette, Y.; Greenberg, E. P., Activity of purified QscR, a *Pseudomonas aeruginosa* orphan quorum-sensing transcription factor. *Mol. Microbiol.* **2006,** *59* (2), 602-9.
5. Eibergen, N. R.; Moore, J. D.; Mattmann, M. E.; Blackwell, H. E., Potent and Selective Modulation of the RhlR Quorum Sensing Receptor by Using Non-native Ligands: An Emerging Target for Virulence Control in *Pseudomonas aeruginosa*. *Chembiochem* **2015,** *16* (16), 2348-56.
6. De Kievit, T. R.; Gillis, R.; Marx, S.; Brown, C.; Iglewski, B. H., Quorum-sensing genes in *Pseudomonas aeruginosa* biofilms: their role and expression patterns. *Appl. Environ. Microbiol.* **2001,** *67* (4), 1865-73.
7. Gerdt, J. P.; McInnis, C. E.; Schell, T. L.; Rossi, F. M.; Blackwell, H. E., Mutational analysis of the quorum-sensing receptor LasR reveals interactions that govern activation and inhibition by nonlactone ligands. *Chem. Biol.* **2014,** *21* (10), 1361-9.
8. Schuster, M.; Urbanowski, M. L.; Greenberg, E. P., Promoter specificity in *Pseudomonas aeruginosa* quorum sensing revealed by DNA binding of purified LasR. *Proc. Natl. Acad. Sci. U. S. A.* **2004,** *101* (45), 15833-9.
9 O'Reilly, M. C.; Blackwell, H. E., Structure-Based Design and Biological Evaluation of Triphenyl Scaffold-Based Hybrid Compounds as Hydrolytically Stable Modulators of a LuxR-Type Quorum Sensing Receptor. *ACS. Infect. Dis.* **2016,** *2* (1), 32-38.
10. Mattmann, M. E.; Shipway, P. M.; Heth, N. J.; Blackwell, H. E., Potent and selective synthetic modulators of a quorum sensing repressor in *Pseudomonas aeruginosa* identified from second-generation libraries of *N*-acylated L-homoserine lactones. *Chembiochem* **2011,** *12* (6), 942-9.
11. Gerdt, J. P.; McInnis, C. E.; Schell, T. L.; Blackwell, H. E., Unraveling the contributions of hydrogen-bonding interactions to the activity of native and non-native ligands in the quorum-sensing receptor LasR. *Org. Biomol. Chem.* **2015,** *13* (5), 1453-62.
12. Griffith, K. L.; Wolf, R. E., Jr., Measuring beta-galactosidase activity in bacteria: cell growth, permeabilization, and enzyme assays in 96-well arrays. *Biochem. Biophys. Res. Commun.* **2002,** *290* (1), 397-402.
13. Moore, J. D.; Rossi, F. M.; Welsh, M. A.; Nyffeler, K. E.; Blackwell, H. E., A Comparative Analysis of Synthetic Quorum Sensing Modulators in *Pseudomonas aeruginosa*: New Insights into Mechanism, Active Efflux Susceptibility, Phenotypic Response, and Next-Generation Ligand Design. *J. Am. Chem. Soc.* **2015,** *137* (46), 14626-39.
14. Bradford, M. M., A rapid and sensitive method for the quantitation of microgram quantities of protein utilizing the principle of protein-dye binding. *Anal. Biochem.* **1076,** *72*, 248-254.

15. McInnis, C. E.; Blackwell, H. E., Design, synthesis, and biological evaluation of abiotic, non-lactone modulators of LuxR-type quorum sensing. *Bioorg. Med. Chem.* **2011,** *19* (16), 4812-9.

**[1]H- and [13]C-NMR spectra for V-06-018 (26) and all new compounds (7–37 and 39–44)**

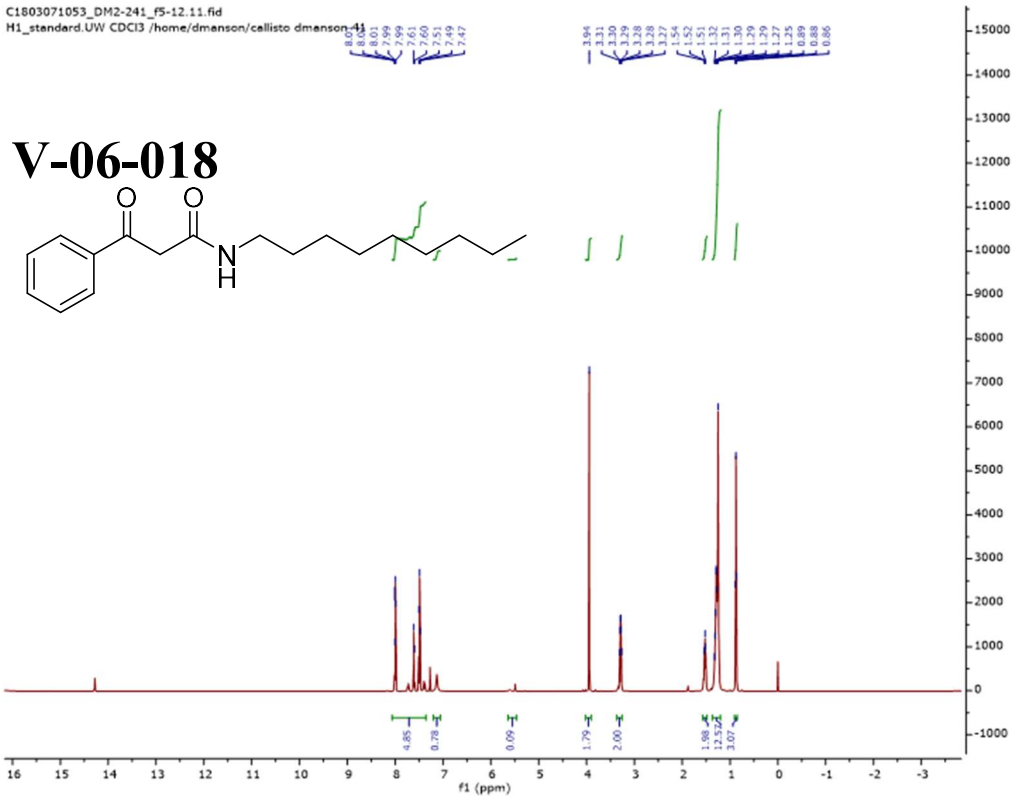


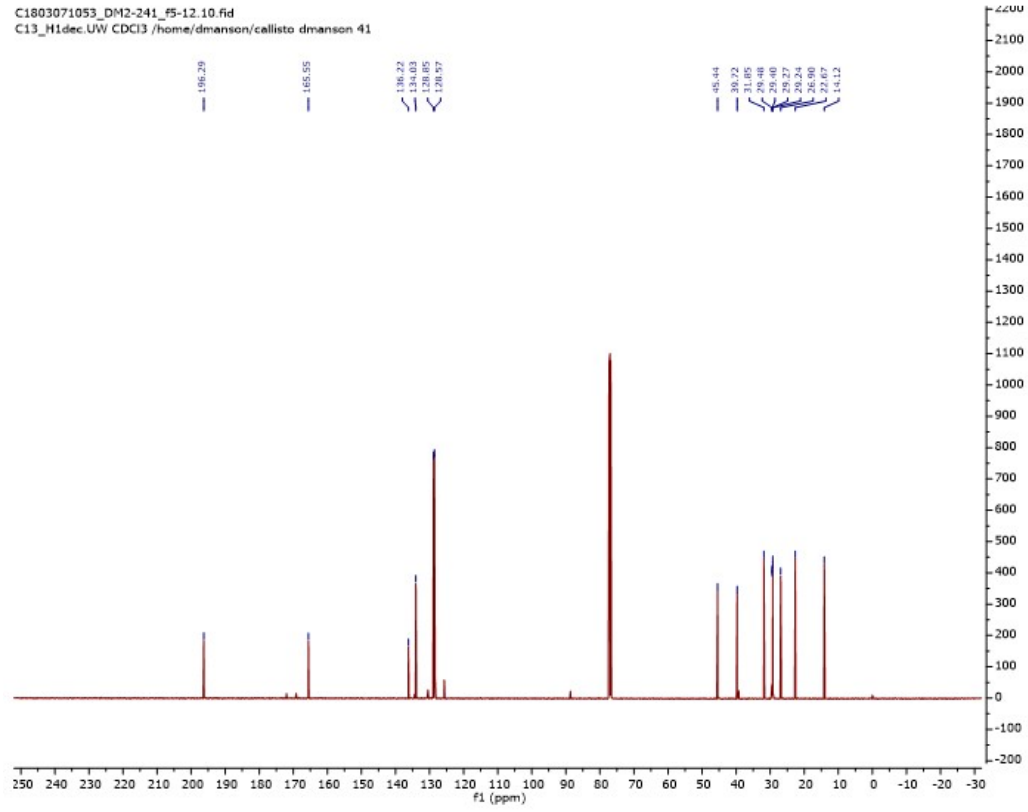

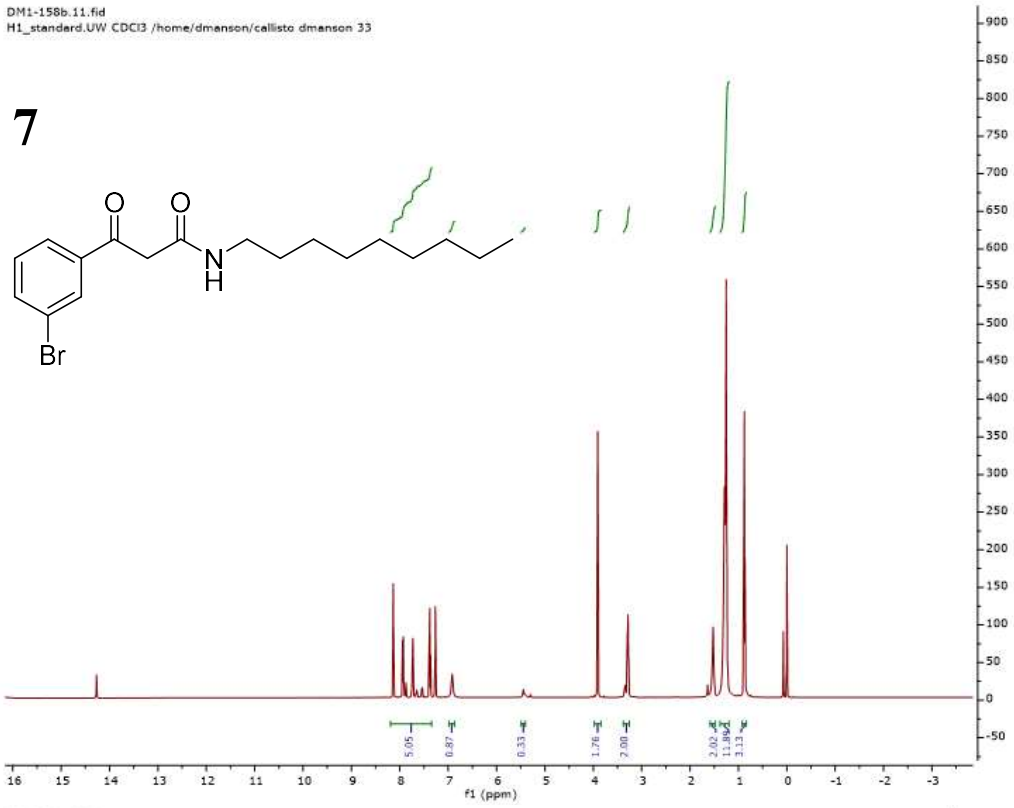
DM1-158b.11.fid
H1_standard.UW CDCl3 /home/dmanson/callisto dmanson 33
7
O
O
N
H
Br
5.05
0.87
0.33
1.76
2.00
2.02
11.80
3.13
f1 (ppm)

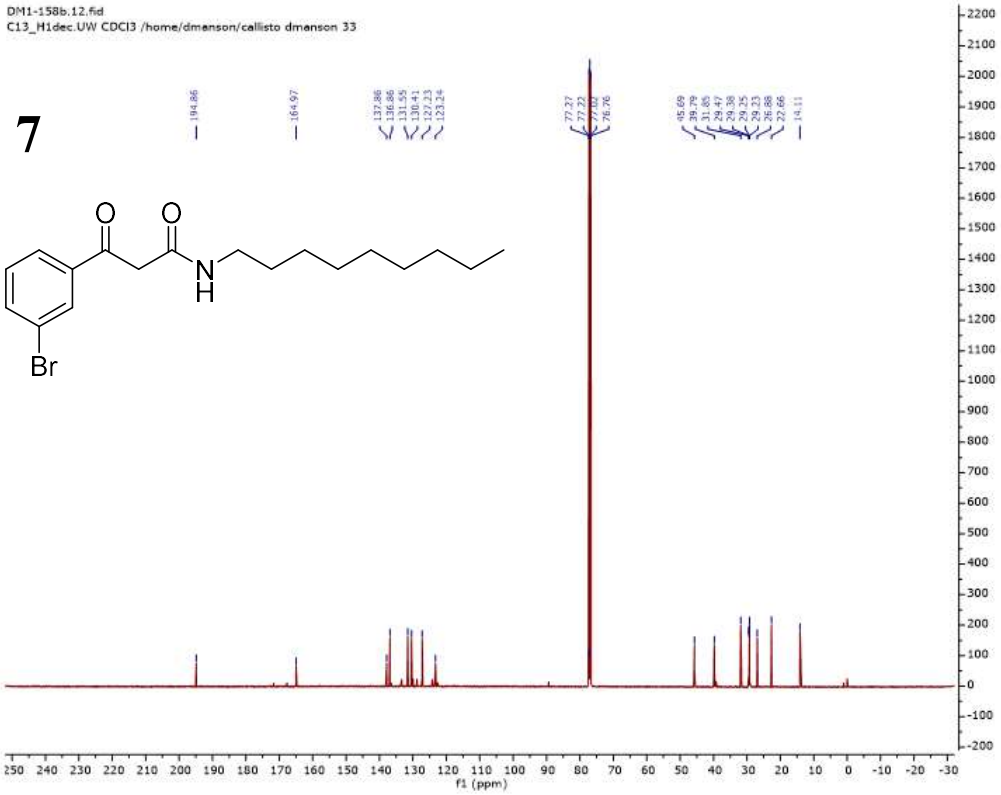
DM1-158b.12.fid
C13_H1dec.UW CDCl3 /home/dmanson/callisto dmanson 33
7
O
O
N
H
Br
194.86
164.97
137.86
136.46
131.55
130.41
127.23
123.24
77.27
77.23
77.02
76.76
65.69
39.79
31.85
29.47
29.38
29.25
29.23
29.08
22.66
14.11
f1 (ppm)

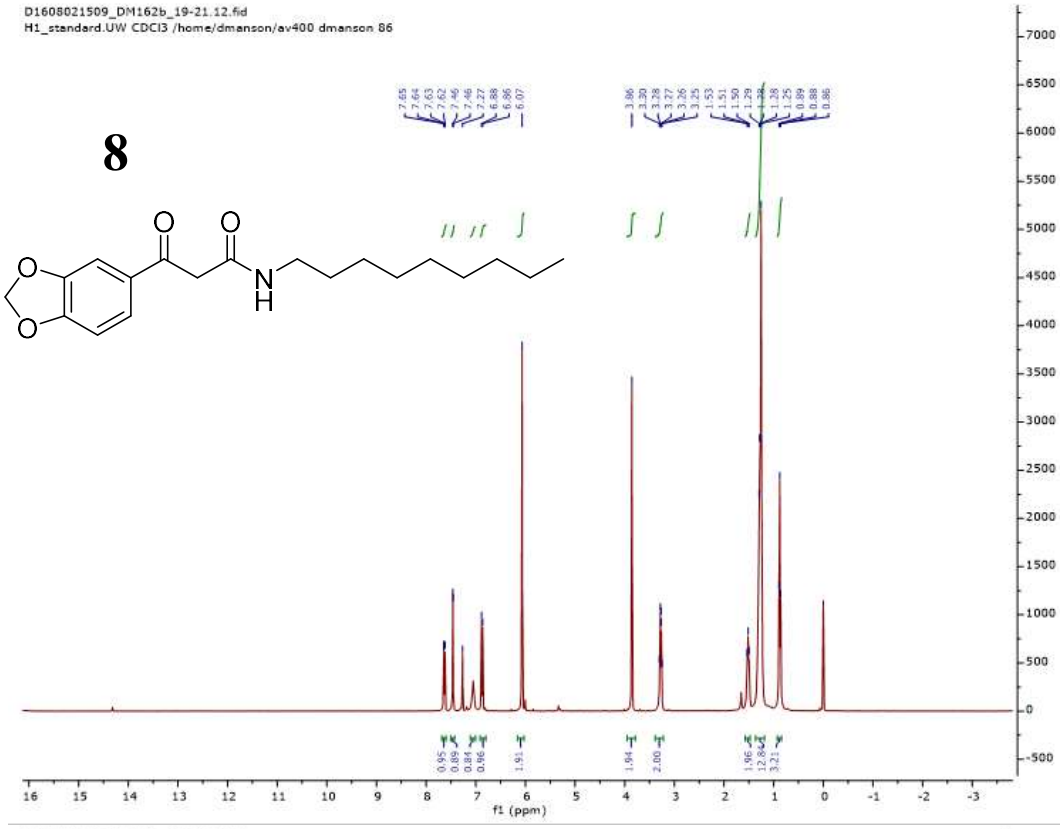
D1608021509_DM162b_19-21.12.fid
H1_standard.UW CDCl3 /home/dmanson/av400 dmanson 86
8
f1 (ppm)

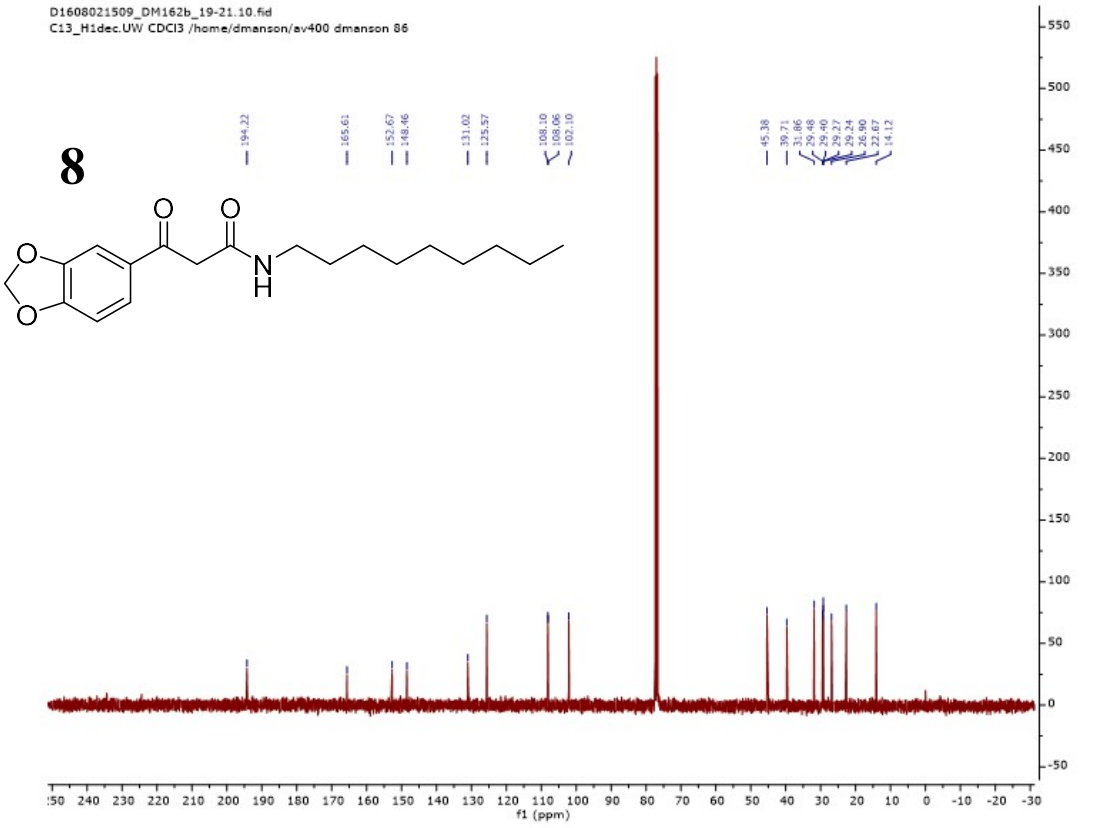
D1608021509_DM162b_19-21.10.fid
C13_H1dec.UW CDCl3 /home/dmanson/av400 dmanson 86
8
f1 (ppm)

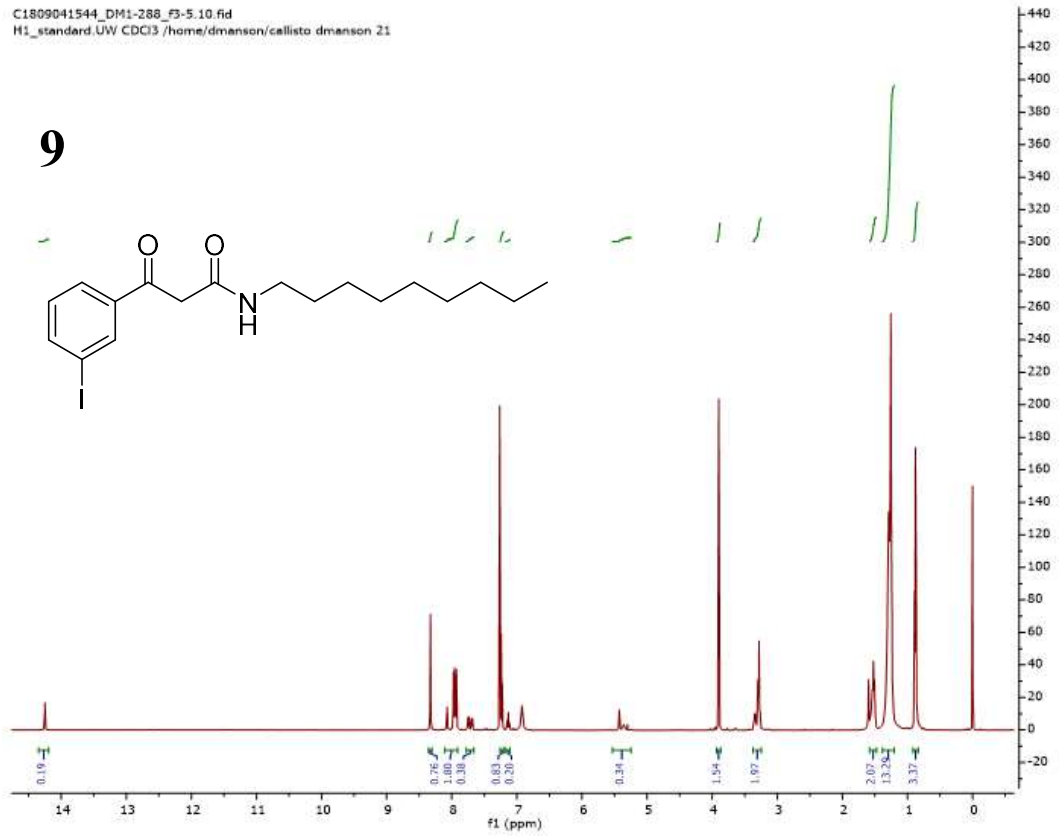
C1809041544_DM1-288_f3-5.10.fid
H1_standard.UW CDCl3 /home/dmanson/callisto dmanson 21
9
f1 (ppm)

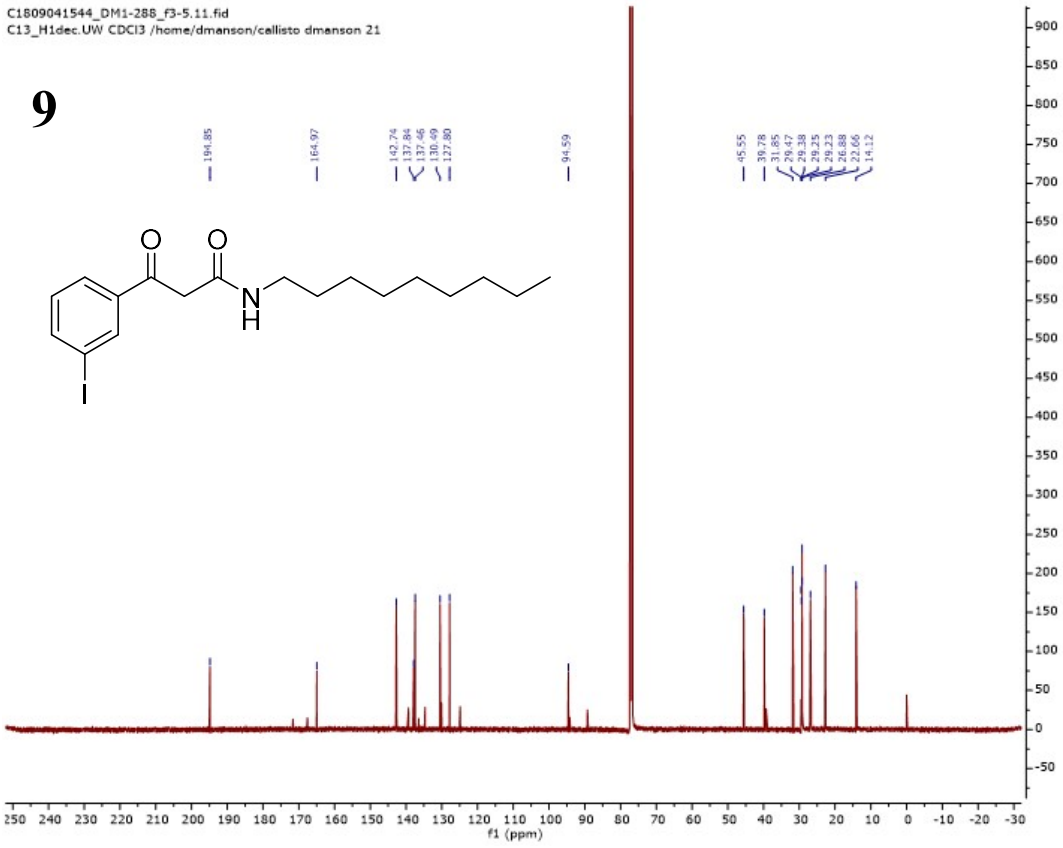
C1809041544_DM1-288_f3-5.11.fid
C13_H1dec.UW CDCl3 /home/dmanson/callisto dmanson 21
9
194.85
164.97
142.74
137.84
137.46
130.49
127.80
94.59
45.55
39.78
31.85
29.47
29.38
29.25
29.23
26.88
22.66
14.12
f1 (ppm)

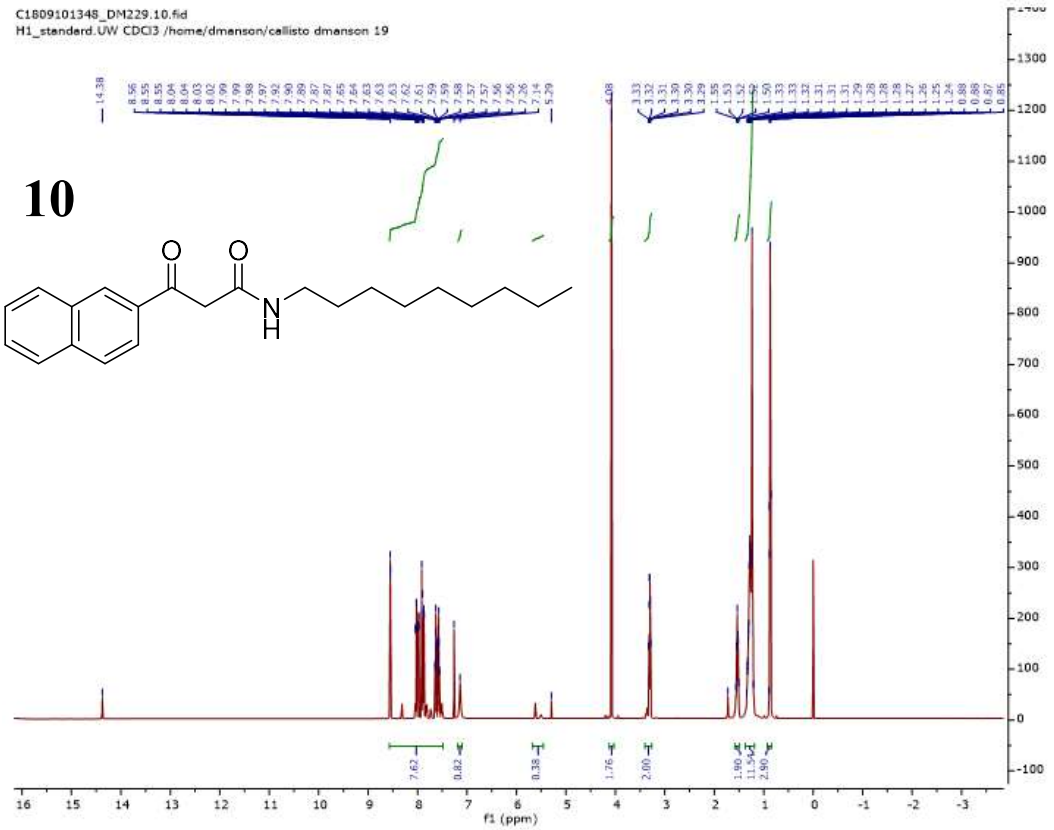
C1809101348_DM229.10.fid
H1_standard.UW CDCl3 /home/dmanson/callisto dmanson 19
10
f1 (ppm)

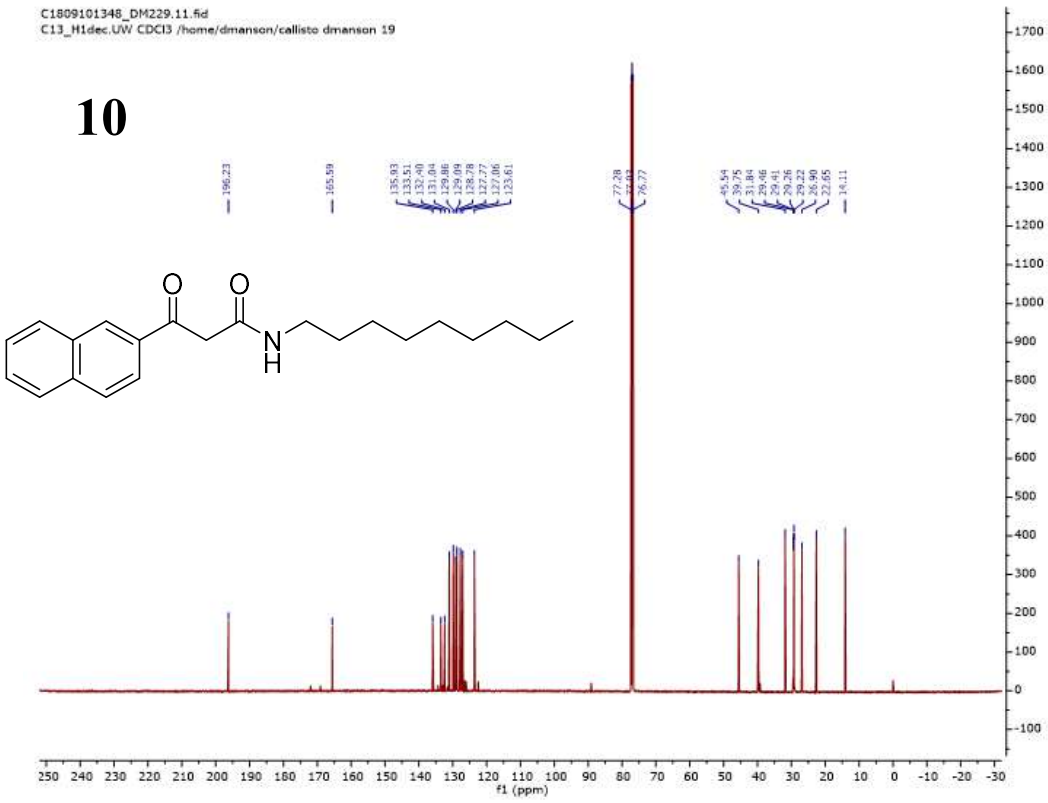
C1809101348_DM229.11.fid
C13_H1dec.UW CDCl3 /home/dmanson/callisto dmanson 19
10
f1 (ppm)

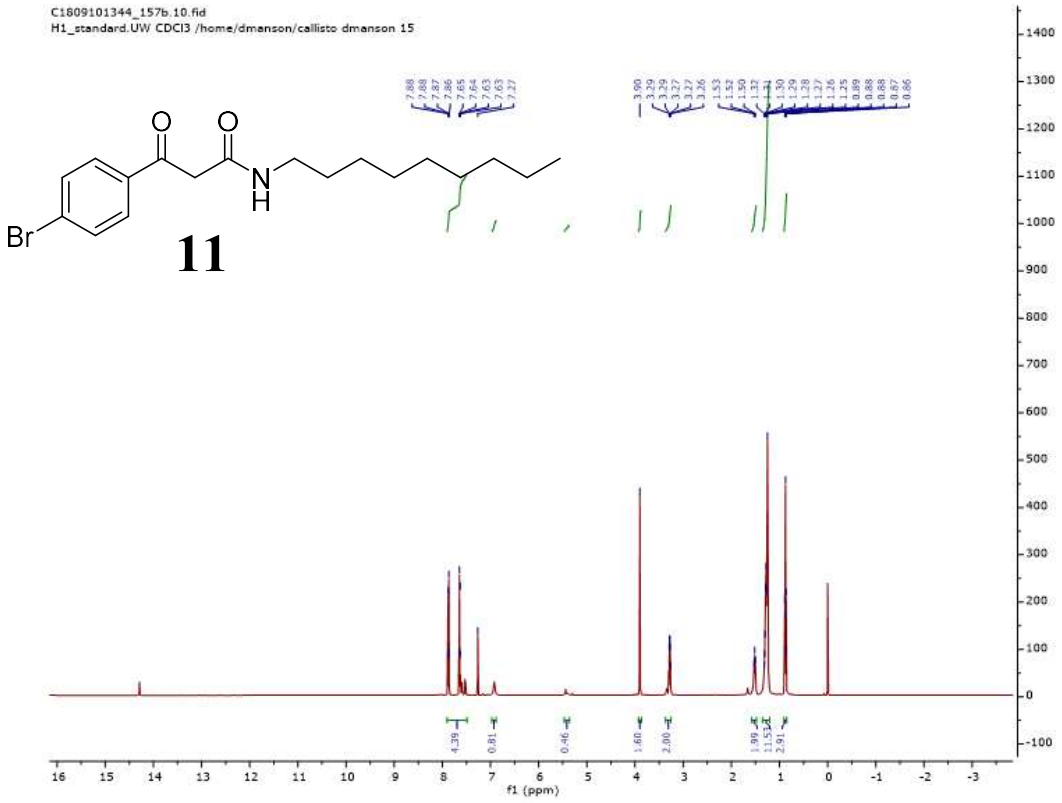
C1809101344_157b.10.fid
H1_standard.UW CDCl3 /home/dmanson/callisto dmanson 15
O
O
N
H
Br
11
f1 (ppm)

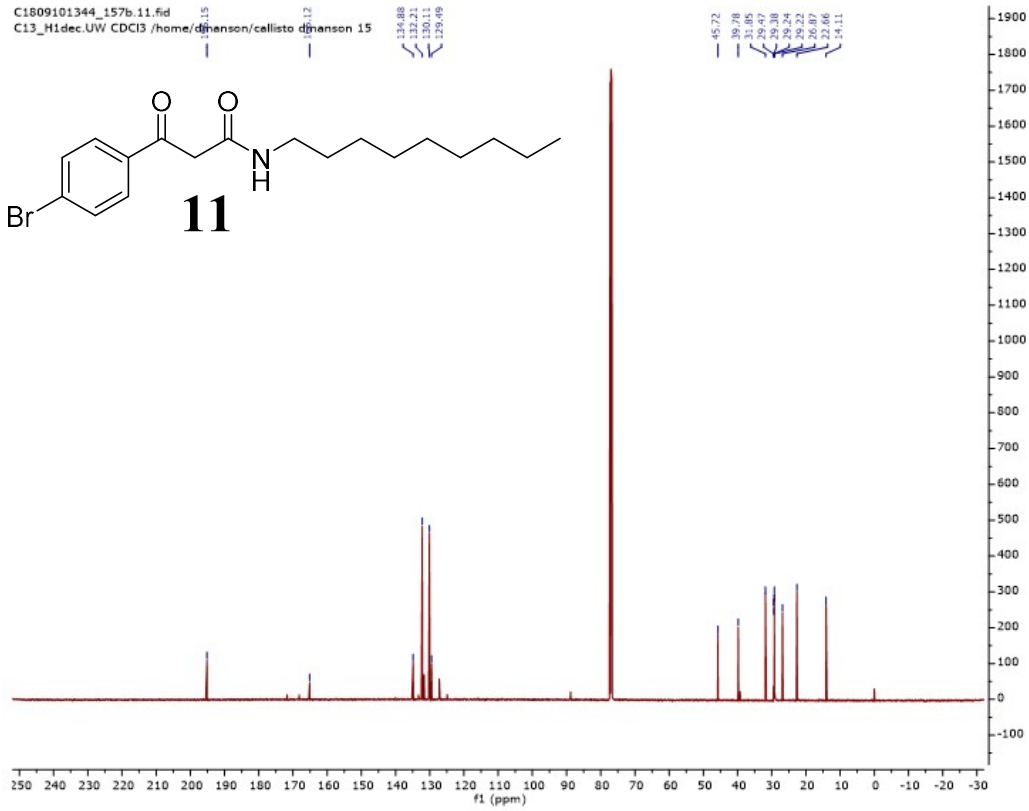
C1809101344_157b.11.fid
C13_H1dec.UW CDCl3 /home/dmanson/callisto dmanson 15
O
O
N
H
Br
11
f1 (ppm)

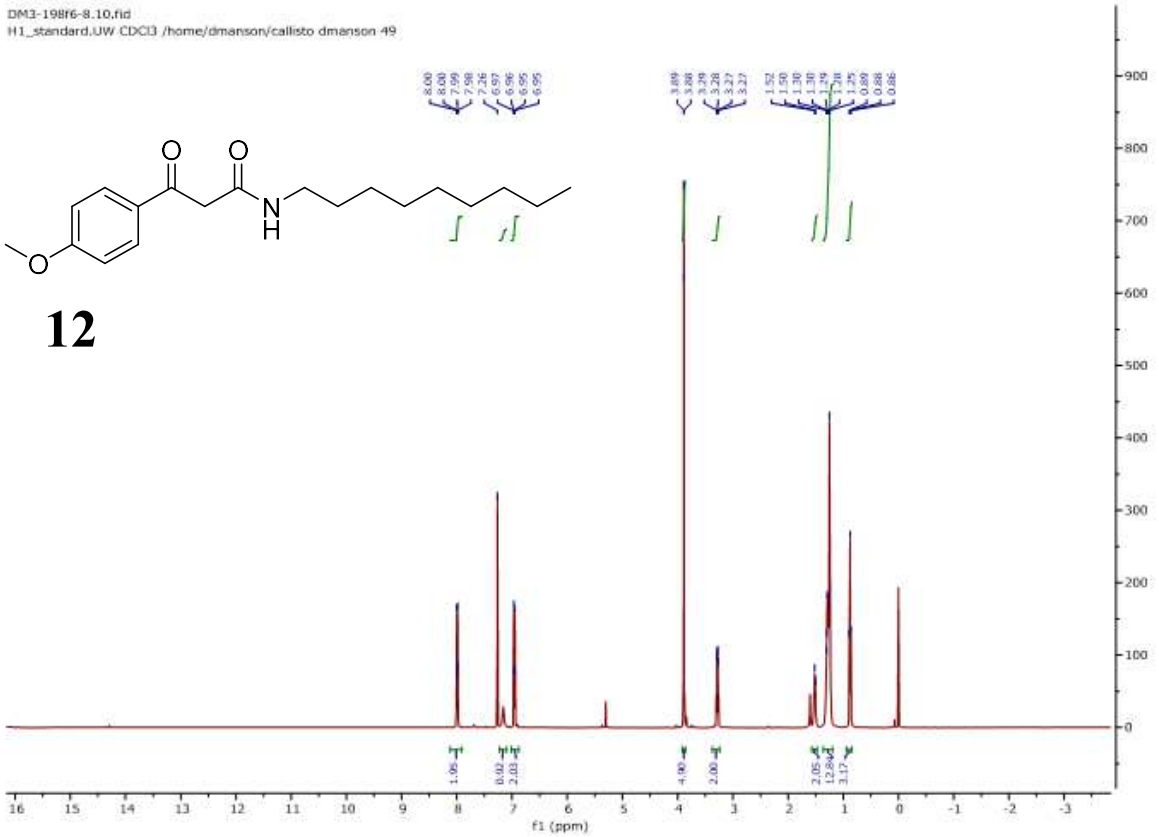
DM3-198f6-8.10.fid
H1_standard.UW CDCl3 /home/dmanson/callisto dmanson 49
12
f1 (ppm)

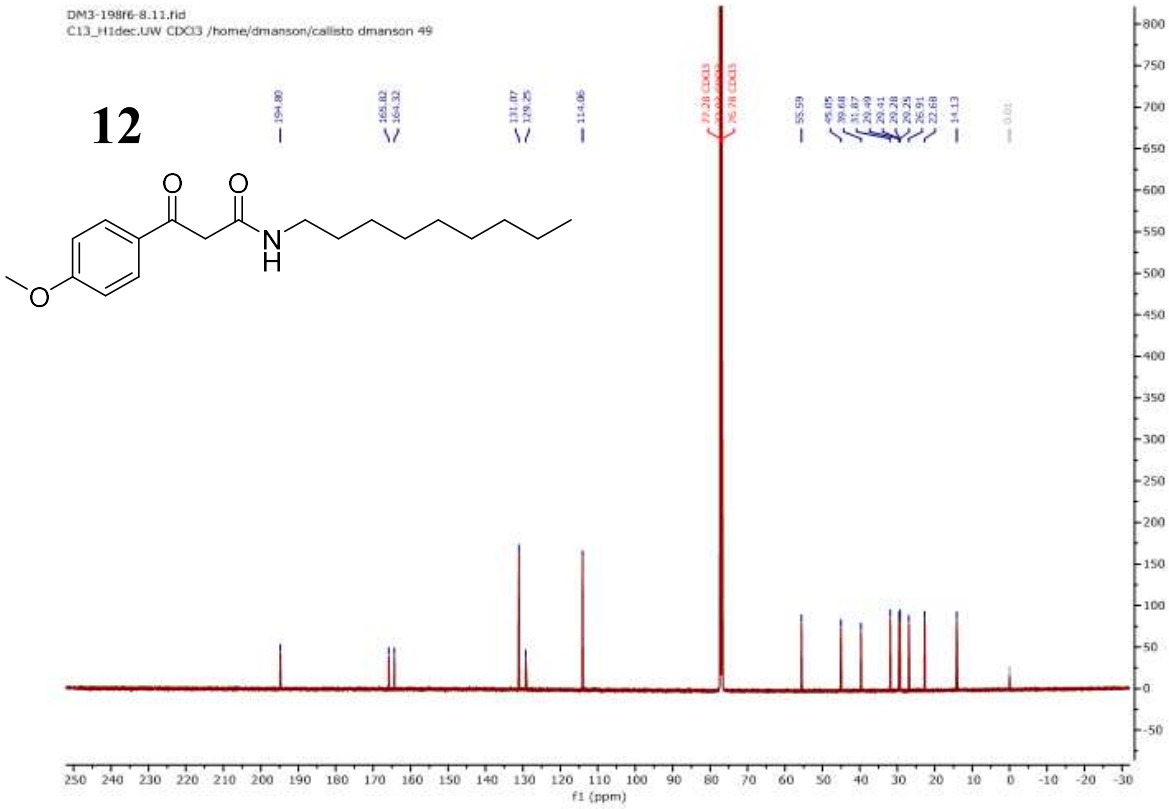
DM3-198f6-8.11.fid
C13_H1dec.UW CDCl3 /home/dmanson/callisto dmanson 49
12
f1 (ppm)

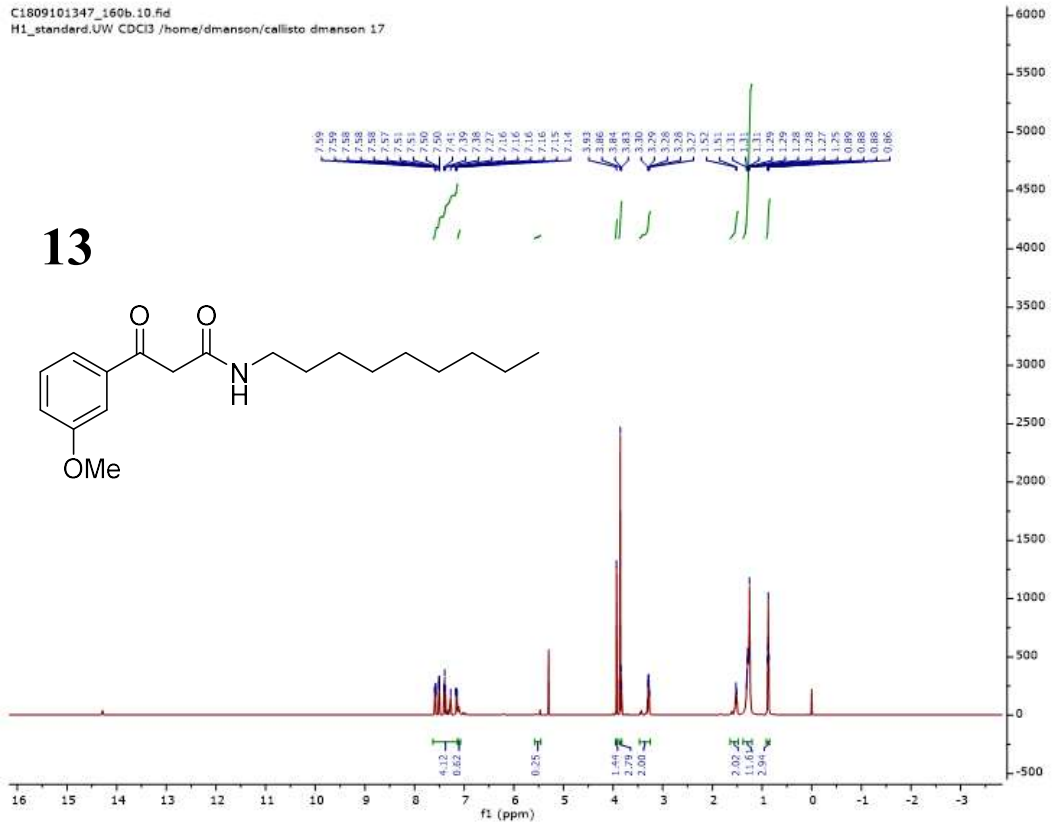
C1809101347_160b.10.fid
H1_standard.UW CDCl3 /home/dmanson/callisto dmanson 17
13
O
O
N
H
OMe
f1 (ppm)

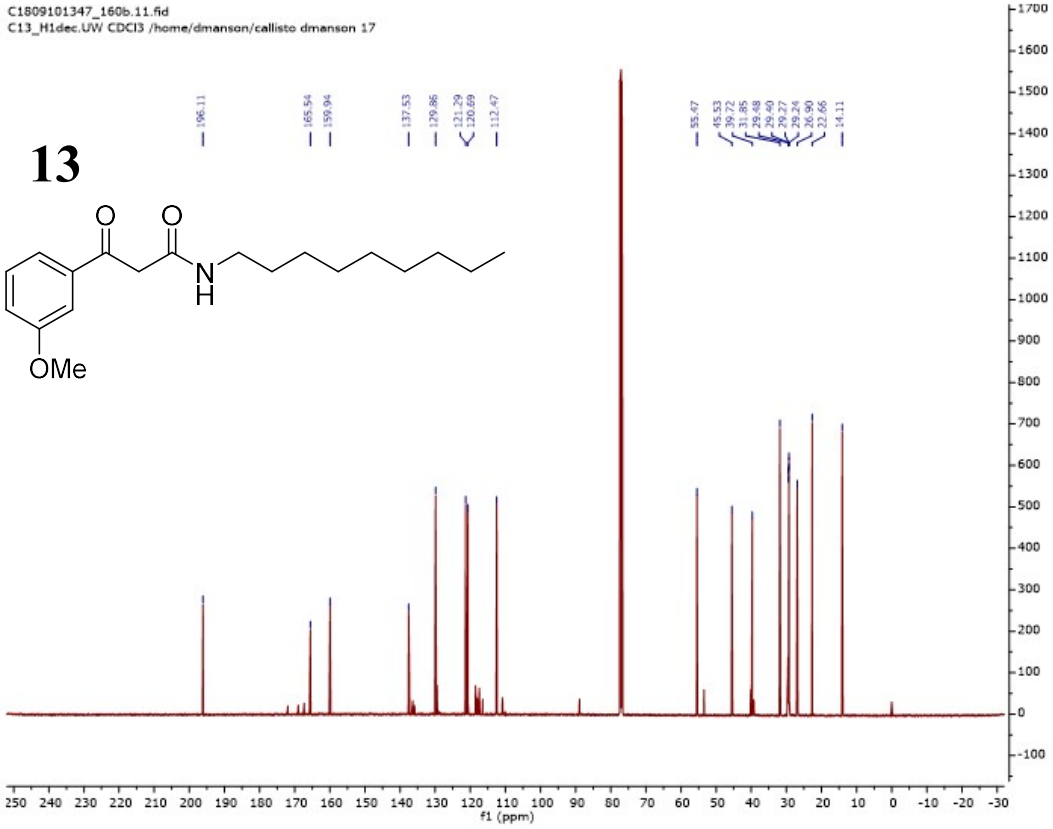
C1809101347_160b.11.fid
C13_H1dec.UW CDCl3 /home/dmanson/callisto dmanson 17
13
O
O
N
H
OMe
f1 (ppm)

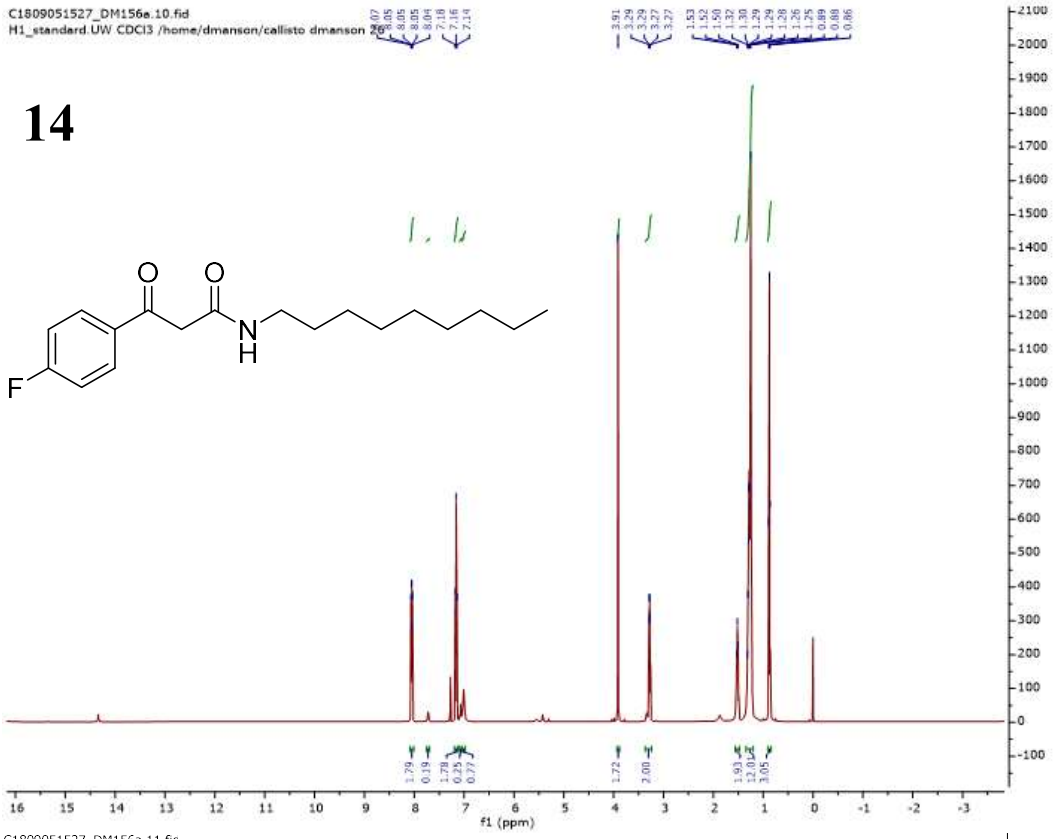
C1809051527_DM156a.10.fid
H1_standard.UW CDCl3 /home/dmanson/callisto dmanson 26
14
f1 (ppm)

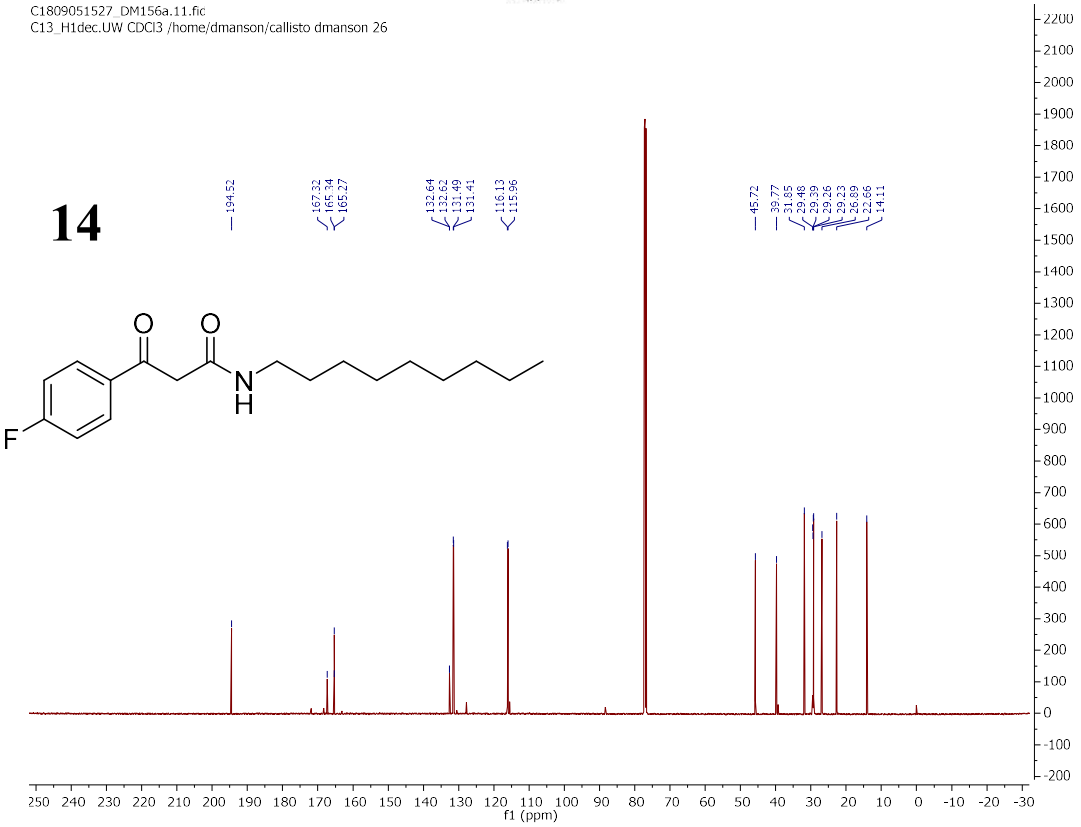
C1809051527_DM156a.11.fic
C13_H1dec.UW CDCl3 /home/dmanson/callisto dmanson 26
14
f1 (ppm)

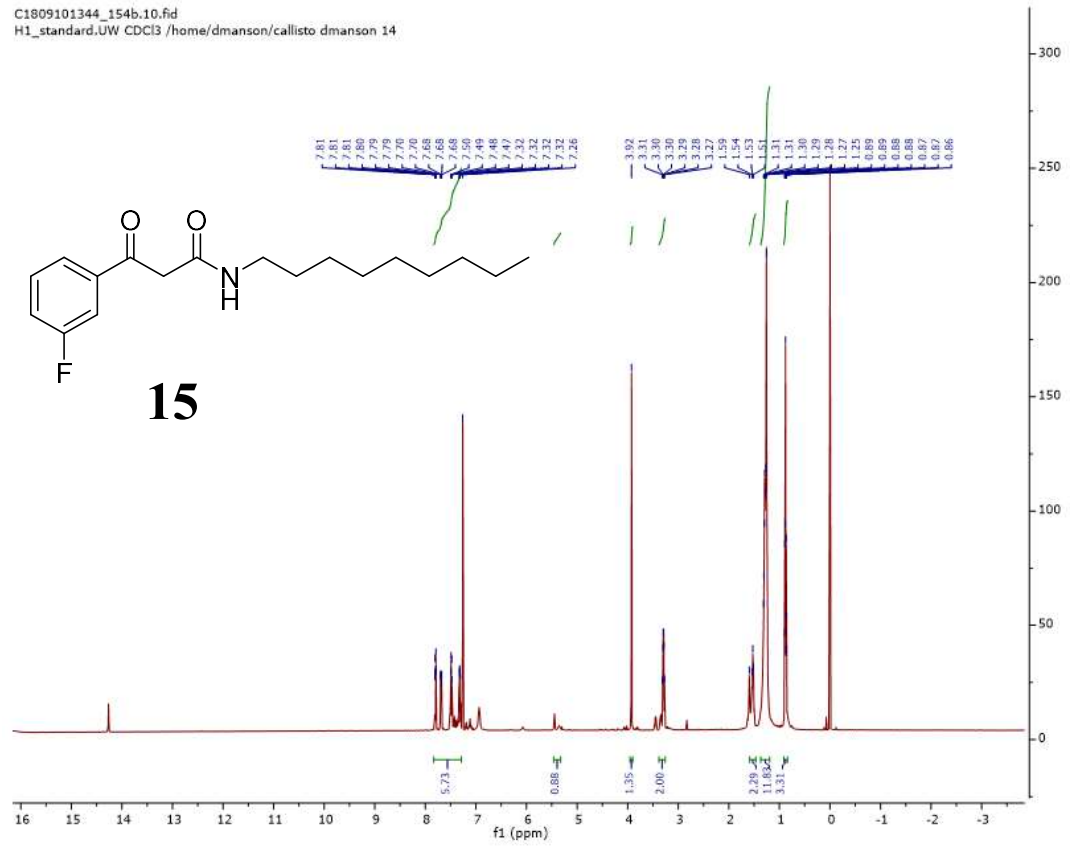
C1809101344_154b.10.fid
H1_standard.UW CDCl3 /home/dmanson/callisto dmanson 14
O
O
N
H
F
15
f1 (ppm)

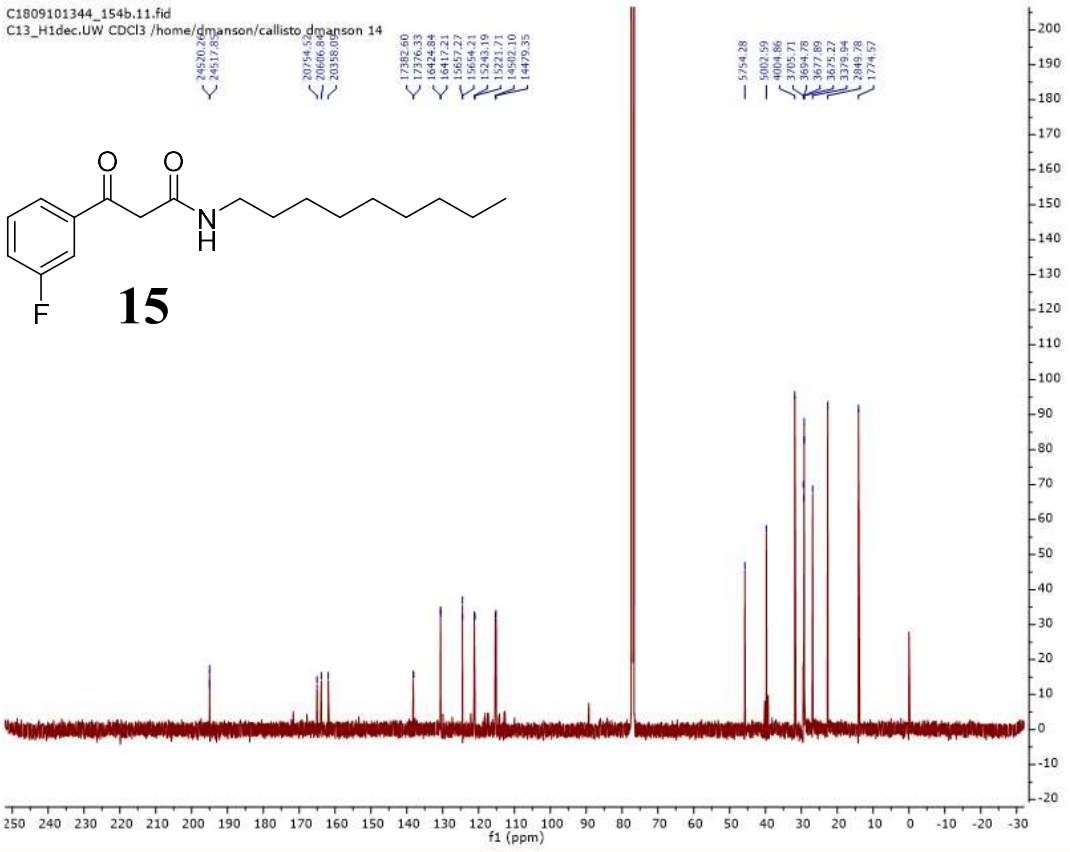
C1809101344_154b.11.fid
C13_H1dec.UW CDCl3 /home/dmanson/callisto dmanson 14
O
O
N
H
F
15
f1 (ppm)

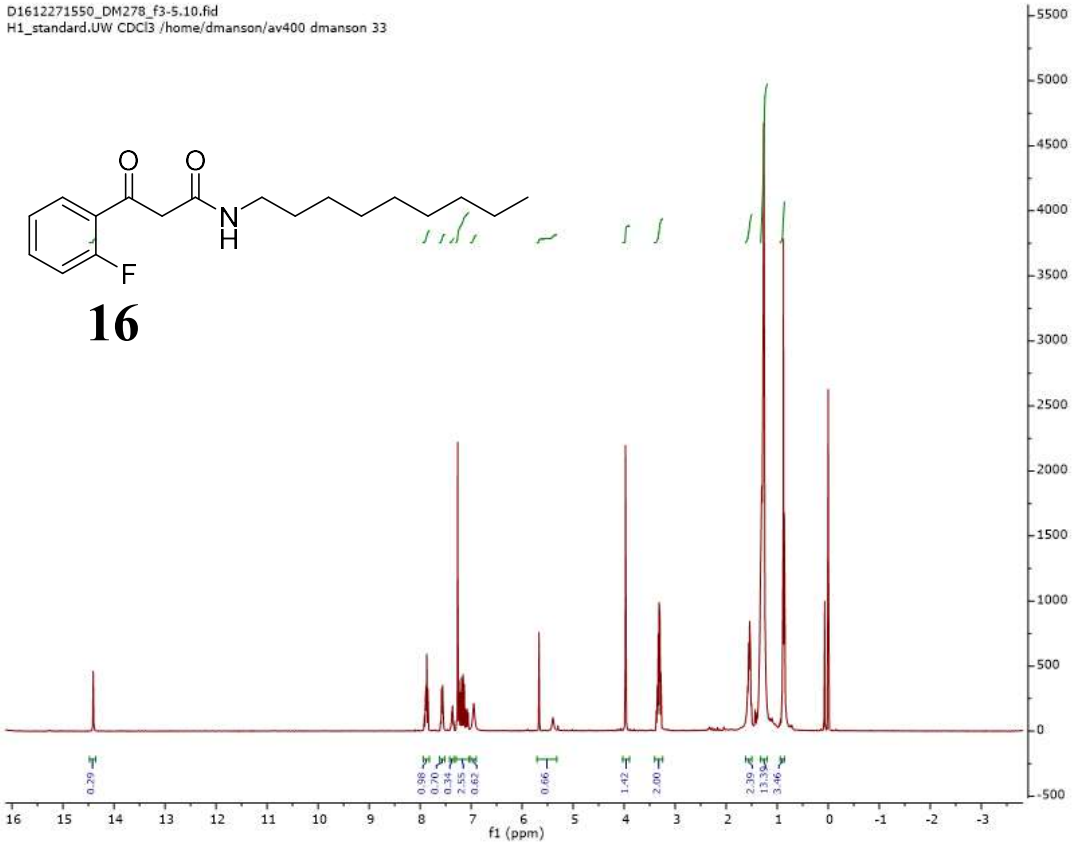
D1612271550_DM278_f3-5.10.fid
H1_standard.UW CDCl3 /home/dmanson/av400 dmanson 33
O
O
N
H
F
16
f1 (ppm)

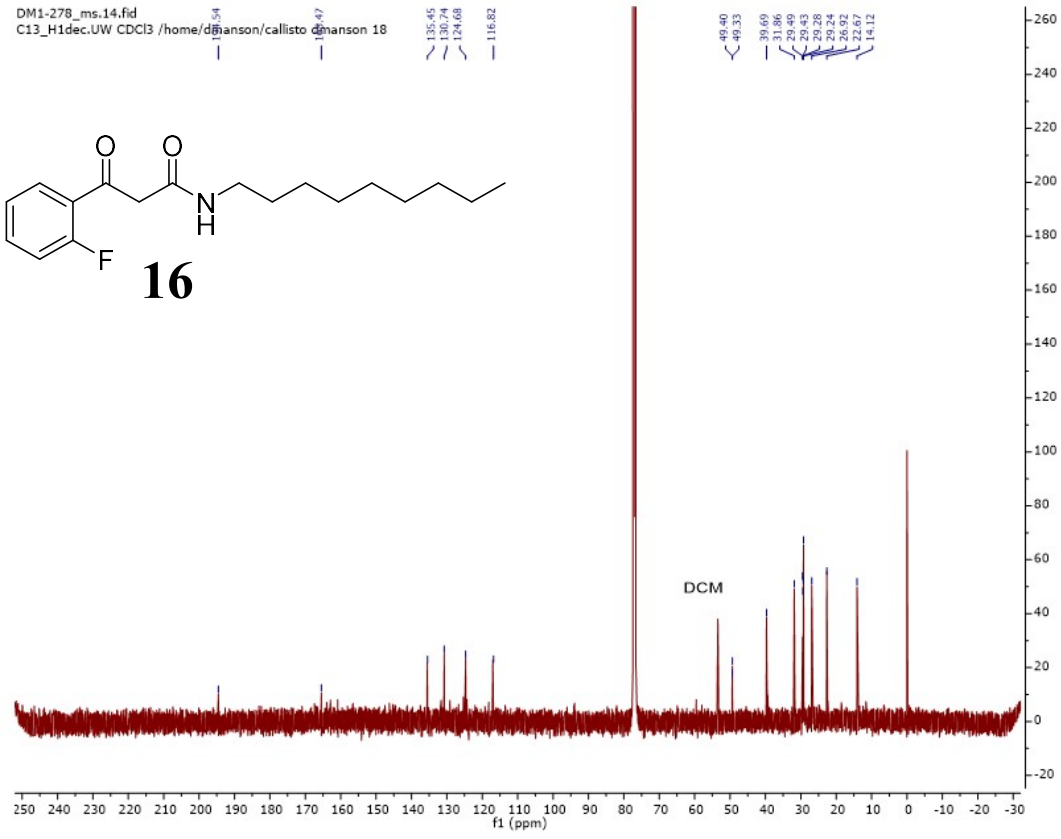
DM1-278_ms.14.fid
C13_H1dec.UW CDCl3 /home/dmanson/callisto dmanson 18
135.45
130.74
124.68
116.82
49.40
49.33
39.69
31.86
29.49
29.43
29.28
29.24
26.92
22.67
14.12
O
O
N
H
F
16
DCM
f1 (ppm)

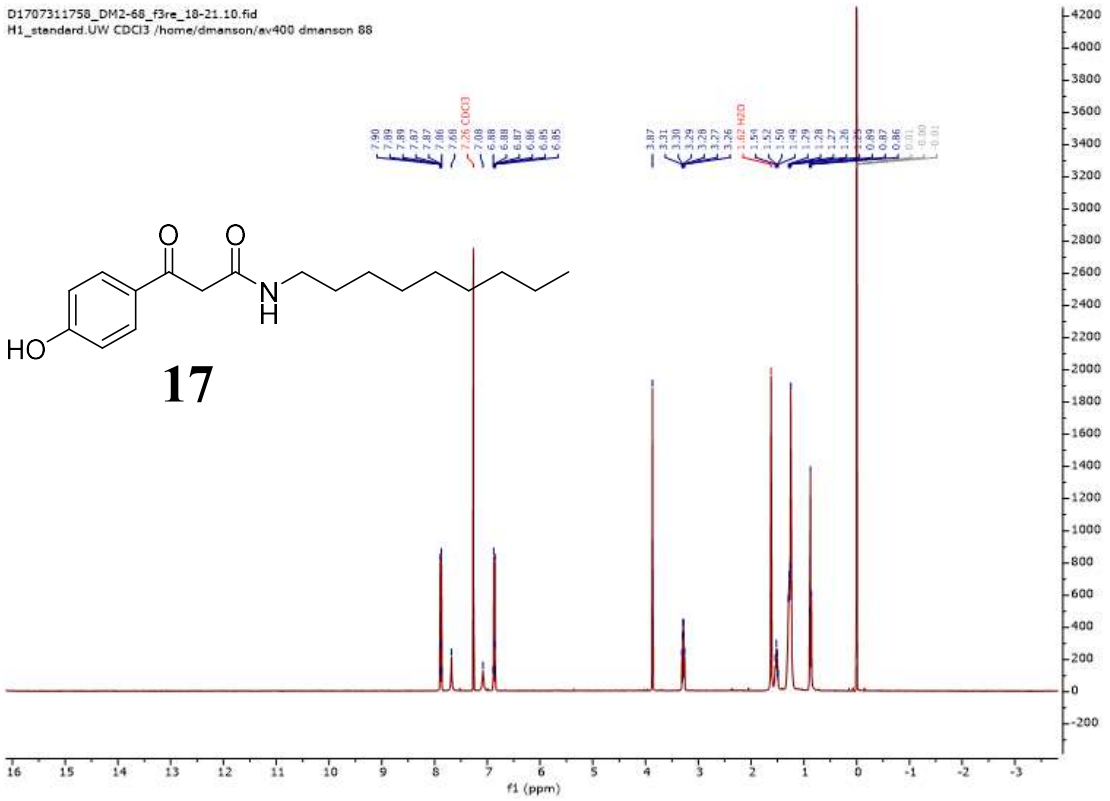
D1707311758_DM2-68_f3re_18-21.10.fid
H1_standard.UW CDCl3 /home/dmanson/av400 dmanson 88
7.90
7.89
7.88
7.87
7.87
7.86
7.68
7.26 CDCl3
7.08
6.88
6.87
6.86
6.85
6.85
3.87
3.31
3.30
3.29
3.28
3.27
3.26
1.62 H2O
1.54
1.52
1.50
1.49
1.29
1.28
1.27
1.26
0.89
0.87
0.86
0.01
-0.00
-0.01
O
O
N
H
HO
17
f1 (ppm)

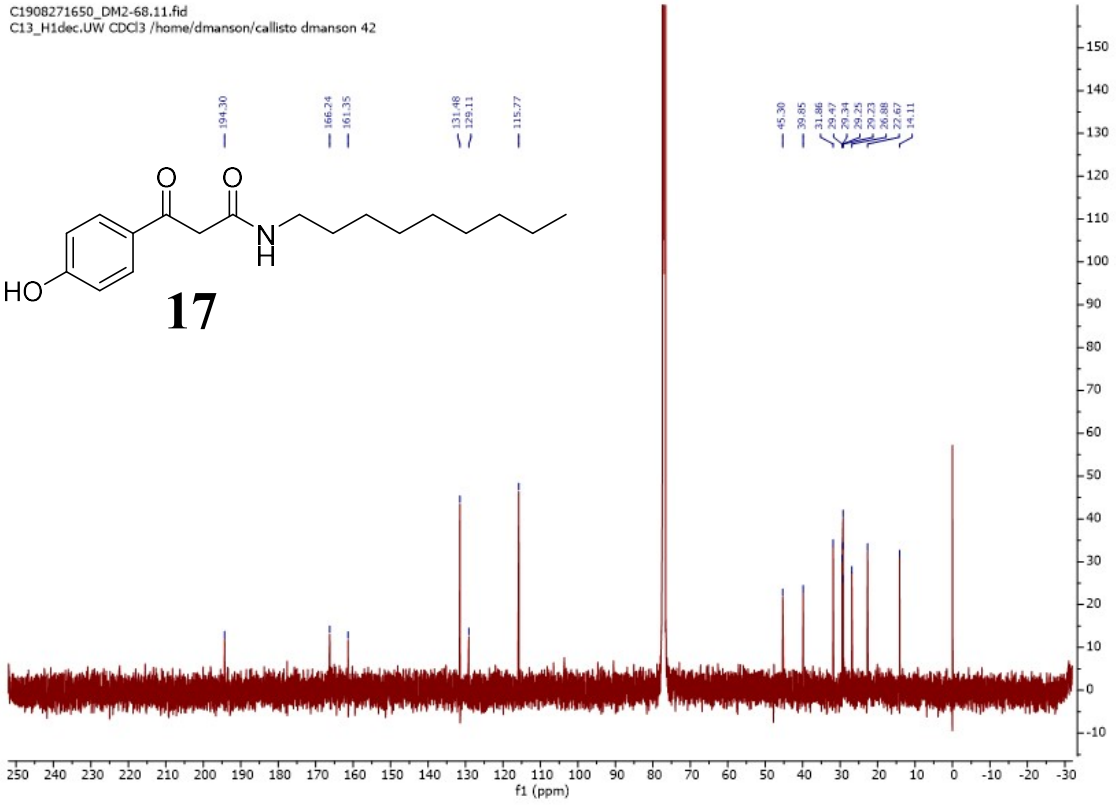
C1908271650_DM2-68.11.fid
C13_H1dec.UW CDCl3 /home/dmanson/callisto dmanson 42
194.30
166.24
161.35
131.48
129.11
115.77
45.30
39.85
31.86
29.47
29.34
29.25
29.23
26.88
22.67
14.11
O
O
N
H
HO
17
f1 (ppm)

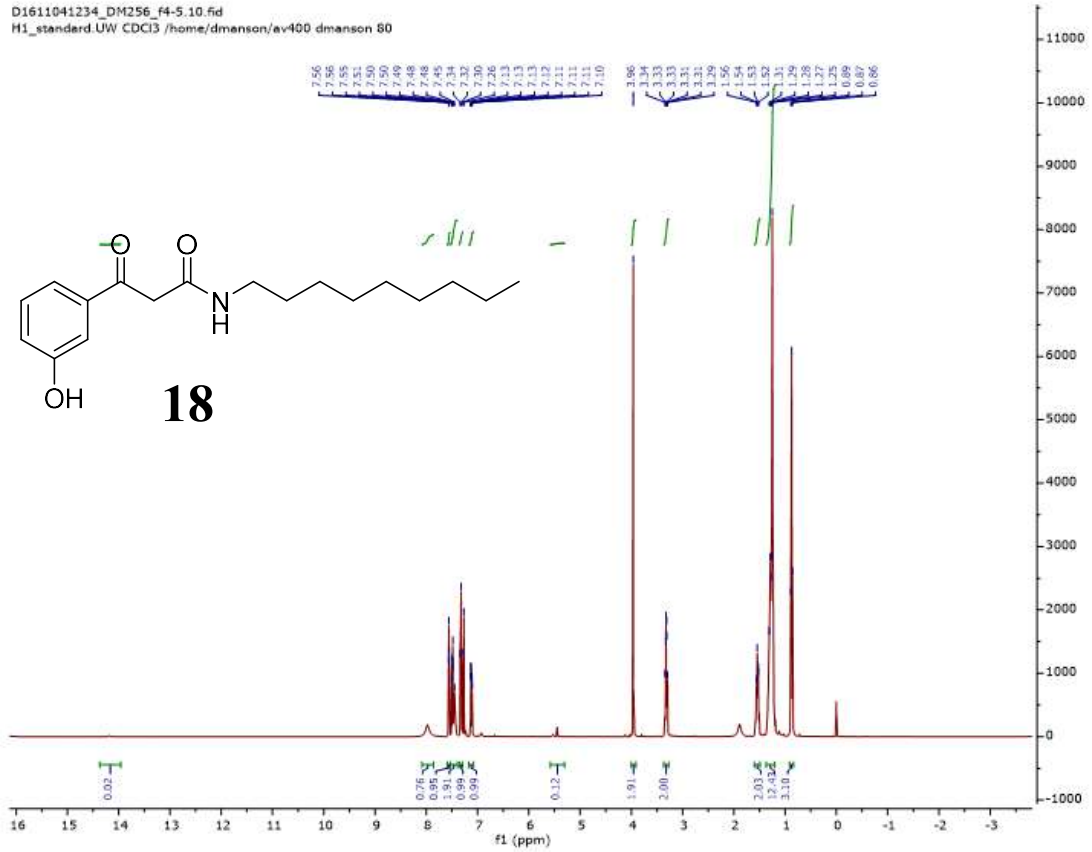
D1611041234_DM256_f4-5.10.fid
H1_standard.UW CDCl3 /home/dmanson/av400 dmanson 80
18
f1 (ppm)

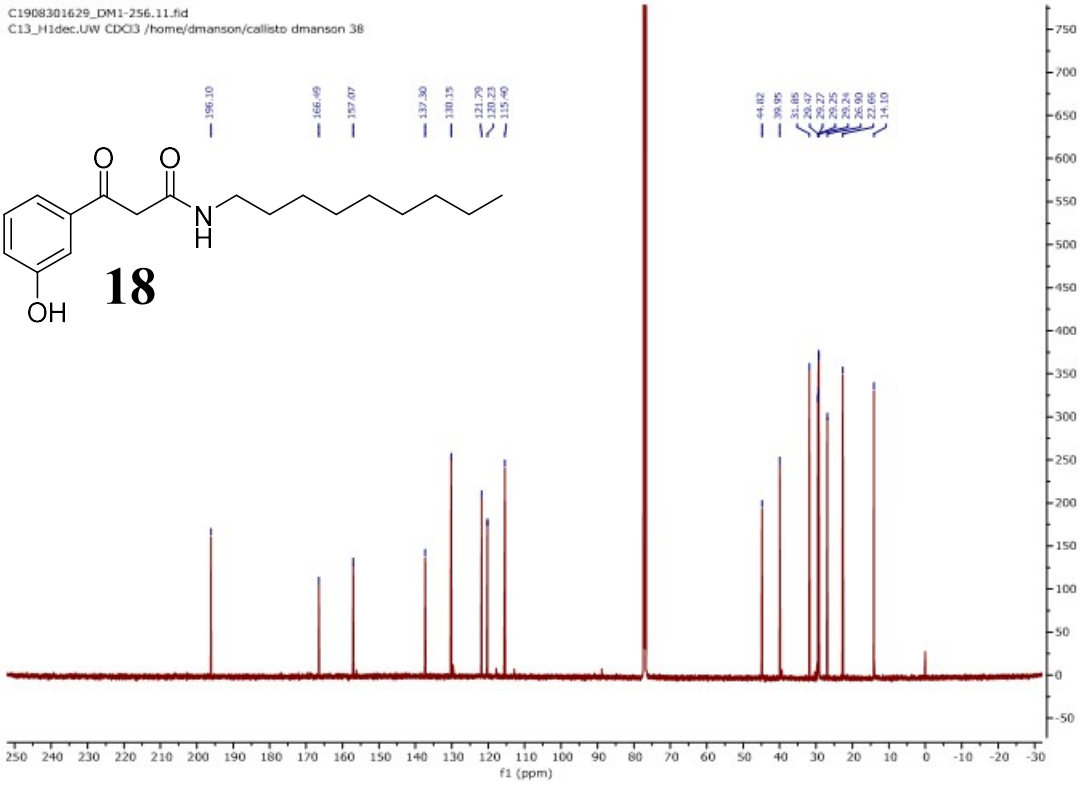
C1908301629_DM1-256.11.fid
C13_H1dec.UW CDCl3 /home/dmanson/callisto dmanson 38
18
f1 (ppm)

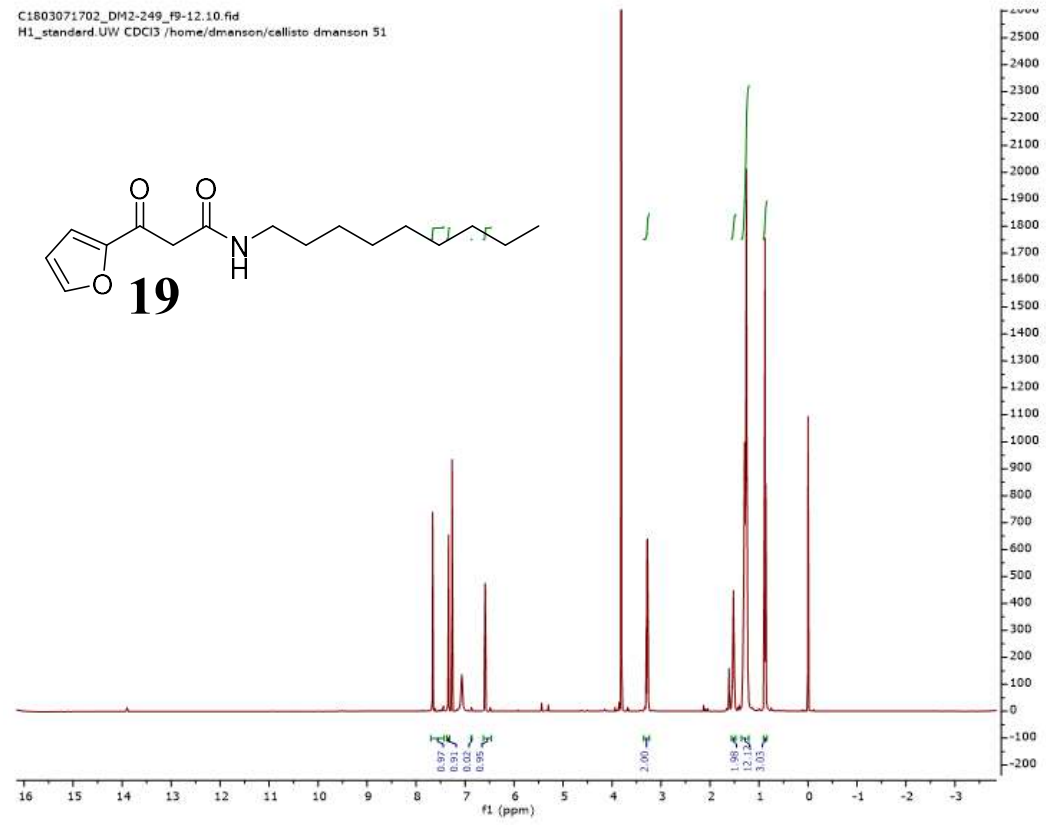
C1803071702_DM2-249_f9-12.10.fid
H1_standard.UW CDCl3 /home/dmanson/callisto dmanson 51
19
f1 (ppm)

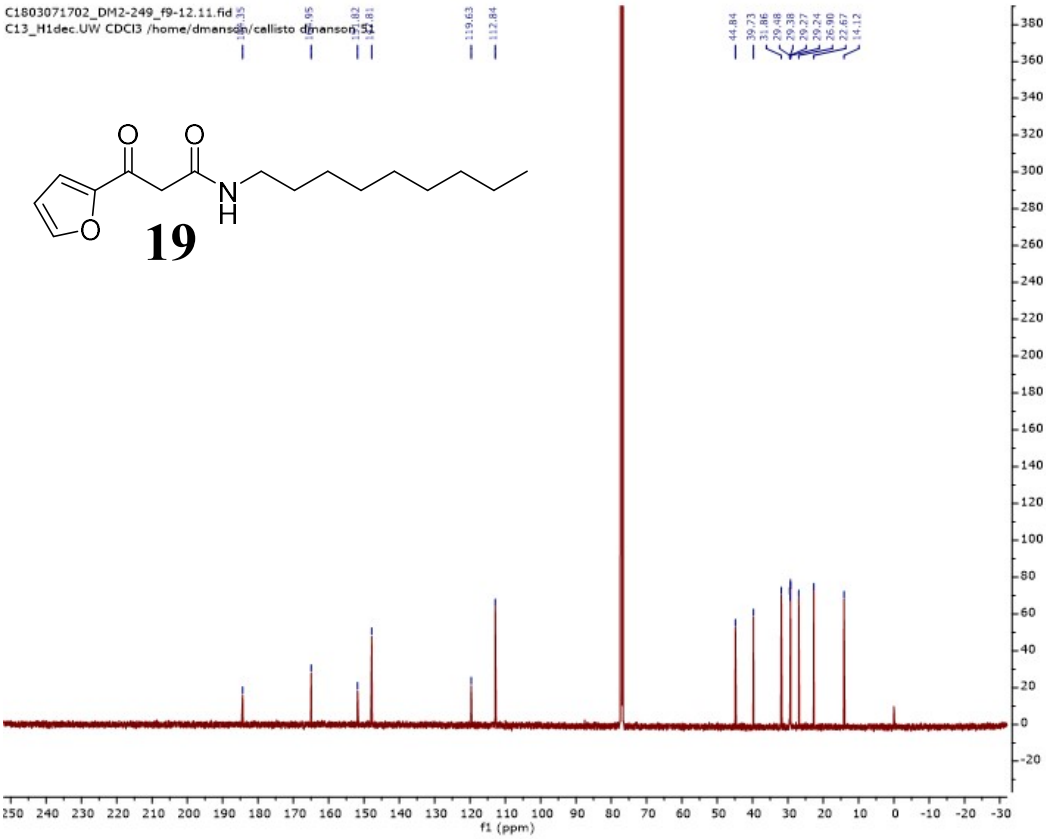
C1803071702_DM2-249_f9-12.11.fid
C13_H1dec.UW CDCl3 /home/dmanson/callisto dmanson 51
19
f1 (ppm)

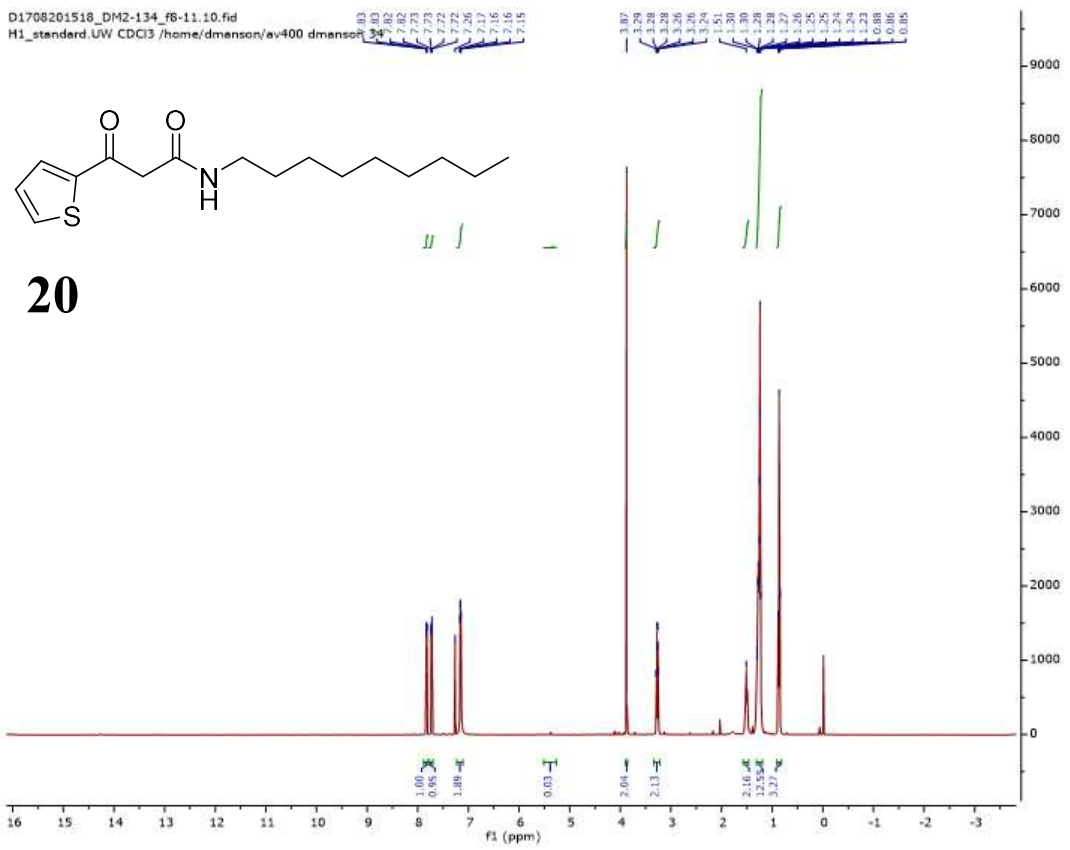
D1708201518_DM2-134_f8-11.10.fid
H1_standard.UW CDCl3 /home/dmanson/av400 dmanson 34
f1 (ppm)

**20**

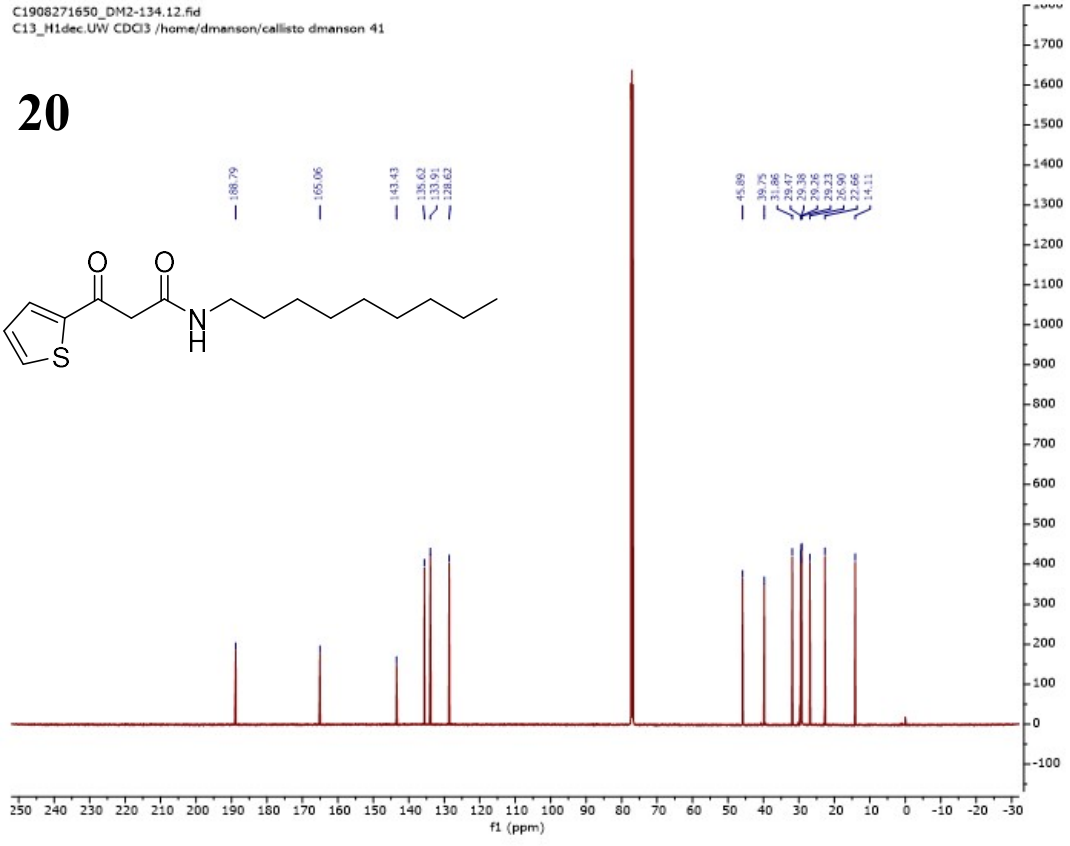
C1908271650_DM2-134.12.fid
C13_H1dec.UW CDCl3 /home/dmanson/callisto dmanson 41
f1 (ppm)

**20**

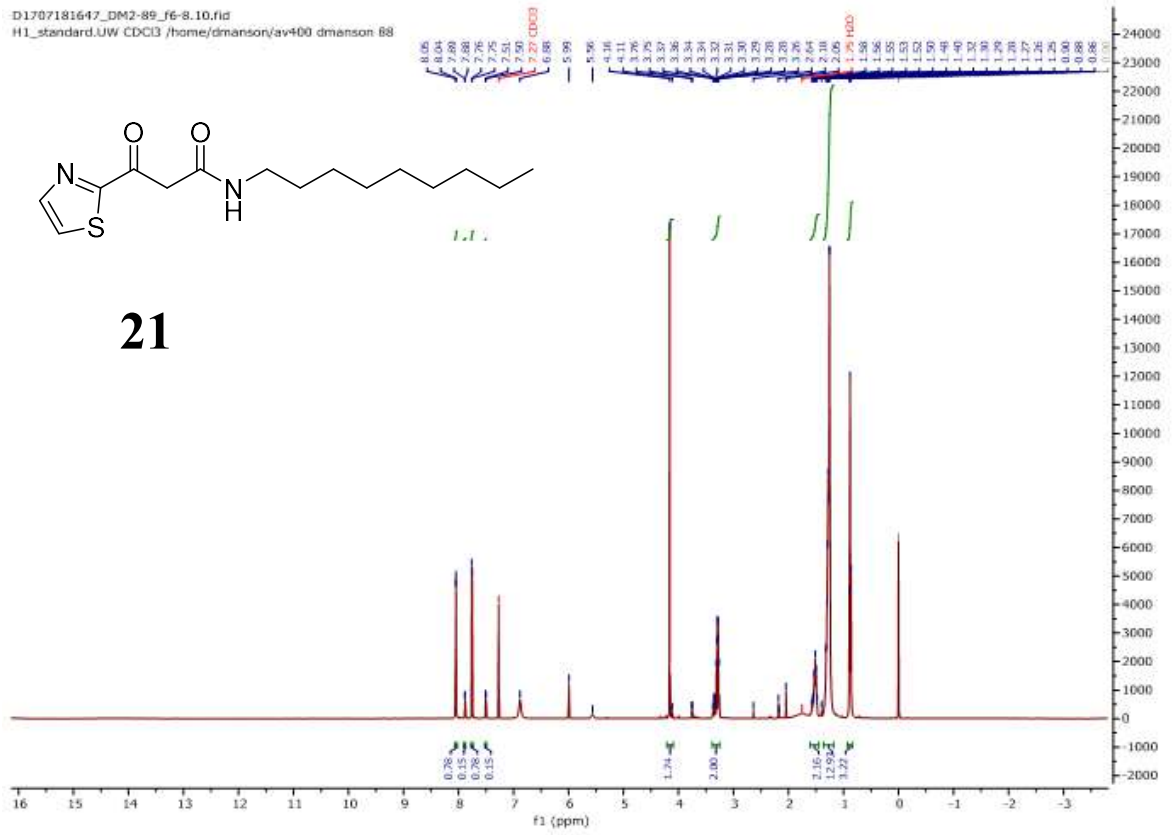
D1707181647_DM2-89_f6-8.10.fid
H1_standard.UW CDCl3 /home/dmanson/av400 dmanson 88
f1 (ppm)

**21**

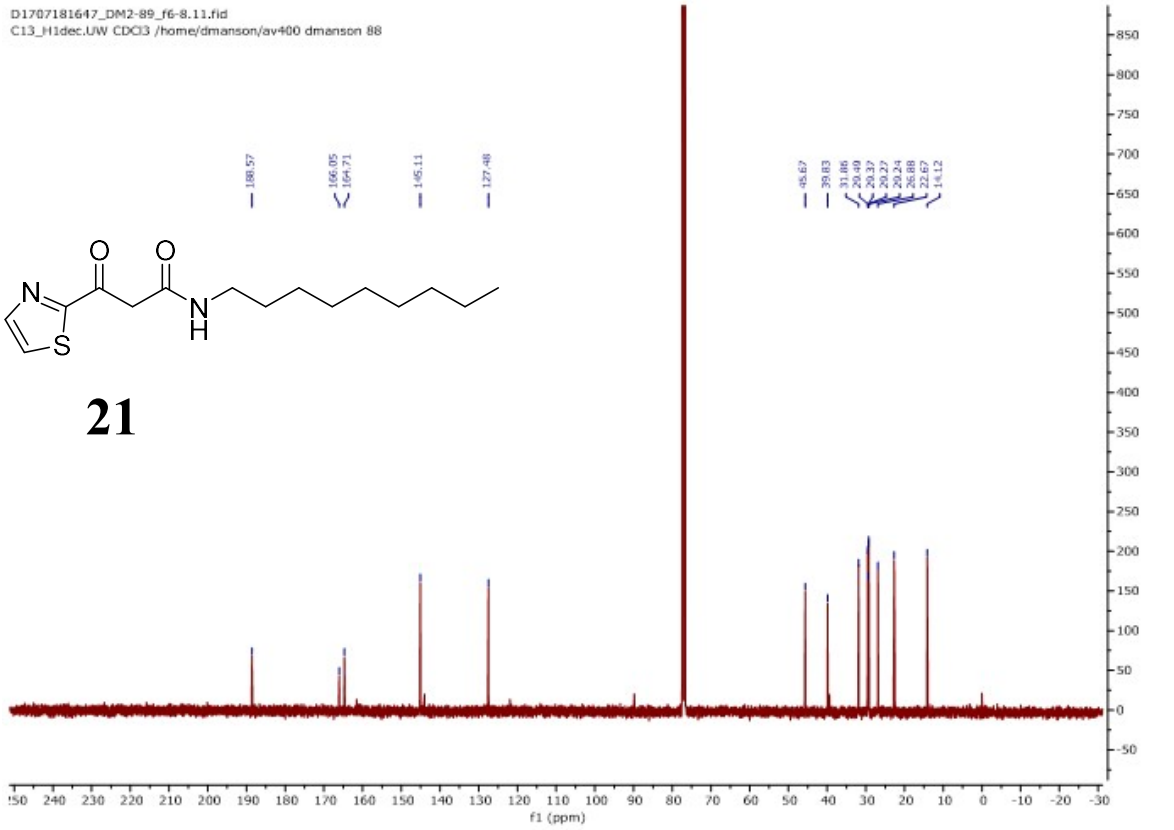
D1707181647_DM2-89_f6-8.11.fid
C13_H1dec.UW CDCl3 /home/dmanson/av400 dmanson 88
f1 (ppm)

**21**

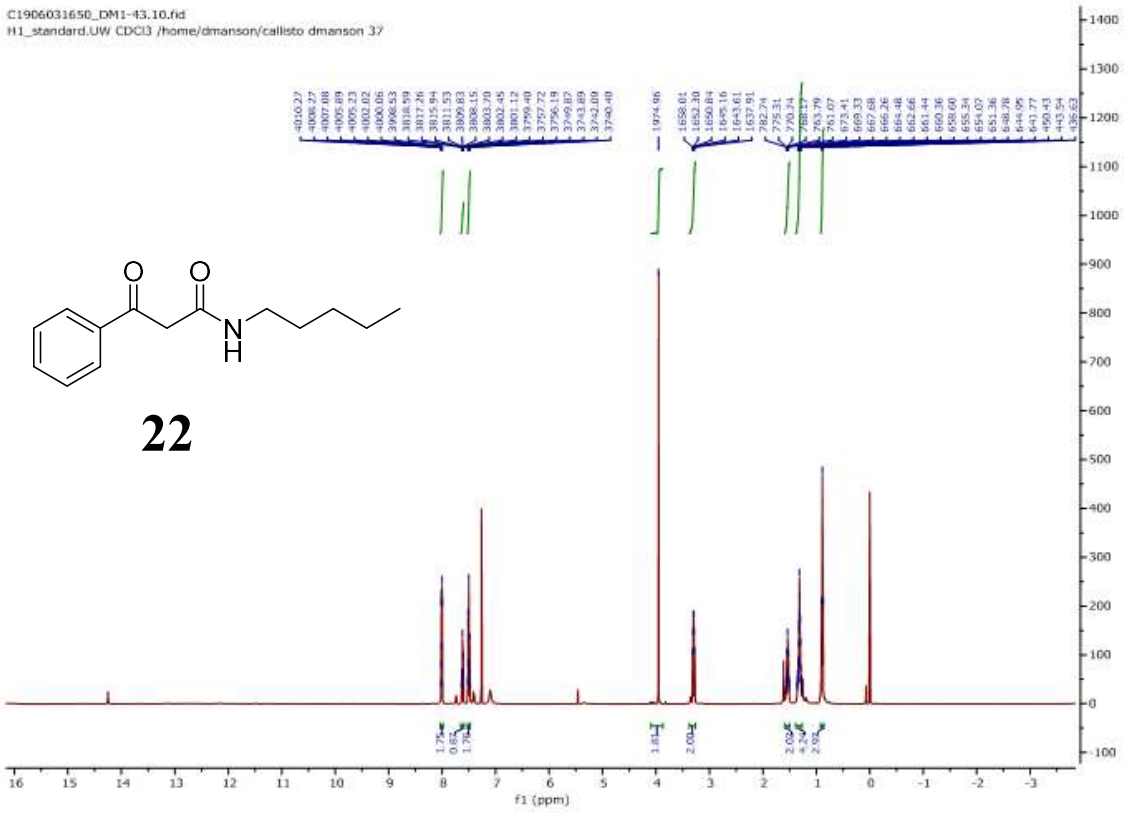
C19D6031650_DM1-43.10.fid
H1_standard.UW CDCl3 /home/dmanson/callisto dmanson 37
22
f1 (ppm)

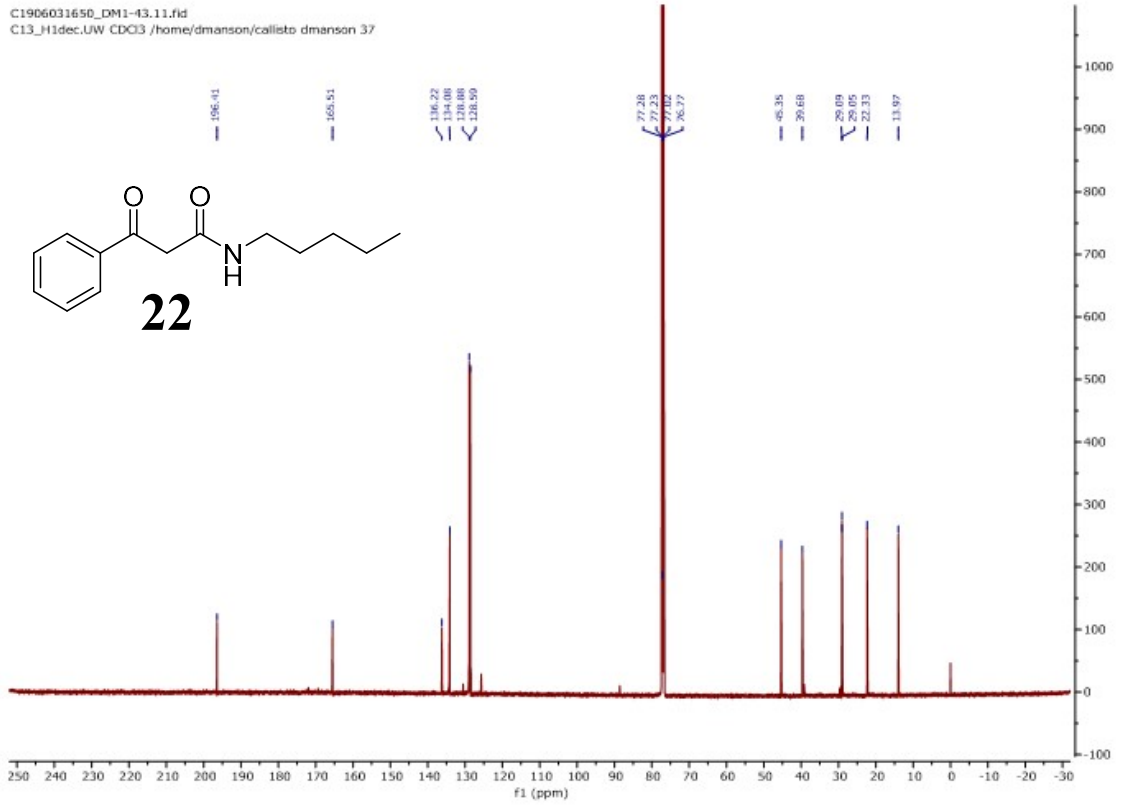
C19D6031650_DM1-43.11.fid
C13_H1dec.UW CDCl3 /home/dmanson/callisto dmanson 37
22
f1 (ppm)

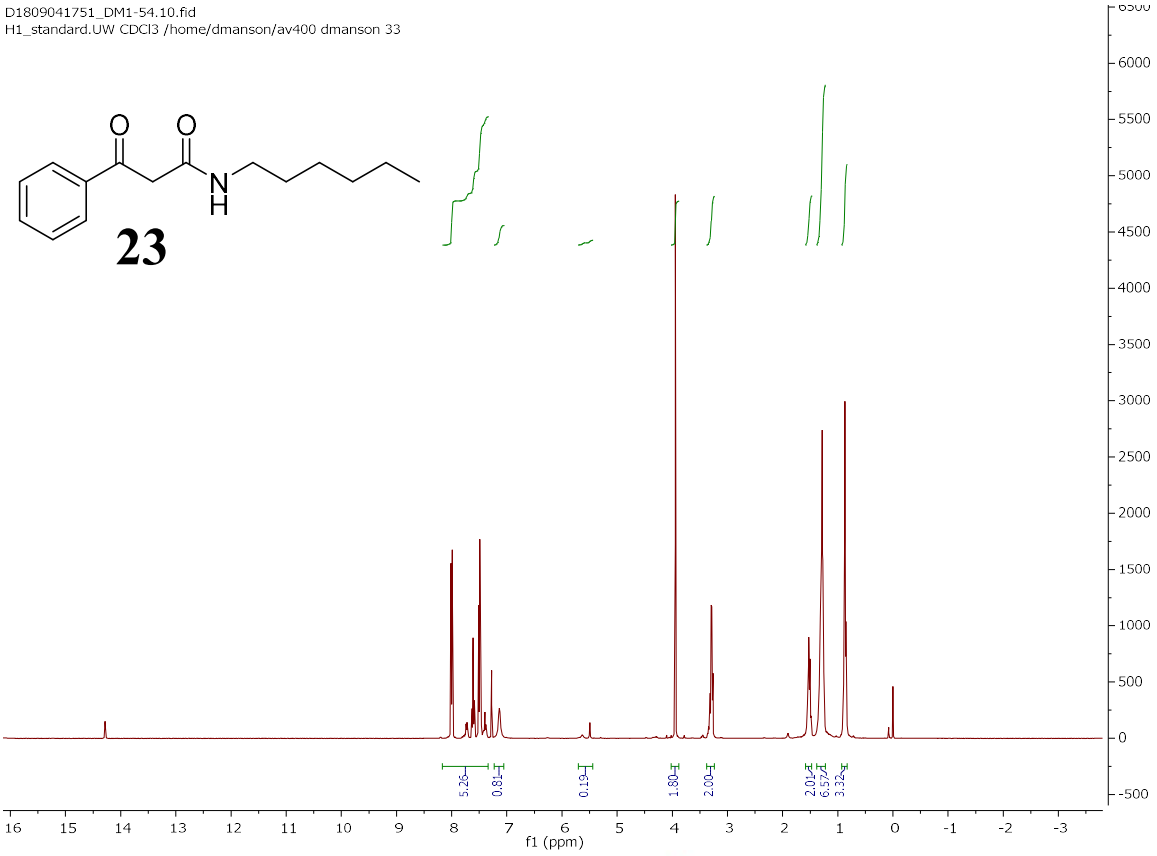
D1809041751_DM1-54.10.fid
H1_standard.UW CDCl3 /home/dmanson/av400 dmanson 33
23
f1 (ppm)

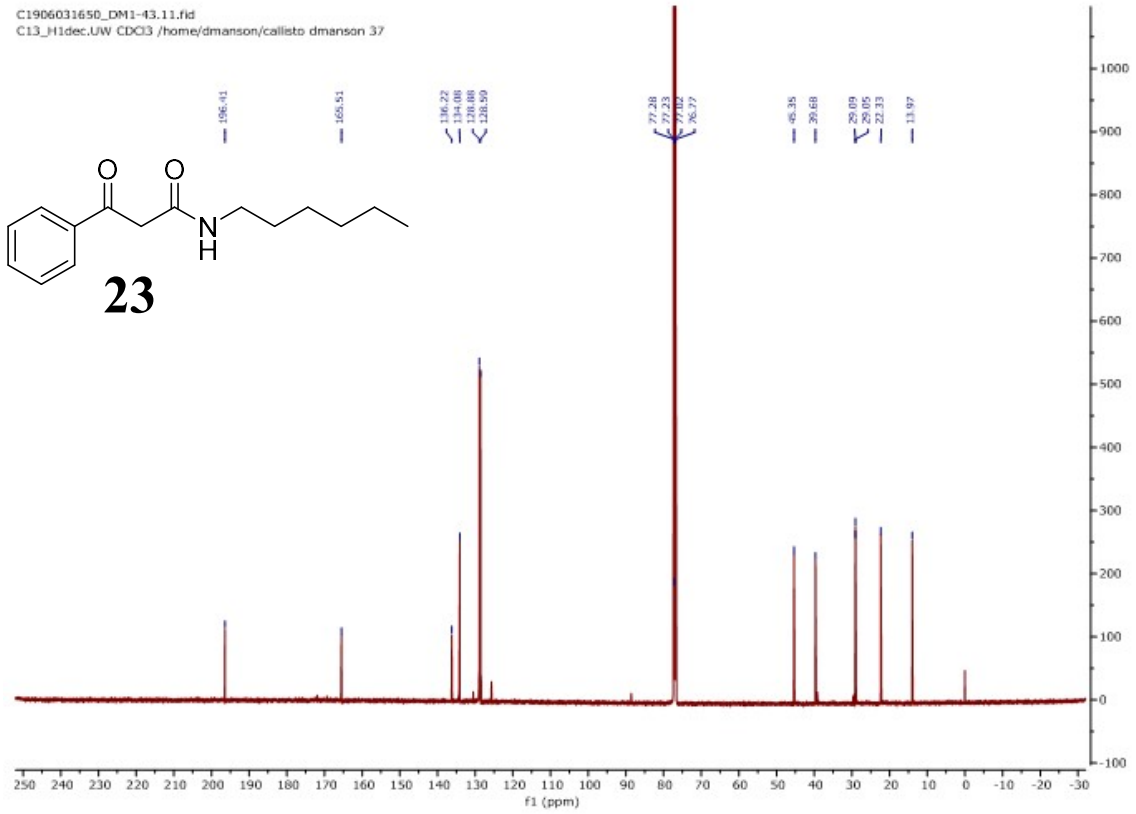
C1906031650_DM1-43.11.fid
C13_H1dec.UW CDCl3 /home/dmanson/callisto dmanson 37
23
f1 (ppm)

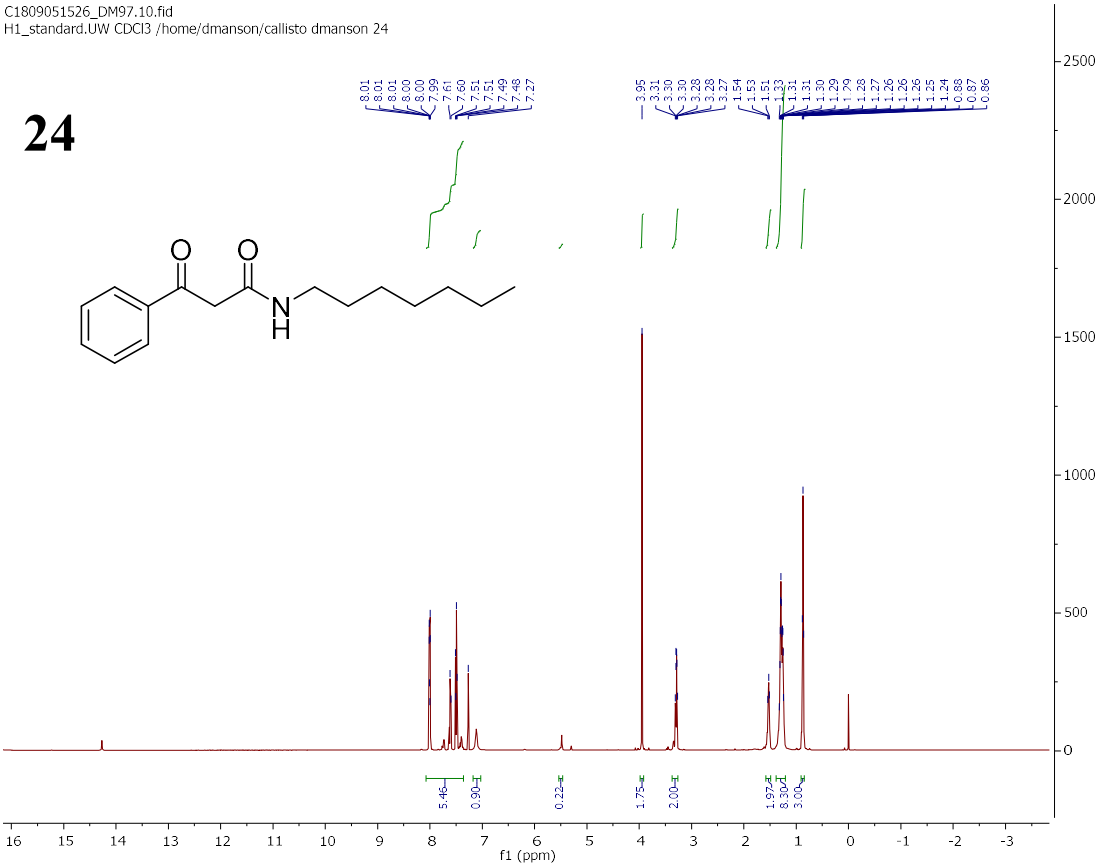
C1809051526_DM97.10.fid
H1_standard.UW CDCl3 /home/dmanson/callisto dmanson 24
24
f1 (ppm)

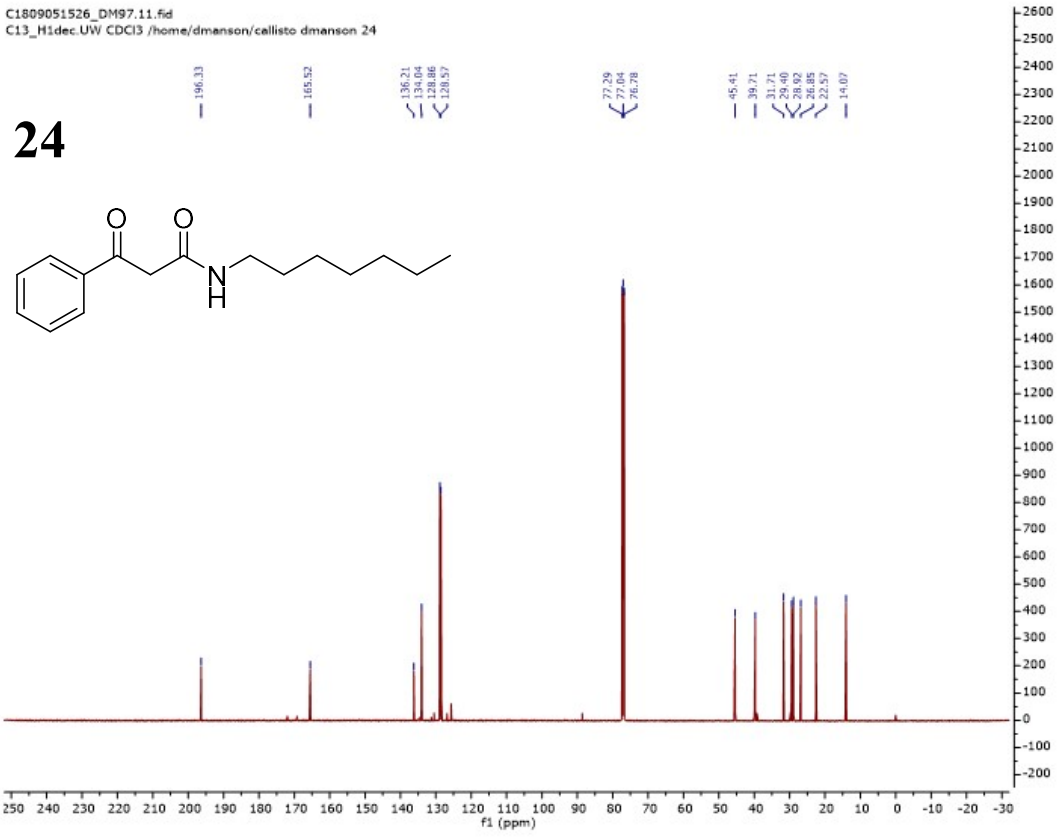
C1809051526_DM97.11.fid
C13_H1dec.UW CDCl3 /home/dmanson/callisto dmanson 24
24
f1 (ppm)

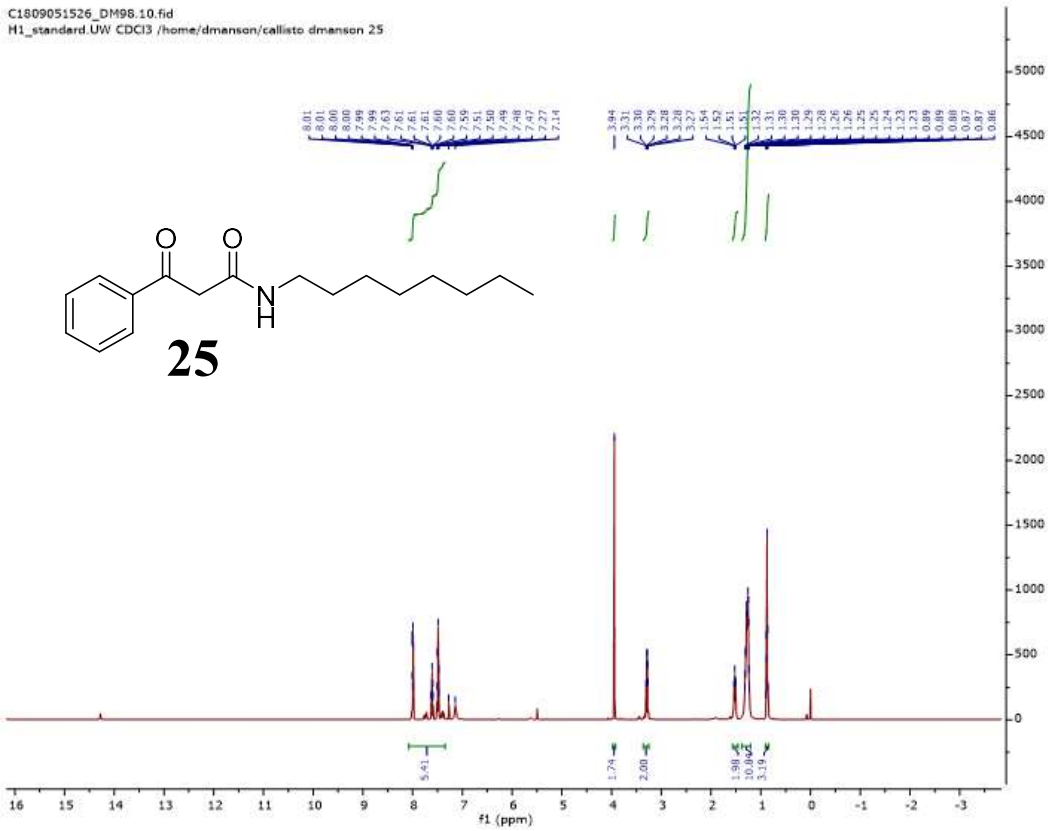
C1809051526_DM98.10.fid
H1_standard.UW CDCl3 /home/dmanson/callisto dmanson 25
25
f1 (ppm)

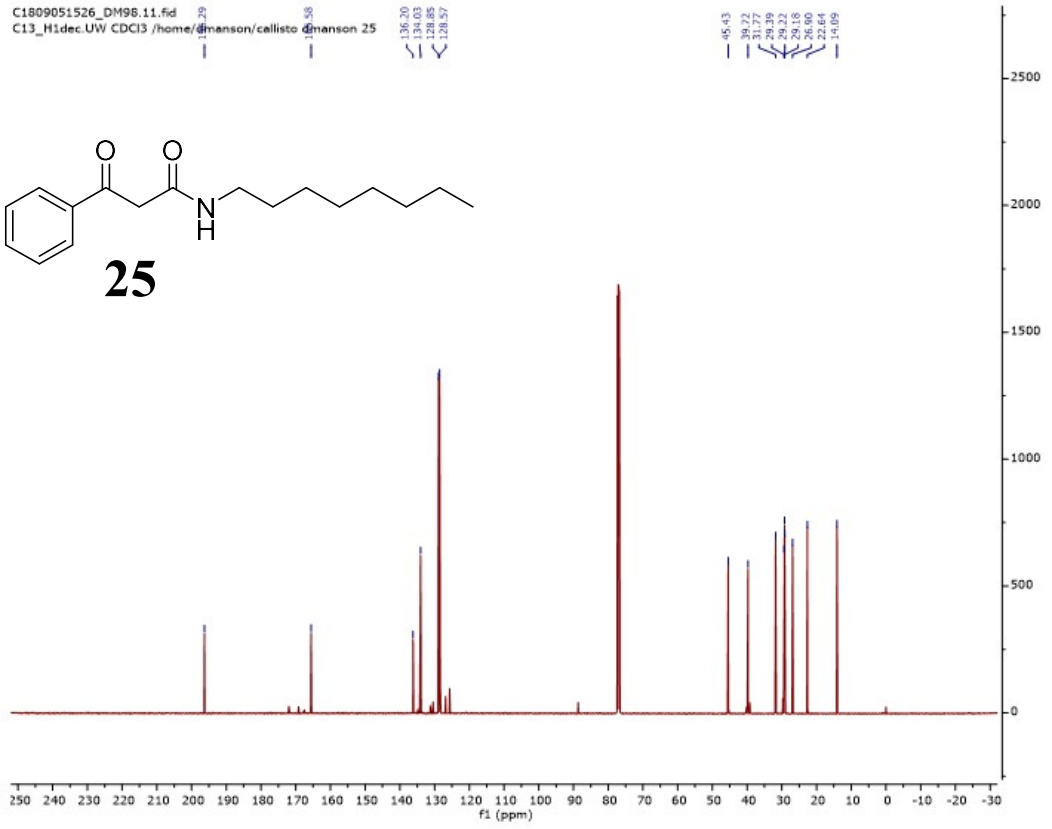
C1809051526_DM98.11.fid
C13_H1dec.UW CDCl3 /home/dmanson/callisto dmanson 25
25
f1 (ppm)

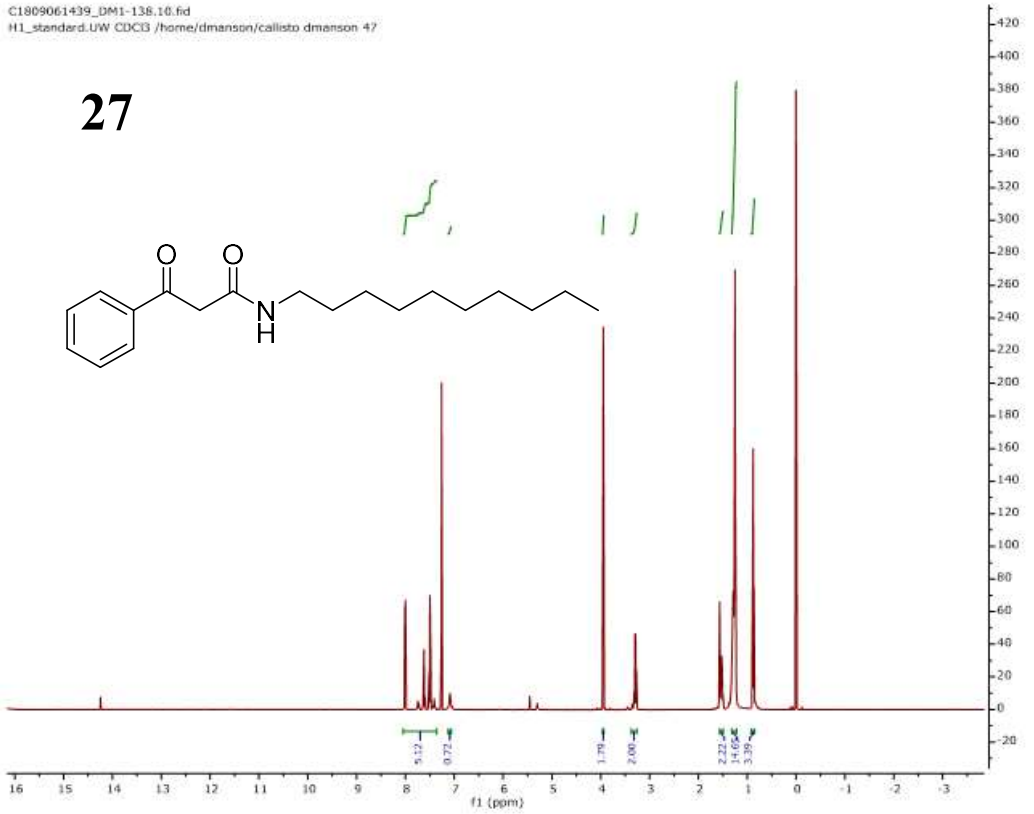
C1809061439_DM1-138.10.fid
H1_standard.UW CDCl3 /home/dmanson/callisto dmanson 47
27
f1 (ppm)

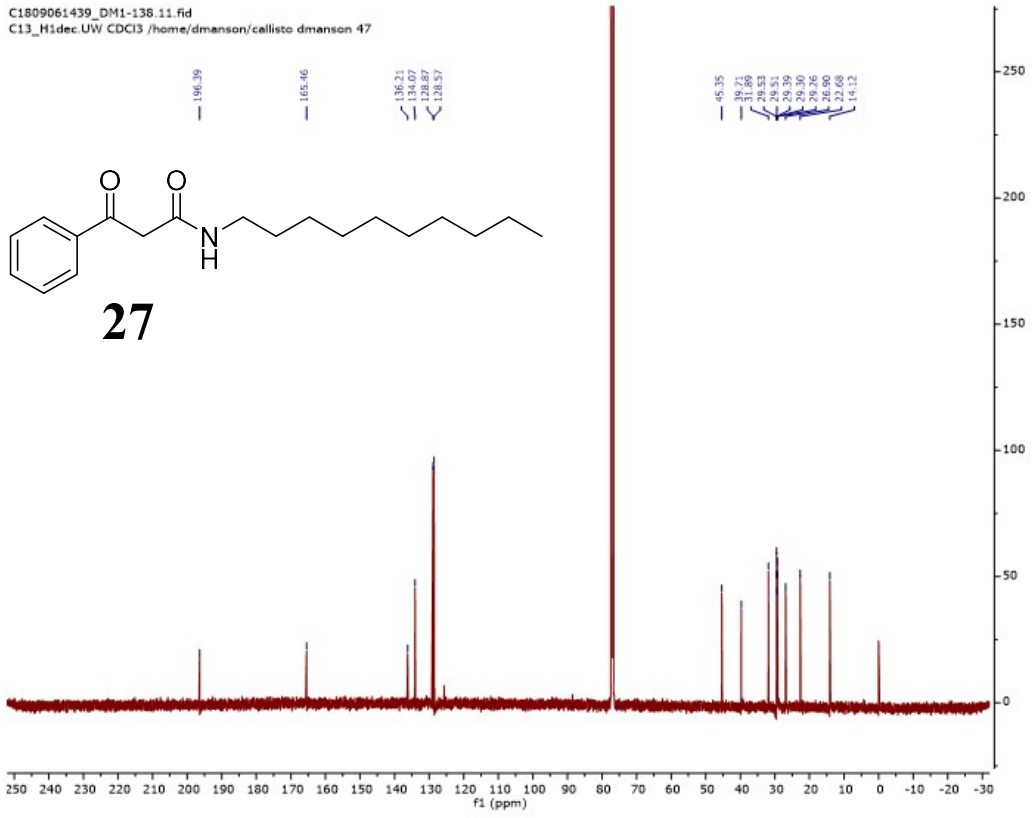
C1809061439_DM1-138.11.fid
C13_H1dec.UW CDCl3 /home/dmanson/callisto dmanson 47
196.39
165.46
136.21
134.07
128.87
128.57
45.35
39.71
31.89
29.53
29.51
29.39
29.30
29.26
26.90
22.68
14.12
27
f1 (ppm)

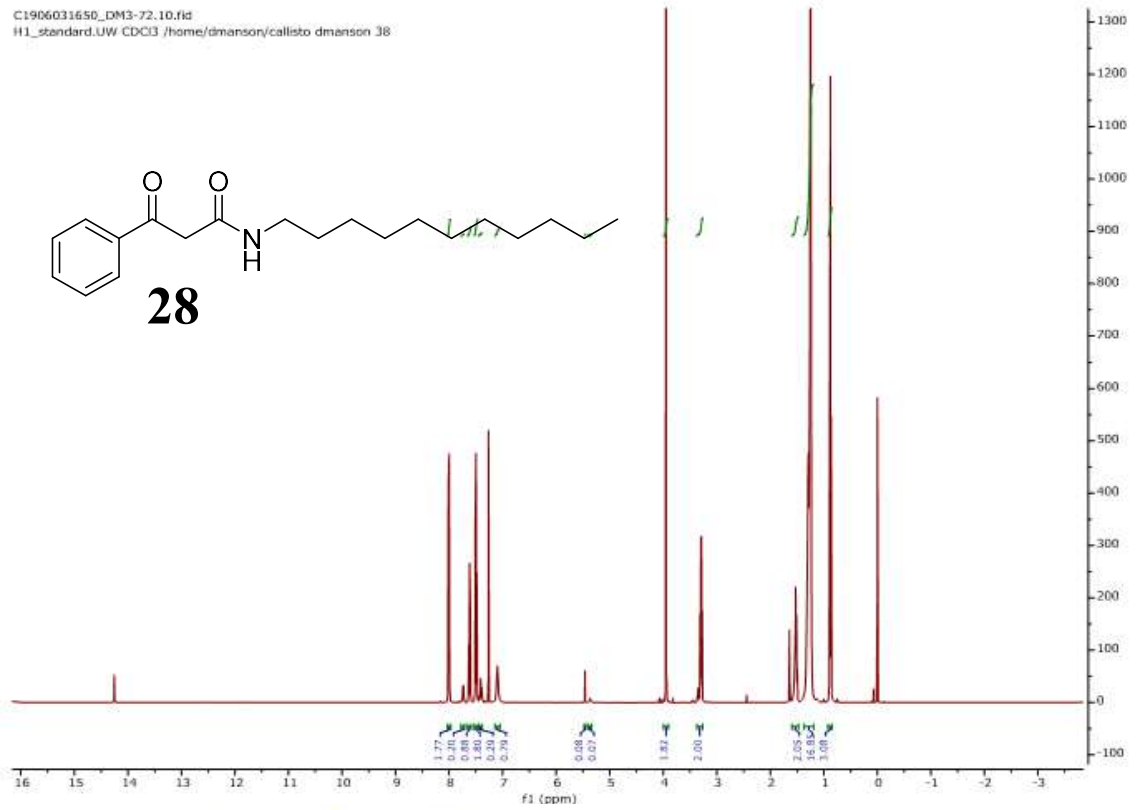
C19060316S0_DM3-72.10.fid
H1_standard.UW CDCl3 /home/dmanson/callisto dmanson 38
O
O
N
H
28
f1 (ppm)

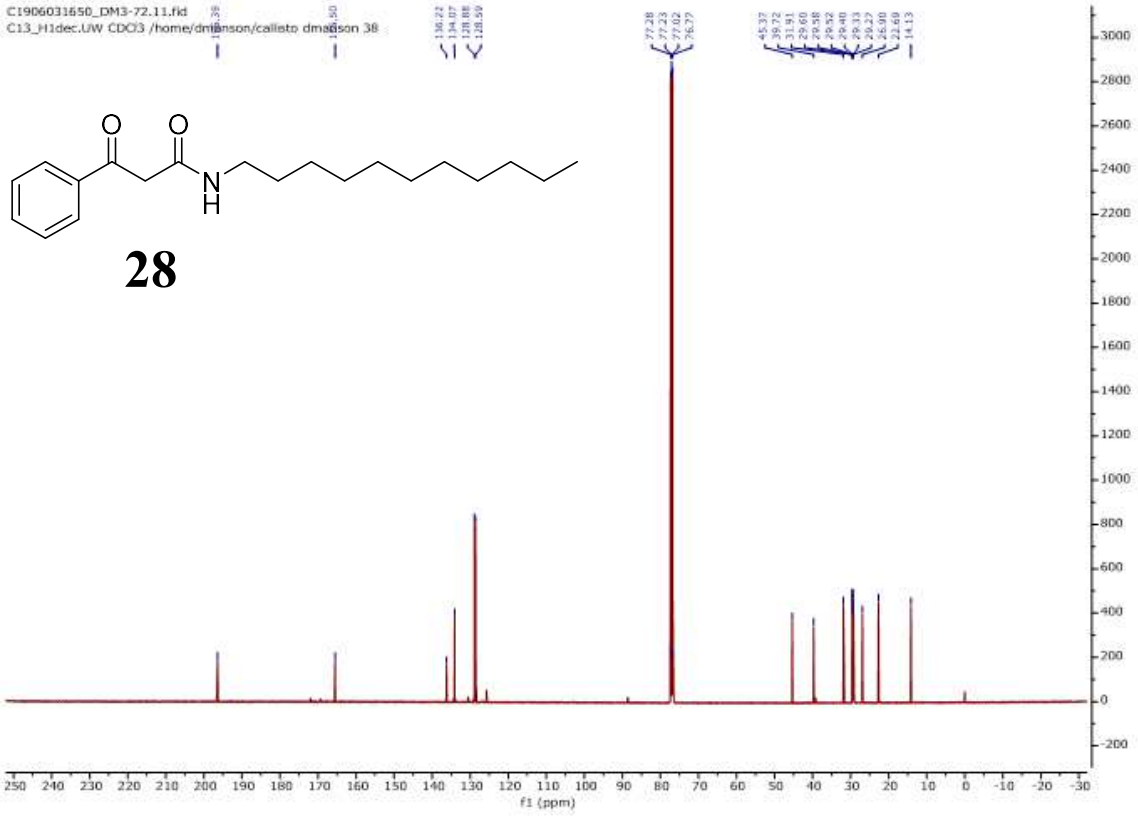
C19060316S0_DM3-72.11.fid
C13_H1dec.UW CDCl3 /home/dmanson/callisto dmanson 38
O
O
N
H
28
f1 (ppm)

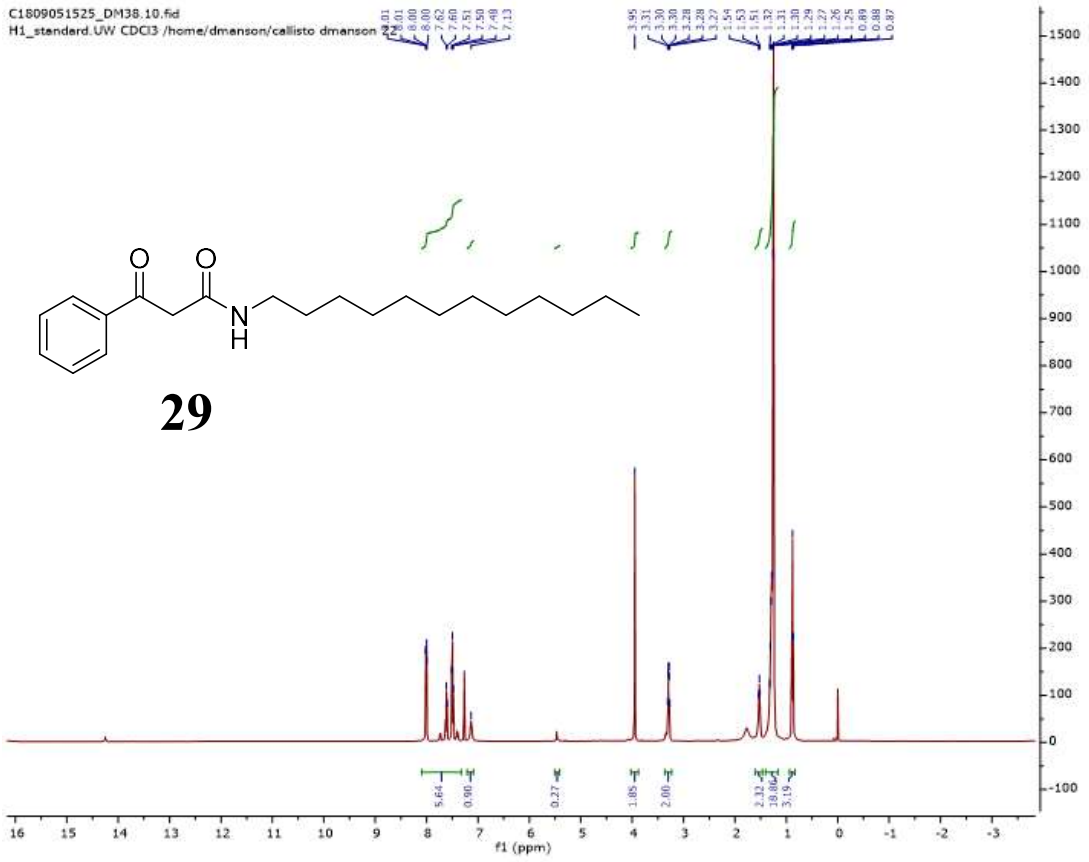
C1809051525_DM38.10.fid
H1_standard.UW CDCl3 /home/dmanson/callisto dmanson 22
f1 (ppm)

**29**

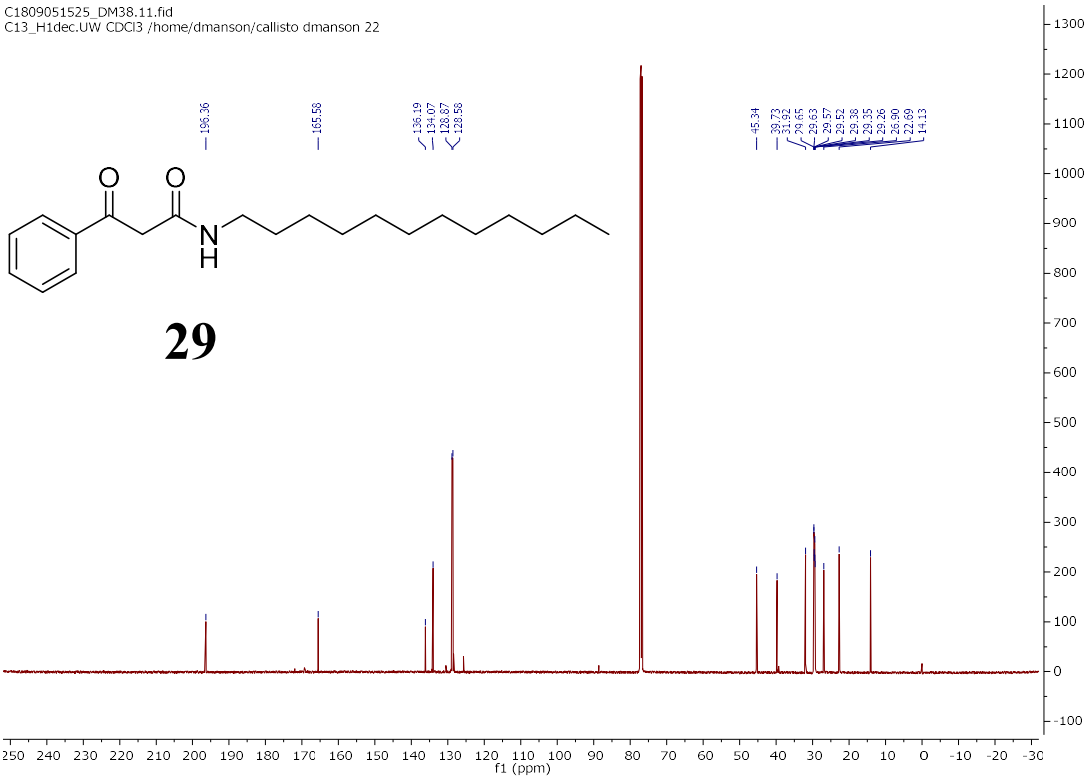
C1809051525_DM38.11.fid
C13_H1dec.UW CDCl3 /home/dmanson/callisto dmanson 22
f1 (ppm)

**29**

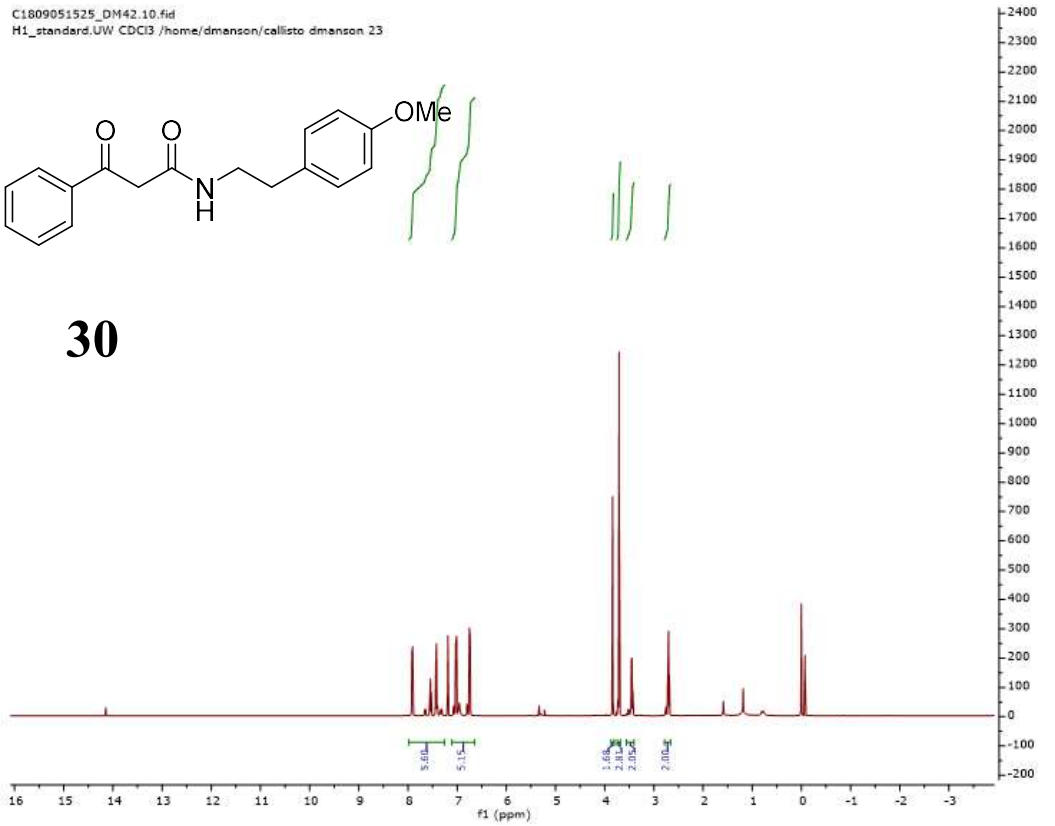
C1809051525_DM42.10.fid
H1_standard.UW CDCl3 /home/dmanson/callisto dmanson 23
OMe
O
O
N
H
f1 (ppm)

**30**

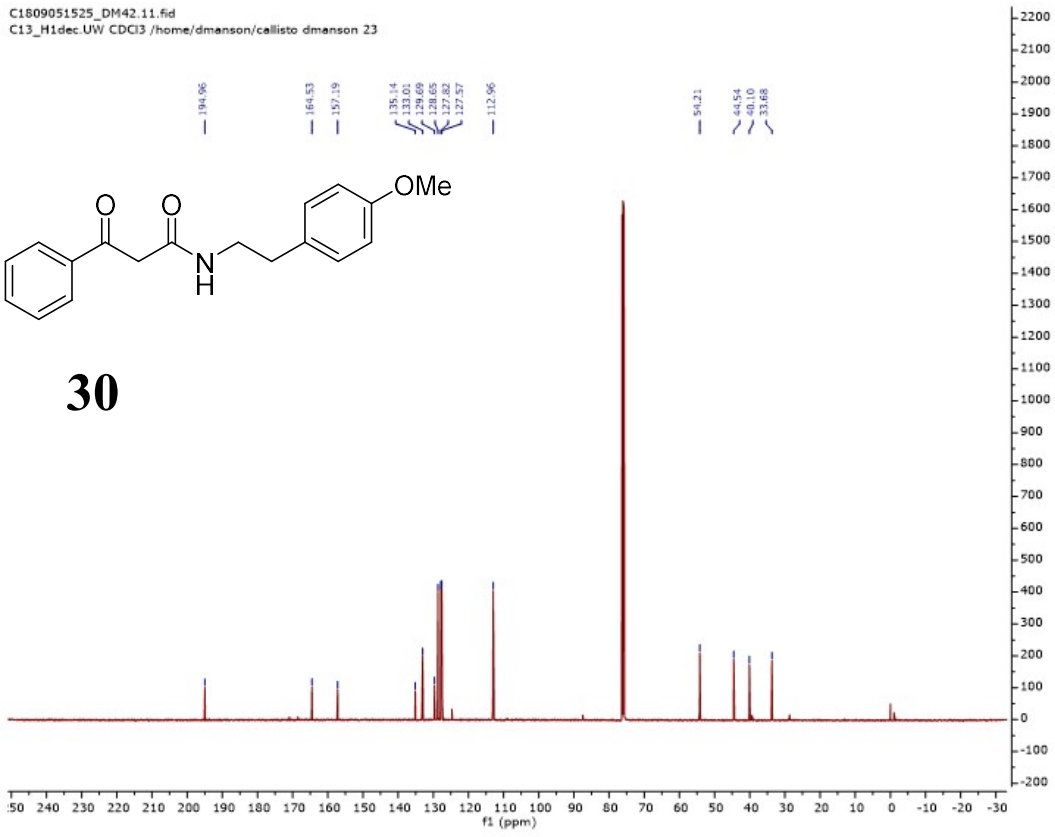
C1809051525_DM42.11.fid
C13_H1dec.UW CDCl3 /home/dmanson/callisto dmanson 23
194.96
164.53
157.19
135.14
133.01
129.69
128.65
127.82
127.57
112.96
54.21
44.54
40.10
33.68
OMe
O
O
N
H
f1 (ppm)

**30**

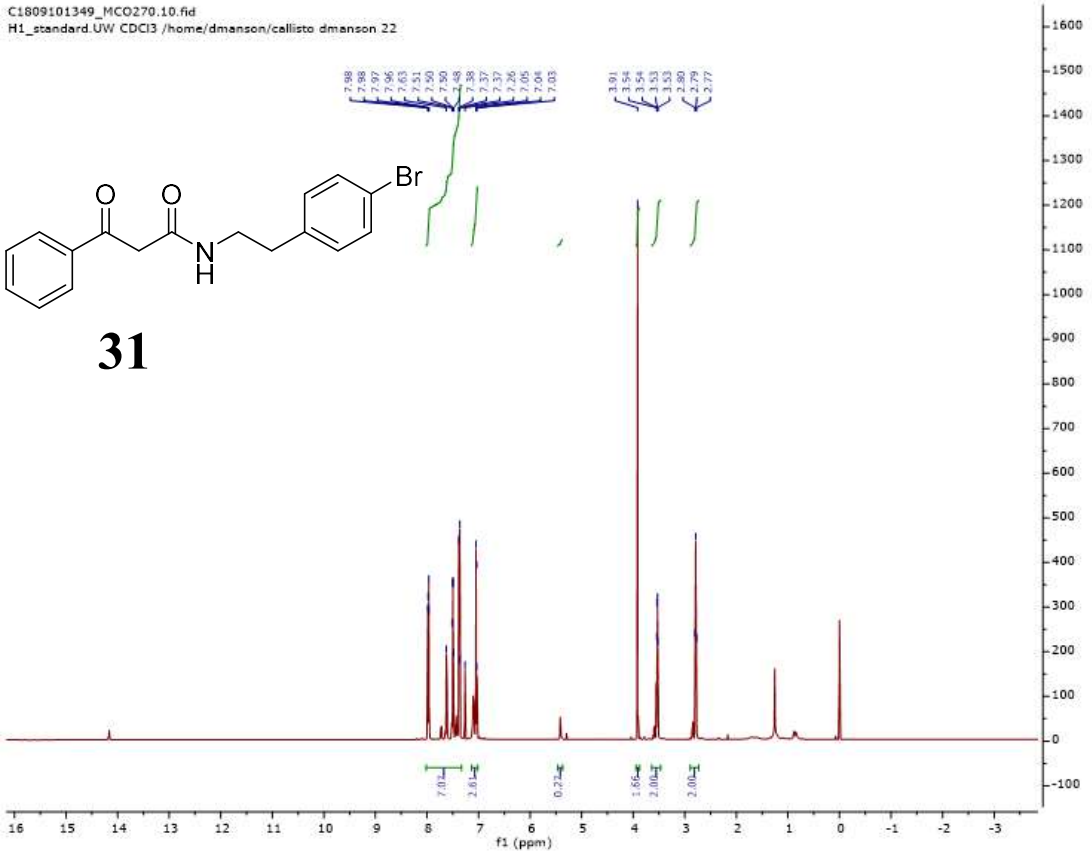
C1809101349_MCO270.10.fid
H1_standard.UW CDCl3 /home/dmanson/callisto dmanson 22
Br
O
O
N
H
f1 (ppm)

**31**

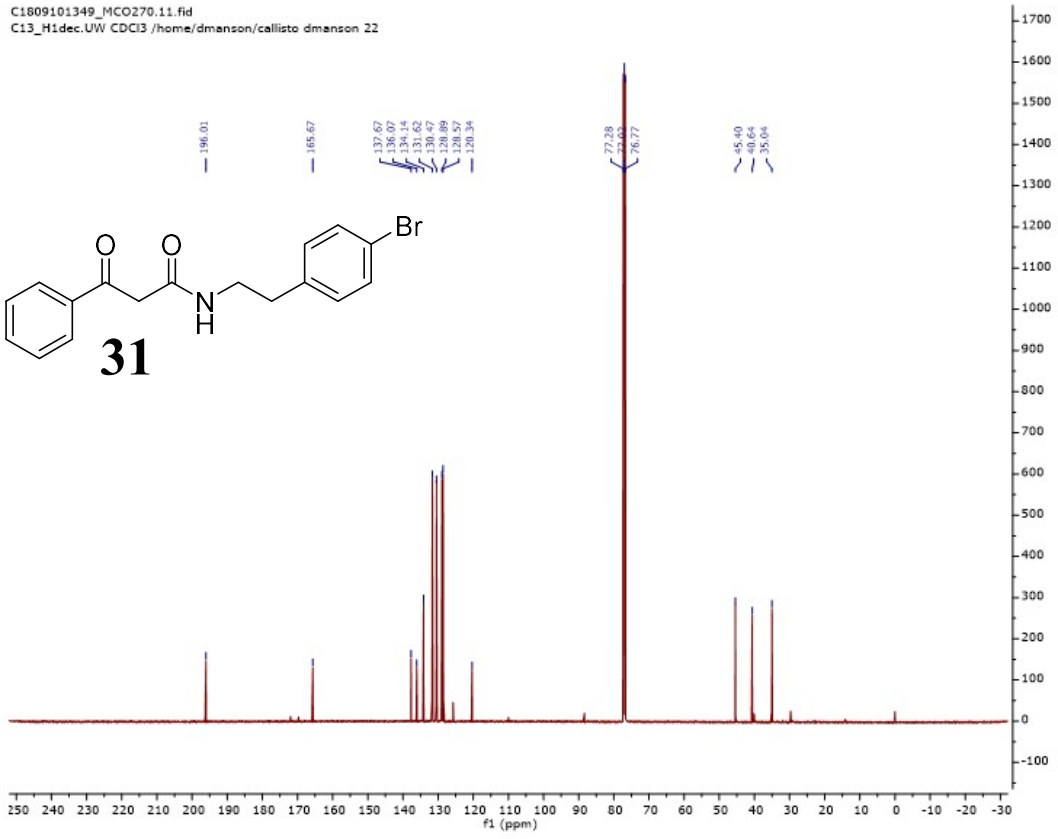
C1809101349_MCO270.11.fid
C13_H1dec.UW CDCl3 /home/dmanson/callisto dmanson 22
Br
O
O
N
H
f1 (ppm)

**31**

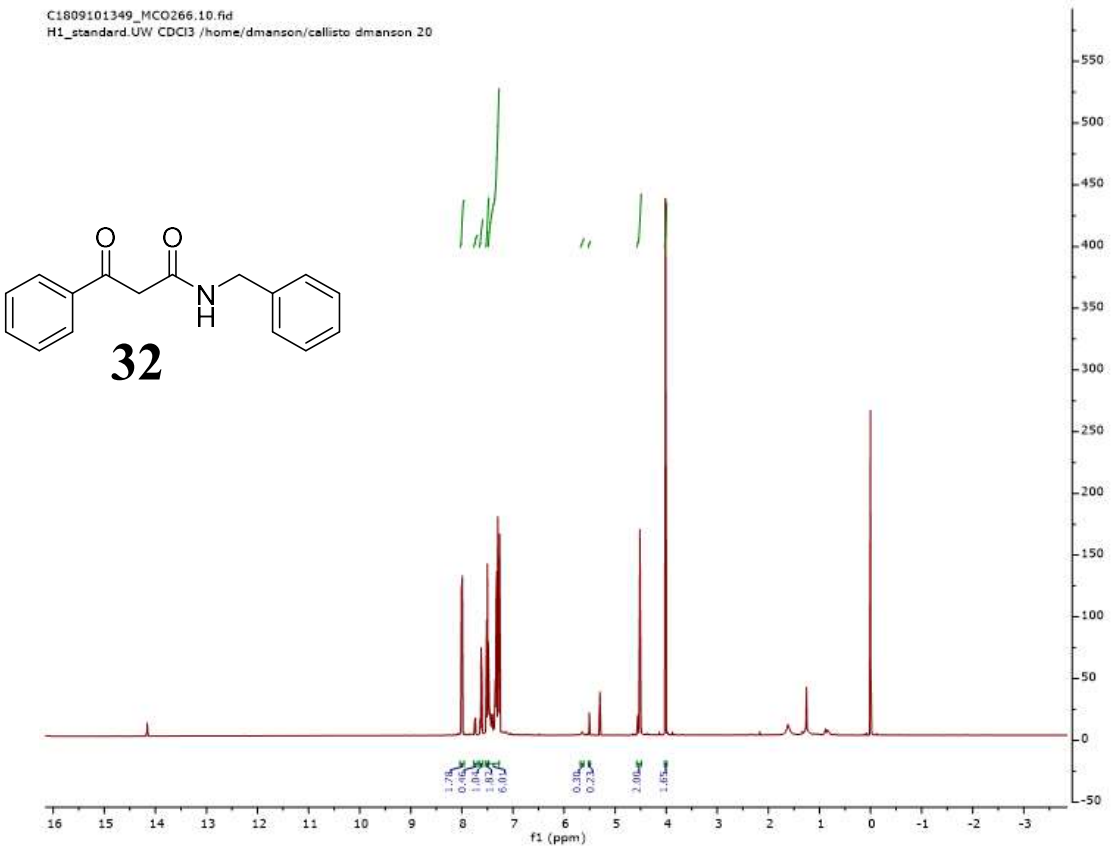
C1809101349_MCO266.10.fid
H1_standard.UW CDCl3 /home/dmanson/callisto dmanson 20
f1 (ppm)

**32**

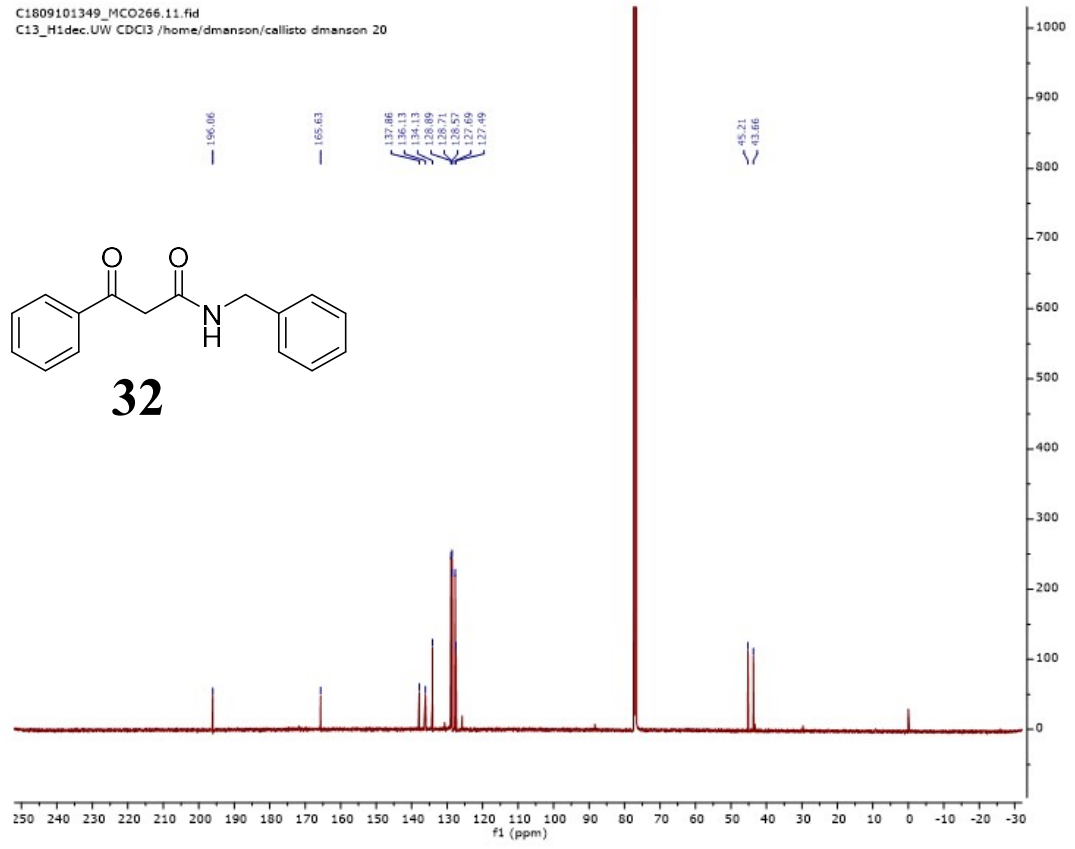
C1809101349_MCO266.11.fid
C13_H1dec.UW CDCl3 /home/dmanson/callisto dmanson 20
196.06
165.63
137.86
136.13
134.13
128.89
128.71
128.57
127.69
127.49
45.21
43.66
f1 (ppm)

**32**

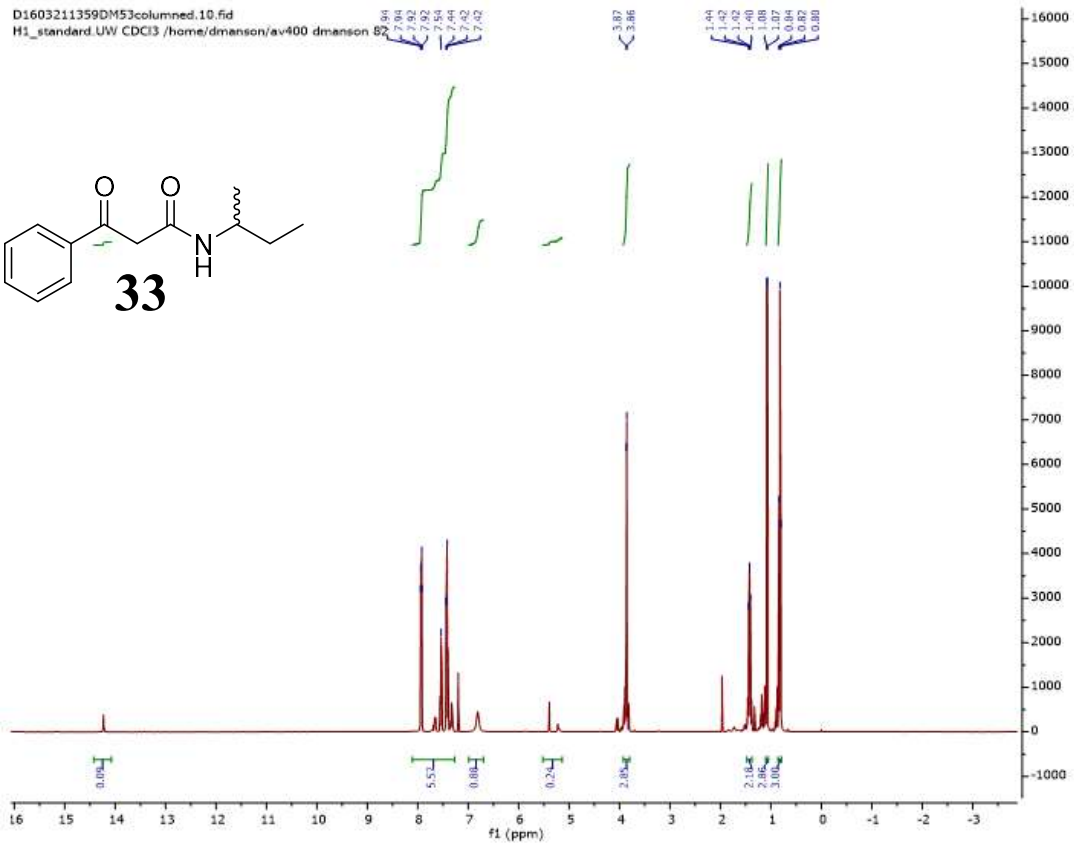
D1603211359DM53columned.10.fid
H1_standard.UW CDCl3 /home/dmanson/av400 dmanson 82
33
f1 (ppm)

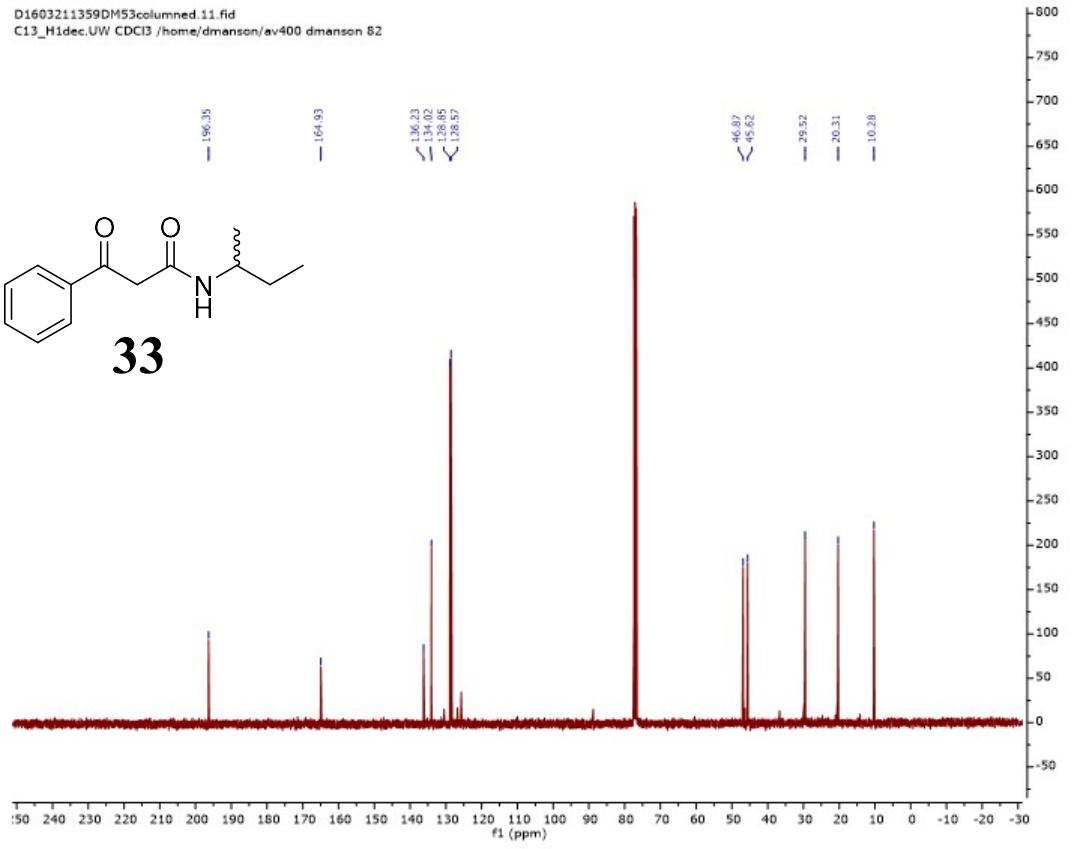
D1603211359DM53columned.11.fid
C13_H1dec.UW CDCl3 /home/dmanson/av400 dmanson 82
196.35
164.93
136.23
134.02
128.85
128.57
46.87
45.62
29.52
20.31
10.28
33
f1 (ppm)

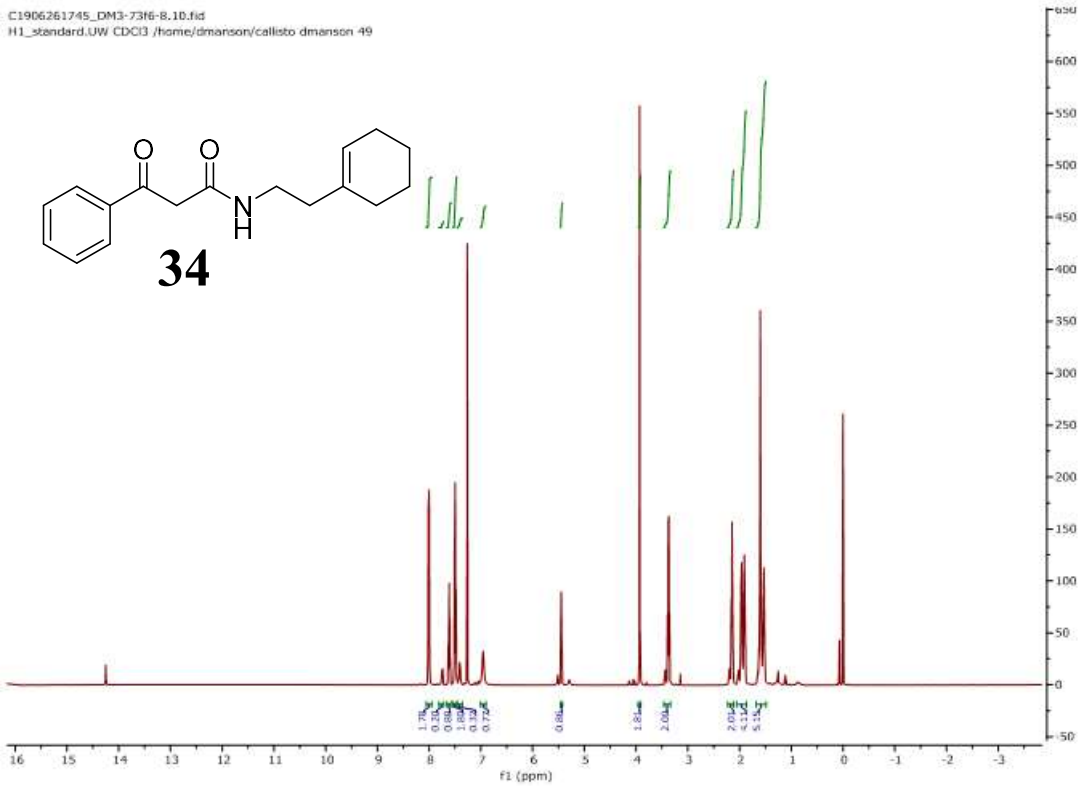
C1906261745_DM3-73f6-8.10.fid
H1_standard.UW CDCl3 /home/dmanson/callisto dmanson 49
34
f1 (ppm)

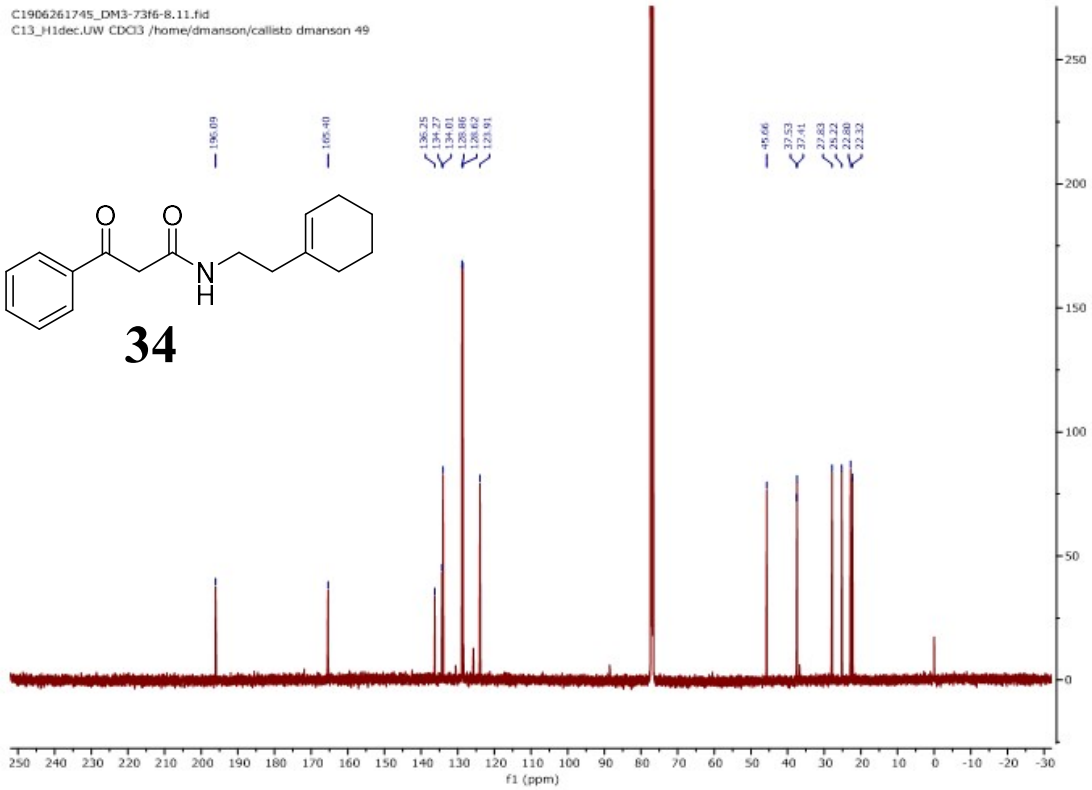
C1906261745_DM3-73f6-8.11.fid
C13_H1dec.UW CDCl3 /home/dmanson/callisto dmanson 49
196.69
165.40
136.35
134.27
134.01
128.86
128.62
123.91
45.66
37.53
37.41
27.83
25.22
22.80
22.32
34
f1 (ppm)

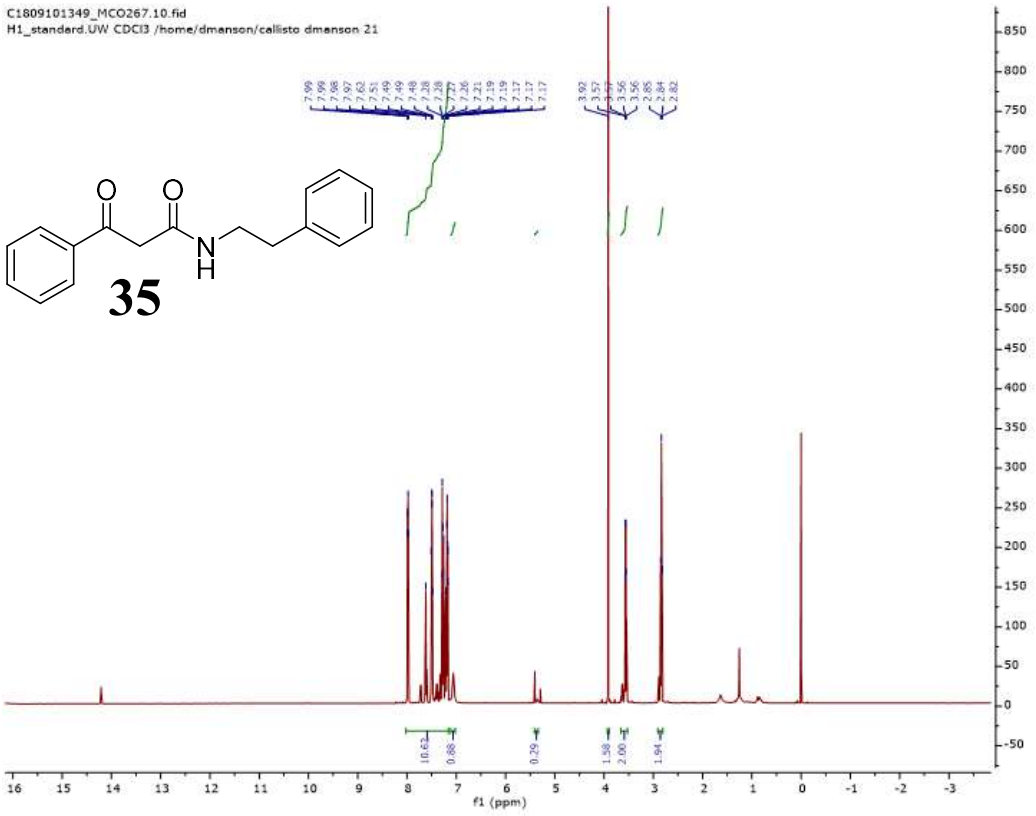
C1809101349_MCO267.10.fid
H1_standard.UW CDCl3 /home/dmanson/callisto dmanson 21
35
f1 (ppm)

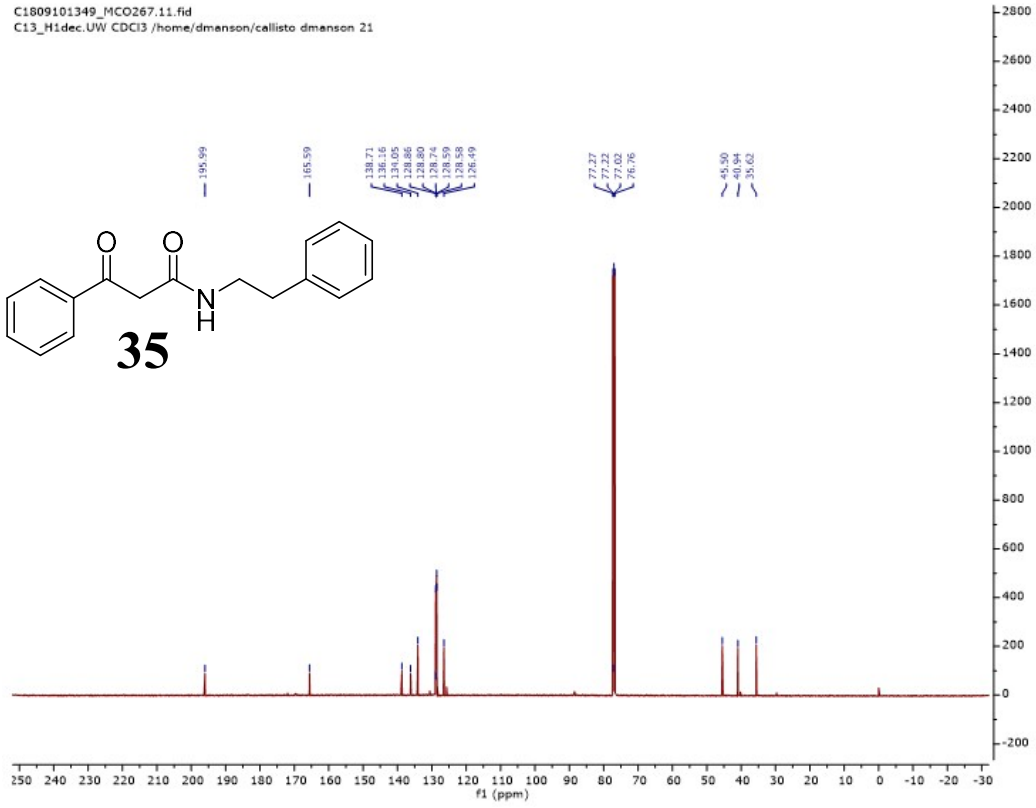
C1809101349_MCO267.11.fid
C13_H1dec.UW CDCl3 /home/dmanson/callisto dmanson 21
35
f1 (ppm)

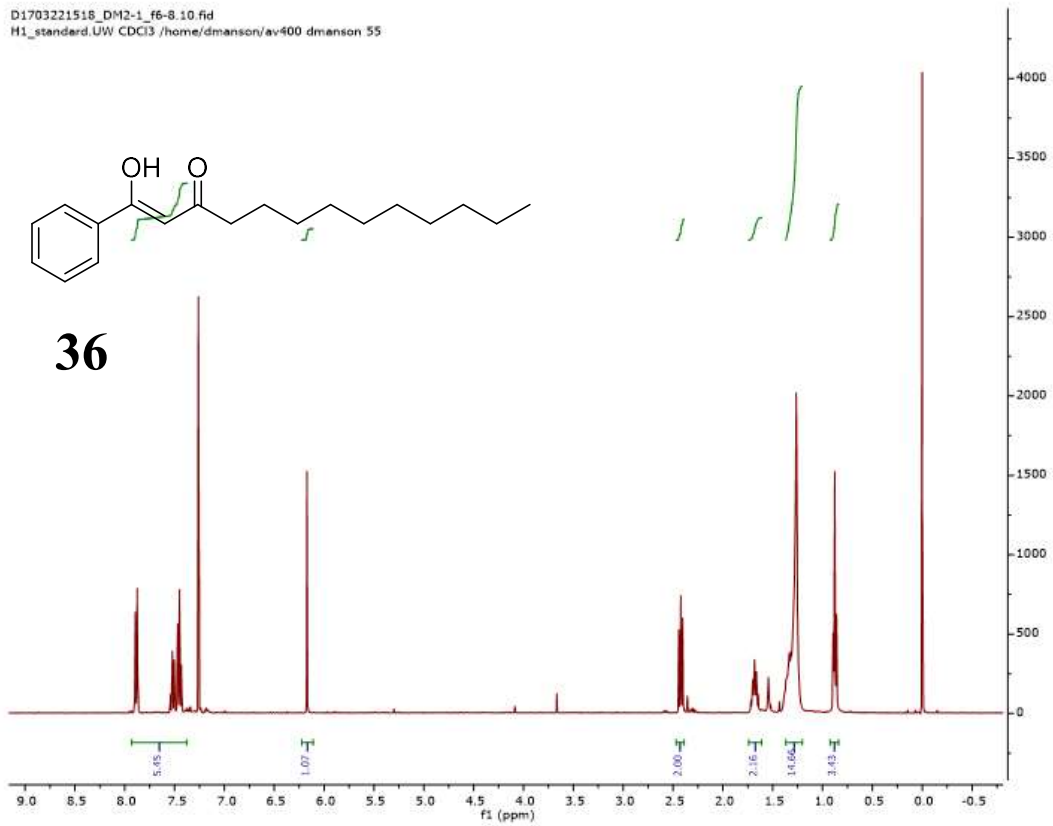
D1703221518_DM2-1_f6-8.10.fid
H1_standard.UW CDCl3 /home/dmanson/av400 dmanson 55
OH
O
36
f1 (ppm)

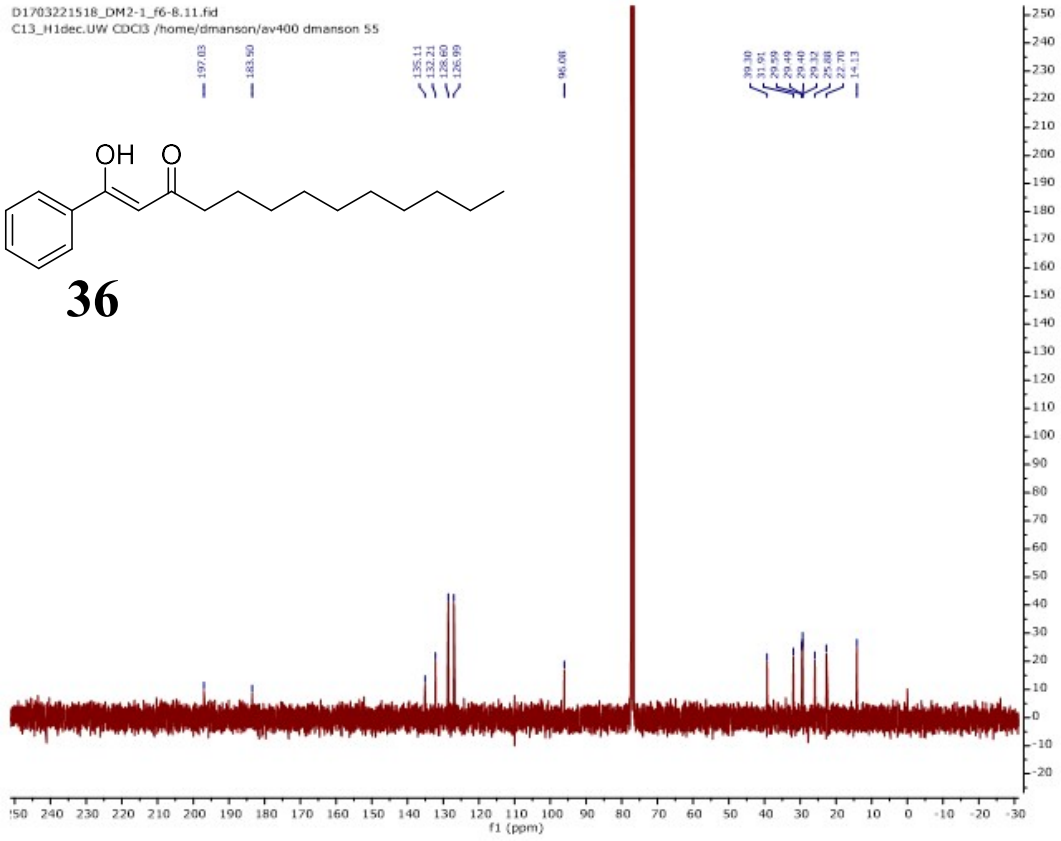
D1703221518_DM2-1_f6-8.11.fid
C13_H1dec.UW CDCl3 /home/dmanson/av400 dmanson 55
OH
O
36
f1 (ppm)

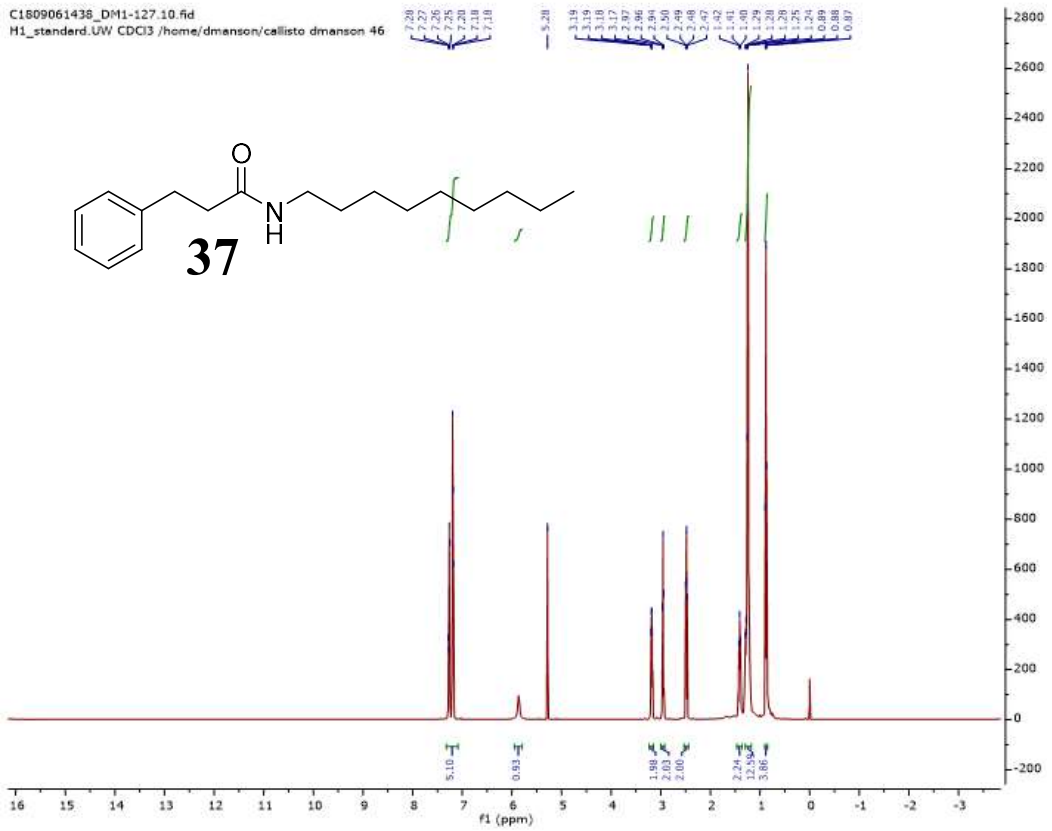
C1809061438_DM1-127.10.fid
H1_standard.UW CDCl3 /home/dmanson/callisto dmanson 46
O
N
H
37
f1 (ppm)

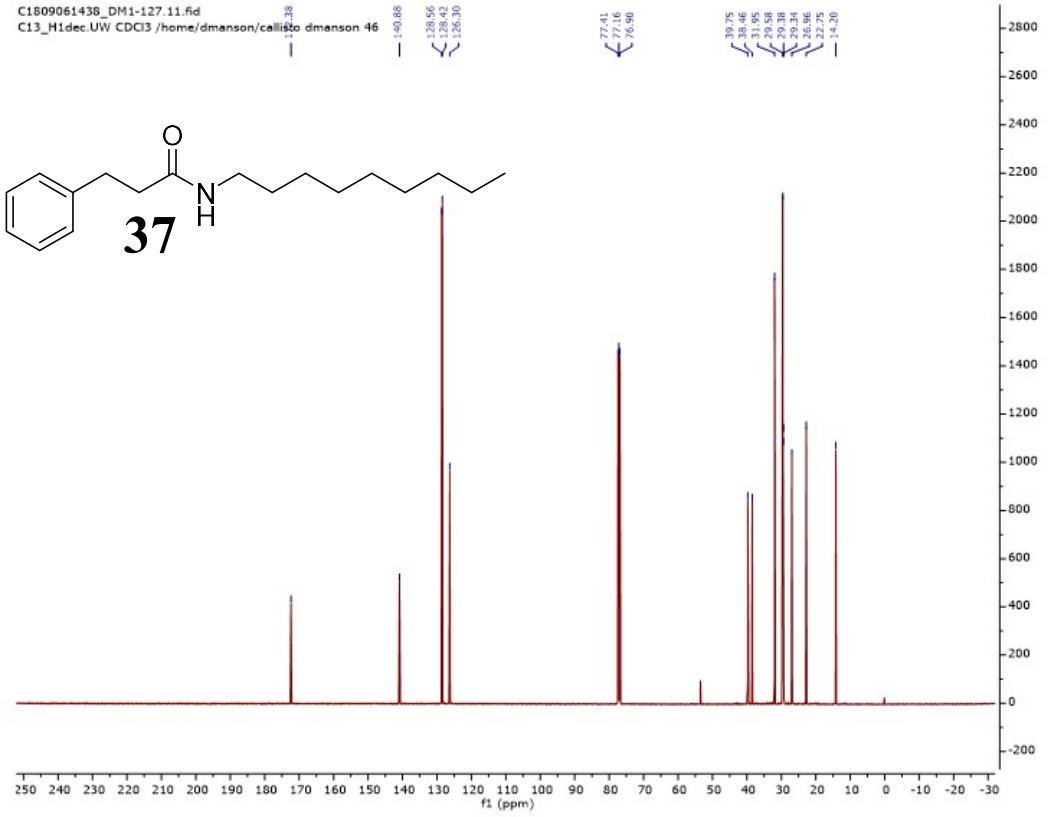
C1809061438_DM1-127.11.fid
C13_H1dec.UW CDCl3 /home/dmanson/callisto dmanson 46
O
N
H
37
f1 (ppm)

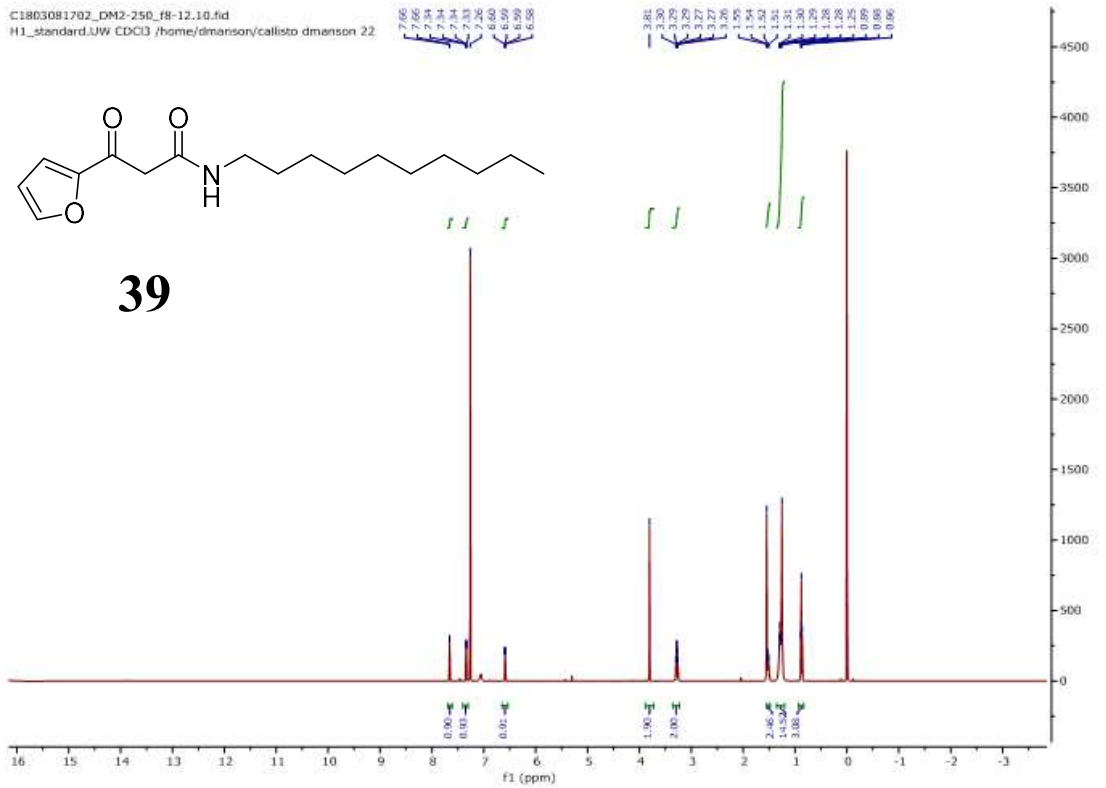
C1803081702_DM2-250_f8-12.10.fid
H1_standard.UW CDCl3 /home/dmanson/callisto dmanson 22
O
O
N
H
O
39
f1 (ppm)

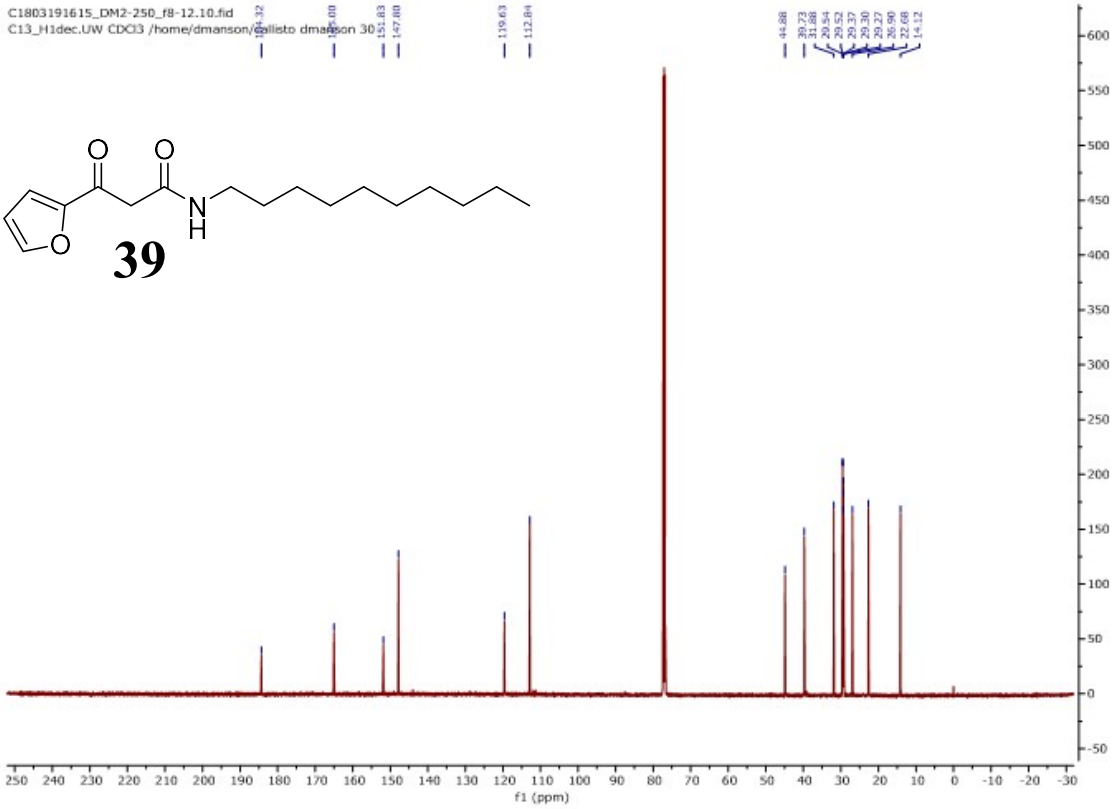
C1803191615_DM2-250_f8-12.10.fid
C13_H1dec.UW CDCl3 /home/dmanson/callisto dmanson 30
O
O
N
H
O
39
f1 (ppm)

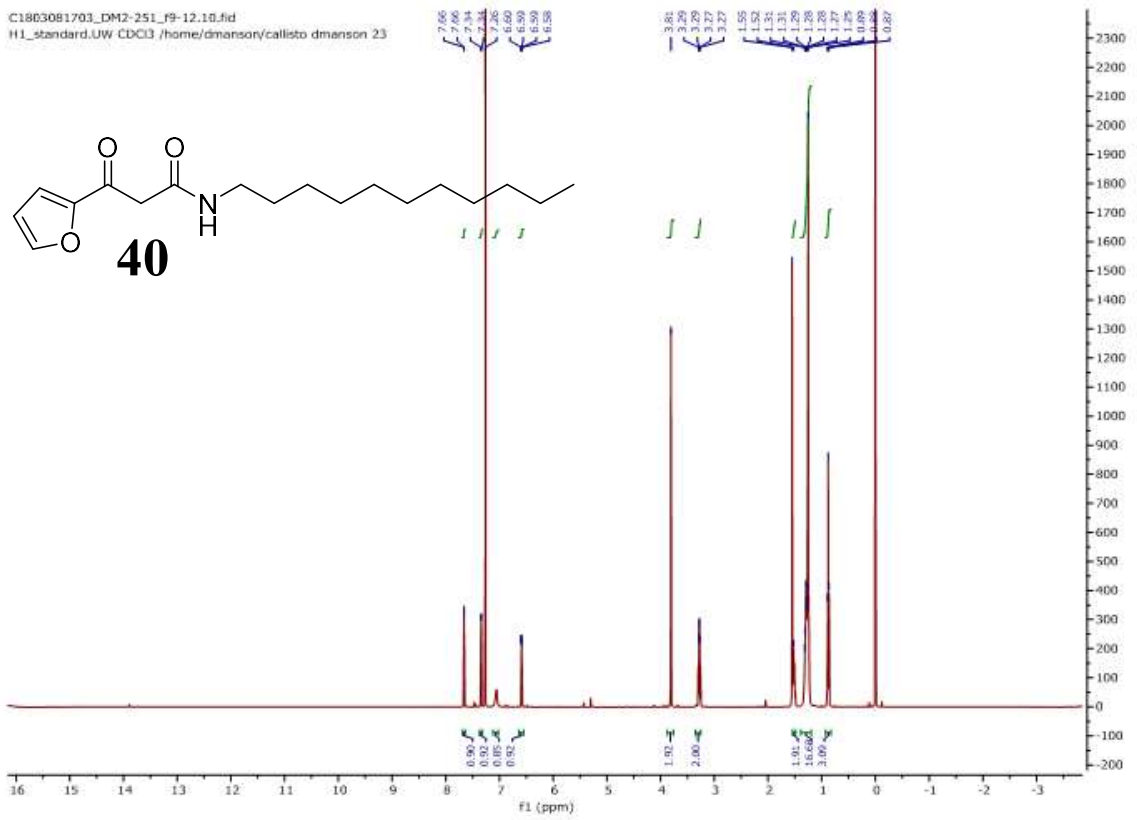
C1803081703_DM2-251_f9-12.10.fid
H1_standard.UW CDCl3 /home/dmanson/callisto dmanson 23
40
f1 (ppm)

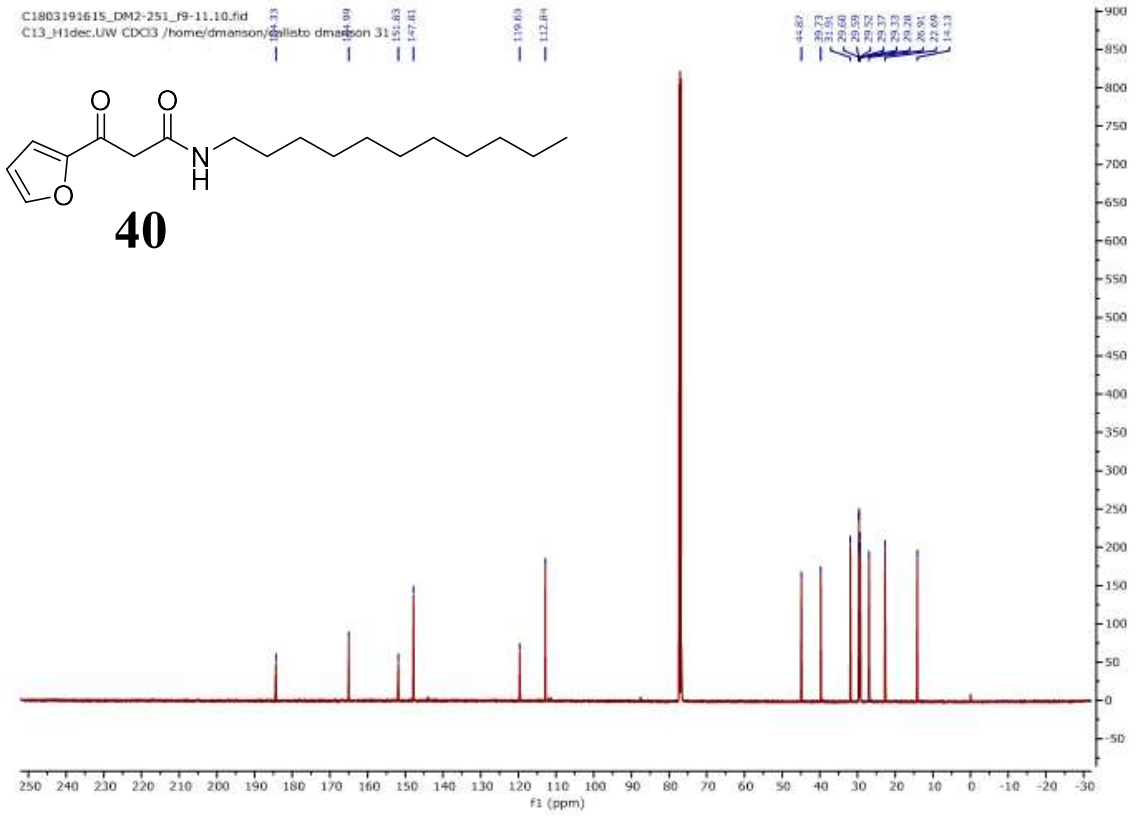
C1803191615_DM2-251_f9-11.10.fid
C13_H1dec.UW CDCl3 /home/dmanson/callisto dmanson 31
40
f1 (ppm)

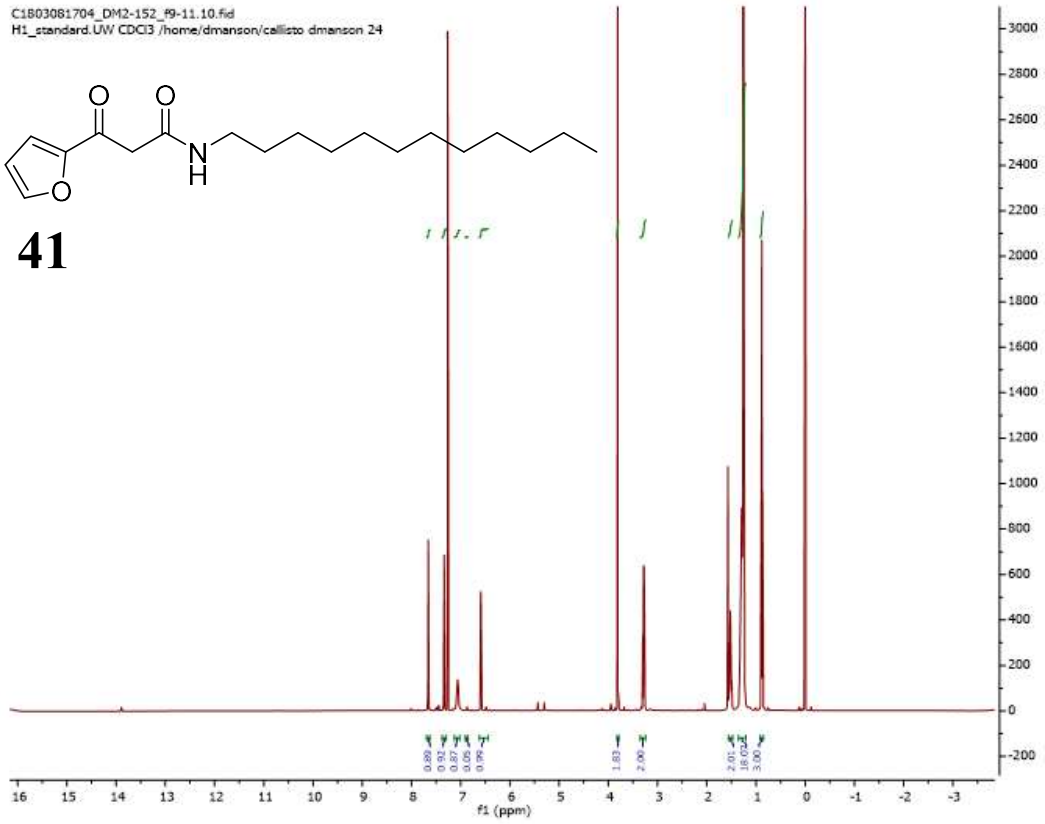
C1803081704_DM2-152_f9-11.10.fid
H1_standard.UW CDCl3 /home/dmanson/callisto dmanson 24
f1 (ppm)

**41**

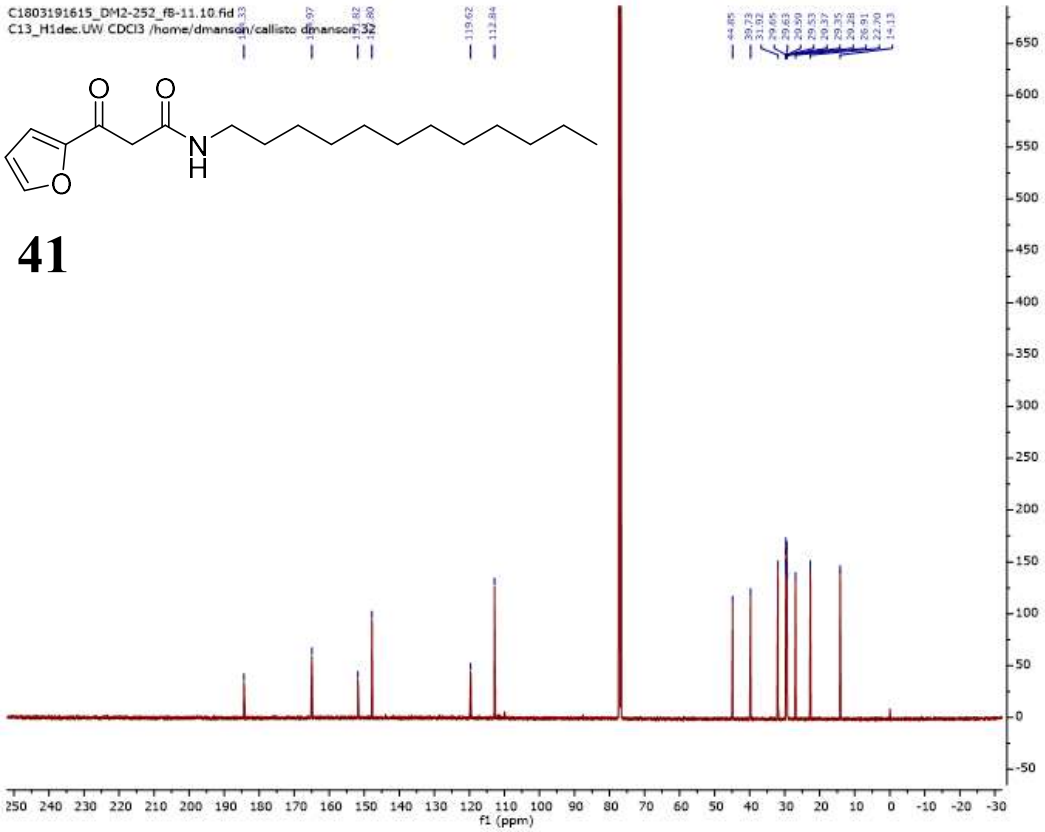
C1803191615_DM2-252_f8-11.10.fid
C13_H1dec.UW CDCl3 /home/dmanson/callisto dmanson 32
f1 (ppm)

**41**

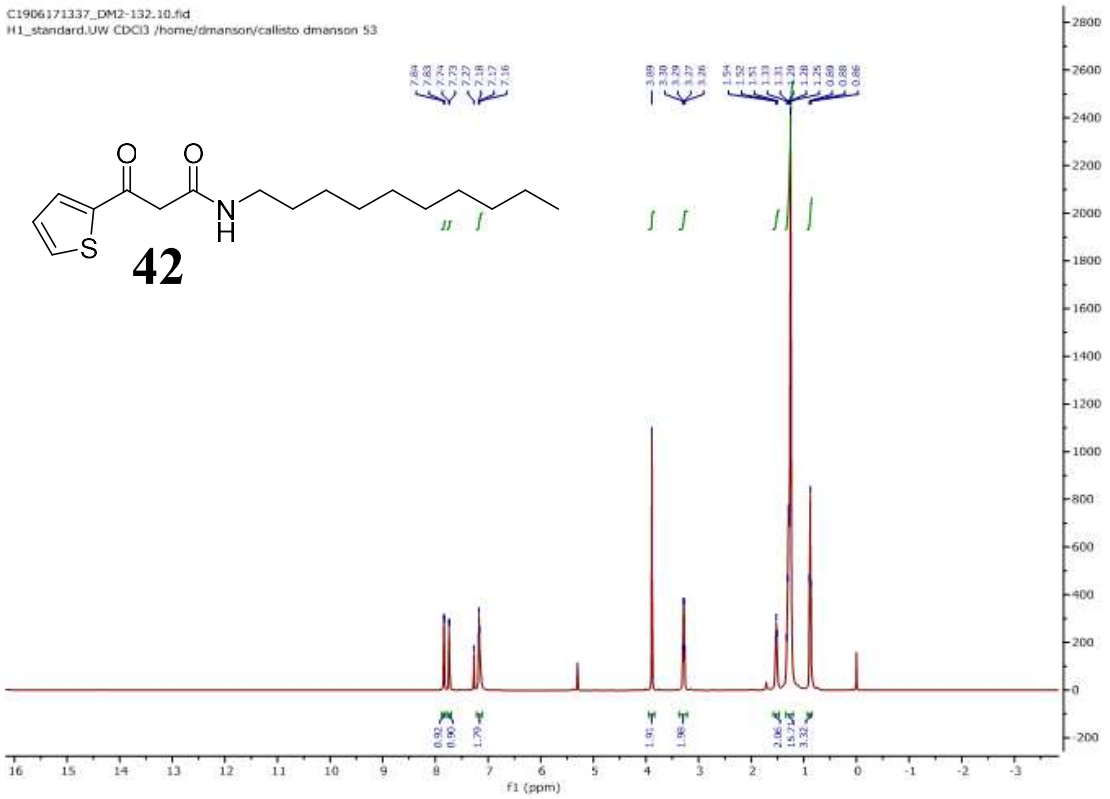
C1906171337_DM2-132.10.fid
H1_standard.UW CDCl3 /home/dmanson/callisto dmanson 53
42
f1 (ppm)

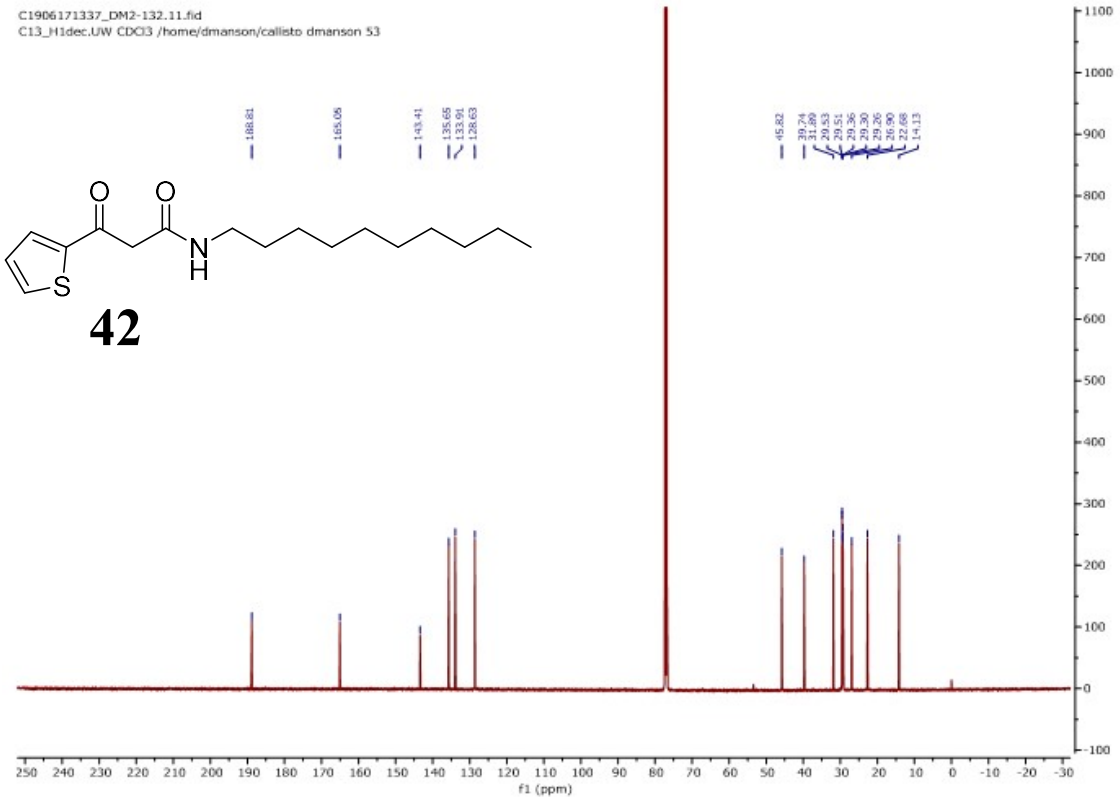
C1906171337_DM2-132.11.fid
C13_H1dec.UW CDCl3 /home/dmanson/callisto dmanson 53
42
f1 (ppm)

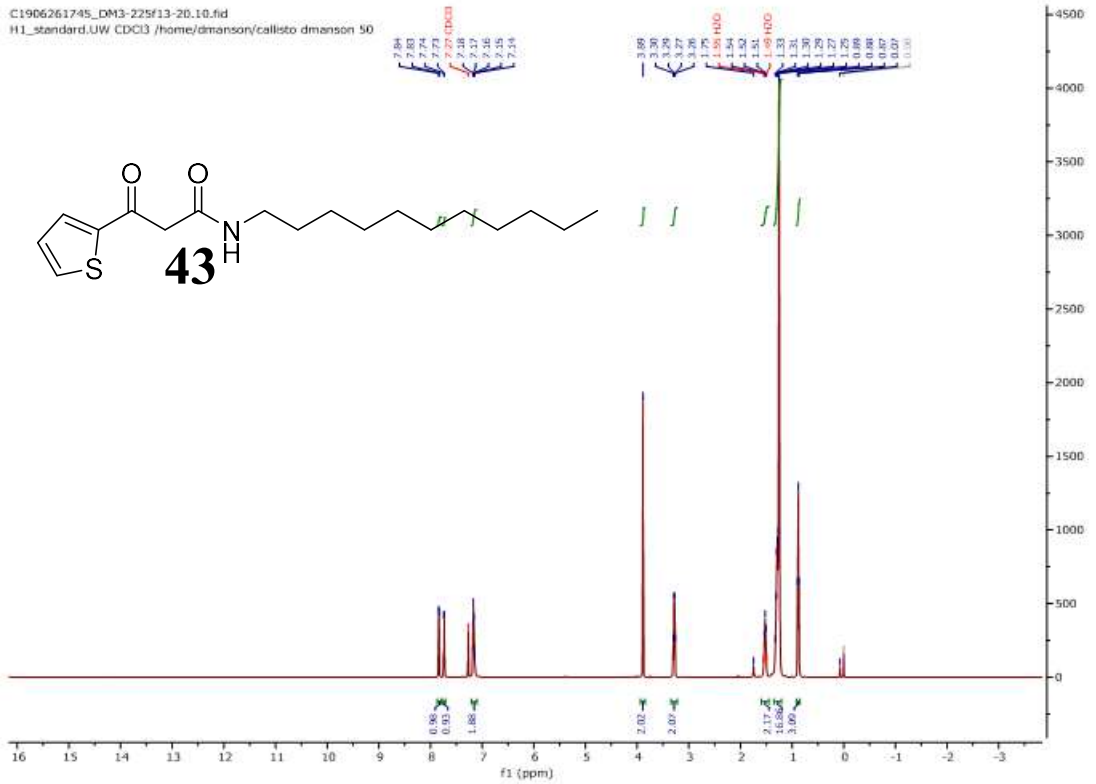
C1906261745_DM3-225f13-20.10.fid
H1_standard.UW CDCl3 /home/dmanson/callisto dmanson 50
43
f1 (ppm)

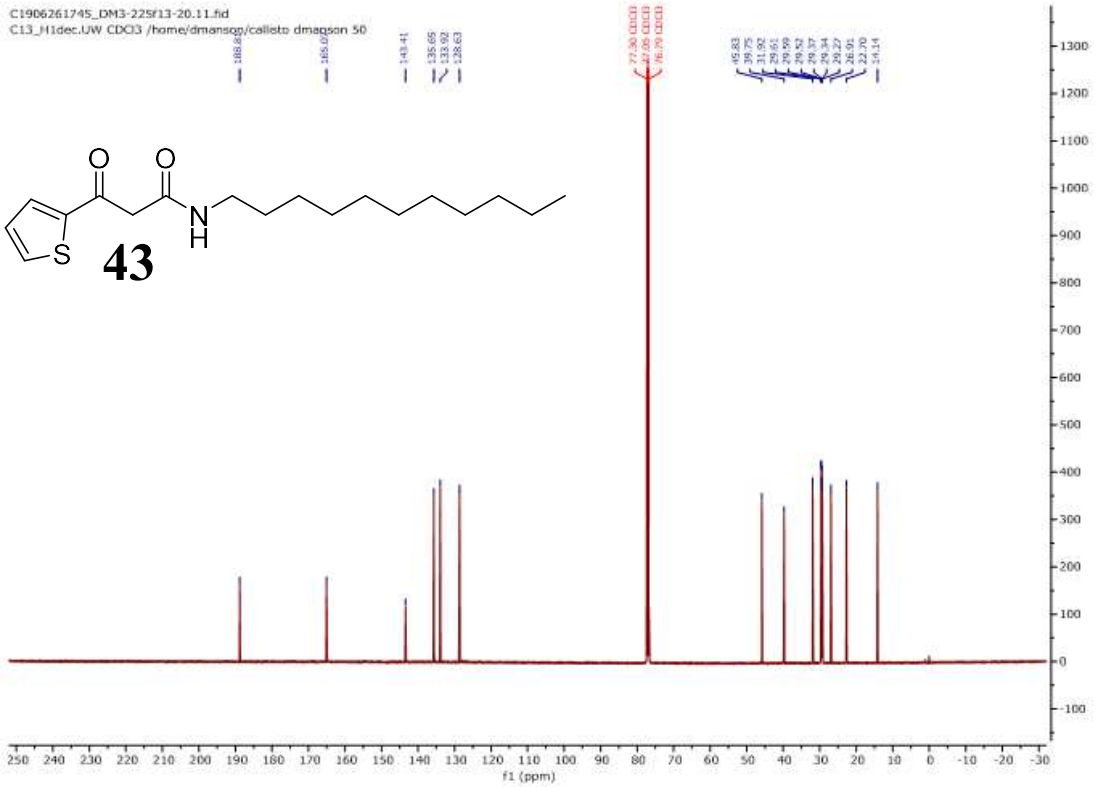
C1906261745_DM3-225f13-20.11.fid
C13_H1dec.UW CDCl3 /home/dmanson/callisto dmanson 50
43
f1 (ppm)

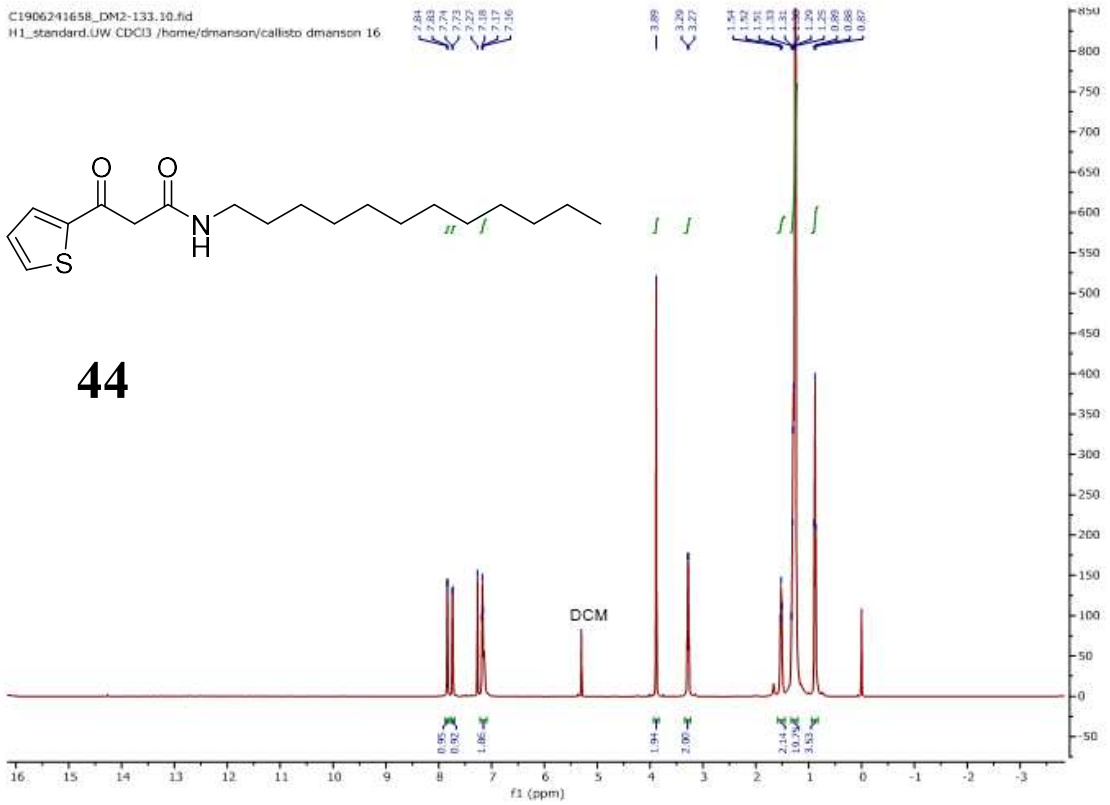
C19062416S8_DM2-133.10.fid
H1_standard.UW CDCl3 /home/dmanson/callisto dmanson 16
DCM
f1 (ppm)

**44**

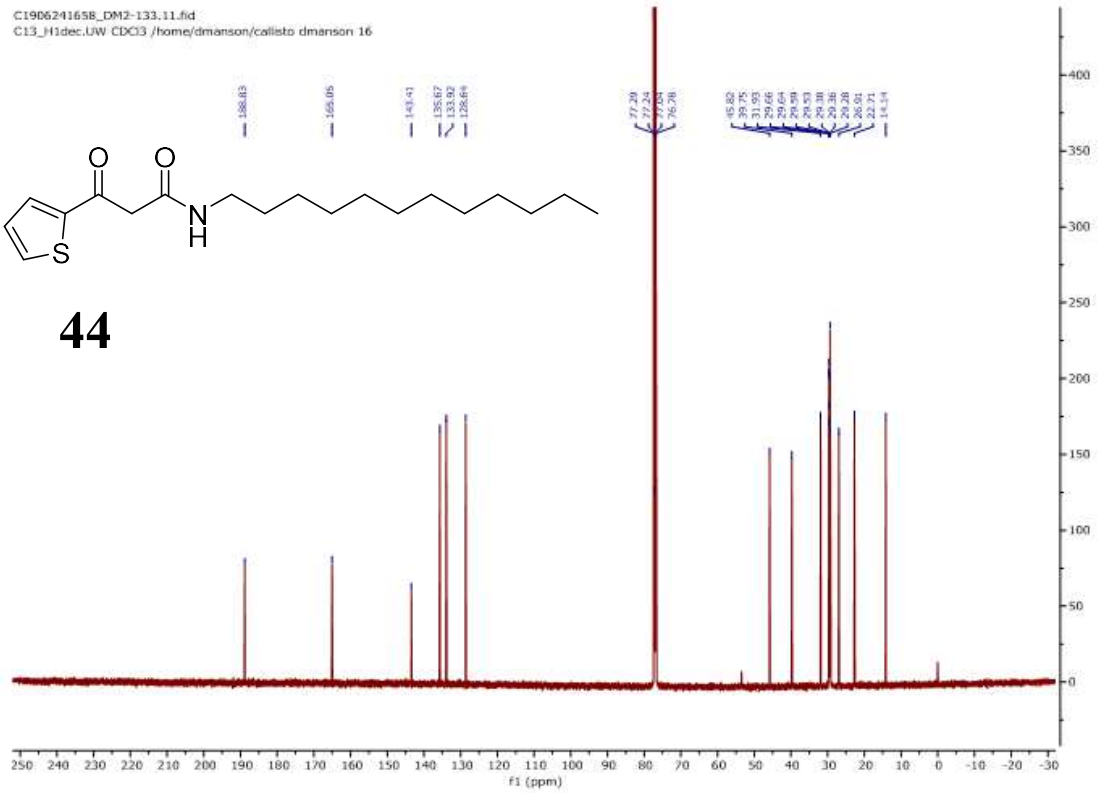
C19062416SB_DM2-133.11.fid
C13_H1dec.UW CDCl3 /home/dmanson/callisto dmanson 16
f1 (ppm)

**44**

**References**


1. Brown, E. D.; Wright, G. D., Antibacterial drug discovery in the resistance era. *Nature* **2016,** *529* (7586), 336-43.
2. Nathan, C.; Card, O., Antibiotic Resistance - Problems, Progress, and Prospects. *New Engl. J. of Med.* **2014,** *371*, 1761-1763.
3. Allen, R. C.; Popat, R.; Diggle, S. P.; Brown, S. P., Targeting virulence: can we make evolution-proof drugs? *Nat. Rev. Microbiol.* **2014,** *12* (4), 300-8.
4. Whiteley, M.; Diggle, S. P.; Greenberg, E. P., Progress in and promise of bacterial quorum sensing research. *Nature* **2017,** *551* (7680), 313-320.
5. Rutherford, S. T.; Bassler, B. L., Bacterial quorum sensing: its role in virulence and possibilities for its control. *Cold Spring Harb. Perspect. Med.*. **2012,** *2* (11).
6. Fuqua, C.; Greenberg, E. P., Listening in on bacteria: acyl-homoserine lactone signalling. *Nat. Rev. Mol. Cell. Biol.* **2002,** *3* (9), 685-95.
7. Galloway, W. R.; Hodgkinson, J. T.; Bowden, S. D.; Welch, M.; Spring, D. R., Quorum Sensing in Gram-Negative Bacteria: Small-Molecule Modulation of AHL and AI-2 Quorum Sensing Pathways. *Chem. Rev.* **2011,** *111*, 28-67.
8. Sintim, H. O.; Smith, J. A.; Wang, J.; Nakayama, S.; Yan, L., Paradigm shift in discovering next-generation anti-infective agents: targeting quorum sensing, c-di-GMP signaling and biofilm formation in bacteria with small molecules. *Future Med. Chem.* **2010,** *2* (6), 1005-1035.
9. Welsh, M. A.; Blackwell, H. E., Chemical Genetics Reveals Environment-Specific Roles for Quorum Sensing Circuits in Pseudomonas aeruginosa. *Cell Chem. Biol.* **2016,** *23* (3), 361-9.
10. Welsh, M. A.; Eibergen, N. R.; Moore, J. D.; Blackwell, H. E., Small molecule disruption of quorum sensing cross-regulation in pseudomonas aeruginosa causes major and unexpected alterations to virulence phenotypes. *J. Am. Chem. Soc.* **2015,** *137* (4), 1510-9.
11. Tal-Gan, Y.; Ivancic, M.; Cornilescu, G.; Yang, T.; Blackwell, H. E., Highly Stable, Amide-Bridged Autoinducing Peptide Analogues that Strongly Inhibit the AgrC Quorum Sensing Receptor in Staphylococcus aureus. *Angew. Chem. Int. Ed. Engl.* **2016,** *55* (31), 8913-7.
12. Wang, B.; Muir, T. W., Regulation of Virulence in Staphylococcus aureus: Molecular Mechanisms and Remaining Puzzles. *Cell Chem. Biol.* **2016,** *23* (2), 214-224.
13. Starkey, M.; Lepine, F.; Maura, D.; Bandyopadhaya, A.; Lesic, B.; He, J.; Kitao, T.; Righi, V.; Milot, S.; Tzika, A.; Rahme, L., Identification of anti-virulence compounds that disrupt quorum-sensing regulated acute and persistent pathogenicity. *PLoS Pathog.* **2014,** *10* (8), e1004321.
14. Hodgkinson, J. T.; Galloway, W. R.; Wright, M.; Mati, I. K.; Nicholson, R. L.; Welch, M.; Spring, D. R., Design, synthesis and biological evaluation of non-natural modulators of quorum sensing in Pseudomonas aeruginosa. *Org. Biomol. Chem.* **2012,** *10* (30), 6032-44.
15. Amara, N.; Mashiach, R.; Amar, D.; Krief, P.; Spieser, S. A. H.; Bottomley, M. J.; Aharoni, A.; Meijler, M. M., Covalent Inhibition of Bacterial Quorum Sensing. *J. Am. Chem. Soc.* **2009**.
16. Moore, J. D.; Gerdt, J. P.; Eibergen, N. R.; Blackwell, H. E., Active efflux influences the potency of quorum sensing inhibitors in Pseudomonas aeruginosa. *Chembiochem* **2014,** *15* (3), 435-42.

17. Wagner, V. E.; Bushnell, D.; Passador, L.; Brooks, A. I.; Iglewski, B. H., Microarray Analysis of Pseudomonas aeruginosa Quorum-Sensing Regulons: Effects of Growth Phase and Environment. *J. Bacteriol.* **2003,** *185* (7), 2080-2095.
18. Schuster, M.; Greenberg, E. P., A network of networks: quorum-sensing gene regulation in Pseudomonas aeruginosa. *Int. J. Med. Microbiol.* **2006,** *296* (2-3), 73-81.
19. De Kievit, T. R.; Gillis, R.; Marx, S.; Brown, C.; Iglewski, B. H., Quorum-sensing genes in Pseudomonas aeruginosa biofilms: their role and expression patterns. *Appl. Environ. Microbiol.* **2001,** *67* (4), 1865-73.
20. The structure of TP1 was originally reported in 2006 (see ref. 25). In 2011, its structure was revised, from TP1-P (TP1- previous) to TP1-R (TP1- revised). Both isomers are bioactive and have similar activities. In the present study, we depict TP1-P and report a measurement of its $EC_{50}$ previously made by our lab. See: Zakhari, J.S.; Kinoyama, I.; Struss, A.K.; Pullanikat, P.; Lowery, C.A.; Lardy, M.; Janda, K.D. *J. Am. Chem. Soc.*, **2011** *133* (11), 3840-3842.
21. Christensen, Q. H.; Grove, T. L.; Booker, S. J.; Greenberg, E. P., A high-throughput screen for quorum-sensing inhibitors that target acyl-homoserine lactone synthases. *Proc. Natl. Acad. Sci. U. S. A.* **2013,** *110* (34), 13815-20.
22. Amara, N.; Krom, B. P.; Kaufmann, G. F.; Meijler, M. M., Macromolecular Inhibition of Quorum Sensing: Enzymes, Anbitodies, and Beyond. *Chem. Rev.* **2011,** *111*, 195-208.
23. Welsh, M. A.; Blackwell, H. E., Chemical probes of quorum sensing: from compound development to biological discovery. *FEMS Microbiol. Rev.* **2016,** *40* (5), 774-94.
24. O'Loughlin, C. T.; Miller, L. C.; Siryaporn, A.; Drescher, K.; Semmelhack, M. F.; Bassler, B. L., A quorum-sensing inhibitor blocks Pseudomonas aeruginosa virulence and biofilm formation. *Proc. Natl. Acad. Sci. U. S. A.* **2013,** *110* (44), 17981-6.
25. Muh, U.; Hare, B. J.; Duerkop, B. A.; Schuster, M.; Hanzelka, B. L.; Heim, R.; Olson, E. R.; Greenberg, E. P., A structurally unrelated mimic of a Pseudomonas aeruginosa acyl-homoserine lactone quorum-sensing signal. *Proc. Natl. Acad. Sci. U. S. A.* **2006,** *103* (45), 16948-52.
26. O'Reilly, M. C.; Blackwell, H. E., Structure-Based Design and Biological Evaluation of Triphenyl Scaffold-Based Hybrid Compounds as Hydrolytically Stable Modulators of a LuxR-Type Quorum Sensing Receptor. *ACS Infect. Dis.* **2016,** *2* (1), 32-38.
27. Geske, G. D.; O'Neill, J. C.; Miller, D. M.; Wezeman, R. J.; Mattmann, M. E.; Lin, Q.; Blackwell, H. E., Comparative analyses of N-acylated homoserine lactones reveal unique structural features that dictate their ability to activate or inhibit quorum sensing. *Chembiochem* **2008,** *9* (3), 389-400.
28. Geske, G. D.; O'Neill, J. C.; Miller, D. M.; Mattman, M.E.; Blackwell, H. E., Modulation of Bacterial Quorum Sensing with Synthetic Ligands: System Evaluation of N-Acylated Homoserine Lactones in Multiple Species and New Insights into Their Mechanisms of Action. *J. Am. Chem. Soc.* **2007,** *129*, 13613-13625.
29. We note that Lipoxin A has been reported to inhibit LasR using an E. coli LasR reporter strain with a nanomolar IC50, but it only lowered LasR activity to 80% (relative to 100% activation by the native ligand). We are unaware of any other compound with a sub-micromolar IC50 in LasR and active in P. aeruginosa. See: Wu, B.; Capilato, J.N.; Pham, M.P.; Walker, J.; Spur, B.; Rodriguez, A.; Perez, L.J.; Yin, K. *FASEB J.*, **2016**, *30* (6), 2400-2410.

30. Moore, J. D.; Rossi, F. M.; Welsh, M. A.; Nyffeler, K. E.; Blackwell, H. E., A Comparative Analysis of Synthetic Quorum Sensing Modulators in Pseudomonas aeruginosa: New Insights into Mechanism, Active Efflux Susceptibility, Phenotypic Response, and Next-Generation Ligand Design. *J. Am. Chem. Soc.* **2015,** *137* (46), 14626-39.
31. Yates, E. A.; Philipp, B.; Buckley, C.; Atkinson, S.; Chhabra, S. R.; Sockett, R. E.; Goldner, M.; Dessaux, Y.; Camara, M.; Smith, H.; Williams, P., N-Acylhomoserine Lactones Undergo Lactonolysis in a pH-, Temperature-, and Acyl Chain Length-Dependent Manner during Growth of Yersinia pseudotuberculosis and Pseudomonas aeruginosa. *Infect. Immun.* **2002,** *70* (10), 5635-5646.
32. Yang, F.; Wang, L. H.; Wang, J.; Dong, Y. H.; Hu, J. Y.; Zhang, L. H., Quorum quenching enzyme activity is widely conserved in the sera of mammalian species. *FEBS Lett.* **2005,** *579* (17), 3713-7.
33. Muh, U.; Schuster, M.; Heim, R.; Singh, A.; Olson, E. R.; Greenberg, E. P., Novel Pseudomonas aeruginosa quorum-sensing inhibitors identified in an ultra-high-throughput screen. *Antimicrob. Agents. Chemother.* **2006,** *50* (11), 3674-9.
34. Jiang, Y.; Chen, X.; Zheng, Y.; Xue, Z.; Shu, C.; Yuan, W.; Zhang, X., Highly diastereoselective and enantioselective synthesis of alpha-hydroxy beta-amino acid derivatives: Lewis base catalyzed hydrosilylation of alpha-acetoxy beta-enamino esters. *Angew. Chem. Int. Ed. Engl.* **2011,** *50* (32), 7304-7.
35. Gerdt, J. P.; McInnis, C. E.; Schell, T. L.; Rossi, F. M.; Blackwell, H. E., Mutational analysis of the quorum-sensing receptor LasR reveals interactions that govern activation and inhibition by nonlactone ligands. *Chem. Biol.* **2014,** *21* (10), 1361-9.
36. Bottomley, M. J.; Muraglia, E.; Bazzo, R.; Carfi, A., Molecular insights into quorum sensing in the human pathogen Pseudomonas aeruginosa from the structure of the virulence regulator LasR bound to its autoinducer. *J. Biol. Chem.* **2007,** *282* (18), 13592-600.
37. Paczkowski, J. E.; McCready, A. R.; Cong, J. P.; Li, Z.; Jeffrey, P. D.; Smith, C. D.; Henke, B. R.; Hughson, F. M.; Bassler, B. L., An Autoinducer Analogue Reveals an Alternative Mode of Ligand Binding for the LasR Quorum-Sensing Receptor. *ACS Chem. Biol.* **2019,** *14* (3), 378-389.
38. McCready, A. R.; Paczkowski, J. E.; Henke, B. R.; Bassler, B. L., Structural determinants driving homoserine lactone ligand selection in the Pseudomonas aeruginosa LasR quorum-sensing receptor. *Proc Natl Acad Sci U. S. A.* **2019,** *116* (1), 245-254.
39. Passador, L.; Tucker, K. D.; Guertin, K. R.; Journet, M. P.; Kende, A. S.; Iglewski, B. H.; Functional Analysis of the *Pseudomonas aeruginosa* Autoinducer PAI. *J. Bacteriol.* **1996,** *178 (*20*)* 5995-6000.
40. McInnis, C. E.; Blackwell, H. E., Design, synthesis, and biological evaluation of abiotic, non-lactone modulators of LuxR-type quorum sensing. *Bioorg. Med. Chem.* **2011,** *19* (16), 4812-9.
41. Pearson, J. P.; Pesci, E. C.; Iglewski, B. H., Roles of *Pseudomonas aeruginosa las* and *rhl* Quorum-Sensing Systems in Control of Elastase and Rhamnolipid Biosynthesis Genes. *J. Bacteriol.* **1997,** *179* (18), 5756-5767.
42. Chugani, S. A.; Whiteley, M.; Lee, K. M.; D'Argenio, D.; Manoil, C.; Greenberg, E. P., QscR, a modulator of quorum-sensing signal synthesis and virulence in Pseudomonas aeruginosa. *Proc. Natl. Acad. Sci. U. S. A.* **2001,** *98* (5), 2752-7.
43. Lindsay, A.; Ahmer, B. M., Effect of sdiA on biosensors of N-acylhomoserine lactones. *J. Bacteriol.* **2005,** *187* (14), 5054-8.

44. Lee, J. H.; Lequette, Y.; Greenberg, E. P., Activity of purified QscR, a Pseudomonas aeruginosa orphan quorum-sensing transcription factor. *Mol. Microbiol.* **2006,** *59* (2), 602-9.
45. Wellington, S.; Greenberg, E. P., Quorum Sensing signal selectivity and the potential for interspecies cross talk. *mBio* **2019,** *10* (2), e00146-19.
46. Churchill, M. E. A.; Chen, L., Structural Basis of Acyl-homoserine Lactone-Dependent Signaling. *Chem. Rev.* **2011,** *111*, 68-85.
47. O'Reilly, M. C.; Dong, S. H.; Rossi, F. M.; Karlen, K. M.; Kumar, R. S.; Nair, S. K.; Blackwell, H. E., Structural and Biochemical Studies of Non-native Agonists of the LasR Quorum-Sensing Receptor Reveal an L3 Loop "Out" Conformation for LasR. *Cell Chem. Biol.* **2018**.
48. Zou, Y.; Nair, S. K., Molecular basis for the recognition of structurally distinct autoinducer mimics by the Pseudomonas aeruginosa LasR quorum-sensing signaling receptor. *Chem. Biol.* **2009,** *16* (9), 961-70.
49. Wysoczynski-Horita, C. L.; Boursier, M. E.; Hill, R.; Hansen, K.; Blackwell, H. E.; Churchill, M. E. A., Mechanism of agonism and antagonism of the Pseudomonas aeruginosa quorum sensing regulator QscR with non-native ligands. *Mol. Microbiol.* **2018,** *108* (3), 240-257.
50. Chen, G.; Swem, L. R.; Swem, D. L.; Stauff, D. L.; O'Loughlin, C. T.; Jeffrey, P. D.; Bassler, B. L.; Hughson, F. M., A strategy for antagonizing quorum sensing. *Mol. Cell* **2011,** *42* (2), 199-209.
51. Suneby, E. G.; Herndon, L. R.; Schneider, T. L., Pseudomonas aeruginosa LasR.DNA Binding Is Directly Inhibited by Quorum Sensing Antagonists. *ACS Infect. Dis.* **2017,** *3* (3) 183-189.
52. Morkunas, B.; Galloway, W. R.; Wright, M.; Ibbeson, B. M.; Hodgkinson, J. T.; O'Connell, K. M.; Bartolucci, N.; Della Valle, M.; Welch, M.; Spring, D. R., Inhibition of the production of the Pseudomonas aeruginosa virulence factor pyocyanin in wild-type cells by quorum sensing autoinducer-mimics. *Org. Biomol. Chem.* **2012,** *10* (42), 8452-64.
53. Sappington, K. J.; Dandekar, A. A.; Oinuma, K.; Greenberg, E. P., Reversible signal binding by the Pseudomonas aeruginosa quorum-sensing signal receptor LasR. *MBio* **2011,** *2* (1), e00011-11.
54. Gerdt, J. P.; McInnis, C. E.; Schell, T. L.; Blackwell, H. E., Unraveling the contributions of hydrogen-bonding interactions to the activity of native and non-native ligands in the quorum-sensing receptor LasR. *Org. Biomol. Chem.* **2015,** *13* (5), 1453-62.
55. Gerdt, J. P.; Blackwell, H. E., Competition studies confirm two major barriers that can preclude the spread of resistance to quorum-sensing inhibitors in bacteria. *ACS Chem. Biol.* **2014,** *9* (10), 2291-9.
56. Sully, E. K.; Malachowa, N.; Elmore, B. O.; Alexander, S. M.; Femling, J. K.; Gray, B. M.; DeLeo, F. R.; Otto, M.; Cheung, A. L.; Edwards, B. S.; Sklar, L. A.; Horswill, A. R.; Hall, P. R.; Gresham, H. D., Selective chemical inhibition of agr quorum sensing in Staphylococcus aureus promotes host defense with minimal impact on resistance. *PLOS Pathog.* **2014,** *10* (6), e1004174.

# CHAPTER 3: New abiotic inhibitors of the *Pseudomonas aeruginosa* quorum sensing receptor LasR discovered in a high-throughput screen

Daniel E. Manson, Gene E. Ananiev, Song Guo, Spencer S. Erickson, and Helen E. Blackwell

To be submitted to *ACS Chemical Biology*

D.E. Manson and H.E. Blackwell designed experiments. G.E. Ananiev and S. Guo assisted with expertise for conducting the high throughput screen. S. S. Erickson conducted molecular docking experiments. D.E. Manson performed reporter gene experiments and analyzed the data. D.E. Manson and H.E. Blackwell wrote the chapter.

## Abstract

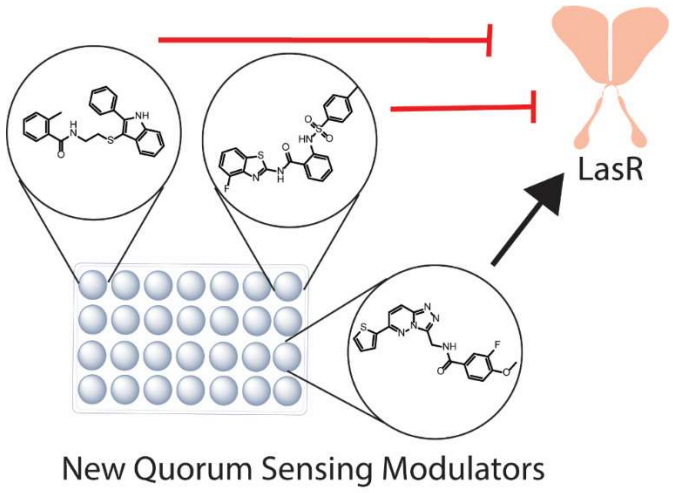


The opportunistic pathogen *Pseudomonas aeruginosa* controls myriad aspects of virulence via a bacterial cell-to-cell chemical communication system known as quorum sensing (QS). Small molecules that inhibit QS in *P. aeruginosa* would be useful tool compounds to study the role of this signaling pathway in infection and interrogate its viability of as an approach to block virulence. However, nearly all compounds known to target QS in *P. aeruginosa* are of low potency and have structural liabilities that limit their application in biologically relevant environments. Here, we report the results of a high-throughput screen for new small molecules that target LasR, a key QS regulator in *P. aeruginosa*. We screened a 25,000-compound library and discovered four new structural classes of LasR modulators. These compounds include antagonists that surpass the potency of all known *N*-acylated homoserine lactone-based antagonists and could serve as robust starting points as scaffolds for further probe optimization.

**Introduction**

Many bacteria communicate using low molecular weight molecules, or "autoinducers", in a phenomenon known as quorum sensing (QS).[1] This cell-to-cell signaling process allows populations of bacteria to gauge their local densities and engage in group-beneficial behaviors at high number, some of which are relevant to human health, agriculture, and industrial processes.[2] Our research group and others are actively involved in the development of small molecule and peptide tools to intercept these pathways and understand their role in infection and host-microbe interactions.[3]

The archetypal QS circuit in Gram-negative bacteria is the LuxI/LuxR receptor/synthase pair, first characterized in the bioluminescent marine symbiont *Vibrio fischeri.*[4, 5] LuxI-type synthase enzymes catalyze the formation of *N*-acyl L-homoserine lactone (AHLs), which is produced at low basal levels at low cell density. At a sufficient concentration of AHL (and thus bacterial cell number), these low molecular weight ligands bind to and activate intracellular LuxR-type receptors. Once complexed with their AHL signal, these transcription factors then typically dimerize and bind to DNA in response, altering QS controlled gene expression.

*P. aeruginosa* is a common Gram-negative pathogen that regulates much of its virulence (i.e., ability to infect) via QS.[6, 7] It has a high rate of antibiotic resistance and is dangerous to immunocompromised, particularly cystic fibrosis (CF), patients. The intimate relationship between virulence and QS in *P. aeruginosa* has motivated considerable research toward the discovery of chemical entities capable of blocking QS in this pathogen, and thereby potentially infections.[8-13]

The QS circuity in *P. aeruginosa* is comprised of at least two complete LuxI/R pairs (LasI/R and RhlI/R), QscR (an "orphan" LuxR type receptor without a related synthase), and

PqsE (a LysR-type receptor). LasI produced *N*-(3-oxo)-dodecanoyl L-homoserine lactone (OdDHL), which is bound by both LasR and QscR.[14] RhlI produces *N*-butyryl L-homoserine lactone (BHL), which is bound by RhlR.[15] PqsR binds the Pseudomonas Quinolone Signal (PQS), 2-heptyl-3-hydroxy-4-(1*H)*-quinolone, which is synthesized by a dedicated biosynthetic gene cluster.[16] These four receptors work together to finely tune *P. aeruginosa* QS in response to environmental queues.[17]

Among these interconnected QS systems, LasR plays a prominent role in *P. aeruginosa*.[15] The receptor regulates the production of virulence factors such as elastase B and alkaline protease.[14] It also upregulates production of rhamnolipid, HCN, and pyocyanin via control of the Rhl and Pqs systems.[6] Accordingly, significant effort has been devoted to the identification of small molecules that can antagonize the activity of LasR, the most common mechanism being to block its native AHL signal, OdDHL, from binding. To find such ligands, the OdDHL scaffold has been studied and derivatized extensively.[18-20] However, these efforts focused on AHL type ligands have failed to produce a LasR antagonist with an $IC_{50}$ value under 10 μM in *P. aeruginosa* based on LasR gene reporter assays.[10] This failure is at least in part due to chemical and biological liabilities inherent to the AHL scaffold. AHLs, both naturally occurring and non-native, are actively effluxed from *P.* aeruginosa by the MexAB-OpRM multidrug efflux pump.[21, 22] Additionally, the lactone ring is prone to hydrolysis in aqueous media, and *P. aeruginosa* contains enzymes that hydrolyze the lactone and amide bonds, rendering the compounds inactive.[23] These liabilities have motivated our laboratory[24, 25] and others[26, 27] to develop QS modulators of Gram-negative bacteria that are not based on the AHL scaffold.[24]

Past work has shown that high-throughput screening (HTS) of small molecule libraries can provide a strategy to discover non-AHL-type QS modulators (**Figure 2.1**). LasR has been the focus of all past HTS efforts to uncover antagonists and agonists of LuxR-type receptors in *P. aeruginosa*. The Greenberg lab has made notable contributions in this area, discovering both V-06-018, the most potent LasR antagonist known at the time of its discovery in 2006 (LasR $IC_{50}$ = 2 μM) and the triphenyl (TP) series of ligands.[28, 29] This series contains the agonist TP-1, which surpasses LasR's native ligand OdDHL in potency ($EC_{50}$ = 70 nM), and TP-5, a LasR antagonist with modest ($IC_{50}$ = 69 μM) potency. Rahme and co-workers have applied HTS very successfully to develop inhibitors of PqsR, such as M64.[11] Virtual screening has also been applied to identify QS modulators in *P. aeruginosa*. 8-Azaguanine, identified *in silico* to bind LasR, was found to antagonize LasR in cell-based gene reporter assays and abrogate QS-controlled phenotypes in *P. aeruginosa*, albeit at high μM concentrations.[30] Many other compounds have been predicted *in silico* to bind LasR, but have yet to be validated experimentally.[31]

Several modulators of LasR discovered via HTS have served as starting points for the development compounds with improved activities or alter properties, including the TP series[25, 32, 33] and V-06-018. Very recently, our laboratory reported a LasR antagonist with a submicromolar $IC_{50}$ that we developed while studying the structure-activity relationships (SARs) surrounding V-06-018's activity profile in LasR.[34] However, improved potency is not everything; the lead compounds from that study are highly lipophilic and cannot be readily diversified further, which will limit their application as probes in certain biological settings. We therefore remain interested in discovering novel non-AHL scaffolds that are (1) highly potent at modulating LasR in *P. aeruginosa* based assays ($IC_{50}$ values in the single-digit μM or lower), (2) free of hydrolytically

and enzymatically labile bonds, (3) readily soluble in aqueous media, and (4) comprised of a structure that is amenable to further chemical diversification.

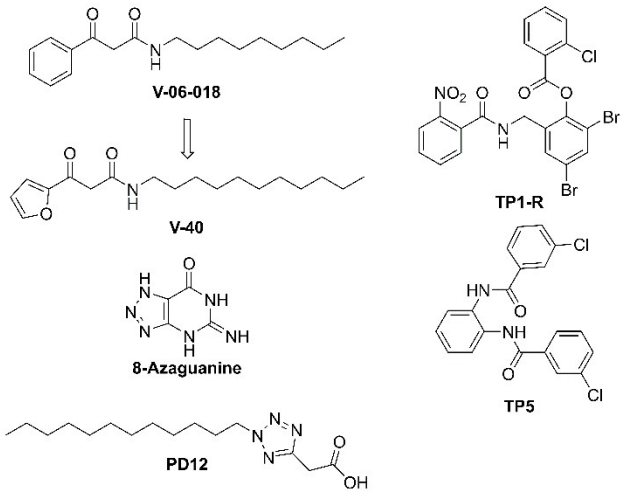


**Figure 3.1.** Selected abiotic small molecules discovered in high throughput screens that modulate the activity of LasR in *P. aeruginosa*. V-06-018,[29] PD12,[29] TP5,[28] and 8-Azaguanine[30] antagonize LasR; TP1-R[28] agonizes LasR.

The present study describes our pursuit of this goal via the screening a 25,000-compound library in a *P. aeruginosa*-based LasR gene reporter assay. We describe the discovery of nine of structurally distinct LasR modulators, including several antagonists with $IC_{50}$ values below 1 μM. We also provide insight into the possible binding mode of these compounds to LasR via molecular docking experiments.

**Results**

**Implementation and execution of a high throughput screen.**

We chose to perform our HTS study in the commonly used *P. aeruginosa*-based LasR gene reporter strain PAO-JP2 (△*lasIrhlI*).[14] This mutant strain lacks the ability to synthesize its own AHLs, but contains the MexAB-OprM efflux pump mentioned above.[21] We wanted the pump to be present in our screening system, as we were most interested in chemical scaffolds that are not

readily effluxed from *P. aeruginosa*. We initiated our study by miniaturizing the assay from a 96- to 384-well microplate format. The principal difficulty in this process was the accumulation of biofilm in the low volume wells, which was overcome by starting the assay at a low cell density (see Experimental section).

We screened the commercial 25,000 compound LifeChem 4 diversity library at a concentration of 10 μM. We identified 172 structures (~0.7% hit rate) that either inhibited *or increased* LasR activity ≥15% relative to our controls. These compounds then were selected for secondary screening in the reporter assay over a range of concentrations to obtain dose-response profiles. We approached our screening data cognizant of the danger posted by pan-assay interference compounds,[35, 36] and removed suspect structures as we triaged our hit compounds. Ultimately, we purchased a selection of the most potent hits and several of their commercially available analogues, in order to fully characterize their LasR activity profiles.

**Structures and activities of hit compounds.**

The structures of the nine hit compounds and related analogs are shown in **Figure 2.2,** and their antagonism and agonism activity profiles in LasR are listed in Table 2.1 (**Figure S1-2**). To the best of our knowledge, none of these compounds have been previously reported to modulate LuxR-type proteins or any other biological targets.

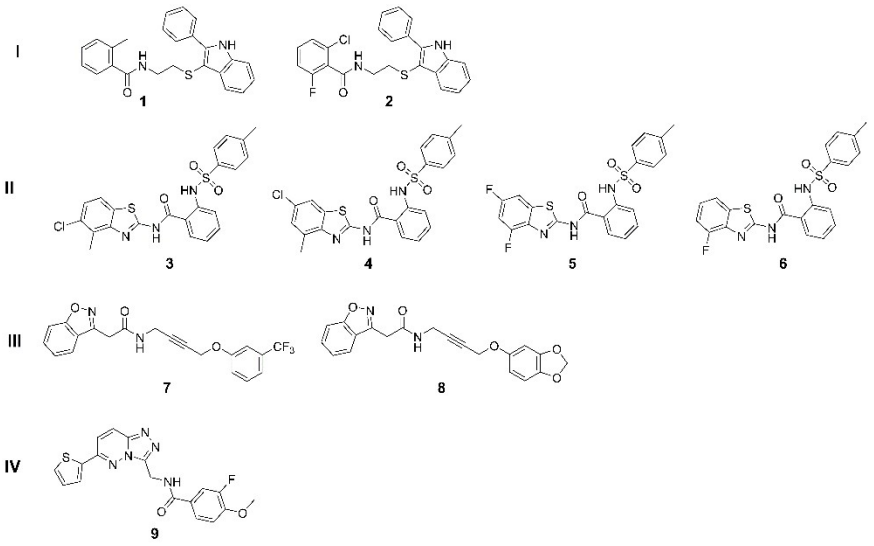


**Figure 3.2** Compounds the LifeChem 4 library that modulate LasR activity can be divided into four structural classes. Classes I–III (compounds **1**–**8**) antagonize LasR, while class IV (**9**) agonizes LasR.

**Table 3.1.** Potency and maximum LasR inhibition (efficacy) for HTS compounds and selected control compounds in *P. aeruginosa* reporter PAO-JP2[a]

| Compound | IC/$EC_{50}$ (μM)[b] | 95% CI (μM)[c] | Maximum Inhibition / Activation (%)[d] |
|---|---|---|---|
| | | *Antagonism* | |
| **1** | 3.5 | 2.5 – 4.9 | 51 |
| **2** | 2.7 | 1.6 – 4.6 | 55 |
| **3** | 0.8 | 0.3 – 2.1 | 38 |
| **4** | 2.4 | 1.2 – 4.7 | 38 |
| **5** | 1.0 | 0.6 – 1.6 | 54 |
| **6** | 1.8 | 1.4 – 2.4 | 72 |
| **7** | 0.4 | 0.3 – 0.6 | 62 |
| **8** | 18 | 13 – 25 | 84 |
| **9** | - | - | - |
| **CL**[e] | 21 | 11-39 | 55 |
| **V40**[f] | 0.2 | 0.2 – 0.3 | 85 |
| | | *Agonism* | |
| **1** | - | - | - |
| **2** | - | - | - |
| **3** | - | - | - |
| **4** | - | - | - |
| **5** | - | - | - |
| **6** | - | - | - |
| **7** | - | - | - |
| **8** | - | - | - |
| **9** | 0.7 | 0.6 – 1.0 | 100 |
| **OdDHL**[e] | 0.1 | 0.1 – 0.2 | 100 |
| **TP-1**[e] | 0.07 | 0.04 – 0.1 | 100 |

[a] See Experimental section for details of the reporter assay and data work-up. [b] Compounds **1**–**8** screened over a range of concentrations (100 μM – 46 nM); compound **9** screened for agonism over an expanded range (100 uM – 0.01 nM). Antagonism experiments conducted in competition against a fixed concentration of OdDHL (100 nM) and reported relative to activation by that concentration of OdDHL. Agonism data is reported relative to the activity of a saturating concentration of OdDHL (100 μM). $IC_{50}$ and $EC_{50}$ values calculated from three independent biological replicates. For full dose-response curves, see Figures S1 and S2. [c] CI = 95% confidence interval. [d] Maximum agonism and antagonism values represent the top and bottom values of the fitted curves. [e]Data from Moore *et al* 2015 using analogous assay conditions.[10] [f]Data from Manson *et al* 2020 using analogous assay conditions.[34]

We found three classes (I–III) of potent and efficacious LasR antagonists in our set of HTS hits (**Figure 2.2**). These antagonists have superior potencies in the *P. aeruginosa* experiment relative to all known AHL-based antagonists.[37] None of these compounds had an

effect on *P. aeruginosa* growth. (**Figure S3**). For comparison, we have included data for the most potent known AHL agonist and antagonist (OdDHL and CL [chlorolactone],[38] respectively), and non-AHL agonist and antagonist (TP-1 and V-40, respectively)[34] in Table 2.1.

Class I (**1** and **2**) had indistinguishable potencies of approximately 3 □M, suggesting a variety of *ortho* substituents on the benzamide moiety can be tolerated. Class II (**3**–**6**), which we term "triaryl" based on their resemblance to the TP series of ligands, had indistinguishable $IC_{50}$ values between 1 and 3 □M. These compounds differed, however, in maximum LasR inhibition; compound **6** had a higher efficacy than compounds **3** and **4**. We were struck by the structural similarity between compounds **3**–**6** and TP5 (**Figure 2.1**).[28] As in compounds **3**–**6**, the central ring of TP5 is unsubstituted apart from the linkers to the other rings. In contrast, the central ring of TPs 1-4, all of which are LasR agonists, are brominated at positions 2 and 4. Additionally, compounds **3**–**6**, like TP5, are linked by two-atom functional groups (an amide and a sulfonamide for **3**–**6** vs. two amides for TP5). The agonist TPs 1-4, however, have an extra methylene unit in the linker between the first and second ring, and an ester linking the second and third ring. Perhaps most notably, the triaryl compounds we report here are approximately 30x more potent than TP5 in *P. aeruginosa* (TP-5 $IC_{50}$ = 69 μM). Further synthetic chemistry can clarify whether this improvement in potency is a function of the different ring identity (phenyl vs. benzothiazole), substituents on the rings, or the functional groups that link them (i.e., ester vs. sulfonamide).

The class III compounds contained both our most potent LasR antagonist, **7**, and our most efficacious LasR antagonist, **8** (**Figure 2.2, Table 2.1**). Despite its efficacy, **8** was the least potent of the hit compounds we evaluated. These results for **7** and **8** indicate that substitution on

the aryl ether moiety plays a large role in determining the activity profile of this class of compound.

The single class IV compound **9**, when screened in a competitive antagonism experiment, was actually found to *increase* GFP production relative to controls (Figure S1). We therefore quantified its LasR agonism profile, along with those of compounds **1**-**8** to complete their assessment. Only compound **9** had activity in this assay, and was found to be relatively potent LasR agonist ($EC_{50}$ = 0.7 μM; **Figure S2**). To our knowledge, only OdDHL, very closely related AHL analogues (i.e., 3-oxo-C11 HL) and TP-1 have sub-micromolar agonism potencies in *P. aeruginosa* reporter systems. Compound **9** therefore represents an important new LasR agonist scaffold with substantial potential for derivatization.

**Screening in *E. coli* confirms hit activity in LasR.**

We conducted our primary screen in a *P. aeruginosa* strain because we are interested in the use of these compounds as probes of LasR in its native environment. To verify that these compounds target LasR directly, we used a heterologous (*E. coli*) LasR reporter system (i.e., the △*SdiA* strain JLD271, harboring pJN105L + pSC11-L; see Experimental sections),[39] in which LasR is isolated from the remainder of the *P. aeruginosa* QS circuitry. Our compounds largely retained their activities in this system, confirming that they target LasR directly (**Figure S4 and S5, Table S2**).[40]

We do note that the potency and efficacy of compounds **1**–**8** was reduced in the *E. coli* LasR reporter relative to in the *P. aeruginosa* LasR reporter system. We ascribe this phenomenon, which we have observed previsisuly,[10, 34] to the increased amount of LasR produced in the heterologous system relative to native production from the bacterial genome.[34, 41]

In turn, receptor overexpression has been shown previously to *increase* the apparent potency of agonists.[41] Indeed, agonist **9** was two orders of magnitude more potent in *E. coli* relative to *P. aeruginosa* ($EC_{50}$ values of 700 vs. 8 nM, respectively). Additionally, compounds **6**–**8**, all of which were incapable of agonizing LasR in the *P. aeruginosa* system were found to moderately agonize it in the *E. coli* system (**Figure S4**). These compounds are therefore best characterized as partial agonists, with agonism profiles too weak to be measured in the *P. aeruginosa* background.

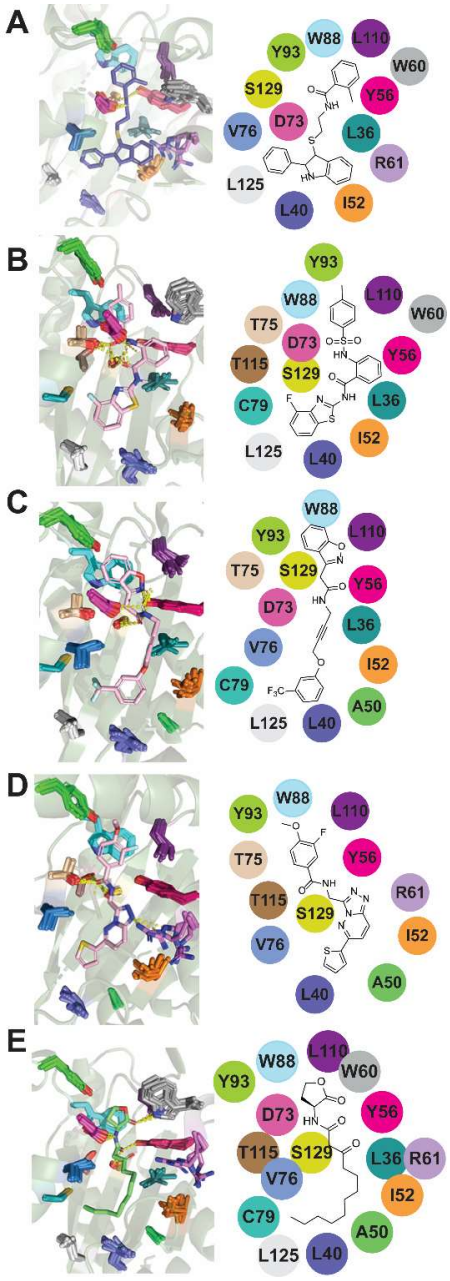


**Figure 3.3.** Views of representative compounds from each structure class computationally docked into an ensemble of LasR LBD structures (PDB IDs 2UV0, 3IX3, 3IX4, 3IX8, 3JPU, 6D6A, 6D6B, 6D6C, 6D6D, 6D6L, 6D6M, 6D6N, 6D6O, 6D6P, 6MWH, 6MWL, 6MWW ).[42] (**A**) Compound **1**; (**B**) compound **6**; (**C**) compound **7**, and (**d**) compound **9**. A view of OdDHL from the [LasR LBD:OdDHL]$_2$ crystal structure[43] is included for comparison in (**E**). Three-dimensional and two-dimensional views are shown at left and right, respectively; residues that flank the compound are indicated in each view in matching colors. Putative hydrogen-bonding interactions are indicated by yellow dashes. These poses represent the highest-docking-score (i.e., lowest energy) poses for each ligand. See Methods section for experimental details regarding docking experiments.

**Molecular docking provides insights into protein-ligand interactions**.

To investigate molecular details of the LasR:ligand interaction, we docked selected hit compounds from each structural class (**1**, **6**, **7,** and **9**) into the OdDHL binding site of LasR (**Figure 2.3**). We used the reported LasR ligand-binding domain (LBD):OdDHL structures reported by the Carfi, Bassler, Nair, and our own groups.[32, 43-45] Given that all reported structures of LuxR-type proteins complexed with both AHL and non-AHL ligands show the small molecule bound to the AHL-binding site,[43, 46, 47] we reasoned that our new ligands likely bind there as well in LasR.

Our docking experiments enabled us to identify portions of the molecules that are analogous to the AHL "head group" and "tail". The AHL:LasR interaction is mediated in part by a series of hydrogen bonds, the most important of which is between the amide N-H and Asp 73.[48, 49] Our docking indicate that analogous hydrogen bonds exist between the amide N-H protons in **1**, **7**, and **9**, and the sulfonamide N-H proton in **6**, and LasR residues including Asp 73, Thr 115, and Ser 129. These residues are also known to form hydrogen bonds with other heteroatoms in the AHL. Compounds **1**, **7**, and **9** extend into the portion of the binding cavity filled by the aliphatic acyl tail of OdDHL and abut against the hydrophobic residues that seal the binding site (i.e., Leu 40, Leu 125, A50). These docking data indicate that these LasR residues likely bind **1**, **6**, **7,** and **9** in a manner that is broadly similar to AHLs (i.e., mediated by the same residues and analogous hydrogen bonds). Further characterization of this binding interaction (i.e., structural experiments and mutagenesis) are ongoing in our laboratory and will be reported in due course.

**Discussion**

This project was motivated by the need for potent and efficacious tool compounds that inhibit the key QS regulator LasR in the opportunistic pathogen *P. aeruginosa*. AHL-based antagonists are poorly active in *P. aeruginosa*-based assays, and few non-AHL antagonists are known. Here, we report the discovery of eight new LasR antagonists and one new LasR agonist that are distinct from the AHL structure. Each of these antagonists exceeds the potency of all known AHL-based LasR antagonists in a *P. aeruginosa* cell-based gene reporter experiment, underscoring the advantage of non-AHL-derived antagonists. We believe that the activity of molecules based on each of these scaffolds can likely be enhanced by synthetic chemistry campaigns.

The similarity between the Class II compounds reported here and the previously reported TP series of ligands is striking; the reoccurrence of this chemotype in two different high throughput screens underscores its utility as a modulator of LasR activity. Our docking data indicate that the ligands from classes I, III, and IV likely adopt poses that are analogous to AHLs, with a carbocyclic or heterocyclic "headgroup" packed into the same residues that surround the homoserine lactone, and an amide bond (or sulfonamide) making polar contacts with polar residues that hydrogen bond the amide joining the HSL to the acyl tail (i.e., Asp 73, Ser 129, and Thr 115). It is likely that screening additional, larger libraries could result in the discovery of related classes of molecules (i.e., cyclic moieties joined by amides and other carbonyl functional groups); of course, completely new scaffolds could be identified also. The discovery and exploitation of such compounds represents a path forward for the QS field to move away from AHL-based antagonists and develop highly potent and chemically robust modulators of QS in Gram-negative bacteria.

**Acknowledgements**
Financial support for this work was provided by the NIH (R35 GM131817).

## Materials and Methods

### Compound handling

Compounds stocks were prepared at appropriate concentrations in DMSO and kept frozen at -20 °C until use.

### Biology

A list of bacterial strains and plasmids used in this study is included in the supplemental information (Table S1). Bacteria were cultured in Luria-Bertani (LB) medium and grown at 37 °C. Cell growth was measured by absorbance at 600 nm ($OD_{600}$). Absorbance and fluorescence measurements were made on a ThermoFisher Nanodrop 2000, a CLARIOstar® plate reader running MARS data analysis software, and a PerkinElmer EnVision plate reader running Envision Manger software. Dose response curves were prepared using GraphPad Prism version 8.3.1.

### *P. aeruginosa* Assay protocol

A 2 mL culture of LB media with 300 μg/mL carbenicillin was inoculated with a single colony of *P. aeruginosa* reporter strain PAO-JP2 and grown overnight. The next morning, overnight culture was diluted 1:100 into fresh LB and grown until $A_{600}$, measured on a nanodrop, = 0.3 AU. While the subculture was growing, 2 μL of compound stocks at appropriate concentrations were manually dispensed into the interior wells of a black 96 well plate. When culture reached the appropriate density, 198 μL were dispensed into the interior wells. Plates were incubated for 6h at 37 °C, at which point fluorescence and absorbance were read. See supplemental

information for modified high throughput screening assay protocol and additional experimental details.

### *E. coli Assay* protocol

A 10 mL culture of LB media with 100 µg/mL and 10 µg/mL gentamicin was inoculated with a single colony of *E. coli* reporter strain JLD271 (pJN105-L, pSC11-L) and grown overnight. The next morning, overnight culture was diluted 1:10 into fresh LB and supplemented with fresh antibiotics. Culture was grown until $A_{600}$, measured on a nanodrop, reached 0.5, at which point 0.4% w/v arabinose was added. While culture grew, 2 µL of compound stocks in DMSO at the appropriate concentration was added to the interior wells of a clear 96 well plate. 198 µL of culture was added, and plate were incubated for 4h. After incubation, miller assay was performed as described previously.[34] See the experimental section for additional details.

### Molecular Docking

Compounds **1-9** were docked into an ensemble of LasR crystal structures using SMINA.[50, 51] The resultant poses were clustered by the Butina-Taylor[52] method and the best-scored pose from the largest cluster is shown in Figure 2.3. See SI for a detailed description of docking methods.

## ASSOCIATED CONTENT

Supplemental information (Details on strains and plasmids, expanded experimental protocols and full dose-response curves) is available free online.

## General instrumentation information

Absorbance measurements were made using a Fisher Scientific Nanodrop 2000, absorbance and fluoresence measurements were made using a CLARIOstar® plate reader running MARS data analysis software, and a PerkinElmer Envision plate reader running Envision Manager Software.

**Table S3.1:** Bacterial strains and plasmids used in this study[a]

| Strain or Plasmid | Description | Ref. |
|---|---|---|
| *E. coli* | | |
| JLD271 | K-12 Δ*lacX74 sdiA271*::CAM; $Cl^R$ | [1] |
| *P. aeruginosa* | | |
| PAO-JP2 | PAO1 *lasI::Tet rhlI::Tn501-2;* $Hg^R$ $Tc^R$ | [2] |
| *Plasmids* | | |
| p*lasI*-LVAGFP | *lasI'-gfp* [LVA] transcriptional fusion; $Cb^R$ | [3] |
| pSC11-L | Broad host range *lasI'-lacZ* reporter; $Ap^R$ | [4] |
| pJN105L | Arabinose-inducible *lasR* expression vector; pBBRMCS backbone; $Gm^R$ | [5] |

[a]Abbreviations: $Cl^R$ = Chloramphenicol resistance; $Hg^R$ = Mercury resistance; $Tc^R$ = tetracycline resistance; $Ap^R$ = Ampicillin resistance; $Gm^R$ = Gentamicin resistance; $Cb^R$ = Carbenicillin resistance

## Reporter assay protocols

### *E. coli* reporter assays (β-galactosidase)

LasR activity was measured in *E. coli* reporter strain JLD271 as previously described.[6-10]. A 10 mL culture of LB with 100 µg/mL ampicillin and 10 µg/mL gentamicin was inoculated with a single colony of JLD271 transformed with pSC11-L (*lacZ* reporter plasmid, **Table S1**) and pJN105-l (LasR) and grown overnight at 37 °C with shaking at 200 rpm. The next day, overnigh culture was diluted 1:10 in fresh LB medium with fresh antibiotics to $A_{600}$ = 0.5 as measured on

a Nanodrop 2000. Compound stock solution in DMSO were added to the interior wells of a clear 96-well microtiter plate (Costar 3370), with final DMSO concentrations <1%.

*For antagonism assays*, DMSO was dispensed into 12 wells on each plate (for use as positive and negative controls). Once subculture reached the appropriate density, 0.4% (w/v) arabinose was added to induce expression of pJN105. Six DMSO containing wells were filled with 198 µL of this subculture as a negative control. The remainder of the culture was adjusted to a final concentration of 2 nM OdDHL and 198 µL aliquots of treated culture were added to all experimental wells and DMSO wells (as a positive control). The outer wells of the plate were filled with 200 µL of water (to help maintain the plate humidity and slow evaporation). Plates were incubated at 37 °C with shaking at 200 rpm for 4 h.

*For agonism assays,* 2 µL DMSO was added to six wells (for negative controls), and 2 µL of 10 mM OdDHL in DMSO were added to another six wells (for positive controls). Once subculture reached the appropriate $A_{600}$, arabinose was added to a final concentration of 0.4% (w/v). Aliquots (198 µL) of this subculture were dispensed into all internal wells. The outer wells of the plate were filled with 200 µL of water (to help maintain the plate humidity/environment and slow evaporation). Plates were incubated at 37 °C with shaking at 200 rpm for 4 h.

Approximately 20 minutes before the end of the incubation period, each interior well of a fresh, chemical-resistant 96 well plate (Costar 3879) was filled with 200 µL Z buffer, 8 µL $CHCl_3$, and 4 µL 0.1% aqueous SDS. After incubation ended, the $OD_{600}$ of each culture plate was measured on a PerkinElmer Envision plate reader. A 50-µL aliquot of each culture-containing well in the

initial plate was transferred to the lysis-buffer containing chemical resistant plate and lysed by aspirating 20 times.

A 100-µL aliquot from each well was transferred to a fresh, clear-bottom 96-well plate. The Miller assay[11] was started by adding 20 µL of substrate *ortho*-nitrophenyl-β-galactoside (ONPG, 0.4% [w/v] in phosphate buffer) to each well. Then, the plates were incubated static at 30 °C for 30 minutes. The reaction was quenched by the addition of 50 µL of sodium carbonate (1M in water) to each well. Absorbances at 420 and 550 nm were measured for each well. Miller units were calculated according to the following formula:

$$Miller\ unit = \frac{1000 * \left(A420 - (1.75 * A550)\right)}{t * v * OD600}$$

$t$ = time ONPG incubated with lysate in min (30)

$v$ = volume of culture lysed in mL (0.05)

Miller units were reported as a percentage relative to the OdDHL containing wells (*i.e.*, wells containing only agonist = 100% activity). All assays were conducted as technical triplicates and performed at least three times (*i.e.*, three biological replicates). Dose-response curves were generated using three-parameter fits with Graphpad Prism software (version 8).

***P. aeruginosa* PAO-JP2 reporter assay (GFP*)***

**High throughput screening (i.e. 384 well plate) protocol**

The LasR assay in *P. aeruginosa* PAO-JP2 was adapted to 384 well plates for screening the LifeChem 4 diversity library. Appropriate volumes of DMSO stocks of experimental and control compounds were dispensed into black 384 well plates using an Echo 550 liquid handler from LabCyte Inc. All primary screening was conducted at 10 μM. Each plate contained wells with only a known antagonist (V-06-018), only DMSO, and only a known antibiotic (ciprofloxacin). The night prior to initiating a primary screening experiment, 2 mL of LB media was inoculated with a single colony of PAO-JP2 (p*lasI*-LVAGFP) and 300 μg/mL carbenicillin. The next day, overnight culture was diluted in fresh LB to OD = 0.094, then diluted a further 1:900 fold. This dilute culture was then divided, and a portion was treated with OdDHL to a final concentration of 300 nM.

This dilute culture was plated into 384 well plates using a Thermo Scientific Multidrop liquid handling robot. Culture treated with OdDHL was dispensed into wells containing experimental compounds and V-06-018; untreated culture was dispensed into wells containing ciprofloxacin and DMSO. Plates were then incubated static for approximately 21 hours, at which point GFP (excitation at 470 nm, emission at 515 nm) and $A_{600}$ were read. Data analysis was performed using the Collaborative Drug Discovery Vault platform.

After conducting the primary screen we conducted triage by secondary screening in dose/response format. The procedure was the same, except experimental compounds were plated at a variety of concentrations instead of 10 μM only.

**96 well plates protocol**

The *P. aeruginosa* PAO-JP2 LasR assay was performed as previously described with the following modifications.[10, 12] A 2-mL sample of LB medium containing 300 μg/mL Carbenicillin was inoculated with a single colony of PAO-JP2 and grown overnight (~16 h). Overnight culture

was diluted 1:100 in fresh LB medium without antibiotic and grown to an $A_{600}$ = 0.3, measured on a ThermoFisher Nanodrop 2000. Aliquots (2 µL) of test compound stock solution in DMSO were added to the interior wells of a black, clear-bottomed 96-well microtiter plate with final DMSO concentrations <1%. Appropriate controls, depending on assay type (see below) were added as well.

*Antagonism experiments*: DMSO (2 µL) was added to twelve wells on each plate. When subculture reached the appropriate density, it was divided, and OdDHL was added to one portion for a final concentration of 100 nM. Treated subculture (198 µL) was added to half of the DMSO containing wells and all experimental wells; untreated subculture was added to the remaining DMSO wells.

*Agonism experiments:* DMSO (2 µL) was added to six wells, and OdDHL (2 µL of 10 mM stock) was added to six addition wells. Subculture (198 µL with **no** OdDHL added) was dispensed to all experimental and control wells.

The outer wells of each plate were filled with 200 µL of water (to help maintain the plate humidity/environment and slow evaporation overall for the interior wells). Plates were then incubated at 37 °C without shaking for 6 h. After incubation, GFP levels (excitation at 485 nM, emission at 544 nM) and $OD_{600}$ were read using a plate reader. For agonism experiments, fluorescence data were reported relative to OdDHL-containing wells (i.e., wells containing only OdDHL = 100% activity); antagonism data were reported relative to wells containing DMSO and OdDHL-treated subculture (i.e., wells containing only 100 nM OdDHL *in culture* = 100%

activity). All assays were conducted as technical triplicates and performed at least three times (*i.e.*, three biological replicates).[13] Dose-response curves were generated as three-parameter fits to the data using Graphpad Prism software (version 8).

**Ensemble and Pose Consensus Docking.**

*Target Preparation*. 16 LasR protein crystal structure representations were obtained from RCSB (PDB Accession Codes: 2UV0, 3IX3, 3IX4, 3IX8, 3JPU, 6D6A, 6D6B, 6D6C, 6D6D, 6D6L, 6D6M, 6D6N, 6D6O, 6D6P, 6MWH, 6MWL, 6MWW). For structural comparison, given that the LasR crystal structures were typically in homooligomeric arrangements, all individual LasR ligand binding domain chains (with accompanying ligands) were isolated and aligned on an arbitrary reference domain, chain A from PDB accession 2UV0, in built-in cealign function in PyMOL (The PyMOL Molecular Graphics System, Version 1.7.6.0 Schrödinger, LLC). Crystallographic waters and ions were removed. A single chain was selected from each crystal structure to comprise 16 target representations for docking based on ascending chain identifier order in alphabetic sequence. After alignment, all crystallographic ligands in the orthosteric ligand binding pocket were extracted and saved in SD format and the apo protein chains were saved in PDB format. The 16 apo protein structure files were then processed in Chimera[14] (using the Dock Prep function to protonate and assign MMFF partial charges and output in mol2 format.

*Ligand Preparation*. Crystallographic ligands were protonated and assigned partial charges using pkatyper and molcharge (AM1BCC) utilities from OpenEye suite (QUACPAC 2.0.2.2: OpenEye Scientific Software, Santa Fe, NM. http://www.eyesopen.com). Nine additional compounds were

exported from ChemDraw in 2D SD format. The SD files were converted to SMILES using babel-3.3 (OpenEye Scientific), converted to 3D conformations in SD format with Omega2 (Hawkins et al., 2010, OMEGA 3.1.2.2: OpenEye Scientific Software, Santa Fe, NM. http://www.eyesopen.com), and converted to mol2 format with partial charges assigned by molcharge (AM1BCC).

*Ensemble Docking*. Each of the 9 ligands were docked to each of the 16 LasR target representations using Smina,[15] a fork of AutoDock Vina v1.1.2[16] in a typical ensemble approach.[17-18] Smina's autobox_ligand feature was used to specific the docking search space based on the co-crystallized ligand identified for each LasR structure using 5 Angstrom padding.

*Pose Consensus Analysis.* Output poses in SD format were processed using RDKit (RDKit: Open-source cheminformatics; http://www.rdkit.org) to include docking scores, pose rank, compound, and target representation saved as molecular property fields. For each compound, only top 3 scoring poses were saved when docking to each LasR target representation. This provides 16 targets * 3 poses/target = 48 total poses for each compound. Using a pose consensus approach,[19] we selected the most likely binding configurations for each compound based on the largest pose cluster observed among the compound's 48 total poses. The poses were clustered by the Butina-Taylor method[20] using pairwise RMSD as distance matrix and 2.5 Angstrom cutoff.

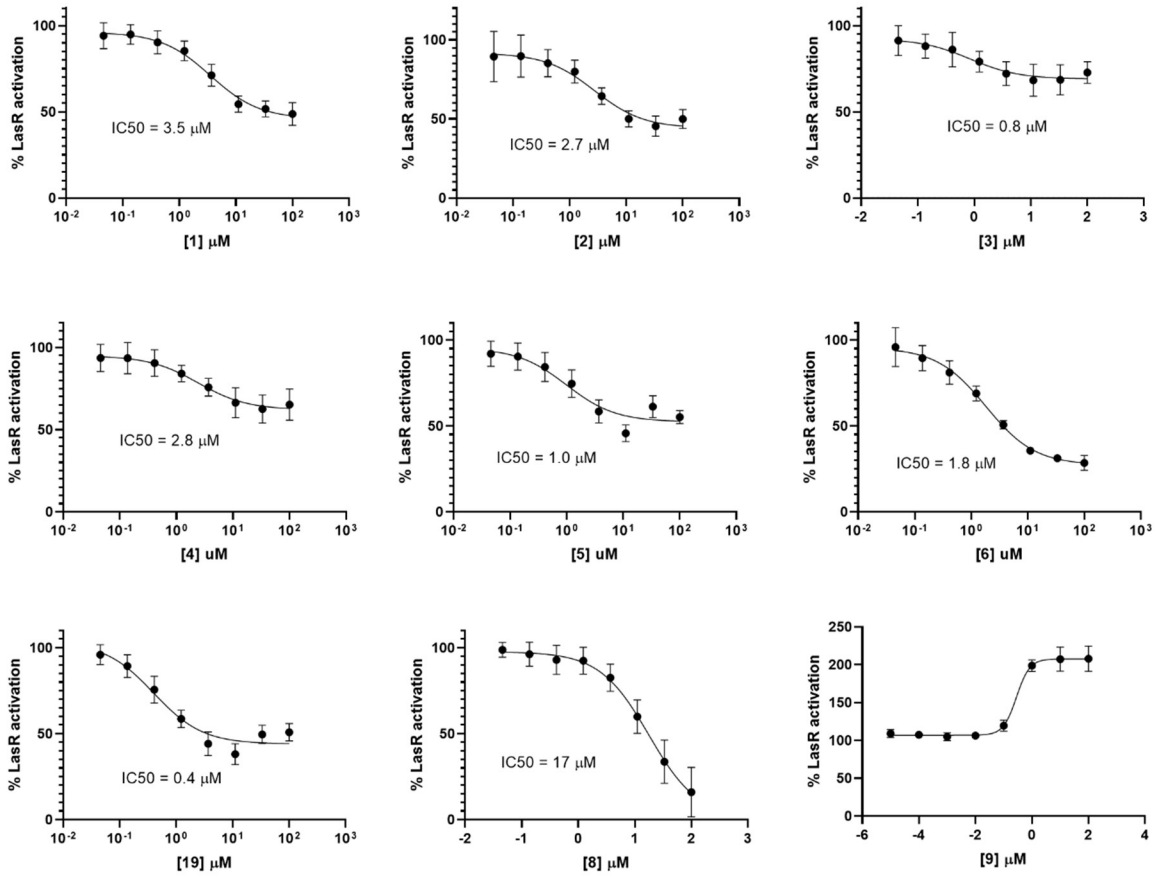


**Figure S3.1:** Dose-response antagonism assay data for selected compounds in the *P. aeruginosa* LasR reporter (PAO-JP2 + pLVA-GFP). Data from three biological replicates are plotted, each performed as three technical replicates. Error bars indicate SD.

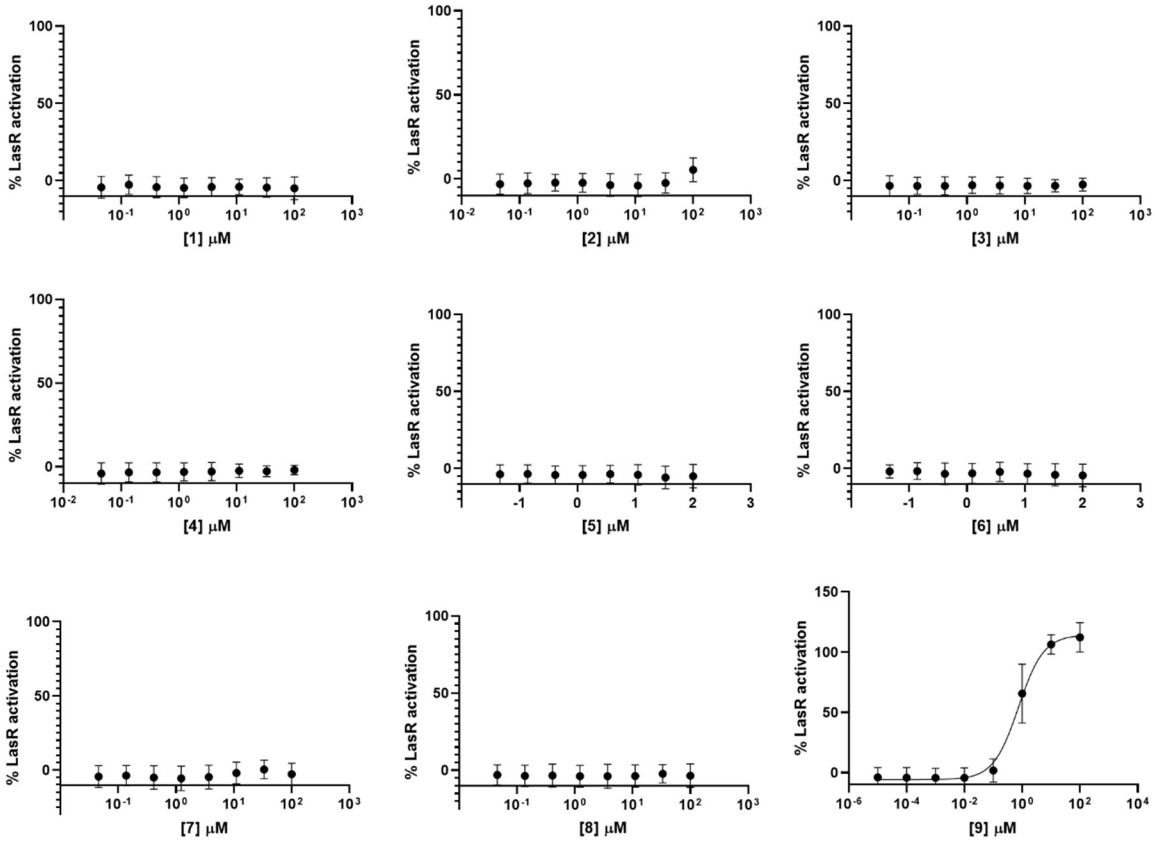


**Figure S3.2:** Dose-response agonism assay data for selected compounds in the *P. aeruginosa* LasR reporter (PAO-JP2 + pLVA-GFP). Data from three biological replicates are plotted, each performed as three technical replicates. Error bars indicate SD.

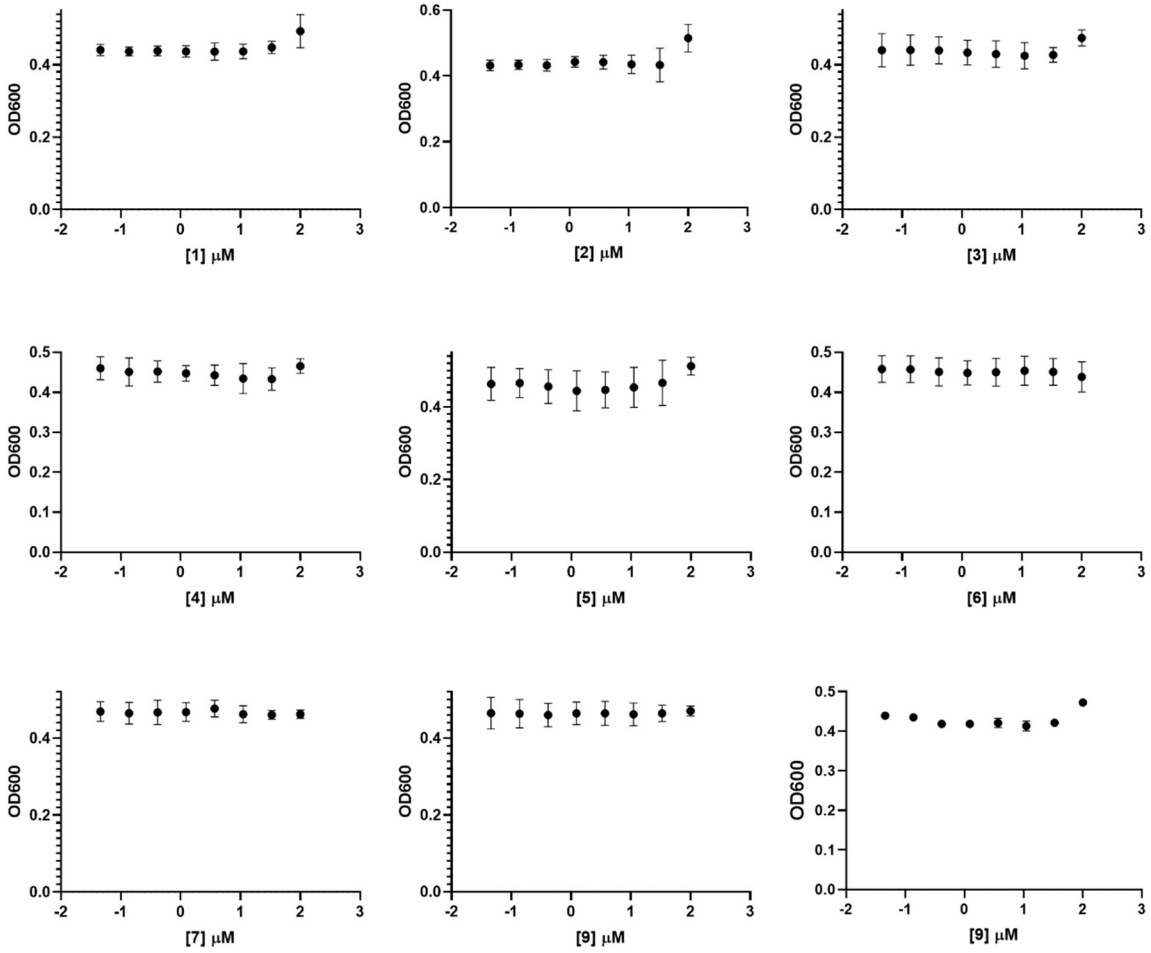


**Figure S3.3.** P. aeruginosa $OD_{600}$ values measured at the end of 6h incubation with compounds **1-9**. Compounds **1-9** did not affect the growth of *P. aeruginosa.*

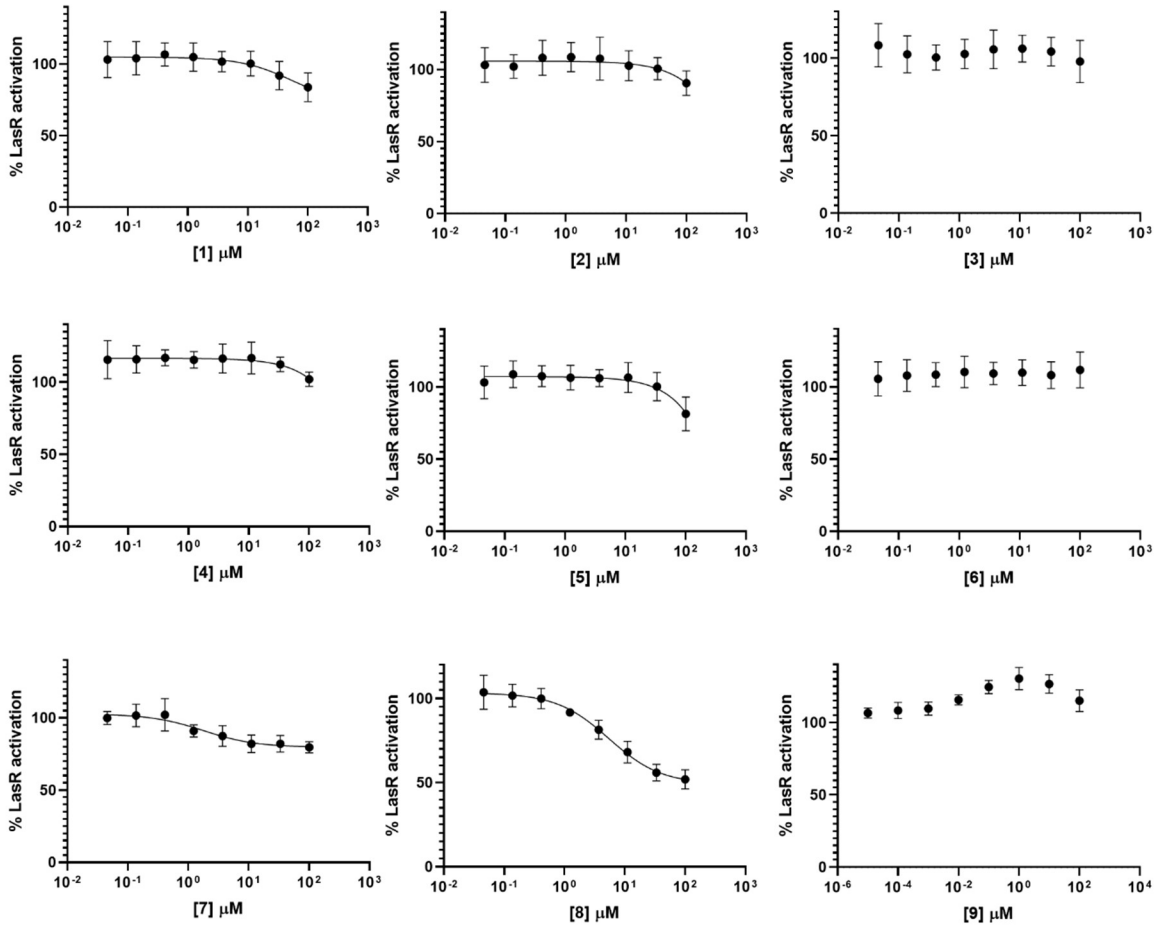


**Figure S3.4:** Dose-response antagonism curves in the *E. coli* LasR JLD271 (pJN105-L + pSC11-L). Data from three biological replicates are plotted, each performed as three technical replicates. Error bars indicate SD.

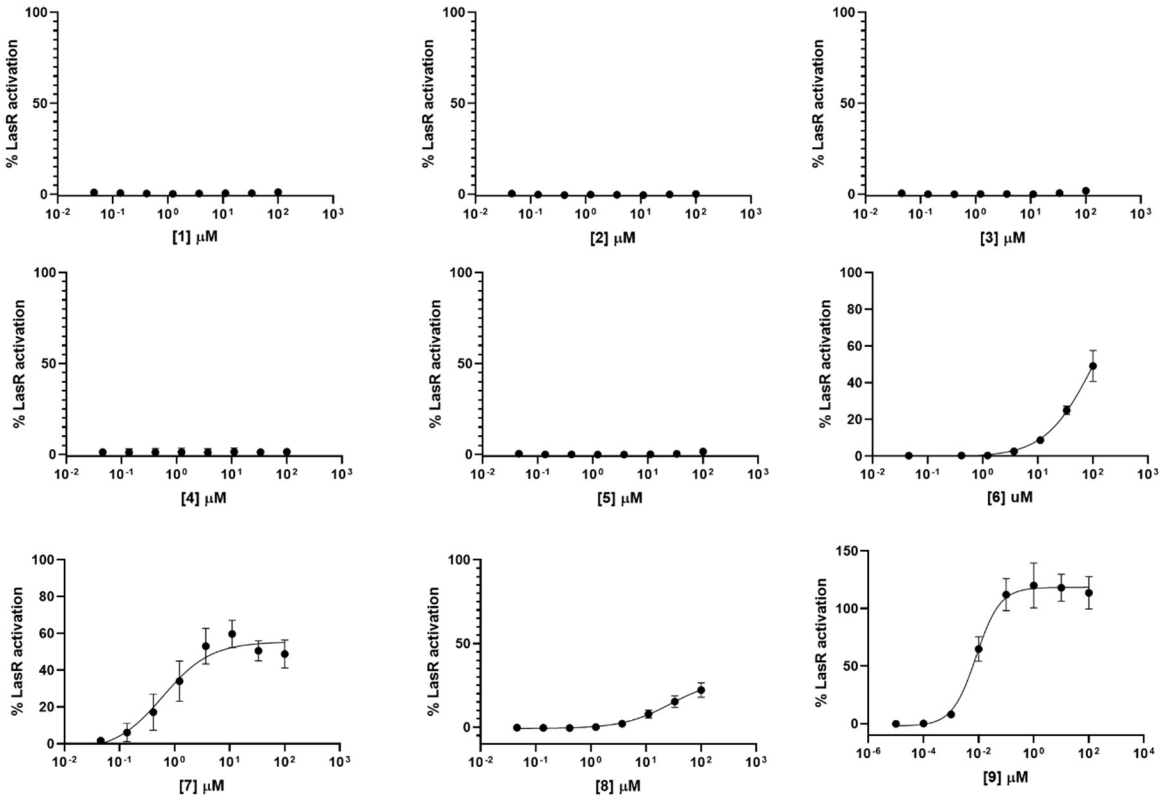


**Figure S3.5:** Dose-response agonism in the *E. coli* LasR JLD271 (pJN105-L + pSC11-L). Data from three biological replicates are plotted, each performed as three technical replicates. Error bars indicate SD.

**Table S3.2:** Potency and efficacy of selected compounds in the *E. coli* LasR reporters (from data in Figure S3 and S4)[a]

| Compound | EC/IC$_{50}$[b] (μM) | 95% CI of EC/IC$_{50}$ (μM)[c] | Maximum Inhibition (%)[d] |
|---|---|---|---|
| -Antagonism | | | |
| 1 | >100 | - | 17 |
| **2** | >100 | - | 10 |
| **4** | >100 | - | 0[e] |
| **5** | >100 | - | 19 |
| **7** | 1.7 | 0.8 – 4.0 | 20 |
| **8** | 5.4 | 3.8 – 7.7 | 49 |
| Agonism | | | |
| **6** | >100 | - | 49 |
| **7** | 0.6 | 0.4 – 0.9 | 48 |
| **8** | 28 | 20-39 | 22 |
| **9** | 0.008 | 0.006 – 0.01 | 100 |

[a]Antagonism experiments performed by competing the compounds against OdDHL at 2 nM. [b] Compounds **1**–**8** screened over a range of concentrations (100 μM – 46 nM); compound **9** screened for agonism over an expanded range (100 uM – 0.01 nM). [c]95% confidence interval is generated form a three-parameter fit to at least three biological replicates. [d]Indicates the maximum inhibition/activation observed at 100 μM. Antagonism % activity is reported relative to 10 nM OdDHL; agonism data is reported relative to 100 μM OdDHL. [e]100 μM of compound **4** modestly antagonized LasR activity relative to low concentrations of **4** (**see Figure S3**); however, error in the assay resulted in all wells with **4** having higher β-galactosidase activity than positive control wells.

**References for materials and methods**


1. Lindsay, A.; Ahmer, B. M., Effect of sdiA on biosensors of N-acylhomoserine lactones. *J Bacteriol* **2005,** *187* (14), 5054-8.
2. Pearson, J. P. P., E.C.; Iglewski, B.H., Roles of *Pseudomonas aeruginosa las* and *rhl* Quorum-Sensing Systems in Control of Elastase and Rhamnolipid Biosynthesis Genes. *Journal of Bacteriology* **1997,** *179* (18), 5756-5767.
3. De Kievit, T. R.; Gillis, R.; Marx, S.; Brown, C.; Iglewski, B. H., Quorum-sensing genes in Pseudomonas aeruginosa biofilms: their role and expression patterns. *Appl Environ Microbiol* **2001,** *67* (4), 1865-73.
4. Chugani, S. A.; Whiteley, M.; Lee, K. M.; D'Argenio, D.; Manoil, C.; Greenberg, E. P., QscR, a modulator of quorum-sensing signal synthesis and virulence in Pseudomonas aeruginosa. *Proc Natl Acad Sci U S A* **2001,** *98* (5), 2752-7.
5. Lee, J. H.; Lequette, Y.; Greenberg, E. P., Activity of purified QscR, a Pseudomonas aeruginosa orphan quorum-sensing transcription factor. *Mol Microbiol* **2006,** *59* (2), 602-9.
6. Eibergen, N. R.; Moore, J. D.; Mattmann, M. E.; Blackwell, H. E., Potent and Selective Modulation of the RhlR Quorum Sensing Receptor by Using Non-native Ligands: An Emerging Target for Virulence Control in Pseudomonas aeruginosa. *Chembiochem* **2015,** *16* (16), 2348-56.
7. O'Reilly, M. C.; Blackwell, H. E., Structure-Based Design and Biological Evaluation of Triphenyl Scaffold-Based Hybrid Compounds as Hydrolytically Stable Modulators of a LuxR-Type Quorum Sensing Receptor. *ACS Infect Dis* **2016,** *2* (1), 32-38.
8. Mattmann, M. E.; Shipway, P. M.; Heth, N. J.; Blackwell, H. E., Potent and selective synthetic modulators of a quorum sensing repressor in Pseudomonas aeruginosa identified from second-generation libraries of N-acylated L-homoserine lactones. *Chembiochem* **2011,** *12* (6), 942-9.
9. Gerdt, J. P.; McInnis, C. E.; Schell, T. L.; Blackwell, H. E., Unraveling the contributions of hydrogen-bonding interactions to the activity of native and non-native ligands in the quorum-sensing receptor LasR. *Org Biomol Chem* **2015,** *13* (5), 1453-62.
10. Manson, D. E.; O'Reilly, M. C.; Nyffeler, K. E.; Blackwell, H. E., Design, synthesis, and biochemical characterization of non-native antagonists of the Pseudomonas aeruginosa quorum sensing receptor LasR with nanomolar IC50 values. *ACS Infect Dis* **2020**.
11. Griffith, K. L.; Wolf, R. E., Jr., Measuring beta-galactosidase activity in bacteria: cell growth, permeabilization, and enzyme assays in 96-well arrays. *Biochem Biophys Res Commun* **2002,** *290* (1), 397-402.
12. Moore, J. D.; Rossi, F. M.; Welsh, M. A.; Nyffeler, K. E.; Blackwell, H. E., A Comparative Analysis of Synthetic Quorum Sensing Modulators in Pseudomonas aeruginosa: New Insights into Mechanism, Active Efflux Susceptibility, Phenotypic Response, and Next-Generation Ligand Design. *J Am Chem Soc* **2015,** *137* (46), 14626-39.
13. Tonge, P. J., Quantifying the Interactions between Biomolecules: Guidelines for Assay Design and Data Analysis. *ACS Infect Dis* **2019**.
14. Huang, C. C., Couch, G.S., Pettersen, E.F., and Ferrin, T.E. In *Chimera: An Extensible Molecular Modeling Application Constructed Using Standard Components.*, Pacific Symposium on Biocomputing, 1996; p 724.
15. Koes, D. R.; Baumgartner, M. P.; Camacho, C. J., Lessons learned in empirical scoring with smina from the CSAR 2011 benchmarking exercise. *J Chem Inf Model* **2013,** *53* (8), 1893-904.

16. Trott, O.; Olson, A. J., AutoDock Vina: improving the speed and accuracy of docking with a new scoring function, efficient optimization, and multithreading. *J Comput Chem* **2010,** *31* (2), 455-61.
17. Knegtel, R. M. A. K., I.D.; Oshiro, C.M., Molecular Docking to Ensembles of Protein Structures. *J. Mol. Biol.* **1997,** *266*, 424-440.
18. Lorber, D. M. S., B.K., Flexible ligand docking using conformational ensembles. *Protein Sci.* **1997,** *7*, 938-950.
19. Bottegoni, C. C., A.; Recanatini, M., A Comparative Study on the Application of Hierarchical-Agglomerative Clustering Approaches to Organize Outputs of Reiterated Docking Runs. *J. Chem. Info. Model.* **2006,** *46*, 852-862.
20. Butina, D., Unsupervised Data Base Clustering Based on Daylight's Fingerprint and Tanimoto Similarity: A Fast and Automated Way To Cluster Small and Large Data Sets. *J. Chem. Inf. Comput. Sci.* **1999,** *39*, 747-750.

**References**

1. Whiteley, M.; Diggle, S. P.; Greenberg, E. P., Progress in and promise of bacterial quorum sensing research. *Nature* **2017,** *551* (7680), 313-320.
2. Rutherford, S. T.; Bassler, B. L., Bacterial quorum sensing: its role in virulence and possibilities for its control. *Cold Spring Harb Perspect Med* **2012,** *2* (11).
3. Welsh, M. A.; Blackwell, H. E., Chemical probes of quorum sensing: from compound development to biological discovery. *FEMS Microbiol Rev* **2016,** *40* (5), 774-94.
4. Schaefer, A., Hanzelka BL, Eberhard A, Greenberg EP, Quorum Sensing in *Vibrio fischeri*: Probing Autoinducer-LuxR Interactions with Autoinducer Analogs. *Journal of Bacteriology* **1996,** *178* (10), 2897-2901.
5. Galloway, R. J. D. H., J.T.; Bowden, S.D.; Welch, M.; Spring, D.R., Quorum Sensing in Gram-Negative Bacteria: Small-Molecule Modulation of AHL and AI-2 Quorum Sensing Pathways. *Chem Rev* **2011,** *111*, 28-67.
6. Balasubramanian, D.; Schneper, L.; Kumari, H.; Mathee, K., A dynamic and intricate regulatory network determines Pseudomonas aeruginosa virulence. *Nucleic Acids Res* **2013,** *41* (1), 1-20.
7. Lee, J.; Zhang, L., The hierarchy quorum sensing network in Pseudomonas aeruginosa. *Protein Cell* **2015,** *6* (1), 26-41.
8. Valastyan, J. S.; Tota, M. R.; Taylor, I. R.; Stergioula, V.; Hone, G. A. B.; Smith, C. D.; Henke, B. R.; Carson, K. G.; Bassler, B. L., Discovery of PqsE Thioesterase Inhibitors for Pseudomonas aeruginosa Using DNA-Encoded Small Molecule Library Screening. *ACS Chem Biol* **2020**.
9. Boursier, M. E.; Moore, J. D.; Heitman, K. M.; Shepardson-Fungairino, S. P.; Combs, J. B.; Koenig, L. C.; Shin, D.; Brown, E. C.; Nagarajan, R.; Blackwell, H. E., Structure-Function Analyses of the N-Butanoyl l-Homoserine Lactone Quorum-Sensing Signal Define Features Critical to Activity in RhlR. *ACS Chem Biol* **2018**.
10. Moore, J. D.; Rossi, F. M.; Welsh, M. A.; Nyffeler, K. E.; Blackwell, H. E., A Comparative Analysis of Synthetic Quorum Sensing Modulators in Pseudomonas aeruginosa: New Insights into Mechanism, Active Efflux Susceptibility, Phenotypic Response, and Next-Generation Ligand Design. *J Am Chem Soc* **2015,** *137* (46), 14626-39.
11. Starkey, M.; Lepine, F.; Maura, D.; Bandyopadhaya, A.; Lesic, B.; He, J.; Kitao, T.; Righi, V.; Milot, S.; Tzika, A.; Rahme, L., Identification of anti-virulence compounds that disrupt quorum-sensing regulated acute and persistent pathogenicity. *PLoS Pathog* **2014,** *10* (8), e1004321.
12. Soukarieh, F.; Liu, R.; Romero, M.; Roberston, S. N.; Richardson, W.; Lucanto, S.; Oton, E. V.; Qudus, N. R.; Mashabi, A.; Grossman, S.; Ali, S.; Sou, T.; Kukavica-Ibrulj, I.; Levesque, R. C.; Bergstrom, C. A. S.; Halliday, N.; Mistry, S. N.; Emsley, J.; Heeb, S.; Williams, P.; Camara, M.; Stocks, M. J., Hit Identification of New Potent PqsR Antagonists as Inhibitors of Quorum Sensing in Planktonic and Biofilm Grown Pseudomonas aeruginosa. *Front Chem* **2020,** *8*, 204.
13. Amara, N. M., R.; Amar, D.; Krief, P.; Spieser, S.A.H.; Bottomley, M.J.; Aharoni, A.; and Meijler, M.M., Covalent Inhibition of Bacterial Quorum Sensing. *J Am Chem Soc* **2009**.
14. Pearson, J. P. P., E.C.; Iglewski, B.H., Roles of *Pseudomonas aeruginosa las* and *rhl* Quorum-Sensing Systems in Control of Elastase and Rhamnolipid Biosynthesis Genes. *Journal of Bacteriology* **1997,** *179* (18), 5756-5767.

15. Pesci, E. C. P., J.P.; Seed, P.C.; Iglewski, B.H, Regulation of *las* and *rhl* Quorum Sensing in *Pseudomonas aeruginosa*. *Journal of Bacteriology* **1997,** *179* (10), 3127-3132.
16. Pesci, E. C. M., J.B.J.; Pearson, J.P.; McKnight, S.; Kende, A.S.; Greenberg, E.P.; Iglewski, B.H., Quinolone signaling in the cell-to-cell communication system of Pseudomonas aeruginosa. *Proc Natl Acad Sci U S A* **1999,** *96*, 11229-11234.
17. Welsh, M. A.; Blackwell, H. E., Chemical Genetics Reveals Environment-Specific Roles for Quorum Sensing Circuits in Pseudomonas aeruginosa. *Cell Chem Biol* **2016,** *23* (3), 361-9.
18. Jog, G. J.; Igarashi, J.; Suga, H., Stereoisomers of P. aeruginosa autoinducer analog to probe the regulator binding site. *Chem Biol* **2006,** *13* (2), 123-8.
19. Mattmann, M. E. Design, synthesis, and evaluation of small molecules for the modulation of quorum sensing in Pseudomonas aeruginosa. 2010., 2010.
20. Morkunas, B.; Galloway, W. R.; Wright, M.; Ibbeson, B. M.; Hodgkinson, J. T.; O'Connell, K. M.; Bartolucci, N.; Della Valle, M.; Welch, M.; Spring, D. R., Inhibition of the production of the Pseudomonas aeruginosa virulence factor pyocyanin in wild-type cells by quorum sensing autoinducer-mimics. *Org Biomol Chem* **2012,** *10* (42), 8452-64.
21. Moore, J. D.; Gerdt, J. P.; Eibergen, N. R.; Blackwell, H. E., Active efflux influences the potency of quorum sensing inhibitors in Pseudomonas aeruginosa. *Chembiochem* **2014,** *15* (3), 435-42.
22. Pearson, J. P. V. D., C.; Iglewski, B.H., Active Efflux and Diffusion are Involved in Transport of *Pseudomonas aeruginosa* Cell-to-Cell Signals. *J Bacteriol* **1999,** *181* (4), 1203-1210.
23. Bokhove, M.; Nadal Jimenez, P.; Quax, W. J.; Dijkstra, B. W., The quorum-quenching N-acyl homoserine lactone acylase PvdQ is an Ntn-hydrolase with an unusual substrate-binding pocket. *Proc Natl Acad Sci U S A* **2010,** *107* (2), 686-91.
24. McInnis, C. E.; Blackwell, H. E., Design, synthesis, and biological evaluation of abiotic, non-lactone modulators of LuxR-type quorum sensing. *Bioorg Med Chem* **2011,** *19* (16), 4812-9.
25. O'Reilly, M. C.; Blackwell, H. E., Structure-Based Design and Biological Evaluation of Triphenyl Scaffold-Based Hybrid Compounds as Hydrolytically Stable Modulators of a LuxR-Type Quorum Sensing Receptor. *ACS Infect Dis* **2016,** *2* (1), 32-38.
26. Hodgkinson, J. T.; Galloway, W. R.; Wright, M.; Mati, I. K.; Nicholson, R. L.; Welch, M.; Spring, D. R., Design, synthesis and biological evaluation of non-natural modulators of quorum sensing in Pseudomonas aeruginosa. *Org Biomol Chem* **2012,** *10* (30), 6032-44.
27. David, S.; Mandabi, A.; Uzi, S.; Aharoni, A.; Meijler, M. M., Mining Plants for Bacterial Quorum Sensing Modulators. *ACS Chem Biol* **2017**.
28. Muh, U.; Hare, B. J.; Duerkop, B. A.; Schuster, M.; Hanzelka, B. L.; Heim, R.; Olson, E. R.; Greenberg, E. P., A structurally unrelated mimic of a Pseudomonas aeruginosa acyl-homoserine lactone quorum-sensing signal. *Proc Natl Acad Sci U S A* **2006,** *103* (45), 16948-52.
29. Muh, U.; Schuster, M.; Heim, R.; Singh, A.; Olson, E. R.; Greenberg, E. P., Novel Pseudomonas aeruginosa quorum-sensing inhibitors identified in an ultra-high-throughput screen. *Antimicrob Agents Chemother* **2006,** *50* (11), 3674-9.
30. Tan, S. Y.; Chua, S. L.; Chen, Y.; Rice, S. A.; Kjelleberg, S.; Nielsen, T. E.; Yang, L.; Givskov, M., Identification of five structurally unrelated quorum-sensing inhibitors of Pseudomonas aeruginosa from a natural-derivative database. *Antimicrob Agents Chemother* **2013,** *57* (11), 5629-41.
31. Kalia, M.; Singh, P. K.; Yadav, V. K.; Yadav, B. S.; Sharma, D.; Narvi, S. S.; Mani, A.; Agarwal, V., Structure based virtual screening for identification of potential quorum sensing

inhibitors against LasR master regulator in Pseudomonas aeruginosa. *Microb Pathog* **2017,** *107*, 136-143.
32. O'Reilly, M. C.; Dong, S. H.; Rossi, F. M.; Karlen, K. M.; Kumar, R. S.; Nair, S. K.; Blackwell, H. E., Structural and Biochemical Studies of Non-native Agonists of the LasR Quorum-Sensing Receptor Reveal an L3 Loop "Out" Conformation for LasR. *Cell Chem Biol* **2018**.
33. O'Brien, K. T.; Noto, J. G.; Nichols-O'Neill, L.; Perez, L. J., Potent Irreversible Inhibitors of LasR Quorum Sensing in Pseudomonas aeruginosa. *ACS Med Chem Lett* **2015,** *6* (2), 162-7.
34. Manson, D. E.; O'Reilly, M. C.; Nyffeler, K. E.; Blackwell, H. E., Design, synthesis, and biochemical characterization of non-native antagonists of the Pseudomonas aeruginosa quorum sensing receptor LasR with nanomolar IC50 values. *ACS Infect Dis* **2020**.
35. Baell, J. B. H., G.A., New Substructure Filters for Removal of Pan Assay Interference Compounds (PAINS) from Screening Libraries and for Their Exclusion in Bioassays. *53* **2010,** (2719-2740).
36. Baell, J. W., M.A., Chemical con artists foil drug discovery. *Nature* **2014,** *513*, 481-483.
37. We note that certain non-monotonic partial agonists have single-digit uM IC50s for the antagonism portion of their profiles; however, we do not include those in this comparison due to their agonism at high concenrations. See Moore et al, JACS 2015, 137, 14626 - 14639
38. O'Loughlin, C. T.; Miller, L. C.; Siryaporn, A.; Drescher, K.; Semmelhack, M. F.; Bassler, B. L., A quorum-sensing inhibitor blocks Pseudomonas aeruginosa virulence and biofilm formation. *Proc Natl Acad Sci U S A* **2013,** *110* (44), 17981-6.
39. Lindsay, A.; Ahmer, B. M., Effect of sdiA on biosensors of N-acylhomoserine lactones. *J Bacteriol* **2005,** *187* (14), 5054-8.
40. Compound 3 does not display appreciable antagonism in the E. coli system. We note that, it was weakly efficacious in the P. aeruginosa system ( ~40% maximum inhibition) and believe that its LasR antagonism is obscured in the E. coli system. Additionally, compound 6 displayed unusual activity in E. coli. It agonized the E. coli system, indicating it interacts directly with LasR, but did not antagonize when competing with a high concentration of OdDHL. Compound 6 may therefore operate via a different mechanism than the remainder of the ligands discussed here.
41. Wellington, S. G., E.P., Quorum Sensing signal selectivity and the potential for interspecies cross talk. *mBio* **2019,** *10* (2), e00146-19.
42. LasR co-crsytals were gathered by the Carfi, Nair, and Bassler labs. See Bottomley et al, J. Biol. Chem (2007), 282, 18, 13592-13600; Zou et al, Chem. Biol. (2009), 16, 9, 961-970; O'Reilly et al, Cell Chem. Biol. (2018), 25, 1128-1139; Paczkowski et al, ACS Chem. Biol. (2019), 14, 378 - 389. PDB IDs: 2UV0, 3IX3, 3IX4, 3IX8, 3JPU, 6D6A, 6D6B, 6D6C, 6D6D, 6D6L, 6D6M, 6D6N, 6D6O, 6D6P, 6MWH, 6MWL, 6MWW
43. Bottomley, M. J.; Muraglia, E.; Bazzo, R.; Carfi, A., Molecular insights into quorum sensing in the human pathogen Pseudomonas aeruginosa from the structure of the virulence regulator LasR bound to its autoinducer. *J Biol Chem* **2007,** *282* (18), 13592-600.
44. Paczkowski, J. E.; McCready, A. R.; Cong, J. P.; Li, Z.; Jeffrey, P. D.; Smith, C. D.; Henke, B. R.; Hughson, F. M.; Bassler, B. L., An Autoinducer Analogue Reveals an Alternative Mode of Ligand Binding for the LasR Quorum-Sensing Receptor. *ACS Chem Biol* **2019,** *14* (3), 378-389.

45. Zou, Y.; Nair, S. K., Molecular basis for the recognition of structurally distinct autoinducer mimics by the Pseudomonas aeruginosa LasR quorum-sensing signaling receptor. *Chem Biol* **2009,** *16* (9), 961-70.
46. Churchill, M. E. A. C., L., Structural Basis of Acyl-homoserine Lactone-Dependent Signaling. *Chem Rev* **2011,** *111*, 68-85.
47. Vannini, A. V., C.; Gargioli, C.; Muraglia, E.; Cortese, R.; Francesco, R.D.; Neddermann, P.; Marco, S.D., The crystal structure of the quorum sensing protein TraR bound to its autoinducer and target DNA. *EMBO Journal* **2002,** *21* (17), 4393-4401.
48. Gerdt, J. P.; McInnis, C. E.; Schell, T. L.; Blackwell, H. E., Unraveling the contributions of hydrogen-bonding interactions to the activity of native and non-native ligands in the quorum-sensing receptor LasR. *Org Biomol Chem* **2015,** *13* (5), 1453-62.
49. Gerdt, J. P.; McInnis, C. E.; Schell, T. L.; Rossi, F. M.; Blackwell, H. E., Mutational analysis of the quorum-sensing receptor LasR reveals interactions that govern activation and inhibition by nonlactone ligands. *Chem Biol* **2014,** *21* (10), 1361-9.
50. Knegtel, R. M. A. K., I.D.; Oshiro, C.M., Molecular Docking to Ensembles of Protein Structures. *J. Mol. Biol.* **1997,** *266*, 424-440.
51. Koes, D. R.; Baumgartner, M. P.; Camacho, C. J., Lessons learned in empirical scoring with smina from the CSAR 2011 benchmarking exercise. *J Chem Inf Model* **2013,** *53* (8), 1893-904.
52. Butina, D., Unsupervised Data Base Clustering Based on Daylight's Fingerprint and Tanimoto Similarity: A Fast and Automated Way To Cluster Small and Large Data Sets. *J. Chem. Inf. Comput. Sci.* **1999,** *39*, 747-750.

# CHAPTER FOUR: Structural basis for partial agonism of the *Pseudomonas aeruginosa* LasR quorum sensing receptor by non-native ligands

Daniel E. Manson, Shi-Hui Dong, Satish Nair, and Helen E. Blackwell

To be submitted to *ACS Chemical Biology*

D. E. Manson, S. Dong, S. Nair, and H.E. Blackwell. S. Dong conducted biochemistry and structural biology experiments. D. E. Manson conducted reporter gene experiments and analyzed data. D. E. Manson and H.E. Blackwell wrote the chapter.

**Abstract**

Bacteria coordinate group beneficial behaviors via a chemical communication system known as quorum sensing (QS). In Gram-negative bacteria, QS primarily involves the production and sensing of *N*-acyl L-homoserine lactones, which affect gene expression by binding to and typically activating LuxR-type transcription factors. Limited structural information is available for LuxR-type proteins, especially in complex with non-native, small molecule agonists and antagonists. This paucity of data has hampered the delineation of mechanistic rationales for LuxR-type protein activation and inhibition, along with the design of new compounds that can more effectively modulate the activity of these biologically significant receptors. Here, we report co-crystal structures of the ligand-binding domain of LasR, a master virulence regulator in the opportunistic pathogen *Pseudomonas aeruginosa*, in complex with six non-native ligands. These structural data, in combination with the results of cell-based reporter gene assays, support a mechanism by which the position of the L3 loop, a variable portion of LasR that seals the ligand binding channel, tunes ligand potency for this set of compounds. These results corroborate two other recent studies of LasR, which collectively underscore a role for the L3 loop in the general mechanism of LasR modulation by non-native ligands.

## Introduction

Many bacteria gauge their population density using low molecular weight chemical signals in a process known as quorum sensing (QS).[1, 2] This process controls a variety of group-beneficial bacterial phenotypes that are relevant to human health, agriculture, and industry. In multiple human, animal, and plant pathogens, these phenotypes include many associated with virulence (i.e., ability to initiate infections).[3, 4] The intimate link between QS and virulence has inspired efforts to both develop chemical entities that block QS[5] and elucidate the structures of key biomolecules that mediate this signaling process.[6]

Gram-negative bacteria most commonly utilize LuxI/LuxR-type QS circuits.[7] These systems involve the synthesis of an *N*-acyl L-homoserine lactone (AHL) by a LuxI-type enzyme.[8] The AHL signals are constantly produced at a low basal level and can freely diffuse out of the cell, although in certain cases they are also actively exported.[9] The concentration of AHL signal is proportional to cell number, so at a certain stage of growth (i.e., when a "quorum" of bacteria has amassed), the AHL concentration will be sufficient for productive binding to a cytoplasmic LuxR-type transcription factor. Thereafter, LuxR-type protein:AHL complexes typically dimerize and bind to DNA, causing changes in gene expression levels and, ultimately, phenotypes involved in various group behaviors.[10] In some bacteria, this process can control almost 10% of them genome.[11]

Many questions remain about the mechanism of LuxI/LuxR-type QS. Biochemical studies of LuxR-type proteins have been slow due to the instabilities of these proteins *in vitro*. The isolation of LuxR-type proteins typically requires that a stabilizing ligand, often their native AHL, be present at each stage of purification.[10, 12] This requirement precludes the possibility of gathering *apo* (ligand-less) structures of these proteins.[13] Even in the presence of native ligands,

these proteins have relatively short half-lives.[14, 15] Despite these difficulties, a small set of LuxR-type proteins have been co-crystalized with a variety of native and non-native AHL ligands, providing a three-dimensional view to guide mechanistic hypotheses.[15-17]

Prior biochemical studies, albeit limited, have provided other useful information on LuxR-type proteins. Notably, the thermal stability of LuxR-type receptor:ligand complexes has been related to the potency with which the ligand activates transcription—that is, LuxR-type proteins in complex with strongly-activating ligands have enhanced thermal stability relative to the same LuxR-type protein bound to weakly-activating ligands.[18] We note that the causal relationship at play is likely the reverse: ligands that cause LuxR-type proteins to adopt stable conformations that are capable of binding DNA are those that can initiate transcription in gene reporter experiments at low concentrations (i.e., high potency ligands).

The vast majority of attempts to isolate LuxR type proteins with synthetic antagonists have yielded insoluble protein,[19] which has hindered most mechanistic studies of LuxR-type protein antagonism. This finding, along with the lower thermal stability of LuxR-type receptors in complex with weakly activating ligands, has inspired the hypothesis that antagonists may function at least in part by promoting misfolding of the protein.[15] CviR, from *Chromobacterium violacein*, is the only LuxR-type protein to be crystalized in complex with a non-native AHL-based antagonist (the chlorolactone AHL analog, CL).[20] The X-ray structure showed the $[CviR:CL]_2$ complex adopted a distinct, "crossed" conformation that is presumed to be incapable of binding DNA (as supported by *in vitro* experiments showing the complex incapable of initiating transcription). Studies to determine if the distinct "crossed conformation is a unique feature of the CviR:CL interaction or a general mechanism of LuxR-type antagonism are ongoing, including in our laboratories.

In the current study, we focus on LasR, a master QS regulator and LuxR-type protein in the opportunistic pathogen *Pseudomonas aeruginosa*. Significant effort has been dedicated to the development of probe compounds that can antagonize LasR, for use as tools to study QS and to potentially attenuate virulence phenotypes.[21-24] However, attempts to purify LasR in complex with antagonists have been met only with insoluble protein.[19] While full-length LasR has proven intractable to crystallization, even in complex with strongly activating ligands, the LasR ligand binding domain (LBD, a construct that lacks the 60 C-terminal residues comprising the helix-turn-helix DNA-binding domain) has been successfully crystalized in complex with a variety of ligands.[25]

Recently, our research groups have reported a series of LasR LBD structures in complex with non-native ligands based on the triphenyl (TP) series of abiotic LasR agonists first reported by the Greenberg lab (**Figure 1**).[26] We identified a region of LasR, the L3 loop (residues Leu 40 – Phe 51) that flanks the opening of the ligand binding pocket and changes position in a manner correlated with the agonism potency of the bound ligand. When complexed with more potent ligands, the loop positions against the LBD and seals the entrance to the ligand binding pocket; however, when in complex with less potent or efficacious ligands (i.e., partial agonists), the L3 loop moves away from the protein, leaving the binding pocket solvent exposed. Homology modeling using the LBD of LasR and the full-length crystal structure of the homologue QscR (that recognizes a similar natural ligand, 3-oxo-C12 AHL (OdDHL)) indicated that this loop is likely in close proximity to the LasR DNA binding domain. This proximity and motion raises the intriguing possibility that the L3 loop plays a role in transmitting information between the two domains, and thereby tuning transcriptional activation. In a concurrent study by Bassler and coworkers, the position of the L3 loop was also shown to play a role in how discriminating LasR

is for activation by AHL-based ligands,[27] further supporting a role for this loop in LasR:ligand interactions.

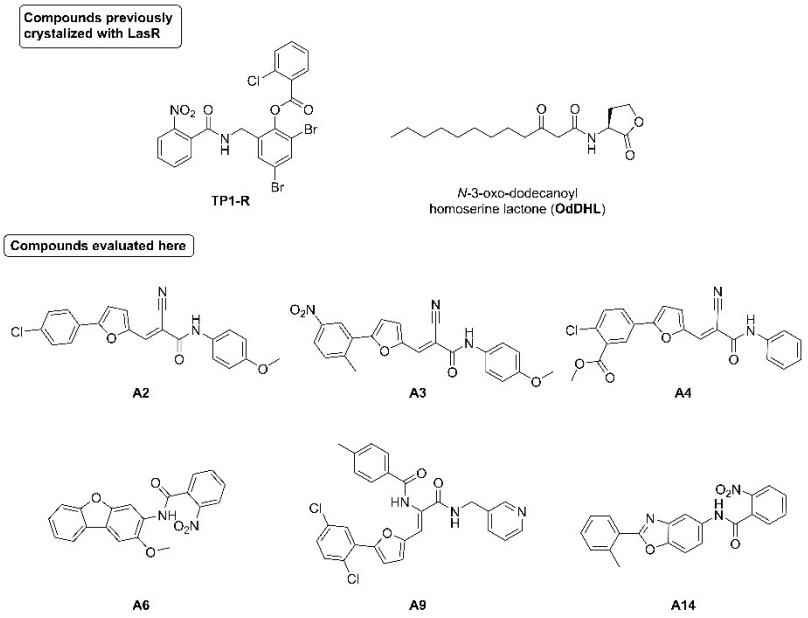


**Figure 4.1.**Selected LasR modulators. **TP1-R**, discovered by the Greenberg lab, structure revised by the Janda lab.[28, 29] OdDHL is the biological ligand of LasR. Compounds **A2**–**A4**, **A5**, **A6** and **A14** were discovered jointly by the Blackwell and Handelsman research groups.[30] Compound naming is preserved from the original report of their discovery.

In seeking new ligands with which to continue our structural investigations into the mechanism of LasR modulation by non-native molecules, we turned to a set of LasR modulators uncovered by our laboratory in 2010 in a high throughput screen (selected compounds shown in **Figure 1**).[30] At that time, those compounds were shown in a cell-based gene reporter experiment to activate LasR at relatively high concentrations (0.5 – 10 μM). These "A-type" compounds are structurally unrelated to all known modulators of LasR, and therefore represent an opportunity to probe the generality of the correlation between the position of the L3 loop with ligand potency in LasR. Here, we further quantified the bioactivity of these compounds and crystalized each of them in complex to the LasR LBD. Analysis of these structures by X-ray crystallography reveal that the compounds bind to LasR analogously to the TP series and AHL-based ligands, and that

the position of the L3 loop varies with ligand potency in a manner consistent with our previous results. These results serve to underscore the importance of the L3 loop in tuning the agonistic activity of small molecule LasR modulators, along with demonstrating the impact of structural data on the mechanistic understanding of LuxR-type protein function. Our findings suggest a route toward the design of both new agonists and antagonists of this important QS receptor.

## Results and Discussion

### Structure and bioactivity of selected probe compounds.

We initiated our study by fully characterizing the activity profiles of our compound set in LasR (**Figure 1**).[30] At the time of their discovery, we did not quantify the potency of these compounds via dose-response analysis; to obtain quantitative data about their relative LasR activity profiles, we did so here. We selected a representative subset of compounds for study that, in the initial report, varied in their agonism efficacy (i.e., the maximum extent to which they activated LasR). These compounds are comprised of three or more carbocyclic or heterocyclic aromatic rings that are either directly bonded to each other (i.e., via C-C bond between rings) or joined by amide or alkene linkers. Compounds **A2**, **A3**, **A4**, and **A9** are analogues of each other. While compounds **A2**–**A4** vary only in the substitution of their aryl rings, **A9** differs in ring substitution and in the substituent on the alkene carbon α to the amide carbonyl. Compounds **A6** and **A14** both share an *ortho*-nitro aryl amide group, analogous to TPI-R, yet have differing heterocyclic substituents on the amide nitrogen.

We used a heterologous LasR reporter system (i.e., in *E. coli*) to quantify the bioactivity of these compounds (**Table 1**).[31] We found that they are moderately potent LasR agonists, with $EC_{50}$ values one to two orders of magnitude above (i.e., less potent than) that of the native ligand of LasR, OdDHL. These activity trends largely correlate with the trends we observed in our original report.[30] We note that we observed higher maximum activation for compounds **A3**, **A4**,

and **A11** than in the 2010 report; however, this was likely due to testing them at high concentrations here (maximum concentrations of 100 μM in this study vs previously 10 μM). We were interested to observe that although compounds **A4** and **A9** were approximately an order of magnitude less potent than **A2**, they were equally as efficacious as **A2** (or, in the case of **A9**, slightly more efficacious). This result suggests that these properties – efficacy and potency – can vary at least somewhat independently of each other for this class of compounds .

The maximum LasR activation (i.e., the efficacy) of all compounds was reduced relative to OdDHL (**Table 1**); notably, **A14**, the weakest agonist, was only capable of ~60% LasR activation. This poor agonism efficacy suggested that, in a competitive binding assay with OdDHL, **A14** would likely reduce LasR activity relative to OdDHL, and thereby is best classified as a partial agonist. Screening compound **A14** in competition with OdDHL at 15 nM (i.e., it's approximate $EC_{90}$ in this LasR reporter system) revealed this to be the case, confirming that **A14** is a LasR partial agonist (i.e., it can either activate or inhibit LasR activity depending on the screening conditions (**Figure 2a-b**)**.** We performed the same experiment with the second-poorest activator, compound **A6** (capable of approximately 70% LasR activation), and found that it also antagonized LasR relative to OdDHL, albeit to a lesser extent (**Figure 2c**).[32] Despite its less-than-maximal activation, we did not observe the same antagonism with **A3** (data not shown). Its improved efficacy relative to **A14** and **A6** indicates that any repression relative to the $EC_{90}$ of OdDHL would be very subtle and may only occur at unfeasibly high compound concentrations (i.e., higher than the solubility limit of **A3** in LB media).

**Table 4.1**. Bioactivity of ligands screened in a heterologous LasR reporter system[a]

| Compound | $EC_{50}$ (nM)[b] | 95% CI (μM)[c] | Maximum Activation (%)[d] |
|---|---|---|---|
| **A2** | 25 | 16-39 | 87 |
| **A3** | 100 | 68-150 | 82 |
| **A4** | 630 | 538-740 | 89 |
| **A6** | 230 | 171-296 | 71 |
| **A9** | 167 | 130-220 | 93 |
| **A14** | 710 | 590-840 | 63 |

[a] All screening was conducted in *E. coli* LasR reporter strain JLD271 (*SdiA*)[33] [b] Compounds were screened over a range of concentrations (100 μM – 0.01 nM) and a three-parameter nonlinear curve was fit to the resulting curve. See **Figure S1** for full dose-response curves. [c] 95% CI = 95% confidence interval, derived from three independent biological replicates; [d] Represents the best-fit top of the dose-response curve. 100% = 100 μM OdDHL.

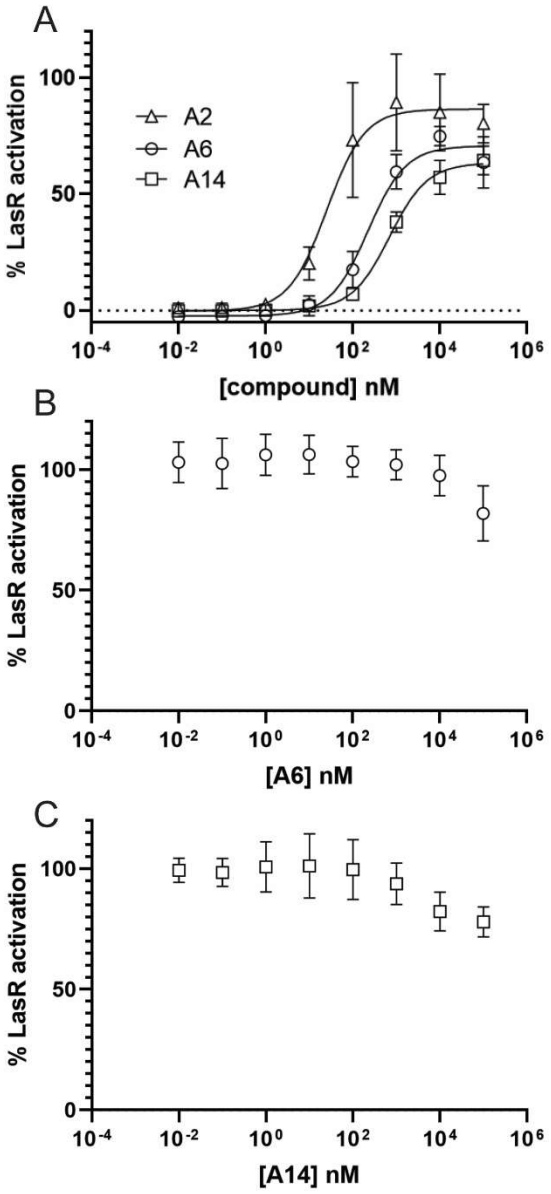


**Figure 4.2.** Compound **A2** is a full agonist and compounds **A6** and **A14** are partial agonists of LasR. (**A**) Agonism experiment with compounds **A2**, **A6**, and **A14. A2** is approximately 9-fold more potent than **A6** and 30-fold more potent than **A14**. Compounds **A6** and **A14** fail to maximally activate LasR. (**B**-**C**) Compounds **A6** and **A14**, respectively, screened in competition against the approximate $EC_{90}$ concentration of OdDHL. Both ligands antagonize LasR activity relative to that level of activation by OdDHL.

**Purification and co-crystallization of LasR with compounds A2–A4, A5, A6 and A14.**

We were interested to characterize the binding interactions between these A-type compounds and LasR further to gain insight into their mechanisms of LasR agonism. To do so, we isolated and purified the LasR LBD in complex with each of the compounds in Table 1 using reported procedures (see Methods). Co-crystals were obtained for the LasR LBD complexed to **A2**–**A4**, **A5**, **A6** and **A14** that provided high quality X-ray diffraction data (<2 Å resolution in each case).

**Ligands place LasR LBD into a conformation closely resembling the LasR LBD:OdDHL dimer.**

We examined the overall fold of the LasR LBD in complex with each of the A-type ligands (**Figure 2C-F**, figure **S2**). We anticipated that if large perturbations to the overall structure of the LBD were to exist, they would be most evident when contrasting our most potent compound **A2** to our least potent compound **A14.** However, we found that all of the compounds placed LasR in an overall conformation that was equivalent to that of the LasR LBD in complex with OdDHL (RMSD difference between all dimers with experimental compounds and the $[LasR:OdDHL]_2$ dimer were>0.6 Å, **Figure 3A-C, Figure S2**).[34] The LBD dimers with the A-type ligands were therefore also similar to each other; the largest difference we observed was between the **A2** and the **A14** complexes (RMSD = 0.702 Å, see **Table S2** for full analysis). Indeed, the only portion of the protein that adopted a different conformation when bound to different ligands was the L3 loop (see discussion below). As each of these compounds are capable of causing LasR to initiate transcription in a reporter gene experiment, it is perhaps unsurprising that they do not cause a major perturbation to the LasR structure.

We note that the minimum crystallographic unit (MCU) for the LasR LBD:**A6** complex contained multiple non-equivalent dimers. There are four dimers in the MCU; of those, three

superimpose on each other, but one does not (RMSD = 21.85 A between the two sets of dimers). Monomers within the two sets **are** superimposable on each other, indicating that the difference resides in the interface between the two monomers. Curiously, the dimer that was **not** superimposable with the remainder of dimers in the minimum crystallographic unit **was** superimposable with the OdDHL dimer (and all other dimers evaluated here). Our analysis of this apparent irregularity is ongoing and will be resolved with input from our collaborators from the Nair lab.

**The position of the L3 loop varies with ligand potency.**

We were curious to examine whether the previously observed correlation between ligand potency and the LasR L3 loop positioning existed within this set of A-type ligands. Again, the L3 loop comprises residues **4051 r**esidues in LasR, sealing the ligand-binding site from solvent when positioned 'in' towards the protein. Contrasting the co-crystal structures of the LasR LBD with our most potent ligand, **A2**, with that of our least potent ligand, partial agonist **A14**, revealed that the correlation was indeed maintained (**Figure 2G-J**). Relative to the LasR LBD:**A2** and LasR LBD:**OdDHL** co-crystal structures,[19] the L3 loop is positioned "out" (i.e., towards solvent) in the **A14** co-crystal structure. In the **A2** structure, the loop is packed "in" against the protein, comparable to the OdDHL structure. In complex with the remaining ligands (**A3**, **A4**, **A6**, and **A9**), the L3 loop varies between its position in the **A2** and **A14** structures (see **Figure S3**). The potencies of these compounds in the reporter assay were also between that of **A2** and that of **A14** (Table 1; Figure S1), which corroborates with the intermediate placement of the L3 loop in their structures.

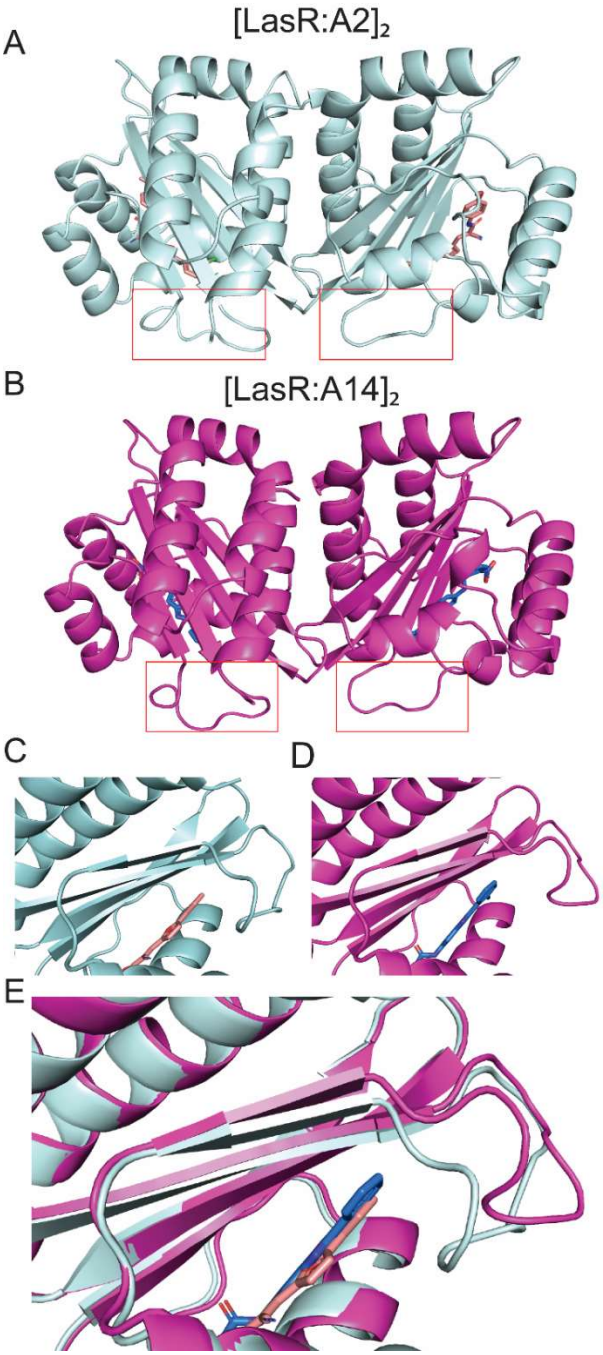


**Figure 4.3.** Selected views of the LasR ligand binding domain in complex with compounds **A2** and **A14**. **(A)** LasR LBD in complex with compound **A2**. The L3 loop is highlighted with a red box. (**B**) The LasR LBD in complex with compound **A14**. The L3 loop is highlighted with a red box. (C-D) Closeup views of the L3 loop from the **A2** and **A14** dimers. **(E)** Expanded overlay of panels C and D. When bound to ligand **A2** (shown in light orange) the L3 loop packs towards the protein, while bound to **A14** (shown in dark blue) it is oriented away from the protein, towards solvent.

**Ligands make similar contacts with LasR as AHLs.**

The crystal structures revealed that each of these non-native ligands bound to the AHL binding site on LasR (**Figure 3A-C**, Figure S4). OdDHL, other AHLs, and various non-AHL ligands (i.e., the TP series) bind to LasR in part by forming a series of hydrogen bonds with polar residues that line the ligand binding channel.[35, 36] These A-type compounds bind in an analogous fashion; they each contain a cyclic moiety that mimics the homoserine lactone "head group" and form polar contacts with the same set of residues (i.e., Asp73, Trp60, Ser129, Tyr56, Arg61, and Thr75, **Figure 4A-C**). In certain cases, these interactions are mediated by one or more molecules of water, as is the case in the LasR LBD:OdDHL structure. In addition, the kinked acyl tail of OdDHL present in the LasR LBD:OdDHL structure is mimicked in each A-type compound by a carbocycle that abuts against residues Leu125 and Leu 40, which form the end of the ligand binding pocket.

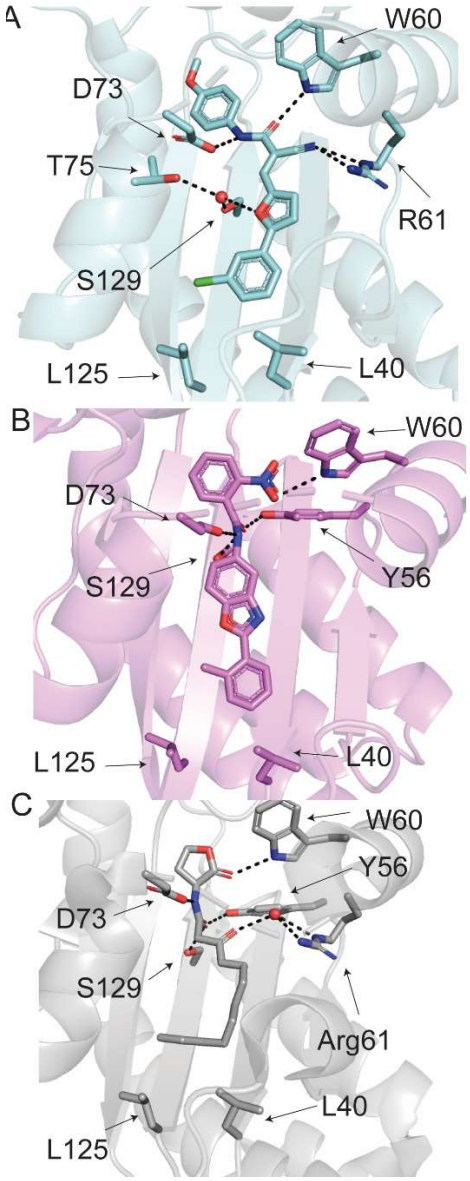


**Figure 4.4.** View of the residues surrounding the ligands **(A) A2**; **(B) A14**; and **(C)** OdDHL (from PDB ID 3IX3).[19] Both **A2** and **A14** makes contacts with polar residues that are analogous to those made by OdDHL. Carbocyclic rings in **A2** and **A14** fill the space occupied by the kinked aliphatic tail in OdDHL. Red spheres represent water molecules.

**Conclusions**

The development of mechanistic hypotheses regarding the activation and inhibition of LuxR-type proteins by native and non-native ligands has been hampered by a lack of structural data. Here, we present six novel co-crystal structures of the LasR LBD in complex with non-native small molecules that were discovered as LasR agonists in a high throughput screen. We found that each of these molecules binds to LasR in a manner that closely resembles the interaction between LasR and AHLs. However, we found that the level of agonism potency (as determined in a LasR transcriptional reporter assay) by these compounds and the position of the LasR L3 loop was correlated in this set of crystal structures. In complex with **A2**, the most potent agonist, the loop packed against LasR, but when bound to **A14**, a relatively weak and partial agonist, the loop was positioned towards solvent. (i.e., away from LasR). Compound **A14** reduces LasR activity relative to its native ligand, raising the possibility that, upon competitive exchange of an agonist for an antagonist in the ligand binding site, an "outward" motion of the L3 loop represents one step in the mechanism by which LasR transitions from an active to an inactive (i.e. not DNA-binding) conformation.

The combined structural and screening data reported herein, gathered with a set of ligands structurally unrelated to any known LasR modulators, suggests that the L3 loop may play a role in the binding of diverse, non-AHL ligands to LasR, and potentially in other LuxR homologues in which it is present. For example, a similar loop has been reported in the structure of SdiA from *E. coli* and QscR from *P. aeruginosa*. [37] Experiments to further elucidate the importance of the L3 loop (e.g., structural studies of full length LasR, and mutagenesis of residues that make up the loop) are ongoing in our laboratories and will be reported in due course.

## Materials and Methods

### Compound Handling

Compounds were stored as solids at -20 °C until ready to use, at which point DMSO stocks were prepared at appropriate concentrations and stored at -20 °C.

### Biology

Bacteria were cultured in Luria-Bertani media and grown at 37 °C. Bacterial growth was quantified by absorbance at 600 nm ($OD_{600}$).

### *E. coli* LasR assay protocol.

The *E. coli* LasR reporter experiment as performed as described previously; see SI for detailed experimental protocols. [31]

**Table S4.1:** Bacterial strains and plasmids used in this study[a]

| Strain or Plasmid | Description | Ref. |
|---|---|---|
| *E. coli* | | |
| JLD271 | K-12 Δ*lacX74 sdiA271*::CAM; $Cl^R$ | [1] |
| *Plasmids* | | |
| pPROBE-KL | *lasI'-gfp*[LVA] transcriptional fusion; $Km^R$ | [2] |
| pJN105L | Arabinose-inducible *lasR* expression vector; pBBRMCS backbone; $Gm^R$ | [3] |

Abbreviations: $Cl^R$ = Chloramphenicol resistance; $Km^R$ = Kanamycin resistance; $Gm^R$ = Gentamicin resistance.

**E. coli LasR reporter protocol**

The heterologous LasR gene reporter assay was performed as described previously.[2] Briefly, the night before an experiment an appropriate volume of LB media supplemented with 50 μg/mL kanamycin and 10 μg/mL gentamicin was inoculated with a single colony of *E. coli* LasR reporter strain JLD271 + pJN105L + pPROBE-KL. The next day, the overnight culture was diluted 1:10 into fresh LB with fresh antibiotic. This culture was grown to an OD = 0.25 with pathlength correction applied. While subculture was growing, 2 μL of compound stocks at the appropriate concentrations was dispensed into the interior wells of black 96 well plate. When culture reached the appropriate density, 0.4% w/v arabinose was added to start expression of pJN105-L.

*For agonism experiments*: Six wells on each plate were filled with 2 μL of DMSO (to serve as negative control), and six wells were filled with 2 μL of a 10 mM OdDHL stock (to serve as positive control). 198 μL of arabinose-induced culture was then dispensed into every well, and plates were incubated for 4h at 37 °C with shaking at 200 RPM.

*For experiments in competition with the OdDHL $EC_{90}$*: Twelve wells on each plate were filled with 2 μL DMSO. The arabinose-induced culture was divided, and to one portion was added the appropriate amount of OdDHL to reach a final concentration of 15 nM. This treated subculture was added to half of the DMSO-containing wells (to serve as a positive control) and all experimental wells. The untreated portion of the subculture was added to the remaining DMSO-containing wells. Plates were then incubated as described previously.

After incubation, GFP (excitation at 485 nm, emission at 544 nm) and $OD_{600}$ (absorbance at 600 nm) was read for each plate. Data analysis was performed using Microsoft Excel and Graphpad Prism (version 8). Compound activities were background-corrected to negative control wells

(i.e., wells containing only DMSO) and reported as a percent relative to the positive control wells (i.e., wells containing only OdDHL, either at 10 μM or 15 nM).

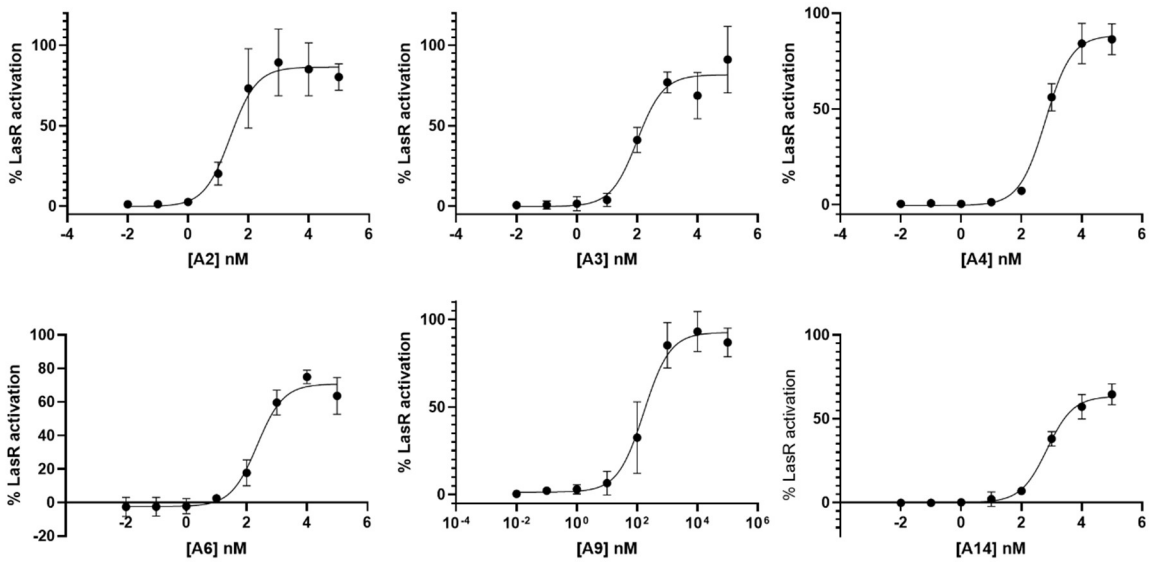


**Figure S4.1.** *E. coli* (JLD271 + pJN105-L + pPROBEKL) screening of compounds **A2-A4**, **A6**, **A9**, and **A14**. Curves are made up of at least three biological replicates. Error bars indicate SD.

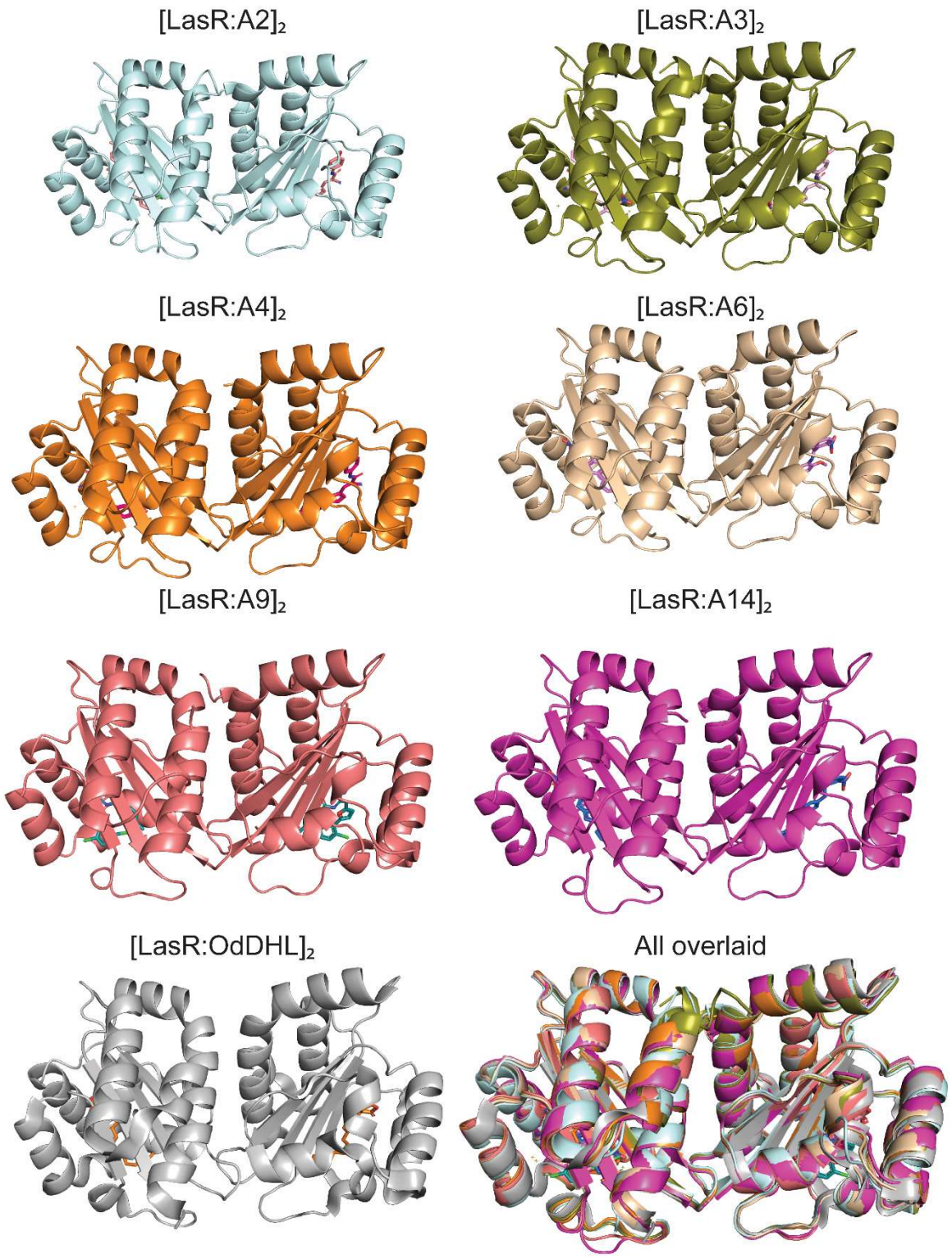


**Figure S4.2.** The LasR ligand binding domain in complex with ligands **A2-A4**, **A6**, **A9**, **A14**, and OdDHL (PDB ID 3IX3).[4]

**Table S4.2.** RMSD analysis of overall dimer similarity

| | A2 | A3 | A4 | A6 | A9 | A14 | OdDHL |
|---|---|---|---|---|---|---|---|
| **A2** | X | X | x | x | X | x | X |
| **A3** | 0.390 Å (292 to 292 atoms) | X | x | x | x | x | X |
| **A4** | 0.568 Å (290 to 290 atoms) | 0.364 Å (287 to 287 atoms) | X | x | x | x | X |
| **A6** | 0.549 Å (288 to 288 atoms) | 0.440 Å (271 to 271 atoms) | 0.326 Å (283 to 283 atoms) | X | x | x | X |
| **A9** | 0.623 Å (299 to 299 atoms) | 0.412 Å (275 to 275 atoms) | 0.438 Å (291 to 291 atoms) | 0.328 (260 to 260 atoms) | x | x | X |
| **A14** | 0.702 Å (282 to 282 atoms) | 0.540 Å (286 to 286 atoms) | 0.272 Å (267 to 267 atoms) | 0.407 Å (304 to 304 atoms) | 0.505 Å (273 to 273 atoms) | X | x |
| **OdDHL (3IX3)** | 0.585 Å (297 to 287 atoms) | 0.585 Å A (284 to 284 atoms) | 0.422 Å (280 to 280 atoms) | 0.342 Å (288 to 288 atoms) | 0.472 Å (278 to 278 atoms) | 0.472 Å (270 to 270 atoms) | X |

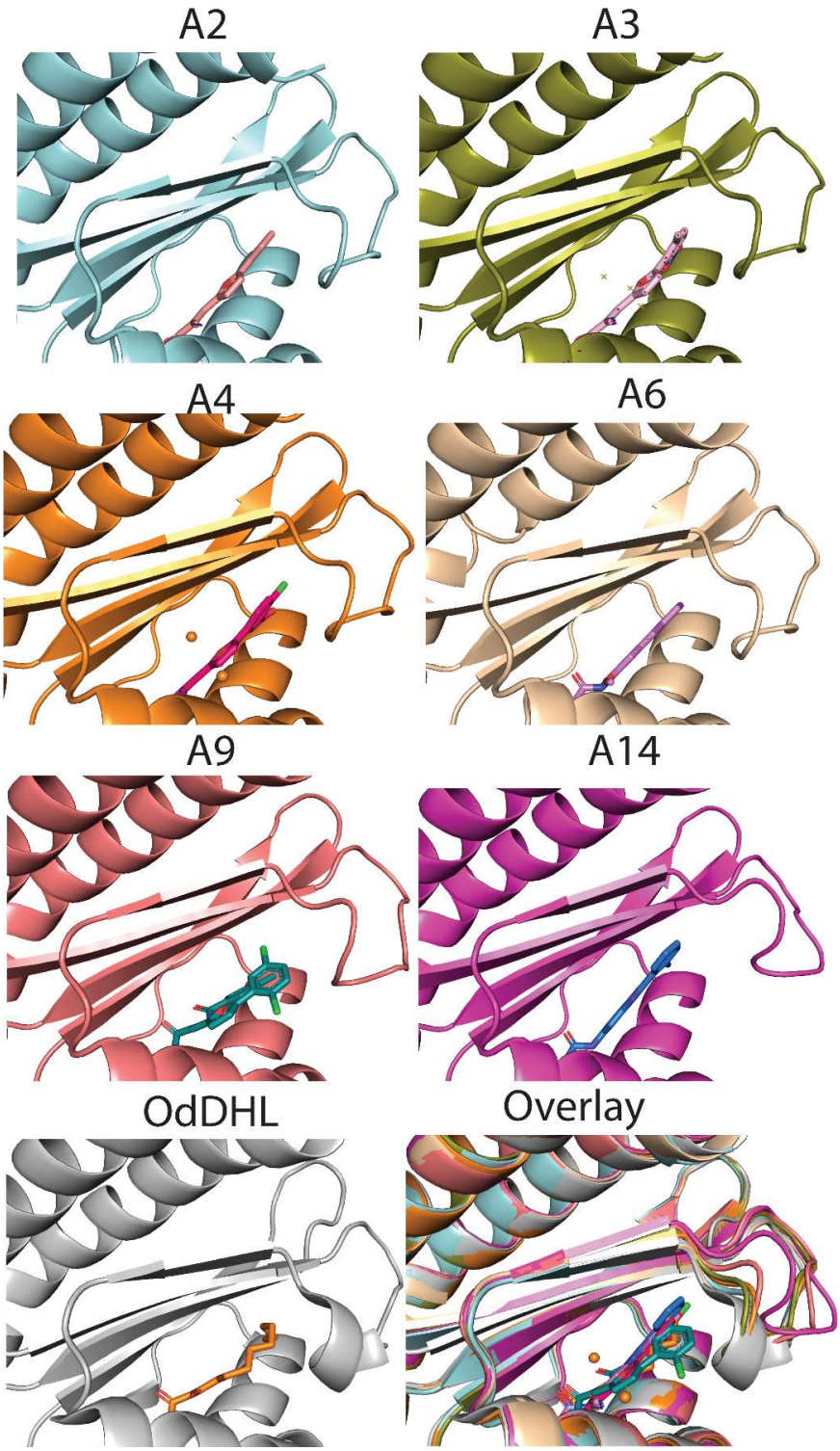


**Figure S4.3.** The L3 loop from the LasR LBD bound to the indicated small molecules. The loop is most-outward when bound to A14, and most-inward when bound to OdDHL, A2, A3, and A6. PDB ID for OdDHL structure is 3IX3.

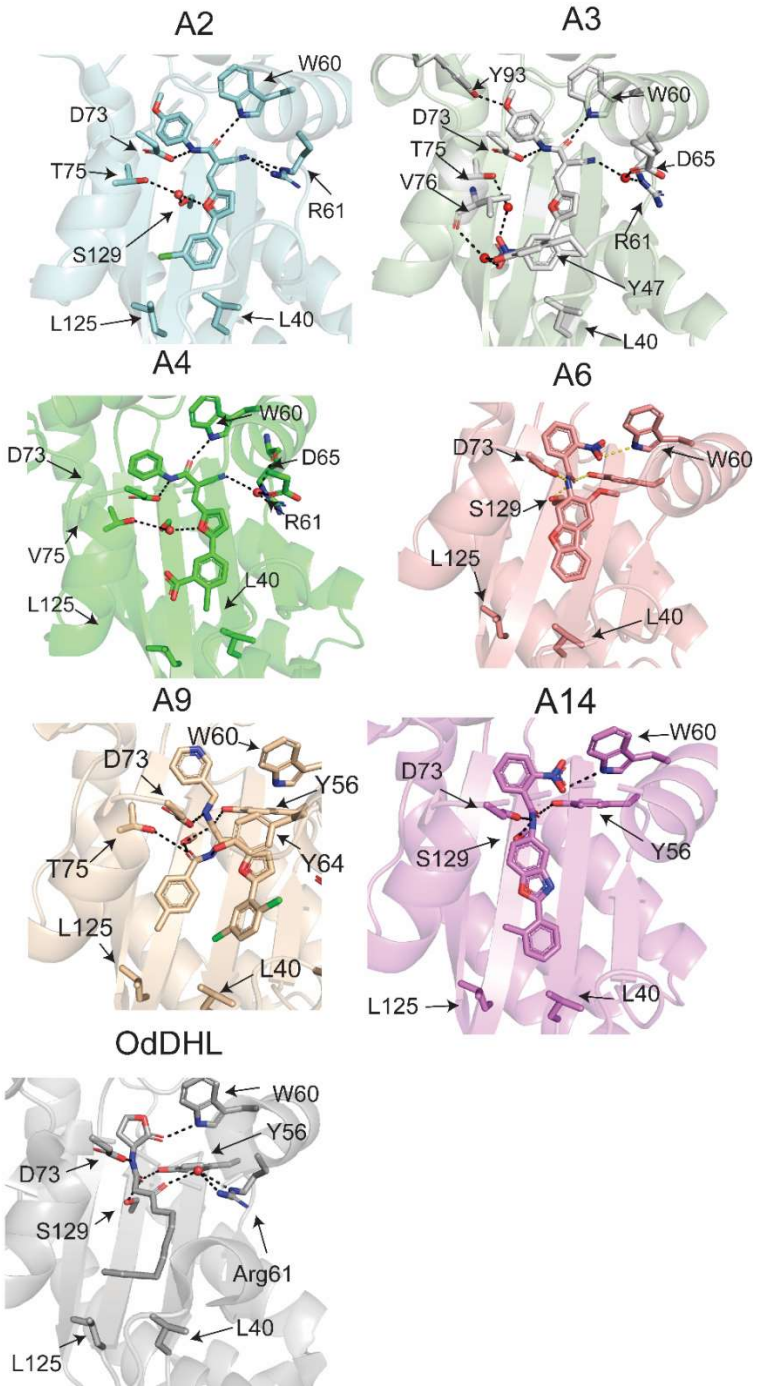


**Figure S4.4** Selected view of ligands **A2** – **A4**, **A6**, **A9**, **A14** and OdDHL in the LasR ligand binding pocket.

**References for materials and methods**

1. Lindsay, A.; Ahmer, B. M., Effect of sdiA on biosensors of N-acylhomoserine lactones. *J Bacteriol* **2005,** *187* (14), 5054-8.
2. Moore, J. D.; Gerdt, J. P.; Eibergen, N. R.; Blackwell, H. E., Active efflux influences the potency of quorum sensing inhibitors in Pseudomonas aeruginosa. *Chembiochem* **2014,** *15* (3), 435-42.
3. Lee, J. H.; Lequette, Y.; Greenberg, E. P., Activity of purified QscR, a Pseudomonas aeruginosa orphan quorum-sensing transcription factor. *Mol Microbiol* **2006,** *59* (2), 602-9.
4. Zou, Y.; Nair, S. K., Molecular basis for the recognition of structurally distinct autoinducer mimics by the Pseudomonas aeruginosa LasR quorum-sensing signaling receptor. *Chem Biol* **2009,** *16* (9), 961-70.

**References**

1. Whiteley, M.; Diggle, S. P.; Greenberg, E. P., Progress in and promise of bacterial quorum sensing research. *Nature* **2017,** *551* (7680), 313-320.
2. Rutherford, S. T.; Bassler, B. L., Bacterial quorum sensing: its role in virulence and possibilities for its control. *Cold Spring Harb Perspect Med* **2012,** *2* (11).
3. Wang, B.; Muir, T. W., Regulation of Virulence in Staphylococcus aureus: Molecular Mechanisms and Remaining Puzzles. *Cell Chem Biol* **2016,** *23* (2), 214-224.
4. Balasubramanian, D.; Schneper, L.; Kumari, H.; Mathee, K., A dynamic and intricate regulatory network determines Pseudomonas aeruginosa virulence. *Nucleic Acids Res* **2013,** *41* (1), 1-20.
5. Welsh, M. A.; Blackwell, H. E., Chemical probes of quorum sensing: from compound development to biological discovery. *FEMS Microbiol Rev* **2016,** *40* (5), 774-94.
6. Churchill, M. E. A. C., L., Structural Basis of Acyl-homoserine Lactone-Dependent Signaling. *Chem Rev* **2011,** *111*, 68-85.
7. Galloway, W. R., Hodgkinson, J.T., Bowden, S.D., Welch, M. Spring, D.R., Quorum Sensing in Gram-Negative Bacteria: Small-Molecule Modulation of AHL and AI-2 Quorum Sensing Pathways. *Chem Rev* **2011,** *111*, 28-67.
8. Dong, S. F., N.D.; Christensen, Q.H.; Greenberg, E.P.; Nagarajan, R.; Nair, S.K., Molecular basis for the substrate specificity of quorum signal synthases. *Proc Natl Acad Sci U S A* **2017,** *114* (34), 9027-9097.
9. Pearson, J. P. V. D., C.; Iglewski, B.H., Active Efflux and Diffusion are Involved in Transport of *Pseudomonas aeruginosa* Cell-to-Cell Signals. *J Bacteriol* **1999,** *181* (4), 1203-1210.
10. Sappington, K. J.; Dandekar, A. A.; Oinuma, K.; Greenberg, E. P., Reversible signal binding by the Pseudomonas aeruginosa quorum-sensing signal receptor LasR. *MBio* **2011,** *2* (1), e00011-11.
11. Wagner, V. E.; Bushnell, D.; Passador, L.; Brooks, A. I.; Iglewski, B. H., Microarray Analysis of Pseudomonas aeruginosa Quorum-Sensing Regulons: Effects of Growth Phase and Environment. *Journal of Bacteriology* **2003,** *185* (7), 2080-2095.
12. Lee, J. H.; Lequette, Y.; Greenberg, E. P., Activity of purified QscR, a Pseudomonas aeruginosa orphan quorum-sensing transcription factor. *Mol Microbiol* **2006,** *59* (2), 602-9.
13. SdiA, LuxR type receptor for enterohemorrhagic E. coli (EHEC) has been co-crystalized with a molecule of 1-octanoyl-rac-glycerol in its ligand binding pocket in lieu of an AHL. See Nguyen et al., mBio, 2015, 6 (2), doi.org/10.1128/mBio.02429-14
14. Oinuma, K.; Greenberg, E. P., Acyl-homoserine lactone binding to and stability of the orphan Pseudomonas aeruginosa quorum-sensing signal receptor QscR. *J Bacteriol* **2011,** *193* (2), 421-8.
15. Wysoczynski-Horita, C. L.; Boursier, M. E.; Hill, R.; Hansen, K.; Blackwell, H. E.; Churchill, M. E. A., Mechanism of agonism and antagonism of the Pseudomonas aeruginosa quorum sensing regulator QscR with non-native ligands. *Mol Microbiol* **2018,** *108* (3), 240-257.
16. Lintz, M. J.; Oinuma, K.; Wysoczynski, C. L.; Greenberg, E. P.; Churchill, M. E., Crystal structure of QscR, a Pseudomonas aeruginosa quorum sensing signal receptor. *Proc Natl Acad Sci U S A* **2011,** *108* (38), 15763-8.
17. Kim, Y.; Chhor, G.; Tsai, C. S.; Fox, G.; Chen, C. S.; Winans, N. J.; Jedrzejczak, R.; Joachimiak, A.; Winans, S. C., X-ray Crystal Structures of the Pheromone-binding Domains of

Two Quorum-Hindered Transcription Factors, YenR of Yersinia enterocolitica and CepR2 of Burkholderia cenocepacia. *Proteins* **2017**.
18. Paczkowski, J. E.; McCready, A. R.; Cong, J. P.; Li, Z.; Jeffrey, P. D.; Smith, C. D.; Henke, B. R.; Hughson, F. M.; Bassler, B. L., An Autoinducer Analogue Reveals an Alternative Mode of Ligand Binding for the LasR Quorum-Sensing Receptor. *ACS Chem Biol* **2019,** *14* (3), 378-389.
19. Zou, Y.; Nair, S. K., Molecular basis for the recognition of structurally distinct autoinducer mimics by the Pseudomonas aeruginosa LasR quorum-sensing signaling receptor. *Chem Biol* **2009,** *16* (9), 961-70.
20. Chen, G.; Swem, L. R.; Swem, D. L.; Stauff, D. L.; O'Loughlin, C. T.; Jeffrey, P. D.; Bassler, B. L.; Hughson, F. M., A strategy for antagonizing quorum sensing. *Mol Cell* **2011,** *42* (2), 199-209.
21. Amara, N.; Gregor, R.; Rayo, J.; Dandela, R.; Daniel, E.; Liubin, N.; Willems, H. M.; Ben-Zvi, A.; Krom, B. P.; Meijler, M. M., Fine-Tuning Covalent Inhibition of Bacterial Quorum Sensing. *Chembiochem* **2016,** *17* (9), 825-35.
22. Hodgkinson, J. T.; Galloway, W. R.; Wright, M.; Mati, I. K.; Nicholson, R. L.; Welch, M.; Spring, D. R., Design, synthesis and biological evaluation of non-natural modulators of quorum sensing in Pseudomonas aeruginosa. *Org Biomol Chem* **2012,** *10* (30), 6032-44.
23. O'Reilly, M. C.; Blackwell, H. E., Structure-Based Design and Biological Evaluation of Triphenyl Scaffold-Based Hybrid Compounds as Hydrolytically Stable Modulators of a LuxR-Type Quorum Sensing Receptor. *ACS Infect Dis* **2016,** *2* (1), 32-38.
24. Manson, D. E.; O'Reilly, M. C.; Nyffeler, K. E.; Blackwell, H. E., Design, synthesis, and biochemical characterization of non-native antagonists of the Pseudomonas aeruginosa quorum sensing receptor LasR with nanomolar IC50 values. *ACS Infect Dis* **2020**.
25. Bottomley, M. J.; Muraglia, E.; Bazzo, R.; Carfi, A., Molecular insights into quorum sensing in the human pathogen Pseudomonas aeruginosa from the structure of the virulence regulator LasR bound to its autoinducer. *J Biol Chem* **2007,** *282* (18), 13592-600.
26. O'Reilly, M. C.; Dong, S. H.; Rossi, F. M.; Karlen, K. M.; Kumar, R. S.; Nair, S. K.; Blackwell, H. E., Structural and Biochemical Studies of Non-native Agonists of the LasR Quorum-Sensing Receptor Reveal an L3 Loop "Out" Conformation for LasR. *Cell Chem Biol* **2018**.
27. McCready, A. R.; Paczkowski, J. E.; Henke, B. R.; Bassler, B. L., Structural determinants driving homoserine lactone ligand selection in the Pseudomonas aeruginosa LasR quorum-sensing receptor. *Proc Natl Acad Sci U S A* **2019,** *116* (1), 245-254.
28. Zakhari, J. S.; Kinoyama, I.; Struss, A. K.; Pullanikat, P.; Lowery, C. A.; Lardy, M.; Janda, K. D., Synthesis and molecular modeling provide insight into a Pseudomonas aeruginosa quorum sensing conundrum. *J Am Chem Soc* **2011,** *133* (11), 3840-2.
29. Muh, U.; Hare, B. J.; Duerkop, B. A.; Schuster, M.; Hanzelka, B. L.; Heim, R.; Olson, E. R.; Greenberg, E. P., A structurally unrelated mimic of a Pseudomonas aeruginosa acyl-homoserine lactone quorum-sensing signal. *Proc Natl Acad Sci U S A* **2006,** *103* (45), 16948-52.
30. Borlee, B. R.; Geske, G. D.; Blackwell, H. E.; Handelsman, J., Identification of synthetic inducers and inhibitors of the quorum-sensing regulator LasR in Pseudomonas aeruginosa by high-throughput screening. *Appl Environ Microbiol* **2010,** *76* (24), 8255-8.
31. Moore, J. D.; Gerdt, J. P.; Eibergen, N. R.; Blackwell, H. E., Active efflux influences the potency of quorum sensing inhibitors in Pseudomonas aeruginosa. *Chembiochem* **2014,** *15* (3), 435-42.

32. Moore, J. D.; Rossi, F. M.; Welsh, M. A.; Nyffeler, K. E.; Blackwell, H. E., A Comparative Analysis of Synthetic Quorum Sensing Modulators in Pseudomonas aeruginosa: New Insights into Mechanism, Active Efflux Susceptibility, Phenotypic Response, and Next-Generation Ligand Design. *J Am Chem Soc* **2015,** *137* (46), 14626-39.
33. Lindsay, A.; Ahmer, B. M., Effect of sdiA on biosensors of N-acylhomoserine lactones. *J Bacteriol* **2005,** *187* (14), 5054-8.
34. LasR:A2 - LasR:OdDHL RMSD = 0.585 A, 287 to 287 atoms; LasR:A3 - LasR:OdDHL RMSD = 0.585 A, 284 to 284 atoms; LasR:A4 - LasR:OdDHL RMSD = 0.52 A, 286 to 285 atoms; LasR:A6.1 - LasR:OdDHL RMSD = 0.323 A, 279 to 279 atoms; LasR:A6.2 - LasR:OdDHL RMSD = 20.854, 318 to 318 atoms; LasR:A9 - LasR:OdDHL RMSD = 0.462 A, 275 to 275 atoms; LasR:A14 - LasR:OdDHL RMSD = 0.427 A, 270 to 270 atoms
35. Gerdt, J. P.; McInnis, C. E.; Schell, T. L.; Blackwell, H. E., Unraveling the contributions of hydrogen-bonding interactions to the activity of native and non-native ligands in the quorum-sensing receptor LasR. *Org Biomol Chem* **2015,** *13* (5), 1453-62.
36. Gerdt, J. P.; McInnis, C. E.; Schell, T. L.; Rossi, F. M.; Blackwell, H. E., Mutational analysis of the quorum-sensing receptor LasR reveals interactions that govern activation and inhibition by nonlactone ligands. *Chem Biol* **2014,** *21* (10), 1361-9.
37. Nguyen, Y.; Nguyen, N. X.; Rogers, J. L.; Liao, J.; MacMillan, J. B.; Jiang, Y.; Sperandio, V., Structural and mechanistic roles of novel chemical ligands on the SdiA quorum-sensing transcription regulator. *mBio* **2015,** *6* (2).

# Chapter 5: Profiling the specificity and promiscuity of LuxR-type receptors with a library of *N*-acylated homoserine lactones that vary in aliphatic acyl tail length

Daniel E. Manson, Akshish K. Madepally, and Helen E. Blackwell

D. E. Manson and H.E. Blackwell designed experiments. D. E. Manson and A. K. Mandepally synthesized compounds and conducted screening experiments. D. E. Manson analyzed data. D. E. Manson and H.E. Blackwell wrote the chapter.

## Abstract

Bacteria can communicate via the exchange of low molecular weight signaling molecules in a process known as quorum sensing (QS). Many Gram-negative bacteria utilize *N*-acylated L-homoserine lactones (AHLs) as their primary signaling molecules, which are sensed by LuxR-type receptors. While bacteria that both synthesize and respond to their own AHL have been studied the most extensively, 76% of bacteria that contain LuxR-type receptors do not synthesize AHL signals, raising the intriguing possibility that these bacteria can "eavesdrop" on their AHL-producing neighbors, or they sense alternate signals. Here, we systematically synthesized and screened a focused library of AHLs that vary in the number of carbons (1–20) in their acyl tails, containing both native and non-native signals, in a panel of LuxR-type receptors. Such a fundamental study of aliphatic AHLs, even in one LuxR-type receptor, is surprisingly yet to be reported. Our results (1) inform the fundamental SAR trends surrounding activation and inhibition by AHLs of varying tail lengths; (2) provide a view of the relative promiscuity of "solo" vs. "paired" LuxR-receptors; and (3) identify AHLs that could be useful as tools in manipulating QS in a mixed community of microbes.

## Introduction

Many common bacteria engage in a chemically-mediated signaling system known as quorum sensing (QS).[1] Described in detail in earlier chapters, QS involves the regulation of gene expression and group-beneficial phenotypes via the production and sensing of autoinducer molecules.[2] Phenotypes controlled by QS vary by species, and are connected to virulence (i.e., the ability to infect) in multiple "ESKAPE" pathogens.[3] This link between QS and human health has motivated the development of synthetic molecules that block QS. Examples of such compounds are described at length in Chapters 1–3 of this thesis.

Gram-negative bacteria primarily use *N*-acylated L-homoserine lactones (AHLs) as their autoinducers (see Chapter 1 for a discussion of naturally occurring and synthetic AHLs).[4] These small molecule signals are synthesized by LuxI-type enzymes from *S*-adenosyl methionine and fatty acids.[5] AHLs passively diffuse out of cells,[6] although in certain cases they are also actively exported.[7] At a threshold high cell density, the AHL concentration reaches a sufficient level for binding its cytosolic target, a LuxR-type protein, which are a class of transcription factors that typically dimerize and bind to DNA in a ligand-dependent manner.[8,9]

Over 200 LuxR-type receptors have been identified thus far in bacteria.[10] This accounting is a function of the number of species to be cultured and sequenced; the true number that exist in Nature may be much higher. Intriguingly, 76% with identified *luxR* genes lack corresponding *luxI* genes, implying that these bacteria do not produce their own AHLs.[10] This raises the possibility that a large proportion of QS capable Gram-negative bacteria use their "solo" or "orphan" receptors to "eavesdrop" on other species' AHL-mediated "conversations", and/or they sense other types of signals (self- or non-self-produced). Indeed, multiple bacteria that use AHL-

mediated QS are known to live together in polymicrobial communities.[11] Furthermore, in certain cases, multiple QS-capable pathogens co-infect humans.[12] Our research group is highly interested in the development of small molecules that could selectively manipulate QS in individual bacterial species, as such compounds could serve as tools to interrogate the role of QS in polymicrobial communities and coinfections.

Despite the potential for interspecies interactions via AHL-type signals, research into the selectivity of different LuxR-type receptors for different AHL signals, naturally-occurring and non-natural, is sparse. Such investigations in natural environments (e.g., in or on a host, in the soil, water, etc.) are largely unreported. Likewise, fundamental studies of the effects of AHL structure on bioactivity—i.e., variance in acyl chain carbon number—even in one LuxR-type receptor, are surprisingly lacking in the literature. Previous studies have focused only on a subset of naturally occurring AHLs with an even number of carbons and excluded odd-numbered AHLs (most likely due to the wider availability of the precursor fatty acids). Interestingly, in some of the earliest studies of non-native AHLs and LuxR-type receptors, C7 HSL was shown to be a highly active antagonist of TraR in *Agrobacterium tumefaciens*;[13] we subsequently observed it to be an antagonist of LasR in *P. aeruginosa*.[14] These findings for C7 HSL suggest that more scrutiny of such compounds could be valuable.

Here, we describe our systematic screening and evaluation of a set of AHLs that vary simply in the length of their carbon tails (from 1–20 carbons). We conducted this study in the pursuit of three goals: (i) a study of the basic SAR surrounding acyl tail length for activation and inhibition of multiple different LuxR-type receptors; (ii) evaluating differences in the promiscuity of "solo" vs. synthase "paired" LuxR-type receptors; and (iii) discovering AHLs that could be useful as research probes in the manipulation of mixed microbial cultures.

**Results and Discussion**

We initiated our study by synthesizing a focused library of AHLs that vary in the length of their acyl tail (from 1–20 carbons). Most of these compounds were synthesized by standard carbodiimide-facilitated couplings of the L-homoserine lactone "headgroup"' and the appropriate carboxylic acid (**Scheme 1**). We also examined a series of AHLs with ketones (i.e., 3-oxo groups) at the 3rd carbon of the acyl tail (from 8–13 carbons). 3OC8, 3OC10, and 3OC12 HSL are commercially available and were in stock in our lab. We supplemented these compounds by synthesizing 3OC7, 3OC9, 3OC11, and 3OC13 HSL using the Meldrum's acid strategy first applied by Spring and coworkers (Scheme 1, see Methods section).[15]

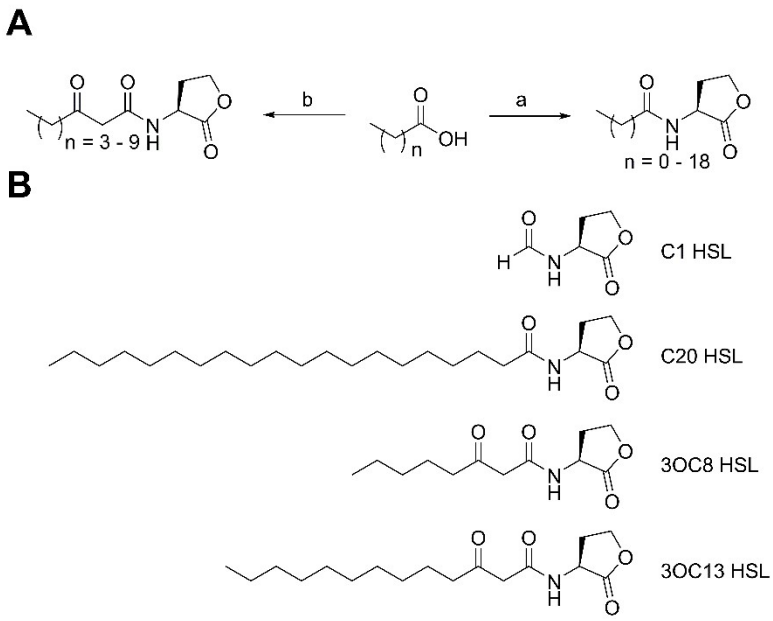


**Scheme 5.1.** (A) Synthesis of straight-chain and 3-oxo aliphatic AHLs, n = 0–18. (a) = EDC·HCl, DMAP, DCM, HSL·HBr; (b) = (1) EDC·HCl, DMAP, DCM, Meldrum's Acid, (2) = △, HSL·HBr, DMF. See experimental section for experimental details. (B) Selected AHLs synthesized for this study.

With our library of compounds in hand, we considered which LuxR-type receptors to evaluate. We chose a variety of "paired" and "solo" LuxR-type receptors for which heterologous

(i.e., *E. coli*) reporter gene screening systems are already used in our laboratory (**Table 1**). We routinely use such heterologous systems, as they are useful for isolating LuxR-type proteins away from confounding pathways (e.g., other LuxR-type receptors[16]or QS systems) present in the native organism. We evaluated four "paired" LuxR-type receptors: LasR and RhlR from *P. aeruginosa;* CviR, from *Chromobacterium violacein;* and CepR from *Burkholderia cepacia*, as well as three "solo" LuxR-type receptors: QscR from *P. aeruginosa*; $SdiA_{SE}$ from *Salmonella enterica* serovar Typhimurium, and $SdiA_{EC}$ from *E. coli*, the latter two of which are 72% identical (Genebank IDs AAC08299.1 and AWF10864.1, respectively). The native or preferred ligand (i.e., capable of maximum activation) of these LuxR receptors varied from four[17] to 12[18] carbons.

**Table 5.1.** LuxR-type proteins evaluated in this study[a]

| Receptor | Native organism | Native or preferred ligand | Ref. for reporter strain |
|---|---|---|---|
| LasR | *Pseudomonas aeruginosa* | 3OC12 HSL | [19] |
| QscR | *Pseudomonas aeruginosa* | 3OC12 HSL[b] | [19] |
| RhlR | *Pseudomonas aeruginosa* | C4 HSL | [20] |
| CviR | *Chromobacterium violacein* | C6 HSL | Unpublished |
| CepR | *Burkholderia cepacia* | C8 HSL | [21] |
| $SdiA_{SE}$ | *Salmonella enterica* | 3OC8 HSL [c] | [22] |
| $SdiA_{EC}$ | *Escherichia coli* | 3OC8 HSL [c] | Unpublished |

[a] All receptors were expressed and screened in *E. coli* strain JLD271 (△*sdiA*).[23] [b]QscR lacks a cognate synthase, but responds maximally to 3OC12 HSL, which is a native AHL signal produced by *P. aeruginosa* (for LasR). [c]SdiA also lacks a cognate synthase, but responds maximally to 3OC8 HSL.

We screened our straight chain aliphatic AHL library for both agonism and antagonism at 10 μM in each of the aforementioned reporter strains (see Supplemental Figures 1-7; antagonism

assays performed in competition against native or preferred AHL), and first visualized the resulting data as a heat map to qualitatively analyze broad activity trends across the receptors (**Figure 1**).[24] We saw that LasR (cognate signal 3OC12 HSL) was activated primarily by AHLs between nine and 15 carbons in length. Given its native preference for 3OC12 HSL, it was somewhat surprising that it was also activated by C5 HSL and C2 HSL, albeit to a lesser extent. It is known, however, that LasR can be activated by short AHL scaffolds that bear a carbocycle on their acyl tails (i.e., phenylacetyl homoserine lactones, PHLs).[14] C7 HSL is a known LasR antagonist,[25] so the discovery that C6 and C8 HSL also inhibited LasR was unsurprising. It is curious, however, to consider the physical contacts that make C7 HSL a LasR antagonist (with no observable activation) and C8 HSL a partial agonist (activation *and* inhibition under the conditions tested). QscR, which like LasR also preferentially binds 3OC12 HSL, was activated by all AHLs from C5 to C16. It was inhibited by all AHLs C4 and shorter.

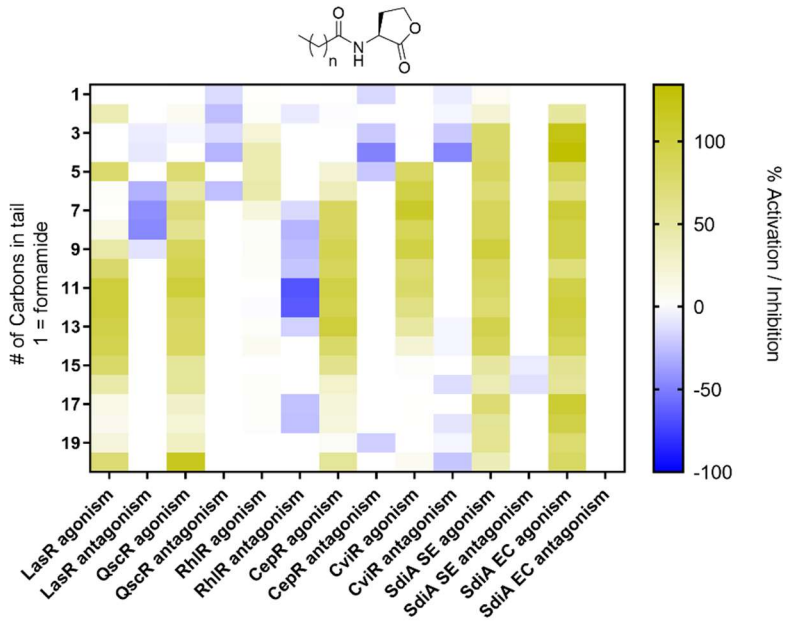


**Figure 5.2.** Heat map depiction of activation and inhibition of various LuxR-type receptors by straight-chain AHLs. For agonism experiments, activity is reported relative to a saturating concentration of native ligand. For antagonism experiments, activity is reported relative to the $EC_{50}$ of native or preferred ligand.

RhlR was unique among the receptors evaluated for (1) the paucity of ligands by which it was activated, and (2) the low extent to which it was activated by those that *were* active (approximately 50% activation by 10 μM of its native ligand, **Figure S3**). RhlR ligands were found to be considerably less potent than those for LasR; the $EC_{50}$ for activation of RhlR by its native ligand, C4 HSL, is ~10 μM,[20] which is three orders of magnitude less than LasR's $EC_{50}$ for activation by 3OC12 HSL (~2 nM).[14] Hydrophobic interactions between the acyl tail of 3OC12 HSL and nonpolar residues that line its binding pocket are important for the LasR – 3OC12 HSL binding interaction,[26] so perhaps the small size of C4 HSL explains its relatively weak affinity for RhlR. In any case, RhlR was only activated by the AHLs closest tail length to C4 HSL and was inhibited by medium to long chain AHLs.

CepR from *B. cepacia* (and conserved in many other Burkholderia species) natively binds to C8 HSL. CepR was activated by AHLs that varied in length from six to 16 carbons. Like QscR, it was inhibited by short-chain AHLs (four carbons and fewer). CviR had similar preferences; it was activated by AHLs between four and 14 carbons in length and inhibited by the ≤4 carbon AHLs. However, unlike CepR, CviR was also weakly inhibited by very long chained AHLs.

Both SdiA variants were more promiscuous than all of the other LuxR-type receptors evaluated herein; they were activated by all AHLs except C1 AHL. They were also antagonized by fewer AHLs than any of the other receptors; in fact, $SdiA_{EC}$ was not antagonized by any of the tested AHLs, and $SdiA_{EC}$ was only weakly antagonized (~10% inhibition) by the C15 and C16 HSLs. SdiA is unusually stable for a LuxR-type receptor; it retains transcriptional activity (i.e.,. it adopts an active, DNA-binding conformation) in the absence of AHLs (in apo-form).[27]

These results for $SdiA_{SE}$ are congruent with a previous study by our lab that also demonstrated it is activated by a far broader range of AHLs than those that inhibit it.[22]

We were surprised to find that the C20 HSL activated most of receptors in which we tested it. Although this AHL does occur naturally,[28] it was strange that activation in LasR, QscR, and CepR, first decreased as chain length passed that of the native ligand, but then increased again at the C20 AHL. A recent collaborative study from our lab and the Lynn research lab indicates that C20 HSL is almost certainly an aggregate at 10 μM in LB medium.[29] Further experiments are required to elucidate whether the observed activity is the result of the binding of a discrete molecule of C20 HSL with a receptor, or the action of an aggregate.

We were curious to conduct an analogous systematic study of the effect of 3-oxo HSL chain length on receptor activation. We screened our smaller library of these derivatives (Scheme 1) in the LasR and QscR reporters (**Figures S8, S9**). We found that each of these ligands activated LasR to roughly the same extent as the straight-chain AHLs (Figure 2; **Figures S1, S8**). However, while C8 HSL was a partial agonist of LasR, 3OC8 HSL was purely an agonist. This finding makes us extremely curious to test 3OC7 HSL in LasR when possible.[30] Each of these 3-oxo HSLs agonized QscR (as did their straight-chain analogs; see above).

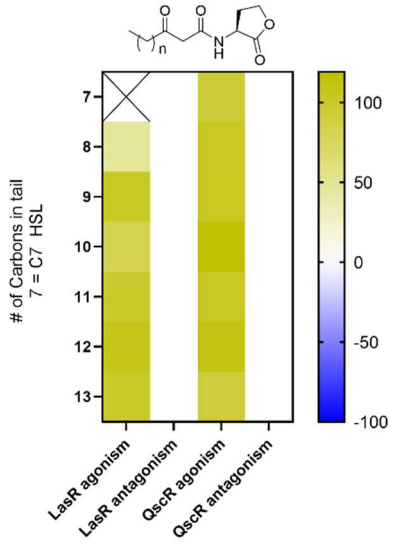


**Figure 5.3.** Heat map depiction of activation and inhibition of various LuxR type receptors by 3-oxo AHLs. 3OC7 HSL was not screened in LasR agonism experiments.

The activity profile of C7 HSL is quite noteworthy. We found it antagonized LasR, antagonized RhlR, and agonized QscR. As LasR and RhlR positively regulate QS and QscR negatively regulates it, this compound should inhibit QS in *P. aeruginosa*. It should also agonize QS in Bcc, as it activated CepR. This compound should therefore be useful in manipulating QS of these two organisms in a co-culture setting – we predict it should boost QS in Burkholderia, and repress it in *P. aeruginosa*. *P. aeruginosa* and Burkholdera are known to coinfect humans,[12] elevating the relevance of this finding.

In summary, we systematically evaluated the AHL-binding "preferences" of a collection of LuxR receptors for AHLs that vary in acyl tail length from one to 20 carbons. The orphan LuxRs that we screened (i.e., QscR/SdiA vs. LasR/CepR/CviR) were more promiscuous than the synthase "paired" receptors. This set of experiments also highlighted the unusual AHL preferences of RhlR. Ongoing structural studies of RhlR may reveal the basis for its limited capacity for activation relative to its homologues.

In closing, we note that a recent study by the Greenberg lab found that heterologous screening systems like the ones used here can overestimate receptor promiscuity, likely due to the overexpression of the LuxR-type protein relative to the levels found in native organisms.[31] This finding must be addressed for the conclusions reached herein to be meaningful. The obvious experiment is to screen these AHL libraries in native screening systems (e.g., screen for CviR activity in a *C. violacein* – based reporter). The high degree of inter-regulation between *P. aeruginosa*'s QS receptors will confound data gathered in that system; we therefore simply recommend screening CviR and SdiA in their native background environments (native screening systems for those receptors exist in the Blackwell lab) to complete this study.

Finally, the AHLs described in this Chapter so far are by no means the only structures of interest for screening against this panel of LuxR-type receptors. Completion of the 3-oxo library (C5-C20), and the asymmetric reduction of the ketone in 3-oxo AHLs to yield the 3-OH species, would provide important sets of AHLs to round out this study. With regard to the 3-OH AHLs, both resultant diastereomers could be screened, clarifying the stereochemical preference of various receptors for a hydroxyl group at that position (if such a preference exists). This synthesis project could provide opportunities for new lab members and undergraduates to "learn the ropes" of AHL preparation, basic microbiology, and cell-based screening. Ultimately, we envision the ultimate success of this project as the perturbation of a mixed-species interaction by a compound chosen from in-cell screening. The deployment of C7 HSL in a nematode model of *P. aeruginosa* /Burkholderia coinfection would represent a promising first attempt.

**Materials and Methods**

**Chemistry**

All reagents were purchased from Sigma Aldrich or Acros organics and were used without further purification, except for dichloromethane, ethyl acetate, and hexanes, which were distilled before use. AHLs were synthesized according to previously published procedures.[15] See SI for detailed synthetic methods. Analytical thin layer chromatography (TLC) was performed on 250 μm glass backed silica plates with F-254 fluorescent indicator from Silicycle and visualized with UV light or potassium permanganate solution. Compounds were stored as powders at -20 °C until needed for experiments. When needed for experiments, DMSO stocks were made at the appropriate concentration and stored at -20°C. See SI for compound characterization data.

**Biology**

Bacteria were cultured in Luria Bertani media and grown at 37°C. Growth was quantified by absorbance at 600 nm ($OD_{600}$). A list of bacterial strains and plasmids used in this project is included in the SI (**Table S1**). Detailed procedures for the heterologous (*E. coli*) reporter experiments are included in the SI. Data analysis was performed using Microsoft Excel and Graphpad Prism (version 8.1).

**General instrumentation information**

NMR spectra were recorded in deuterated solvents at 400 MHz on a Bruker-Avance spectrometer equipped with a BFO probe, and at 500 MHz on a Bruker Avance spectrometer equipped with a DCH cryoprobe. Chemical shifts are reported in parts per million using residual solvent peaks or tetramethylsilane (TMS) as a reference. Couplings are reported in hertz (Hz). Electrospray ionization–exact mass measurement (ESI-EMM) mass spectrometry data were collected on a Waters LCT instrument. Absorbance and fluorescence measurements were obtained on a Biotek Synergy 2 plate reader using Gen5 analysis software.

**Table S5.1** Bacterial strains and plasmids used in this study.

| Strain or Plasmid | Description | Ref |
|---|---|---|
| *E. coli* | | |
| JLD271 | K-12 Δ*lacX74 sdiA271*::CAM; $Cl^R$ | |
| *Plasmids* | | |
| pSC11-L | Broad host range *lasI'-lacZ* reporter; $Ap^R$ | [1] |
| pSC11-Q | Broad host range *PA1897'-lacZ* reporter; $Ap^R$ | [1] |
| pSC11-R | Broad host range *rhlI'-lacZ* reporter; $Ap^R$ | [2] |
| pSC11-CviR | Broad host range *cviI'-lacZ* reporter; $Ap^R$ | Unpublished |
| pSC11-CepR | Broad host range *cepI''-lacZ* reporter; $Ap^R$ | [3] |
| pSC11-$SdiA_{SE}$ | Broad host range *srgE'-lacZ* reporter; $Ap^R$ | [4] |
| pSC11-$SdiA_{EC}$ | Broad host range *gadW'-lacZ* reporter; $Ap^R$ | Unpublished |
| pJN105L | Arabinose-inducible *lasR* expression vector; pBBRMCS backbone; $Gm^R$ | [5] |
| pJN105Q | Arabinose-inducible *qscR* expression vector; pBBRMCS backbone; $Gm^R$ | [5] |
| pJN105R | Arabinose-inducible *rhlR* expression vector; pBBRMCS backbone; $Gm^R$ | [2] |
| pJN105-CviR | Arabinose-inducible *cviR* expression vector; pBBRMCS backbone; $Gm^R$ | Unpublished |
| pJN105-CepR | Arabinose-inducible *cepR* expression vector; pBBRMCS backbone; $Gm^R$ | [3] |
| pJN105- $SdiA_{SE}$ | Arabinose-inducible $sdiA_{SE}$ expression vector; pBBRMCS backbone; $Gm^R$ | [4] |
| pJN105- $SdiA_{EC}$ | Arabinose-inducible $sdiA_{EC}$ expression vector; pBBRMCS backbone; $Gm^R$ | Unpublished |

$Cl^R$ = Chloramphenicol resistance; $Ap^R$ = Ampicillin resistance; $Gm^R$ = Gentamicin resistance

**Representative Synthetic Protocols**

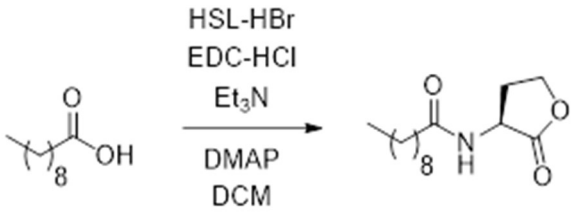


*Synthesis of C10 HSL*

To a solution of decanoic acid (93 mg, 0.5 mmol) in dichloromethane (5 mL) was added EDC-HCl (144 mg, 0.75 mmol), DMAP (9 mg, 0.075 mmol), $Et_3N$ (104 μL, 0.75 mmol) and HSL-HBr (109 mg, 0.6 mmol). The reaction mixture was stirred overnight at room temperature. The following day, the reaction mixture was partitioned with 1M HCl (10 mL). The organic portion was washed with again with 1M HCl (2 x 10 mL), saturated $NaHCO_3$ (3 x 10 mL) and brine (3 x 10 mL), dried over $MgSO_4$ and concentrated under reduced pressure. The resultant material was purified via flash silica gel chromatography with ethyl acetate and hexanes as eluent to yield a white solid (51 mg, 40% isolated yield).

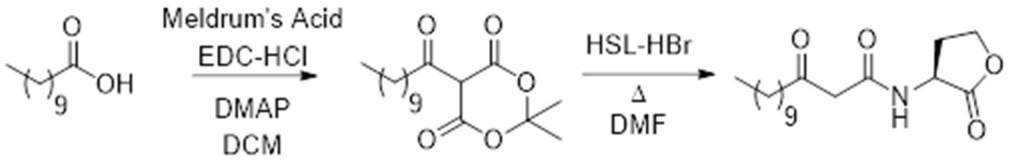


*Synthesis of 3OC12 HSL*

To a solution of decanoic acid (5 mmol, 864 mg) in dichloromethane (50 mL) was added meldrum's acid (721 mg, 5 mmol), EDC-HCl, (1.054 g, 5.5 mmol), and DMAP (610 mg, 5 mmol). The reaction mixture was stirred overnight at RT. The next morning, the reaction was partitioned with 1M HCl (50 mL) and the organic portion was washed a further two times with

1M HCl (50 mL), saturated $NaHCO_3$ (3 x 50 mL), and brine (3 x 50 mL), dried over $MgSO_4$, and concentrated under reduced pressure to yield an oil (1.16 g). This oil was dissolved in DMF (7 mL), and HSL-HBr (0.91g, 5 mmol) was added. The reaction was heated to reflux for 3h, after which the mixture was diluted in ethyl acetate (20 mL), washed with water (3x 20 mL) and brine (3 x 20 mL), then dried over $MgSO_4$ and concentrated under reduced pressure. The resultant material was purified by silica gel chromatography using ethyl acetate and hexanes as solvent to yield a white powder (285 mg, 19% isolated yield over 2 steps).

**_E. coli_ β-galactosidase assay protocol**

The activity of LuxR type proteins was quantified using heterologous (*E. coli*) based reporter gene experiments as previously described.[2-4, 6]

An appropriate volume of LB media supplemented with 100 µg/mL ampicillin and 10 µg/mL gentamicin was inoculated with a single colony of the appropriate reporter strain and grown overnight at 37 °C and shaking at 200 RPM. The next morning, overnight culture was diluted 1:10 info fresh LB and supplemented with fresh antibiotic. This culture was grown to $OD_{600}$ = 0.25, without pathlength correction applied. When culture reached this density, arabinose (0.4% w/v) was added to activate expression of the receptor expression (pJN105) plasmid.

While culture was growing, compound (2 µL of an appropriate stock solution) was dispensed into the interior wells of a clear 96 well plate.

*For agonism assays*

Six wells on each plate were filled with 2 µL of DMSO only (to serve as negative controls) and six wells on each plate were filled with 2 µL of native/preferred ligand to serve as a positive control. For each receptor, those were:

- LasR: 10 mM OdDHL
- QscR: 10 mM OdDHL
- RhlR: 100 mM BHL
- CviR: 10 mM C6 HSL
- CepR: 10 mM C8 HSL
- SdiA (both variants): 10 mM 3OC8 HSL

All other interior wells were filled with 2 µL of 1 mM stock solution of experimental compounds.198 µL of arabinose-induced culture was dispensed into all control and experimental wells and plates were incubated for 4h at 37 °C with shaking at 200 RPM.

*For antagonism assays.*

Twelve wells on each plate were filled with 2 µL of DMSO; half of these served as positive controls, and half as negative controls. All other internal wells were filled with 2 µL of 1 mM stock solution of experimental compounds.

The arabinose-induced culture was partitioned, and to one portion was added an appropriate volume of native/preferred ligand to make the following final concentrations in solution:

- LasR: 2 nM OdDHL
- QscR: 2 nM OdDHL
- RhlR: 10 µM OdDHL
- CviR: 330 nM C6 HSL
- CepR: 2.6 nM C8 HSL
- $SdiA_{SE}$ 1 nM 3OC8 HSL
- $SdiA_{EC}$ 1.5 nM 3OC8 HSL

198 µL of compound-treated subculture was dispensed to all experimental wells and half of the DMSO containing wells (to serve as positive control). The untreated portion of the subculture was then dispensed to the remaining DMSO-containing wells (negative control wells). Water was then dispensed into the exterior wells (to maintain humidity and slow evaporation in the plate) and the plates were incubated at 37 °C for 4h with shaking at 200 RPM.

During incubation, 200 µL of lysis buffer (prepared as described elsewhere)[7] and 8 µL of chloroform was added to the interior wells of an appropriate number chemically resistant 96 well plates.

After incubation, the $OD_{600}$ of all culture plates was read. 50 µL of cell culture from each well was transferred to the plates containing lysis buffer, and cells were lysed by aspirating 20 times. Lysed cell culture (100 µL for LasR and both SdiA variants, 150 µL for all other strains) was transferred to a fresh, clear 96 well plate. B-galactosidase substrate (20 µL of 0.4% w/v *ortho*-nitro phenol galactoside [ONPG] for LasR, 25 µL of ONPG for both SdiA variants, 25 µL of 0.4% w/v chlorophenol red chlorophenol red-β-d-galactopyranoside [CPRG] for all other strains) was added to the same wells, and the plates were incubated according to the following conditions:

- LasR: 30 minutes at 30 °C
- QscR: 45 minutes at 30 °C
- RhlR: 30 minutes at 30 °C
- CviR: 10 minutes at RT
- CepR: 30 minutes at 37 °C
- SdiA (both variants) 20 minutes at 30 °C

After incubation, the assay was quenched by addition of 50 µL of 1M $Na_2CO_3$. For assays using ONPG as substrate, absorbances at 550 and 420 nm was read on a Biotek Synergy 2 plate reader running Gen 5 software (version 1.05); for assays using CPRG, absorbance at 570 nm was read on the same plate reader.

Miller units were calculated according to the following formulae:

For assays using ONPG:

$$Miller\ unit = \frac{1000 * \left(A420 - (1.75 * A550)\right)}{t * v * OD600}$$

Where $t$ = time incubated with substrate (minutes), and $v$ = volume of lysed cells in mL

For assays using CPRG:

$$Miller\ unit = \frac{1000 * (A570)}{t * v * OD600}$$

Data workup was performed using GraphPad Prism (version 8.1.2). Receptor activities were normalized to the average activity in each negative control well, and are reported as percent relative to the average of all positive control wells.

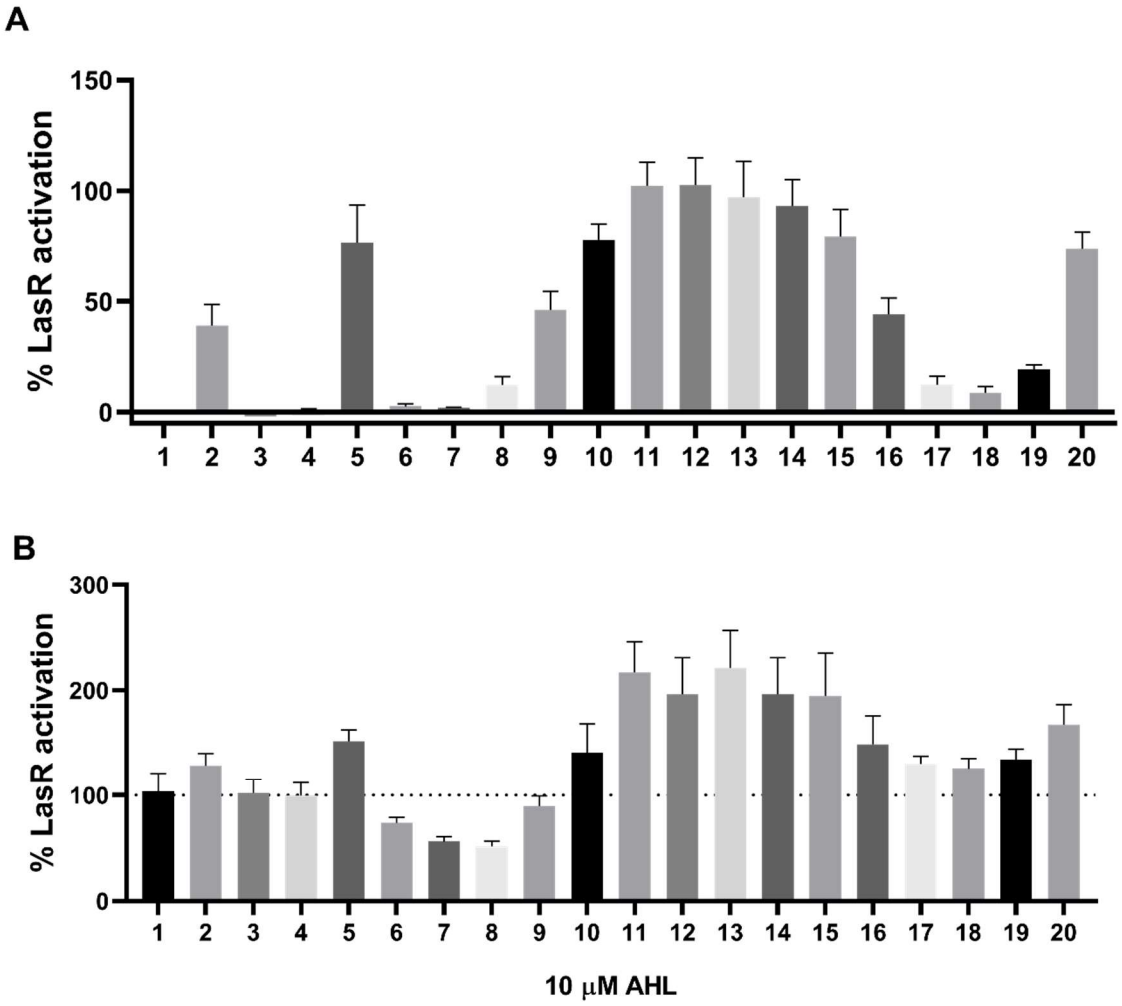


**Figure S5.1.** Single point screening of the 1-20 straight chain library in the *E. coli* LasR reporter (JLD271 + pJN105-L + pSC11-L, see **Table S1**). **(A)** Agonism experiment, 100% = 100 μM OdDHL, n = 3; **(B)** Antagonism experiment; 100% = 2 nM OdDHL, n = 3.

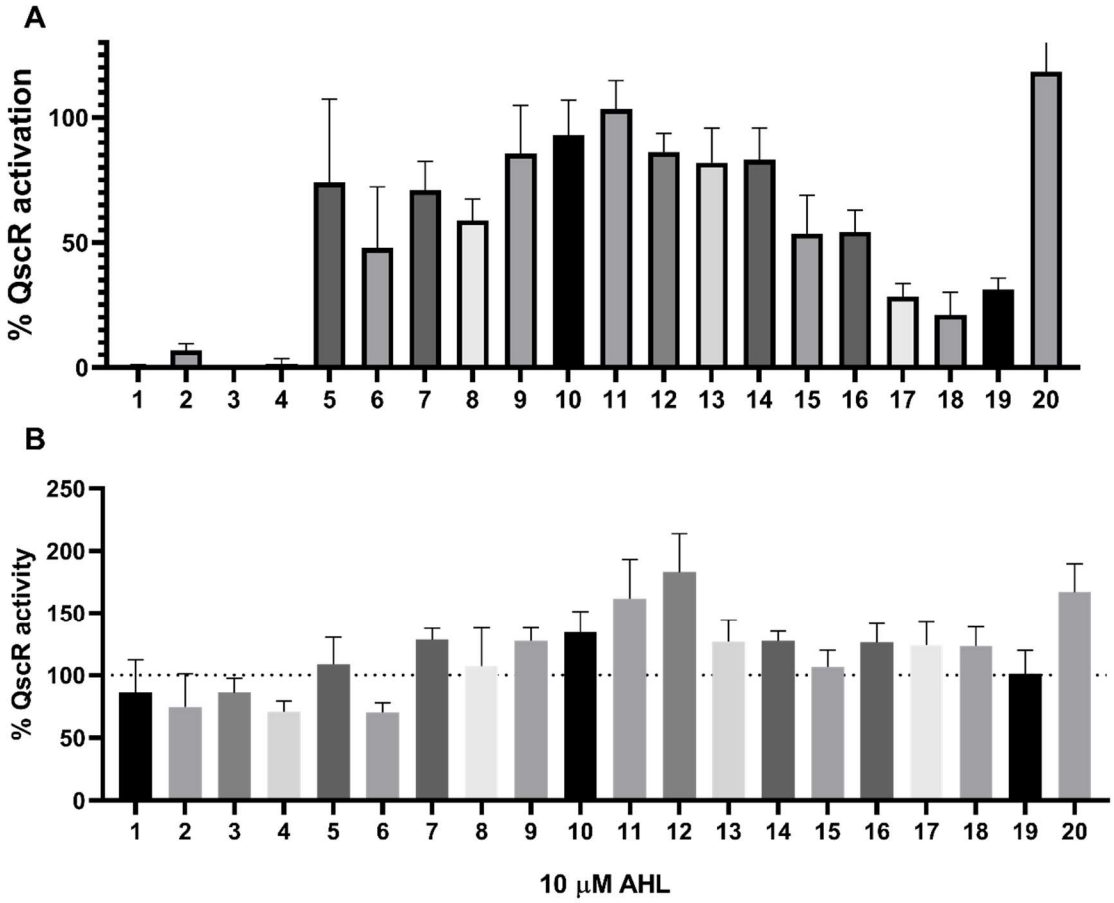


**Figure S5.2.** Single point screening of the 1-20 straight chain library in the *E. coli* QscR reporter (JLD271 + pJN105-Q + pSC11-Q, see **Table S1**). **(A)** Agonism experiment, 100% = 100 μM OdDHL, n = 2; **(B)** Antagonism experiment; 100% = 15 nM OdDHL, n = 2.

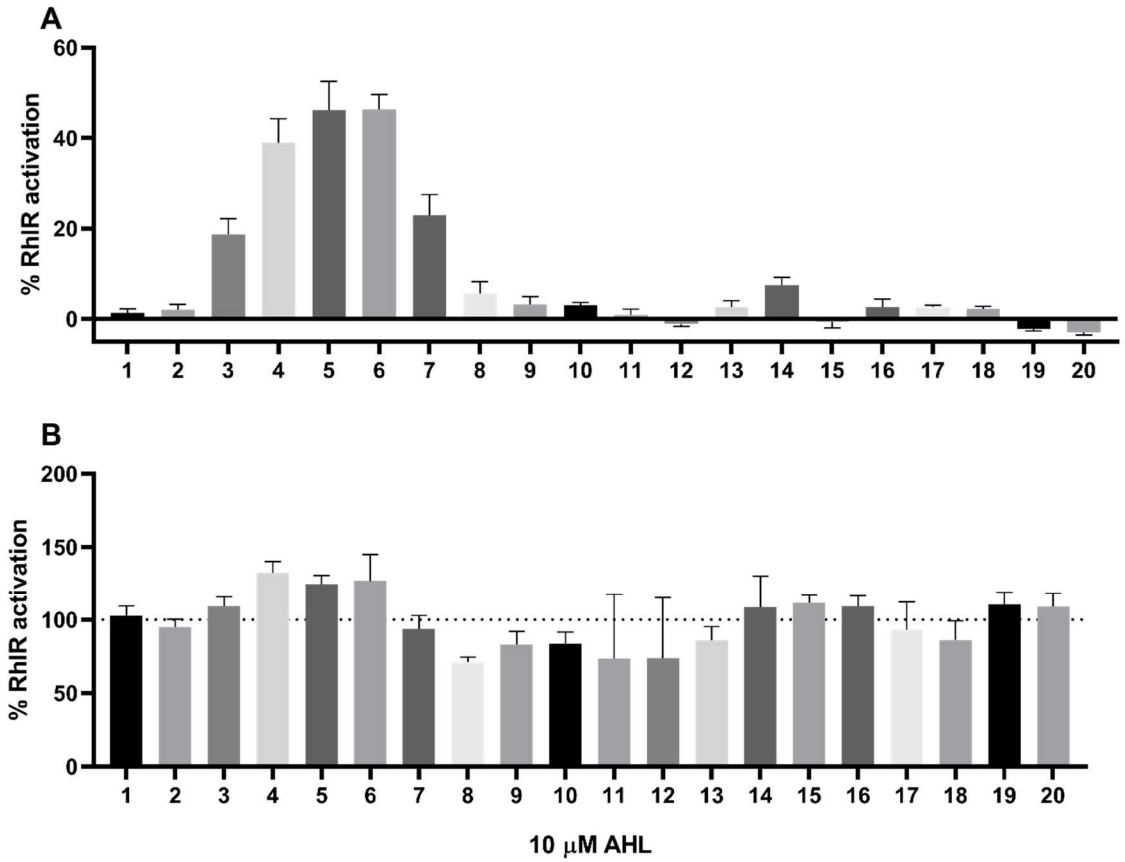


**Figure S5.3.** Single point screening of the 1-20 straight chain library in the *E. coli* RhlR reporter (JLD271 + pJN105-R + pSC11-R, see **Table S1**). **(A)** Agonism experiment, 100% = 1 mM BHL, n = 2; **(B)** Antagonism experiment; 100% = 10 μM BHL, n = 2.

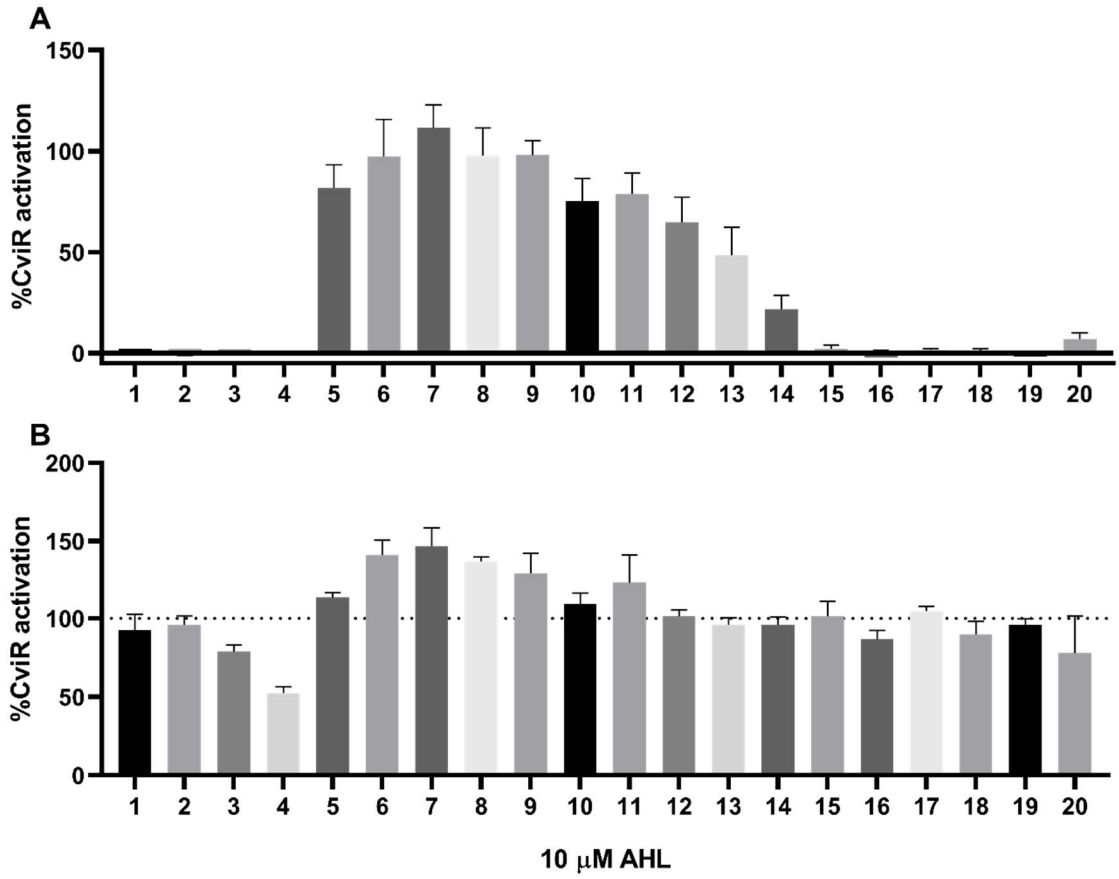


**Figure S5.4.** Single point screening of the 1-20 straight chain library in the *E. coli* CviR reporter (JLD271 + pJN105-CviR + pSC11-CviR, see **Table S1**). **(A)** Agonism experiment, 100% = 100 μM HHL, n = 3; **(B)** Antagonism experiment; 100% = 330 nM HHL, n = 1.

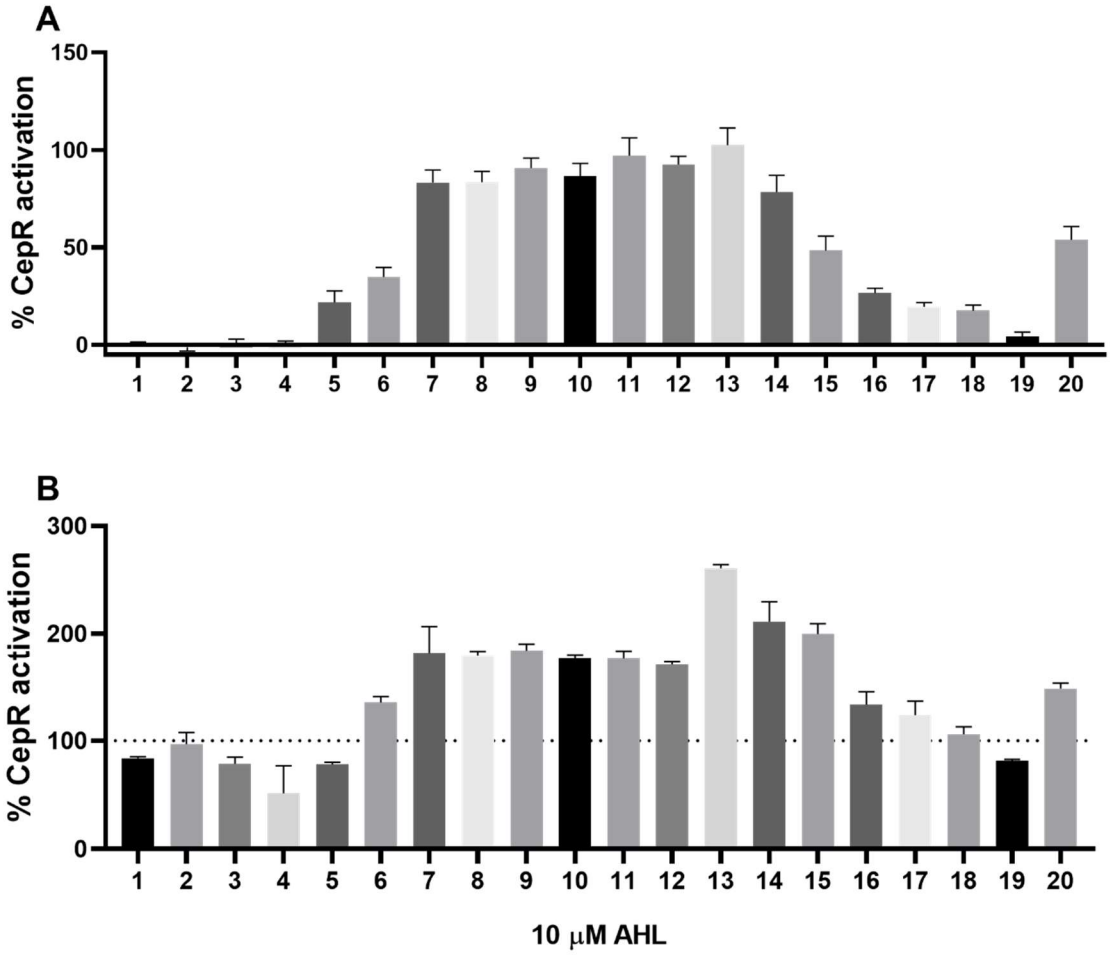


**Figure S5.5.** Single point screening of the 1-20 straight chain library in the *E. coli* CepR reporter (JLD271 + pJN105-CepR + pSC11-CepR, see **Table S1**). **(A)** Agonism experiment, 100% = 100 μM OHL, n = 3; **(B)** Antagonism experiment; 100% = 2.6 nM OHL, n = 1.

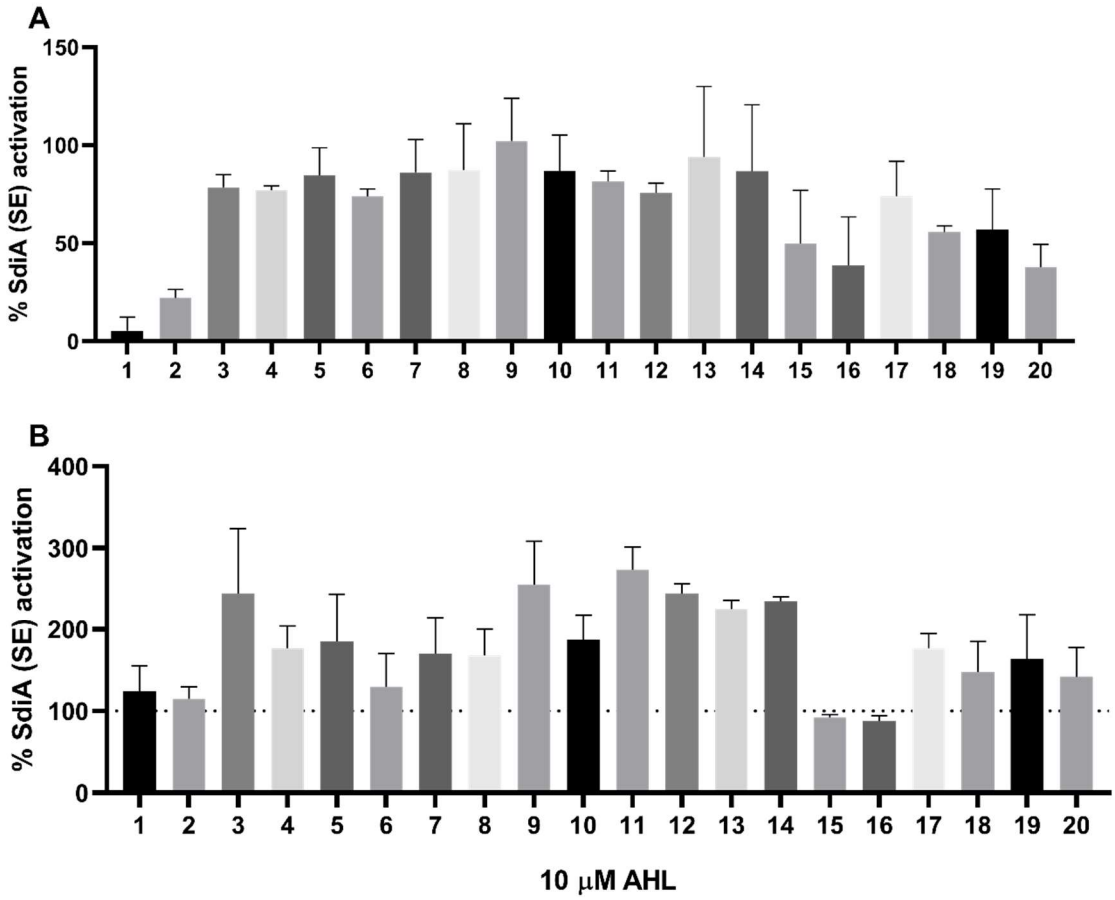


**Figure S5.6.** Single point screening of the 1-20 straight chain library in the *E. coli* $SdiA_{SE}$ reporter (JLD271 + pJN105- $SdiA_{SE}$ + pSC11- $SdiA_{SE}$, see **Table S1**). **(A)** Agonism experiment, 100% = 100 μM OOHL, n = 2; **(B)** Antagonism experiment; 100% = 1 nM OOHL, n = 2.

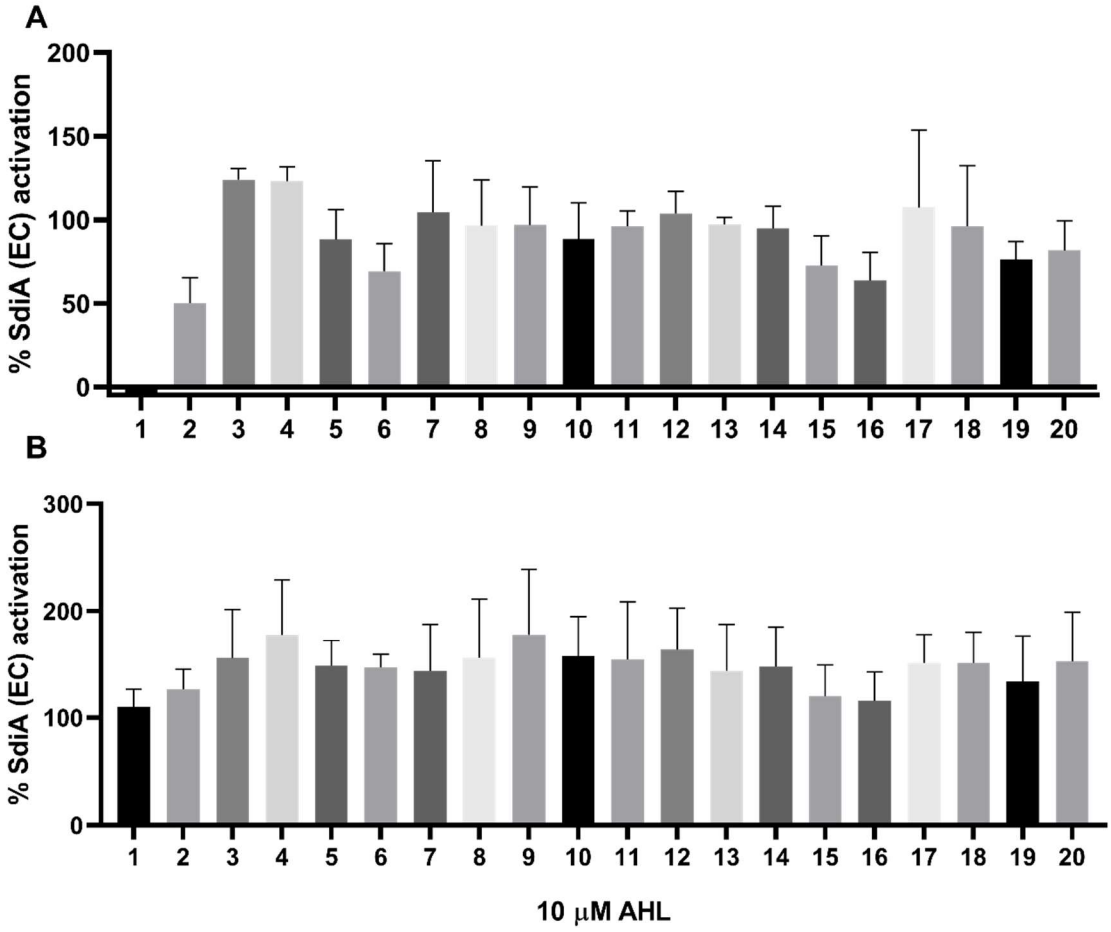


**Figure S5.7.** Single point screening of the 1-20 straight chain library in the *E. coli* $SdiA_{EC}$ reporter (JLD271 + pJN105- $SdiA_{EC}$ + pSC11- $SdiA_{EC}$, see **Table S1**). **(A)** Agonism experiment, 100% = 100 μM OOHL, n = 2; **(B)** Antagonism experiment; 100% = 1.5 nM OOHL, n = 2.

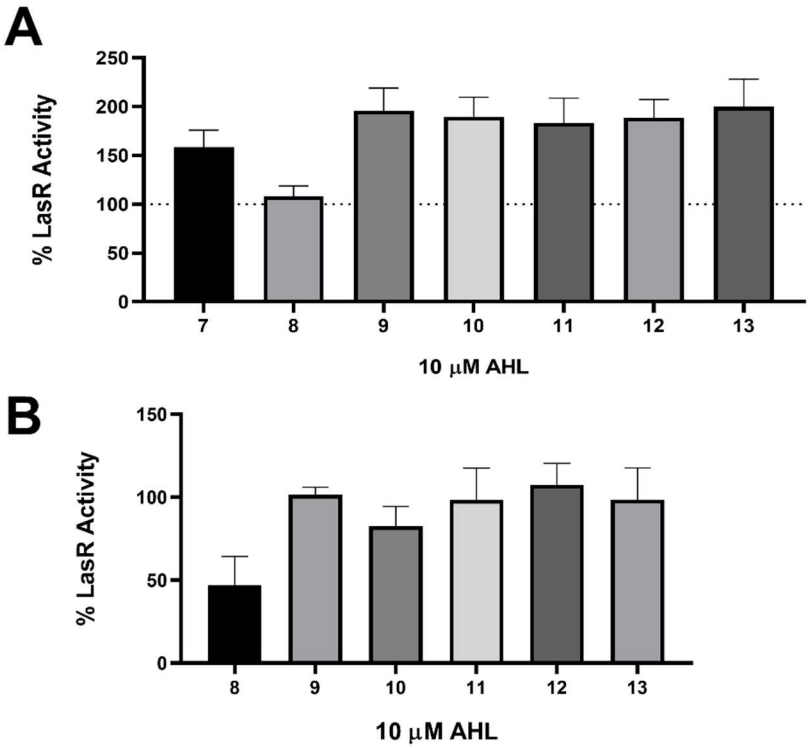


**Figure S5.8.** Single point screening of the 8-13 3-oxo library in the *E. coli* LasR reporter (JLD271 + pJN105-L + pSC11-L, see **Table S1**). **(A)** Agonism experiment, 100% = 100 μM OdDHL, n = 3; **(B)** Antagonism experiment; 100% = 2 nM OdDHL, n = 3.

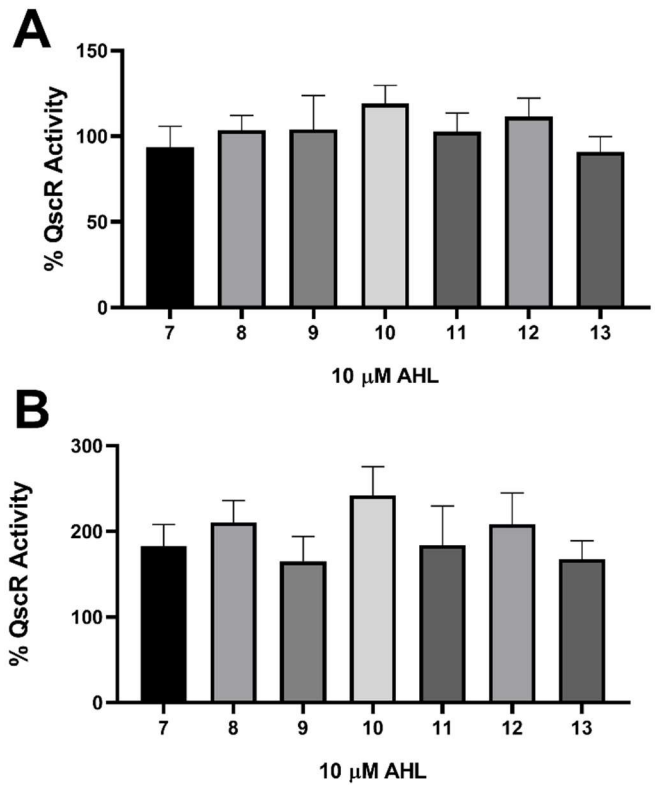


**Figure S.9.** Single point screening of the 8-13 3-oxo library in the *E. coli* QscR reporter (JLD271 + pJN105-Q + pSC11-Q, see **Table S1**). **(A)** Agonism experiment, 100% = 100 μM OdDHL, n = 3; **(B)** Antagonism experiment; 100% = 15 nM OdDHL, n = 3.

**COMPOUND CHARACTERIZATION DATA**

3C HSL

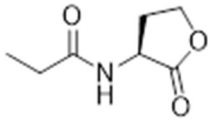

$^{1}$H NMR (400 MHz, Chloroform-*d*) δ 6.06 (s, 1H), 4.56 (ddd, *J* = 11.6, 8.6, 5.8 Hz, 1H), 4.48 (td, *J* = 9.1, 1.2 Hz, 1H), 4.29 (ddd, *J* = 11.4, 9.3, 5.8 Hz, 1H), 2.86 (dddd, *J* = 12.5, 8.5, 5.8, 1.2 Hz, 1H), 2.30 (qd, *J* = 7.6, 1.3 Hz, 2H), 2.14 (dtd, *J* = 12.5, 11.5, 8.8 Hz, 1H), 1.18 (t, *J* = 7.6 Hz, 3H). ESI-EMM: $[M+H]^+$ calculated [m+h] 158.0812; measured 158.081, 1.3 ppm.

4C HSL

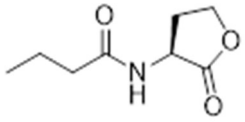

$^{1}$H NMR (500 MHz, Chloroform-*d*) δ 6.11 (s, 1H), 4.57 (ddd, *J* = 11.6, 8.6, 5.9 Hz, 1H), 4.47 (td, *J* = 9.1, 1.2 Hz, 1H), 4.29 (ddd, *J* = 11.3, 9.3, 5.8 Hz, 1H), 2.85 (dddd, *J* = 13.4, 12.2, 6.7, 3.8 Hz, 1H), 2.24 (td, *J* = 7.4, 2.1 Hz, 2H), 2.14 (dtd, *J* = 12.5, 11.5, 8.8 Hz, 1H), 1.69 (h, *J* = 7.4 Hz, 2H), 0.97 (t, *J* = 7.4 Hz, 3H). $^{13}$C NMR (126 MHz, $CDCl_3$) δ 175.61, 173.62, 66.13, 49.23, 38.04, 30.63, 18.88, 13.68, 1.03 ESI- EMM $[m+h]^+$ calculated 172.0968; measured 172.1967, 0.6 ppm

5C HSL

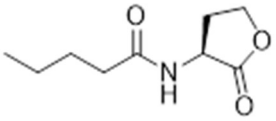

$^{1}$H NMR (500 MHz, Chloroform-*d*) δ 6.05 (s, 1H), 4.63 – 4.41 (m, 2H), 4.29 (ddd, *J* = 11.2, 9.3, 5.9 Hz, 1H), 2.86 (dddd, *J* = 12.7, 8.5, 5.9, 1.2 Hz, 1H), 2.26 (td, *J* = 7.4, 1.5 Hz, 2H), 2.18 – 2.08 (m, 1H), 1.64 (p, *J* = 7.6 Hz, 2H), 1.43 – 1.30 (m, 2H), 0.93 (t, *J* = 7.3 Hz, 3H). $^{13}$C NMR (126 MHz, $CDCl_3$) δ 175.57, 173.75, 66.12, 49.26, 35.91, 30.67, 27.50, 22.32, 13.77. ESI-EMM: calculated [m+h] 186.1125; measured 186.1123 1.1 ppm

6C HSL

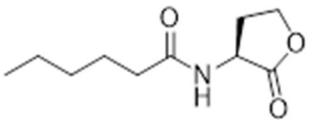

$^{1}$H NMR (500 MHz, Chloroform-*d*) δ 6.10 (d, *J* = 5.8 Hz, 1H), 4.56 (ddd, *J* = 11.6, 8.6, 5.9 Hz, 1H), 4.47 (td, *J* = 9.1, 1.1 Hz, 1H), 4.29 (ddd, *J* = 11.3, 9.2, 5.8 Hz, 1H), 2.93 – 2.81 (m, 1H), 2.25 (td, *J* = 7.4, 1.6 Hz, 2H), 2.14 (qd, *J* = 11.8, 8.8 Hz, 1H), 1.64 (d, *J* = 7.3 Hz, 3H), 1.32 (td, *J* = 6.9, 5.8, 3.3 Hz, 4H), 0.90 (t, *J* = 6.8 Hz, 3H). $^{13}$C NMR (126 MHz, $CDCl_3$) δ 175.62, 173.79, 66.14, 49.25, 36.16, 31.36, 30.65, 25.12, 22.37, 13.92. ESI-EMM: calculated [m+h] 200.1281; measured 200.1279 1.0 ppm

7C HSL

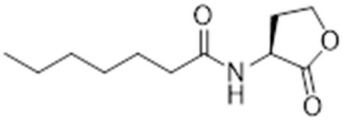

$^{1}$H NMR (500 MHz, Chloroform-*d*) δ 6.02 – 5.92 (m, 1H), 4.59 – 4.41 (m, 2H), 4.28 (ddd, *J* = 11.3, 9.3, 5.8 Hz, 1H), 2.87 (dddd, *J* = 12.6, 8.5, 5.8, 1.2 Hz, 1H), 2.25 (td, *J* = 7.4, 1.6 Hz, 2H), 2.12 (dtd, *J* = 12.4, 11.5, 8.8 Hz, 1H), 1.72 – 1.59 (m, 2H), 1.40 – 1.23 (m, 6H), 0.88 (t, *J* = 6.7 Hz, 3H). $^{13}$C NMR (126 MHz, $CDCl_3$) δ $^{13}$C NMR (126 MHz, $CDCl_3$) δ 175.51, 173.75, 66.12, 49.30, 36.21, 31.48, 30.75, 28.87, 25.39, 22.47, 14.02. ESI-EMM: calculated [m+h] 214.1438; measured 214.1435 1.4 ppm

8C HSL

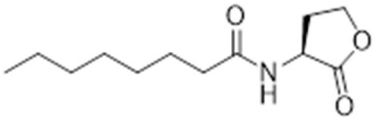

$^{1}$H NMR (500 MHz, Chloroform-*d*) δ 6.25 (d, *J* = 6.1 Hz, 1H), 4.57 (ddd, *J* = 11.6, 8.6, 6.2 Hz, 1H), 4.45 (td, *J* = 9.0, 1.2 Hz, 1H), 4.27 (ddd, *J* = 11.2, 9.2, 5.9 Hz, 1H), 2.81 (dddd, *J* = 14.2, 8.8, 6.0, 1.3 Hz, 1H), 2.29 – 2.08 (m, 3H), 1.62 (q, *J* = 7.3 Hz, 2H), 1.36 – 1.20 (m, 8H), 0.90 – 0.82 (m, 3H). $^{13}$C NMR (126 MHz, $CDCl_3$) δ 175.73, 173.82, 66.13, 49.15, 36.17, 31.65, 30.48, 29.17, 28.98, 25.45, 22.60, 14.07. ESI-EMM: calculated [m+h] 228.1594; measured 228.1593 0.4 ppm

9C HSL

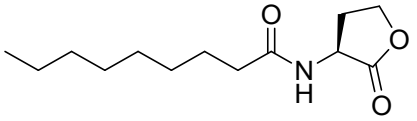

$^{1}$H NMR (500 MHz, Chloroform-*d*) δ 4.94 (s, 1H), 4.58 – 4.44 (m, 2H), 4.29 (ddd, *J* = 11.2, 9.3, 5.8 Hz, 1H), 2.88 (dddd, *J* = 12.6, 8.5, 5.8, 1.2 Hz, 1H), 2.25 (td, *J* = 7.5, 1.7 Hz, 2H), 2.17 – 2.07 (m, 1H), 1.65 (t, *J* = 7.3 Hz, 2H), 1.38 – 1.20 (m, 10H), 0.88 (t, *J* = 6.8 Hz, 3H). $^{13}$C NMR (126 MHz, $CDCl_3$) δ 175.48, 173.73, 66.12, 49.31, 36.22, 31.80, 30.78, 29.27, 29.21, 29.11, 25.43, 22.64, 14.10, ESI-EMM: calculated [m+Na] 264.1570; measured 264.1586, 1.5 ppm

10C HSL

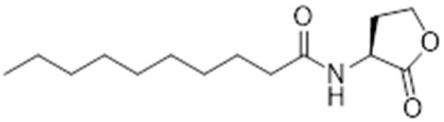

$^{1}$H NMR (500 MHz, Chloroform-*d*) δ 6.27 (d, *J* = 6.2 Hz, 1H), 4.59 (ddd, *J* = 11.6, 8.7, 6.1 Hz, 1H), 4.47 (t, *J* = 9.0 Hz, 1H), 4.29 (ddd, *J* = 11.3, 9.2, 5.9 Hz, 1H), 2.82 (ddd, *J* = 11.9, 8.6, 5.9 Hz, 1H), 2.35 – 2.08 (m, 3H), 1.72 – 1.58 (m, 2H), 1.36 – 1.21 (m, 13H), 0.88 (t, *J* = 6.9 Hz, 3H). $^{13}$C NMR (126 MHz, $CDCl_3$) δ 175.73, 173.82, 66.12, 49.15, 36.18, 31.85, 30.48, 29.42, 29.33, 29.26, 29.22, 25.46, 22.66, 14.11. ESI-EMM: calculated [m+h] 256.1907; measured 256.1904 1.2 ppm

11C HSL

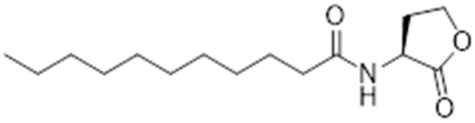

$^1$H NMR (500 MHz, Chloroform-*d*) δ 6.07 (d, *J* = 5.9 Hz, 1H), 4.56 (ddd, *J* = 11.6, 8.5, 5.8 Hz, 1H), 4.50 – 4.44 (m, 1H), 4.29 (ddd, *J* = 11.4, 9.3, 5.9 Hz, 1H), 2.91 – 2.80 (m, 1H), 2.25 (td, *J* = 7.4, 1.6 Hz, 2H), 2.13 (dtd, *J* = 12.5, 11.5, 8.8 Hz, 1H), 1.69 – 1.59 (m, 3H), 1.37 – 1.20 (m, 14H), 0.88 (t, *J* = 6.9 Hz, 3H). $^{13}$C NMR (126 MHz, $CDCl_3$) δ 175.59, 173.78, 66.13, 49.25, 36.21, 31.89, 30.67, 29.56, 29.46, 29.32, 29.30, 29.22, 25.44, 22.68, 14.12 ESI-EMM: calculated [m+h] 270.2064; measured 270.2060 1.5 ppm

12C HSL

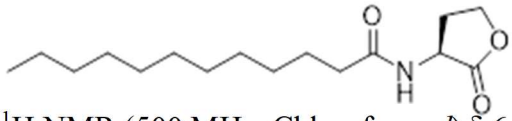

$^1$H NMR (500 MHz, Chloroform-*d*) δ 6.05 (s, 1H), 4.55 (ddd, *J* = 11.6, 8.5, 5.8 Hz, 1H), 4.47 (t, *J* = 9.0 Hz, 1H), 4.29 (ddd, *J* = 11.4, 9.2, 5.8 Hz, 1H), 2.86 (ddd, *J* = 13.2, 8.5, 5.8 Hz, 1H), 2.25 (td, *J* = 7.3, 1.6 Hz, 2H), 2.13 (qd, *J* = 11.7, 8.8 Hz, 1H), 1.65 (d, *J* = 7.2 Hz, 3H), 1.27 (d, *J* = 11.4 Hz, 17H), 0.88 (t, *J* = 6.8 Hz, 3H). $^{13}$C NMR (126 MHz, $CDCl_3$) δ 175.71, 173.91, 66.26, 49.41, 36.35, 32.05, 30.83, 29.74, 29.60, 29.47, 29.46, 29.36, 25.58, 22.83, 14.27. ESI-EMM: calculated [m+h] 284.2220; measured 284.2217, 1.1 ppm

13C HSL

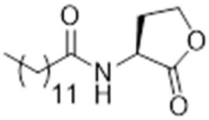

$^1$H NMR (400 MHz, Chloroform-*d*) δ 5.94 (s, 1H), 4.58 – 4.42 (m, 2H), 4.29 (ddd, *J* = 11.4, 9.3, 5.8 Hz, 1H), 2.93 – 2.84 (m, 1H), 2.30 – 2.20 (m, 2H), 2.20 – 2.06 (m, 1H), 1.64 (t, *J* = 7.4 Hz, 2H), 1.27 (d, *J* = 15.1 Hz, 15H), 0.88 (t, *J* = 6.8 Hz, 3H). ESI-EMM: calculated [m+h] 298.2377; measured 298.2374 1.0 ppm

14C HSL

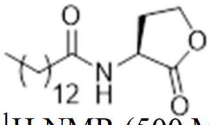

$^1$H NMR (500 MHz, Chloroform-*d*) δ 5.96 (s, 1H), 4.54 (ddd, *J* = 11.7, 8.5, 5.6 Hz, 1H), 4.47 (td, *J* = 9.1, 1.1 Hz, 1H), 4.29 (ddd, *J* = 11.3, 9.3, 5.8 Hz, 1H), 2.88 (dddd, *J* = 12.5, 8.6, 5.8, 1.1 Hz, 1H), 2.25 (td, *J* = 7.3, 1.7 Hz, 2H), 2.12 (qd, *J* = 11.8, 8.8 Hz, 1H), 1.70 – 1.60 (m, 2H), 1.25 (s, 20H), 0.88 (t, *J* = 6.9 Hz, 3H). $^{13}$C NMR (126 MHz, $CDCl_3$) δ 175.49, 173.75, 66.12, 49.31, 36.22, 31.92, 30.77, 29.68, 29.65, 29.60, 29.46, 29.36, 29.31, 29.21, 25.43, 22.70, 14.13 ESI-EMM: calculated [m+h] 312.2533; measured 312.2527 1.9 ppm

15C HSL

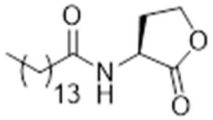

$^1$H NMR (400 MHz, Chloroform-*d*) δ 6.21 (d, *J* = 6.1 Hz, 1H), 4.58 (ddd, *J* = 11.6, 8.6, 6.0 Hz, 1H), 4.47 (td, *J* = 9.0, 1.2 Hz, 1H), 4.29 (ddd, *J* = 11.3, 9.3, 5.9 Hz, 1H), 2.89 – 2.78 (m, 1H), 2.31 – 2.21 (m, 2H), 2.14 (qd, *J* = 11.6, 8.8 Hz, 1H), 1.65 (q, *J* = 7.4 Hz, 2H), 1.36 – 1.25 (m, 8H), 1.25 (s, 12H), 0.88 (t, *J* = 6.7 Hz, 3H). ESI-EMM: calculated [m+h] 326.2690; measured 326.2686 1.2 ppm

16C HSL

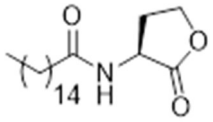

$^1$H NMR (400 MHz, Chloroform-*d*) δ 6.33 (d, *J* = 6.1 Hz, 1H), 4.58 (ddd, *J* = 11.5, 8.6, 6.1 Hz, 1H), 4.47 (td, *J* = 9.1, 1.3 Hz, 1H), 4.28 (ddd, *J* = 11.2, 9.2, 5.9 Hz, 1H), 2.88 – 2.77 (m, 2H), 2.28 – 2.11 (m, 3H), 1.64 (p, *J* = 7.5 Hz, 2H), 1.37 – 1.21 (m, 23H), 0.92 – 0.83 (m, 3H). ESI-EMM: calculated [m+h] 340.2846; measured 340.2843 0.9 ppm

17C HSL

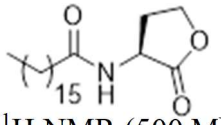

$^1$H NMR (*500* MHz, Chloroform-*d*) δ 5.94 (s, 1H), 4.58 – 4.44 (m, 2H), 4.29 (ddd, *J* = 11.2, 9.3, 5.8 Hz, 1H), 2.88 (dddd, *J* = 12.6, 8.5, 5.8, 1.1 Hz, 1H), 2.25 (td, *J* = 7.4, 1.7 Hz, 2H), 2.12 (qd, *J* = 11.7, 8.7 Hz, 1H), 1.64 (t, *J* = 7.3 Hz, 2H), 1.25 (s, 26H), 0.88 (t, *J* = 6.8 Hz, 3H). $^{13}$C NMR (126 MHz, $CDCl_3$) δ 175.48, 173.75, 66.12, 49.32, 36.23, 31.93, 30.78, 29.70, 29.68, 29.67, 29.65, 29.61, 29.46, 29.37, 29.32, 29.22, 25.43, 22.70, 14.14 ESI-EMM: calculated [m+h] 354.3003; measured 354.2997 1.7 ppm

18C HSL

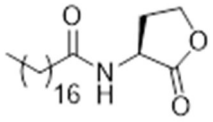

$^1$H NMR (500 MHz, Chloroform-*d*) δ 5.99 (d, *J* = 5.6 Hz, 1H), 4.54 (ddd, *J* = 11.6, 8.5, 5.7 Hz, 1H), 4.47 (t, *J* = 9.0 Hz, 1H), 4.29 (ddd, *J* = 11.3, 9.3, 5.8 Hz, 1H), 2.87 (ddd, *J* = 13.4, 8.5, 5.8 Hz, 1H), 2.25 (dd, *J* = 8.8, 6.6 Hz, 2H), 2.12 (qd, *J* = 11.8, 8.7 Hz, 1H), 1.64 (q, *J* = 7.4 Hz, 2H), 1.25 (s, 28H), 0.88 (t, *J* = 6.8 Hz, 3H). $^{13}$C NMR (126 MHz, $CDCl_3$) δ 175.46, 173.74, 66.12, 49.33, 36.23, 31.93, 30.80, 29.70, 29.67, 29.65, 29.61, 29.46, 29.37, 29.32, 29.22, 25.43, 22.70, 14.14 ESI-EMM: calculated [m+na] 390.2979 measured 390.2974 1.3 ppm

19C HSL

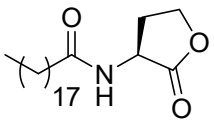

$^{1}$H NMR (500 MHz, Chloroform-*d*) δ 5.93 (d, *J* = 5.6 Hz, 1H), 4.57 – 4.44 (m, 2H), 4.29 (ddd, *J* = 11.3, 9.3, 5.8 Hz, 1H), 2.89 (dtd, *J* = 13.2, 6.2, 3.0 Hz, 1H), 2.25 (td, *J* = 7.4, 1.7 Hz, 2H), 2.12 (qd, *J* = 11.8, 8.8 Hz, 1H), 1.65 (q, *J* = 7.4 Hz, 2H), 1.25 (s, 29H), 0.88 (t, *J* = 6.8 Hz, 3H). $^{13}$C NMR (126 MHz, $CDCl_3$) δ 175.47, 173.75, 66.12, 49.32, 36.23, 31.93, 30.79, 29.71, 29.68, 29.67, 29.65, 29.61, 29.46, 29.37, 29.32, 29.22, 25.43, 22.70, 14.14. ESI-EMM: calculated [m+na] 404.3135 measured 404.3132 0.7 ppm

20C HSL

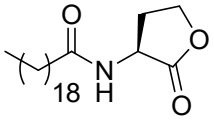

$^{1}$H NMR (500 MHz, Chloroform-*d*) δ 5.91 (s, 1H), 4.53 (ddd, *J* = 11.6, 8.5, 5.5 Hz, 1H), 4.47 (t, *J* = 9.0 Hz, 1H), 4.29 (ddd, *J* = 11.4, 9.3, 5.8 Hz, 1H), 2.89 (ddd, *J* = 13.4, 8.6, 5.8 Hz, 1H), 2.25 (td, *J* = 7.4, 1.7 Hz, 2H), 2.12 (qd, *J* = 11.8, 8.8 Hz, 1H), 1.65 (q, *J* = 7.4 Hz, 2H), 1.25 (s, 32H), 0.88 (t, *J* = 6.8 Hz, 3H). $^{13}$C NMR (126 MHz, $CDCl_3$) δ 175.45, 173.72, 66.11, 49.33, 36.23, 31.93, 30.80, 29.71, 29.68, 29.66, 29.65, 29.61, 29.46, 29.37, 29.31, 29.21, 25.43, 22.70, 14.13. ESI-EMM: calculated [m+na] 418.3292 measured 418.3286 1.4 ppm

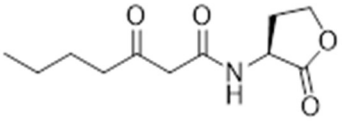

$^{1}$H NMR (500 MHz, Chloroform-*d*) δ 7.69 (d, *J* = 6.7 Hz, 1H), 4.61 (ddd, *J* = 11.4, 8.8, 6.8 Hz, 1H), 4.47 (tq, *J* = 8.9, 1.5 Hz, 1H), 4.32 – 4.24 (m, 1H), 3.48 (s, 2H), 2.78 – 2.69 (m, 1H), 2.54 (t, *J* = 7.4 Hz, 2H), 2.33 – 2.19 (m, 1H), 1.57 (dtd, *J* = 9.1, 7.4, 5.7 Hz, 2H), 1.32 (ht, *J* = 7.3, 1.4 Hz, 2H), 0.91 (tt, *J* = 7.4, 1.5 Hz, 3H). $^{13}$C NMR (126 MHz, $CDCl_3$) δ 206.50, 174.93, 166.53, 65.92, 49.03, 48.26, 43.53, 29.68, 25.40, 22.10, 13.77.

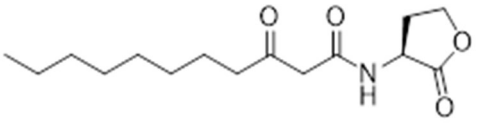

$^{1}$H NMR (500 MHz, Chloroform-*d*) δ 7.66 (d, *J* = 6.7 Hz, 1H), 4.60 (ddd, *J* = 11.4, 8.7, 6.7 Hz, 1H), 4.47 (td, *J* = 9.1, 1.5 Hz, 1H), 4.28 (ddd, *J* = 11.0, 9.2, 6.1 Hz, 1H), 3.47 (s, 2H), 2.79 – 2.71 (m, 1H), 2.53 (t, *J* = 7.3 Hz, 2H), 2.24 (dtd, *J* = 12.5, 11.2, 8.9 Hz, 1H), 1.58 (t, *J* = 7.3 Hz, 2H), 1.34 – 1.20 (m, 11H), 0.88 (t, *J* = 6.9 Hz, 3H). $^{13}$C NMR (126 MHz, $CDCl_3$) δ 206.57, 174.83, 166.39, 65.89, 49.05, 48.15, 43.92, 31.79, 29.81, 29.30, 29.09, 29.00, 23.37, 22.63, 14.08.

**REFERENCES for materials and methods**

1. Chugani, S. A.; Whiteley, M.; Lee, K. M.; D'Argenio, D.; Manoil, C.; Greenberg, E. P., QscR, a modulator of quorum-sensing signal synthesis and virulence in Pseudomonas aeruginosa. *Proc Natl Acad Sci U S A* **2001,** *98* (5), 2752-7.
2. Eibergen, N. R.; Moore, J. D.; Mattmann, M. E.; Blackwell, H. E., Potent and Selective Modulation of the RhlR Quorum Sensing Receptor by Using Non-native Ligands: An Emerging Target for Virulence Control in Pseudomonas aeruginosa. *Chembiochem* **2015,** *16* (16), 2348-56.
3. Slinger, B. L.; Deay, J. J.; Chandler, J. R.; Blackwell, H. E., Potent modulation of the CepR quorum sensing receptor and virulence in a Burkholderia cepacia complex member using non-native lactone ligands. *Sci Rep* **2019,** *9* (1), 13449.
4. Styles, M. J.; Blackwell, H. E., Non-native autoinducer analogs capable of modulating the SdiA quorum sensing receptor in Salmonella enterica serovar Typhimurium. *Beilstein J Org Chem* **2018,** *14*, 2651-2664.
5. Lee, J. H.; Lequette, Y.; Greenberg, E. P., Activity of purified QscR, a Pseudomonas aeruginosa orphan quorum-sensing transcription factor. *Mol Microbiol* **2006,** *59* (2), 602-9.
6. Boursier, M. E.; Manson, D. E.; Combs, J. B.; Blackwell, H. E., A comparative study of non-native N -acyl l -homoserine lactone analogs in two Pseudomonas aeruginosa quorum sensing receptors that share a common native ligand yet inversely regulate virulence. *Bioorganic & Medicinal Chemistry* **2018**.
7. Manson, D. E.; O'Reilly, M. C.; Nyffeler, K. E.; Blackwell, H. E., Design, synthesis, and biochemical characterization of non-native antagonists of the Pseudomonas aeruginosa quorum sensing receptor LasR with nanomolar IC50 values. *ACS Infect Dis* **2020**.

**NMR DATA for 3C HSL – 20C HSL; 3OC7 HSL, and 3OC11 HSL**

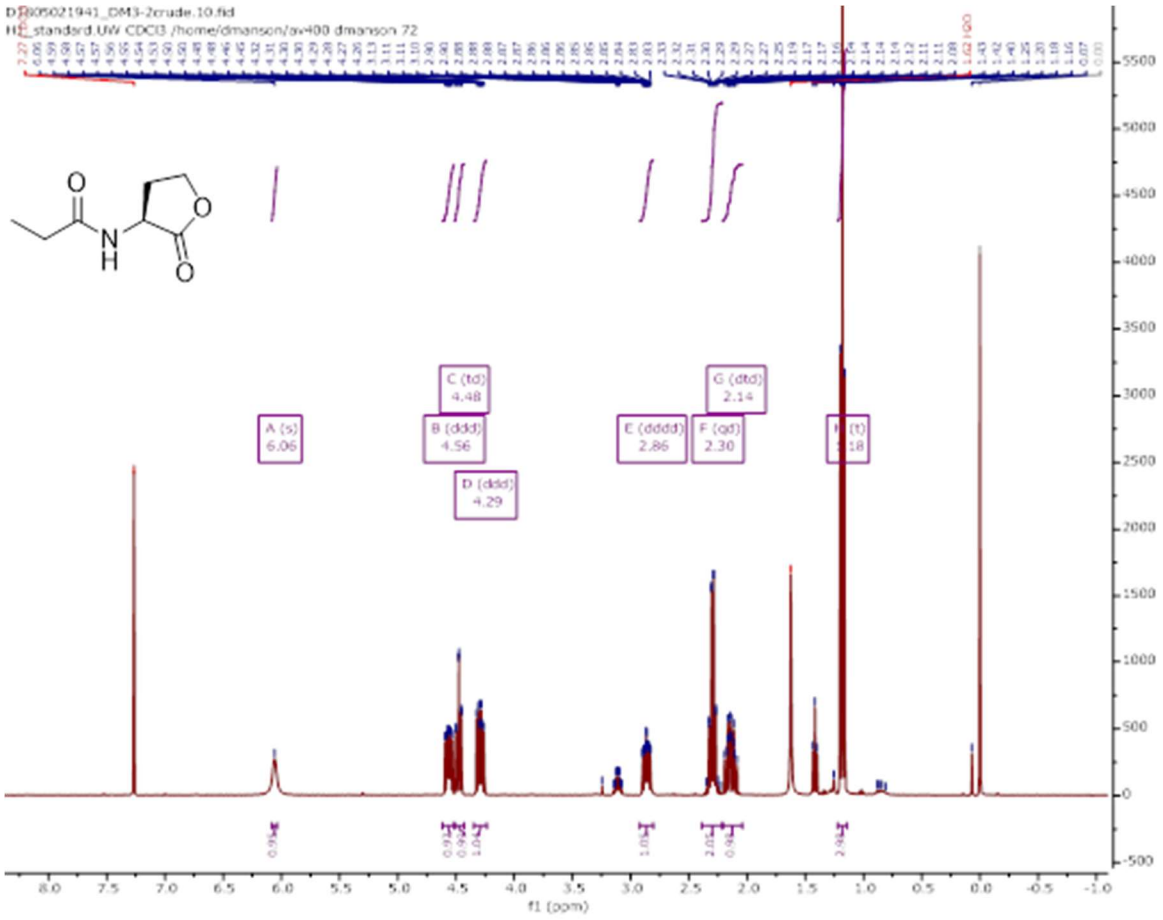

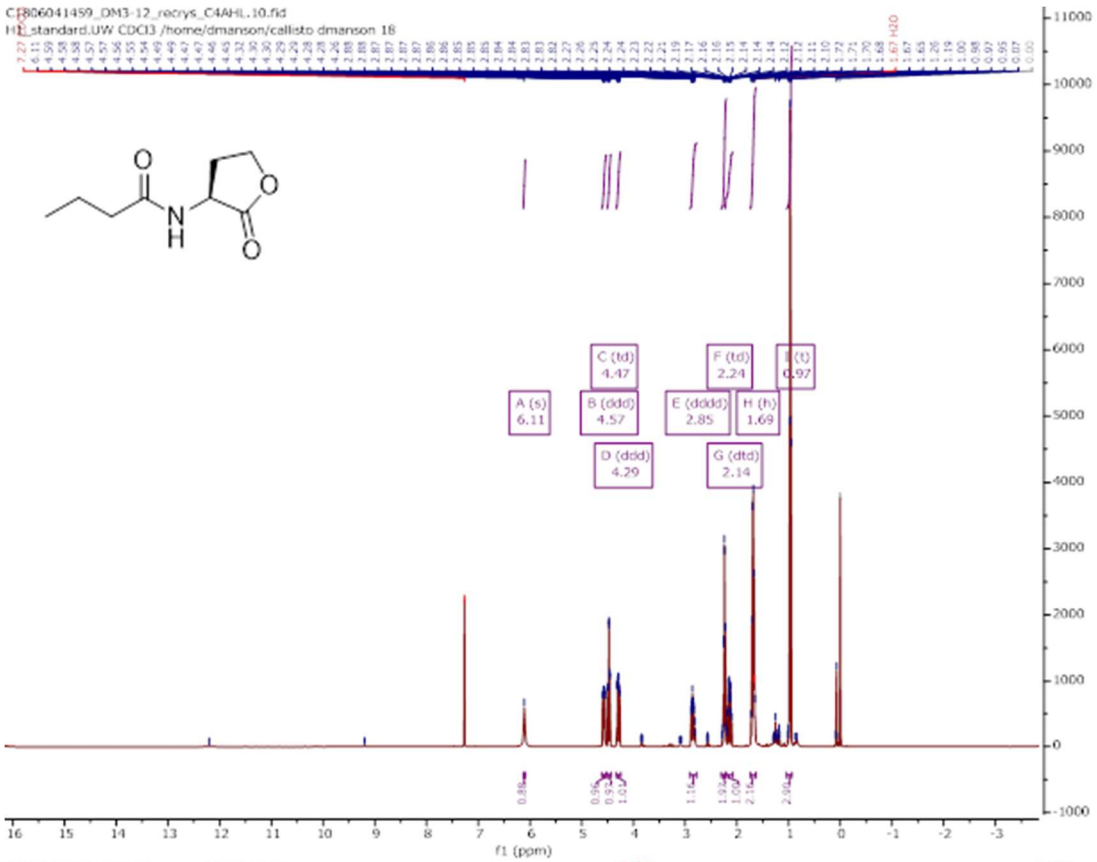
C1806041459_DM3-12_recrys_C4AHL.10.fid
H1_standard.UW CDCl3 /home/dmanson/callisto dmanson 18
A (s) 6.11
B (ddd) 4.57
C (td) 4.47
D (ddd) 4.29
E (dddd) 2.85
F (td) 2.24
G (dtd) 2.14
H (h) 1.69
I (t) 0.97
H2O
f1 (ppm)

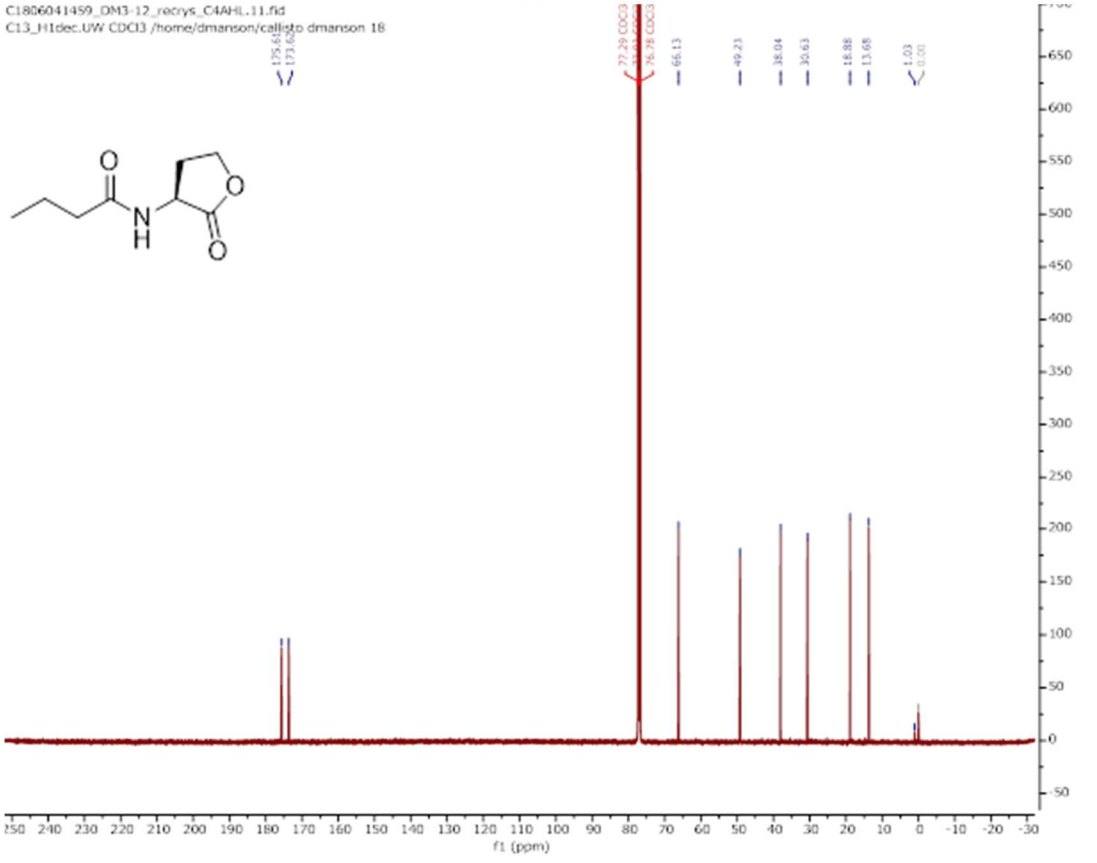
C1806041459_DM3-12_recrys_C4AHL.11.fid
C13_H1dec.UW CDCl3 /home/dmanson/callisto dmanson 18
77.29 CDCl3
76.78 CDCl3
66.13
49.23
38.04
30.63
18.88
13.68
f1 (ppm)

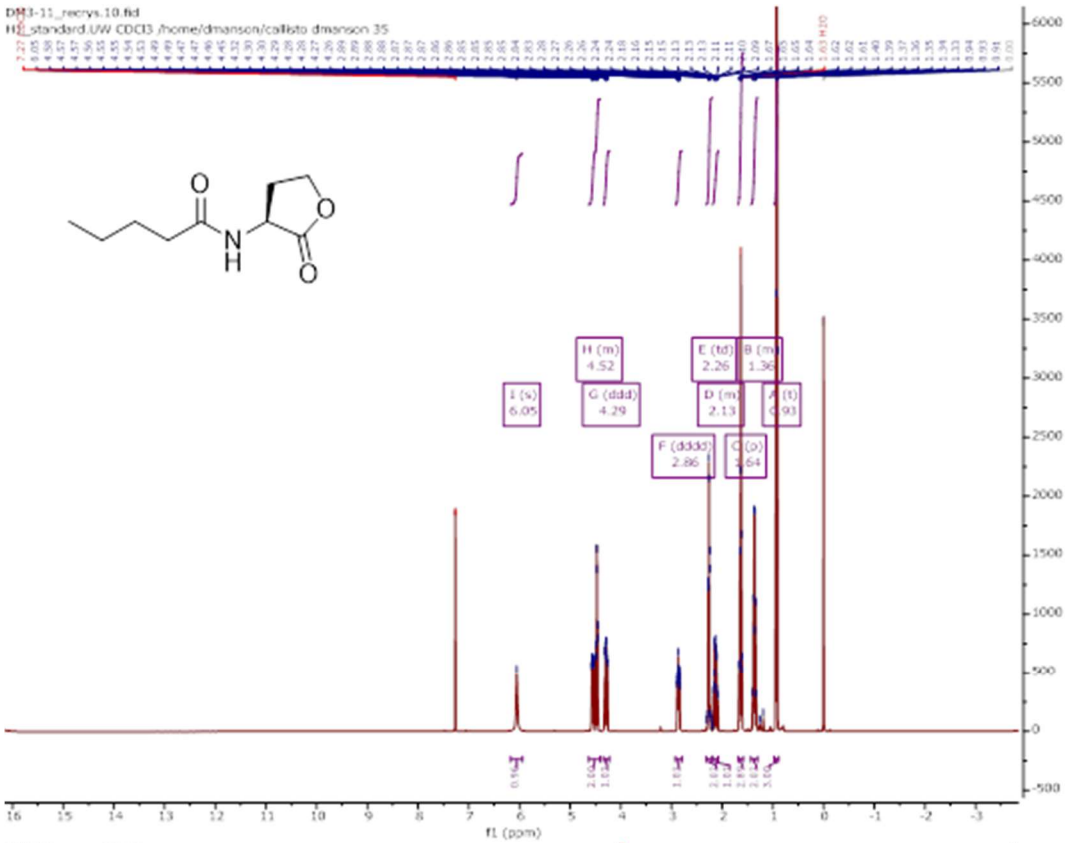
DM3-11_recrys.10.fid
H1_standard.UW CDCl3 /home/dmanson/callisto dmanson 35
I (s)
6.05
H (m)
4.52
G (ddd)
4.29
F (dddd)
2.86
E (td)
2.26
C (o)
2.64
D (m)
2.13
B (m)
1.36
A (t)
0.93
f1 (ppm)

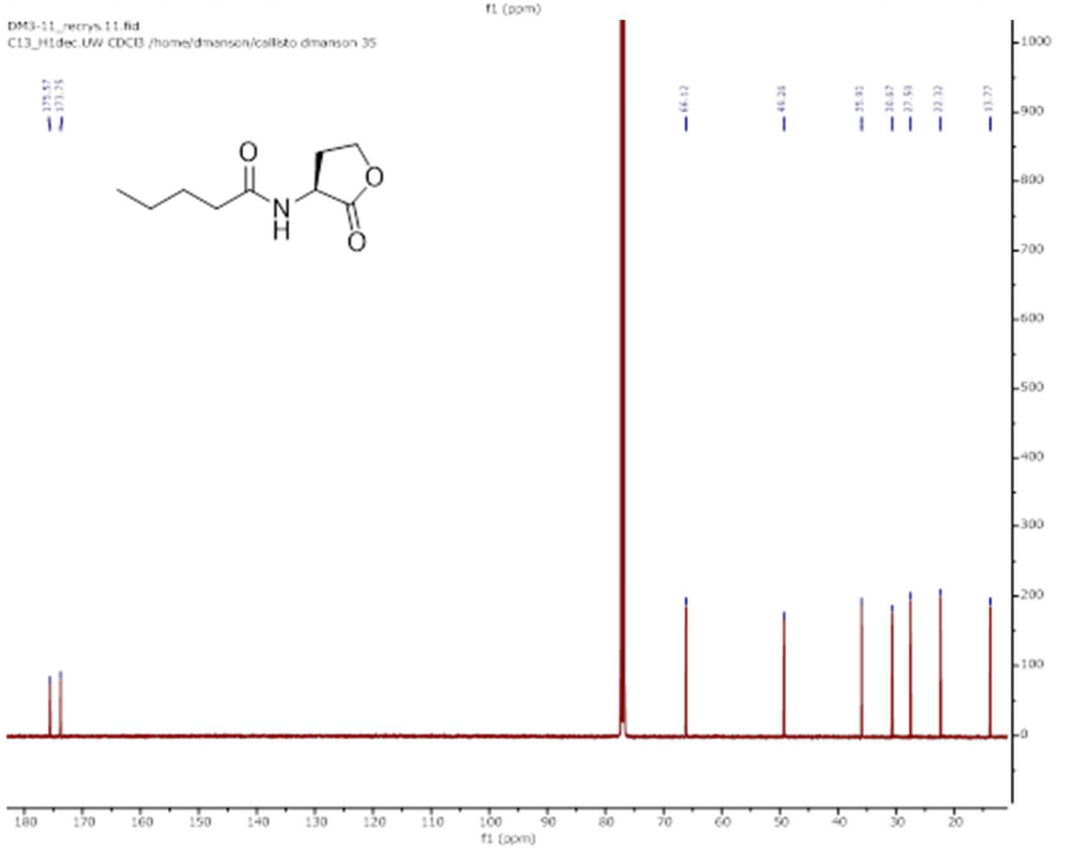
DM3-11_recrys.11.fid
C13_H1dec.UW CDCl3 /home/dmanson/callisto dmanson 35
f1 (ppm)

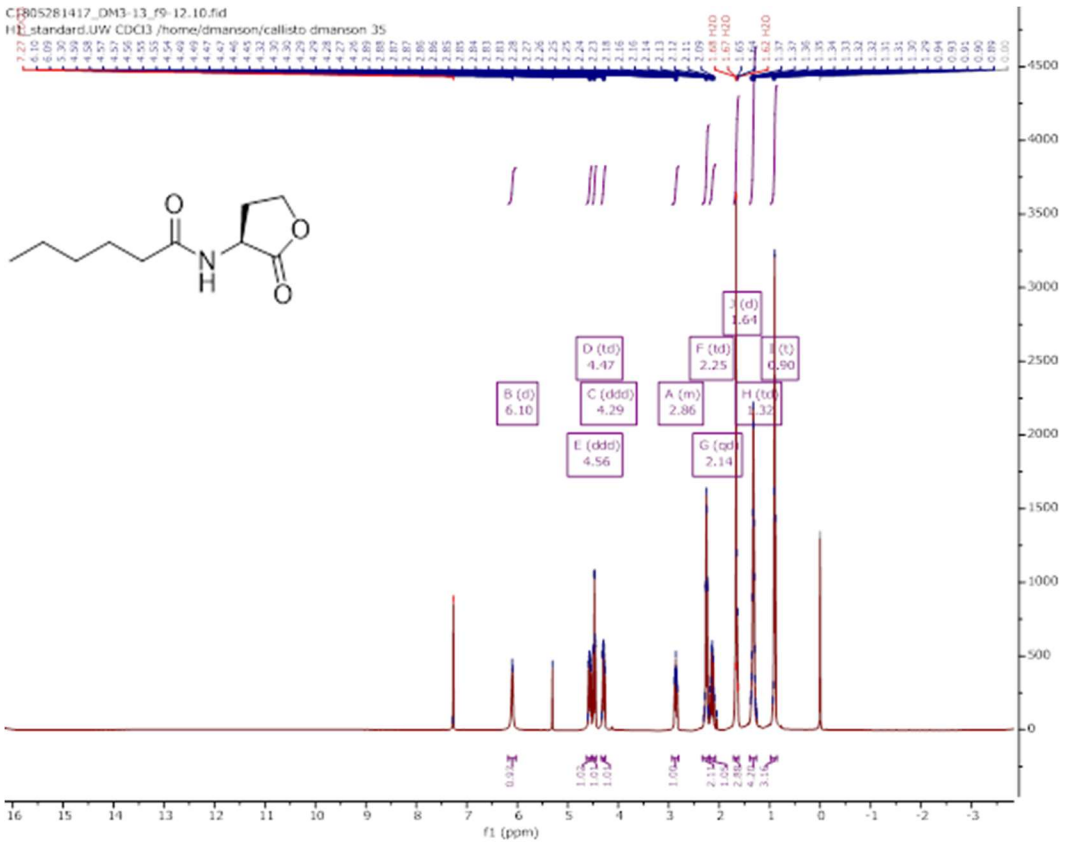
C1805281417_DM3-13_f9-12.10.fid
H1_standard.UW CDCl3 /home/dmanson/callisto dmanson 35
B (d) 6.10
C (ddd) 4.29
D (td) 4.47
E (ddd) 4.56
A (m) 2.86
G (qd) 2.14
H (td) 1.32
F (td) 2.25
I (t) 0.90
J (d) 1.64
f1 (ppm)

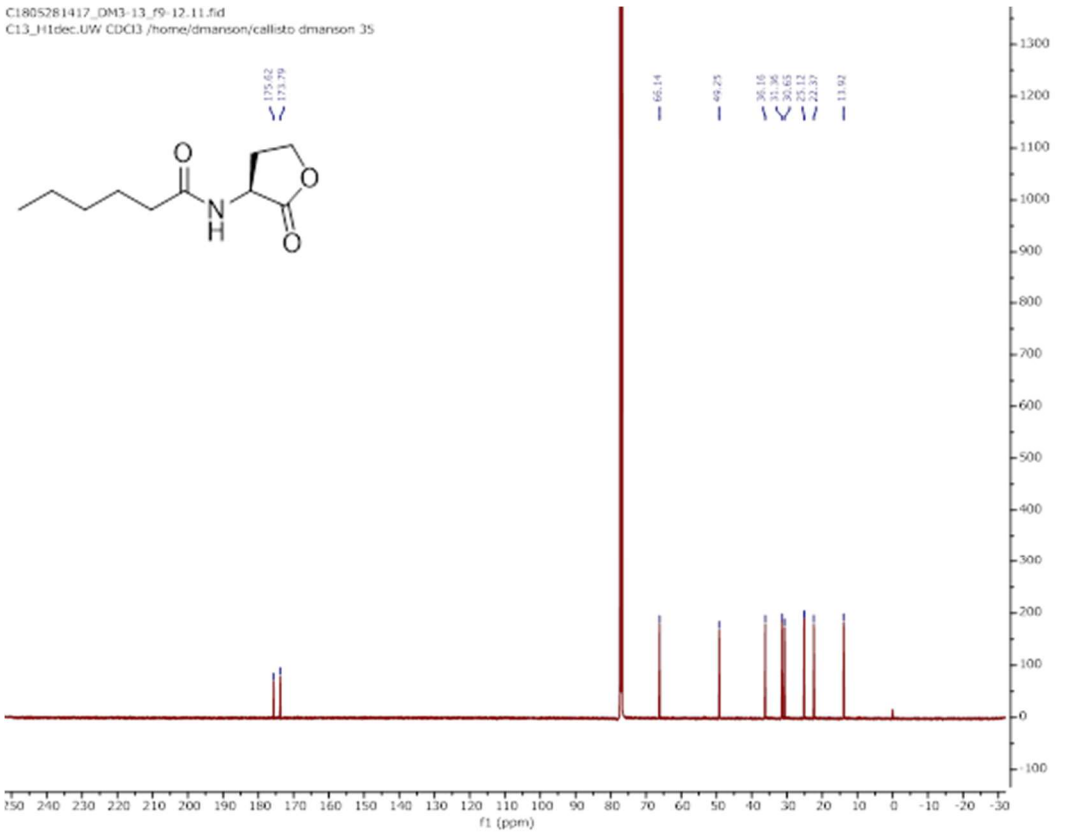
C1805281417_DM3-13_f9-12.11.fid
C13_H1dec.UW CDCl3 /home/dmanson/callisto dmanson 35
175.62
173.79
66.14
49.25
36.16
31.36
30.65
25.12
22.37
13.92
f1 (ppm)

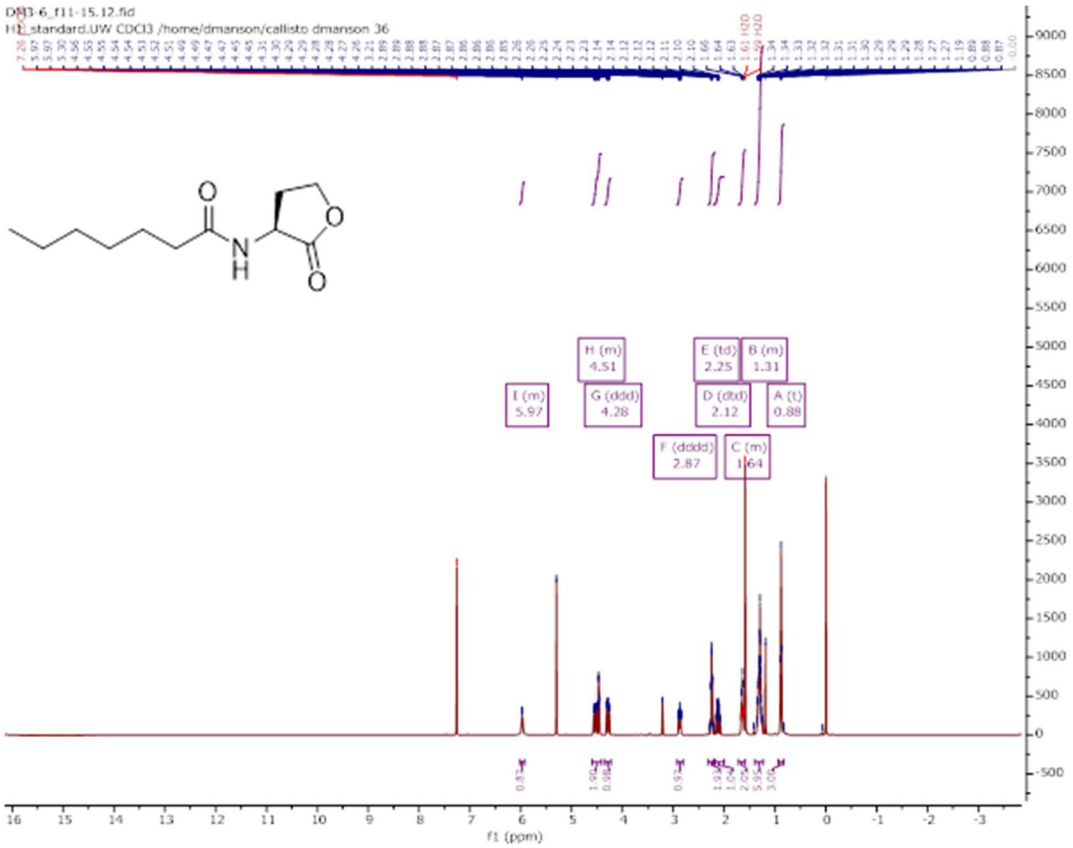
DM3-6_f11-15.12.fid
H1_standard.UW CDCl3 /home/dmanson/callisto dmanson 36
H (m) 4.51
E (td) 2.25
B (m) 1.31
I (m) 5.97
G (ddd) 4.28
D (dtd) 2.12
A (t) 0.88
F (dddd) 2.87
C (m) 1.64
f1 (ppm)

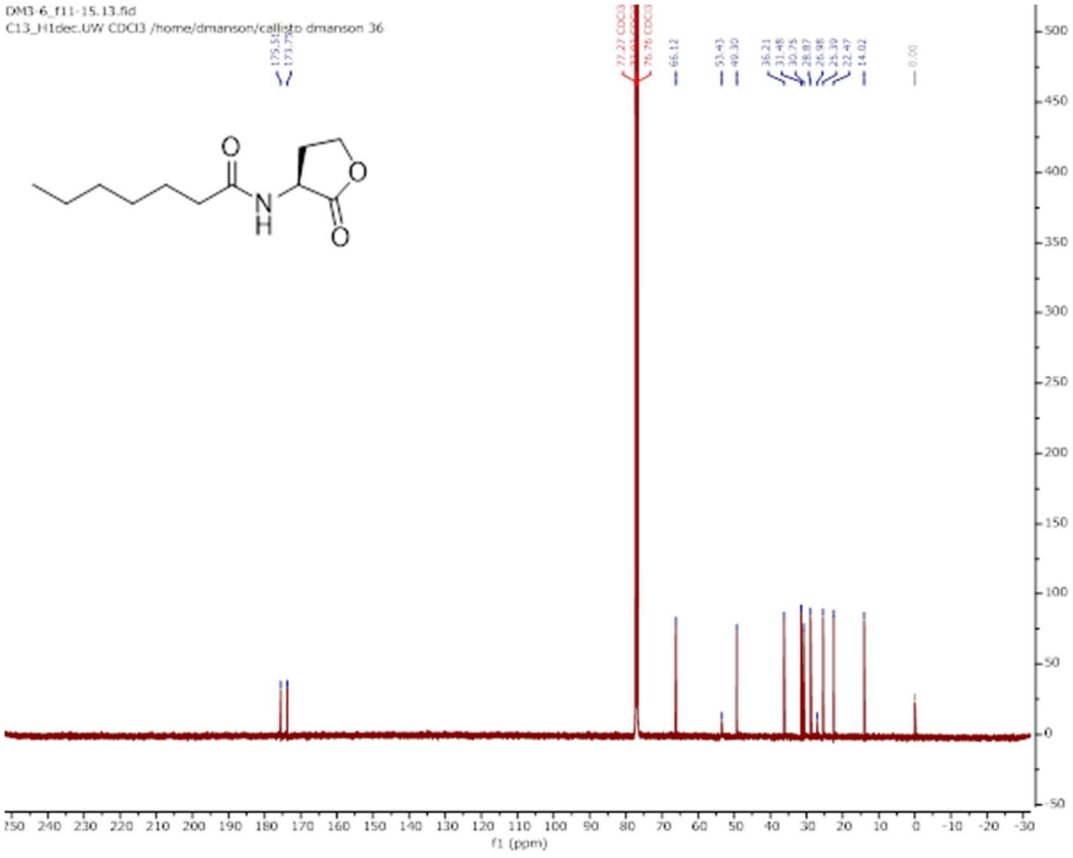
DM3-6_f11-15.13.fid
C13_H1dec.UW CDCl3 /home/dmanson/callisto dmanson 36
f1 (ppm)

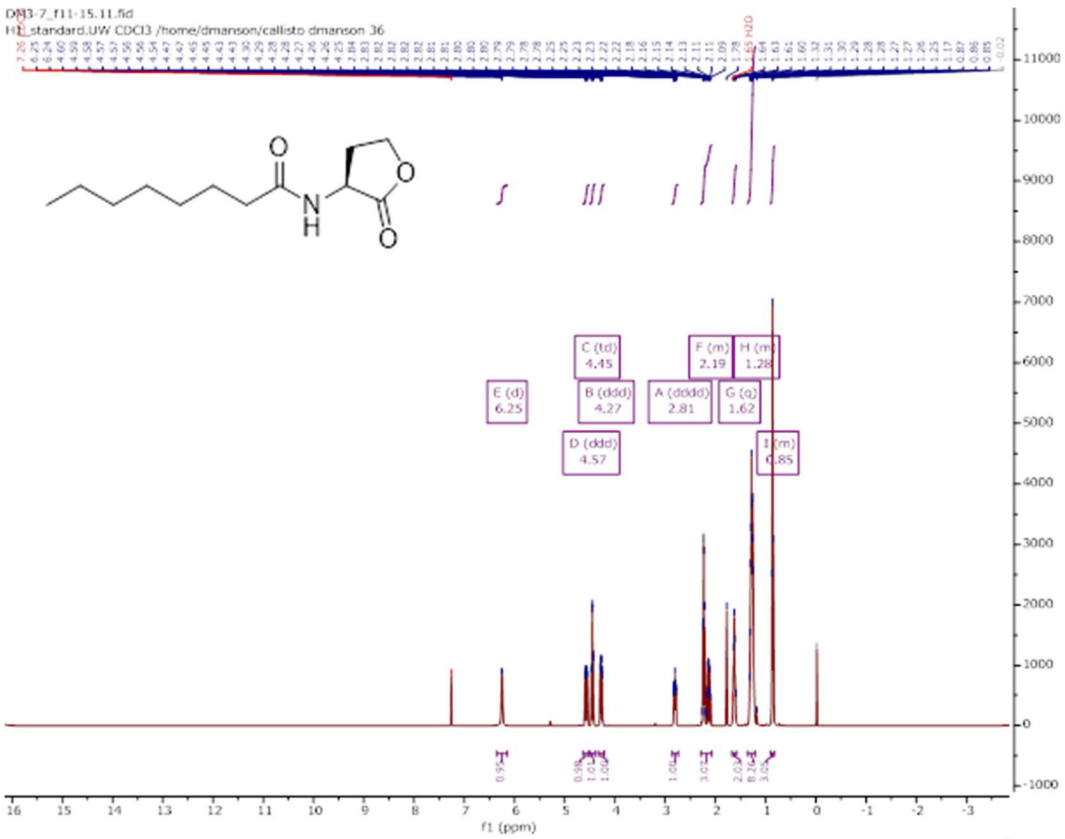
DM3-7_f11-15.11.fid
H1_standard.UW CDCl3 /home/dmanson/callisto dmanson 36
C (td) 4.45
F (m) 2.19
H (m) 1.28
E (d) 6.25
B (ddd) 4.27
A (dddd) 2.81
G (q) 1.62
D (ddd) 4.57
I (m) 0.85
f1 (ppm)

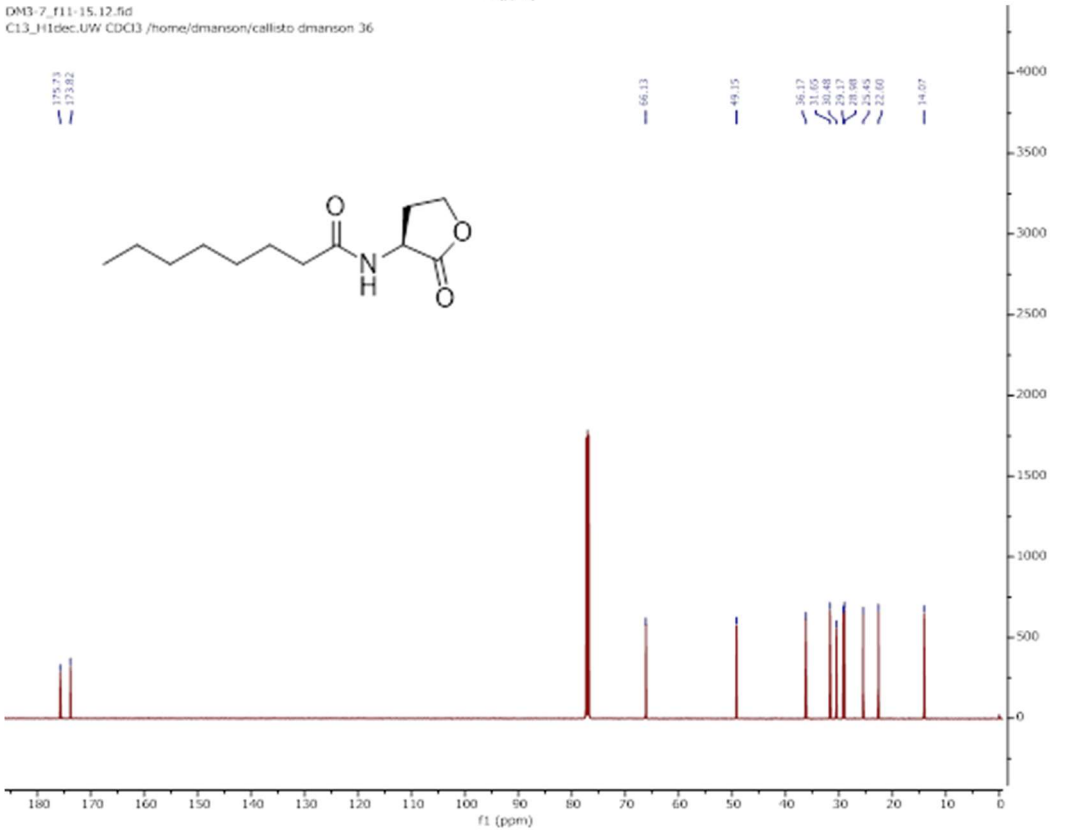
DM3-7_f11-15.12.fid
C13_H1dec.UW CDCl3 /home/dmanson/callisto dmanson 36
175.73
173.82
66.13
49.35
36.17
31.65
30.48
29.17
28.98
25.45
22.60
14.07
f1 (ppm)

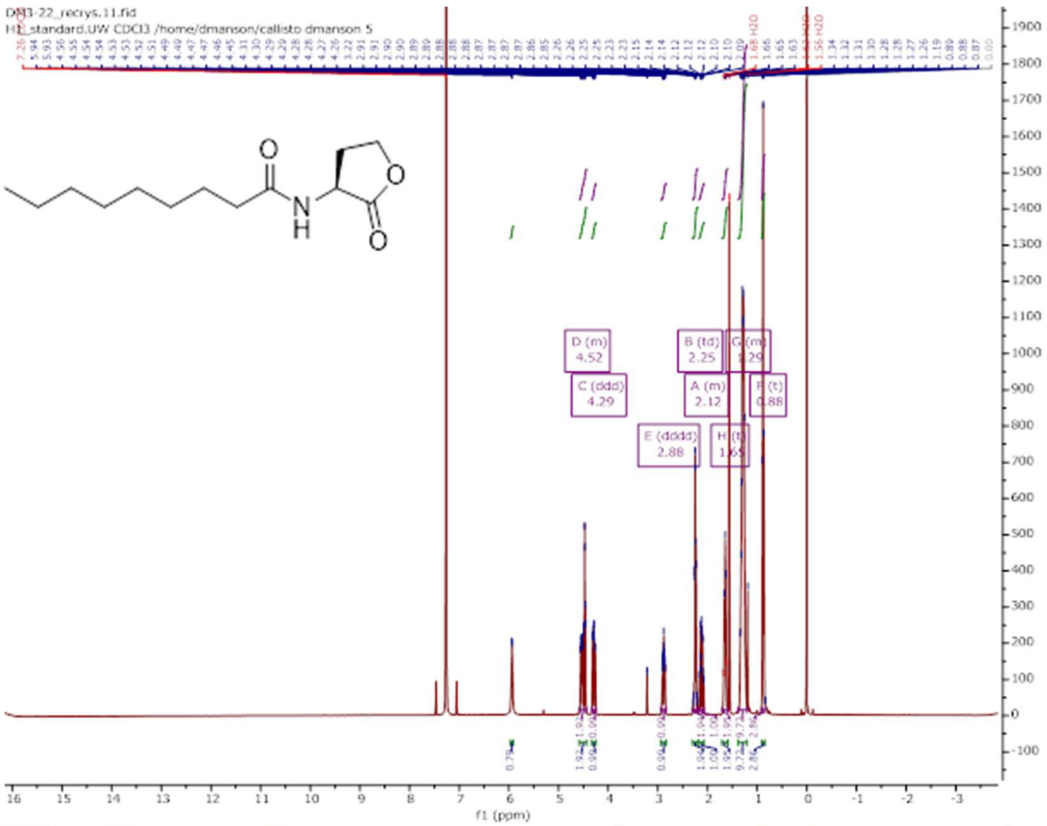
DM3-22_recrys.11.fid
H1_standard.UW CDCl3 /home/dmanson/callisto dmanson 5
D (m) 4.52
C (ddd) 4.29
B (td) 2.25
G (m) 2.29
A (m) 2.12
F (t) 0.88
E (dddd) 2.88
H (t) 1.65
f1 (ppm)

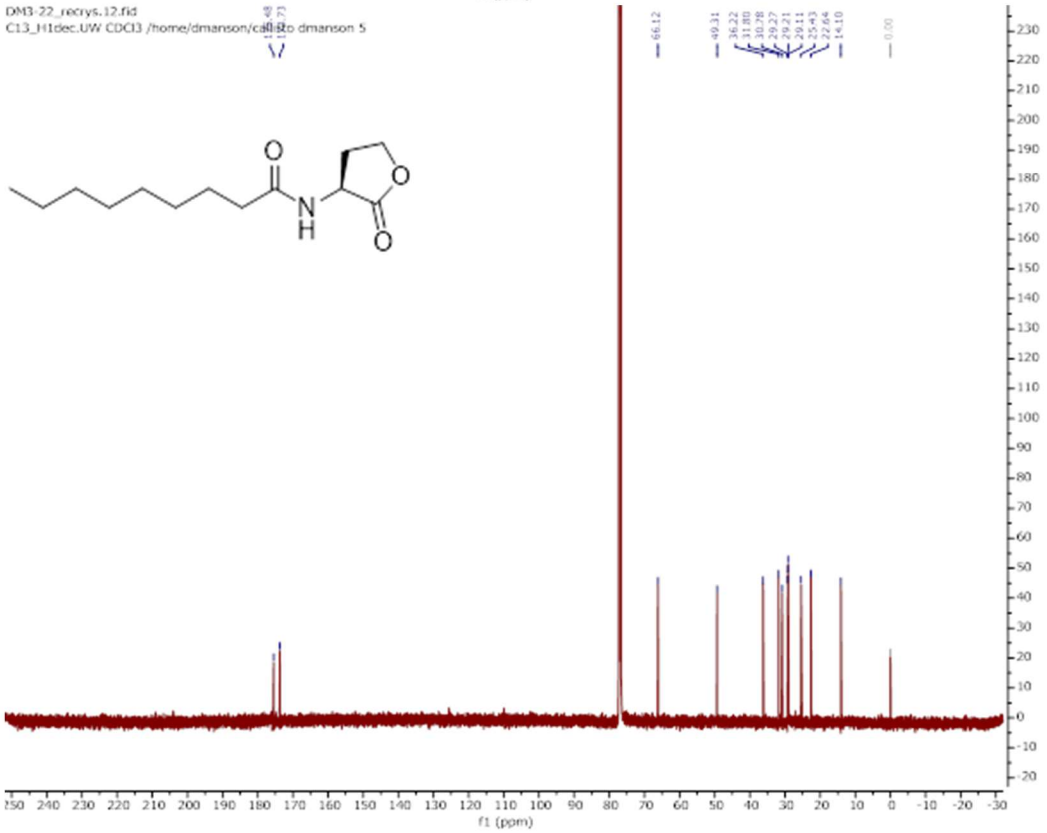
DM3-22_recrys.12.fid
C13_H1dec.UW CDCl3 /home/dmanson/callisto dmanson 5
f1 (ppm)

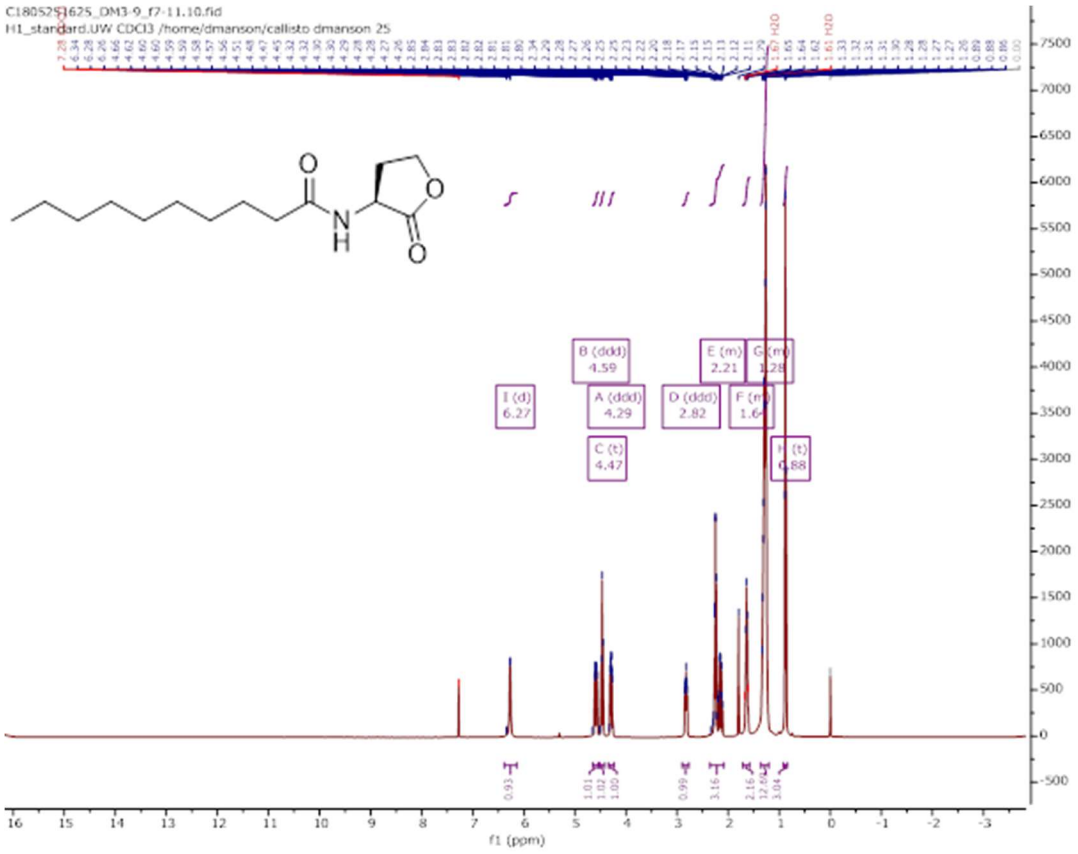
C180525162S_DM3-9_f7-11.10.fid
H1_standard.UW CDCl3 /home/dmanson/callisto dmanson 25
B (ddd) 4.59
E (m) 2.21
G (m) 1.28
I (d) 6.27
A (ddd) 4.29
D (ddd) 2.82
F (m) 1.64
C (t) 4.47
J (t) 0.88
f1 (ppm)

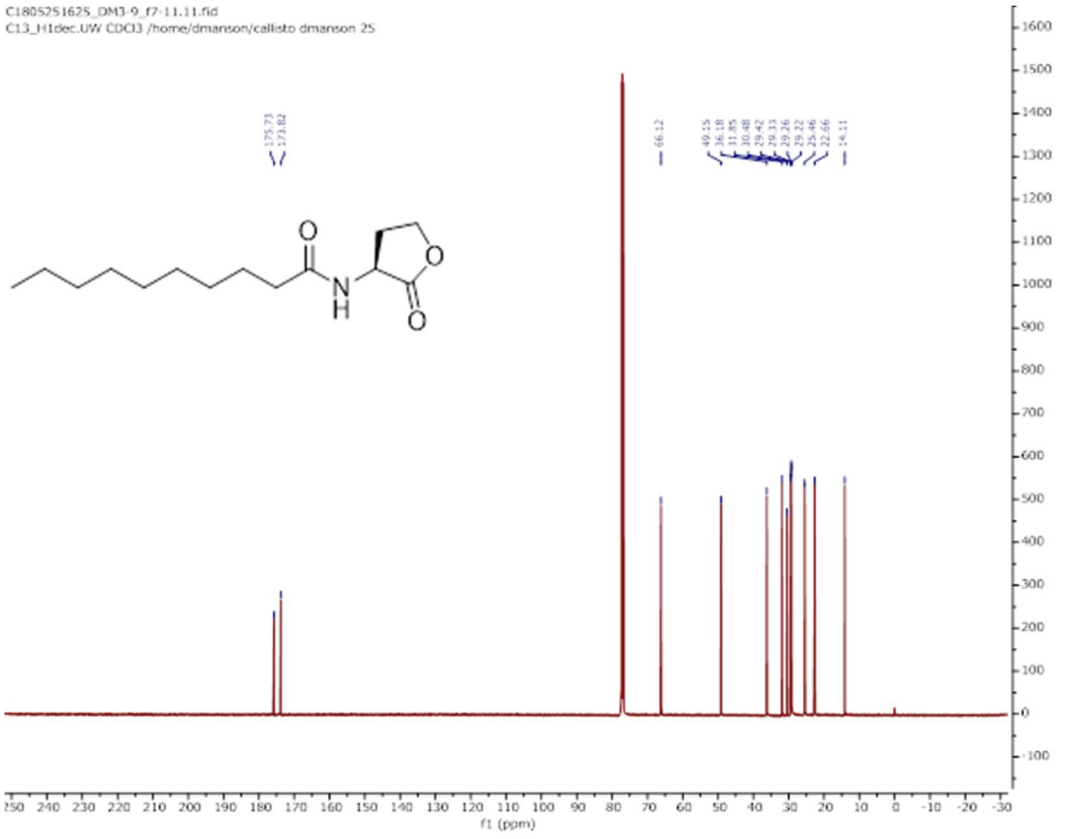
C180525162S_DM3-9_f7-11.11.fid
C13_H1dec.UW CDCl3 /home/dmanson/callisto dmanson 25
175.73
173.82
66.12
49.15
36.18
31.85
30.48
29.42
29.33
29.26
29.22
25.46
22.66
14.11
f1 (ppm)

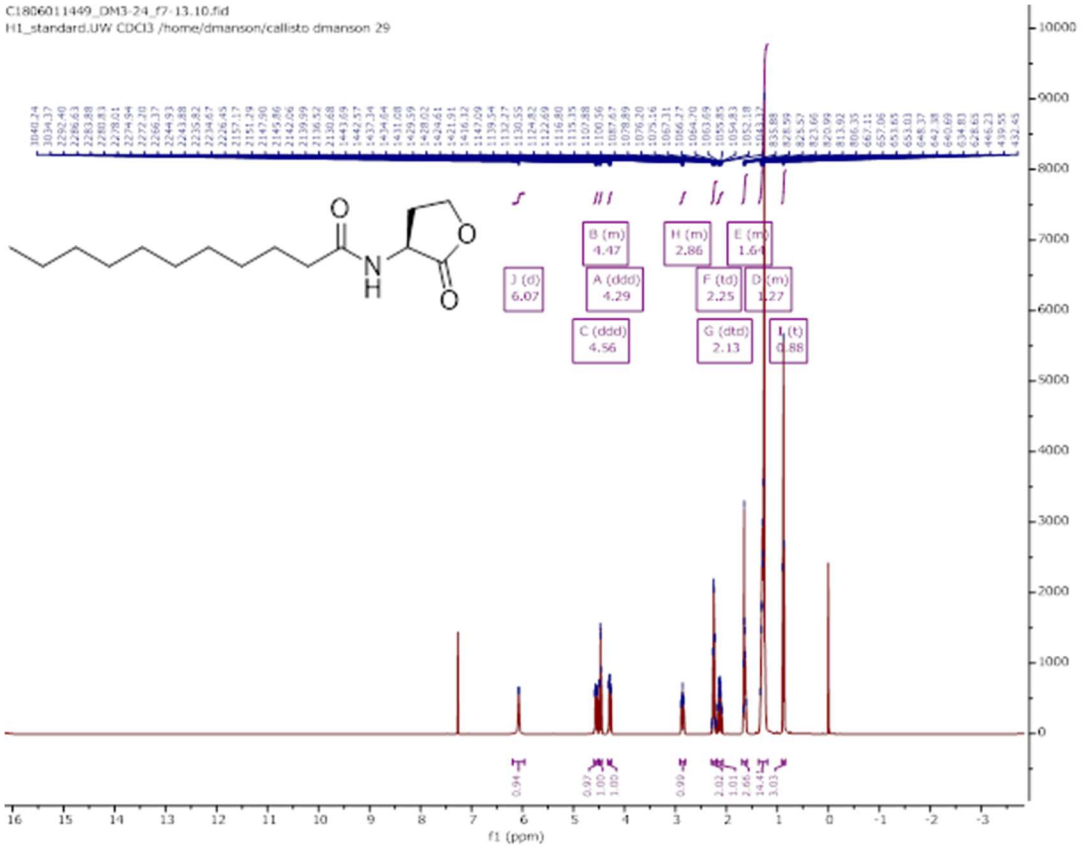
C1806011449_DM3-24_f7-13.10.fid
H1_standard.UW CDCl3 /home/dmanson/callisto dmanson 29
J (d) 6.07
B (m) 4.47
A (ddd) 4.29
C (ddd) 4.56
H (m) 2.86
E (m) 1.64
F (td) 2.25
D (m) 1.27
G (dtd) 2.13
I (t) 0.88
f1 (ppm)

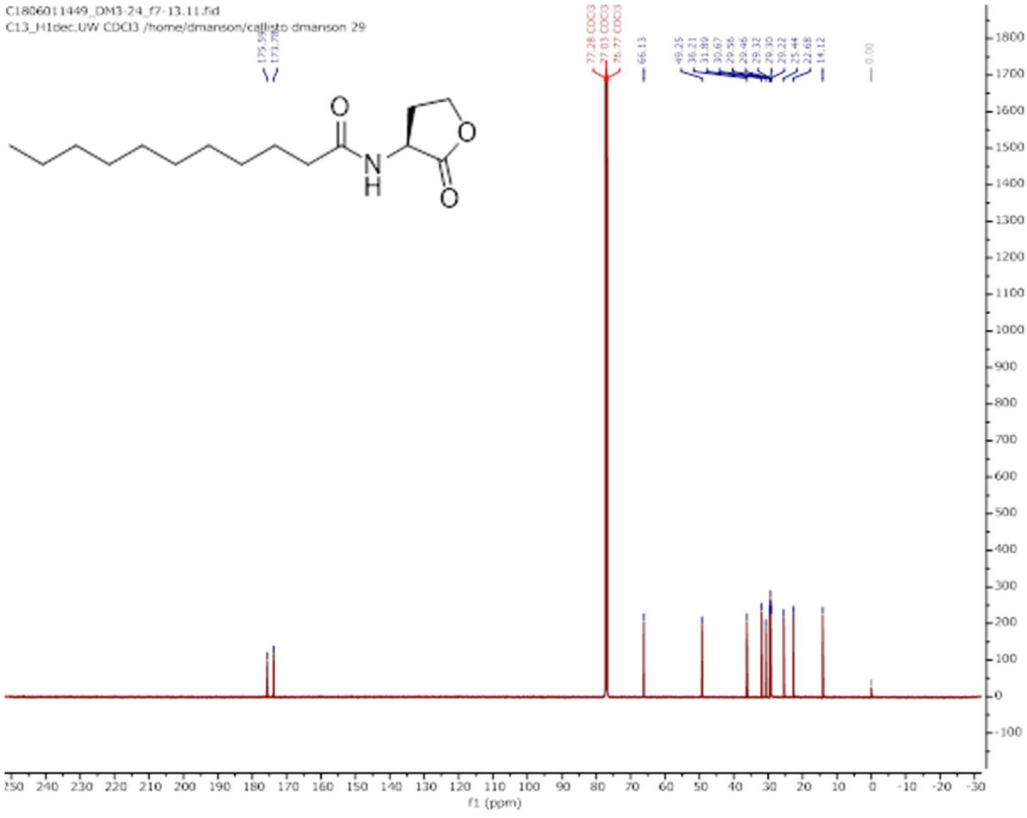
C1806011449_DM3-24_f7-13.11.fid
C13_H1dec.UW CDCl3 /home/dmanson/callisto dmanson 29
f1 (ppm)

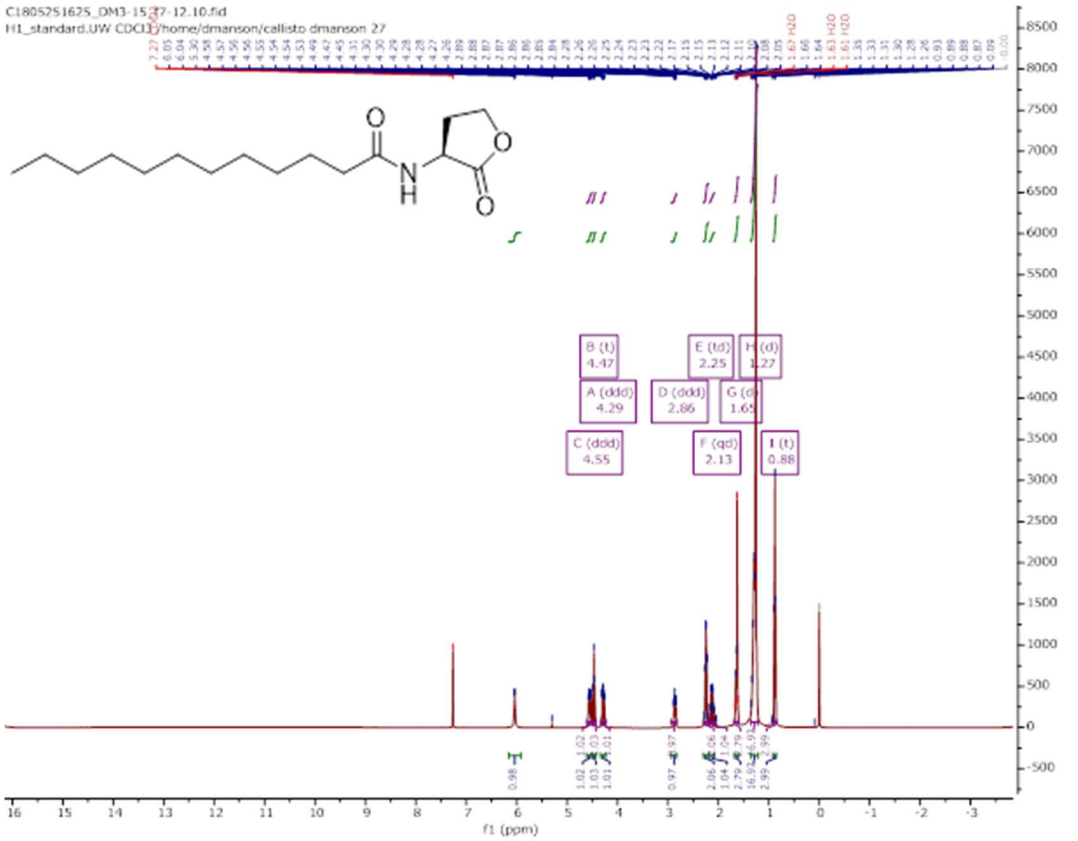
C18052S1625_DM3-15_f7-12.10.fid
H1_standard.UW CDCl3 /home/dmanson/callisto dmanson 27
B (t) 4.47
E (td) 2.25
H (d) 1.27
A (ddd) 4.29
D (ddd) 2.86
G (d) 1.65
C (ddd) 4.55
F (qd) 2.13
I (t) 0.88
f1 (ppm)

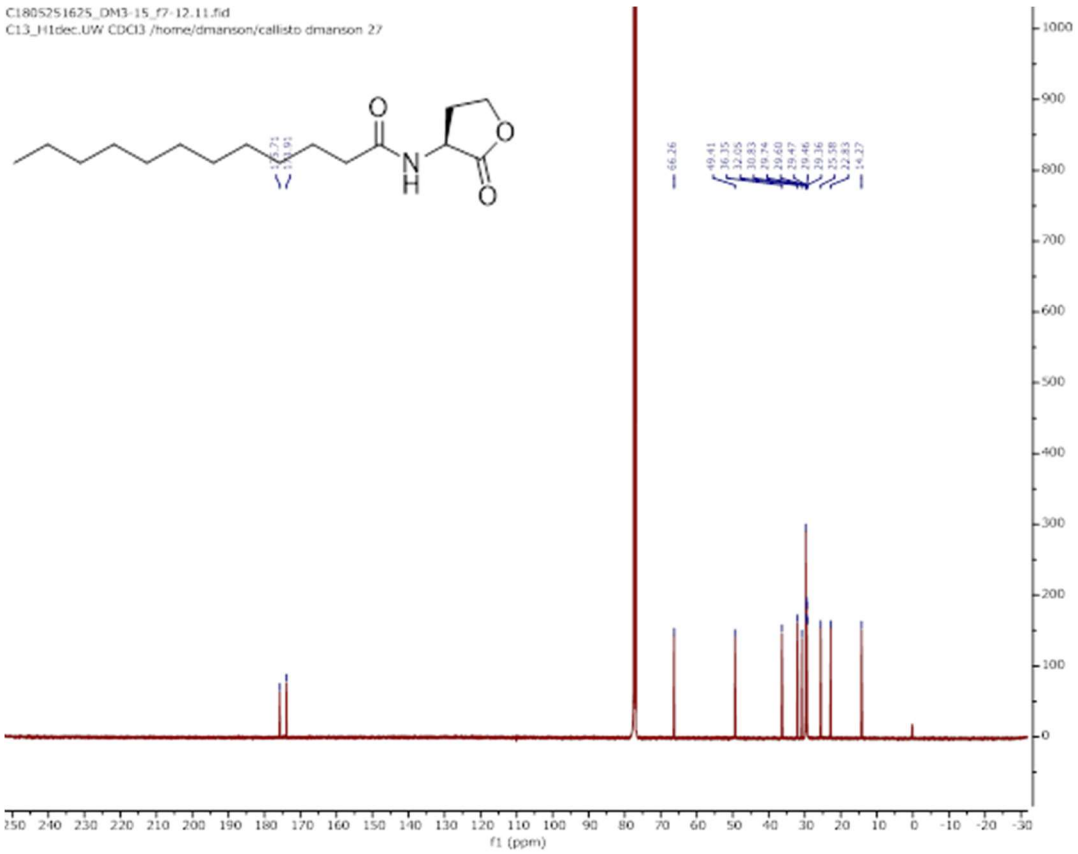
C18052S1625_DM3-15_f7-12.11.fid
C13_H1dec.UW CDCl3 /home/dmanson/callisto dmanson 27
f1 (ppm)

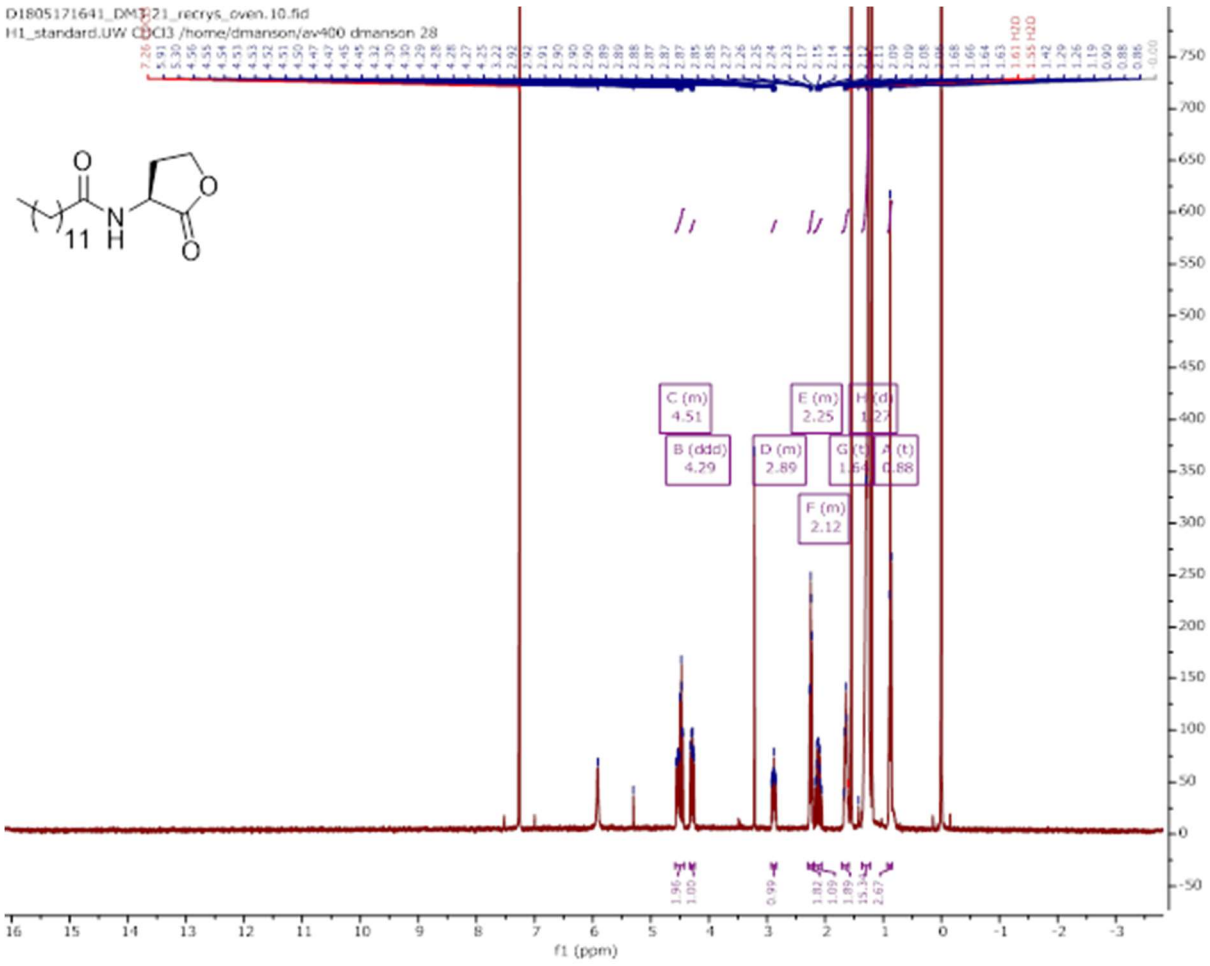
D1805171641_DMS21_recrys_oven.10.fid
H1_standard.UW CDCl3 /home/dmanson/av400 dmanson 28
O
O
N
H
11
O
C (m)
4.51
B (ddd)
4.29
D (m)
2.89
E (m)
2.25
F (m)
2.12
G (t)
1.64
A (t)
0.88
f1 (ppm)

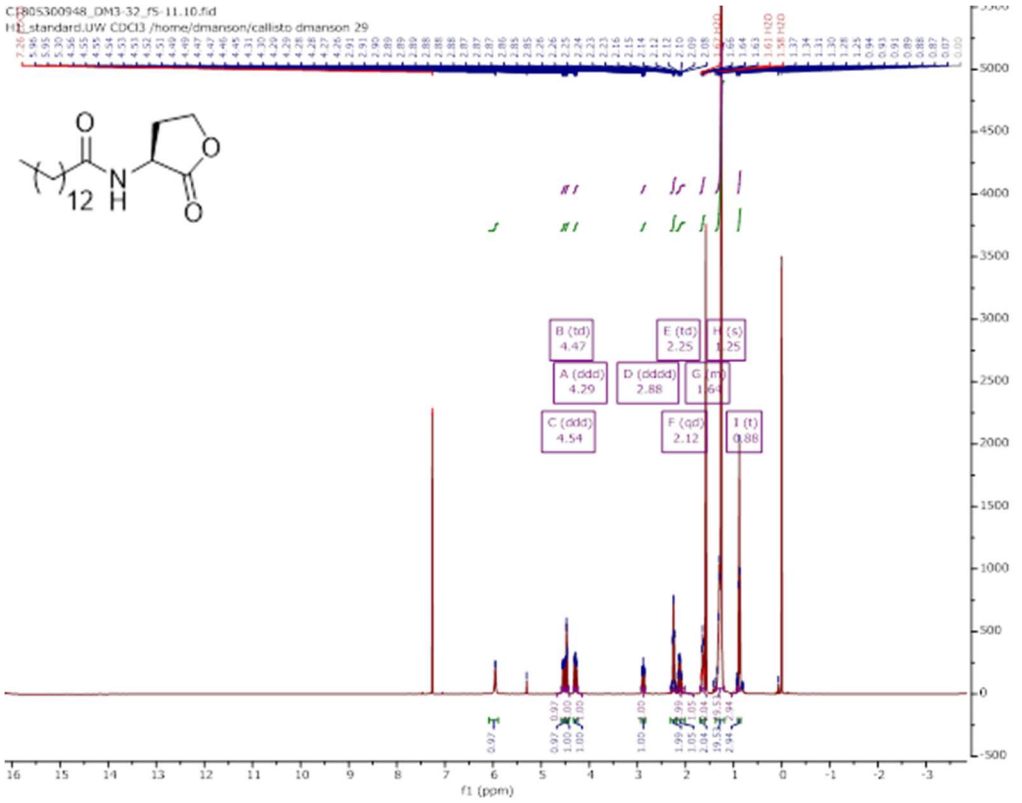
C1805300948_DM3-32_fS-11.10.fid
H1_standard.UW CDCl3 /home/dmanson/callisto dmanson 29
B (td) 4.47
E (td) 2.25
H (s) 1.25
A (ddd) 4.29
D (dddd) 2.88
G (m) 1.64
C (ddd) 4.54
F (qd) 2.12
I (t) 0.88
f1 (ppm)

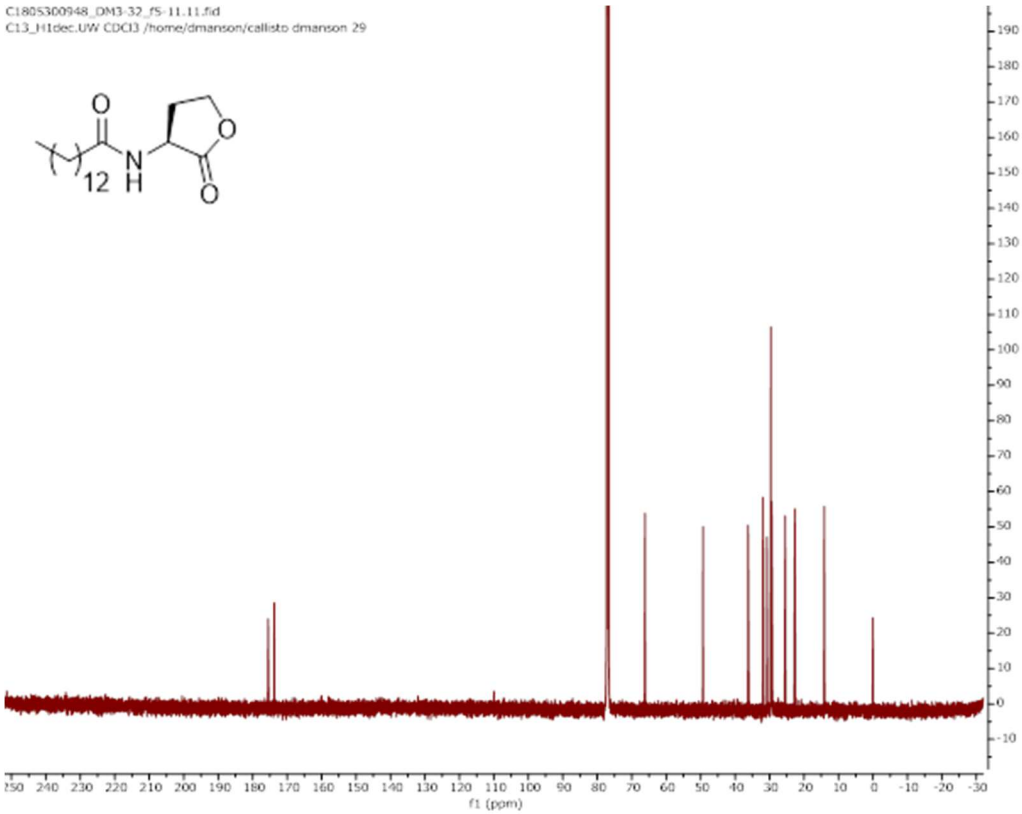
C1805300948_DM3-32_fS-11.11.fid
C13_H1dec.UW CDCl3 /home/dmanson/callisto dmanson 29
f1 (ppm)

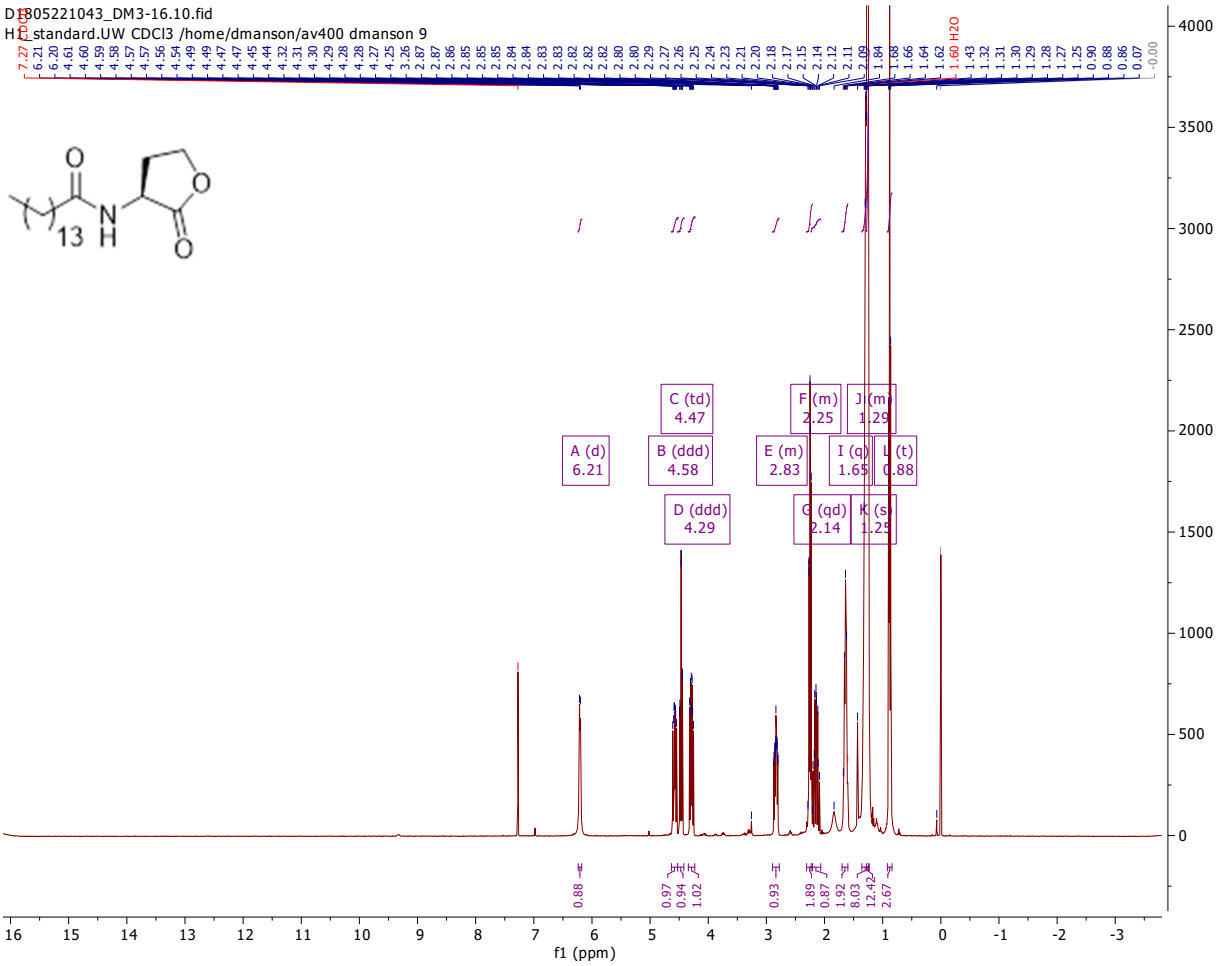
D:\805221043_DM3-16.10.fid
H1 standard.UW CDCl3 /home/dmanson/av400 dmanson 9
A (d) 6.21
B (ddd) 4.58
C (td) 4.47
D (ddd) 4.29
E (m) 2.83
F (m) 2.25
G (qd) 2.14
I (q) 1.65
J (m) 1.29
K (s) 1.25
L (t) 0.88
f1 (ppm)

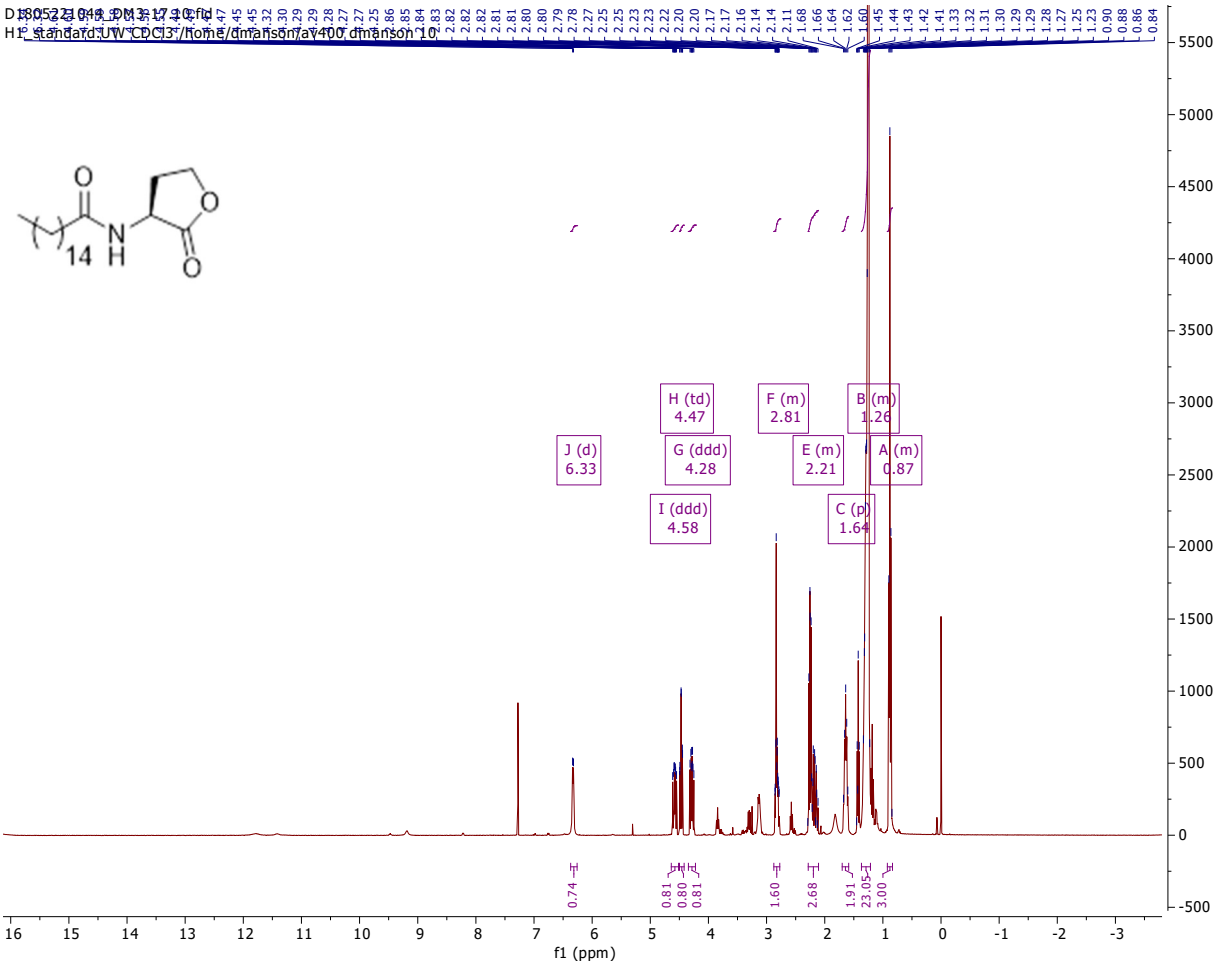
H (td)
4.47
F (m)
2.81
B (m)
1.26
J (d)
6.33
G (ddd)
4.28
E (m)
2.21
A (m)
0.87
I (ddd)
4.58
C (p)
1.64
0.74
0.81
0.80
0.81
1.60
2.68
1.91
23.05
3.00
f1 (ppm)

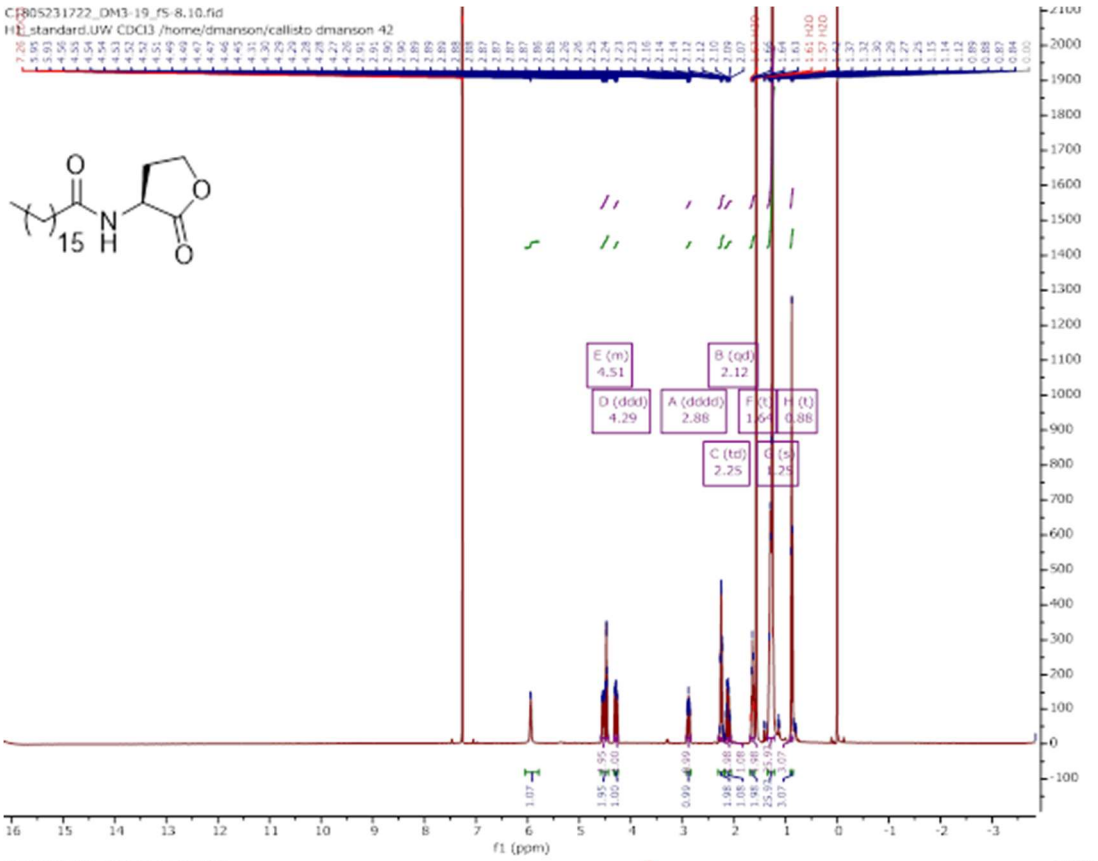
C1805231722_DM3-19_fS-8.10.fid
H1_standard.UW CDCl3 /home/dmanson/callisto dmanson 42
E (m) 4.51
B (qd) 2.12
D (ddd) 4.29
A (dddd) 2.88
C (td) 2.25
G (s) 1.25
H (t) 0.88
f1 (ppm)

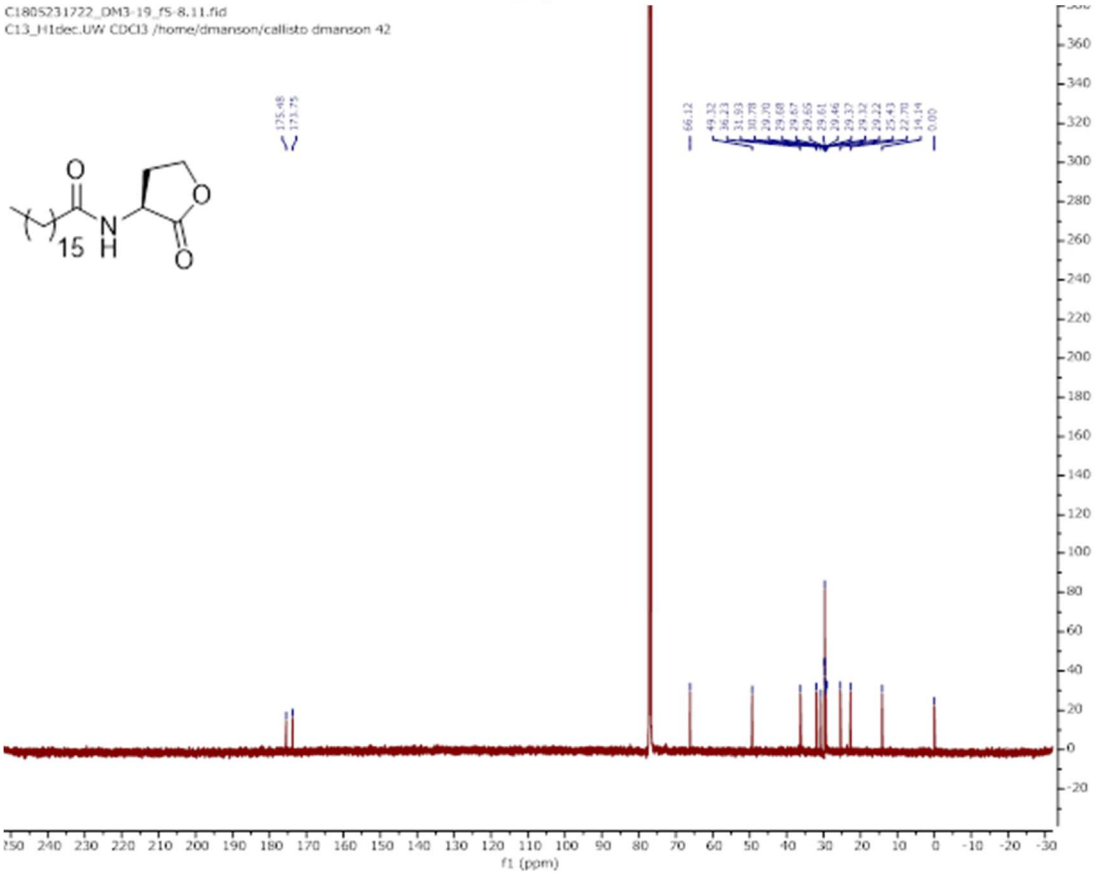
C1805231722_DM3-19_fS-8.11.fid
C13_H1dec.UW CDCl3 /home/dmanson/callisto dmanson 42
175.48
173.75
66.12
49.32
36.23
31.93
30.78
29.70
29.68
29.67
29.65
29.61
29.46
29.37
29.32
29.22
25.43
22.70
14.14
0.00
f1 (ppm)

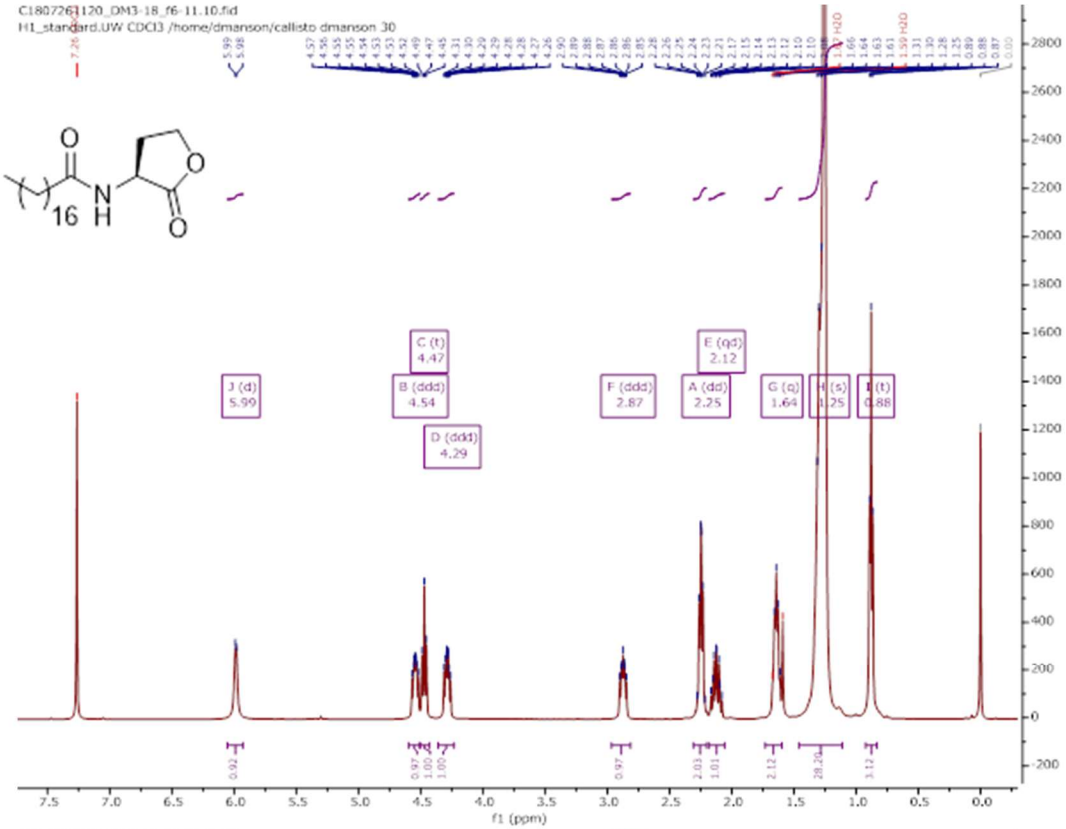
C1807261120_DM3-18_f6-11.10.fid
H1_standard.UW CDCl3 /home/dmanson/callisto dmanson 30
J (d) 5.99
C (t) 4.47
B (ddd) 4.54
D (ddd) 4.29
F (ddd) 2.87
E (qd) 2.12
A (dd) 2.25
G (q) 1.64
H (s) 1.25
I (t) 0.88
f1 (ppm)

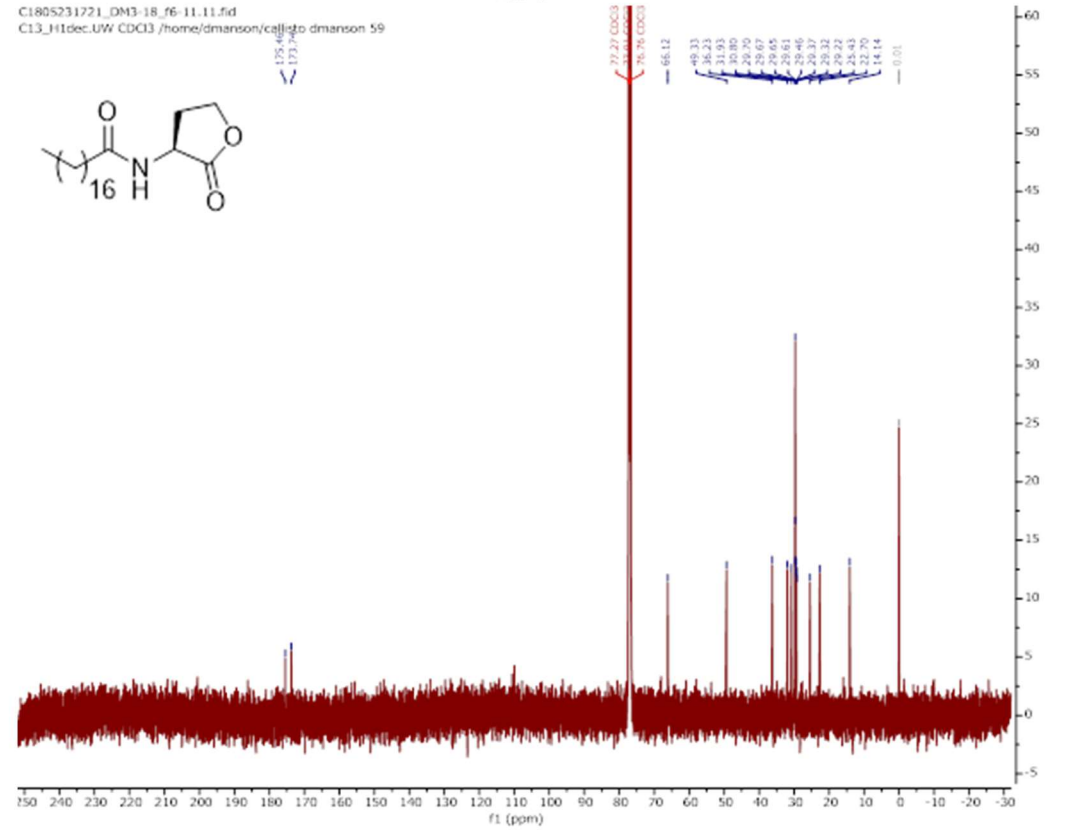
C1805231721_DM3-18_f6-11.11.fid
C13_H1dec.UW CDCl3 /home/dmanson/callisto dmanson 59
f1 (ppm)

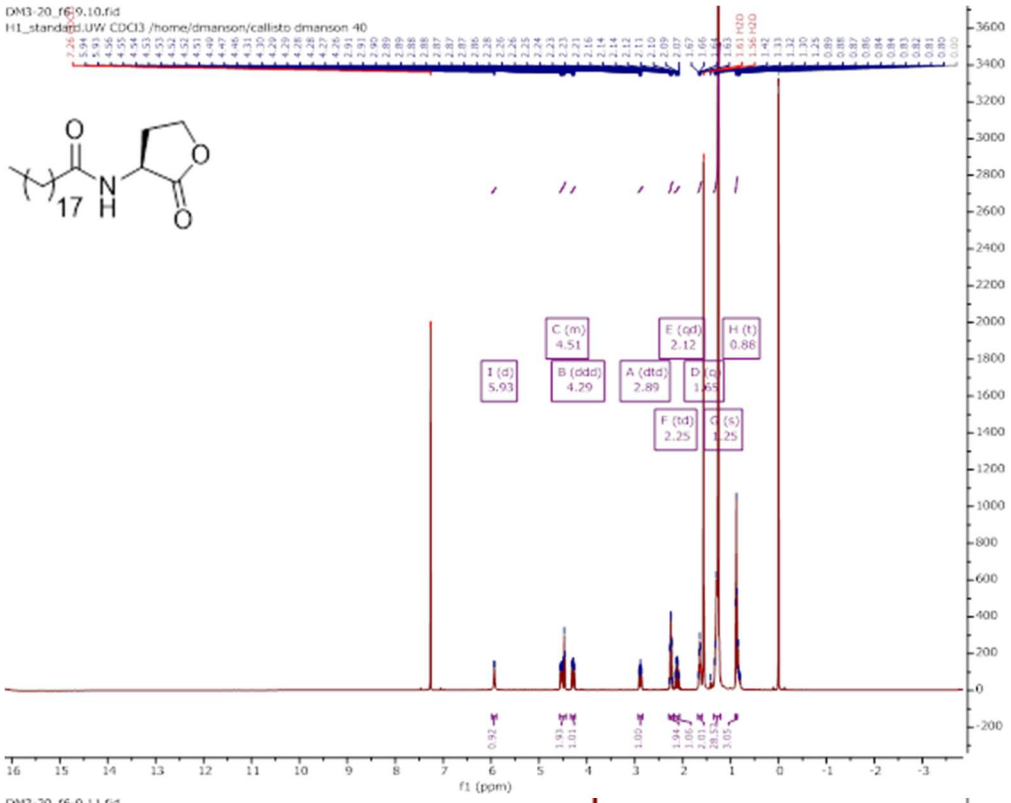
DM3-20_f6-9.10.fid
H1_standard.UW CDCl3 /home/dmanson/callisto dmanson 40
C (m) 4.51
E (qd) 2.12
H (t) 0.88
I (d) 5.93
B (ddd) 4.29
A (dtd) 2.89
D (p) 1.69
F (td) 2.25
G (s) 1.25
f1 (ppm)

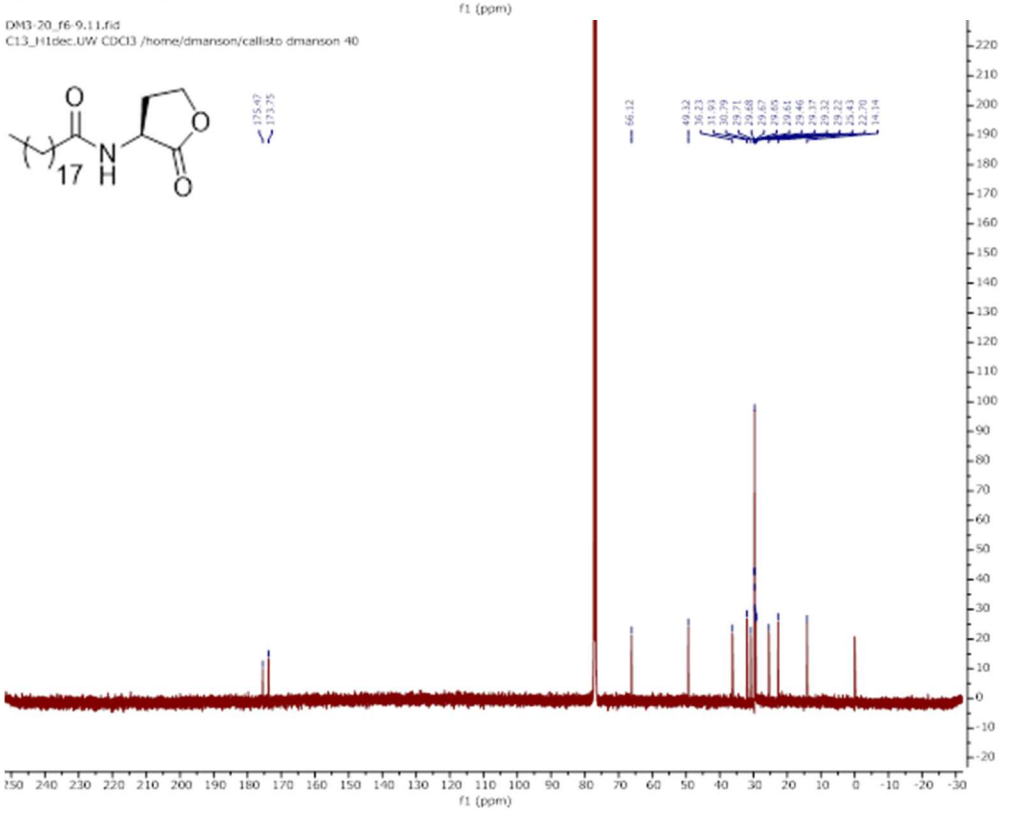
DM3-20_f6-9.11.fid
C13_H1dec.UW CDCl3 /home/dmanson/callisto dmanson 40
f1 (ppm)

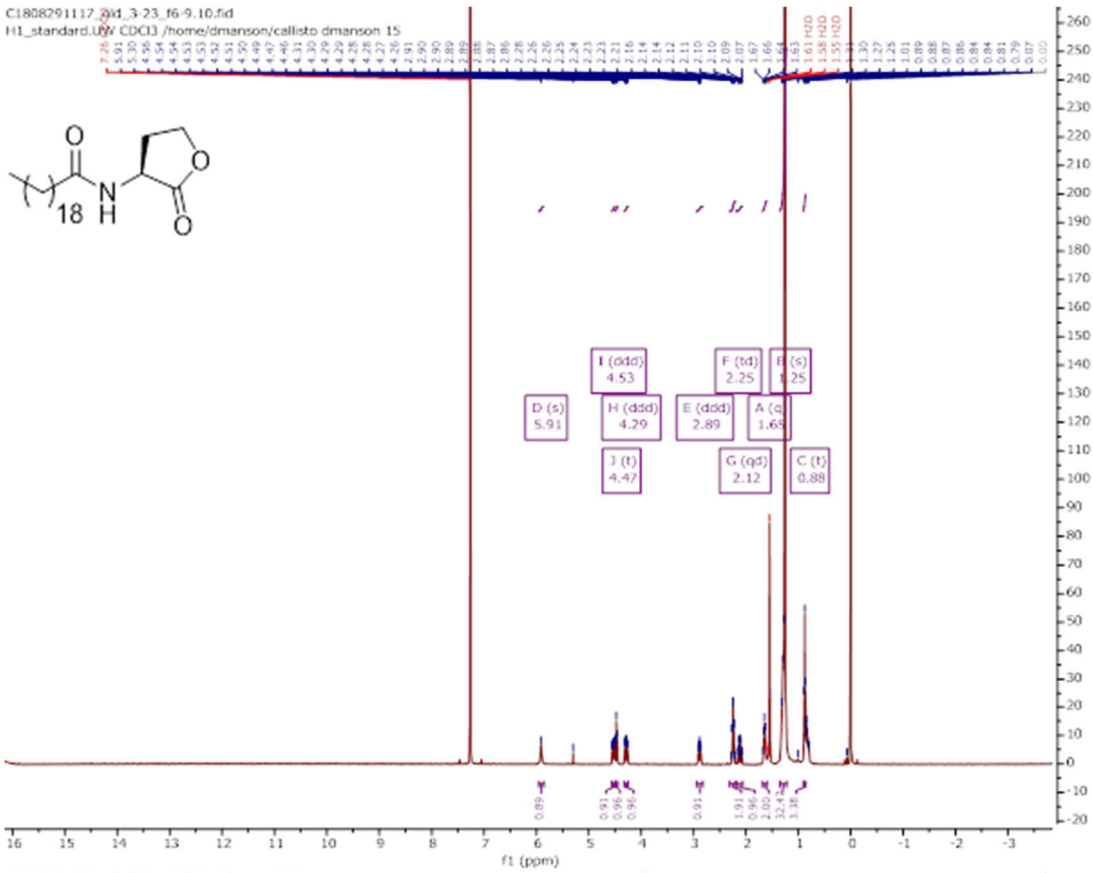
C1808291117_old_3-23_f6-9.10.fid
H1_standard.UW CDCl3 /home/dmanson/callisto dmanson 15
I (ddd) 4.53
F (td) 2.25
H (s) 1.25
D (s) 5.91
H (ddd) 4.29
E (ddd) 2.89
A (q) 1.65
J (t) 4.47
G (qd) 2.12
C (t) 0.88
f1 (ppm)

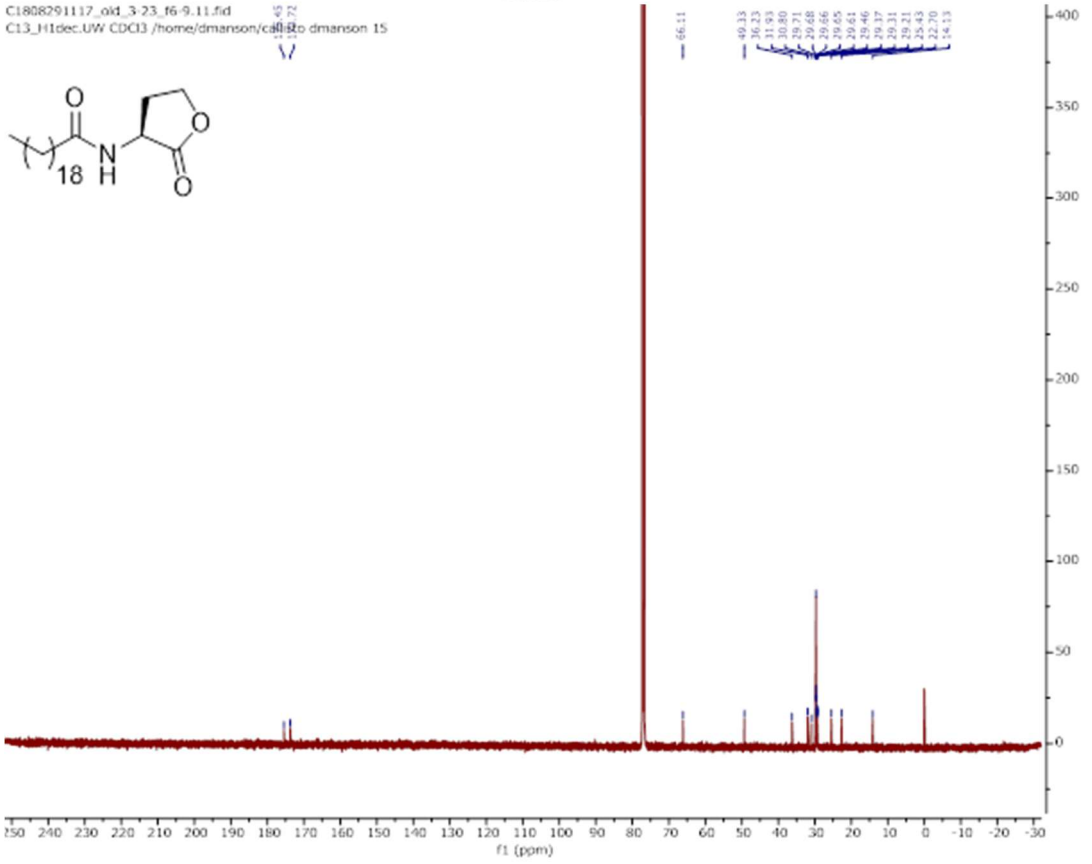
C1808291117_old_3-23_f6-9.11.fid
C13_H1dec.UW CDCl3 /home/dmanson/callisto dmanson 15
f1 (ppm)

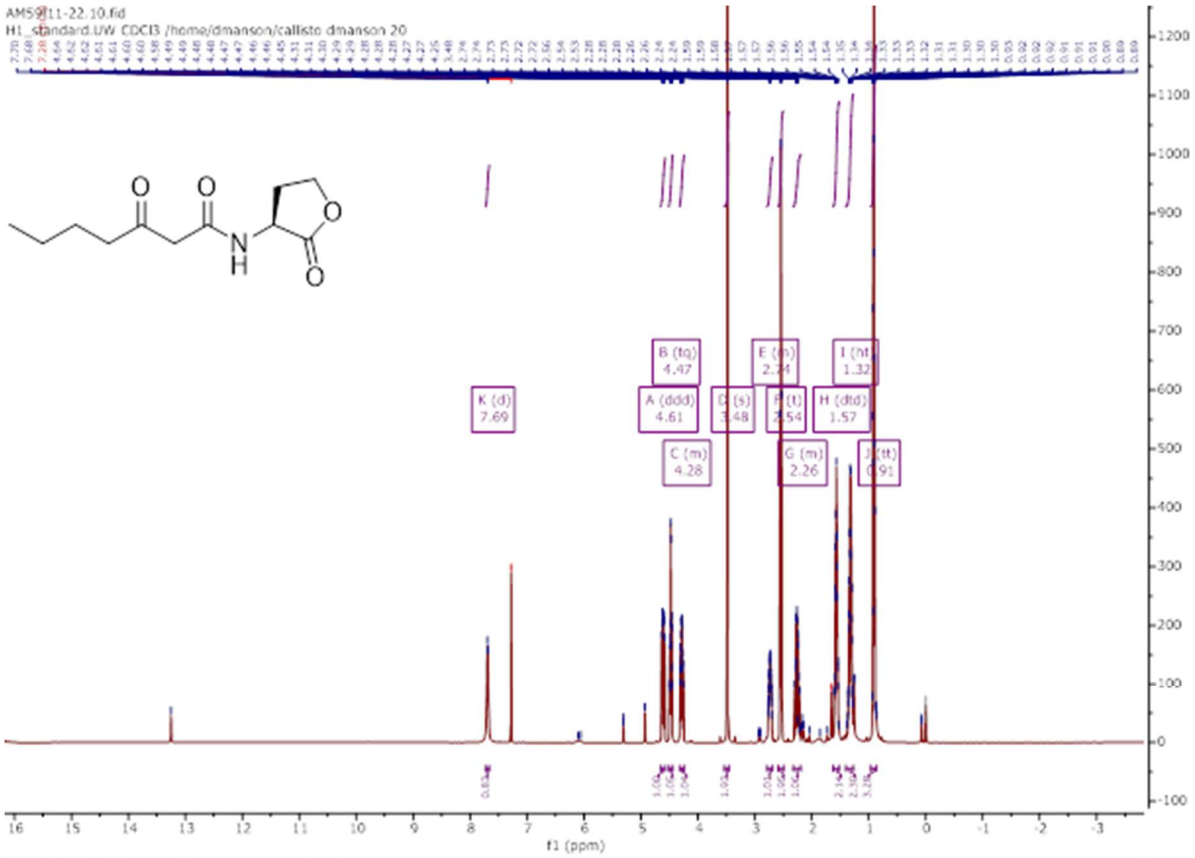
AM59f11-22.10.fid
H1_standard.UW CDCl3 /home/dmanson/calliste dmanson 20
K (d) 7.69
A (ddd) 4.61
B (tq) 4.47
C (m) 4.28
G (s) 3.48
F (t) 2.54
E (m) 2.34
H (dtd) 1.57
G (m) 2.26
I (ht) 1.32
J (tt) 0.91
f1 (ppm)

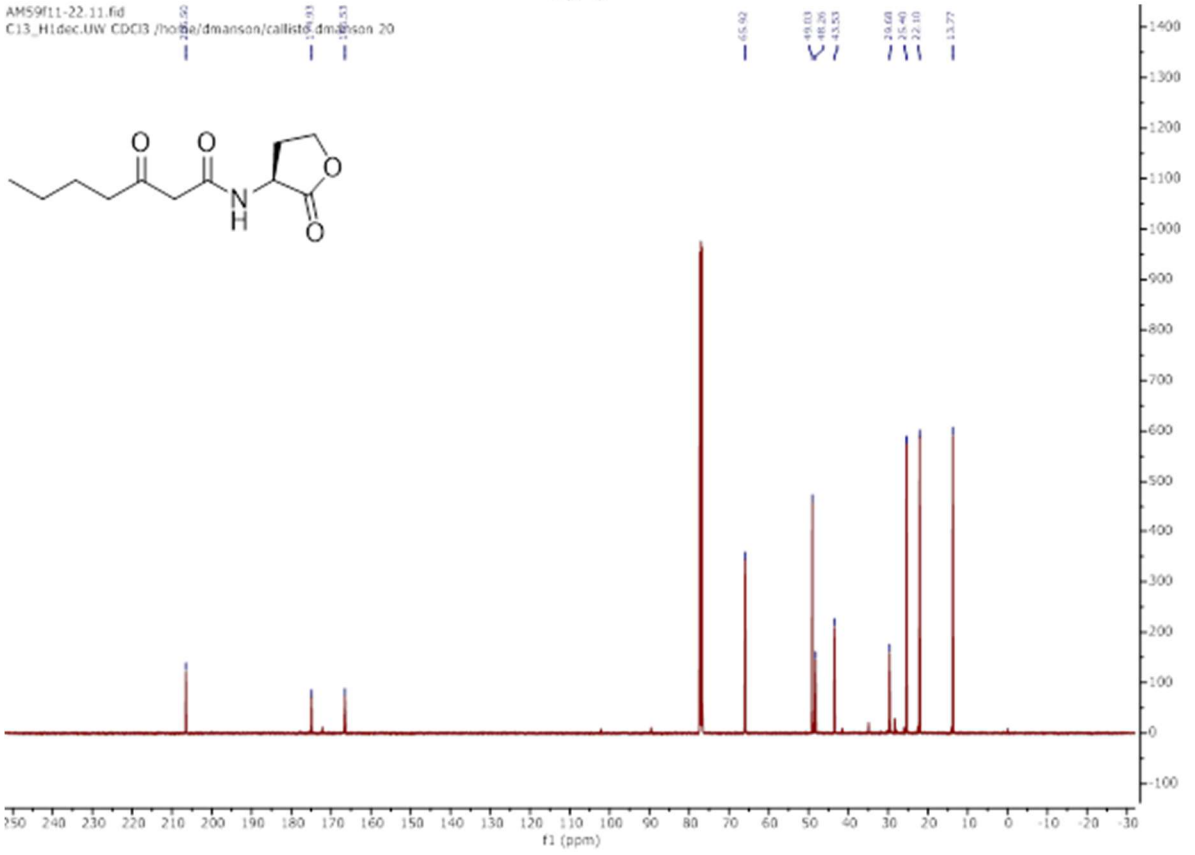
AM59f11-22.11.fid
C13_H1dec.UW CDCl3 /home/dmanson/calliste dmanson 20
f1 (ppm)

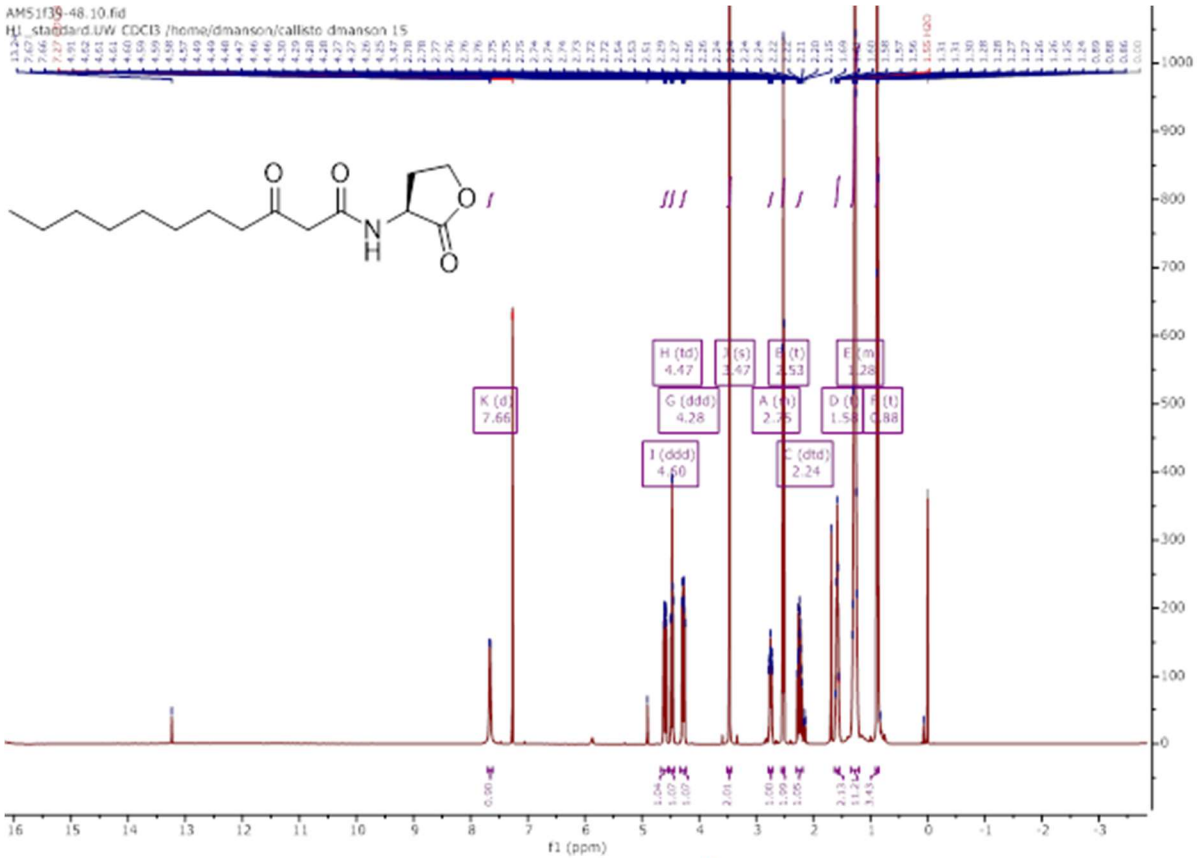
AM51f39-48.10.fid
H1_standard.UW CDCl3 /home/dmanson/callisto dmanson 15
K (d) 7.66
H (td) 4.47
G (ddd) 4.28
I (ddd) 4.60
A (s) 2.25
C (dtd) 2.24
f1 (ppm)

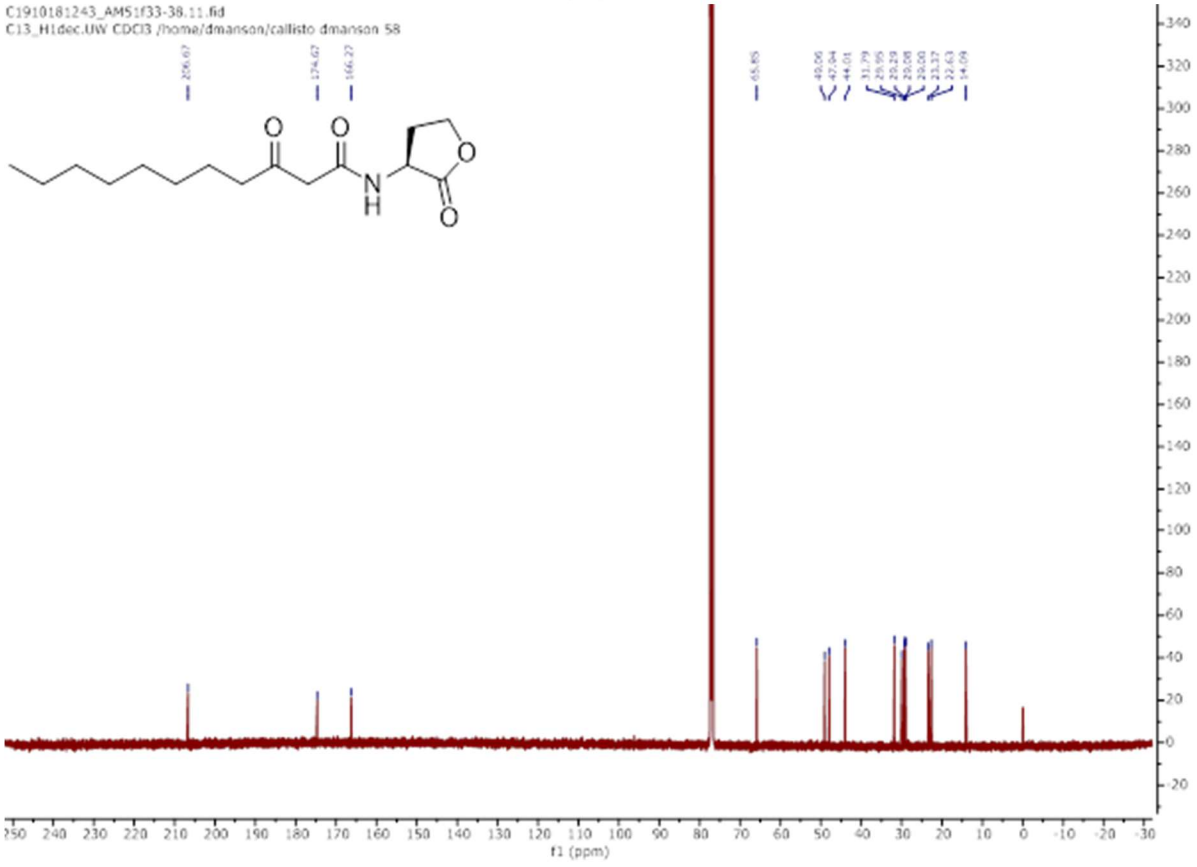
C1910181243_AM51f33-38.11.fid
C13_H1dec.UW CDCl3 /home/dmanson/callisto dmanson 58
206.67
174.67
166.27
65.85
f1 (ppm)

**References**

1. Whiteley, M.; Diggle, S. P.; Greenberg, E. P., Progress in and promise of bacterial quorum sensing research. *Nature* **2017,** *551* (7680), 313-320.
2. Rutherford, S. T.; Bassler, B. L., Bacterial quorum sensing: its role in virulence and possibilities for its control. *Cold Spring Harb Perspect Med* **2012,** *2* (11).
3. Mulani, M. S.; Kamble, E. E.; Kumkar, S. N.; Tawre, M. S.; Pardesi, K. R., Emerging Strategies to Combat ESKAPE Pathogens in the Era of Antimicrobial Resistance: A Review. *Front Microbiol* **2019,** *10*, 539.
4. Fuqua, C. W., S.C.; Greenberg, E.P., Quorum Sensing in Bacteria: the LuxR-LuxI Family of Cell Density-Responsive Transcriptional Regulators. *J. Bacteriol.* **1994,** *176* (2), 269-275.
5. Dong, S. F., N.D.; Christensen, Q.H.; Greenberg, E.P.; Nagarajan, R.; Nair, S.K., Molecular basis for the substrate specificity of quorum signal synthases. *Proc Natl Acad Sci U S A* **2017,** *114* (34), 9027-9097.
6. Pearson, J. P. V. D., C.; Iglewski, B.H., Active Efflux and Diffusion are Involved in Transport of *Pseudomonas aeruginosa* Cell-to-Cell Signals. *J Bacteriol* **1999,** *181* (4), 1203-1210.
7. Blair, J. M.; Piddock, L. J., Structure, function and inhibition of RND efflux pumps in Gram-negative bacteria: an update. *Curr Opin Microbiol* **2009,** *12* (5), 512-9.
8. Churchill, M. E. A. C., L., Structural Basis of Acyl-homoserine Lactone-Dependent Signaling. *Chem Rev* **2011,** *111*, 68-85.
9. Sappington, K. J.; Dandekar, A. A.; Oinuma, K.; Greenberg, E. P., Reversible signal binding by the Pseudomonas aeruginosa quorum-sensing signal receptor LasR. *MBio* **2011,** *2* (1), e00011-11.
10. Hudaiberdiev, S.; Choudhary, K. S.; Vera Alvarez, R.; Gelencser, Z.; Ligeti, B.; Lamba, D.; Pongor, S., Census of solo LuxR genes in prokaryotic genomes. *Front Cell Infect Microbiol* **2015,** *5*, 20.
11. DeLeon, S.; Clinton, A.; Fowler, H.; Everett, J.; Horswill, A. R.; Rumbaugh, K. P., Synergistic interactions of Pseudomonas aeruginosa and Staphylococcus aureus in an in vitro wound model. *Infect Immun* **2014,** *82* (11), 4718-28.
12. Bragonzi, A.; Farulla, I.; Paroni, M.; Twomey, K. B.; Pirone, L.; Lore, N. I.; Bianconi, I.; Dalmastri, C.; Ryan, R. P.; Bevivino, A., Modelling co-infection of the cystic fibrosis lung by Pseudomonas aeruginosa and Burkholderia cenocepacia reveals influences on biofilm formation and host response. *PLoS One* **2012,** *7* (12), e52330.
13. Zhu J, B. J., More MI, Fuqua C, Eberhard A, Winans SC, Analogs of the Autoinducer 3-Oxooctanoyl-Homoserine Lactone Strongly Inhibit Activity of the TraR Protein of *Agrobacterium tumefaciens*. *Journal of Bacteriology* **1998,** *180* (20), 5398-5405.
14. Moore, J. D.; Rossi, F. M.; Welsh, M. A.; Nyffeler, K. E.; Blackwell, H. E., A Comparative Analysis of Synthetic Quorum Sensing Modulators in Pseudomonas aeruginosa: New Insights into Mechanism, Active Efflux Susceptibility, Phenotypic Response, and Next-Generation Ligand Design. *J Am Chem Soc* **2015,** *137* (46), 14626-39.
15. Hodgkinson, J. T.; Galloway, W. R. J. D.; Casoli, M.; Keane, H.; Su, X.; Salmond, G. P. C.; Welch, M.; Spring, D. R., Robust routes for the synthesis of N-acylated-l-homoserine lactone (AHL) quorum sensing molecules with high levels of enantiomeric purity. *Tetrahedron Letters* **2011,** *52* (26), 3291-3294.
16. Schuster, M.; Greenberg, E. P., A network of networks: quorum-sensing gene regulation in Pseudomonas aeruginosa. *Int J Med Microbiol* **2006,** *296* (2-3), 73-81.

17. Brint, J. M. O., D.E., Synthesis of Multiple Exoproducts in *Pseudomonas aeruginosa* Is under the Control of RhlR-RhlI, Another Set of Regulators in Strain PAO1 with Homology to the Autoinducer-Responsive LuxR-LuxI Family. *J Bacteriol* **1995,** *177* (24), 7155-7163.
18. Passador, L. T., K.D.; Buertin, K.R.; Journet, M.P.; Kende, A.S.; Iglewski, B.H., Functional Analysis of the *Pseuomonas aeruginosa* Autoinducer PAI. *J Bacteriol* **1996,** *178* (20), 5995-6000.
19. Lee, J. H.; Lequette, Y.; Greenberg, E. P., Activity of purified QscR, a Pseudomonas aeruginosa orphan quorum-sensing transcription factor. *Mol Microbiol* **2006,** *59* (2), 602-9.
20. Eibergen, N. R.; Moore, J. D.; Mattmann, M. E.; Blackwell, H. E., Potent and Selective Modulation of the RhlR Quorum Sensing Receptor by Using Non-native Ligands: An Emerging Target for Virulence Control in Pseudomonas aeruginosa. *Chembiochem* **2015,** *16* (16), 2348-56.
21. Slinger, B. L.; Deay, J. J.; Chandler, J. R.; Blackwell, H. E., Potent modulation of the CepR quorum sensing receptor and virulence in a Burkholderia cepacia complex member using non-native lactone ligands. *Sci Rep* **2019,** *9* (1), 13449.
22. Styles, M. J.; Blackwell, H. E., Non-native autoinducer analogs capable of modulating the SdiA quorum sensing receptor in Salmonella enterica serovar Typhimurium. *Beilstein J Org Chem* **2018,** *14*, 2651-2664.
23. Lindsay, A.; Ahmer, B. M., Effect of sdiA on biosensors of N-acylhomoserine lactones. *J Bacteriol* **2005,** *187* (14), 5054-8.
24. Synthesis and screening of 3-oxo AHLs was undertaken as an undergraduate research project and only conducted in LasR and QscR.
25. Geske, G. D. W., R.J.; Siegel, A.P.; Blackwell, H.E., Smal Molecule Inhibitors of Bacterial Quorum Sensing and Biofilm Formation. *J Am Chem Soc* **2005,** *127*, 12762-12763.
26. Paczkowski, J. E.; McCready, A. R.; Cong, J. P.; Li, Z.; Jeffrey, P. D.; Smith, C. D.; Henke, B. R.; Hughson, F. M.; Bassler, B. L., An Autoinducer Analogue Reveals an Alternative Mode of Ligand Binding for the LasR Quorum-Sensing Receptor. *ACS Chem Biol* **2019,** *14* (3), 378-389.
27. Kanamaru, K. K., K.; Tatsuno, T.; Tobe, T.; Sasakawa, C., SdiA, an Escherichia colihomologue of quorum-sensing regulators, controls the expression of virulence factors in enterohaemorrhagic Escherichia coli O157:H7. *Mol Microbiol* **2000,** *38* (4), 805-816.
28. Arashida, N.; Shimbo, K.; Terada, T.; Okimi, T.; Kikuchi, Y.; Hashiro, S.; Umekage, S.; Yasueda, H., Identification of novel long chain N-acylhomoserine lactones of chain length C20 from the marine phototrophic bacterium Rhodovulum sulfidophilum. *Biosci Biotechnol Biochem* **2018,** *82* (10), 1683-1693.
29. Gahan, C. G.; Patel, S. J.; Boursier, M. E.; Nyffeler, K. E.; Jennings, J.; Abbott, N. L.; Blackwell, H. E.; Van Lehn, R. C.; Lynn, D. M., Bacterial Quorum Sensing Signals Self-Assemble in Aqueous Media to Form Micelles and Vesicles: An Integrated Experimental and Molecular Dynamics Study. *J Phys Chem B* **2020,** *124* (18), 3616-3628.
30. The last 5 days, June 20-24, 2020, saw the highest single-day counts of new, positive COVID-19 tests in Dane County.
31. Wellington, S. G., E.P., Quorum Sensing signal selectivity and the potential for interspecies cross talk. *mBio* **2019,** *10* (2), e00146-19.

# Chapter 6: A comparative study of non-native *n*-acyl L-homoserine lactone analogs in two *Pseudomonas aeruginosa* quorum sensing receptors that share a common native ligand yet inversely regulate virulence

Michelle E. Boursier, Daniel E. Manson, Joshua B. Combs, Helen E. Blackwell.

**This chapter has been published under the same title** – Reference: Boursier, M.E., Manson, D.E., Combs, J.B., Blackwell, H.E. A comparative study of non-native *N*-acyl L-homoserine lactone analogs in two *Pseudomonas aeruginosa* quorum sensing receptors that share a common native ligand yet inversely regulate virulence. *Bioorg. Med. Chem.* **2018**, *26*, 5336-5342

M.E. Boursier and H. E. Blackwell designed experiments. J. B. Combs synthesized compounds. J.B. Combs and D. E. Manson performed screening experiments. D. E. Manson, M.E. Boursier, and H.E. Blackwell wrote the chapter.

**Abstract**

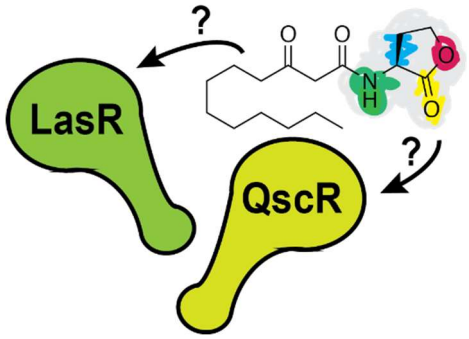


Certain bacteria can coordinate group behaviors via a chemical communication system known as quorum sensing (QS). Gram-negative bacteria typically use *N*-acyl L-homoserine lactone (AHL) signals and their cognate intracellular LuxR-type receptors for QS. The opportunistic pathogen *Pseudomonas aeruginosa* has a relatively complex QS circuit in which two of its LuxR-type receptors, LasR and QscR, are activated by the same natural signal, *N*-(3-oxo)-dodecanoyl L-homoserine lactone. Intriguingly, once active, LasR activates virulence pathways in *P. aeruginosa*, while activated QscR can inactivate LasR and thus repress virulence. We have a limited understanding of the structural features of AHLs that engender either agonistic activity in both receptors or receptor-selective activity. Compounds with the latter active profile could prove especially useful tools to tease out the roles of these two receptors in virulence regulation. A small collection of AHL analogues was assembled and screened in cell-based reporter assays for activity in both LasR and QscR. We identified several structural motifs that bias ligand activation towards each of the two receptors. These findings will inform the development of new synthetic ligands for LasR and QscR with improved potencies and selectivities.

## Introduction

Bacteria can communicate using chemical signals in a process called quorum sensing (QS) [1, 2]. In the canonical LuxI/LuxR systems found in Gram-negative bacteria, *N*-acyl L-homoserine lactones (AHLs) signals (or autoinducers) are produced by LuxI-type synthases at a basal level [3]. At a sufficiently high cell and signal density, the AHL signal will productively bind its cognate intracellular LuxR-type receptor. Thereafter, the activated complex will typically dimerize, bind to various promoters in the bacterial genome, and alter the expression of group beneficial genes. The LuxI/LuxR system is also upregulated, resulting in a positive feedback loop that is a hallmark of QS systems.

### *QS in Pseudomonas aeruginosa*

*P. aeruginosa* is an increasingly antibiotic resistant Gram-negative pathogen that is notorious for infecting cystic fibrosis patients and other immunocompromised individuals [4]. This bacterium regulates almost 10% of its genome via QS [5], including an arsenal of virulence factors, making inhibition of its QS circuit an attractive target for both anti-virulence and fundamental chemical biology research [6-10]. However, the development of ligands that modulate QS in *P. aeruginosa* is challenging due to its relatively complex QS system (Figure 1) [11]. *P. aeruginosa* has two distinct LuxI/LuxR systems, LasR and RhlR, in addition to the unrelated LysR-type Pseudomonas Quinolone System (PQS) [12]. LasR, considered at the top of the QS hierarchy, is activated by *N*-3-(oxo)-dodecanoyl L-homoserine lactone (OdDHL), which is produced by the LasI synthase. This receptor activates the rhl system, composed of the RhlR receptor and the RhlI synthase, the latter of which produces RhlR's cognate signal, *N*-butryl L-homoserine lactone (BHL). Both the las and rhl systems are negatively regulated by an orphan LuxR-type receptor or receptor "solo", QscR, which lacks its own corresponding synthase and native ligand, yet binds

and is maximally activated by OdDHL, the native ligand for LasR [12]. Interestingly, QscR serves as a repressor of both LasR and RhlR activity and suppresses virulence. The mechanism of this repression by QscR is not fully understood, but could include the formation of inactive heterodimers [13].

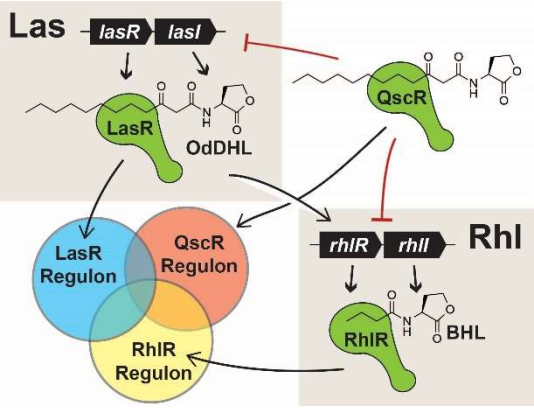


**Figure 6.1.** Simplified schematic of the three LuxR-type receptors in *P. aeruginosa* and their interregulation. LasR, QscR, and RhlR have overlapping regulons that control group beneficial genes, including many involved in virulence.

The three *P. aeruginosa* LuxR-type receptors have overlapping regulons (Figure 1), suggesting some redundancies in their modulation of group-related genes [14-16]. That said, LasR is the primary inducer of many major virulence factors, including elastase, endotoxin A, and alkaline protease [17], whereas RhlR primarily regulates the biosurfactant rhamnolipid [18]. QscR has been shown to directly regulate a number of genes, but their functions are currently unknown [14]. Our laboratory [19-22] and others [23-28] have devoted significant effort to developing non-native small molecules capable of targeting LasR, RhlR, and/or QscR to better delineate their individual roles in virulence progression. Several of these compounds have been shown to reduce virulence factor production in wild-type *P. aeruginosa* [29], and represent useful research tools to study *P. aeruginosa* QS pathways that can be challenging to interrogate using genetic knockouts [30]. To date, ligands relatively selective for LasR and RhlR have been identified [22]; however, the

molecular features that drive the selectivity of non-native ligands for LasR over QscR, and *vice versa*, remain largely unknown [21]. Notably, compounds that display selective QscR agonism could be utilized to antagonize both the las and rhl circuits, and could be useful molecules to modulate virulence; indeed, initial studies have shown that QscR activators can reduce virulence factor production in *P. aeruginosa* [31] and that a *P. aeruginosa* QscR-null mutant is hypervirulent in an insect model [32]. Delineating the structural features of AHLs that engender either agonistic activity in both QscR and LasR or receptor selective activity was one of the broad motivations for this study.

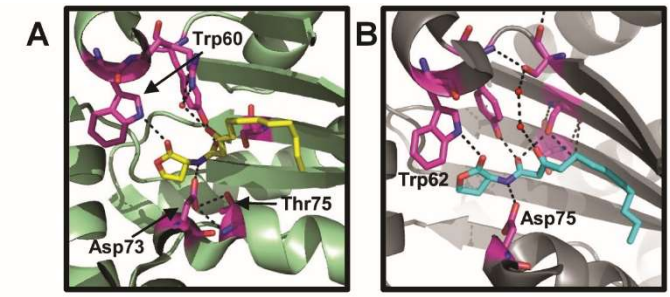


**Figure 6.2.** Views of (A) OdDHL (in yellow) bound to LasR (A) and OdDHL (in cyan) bound QscR (B) from their respective crystal structures [33, 34]. Key residues involved in hydrogen bonds to the KMd 3SZT.5 (QscR).

**Structural differences between LasR and QscR and prior studies of AHL activity profiles in these receptors**

Beyond the development of novel chemical tools for QscR and LasR, understanding the features of AHL-type compounds that selectively modulate either of these receptors (if they exist)is of fundamental interest, as these two receptors are activated maximally by the same natural ligand, OdDHL. This activity trend suggests that their ligand binding sites and/or modes of ligand recognition could be similar. However, structural studies of QscR and LasR have revealed that these two proteins differ in a number of ways [33, 34]. While both receptors possess the nine

highly-conserved amino acids found in the ligand-binding site of most LuxR-type receptors [35], their overall sequence similarity is only 16% [36]. X-ray crystallography of full length QscR and the ligand-binding domain (LBD) of LasR revealed that several of the hydrogen bonding contacts with OdDHL in the two receptors also involve different amino acids (Figure 2); overlays of the QscR and LasR LBDs reveal RMSD differences of 1.97 Å [33]. Additionally, QscR has been shown to be more stable and more amenable to ligand exchange *in vitro* than LasR, allowing for its biochemical manipulation with a variety of AHLs [37]. Indeed, cell-based reporter assays demonstrated that QscR is able to be activated by a wider assortment of native AHLs than LasR, as well as non-native AHLs with sterically bulkier acyl chains [21]. This more relaxed ligand binding capability may be due to QscR's larger ligand binding site and/or the different hydrogen-bonding networks available in QscR relative to LasR (Figure 2) [33, 38].

Most non-native AHLs developed to study LuxR-type receptor activity in *P. aeruginosa* have had varying acyl chains, yet maintain the native L-homoserine lactone "headgroup" [8]. Accordingly, relatively little is known about the effects of AHL analog activity in LasR and QscR with structural variations of the lactone "head group" (*vide infra*). Of the analogs with non-native headgroups that have been examined [27, 28, 39], most are weaker modulators of LasR (and other related receptors) than analogs that retain the lactone headgroup [40]. This trend has been attributed to hydrogen bonding contacts between the lactone and the receptor that are presumably essential for strong binding [41]. For example, structural data for both LasR and QscR highlight a key hydrogen bond between the OdDHL ester carbonyl and a conserved tryptophan side chain (Figure 2) [33, 34]. The OdDHL amide proton also forms a hydrogen bonding contact with a conserved aspartate residue. Replacement of the homoserine lactone with another chemical moiety, however, would be desirable for new probe design, as the lactone is hydrolytically unstable

(half-life of ~4–24 hours; depending on appended acyl chain structure [42]), which reduces their utility for deployment as tools in biologically relevant environments. Further analysis of subtle structural changes to the AHL head group, some of which retain the possibility to engage in hydrogen bonds, could result in compounds with improved stability, activity, and selectivity profiles. We sought to test this hypothesis in the current study in the context of OdDHL analogs and their comparative activity profiles in, and selectivity for, LasR and QscR.

Herein, we report the examination of a set of closely related OdDHL analogs selected to test the effects of systematic structural changes to the lactone headgroup on compound activity and selectivity for LasR and QscR. These compounds were evaluated in cell-based reporter assays that allowed for quantitative study of (i) agonism of LasR and QscR and (ii) competitive antagonism of LasR and QscR in the presence of OdDHL, providing for comparative analysis of ligand potency and selectivity in each receptor. Overall, we found that a subset of these OdDHL analogs with non-native head groups were selective for either receptor. In addition, we also identified analogs with high potencies that should have significantly improved hydrolytic stability in aqueous media relative to lactone derivatives. These compounds begin to teach us the features of AHL analogs that drive receptor selectivity, and will guide the future development of chemical probes to study the QS circuit in *P. aeruginosa*, and likely other related bacteria.

## Results and Discussion

### Compound selection, historical background for certain molecules, and synthesis

We selected compounds for study based on prior reports of OdDHL (**1**) analogs and our own design criteria (Figure 3). All of these compounds retain the 3-oxo-dodecanoyl "tail" group (except for sulfonamide **10**, which still preserves a 12-atom side chain). Of the small set of reported OdDHL analogs with alterations to the lactone headgroup, these derivatives have been examined

in different biological assays and largely only in LasR, thus comparative activity data in LasR or relative to QscR are not available. Of this group, we selected eight compounds that contained largely systematic structural changes to the lactone headgroup (**2**–**6**, **8**, and **10**) for comparative analysis in the current study. Pertinent background information on these compounds is provided here. Iglewski and coworkers first reported the homocysteine thiolactone (**3**) and γ-lactam (**4**) analogs in 1996 [43]. The thiolactone (**3**) was found to agonize LasR comparably to OdDHL (**1**), whereas the lactam was about 100-fold less potent based on $EC_{50}$. The Suga lab later examined non-hydrolyzable cyclopentanone **5** and cyclopentanol **8** derivatives [24]. With the carbonyl group maintained, cyclopentanone **5** retained agonistic activity in LasR but was not nearly as potent as OdDHL (**1**). The reduced analog, cyclopentanol **8**, could also agonize LasR, albeit only at very high concentrations (400 μM). Our lab reexamined thiolactone **3** and performed initial studies on cyclopentyl derivative **6** in LasR in 2011, again confirming the high potency of the thiolactone **3** and demonstrating some agonistic activity for **6** in LasR (but no $EC_{50}$ was calculated) [44, 45]. Sulfonamide variant **10** was the only compounds to be tested in both LasR and QscR [20, 46, 47]. This compound was a mild agonist of QscR, yet was inactive in LasR. Ester **11** and the D-enantiomer of OdDHL, **2**, were reported in 2004 and 2006 respectively, but no biological assay data was reported in LasR [48, 49]. We expanded this set of close OdDHL analogs with tetrahydrofuran (THF) derivatives **7** and **9** (Figure 3), which are new to this study. These compounds were included to maintain an oxygen in the heterocycles yet remove the carbonyl (**7**) and lengthen the head group (**9**). The set of 10 compounds were synthesized in moderate to good yields using standard amide bond coupling procedures or previously described methods (see Experimental Section) [50-52].

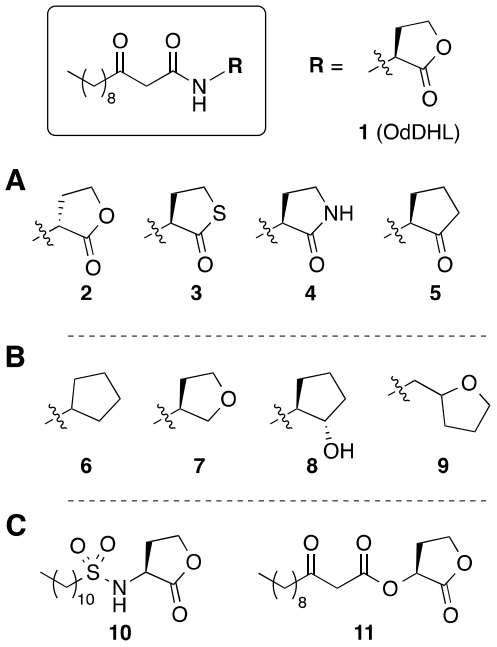


**Figure 6.3**. Structures of the compounds evaluated in this study. Compounds **2**–**9** retained the 3-oxo-dodecanoyl chain of OdDHL (**1**). Structures are loosely grouped based on variation to (A) the lactone stereochemistry or ring oxygen, (B) carbonyl replacement, and (C) amide linker modifications. Certain compounds were reported previously by other laboratories: **2**, Ishiguro and coworkers [49]; **3** and **4**, Iglewski and coworkers; **5**, **8**, and **11** [43]; Suga and coworkers; **6** and **10** [24, 48]; **10**, our laboratory [45].

The 10 OdDHL analogs selected for further analysis were roughly organized into three groups (1–3). Group 1 retained a carbonyl on the head group (Figure 3A). These compounds probed the importance of ring stereochemistry with compound **2**, and the identity of the ring heteroatom with thiolactone **3**, lactam **4**, and ketone **5**. These different atoms modify the size and shape of the ring, as well as the hydrogen bonding ability of the carbonyl and the ring atom itself. Group 2 compounds lacked a carbonyl (Figure 3B). Cyclopentane analog **6** is devoid of endocyclic heteroatoms and has no hydrogen bond acceptors, whereas THF derivative **7** retains an oxygen. Alcohol **8**, the asymmetrically reduced form of ketone **5**, allowed for testing the effects of a hydrogen-bond donor and acceptor versus only an acceptor (as in **5**) on the ring. Compound **9** (made as the racemate) adds a methylene to the THF derivative **7** and extends the head group. Lastly, the Group 3 compounds probed the amide linker between the head group and alkyl chain,

by converting it to either a sulfonamide (**10**) or an ester (**11**) (Figure 3C). The latter compound removes a hydrogen bond donor, while the former also lacks the 3-oxo group.

Biological evaluation in LasR and QscR

**Assay methods**

Cell-based reporter gene assays are routinely used to measure LuxR-type protein activity in the presence of exogenous compound. As *P. aeruginosa* has three LuxR-type receptors that are closely interregulated (Figure 1), measuring the activity of individual receptors in the native background can be challenging. To address this issue, our lab has developed heterologous reporter systems in *E. coli* strain JLD271 (Δ*sdiA*) for all three of the *P. aeruginosa* LuxR-type receptors [22, 30, 32, 38, 53]. Aside from standardizing the receptor expression levels and reporter plasmids, these strains also lack *E. coli*'s native LuxR-type receptor, SdiA, removing a possible ligand "sink" that could alter activity profiles. Using these LasR and QscR reporters and our previously described protocols [22, 39], we examined the agonistic activities of compounds **2–11** over a range of concentrations (1 pM–100 μM; see Experimental Section). Compounds that showed weak agonism (i.e., potency too low to calculate an $EC_{50}$ value) were also screened for their ability to antagonize LasR and QscR in competition with OdDHL (**1**) over a range of concentrations (3.2 nM–250 □M). Screening data were analyzed by examining maximum agonistic and antagonistic activities and calculating $EC_{50}$ and $IC_{50}$ values, and are listed in Table 1.

**Table 6.1.** Compound activity data in *E. coli* LasR and QscR reporter strains. CI = 95% confidence interval. [A]

| | LasR | | | QscR | | |
|---|---|---|---|---|---|---|
| **Agonism** | | | | | | |
| Compound | $EC_{50}$ (nM)[b] | 95% CI (nM) | Activation (%)[c] | $EC_{50}$ (nM)[b] | 95% CI (nM) | Activation (%)[c] |
| **1** (OdDHL) | 1.5 | (0.91 – 2.5) | 100 | 15 | (6.8 – 32) | 100 |
| **2** | 110 | (81 – 150) | 99 | 1380 | (440 – 4300) | 110 |
| **3** | 1.5 | (0.71 – 3.3) | 100 | 80 | (42 – 150) | 110 |
| **4** | 30 | (11– 79) | 110 | 3300 | (1600 – 7000) | 56 |
| **5** | 15 | (7.7 – 29) | 110 | 830 | (450 – 1500) | 77 |
| **6** | 160 | (73 – 360) | 88 | 360 | (230 – 550) | 100 |
| **7** | 910 | (760 – 1100) | 81 | 820 | (530 – 1300) | 74 |
| **8** | 1900 | (1400 – 2500) | 96 | 3500 | (1700 – 6900) | 110 |
| **9** | 260 | (130 – 500) | 96 | –[d] | – | 3.2 |
| **10** | –[d] | – | 6.4 | 1600 | (1000 – 2500) | 72 |
| **11** | –[d] | – | 27 | –[d] | – | 37 |
| **Antagonism** | | | | | | |
| Compound | $IC_{50}$ (μM)[e] | 95% CI (μM) | Inhibition (%)[f] | $IC_{50}$ (μM)[e] | 95% CI (μM) | Inhibition (%)[f] |
| **9** | – | – | – | > 250 | – | 59 |
| **10** | – | – | – | – | – | – |
| **11** | > 250 | – | 53 | > 250 | – | 23 |

[a]For details of reporter strains, see Experimental Section. All assays performed in triplicate; 95% CIs calculated from the SEM of n ≥ 3 trials. Shading in table provided for clarity to highlight Groups 1–3 in the agonism data. [b]For agonism experiments, LasR or QscR activity was measured relative to that of 100 μM OdDHL (**1**). $EC_{50}$ values determined by testing compounds over a range of concentrations (1 pM–100 □M). [c]Denotes the highest value of LasR or QscR activation observed for each compound at any concentration on the dose–response curve. Error = ±10. [d]Not calculated. [e]Antagonism experiments performed by competing the various compounds against OdDHL (**1**) at its $EC_{50}$ in LasR (1.5 nM) or QscR (15 nM), and inhibitory activity was measured relative to receptor activation at this $EC_{50}$. $IC_{50}$ values determined by testing compounds over a range of concentrations (3.2 nM–250 □M). [f]Denotes the highest value of LasR or QscR inhibition observed for each compound at any concentration on the dose–response curve. Full agonism and antagonism dose response curves are shown in the Supp. Info.

**Agonism assay results for Group 1 compounds (2–5)**

All of the compounds in Group 1, which retained a carbonyl in the head group, activated LasR to nearly 100% with $EC_{50}$ values in the low to mid nanomolar range (Table 1). D-OdDHL **2** was the least potent activator in this group ($EC_{50}$ 100-fold higher than L-OdDHL (**1**)), which was

unsurprising based on previous reports of the importance of lactone stereochemistry for LuxR-type receptor activation [51]. Lactam and cyclopentanone variants (**4** and **5**, respectively) were ~10–20-fold less potent than OdDHL (**1**), suggesting that these changes to the ring that either introduce an H-bond donor (lactam **5**) or remove H-bonding capability (ketone **5**) are moderately well tolerated in LasR. Thiolactone **3** was found to be the most potent non-native agonist of LasR in Group 1 (and in this study overall), with a comparable $EC_{50}$ to OdDHL (1.5 nM), corroborating previous reports [43, 44].

The agonism activity trends for Group 1 in QscR were both similar to and different than those in LasR. For instance, D-OdDHL **2** also showed a nearly 100-fold reduction in activity relative to OdDHL (**1**) whilst maintaining full efficacy, suggesting that the two receptors have similar intolerances for the inverted stereochemistry. Larger differences were observed upon varying the carbonyl group to thiolactone, lactam, and ketone. Thiolactone **3** was capable of full QscR activation, while the lactam and lactone showed reduced efficacy. Unlike in LasR, thiolactone **3** was five-fold less potent than OdDHL in QscR. Previous studies have suggested thiolactones to have a stabilizing effect on LasR due to their larger size and capability for hydrogen-bonding [54], so it is possible that the QscR ligand-binding site does not accommodate larger ring sizes well (assuming these closely related analogs also target the same site). This activity trend is supported by the QscR reporter assay data for lactam **4**, which displayed >200-fold reduced potency relative to OdDHL. The lactam nitrogen is closer in size to a sulfur atom than oxygen based on covalent radii [55], and will also interact with the ligand binding pocket differently because of the added hydrogen bond donor. The reduced flexibility of the amide C-N bond (relative to the C-O bond of a lactone) may also play a role in receptor binding. These differences may contribute to lactam **4**'s reduced potency. This trend may also be observed for cyclopentanone **5**; the subtly larger steric

size of the cyclopentanone versus the homoserine lactone (i.e., increased covalent radius of a methylene group vs. an oxygen atom), in addition to the lack of an endocyclic H-bonding acceptor, results in a ~55-fold difference overall. Overall, LasR appeared more tolerant of these head group changes relative to QscR.

**Agonism results for Group 2 compounds (6–9)**

Group 2 compounds, lacking a head group carbonyl (**6**–**9**), exhibited slightly lower efficacies and generally lower potencies in LasR relative to Group 1 (Table 1). Cyclopentane **6**, with a 100-fold loss in potency relative to OdDHL (**1**), was the most potent compound. THF derivative **7**, whilst 600-fold less potent than OdDHL, maintains an oxygen in the head group at a position comparable to the intact homoserine lactone, unlike compound **6**. The presence of this oxygen could possibly result in a disfavored hydrogen bonding interaction. Interestingly, a similar loss in potency is not observed in extended THF-derivative, **9**. Presumably, the added methylene linker places the head group in a more favorable position for ligand binding. Alcohol **8**, with both a hydrogen bond donor and acceptor at the carbonyl position, was the weakest LasR activator in Group 2, with a ~1200-fold higher $EC_{50}$ relative to OdDHL. We hypothesize that this molecule makes drastically changed and/or unfavorable hydrogen binding contacts in the pocket that alter the LasR protein configuration for optimal activity.

Turning to QscR, the Group 2 compounds **6**–**8** had largely similar potencies in QscR and LasR. However, because OdDHL is ~10 times more potent in LasR then QscR using these reporter assays, the similar potencies of **6**–**8** in both receptors indicate that QscR was better able to accommodate these ligands than LasR; we return to this issue when making comparisons between the two receptors below (see also Figure 4). Cyclopentane **6** was still the most potent of the group in QscR, exhibiting only a 24-fold reduction in potency relative to OdDHL. THF variant **7** was

slightly less potent than cyclopentane **6**, possibly indicating this ligand is making an undesirable contact in QscR as well as in LasR. Also similar to LasR, alcohol **8** was a very weak QscR agonist ($EC_{50}$ value in the micromolar range), suggesting its altered H-bonding properties were disfavored in both QscR and LasR. In contrast to LasR, however, the other THF derivative (**9**) showed negligible activity in QscR. This extended head group was apparently not tolerated for QscR agonism.

**Agonism data for group 3 compounds**

The two compounds in Group 3 (**10** and **11**) contained alterations to the amide linker, and both show limited activity in LasR and QscR. Sulfonamide **10** was inactive in LasR and showed only weak agonistic activity in QscR, corroborating previous reported trends [47]. As some of the most potent previously reported agonists and antagonists of QscR contain steric bulk alpha to the amide linker [21], it is perhaps not surprising that the sulfonamide can be tolerated in QscR, albeit engendering very modest ligand activity. In turn, ester **11**, which lacks the ability to donate a hydrogen bond, drastically looses efficacy in LasR and QscR. This loss of activity is supported by prior mutational studies highlighting the importance of Asp73 for LasR activation [54]. The chemical experiment performed here (removing the hydrogen bond donor from the ligand rather than the protein) supports the importance of hydrogen bonding between Asp73 and Thr75 (in LasR) and Asp75 (in QscR) with a ligand as being vital to receptor activation (Figure 2) [33, 34].

**Antagonism screening for compounds with limited activity in agonism experiments**

We reasoned that compounds with limited to no activity in the agonism assays could operate as receptor antagonists instead [56] Therefore, we measured the antagonism profiles of compounds **10** and **11** in LasR and **9** and **11** in QscR, each in competition against OdDHL (**1**). The data resulting from these assays are listed in Table 1. Sulfonamide **10** failed to antagonize LasR,

suggesting that, in concert with its lack of agnostic activity, this linkage alternation simply destroys receptor interactions. Ester **11** was capable of weak LasR antagonism, achieving a maximum inhibition of 53% at the highest concentration tested, but was not sufficiently potent to calculate an $IC_{50}$.

In QscR, extended THF analogue **9** was twice as active as ester **11**, with maximum inhibitory activities of 59% versus 23%, respectively. Neither compound was potent enough to calculate an $IC_{50}$, however. These data reinforce the importance of the Asp73/Asp75 to amide N-H hydrogen bond for LasR or QscR binding and the intolerance of LasR for added steric bulk near the amide bond. Additionally, our results suggest that "elongated" head groups, such as in **9**, may be a useful motif for developing QscR-selective antagonists.

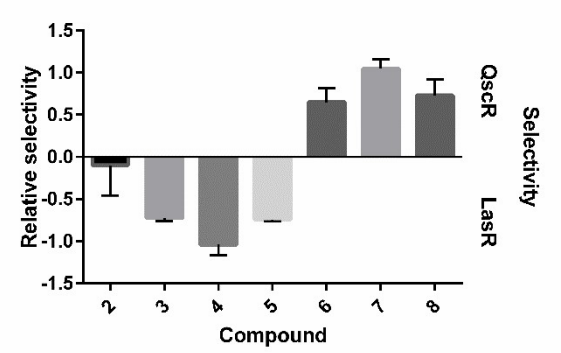


**Figure 6.4.** Relatively selectivity profiles for compounds **2-8** in LasR and QscR. Error bars were generated from the 95% confidence intervals of the $EC_{50}$ values in each receptor. See Supp. Info. for a mathematical definition of relative selectivity.

**Relative selectivity profiles in LasR and QscR**

We were interested in determining if any of the motifs present in our library engendered molecules with selectivity for LasR over QscR, and *vice versa*. As noted above, OdDHL (**1**) is approximately 10-fold more potent in LasR than QscR. Therefore, non-native compounds with similar potencies that are above the $EC_{50}$ value of OdDHL in both receptors (i.e., **6**–**8**) have lost 10-fold *less* potency against QscR than LasR (relative to OdDHL). To quantify this phenomenon

and determine whether our molecules were selective for LasR or QscR relative to OdDHL, we developed a "relative selectivity" metric (see Supp. Info. for mathematical derivation). We applied this metric to all molecules for which we could calculate an $EC_{50}$ in both receptors (**2**–**8**) and excluded compounds with no activity in one receptor (**9**–**11**). These metric data are plotted in Figure 4 and reveal that the presence or absence of a carbonyl in a compound was the main driver of relative selectivity. Carbonyl-containing compounds **3**–**5** showed relative selectivity for LasR, whilst compounds without carbonyls (**6**–**8**) showed relative selectivity for QscR. This selectively trend suggest that receptor contacts with the carbonyl (steric and/or hydrogen-bonding) are favored in LasR over QscR for this set of close OdDHL analogs.

**Conclusion**

The goal of this study was to measure the agonism and antagonism profiles of a set of head group-modified OdDHL (**1**) analogues to identify molecular features important for the differential activation of LasR and QscR. These overall SARs are shown schematically in Figure 5. In general, LasR activity is more greatly affected by the removal of the homoserine lactone carbonyl than QscR. LasR also cannot tolerate steric bulk near the amide carbonyl. In terms of agonism, QscR is less amenable to elongation of the head group (i.e., as in **9**) and changes in identity of the carbonyl-bearing ring (i.e., lactone vs. thiolactone, lactam, or ketone) relative to LasR. Both receptors are equally affected by changes in ring stereochemistry and require a hydrogen bond donor on the ligand linker (i.e., an amide) for appreciable receptor activation. In addition, our study of the antagonism profiles of analogues with limited to no agonistic activity revealed that ester **11**, and THF-derivative **9** and **11**, are mild antagonists of LasR and QscR, respectively. These antagonism data suggest that the incorporation of "elongated" head groups (as in **9**) can generate QscR-selective antagonists.

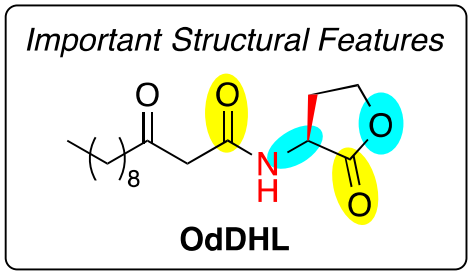


**Figure 6.5.** Structural features important for the activation of LasR and QscR receptors. Features more important for LasR activation are shown in yellow (i.e., removal of the lactone carbonyl, added bulk around amide carbonyl). Features more important for LasR activation are shown in yellow (i.e., removal of the lactone carbonyl, added bulk around amide carbonyl). Features more important for QscR activation are shown in cyan (i.e., increased linker length, heteroatom change). Changes equally detrimental for activation of both receptors are shown in red.

Looking to the future, these investigations have revealed several head groups as potential leads for generating new probe compounds for LasR and QscR with improved hydrolytic stability. Thiolactone **3**, lactam **4**, and cyclopentanone **5** all are relatively more stable than homoserine lactone and maintain potencies in LasR in the mid-nanomolar range. These compounds have increased selectivity for LasR over QscR, making them excellent leads for future compounds targeting this receptor. While changes in the homoserine lactone heteroatom generally result in reduced activity in both LuxR-type receptors, these activity differences may not be as critical if the compounds have longer half-lives in aqueous media, allowing them to remain active over prolonged periods in biologically relevant environments. Homocysteine thiolactone derivatives, like **3**, are particularly interesting in this regard, as we have shown them to remain intact significantly longer than the native lactone head group [44]. Alternatively, QscR selective compounds may benefit from the incorporation of a sulfonamide linker or from the removal of the homoserine lactone carbonyl. Both changes resulted in modest QscR agonists with limited to no activity versus LasR. Further development of the lead compounds and the SARs for OdDHL (**1**) reported here is ongoing in our lab.

## Materials and Methods

### General

All chemical reagents and solvents were purchased from commercial sources and used without further purification, except for dichloromethane (DCM), which was distilled and dried over activated molecular sieves. Water (18 MΩ) was purified using a Thermo Scientific Barnstead Nanopure system. OdDHL (**1**) was purchased from Sigma Aldrich. Chlorophenol red-β-D-galactopyranoside (CPRG) was purchased from Roche. *Ortho*-nitrophenyl-β-galactoside (ONPG) was purchased from Sigma Aldrich. All media and reagents for bacterial culture were purchased from commercial sources and used according to manufacturer's instructions.

### Chemistry

For compounds **2**–**9** and **11**, the acyl "tail group" was introduced via 2-(2-nonyl-1,3-dioxolan-2-yl) acetic acid, which was synthesized according to the method of Spring and coworkers [52]. This acid was coupled to each analog head group using 1-ethyl-3-(3-dimethylaminopropyl)carbodiimide (EDC)–mediated coupling chemistry as reported previously by our laboratory [45]. The resulting product of each coupling reaction was deprotected with trifluoroacetic acid (TFA) to produce the analogs **2**–**4**, **6**, **7**, **9**, and **11** [52]. The head group for compound **4** ((*S*)-3-amino-2-pyrrolidinone) was prepared as previously described [57]. Enantiomerically pure (*S, S*)-2-aminocyclopentanol was used in the preparation of compound **8**. Formation of the amide bond between head groups and tail groups in analogues **5** and **8** required a different reaction solvent than that for **2**–**4**, **6**, **7**, **9**, and **11** (DMF rather than DCM), but otherwise all reaction conditions were identical. Cyclopentanone **5** was prepared via Dess-Martin oxidation of its hydroxyl precursor (**8**) as previously reported [51]. Sulfonamide **10** was synthesized as

described [50]. All products were purified to homogeneity via silica gel chromatography as needed after standard aqueous work-up.

**Bacteriology methods**

Bacteria were cultured in Luria−Bertani medium (LB) at 37 °C. Absorbance measurements were performed in 96-well microtiter plates and path length-corrected using a Biotek Synergy 2 plate reader running Gen 5 software (version 1.05). Bacterial growth was assessed by measuring absorbance at 600 nm ($OD_{600}$).

**Bacterial strains and assay protocols**

The bacterial reporter strains used for this study were the (i) *E. coli* strain JLD271 (Δ*sdiA*) harboring the LasR expression plasmid pJN105L and the *lasI-lacZ* transcriptional fusion reporter pSC11-L, and (ii) *E. coli* strain JLD271 (Δ*sdiA*) harboring the QscR expression plasmid pJN105Q and the p*PA1897-lacZ* transcriptional fusion reporter pSC11-Q. Miller-type □-galactosidase assays were performed in these two *E. coli* reporters using either CPRG or ONPG substrates as previously described [22, 39]. For agonism experiments, LasR or QscR activity was measured relative to that of 100 μM OdDHL (**1**). Antagonism experiments were performed by competing the various compounds against OdDHL (**1**) at its $EC_{50}$ in LasR (1.5 nM) or QscR (15 nM), and inhibitory activity was measured relative to receptor activation at this $EC_{50}$. $EC_{50}$ and $IC_{50}$ values were determined by testing compounds over a range of concentrations (≤ 250 μM).

**Acknowledgements**

Financial support for this work was provided by the NIH (R01 GM109403) and the Burroughs Wellcome Fund. M.E.B. was funded in part by the NSF through a seed grant from the UW–Madison Materials Research Science and Engineering Center (DMR-1121288). NMR facilities in

the UW–Madison Department of Chemistry were supported by the NSF (CHE-0342998) and a gift from Paul J. Bender. MS facilities in the UW–Madison Department of Chemistry were supported by the NSF (CHE-9974839). Korbin H. J. West is acknowledged for helpful discussions.

**Instrumentation and analytical methods**

NMR spectra were recorded in deuterated NMR solvents at 500 MHz on a Bruker Avance-500 spectrometer with DCH cryoprobe and SampleXpress. Chemical shifts are reported in parts per million (ppm, δ) using corresponding solvents or tetramethylsilane (TMS) as a reference. Couplings are reported in hertz (Hz). Electrospray ionization MS measurements were performed on a Waters LCT. Samples were dissolved in acetonitrile and sprayed with a sample cone voltage of 20. For exact mass measurements (EMM), an aliquot of a known compound (lock mass) was added to the sample and resprayed.

**Compound characterization data**

$^{1}$H NMR, $^{13}$C NMR, and ESI MS data are reported below for the new compounds in this study (**7** and **9**). Characterization data for compounds **4** [1] and **11** [2] are included as they have not been fully characterized in past studies reporting their structures. Characterization data for compounds **2** [3], **3** [4], **5** [5], **6** [6], **8** [7], and **10** [8] matched those in prior reports. We note that minor amounts of enol tautomer appear in all spectra; NMR characterization data is reported for the keto tautomer. Copies of the spectra are included at the end of this document.

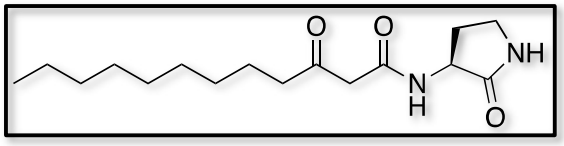


**4:** $^{1}$H NMR (500 MHz, $CDCl_3$) δ 7.56 (s, 1H), 6.38 (d, *J* = 32.2 Hz, 1H), 4.44 (ddd, *J* = 11.0, 8.4, 6.3 Hz, 1H), 3.50 – 3.32 (m, 4H), 2.83 – 2.62 (m, 1H), 2.53 (t, *J* = 7.4 Hz, 2H), 1.98 (dq, *J* = 12.3, 9.8 Hz, 1H), 1.68 – 1.48 (m, 2H), 1.26 (d, *J* = 7.0 Hz, 15H), 0.87 (t, *J* = 6.8 Hz, 3H); $^{13}$C

NMR (126 MHz, $CDCl_3$) δ 206.57, 166.60, 50.76, 48.98, 43.92, 39.35, 31.99, 29.85, 29.78, 29.54, 29.50, 29.39, 29.15, 23.52, 22.80, 14.25; ESI MS: expected $[M+H]^+$: 297.2173, observed: 297.2169.

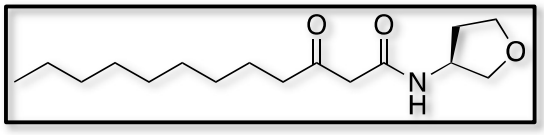

**7:** $^1H$ NMR (500 MHz, $CDCl_3$) δ 4.50 (dtd, *J* = 7.0, 3.7, 1.9 Hz, 1H), 3.93 (dt, *J* = 8.6, 7.3 Hz, 1H), 3.89 – 3.76 (m, 2H), 3.65 (dd, *J* = 9.4, 3.1 Hz, 1H), 3.37 (d, *J* = 1.7 Hz, 2H), 2.50 (t, *J* = 7.3 Hz, 2H), 2.35 – 2.19 (m, 1H), 1.81 (dddd, *J* = 13.1, 7.5, 5.6, 3.4 Hz, 1H), 1.56 (dd, *J* = 13.5, 6.8 Hz, 3H), 1.40 – 1.16 (m, 14H), 0.87 (t, *J* = 6.9 Hz, 3H); $^{13}C$ NMR (126 MHz, $CDCl_3$) δ 207.35, 165.51, 73.49, 67.04, 50.39, 48.58, 44.17, 33.17, 31.98, 29.51, 29.47, 29.37, 29.13, 23.49, 22.79, 14.24; ESI MS: expected $[M+H]^+$: 284.2220, observed: 284.2215.

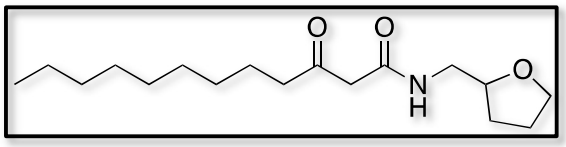

**9:** $^1H$ NMR (500 MHz, $CDCl_3$) δ 7.11 (s, 1H), 3.98 (qd, *J* = 7.0, 3.6 Hz, 1H), 3.88 (dt, *J* = 8.3, 6.6 Hz, 1H), 3.80 – 3.71 (m, 1H), 3.54 (ddd, *J* = 13.7, 6.2, 3.6 Hz, 1H), 3.39 (d, *J* = 2.6 Hz, 2H), 3.22 (ddd, *J* = 13.6, 7.1, 5.2 Hz, 1H), 2.52 (t, *J* = 7.4 Hz, 2H), 2.06 – 1.81 (m, 3H), 1.76 – 1.46 (m, 3H), 1.26 (d, *J* = 6.7 Hz, 12H), 0.87 (t, *J* = 6.9 Hz, 3H); $^{13}C$ NMR (126 MHz, $CDCl_3$) δ 206.85, 165.88, 77.58, 68.35, 49.17, 44.05, 43.39, 32.00, 29.53, 29.49, 29.39, 29.15, 28.80, 26.02, 23.54, 22.80, 14.25; ESI MS: expected $[M+H]^+$: 298.2377, observed: 298.2372.

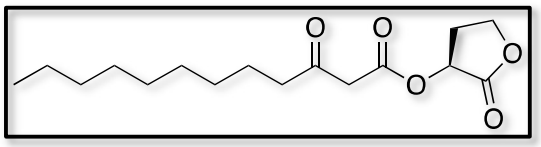

**11:** $^1H$ NMR (500 MHz, $CDCl_3$) 5.44 (t, *J* = 8.9 Hz, 1H), 4.48 (td, *J* = 9.1, 2.7 Hz, 1H), 4.36 – 4.25 (m, 1H), 3.69 – 3.40 (m, 2H), 2.74 (dddd, *J* = 13.1, 9.0, 6.5, 2.7 Hz, 1H), 2.54 (t, *J* = 7.3 Hz, 2H), 2.36 (dq, *J* = 12.9, 9.4 Hz, 1H), 1.58 (h, *J* = 8.3, 7.8 Hz, 2H), 1.27 (dd, *J* = 11.5, 6.2 Hz, 14H), 0.97 – 0.71 (m, 3H); $^{13}C$ NMR (126 MHz, $CDCl_3$) δ 202.24, 172.28, 166.22, 68.37, 65.18, 48.62, 43.18, 31.85, 29.38, 29.34, 29.24, 28.97, 28.77, 23.43, 22.66, 14.11; ESI MS: expected $[M+H]^+$: 316.2119, observed: 316.2114

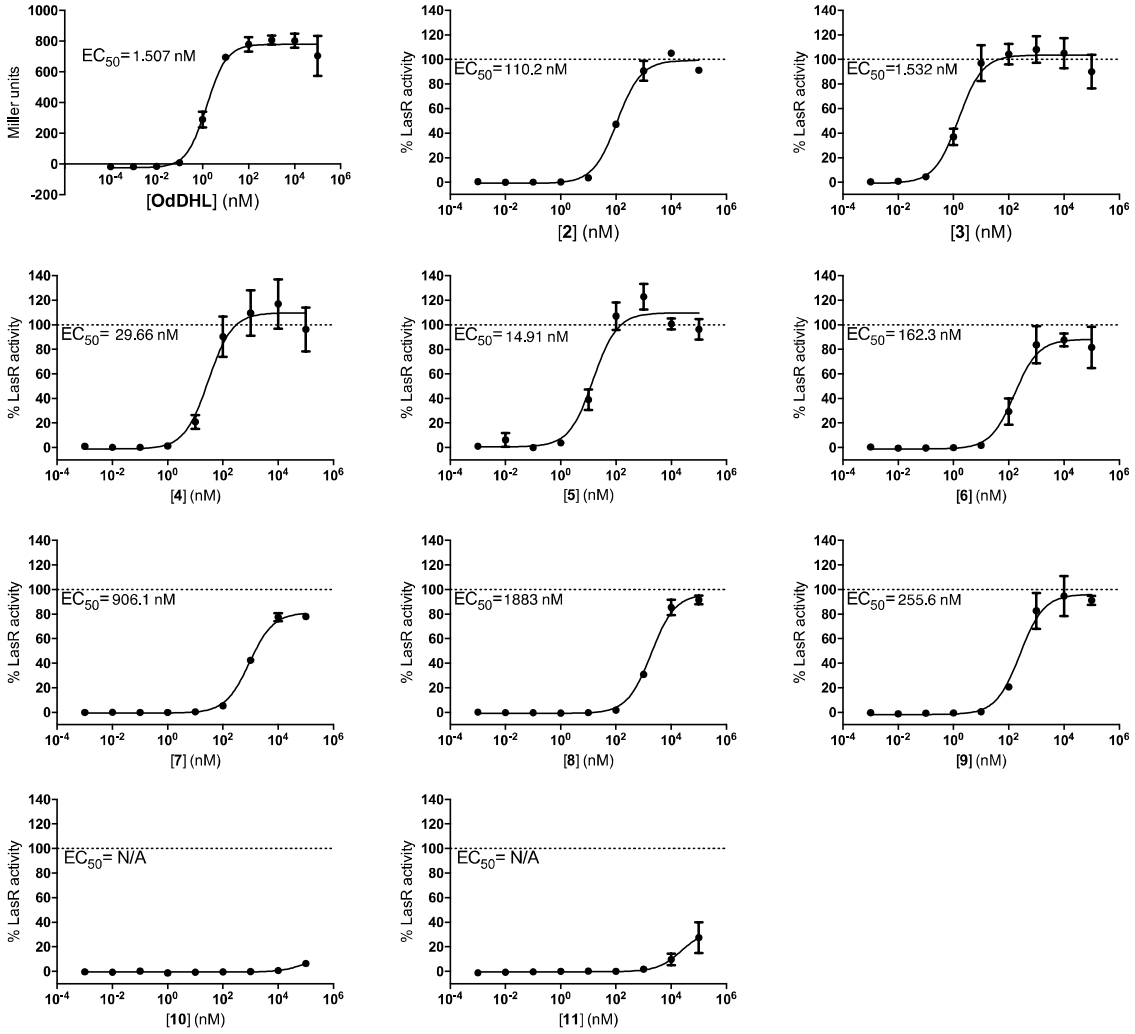


**Figure S6.1**. Dose–response curves for LasR agonism in *E. coli* for all compounds. Assay performed using the *E. coli* JLD271/pJN105L/pSC11 LasR reporter strain. Compounds indicated in the X-axis of each plot. % Activity defined as the activity of the synthetic compound relative to maximum possible LasR activity (i.e., activity effected by OdDHL (**1**) at 100 μM). $EC_{50}$ values and 95% Confidence Intervals (CI; shown in Table 7.1) calculated using GraphPad Prism. Error bars, SEM of n ≥ 3 trials.

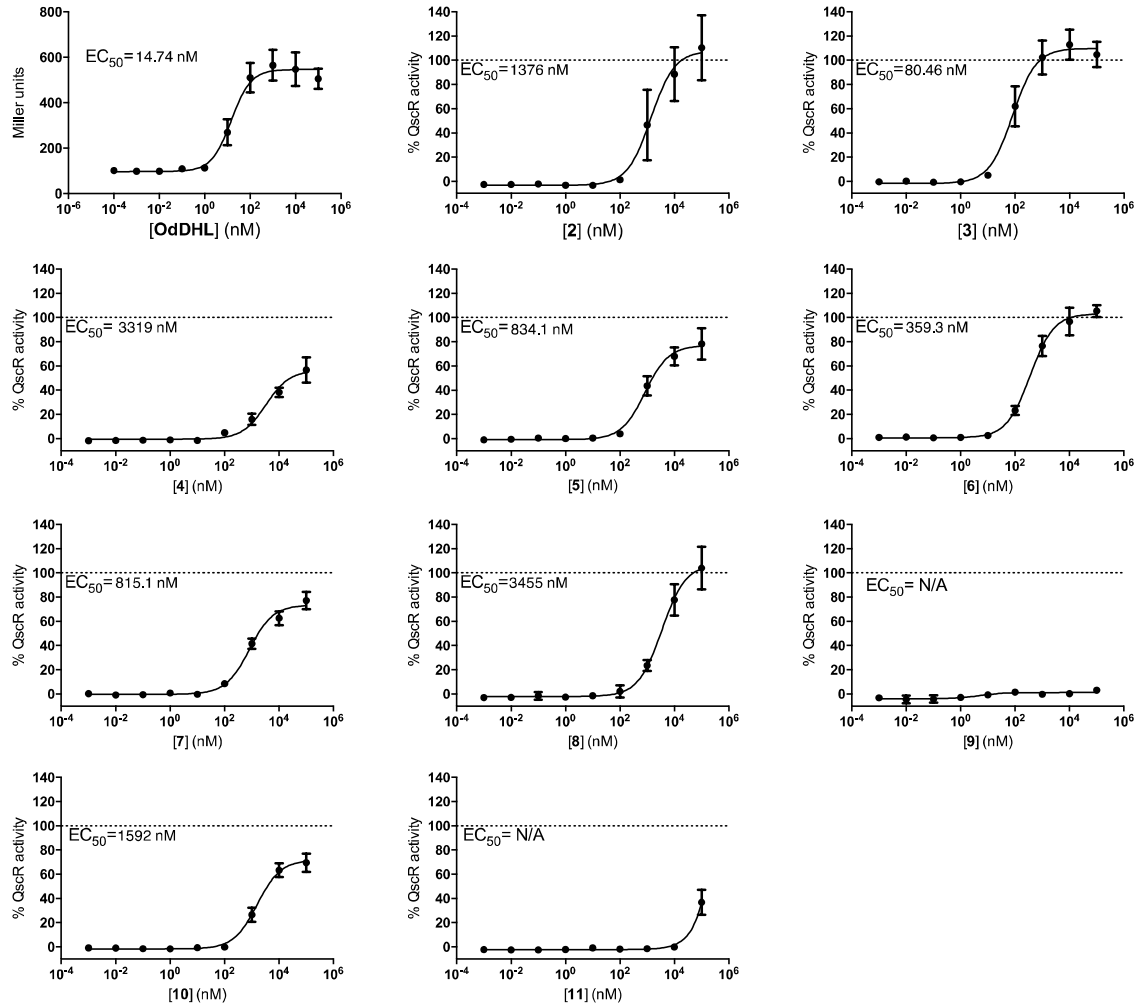


**Figure S6.2**. Dose–response curves for QscR agonism in *E. coli* for all compounds. Assay performed using the *E. coli* JLD271/pJN105Q/pSC11-Q QscR reporter strain. Compounds indicated in the X-axis of each plot. % Activity defined as the activity of the synthetic compound relative to maximum possible QscR activity (i.e., activity effected by OdDHL (**1**) at 100 μM). $EC_{50}$ values and 95% Confidence Intervals (CI; shown in Table 7.1) calculated using GraphPad Prism. Error bars, SEM of n ≥ 3 trials.

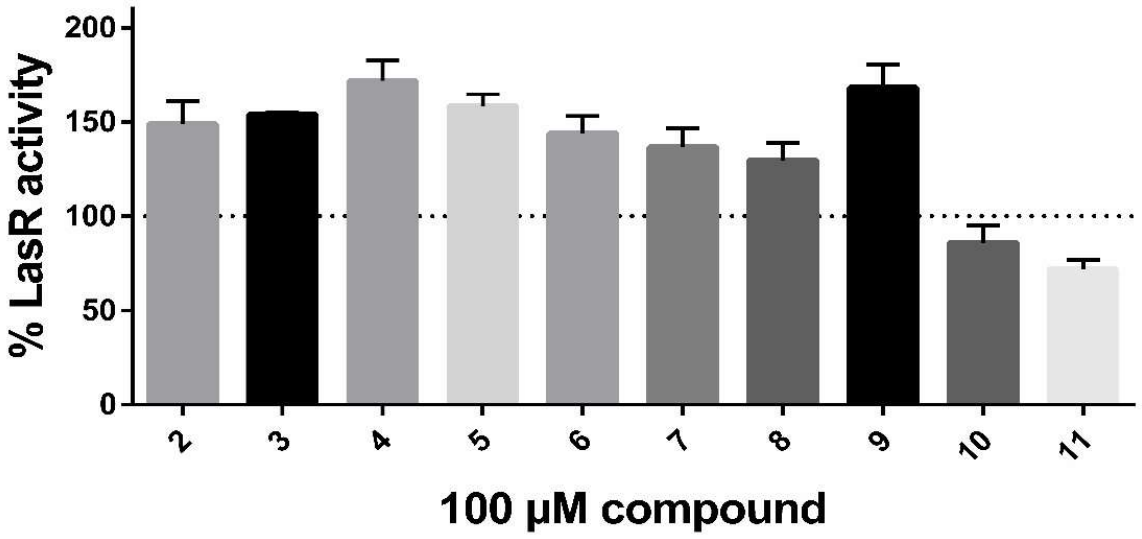


**Figure S6.3**. Single point LasR antagonism data in *E. coli* for all compounds.

Assay performed using the *E. coli* JLD271/pJN105L/pSC11-L LasR reporter strain. Antagonism experiments performed in the presence of the native ligand (OdDHL, **1**) at its $EC_{50}$ value (2 nM). % Activity defined as the activity of the synthetic compound relative to 50% possible LasR activity (i.e., activity effected by OdDHL at its $EC_{50}$). Error bars, SEM of $n \geq 3$ trials.

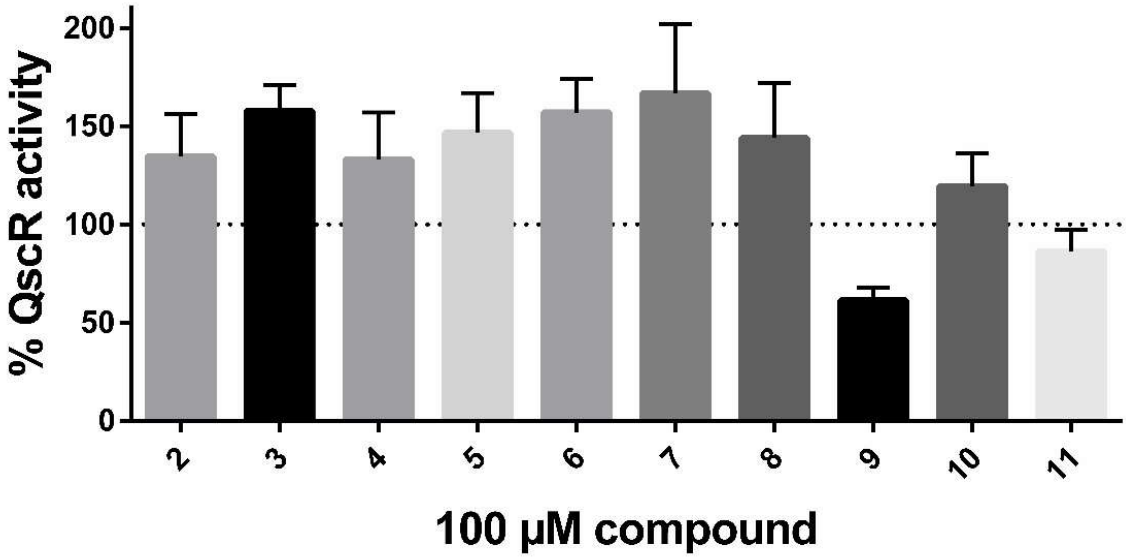


**Figure S6.4**. Single point QscR antagonism data in *E. coli* for all compounds.

Assay performed using the E. coli JLD271/pJN105Q/pSC11-Q QscR reporter strain. Antagonism experiments performed in the presence of the natural ligand (OdDHL, **1**) at its $EC_{50}$ value (15 nM). % Activity defined as the activity of the synthetic compound relative to 50% possible QscR activity (i.e., activity effected by OdDHL at its $EC_{50}$). Error bars, SEM of $n \geq 3$ trials.

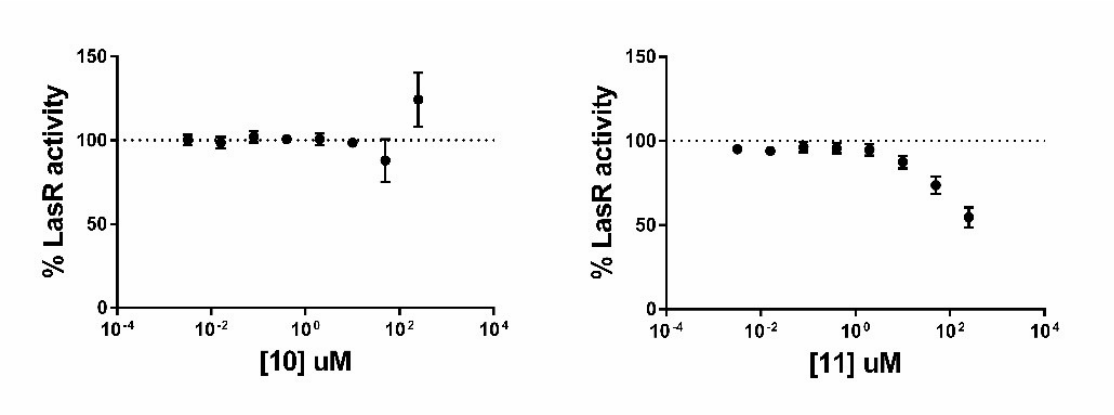


**Figure S6.5.** Dose–response curves for LasR antagonism in *E. coli* for compounds with no LasR agonism activity (10 and 11).

Assay performed using the *E. coli* JLD271/pJN105L/pSC11-L LasR reporter strain. Compounds indicated in the X-axis of each plot. Antagonism experiments performed in the presence of the native ligand (OdDHL,**1**) at its $EC_{50}$ value (2 nM). % Activity defined as the activity of the synthetic compound relative to 50% possible LasR activity (i.e., activity effected by OdDHL at its $EC_{50}$). Error bars, SEM of $n \geq 3$ trials.

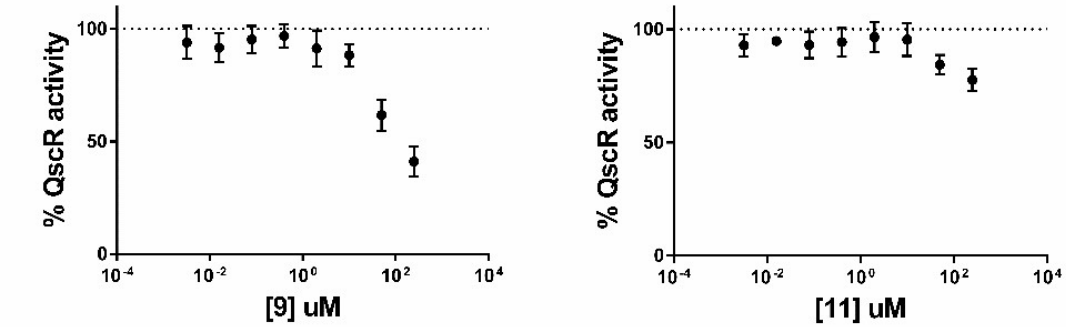


**Figure S6.6.** Dose–response curves for QscR antagonism in *E. coli* for compounds with no QscR agonism activity (9 and 11).

Assay performed using the *E. coli* JLD271/pJN105Q/pSC11-Q QscR reporter strain. Compounds indicated in the X-axis of each plot. Antagonism experiments performed in the presence of the natural ligand (OdDHL, **1**) at its $EC_{50}$ value (15 nM). % Activity defined as the activity of the synthetic AHL relative to 50% possible QscR activity (i.e., activity effected by OdDHL at its $EC_{50}$). Error bars, SEM of $n \geq 3$ trials.

**Definition and discussion of relative selectivity**

OdDHL (**1**), the native ligand for LasR and one of the most active natural AHLs for QscR, activates LasR with approximately 10-fold higher potency than QscR (2 nM vs. 15 nM $EC_{50}$ values, respectively). Accordingly, a non-native agonist with an $EC_{50}$ of 100 nM in both receptors has lost 10-fold less potency in QscR than in LasR (relative to the potency of OdDHL in each receptor). Conversely, a non-native agonist with an $EC_{50}$ of 0.001 nM in both receptors has gained 10-fold more potency in QscR than in LasR (again, relative to OdDHL). To address this issue and identify molecules with a preferential increase/decrease in potency in one receptor over the other, we developed a "relative selectivity" metric defined as follows:

$$\boldsymbol{Relative\ selectivity = log\left(\frac{Compound\ EC_{50}\ in\ LasR}{Compound\ EC_{50}\ in\ QscR} * A^{-1}\right)}$$

$$\boldsymbol{A = \frac{OdDHL\ EC_{50}\ in\ LasR}{OdDHL\ EC_{50}\ in\ QscR}}$$

Key to this metric is A, which is a normalization constant that reflects the increased potency of OdDHL (**1**) in LasR vs. QscR. Taking a logarithm of the product of A and the ratio of a compound's $EC_{50}$ in LasR and QscR returns a value indicating which receptor has a larger increase or decrease in $EC_{50}$ for that compound relative to OdDHL. Accordingly, positive relative selectivity numbers reflect compounds that are said to be QscR selective, and negative relative selectivity numbers are LasR selective.

We believe this metric may be useful in identifying molecular features that are "preferred" by one receptor over the other. For example, in this work compounds **6**–**8** had comparable $EC_{50}$

values in both receptors but lost an order of magnitude *more* potency in LasR than QscR. That loss is reflected by their relative selectivity value of ~1.

**References for materials and methods**

[1] L. Passador, K.D. Tucker, K.R. Guertin, M.P. Journet, a.S. Kende, A.S. Kende, B.H. Iglewski, Functional analysis of the Pseudomonas aeruginosa autoinducer PAI, J. Bacteriol., 178 (1996) 5995-6000.
[2] E. Murray, R. Crowley, A. Truman, S. Clarke, J. Cottam, G. Jadhav, P.O. Shea, C. Lindholm, A. Cockayne, R. Chhabra, W.C. Chan, P. Williams, E.J. Murray, R.C. Crowley, S.R. Clarke, J.A. Cottam, P. Jadhav, V.R. Steele, S. Ram, Targeting Staphylococcus aureus quorum sensing with non-peptidic small molecule inhibitors, J. Med. Chem., 57 (2014) 2813-2819.
[3] G.D.W. Geske, R.J.; Siegel, A.P.; Blackwell, H.E., Smal Molecule Inhibitors of Bacterial Quorum Sensing and Biofilm Formation, J Am Chem Soc, 127 (2005) 12762-12763.
[4] C.E. McInnis, H.E. Blackwell, Thiolactone modulators of quorum sensing revealed through library design and screening, Bioorg. Med. Chem., 19 (2011) 4820-4828.
[5] G.J. Jog, J. Igarashi, H. Suga, Stereoisomers of P. aeruginosa autoinducer analog to probe the regulator binding site, Chem Biol, 13 (2006) 123-128.
[6] C.E. McInnis, H.E. Blackwell, Design, synthesis, and biological evaluation of abiotic, non-lactone modulators of LuxR-type quorum sensing, Bioorg. Med. Chem., 19 (2011) 4812-4819.
[7] K.M. Smith, Y. Bu, H. Suga, Induction and Inhibition of Pseudomonas aeruginosa Quorum Sensing by Synthetic Autoinducer Analogs, Chemistry & Biology, 10 (2003) 81-89.
[8] O.N.J. Geske GD, Miller MM, Mattman ME, Blackwell HE, Modulation of Bacterial Quorum Sensing with Synthetic Ligands: System Evaluation of N-Acylated Homoserine Lactones in Multiple Species and New Insights into Their Mechanisms of Action, J Am Chem Soc, 129 (2007) 13613-13625.

## $^{1}$H- and $^{13}$C-NMR spectra for selected compounds (4, 7, 9 and 11)

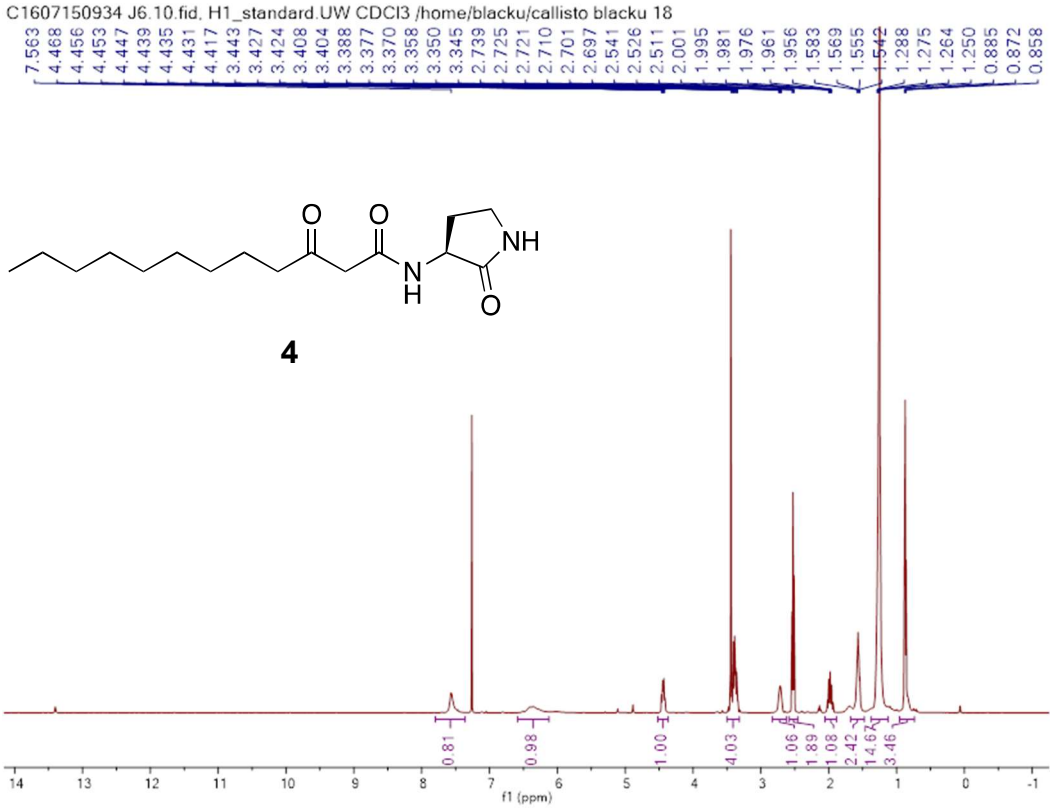


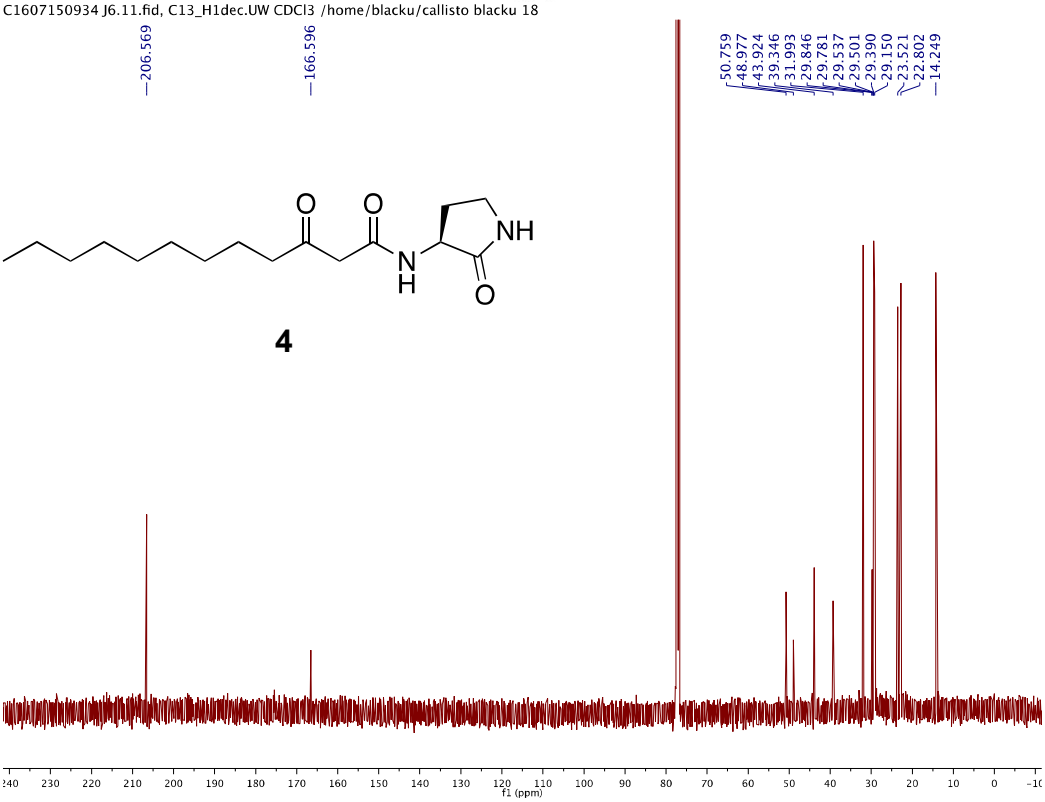

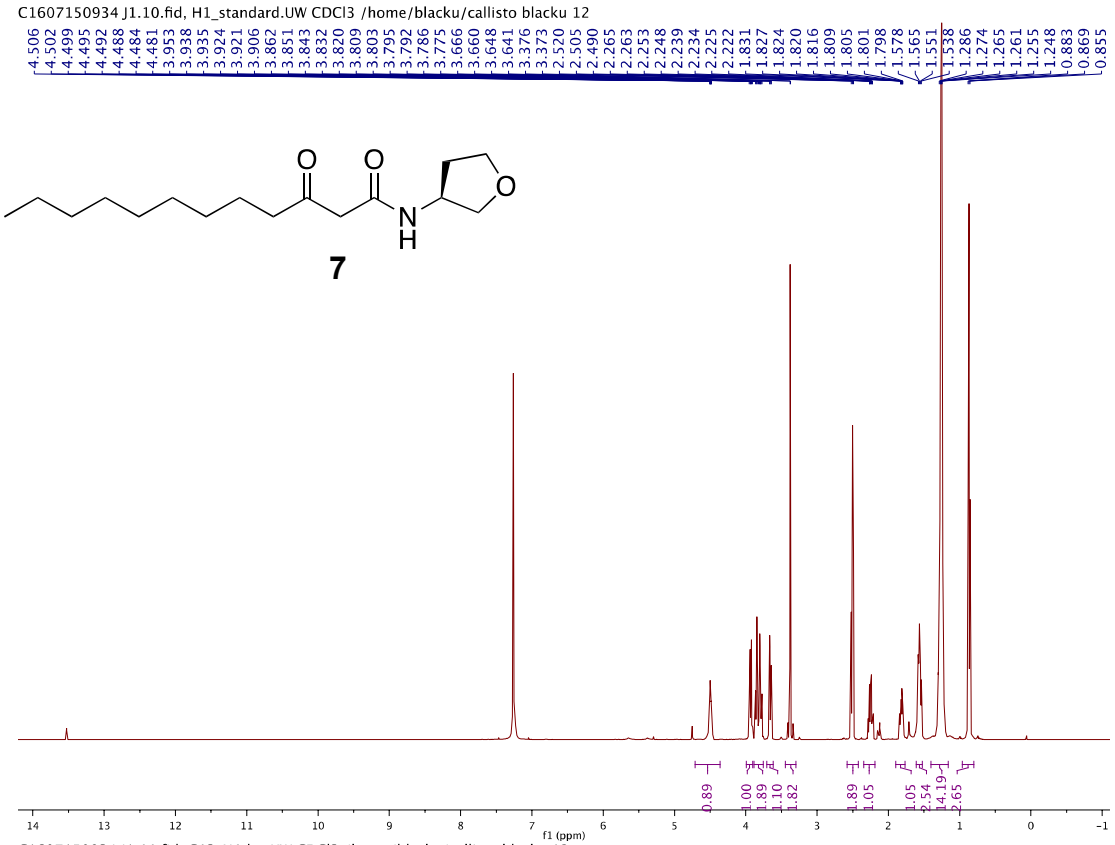
C1607150934 J1.10.fid, H1_standard.UW CDCl3 /home/blacku/callisto blacku 12
4.506
4.502
4.499
4.495
4.492
4.488
4.484
4.481
3.953
3.938
3.935
3.924
3.921
3.906
3.862
3.851
3.843
3.832
3.820
3.809
3.803
3.795
3.792
3.786
3.775
3.666
3.660
3.648
3.641
3.376
3.373
2.520
2.505
2.490
2.265
2.263
2.253
2.248
2.239
2.234
2.225
2.222
1.831
1.827
1.824
1.820
1.816
1.809
1.805
1.801
1.798
1.578
1.565
1.551
1.538
1.286
1.274
1.265
1.261
1.255
1.248
0.883
0.869
0.855
O
O
N
H
O
7
0.89
1.00
1.89
1.10
1.82
1.89
1.05
1.05
2.54
14.19
2.65
f1 (ppm)

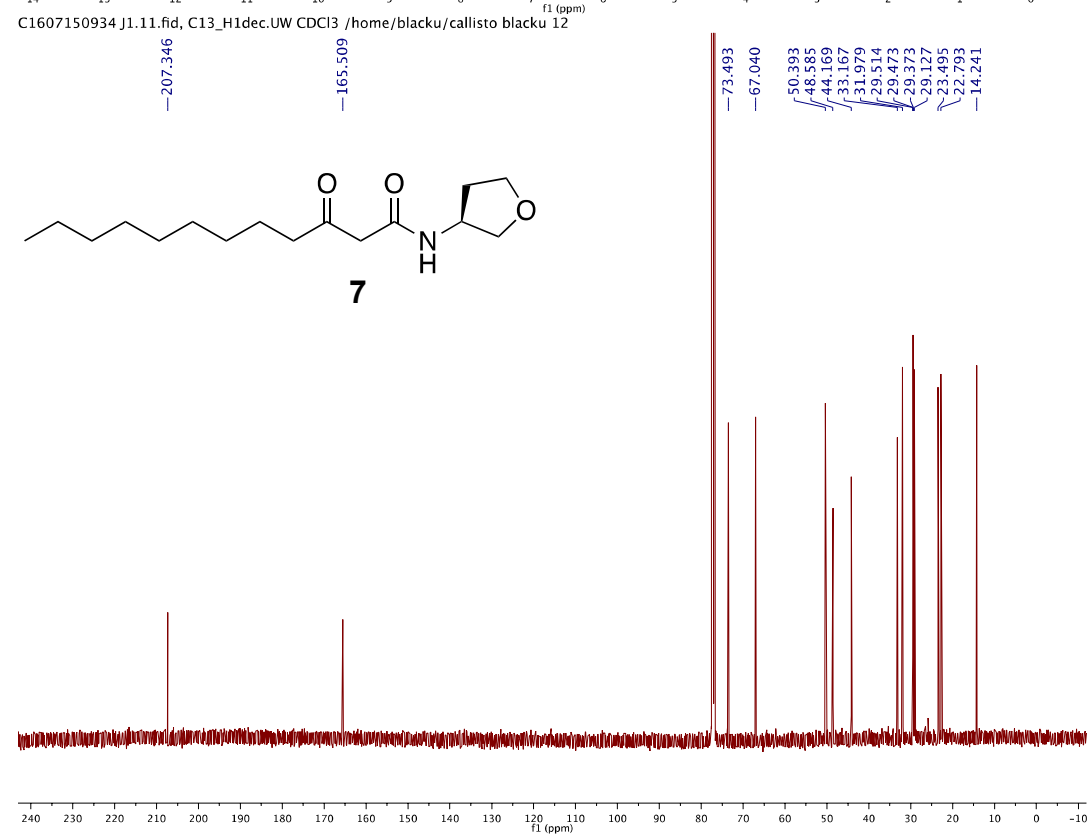
C1607150934 J1.11.fid, C13_H1dec.UW CDCl3 /home/blacku/callisto blacku 12
207.346
165.509
73.493
67.040
50.393
48.585
44.169
33.167
31.979
29.514
29.473
29.373
29.127
23.495
22.793
14.241
O
O
N
H
O
7
f1 (ppm)

C1607150934 J7.10.fid, H1_standard.UW CDCl3 /home/blacku/callisto blacku 19

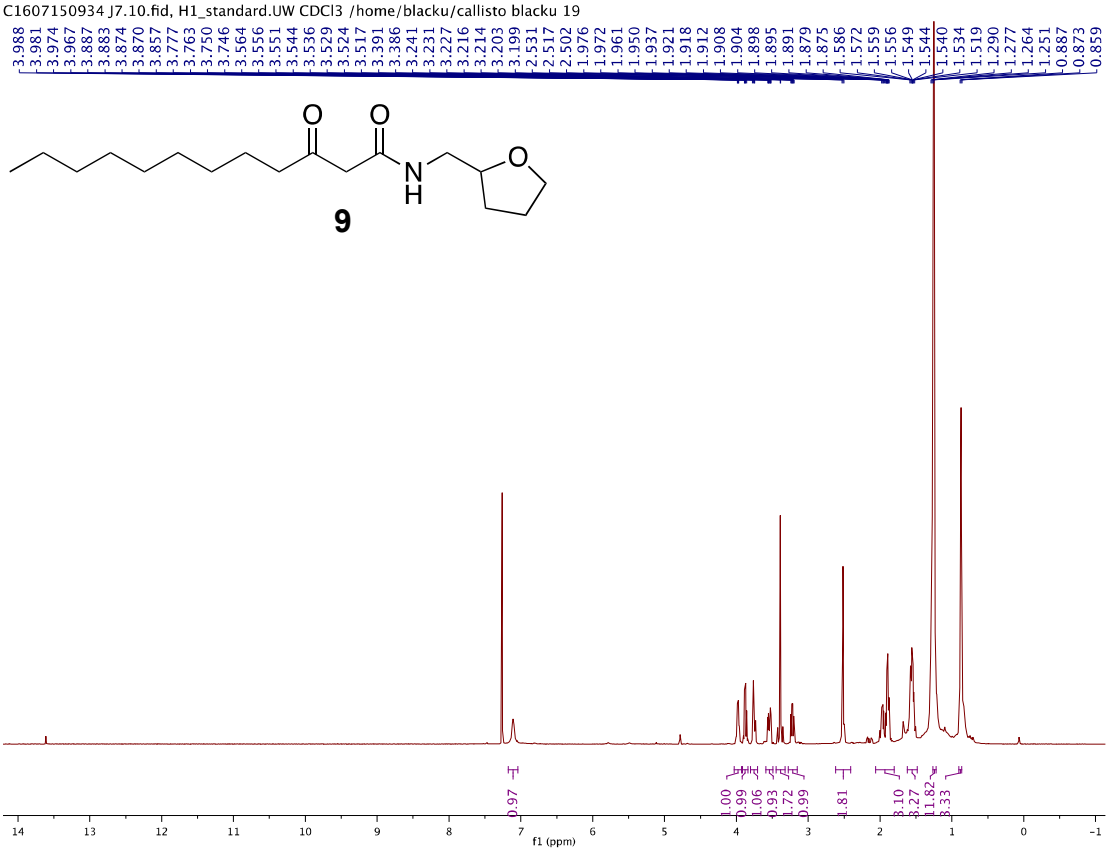


C1607150934 J7.11.fid, C13_H1dec.UW CDCl3 /home/blacku/callisto blacku 19

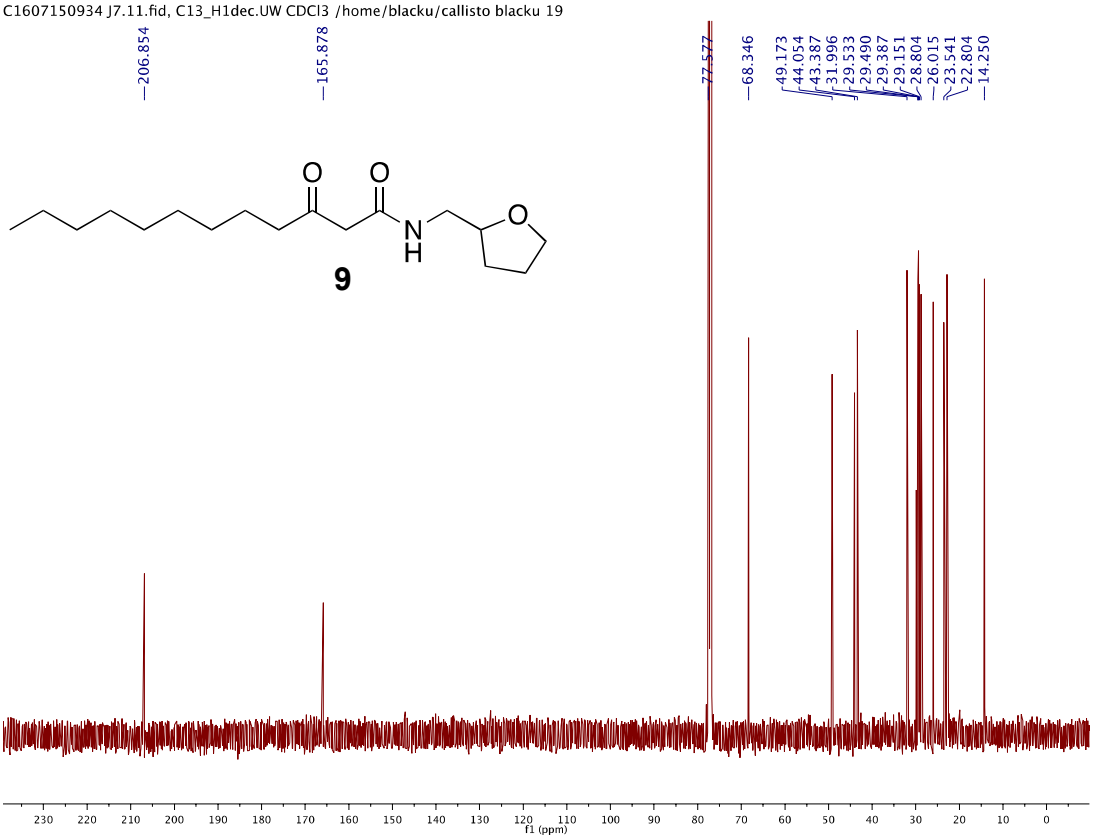

D1605171501-JBC 01-33 1.10.fid, H1_standard.UW CDCl3 /home/dzzz/av400 blacku 93

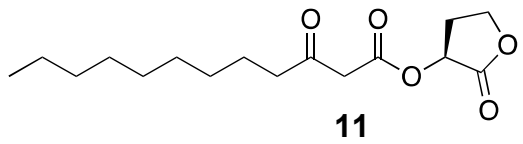

11




C1605181135.11.fid — C13_H1dec.UW CDCl3 /home/blacku/callisto blacku 47

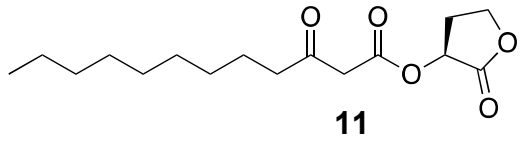

11

**References**

[1] Whiteley, M., Diggle, S.P., Greenberg, E.P., Progress in and promise of bacterial quorum sensing research, Nature, 551 (2017) 313-320.
[2] Rutherford, S.T., Bassler, B.L., Bacterial quorum sensing: its role in virulence and possibilities for its control, Cold Spring Harb. Perspect. Med., 2 (2012) a012427.
[3] Fuqua, C., Greenberg, E.P., Listening in on bacteria: acyl-homoserine lactone signalling, Nat. Rev. Mol. Cell. Biol., 3 (2002) 685-695.
[4] Kerr, K.G., Snelling, A.M., Pseudomonas aeruginosa: a formidable and ever-present adversary, J. Hosp. Infect., 73 (2009) 338-344.
[5] Schuster, M., Greenberg, E.P., LuxR-type proteins in Pseuodomonas aeruginosa quorum sensing: distinct mechanisms with global implications, in: S.C. Winans, B.L. Bassler (Eds.) Chemical communication among bacteria, ASM Press, Washington, DC, 2008, pp. 133-144.
[6] Welsh, M.A., Blackwell, H.E., Chemical probes of quorum sensing: from compound development to biological discovery, FEMS Microbiol. Rev., 40 (2016) 774-794.
[7] Sintim, H.O., Smith, J.A., Wang, J., Nakayama, S., Yan, L., Paradigm shift in discovering next-generation anti-infective agents: targeting quorum sensing, c-di-GMP signaling and biofilm formation in bacteria with small molecules, Future Med. Chem., 2 (2010) 1005-1035.
[8] Galloway, W.R.J.D., Hodgkinson, J.T., Bowden, S.D., Welch, M., Spring, D.R., Quorum sensing in gram-negative bacteria: small molecule modulation of AHL and Al-2 quorum sensing pathways, Chem. Rev., 111 (2011) 28-67.
[9] Galloway, W.R.J.D., Hodgkinson, J.T., Bovvden, S., Welch, M., Spring, D.R., Applications of small molecule activators and inhibitors of quorum sensing in gram-negative bacteria, Trends Microbiol., 20 (2012) 449-458.
[10] Amara, N., Krom, B.P., Kaufmann, G.F., Meijler, M.M., Macromolecular inhibition of quorum sensing: enzymes, antibodies, and beyond, Chem. Rev., 111 (2011) 195-208.
[11] Welsh, M.A., Blackwell, H.E., Chemical genetics reveals environment-specific roles for quorum sensing circuits in Pseudomonas aeruginosa, Cell Chem. Biol., 23 (2016) 361-369.
[12] Schuster, M., Greenberg, E.P., A network of networks: quorum-sensing gene regulation in Pseudomonas aeruginosa, Int. J. Med. Microbiol, 296 (2006) 73-81.
[13] Ledgham, F., Ventre, I., Soscia, C. Foglin, M. Sturgis, J.N. Lazdunski, A., Interactions of the quorum sensing regulator QscR: interaction with itself and the other regulators of Pseudomonas aeruginosa LasR and RhlR, Mol. Microbiol., 48 (2003) 199-210.
[14] Lequette, Y., Lee, J.H., Ledgham, F., Lazdunski, A., Greenberg, E.P., A distinct QscR regulon in the Pseudomonas aeruginosa quorum-sensing circuit, J. Bacteriol., 188 (2006) 3365-3370.
[15] Schuster, M., Lostroh, C.P., Ogi, T., Greenberg, E.P., Identification, timing, and signal specificity of Pseudomonas aeruginosa quorum-controlled genes: a transcriptome analysis, J. Bacteriol., 185 (2003) 2066-2079.
[16] Wagner, V.E., Bushnell, D., Passador, L., Brooks, A.I., Iglewski, B.H., Microarray analysis of pseudomonas aeruginosa quorum-sensing regulons: effects of growth phase and environment, J. Bacteriol., 185 (2003) 2080-2095.
[17] Gambello, M.J., Kaye, S., Iglewski, B.H., LasR of Pseudomonas aeruginosa is a transcriptional activator of the alkaline protease gene (*apr*) and an enhancer of exotoxin A expression, Infect. Immun., 61 (1993) 1180-1184.

[18] Brint, J.M., Ohman, D.E., Synthesis of multiple exoproducts in *Pseudomonas aeruginosa* is under the control of RhlR-RhlI, another set of regulators in strain PAO1 with homology to the autoinducer-responsive LuxR-LuxI family, J. Bacteriol., 177 (1995) 7155-7163.
[19] Mattmann, M.E., Blackwell, H.E., Small molecules that modulate quorum sensing and control virulence in Pseudomonas aeruginosa, J. Org. Chem, 75 (2010) 6737-6746.
[20] Geske G.D., O'Neill, J.C., Miller, D.M., Mattman M.E., Blackwell, H.E., Modulation of bacterial quorum sensing with synthetic ligands: system evaluation of N-acylated homoserine lactones in multiple species and new insights into their mechanisms of action, J. Am. Chem. Soc., 129 (2007) 13613-13625.
[21] Mattmann, M.E., Shipway, P.M., Heth, N.J., Blackwell, H.E., Potent and selective synthetic modulators of a quorum sensing repressor in Pseudomonas aeruginosa identified from second-generation libraries of N-acylated L-homoserine lactones, Chembiochem, 12 (2011) 942-949.
[22] Eibergen, N.R., Moore, J.D., Mattmann, M.E., Blackwell, H.E., Potent and selective modulation of the RhlR quorum sensing receptor by using non-native ligands: an emerging target for virulence control in Pseudomonas aeruginosa, Chembiochem, 16 (2015) 2348-2356.
[23] Amara, N., Mashiach, R., Amar, D., Krief, P., Spieser, S.A.H., Bottomley, M.J., Aharoni, A., Meijler, M.M., Covalent Inhibition of Bacterial Quorum Sensing, J. Am. Chem. Soc., 131 (2009) 10610-10619.
[24] Smith, K.M., Bu, Y.G., Suga, H., Induction and inhibition of Pseudomonas aeruginosa quorum sensing by synthetic autoinducer analogs, Chem. Biol., 10 (2003) 81-89.
[25] Hodgkinson, J.T., Galloway, W., Wright, M., Mati, I.K., Nicholson, R.L., Welch, M., Spring, D.R., Design, synthesis and biological evaluation of non-natural modulators of quorum sensing in Pseudomonas aeruginosa, Org. Biomol. Chem., 10 (2012) 6032-6044.
[26] O'Loughlin, C.T., Miller, L.C., Siryaporn, A., Drescher, K., Semmelhack, M.F., Bassler, B.L., A quorum-sensing inhibitor blocks Pseudomonas aeruginosa virulence and biofilm formation, Proc. Natl. Acad. Sci. U. S. A., 110 (2013) 17981-17986.
[27] Muh, U., Hare, B.J., Duerkop, B.A., Schuster, M., Hanzelka, B.L., Heim, R., Olson, E.R., Greenberg, E.P., A structurally unrelated mimic of a Pseudomonas aeruginosa acyl-homoserine lactone quorum-sensing signal, Proc. Natl. Acad. Sci. U. S. A., 103 (2006) 16948-16952.
[28] Muh, U., Schuster, M., Heim, R., Singh, A., Olson, E.R., Greenberg, E.P., Novel Pseudomonas aeruginosa quorum-sensing inhibitors identified in an ultra-high-throughput screen, Antimicrob. Agents Chemother., 50 (2006) 3674-3679.
[29] Muimhneachain, E.O., Reen, F.J., O'Gara, F., McGlacken, G.P., Analogues of Pseudomonas aeruginosa signalling molecules to tackle infections, Org. Biomol. Chem, 16 (2018) 169-179.
[30] Welsh, M.A., Eibergen, N.R., Moore, J.D., Blackwell, H.E., Welsh, M., Eibergen, N.R., Moore, J.D., Blackwell, H.E., Small molecule disruption of quorum sensing cross- regulation in Pseudomonas aeruginosa causes major and unexpected alterations to virulence phenotypes, J. Am. Chem. Soc., 137 (2015) 1510-1519.
[31] Weng, L.X., Yang, Y.X., Zhang, Y.Q., Wang, L.H., A new synthetic ligand that activates QscR and blocks antibiotic-tolerant biofilm formation in Pseudomonas aeruginosa, Appl. Microbiol. Biotechnol., 98 (2014) 2565-2572.
[32] Chugani, S.A., Whiteley, M., Lee, K.M., D'Argenio, D., Manoil, C., Greenberg, E.P., QscR, a modulator of quorum-sensing signal synthesis and virulence in Pseudomonas aeruginosa, Proc. Natl. Acad. Sci. U. S. A., 98 (2001) 2752-2757.

[33] Lintz, M.J., Oinuma, K., Wysoczynski, C.L., Greenberg, E.P., Churchill, M.E., Crystal structure of QscR, a Pseudomonas aeruginosa quorum sensing signal receptor, Proc. Natl. Acad. Sci. U. S. A., 108 (2011) 15763-15768.
[34] Bottomley, M.J., Muraglia, E., Bazzo, R., Carfi, A., Molecular insights into quorum sensing in the human pathogen Pseudomonas aeruginosa from the structure of the virulence regulator LasR bound to its autoinducer, J Biol Chem, 282 (2007) 13592-13600.
[35] Zhang, R.G., Pappas, K.M., Brace, J.L., Miller, P.C., Oulmassov, T., Molyneaux, J.M., Anderson, J.C., Bashkin, J.K., Winans, S.C., Joachimiak, A., Structure of a bacterial quorum-sensing transcription factor complexed with pheromone and DNA, Nature, 417 (2002) 971-974.
[36] Reche, P., Sequence Identity and Similarity Tool, Secretaria General De Ciencia, Tecnologia E Innovacion of Spain. Available online at http://imed.med.ucm.es/Tools/sias.html, (2017).
[37] Oinuma, K., Greenberg, E.P., Acyl-homoserine lactone binding to and stability of the orphan Pseudomonas aeruginosa quorum-sensing signal receptor QscR, J. Bacteriol., 193 (2011) 421-428.
[38] Lee, J.H., Lequette, Y., Greenberg, E.P., Activity of purified QscR, a Pseudomonas aeruginosa orphan quorum-sensing transcription factor, Mol. Microbiol., 59 (2006) 602-609.
[39] O'Reilly, M.C., Blackwell, H.E., Structure-Based Design and Biological Evaluation of Triphenyl Scaffold-Based Hybrid Compounds as Hydrolytically Stable Modulators of a LuxR-Type Quorum Sensing Receptor, ACS Infect. Dis., 2 (2016) 32-38.
[40] Moore, J.D., Rossi, F.M., Welsh, M.A., Nyffeler, K.E., Blackwell, H.E., A comparative analysis of synthetic quorum sensing modulators in Pseudomonas aeruginosa: new insights into mechanism, active efflux susceptibility, phenotypic response, and next-generation ligand design, J. Am. Chem. Soc., 137 (2015) 14626-14639.
[41] Vannini, A.V., Volpari, C., Gargioli, C., Muraglia, E., Cortese, R., Francesco, R.D., Neddermann, P., Marco, S.D., The crystal structure of the quorum sensing protein TraR bound to its autoinducer and target DNA, EMBO Journal, 21 (2002) 4393-4401.
[42] Glansdorp, F.G., Thomas, G.L., Lee, J.K., Dutton, J.M., Salmond, G.P., Welch, M., Spring, D.R., Synthesis and stability of small molecule probes for Pseudomonas aeruginosa quorum sensing modulation, Org. Biomol. Chem, 2 (2004) 3329-3336.
[43] Passador, L., Tucker, K.D., Guertin, K.R., Journet, M.P., Kende, A.S., Iglewski, B.H., Functional analysis of the Pseudomonas aeruginosa autoinducer PAI, J. Bacteriol., 178 (1996) 5995-6000.
[44] McInnis, C.E., Blackwell, H.E., Thiolactone modulators of quorum sensing revealed through library design and screening., Bioorg. Med. Chem., 19 (2011) 4820-4828.
[45] McInnis, C.E., Blackwell, H.E., Design, synthesis, and biological evaluation of abiotic, non-lactone modulators of LuxR-type quorum sensing, Bioorg. Med. Chem., 19 (2011) 4812-4819.
[46] Geske, G.D., O'Neill, J.C., Miller, D.M., Wezeman, R.J., Mattmann, M.E., Lin, Q., Blackwell, H.E., Comparative analyses of N-acylated homoserine lactones reveal unique structural features that dictate their ability to activate or inhibit quorum sensing, ChemBioChem, 9 (2008) 389-400.
[47] Mattmann, M.E., Geske, G.D., Worzalla, G.A., Chandler, J.R., Sappington, K.J., Greenberg, E.P., Blackwell, H.E., Synthetic ligands that activate and inhibit a quorum-sensing regulator in Pseudomonas aeruginosa, Bioorg. Med. Chem. Lett., 18 (2008) 3072-3075.
[48] Suga, H., Bu, Y., Combinatorial libraries of autoinducer analogs, autoinducer agonists and antagonists, and methods of use thereof (2004) WO 2004016213.

[49] Horikawa, M., Tateda, K., Tuzuki, E., Ishii, Y., Ueda, C., Takabatake, T., Miyairi, S., Yamaguchi, K., Ishiguro, M., Synthesis of Pseudomonas quorum-sensing autoinducer analogs and structural entities required for induction of apoptosis in macrophages, Bioorg. Med. Chem. Lett., 16 (2006) 2130-2133.
[50] Castang, S., Chantegrel, B., Deshayes, C., Dolmazon, R., Gouet, P., Haser, R., Reverchon, S., Nasser, W., Hugouvieux-Cotte-Pattat, N., Doutheau, A., N-Sulfonyl homoserine lactones as antagonists of bacterial quorum sensing., Bioorg. Med. Chem. Lett., 14 (2004) 5145-5149.
[51] Jog, G.J., Igarashi, J., Suga, H., Stereoisomers of P. aeruginosa autoinducer analog to probe the regulator binding site, Chem. Biol., 13 (2006) 123-128.
[52] Hodgkinson, J.T., Galloway, W.R.J.D., Casoli, M., Keane, H., Su, X., Salmond, G.P.C., Welch, M., Spring, D.R., Robust routes for the synthesis of N-acylated-l-homoserine lactone (AHL) quorum sensing molecules with high levels of enantiomeric purity, Tetrahedron Lett., 52 (2011) 3291-3294.
[53] Lindsay, A., Ahmer, B.M., Effect of sdiA on biosensors of N-acylhomoserine lactones, J. Bacteriol., 187 (2005) 5054-5058.
[54] Gerdt, Joseph P., McInnis, Christine E., Schell, Trevor L., Rossi, Francis M., Blackwell, Helen E., Mutational Analysis of the Quorum-Sensing Receptor LasR Reveals Interactions that Govern Activation and Inhibition by Nonlactone Ligands, Chem. Biol., 21 (2014) 1361-1369.
[55] Cordero, B., Gómez, V., Platero-Prats, A.E., Revés, M., Echeverría, J., Cremades, E., Barragán, F., Alvarez, S., Covalent radii revisited, Dalton Trans., (2008) 2832-2838.
[56] Chen, G., Swem, L.R., Swem, D.L., Stauff, D.L., O'Loughlin, C.T., Jeffrey, P.D., Bassler, B.L., Hughson, F.M., A strategy for antagonizing quorum sensing, Mol. Cell., 42 (2011) 199-209.
[57] Skowronek, P., Gawronski, J., Absolute configuration of α-phthalimido carboxylic acid derivatives from circular dichroism spectra, Tetrahedron: Asymmetry, 10 (1999) 4585-4590.

# Chapter 7: Future extensions of work described in this PhD thesis

Daniel E. Manson and Helen E. Blackwell

D.E. Manson and H.E. Blackwell wrote the chapter.

## Abstract

In this thesis, I have described the design and discovery of a variety of non-native small molecules that modulate the activity of LuxR-type receptors in bacteria. Here, I describe a series of experiments that could leverage the discoveries I made as a member of the Blackwell lab for the further development of non-native probes of Gram-negative quorum sensing (QS).

**Further experiments with the V-06-018 scaffold**

In Chapter 2, I described a preliminary exploration of SAR of the V-06-018 scaffold for LasR antagonism. This effort led to the development of LasR antagonists with improved potency relative to V-06-018 (~11x improvement). That study, however, was not an exhaustive investigation of the SAR surrounding V-06-018; fewer than 40 compounds were synthesized and screened. Here, I propose additional analogues to synthesize and an abbreviated synthetic route to attempt to prepare such compounds.

The synthesis of V-06-018 described in Chapter 2 is a four or five step synthetic route, depending if a substituted β-keto ester must be prepared.[1] That synthesis represents nothing more than a functional group interconversion (FGI) from a β-keto ester to a β-keto amide. However, the requisite β-keto ester contains a benzylic ketone that is more reactive than the ester,.For this FGI to work, the ketone must be protected and the ester saponified.

Here, I propose an alternate synthetic route using substituted benzoic acids rather than acetophenones as starting material (Scheme 7.1). This route involves carbodiimide-facilitated carbon-carbon bond formation with Meldrum's acid and subsequent trapping of the thermally-generated ketene by nonylamine (or any other amine of choice). The chief advantage to this route is the reduction in step count. The chief difficulty I envision is a potential side reaction between the benzylic ketone and the amine in step two. I am hopeful that with optimization, this synthetic route can provide quicker access to V-06-018 and its analogues.

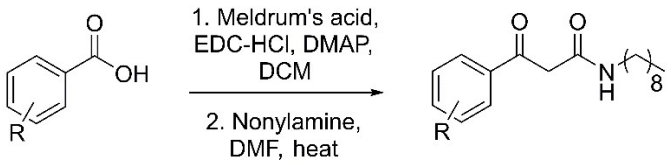


**Scheme 7.1** Proposed abbreviated synthesis of V-06-018 and analogues.

The structure-active relationships (SAR) for V-06-018 uncovered in Chapter 2 indicate that adding steric bulk to the headgroup is unfavorable for LasR antagonism, and that the incorporation of heterocyclic aromatic headgroups could be advantageous. During my second year, I unsuccessfully attempted to synthesize analogues with pyrrole and pyridine headgroups (see chemistry in DM notebook 2, **Figure 7.1**). I was able to synthesize β-keto esters with the appropriate headgroups, but they converted to an unanticipated side product under my ketal installation conditions. I advise an alternative protecting group strategy (i.e., reduction of the ketone, and protecting the resulting alcohol with a silicon protecting group, along with capping of the pyrrole nitrogen), or possibly attempting the chemistry proposed above. Finally, results from my high throughput screen in Chapter 3 indicate that rigidification of the "tail group" by incorporation of an internal alkyne may be advantageous. I am confident that the requisite alkynyl amines can be purchased or readily synthesized.

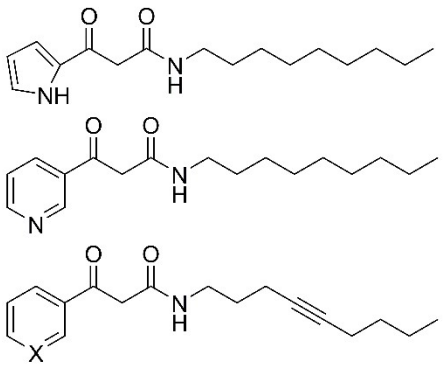


**Figure 7.1** Proposed analogues of V-06-018 to synthesize and evaluate for bioactivity.

Another set of experiments I undertook with the V-06-018 scaffold was the synthesis and screening of analogs with isothiocyanate (ITC) functional groups installed at the end of their acyl tail. These electrophilic handles were intended to react with residue Cys79 in LasR, located at

the end of the AHL binding pocket.[2] One key parameter is the length of the alkyl linker that joining the amide to the ITC group. In my synthesis, this is determined by the number of carbons in the amino alcohol starting material. The six carbon amino alcohol was commercially available; however, linkers of other length should be readily accessible. [3]

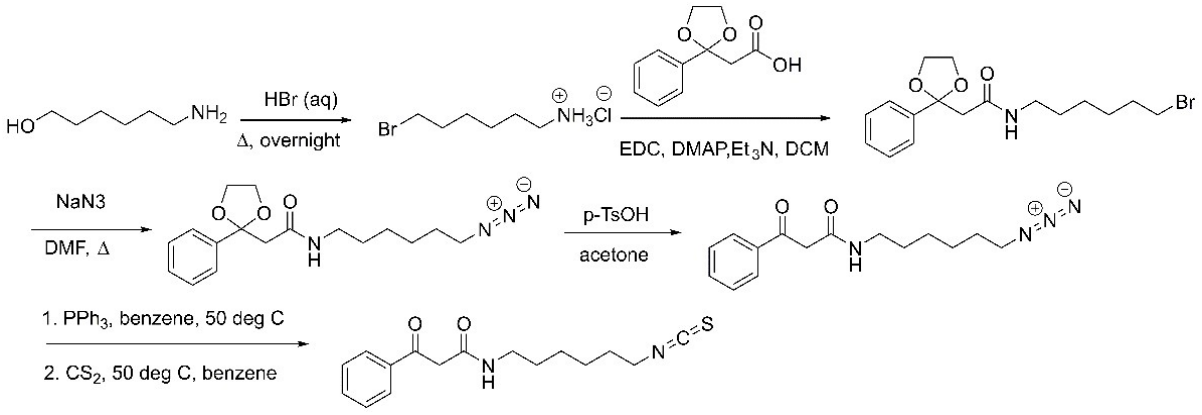


**Scheme 7.2**. Synthesis of isothiocyanate-functionalized V-06-018 analogue. Isothiocyanation conditions are from the Meijler group.[2] Product was obtained in 22% overall yield.

I synthesized the six carbon ITC V-06-018 in a convergent fashion, using the protected carboxylic acid that I had on hand (**Figure 7.2**). In-cell screening of this compound yielded mixed results. In the *E. coli* experiment, the ITC analogue had markedly improved efficacy as a LasR antagonist, while in the *P. aeruginosa* experiment the ITC analogue lost potency relative to its unsubstituted "parent" compound.

LasR antagonists typically display reduced potency and efficacy in the *E. coli* screening system relative to the *P. aeruginosa* system, a phenomenon ascribed to the increased protein levels in the heterologous host (as described in Chapter 2).[4] Here, covalently linking the antagonist to LasR (assuming, for the sake of argument, that the ITC handle works as intended and LasR is covalently modified) led to an improvement in efficacy, but no change in potency in *E. coli*. Covalently binding V-06-018 to LasR prevents the dissociation of V-06-018 from LasR,

but does not increase the affinity with which V-06-018 displaces OdDHL from the binding site; evidently, this results in an improvement in efficacy rather than potency. The source of the unfortunate loss of activity in the *P. aeruginosa* system is unclear; however, I hope that ITC-bearing V-06-018 analogues can be of use in *in vitro* studies of LasR antagonism. I note that the poor result in *P. aeruginosa* is only one experiment – I advise any interested lab members to make another DMSO stock and try again.

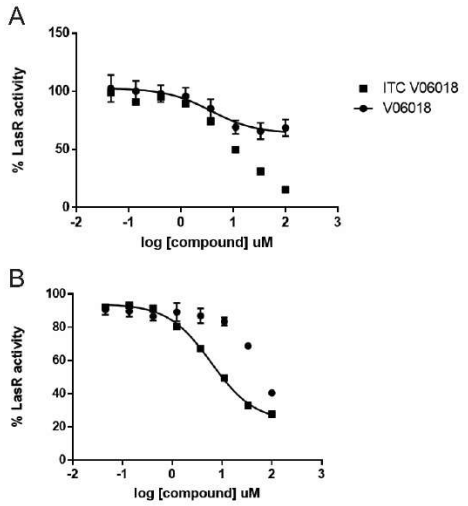


**Figure 7.2** In-cell screening experiments with V-06-018 and its ITC analogue. **(A)** In E. coli strain JLD271, the ITC analogue displayed greater efficacy than V-06-018. (**B**) ITC-V-06-018 lost potency relative to V-06-018 in the *P. aeruginosa* strain PAO-JP2.

Lastly, I attempted to isolate LasR in complex with the lead compounds from my study of V-06-018 SARs. Using a protocol from the Greenberg lab,[5] I was able to isolate LasR in complex with thiophene V-06-018 analogue V42 (DM 4-25, **Figure 7.3**). The successful isolation of LasR in complex with this compound implies that in vitro experiments (i.e., electrophoretic mobility shift assays) and structural studies via NMR or X-ray crystallography should be possible with this ligand.

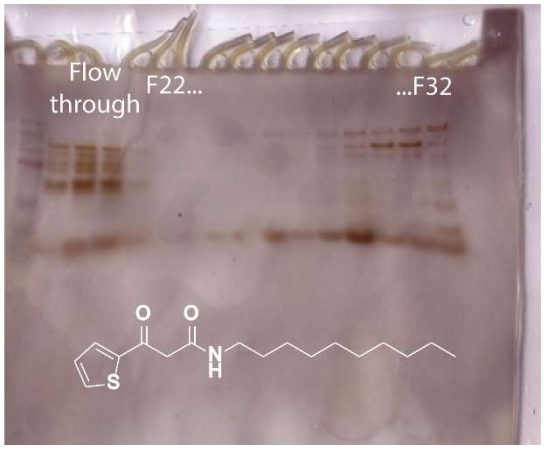


**Figure 7.3** SDS-PAGE gel with fractions from the purification of LasR with thiophene ligand V42 after purification via the method of Schuster et al.[5] Pure LasR was obtained in fractions 22 – 26 of the heparin column, and is the dominant component of fractions 27 and 28.

In summary, I strongly suspect further synthetic chemistry work applied to the V-06-018 scaffold may yield LasR antagonists with improved potency. Additionally, LasR is soluble in complex with highly potent ($IC_{50}$ = 0.2 μM) thiophene-substituted, V-06-018-based non-classical partial agonists, indicating that these ligands may be useful in *in vitro* studies to explore the mechanism of non-classical partial agonism.

## Exploration of SAR for LasR antagonism of compounds discovered in high throughput screening

Chapter 3 of this thesis describes the discovery of eight non-native antagonists of LasR via the screening of a 25,000-compound library. These compounds have structures that are highly amenable to diversification via chemical synthesis. Here, I indicate prospective synthetic routes to each of these compounds to facilitate future SAR studies (**Scheme 2).**

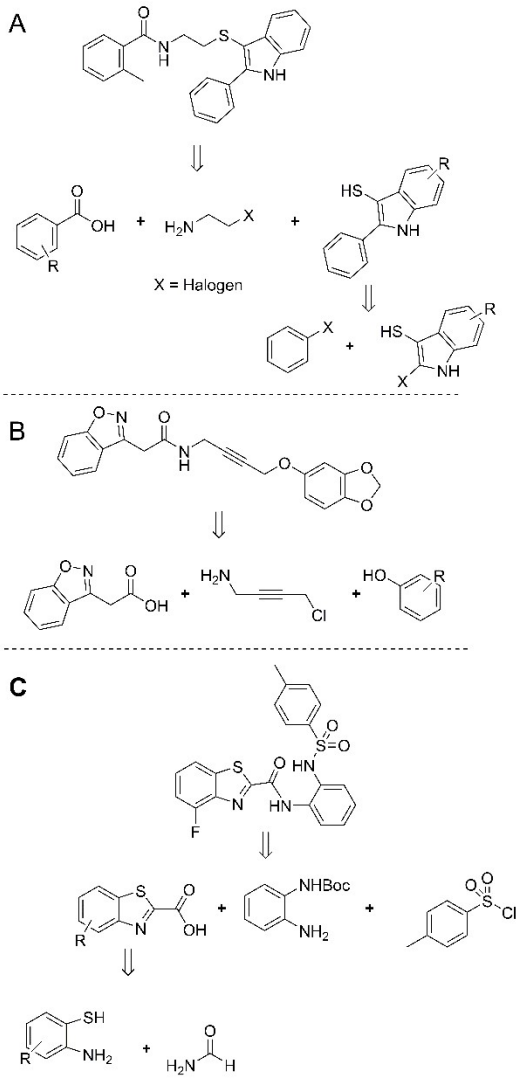


**Scheme 7.3** Retrosynthetic analysis of the three LasR antagonist classes (**A-C**) discovered in Chapter 3. The indicated starting materials are commercially available, and the appropriate forward transformations are precedented.

Select compounds from the general classes shown above had sub-micromolar $IC_{50}$ values in the *P. aeruginosa* LasR gene reporter experiment (see Chapter 3). Synthesizing and screening libraries of analog libraries would clarify the structural features necessary for antagonism and could result in the discovery of new and highly potent LasR antagonists.

**Application of the C7 HSL to probe the role of QS in coinfection by *P. aeruginosa* and *B. cepacia***

In Chapter five, we demonstrated that the C7 HSL is a LasR and RhlR partial agonist, QscR agonist, and CepR agonist. Therefore, this compound should theoretically repress QS in *P. aeruginosa* and activate it in *B. cepacia*. Our lab has developed a *C. elegans* based assay that can be used to measure the severity of infection via worm death, and can quantify the ability of probe molecules to rescue worms from infection.[6] Applying the C7 HSL to a mixed culture of *P. aeruginosa* and *B. cepacia* in the worm assay (and, separately, to mono-culture infections) would demonstrate if perturbing QS in both organisms changes the outcome of a coinfection.

**Synthesis of chemical inducers of dimerization of LuxR type receptors**

Although not described in this thesis, I conducted experiments attempting to synthesize a chemical inducer of dimerization (CID) of LasR. CIDs, popularized by the Schreiber lab and others in the 1990s, [8] are tool compounds that can enforce interactions between proteins that do *not* occur in Nature.[7, 8] If successful, this would be the first chemical inducer of dimerization for LuxR-type proteins, and could be a useful tool to explore mechanistic hypotheses about QS. Asymmetrical (i.e., different "head group" on each end) CIDs also could be useful in promoting the formation of heterodimeric LuxR dimers.

I synthesized a dimeric AHL with an approximately 50 nm polyethylene glycol (PEG) spacer between two homoserine lactone headgroups (**Scheme 7.4**). Purification, however, was challenging. I quenched the reaction by diluting it with water and injecting directly onto a semi-preparative HPLC column (**Figure 7.4a**).

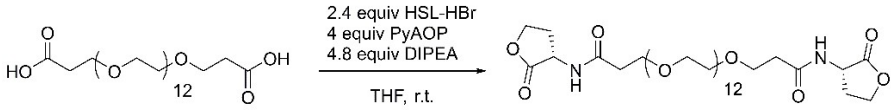


**Scheme 7.4** Synthesis of dimeric AHL with 12 PEG unit spacer.

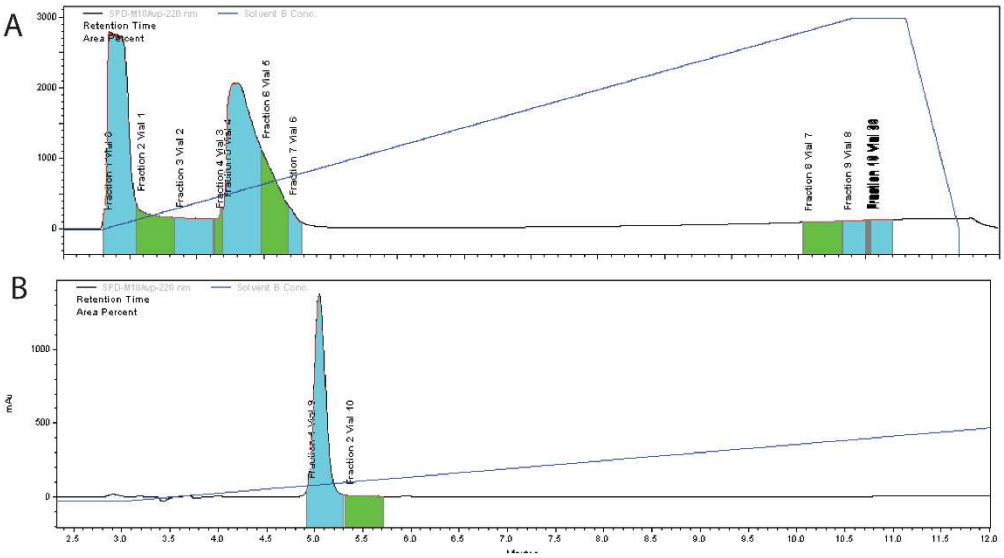


**Figure 7.4** HPLC purification of dimeric AHL. (**A**) Semi-preparative separation of crude reaction mixture. (**B**). Analytical trace of fraction 0 from the semi-preparative run.

Separating fraction 0, which contained most of the mass, on an analytical column yielded a single peak. I identified the presence of my product in that peak by MALDI. However, $^{1}$H NMR analysis of the material indicated that the sample was a mixture with an aromatic compound, almost certainly 1-hydroxy-7-azabenzotriazole from the decomposed pyAOP used for the amide coupling. In conclusion, dimeric AHLs can be synthesized by the conditions shown above; however, further optimization is necessary for the reaction workup and purification conditions.

**References.**

1. Manson, D. E.; O'Reilly, M. C.; Nyffeler, K. E.; Blackwell, H. E., Design, synthesis, and biochemical characterization of non-native antagonists of the Pseudomonas aeruginosa quorum sensing receptor LasR with nanomolar IC50 values. *ACS Infect Dis* **2020**.
2. Amara, N. M., R.; Amar, D.; Krief, P.; Spieser, S.A.H.; Bottomley, M.J.; Aharoni, A.; and Meijler, M.M., Covalent Inhibition of Bacterial Quorum Sensing. *J Am Chem Soc* **2009**.
3. Sawatzky, E.; Al-Momani, E.; Kobayashi, R.; Higuchi, T.; Samnick, S.; Decker, M., A Novel Way To Radiolabel Human Butyrylcholinesterase for Positron Emission Tomography through Irreversible Transfer of the Radiolabeled Moiety. *ChemMedChem* **2016,** *11* (14), 1540-50.
4. Wellington, S. G., E.P., Quorum Sensing signal selectivity and the potential for interspecies cross talk. *mBio* **2019,** *10* (2), e00146-19.
5. Schuster, M.; Urbanowski, M. L.; Greenberg, E. P., Promoter specificity in Pseudomonas aeruginosa quorum sensing revealed by DNA binding of purified LasR. *Proc Natl Acad Sci U S A* **2004,** *101* (45), 15833-9.
6. Slinger, B. L.; Deay, J. J.; Chandler, J. R.; Blackwell, H. E., Potent modulation of the CepR quorum sensing receptor and virulence in a Burkholderia cepacia complex member using non-native lactone ligands. *Sci Rep* **2019,** *9* (1), 13449.
7. Aonbangkhen, C.; Zhang, H.; Wu, D. Z.; Lampson, M. A.; Chenoweth, D. M., Reversible Control of Protein Localization in Living Cells using a Photocaged-Photocleavable Chemical Dimerizer. *Journal of the American Chemical Society* **2018**.
8. Diver, S. T. S., S.L., Single-Step Synthesis of Cell-Permeable Protein Dimerizers That Activate Signal Transduction and Gene Expression. *J. Am. Chem. Soc.* **1997,** *119*, 5106-5109.

# APPENDIX ONE: Liquid crystal emulsions that intercept and report on bacterial quorum sensing

**Benjamin J. Ortiz, Michelle E. Boursier, Kelsey L. Barrett, Daniel E. Manson, Daniel Amador-Noguez, Nicholas L. Abbott, Helen E. Blackwell, David M. Lynn**

Reproduced with permission from:

Ortiz, B.J., Boursier, M.E., Barrett, K.L., Manson, D.E., Amador-Noguez, D., Abbott, N.L., Blackwell, H.E., Lynn, D.M.; *ACS appl. Mater. Interfaces* **2020**, 12, 26, 29056-29065



B. J. Ortiz, and M.E. Boursier, designed and planned experiments. B.J. Ortiz characterized liquid crystal – amphiphile interactions. M.E. Boursier quantified rhamnolipids and performed bacteriology assays. M.E. Boursier and K. Barrett quantified AHL levels. D.E. Manson synthesized HAA. D. Amador-Noguez and N.L. Abbott provided experimental guidance. H.E. Blackwell and D.M. Lynn directed the project. B.J. Ortiz, M.E. Boursier, H.E. Blackwell, and D.M. Lynn directed the project.

ACS APPLIED MATERIALS & INTERFACES

www.acsami.org Research Article

# Liquid Crystal Emulsions That Intercept and Report on Bacterial Quorum Sensing

Benjamín J. Ortiz, Michelle E. Boursier, Kelsey L. Barrett, Daniel E. Manson, Daniel Amador-Noguez, Nicholas L. Abbott, Helen E. Blackwell,* and David M. Lynn*

Cite This: ACS Appl. Mater. Interfaces 2020, 12, 29056−29065 Read Online

ACCESS | Metrics & More | Article Recommendations | Supporting Information



**ABSTRACT:** We report aqueous emulsions of thermotropic liquid crystals (LCs) that can intercept and report on the presence of *N*-acyl-L-homoserine lactones (AHLs), a class of amphiphiles used by pathogenic bacteria to regulate quorum sensing (QS), monitor population densities, and initiate group activities, including biofilm formation and virulence factor production. The concentration of AHL required to promote "bipolar" to "radial" transitions in micrometer-scale droplets of the nematic LC 4′-pentyl-cyanobiphenyl (5CB) decreases with increasing carbon number in the acyl tail, reaching a threshold concentration of 7.1 μM for 3-oxo-C12-AHL, a native QS signal in the pathogen *Pseudomonas aeruginosa*. The LC droplets in these emulsions also respond to biologically relevant concentrations of the biosurfactant rhamnolipid, a virulence factor produced by communities of *P. aeruginosa* under the control of QS. Systematic studies using bacterial mutants support the conclusion that these emulsions respond selectively to the production of rhamnolipid and AHLs and not to other products produced by bacteria at lower (subquorate) population densities. Finally, these emulsions remain configurationally stable in growth media, enabling them to be deployed either in bacterial supernatants or *in situ* in bacterial cultures to eavesdrop on QS and report on changes in bacterial group behavior that can be detected in real time using polarized light. Our results provide new tools to detect and report on bacterial QS and virulence and a materials platform for the rapid and *in situ* monitoring of bacterial communication and resulting group behaviors in bacterial communities.

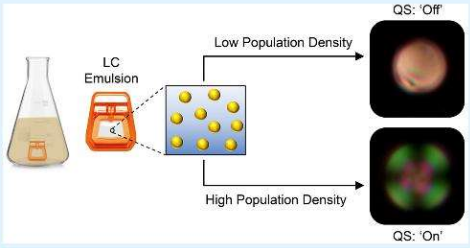


**KEYWORDS:** *liquid crystals, amphiphiles, rhamnolipid, emulsions, bacteria, sensing*

## INTRODUCTION

Many common bacteria coordinate group behaviors and adapt to changing environments using a process known as quorum sensing (QS). This cell−cell communication process is controlled by the production and dissemination of small chemical signals that are "shared" between cells in a population of bacteria.[1,2] In general, the concentration of these signals increases proportionally with the size of the bacterial population until a threshold density of cells (or a "quorum") is reached, at which point QS signal-receptor binding initiates changes in gene expression that lead to changes in group behaviors, including motility,[3] toxin production,[2] and biofilm formation.[4] Several of the most common human, animal, and plant pathogens use QS to control virulence (i.e., initiate infections)[1,2] or form biofilms that are detrimental in medical, industrial, and environmental settings (i.e., surface fouling).[4] The development of strategies that can inhibit QS, enable the monitoring of QS signals, or detect and report on outcomes of QS is, thus, a rapidly growing area of research and has the potential to have impacts in a broad range of contexts.[5−10]

The work reported here was motivated by the potential utility of approaches for the *in situ* monitoring of QS and its outcomes in pathogenic Gram-negative bacteria. Many of these bacteria use amphiphilic molecules as QS signals and produce other amphiphilic species once a quorum is reached.[3,10−12] The opportunistic pathogen *Pseudomonas aeruginosa*, for example, uses amphiphilic *N*-acyl-L-homoserine lactones (AHLs) to regulate QS and produces a class of biosurfactants called rhamnolipids as a virulence factor at high cell densities.[1,2] The L-homoserine lactone headgroup of AHLs is conserved among Gram-negative bacteria, but the aliphatic acyl chain of these signals can vary in both length and chemical structure (Figure 1).[13] *P. aeruginosa* produces two chemically distinct AHLs to regulate QS: a longer-tailed *N*-(3-oxo-

Received: March 28, 2020
Accepted: June 2, 2020
Published: June 2, 2020





https://dx.doi.org/10.1021/acsami.0c05792
ACS Appl. Mater. Interfaces 2020, 12, 29056−29065

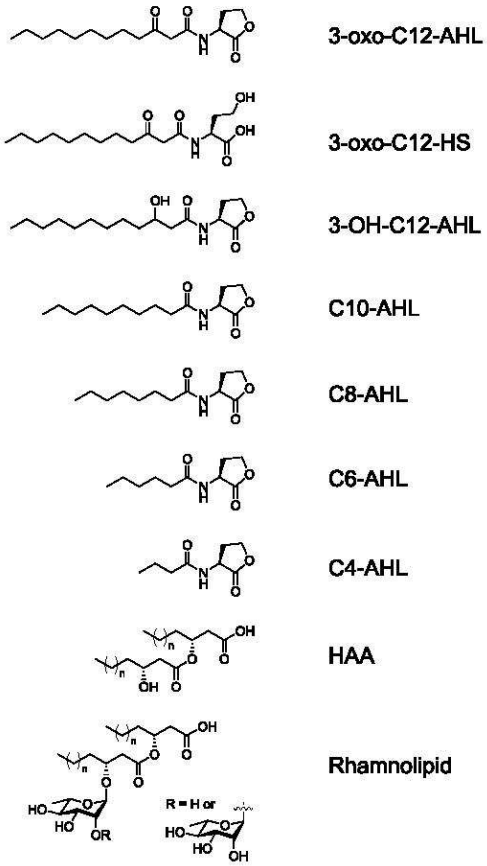


**Figure 1.** Structures of the AHLs and bacterial biosurfactants investigated in this study ($n$ = 3−11 for rhamnolipid and HAA). HAA was evaluated as a mixture of stereoisomers (see Supporting Information (SI)).

dodecanoyl)-L-homoserine lactone (3-oxo-C12-AHL) and a shorter-tailed *N*-butanoyl-L-homoserine lactone (C4-AHL; Figure 1).[14] Past studies have reported methods for the quantification or sensing of AHLs using genetically engineered bacterial biosensors or a variety of analytical methods (e.g., HPLC, MS, NMR, or electrochemical- and fluorescence-based methods).[15−22] However, these approaches often require extraction and/or purification of AHLs from bacterial media prior to analysis, and they can be difficult to apply *in situ* for real-time monitoring of QS in bacterial cultures.

Recent reports reveal that the amphiphilic nature of AHLs permits them to aggregate or self-assemble in solution and at interfaces in ways that are similar to conventional surfactants and lipids.[11,12] For example, long-chained AHLs (e.g., C10-AHL and longer homologues) have been observed to aggregate at sufficiently high concentrations to form micelles and vesicles in aqueous media.[11] In addition, AHLs have been reported to adsorb and assemble at air/water interfaces or insert into phospholipid membranes.[23−25] We reasoned that these behaviors could be leveraged to provide new bases for detecting, monitoring, and quantifying AHLs. Here, we report a conceptually straightforward, scalable, and materials-based strategy for the rapid, real-time, and *in situ* monitoring of AHLs and other amphiphilic products of QS produced by bacteria. Our approach exploits the stimuli-responsive behaviors of oil-in-water emulsions containing micrometer-scale droplets of thermotropic liquid crystals (LCs).

Past studies demonstrate that colloidal droplets of LCs suspended in water can respond to low- or high-molecular-weight amphiphiles that adsorb at the aqueous/LC interface and promote changes in the orientation of the LC that can be readily observed using polarized light.[26−33] These LC-emulsions are easy to prepare and enable the rapid and label-free detection of a range of amphiphilic species, including lipids,[26,28,30] surfactants,[27,31] peptides,[32] and proteins,[33] with sensitivities that depend on the concentration and the structure of the amphiphile. This approach can be remarkably sensitive; past work has reported the detection of lipid A, a six-tailed glycolipid component of bacterial endotoxins, at levels as low as 1 pg/mL in water.[28] Many other one- and two-tailed surfactants and lipids promote LC ordering transitions at concentrations in the range of 10−100 $\mu$g/mL.[28,29,34] In general, these LC droplets can be deployed in aqueous environments as free-floating sensors, or they can be encapsulated in polymer capsules to enhance colloidal stability in complex environments or immobilize them on surfaces.[34−37] This latter approach permits the design of plastic "test strips" that could be used as a basis for the detection of environmental agents using a simple light microscope.[35,36]

This study sought to determine whether bacterial AHLs, and products under their control, could trigger ordering transitions in LC emulsions. We report that AHLs can adsorb at aqueous/LC interfaces and trigger rapid "bipolar-to-radial" transitions in LC droplets that can be readily observed using polarized-light microscopy and, at larger scales, quantified using flow cytometry. We also found that this approach can be used to readily detect and report the presence of bacterial rhamnolipids produced by *P. aeruginosa*. These LC emulsions remain stable in bacterial culture media, permitting them to be used to detect AHLs and rhamnolipid in bacterial supernatants or be deployed *in situ* to report the presence of these products in bacterial cultures. Our results provide new tools for the interception, detection, and reporting of QS regulators and products that are unique to or diagnostic of bacterial communities and thus provide guidance for the development of new approaches to the rapid and *in situ* monitoring of bacterial populations.

## RESULTS AND DISCUSSION

**AHLs and Rhamnolipids Promote Bipolar-to-Radial Transformations in LC Droplet Emulsions.** Bacterial AHLs with long aliphatic acyl tails possess nonionic amphiphilic structures and have been reported to exhibit behaviors characteristic of conventional surfactants and lipids, including the ability to self-assemble in solution and adsorb at interfaces.[11,12,23−25] It was not clear at the outset of these studies, however, whether AHLs would adsorb preferentially at aqueous/LC interfaces or whether adsorption would occur in a manner sufficient to promote changes in the orientation of the LC droplets (e.g., from "bipolar" to "radial" configurations that can be readily observed using polarized light). We thus



https://dx.doi.org/10.1021/acsami.0c05792
ACS Appl. Mater. Interfaces 2020, 12, 29056−29065

performed a series of experiments to determine the influence of AHL concentration and head/tail group structure on the optical configurations of microscale droplets of the model nematic LC 4-cyano-4′-pentylbiphenyl (5CB) dispersed in PBS. For these studies, we selected a series of naturally occurring and common AHLs with acyl chains ranging from 4 to 12 carbons (Figure 1 and Table 1, below).[38,39] This series included 3-oxo-C12-AHL and C4-AHL, the native AHL signals of *P. aeruginosa*. To understand how changes in the headgroup structure could affect the anchoring of the LC, we also included AHLs having different oxidation states at the third carbon of the acyl chain and a hydrolyzed, ring-opened form of 3-oxo-C12-AHL containing an ionizable homoserine group (referred to as 3-oxo-C12-HS; Figure 1). The hydrolysis of the AHL headgroup occurs naturally in aqueous solutions, and hydrolyzed AHL is present, albeit QS-inactive, in bacterial cultures.[40] 3-oxo-C12-HS was thus also included here to understand whether this byproduct of QS could also be used as a marker to monitor bacterial populations. Finally, we also examined rhamnolipid and 3-(3-hydroxyalkanoyloxy)alkanoic acid (HAA), an amphiphilic species produced by *P. aeruginosa* as a precursor during rhamnolipid biosynthesis.[41]

**Table 1. $BR_{50}$ Values for AHLs, Rhamnolipids, and HAA[a]**

| amphiphiles | $BR_{50}$ values ($\mu$M)[a] | 95% CI ($\mu$M) |
|---|---|---|
| 3-oxo-C12-AHL | 7.1 | 6.7−7.6 |
| 3-oxo-C12-HS | 20 | 14−29 |
| 3-OH-C12-AHL | 16 | 13−20 |
| C10-AHL | >72 | |
| C8-AHL | >360 | |
| C6-AHL | | |
| C4-AHL | | |
| HAA | 2.3 $\mu$g/mL (8 $\mu$M) | 2.1−2.5 $\mu$g/mL |
| rhamnolipids | 5.9 $\mu$g/mL (~7−20 $\mu$M)[b] | 5.1−6.9 $\mu$g/mL |

[a]$BR_{50}$ is defined as the minimum concentration required to induce changes from bipolar to radial states in at least 50% of LC droplets. Values were obtained from sigmoidal regressions to the data plotted in Figures 3 and S2. CI = confidence interval. [b]We estimate the molar concentration of a 6 $\mu$g/mL mixture of commercial rhamnolipids to be in this micromolar range; see SI for additional details.

We began by characterizing the influence of 3-oxo-C12-AHL on the anchoring of microscale droplets of LC in a defined aqueous buffer. We prepared emulsions of 5CB in phosphate-buffered solution (PBS) and used polarized-light microscopy and flow cytometry to characterize transitions in the LC droplets from bipolar to radial configurations.[27,42] Droplets of 5CB suspended in PBS exhibit so-called bipolar configurations that have the diagnostic appearance shown in Figure 2B and 2C when viewed by bright-field or polarized-light microscopy.[32,45] In bipolar droplets, the director of the LC is aligned tangentially to the surface, which results in two topological defects at opposite poles of the droplet; a cartoon illustrating the director profile in a bipolar LC droplet is shown in Figure 2A.[32,45] Upon the addition of 3-oxo-C12-AHL at a concentration of 50 $\mu$M, these bipolar droplets were observed to change rapidly (within 1−2 s) and uniformly (approximately all droplets in any random field of view) to a so-called radial configuration exemplified by the images shown in Figures 2D and 2E. In radial droplets, the director of the LC is aligned normal to the surface, with a single defect at the center of the droplet (see Figure 2A).[32,45] This bipolar-to-radial transition is consistent with results observed in past studies on LC droplets in contact with conventional surfactants[27,29,31,42] and reveals that this nonionic amphiphile can adsorb at aqueous/LC interfaces and trigger diagnostic changes in the optical properties of the LC droplets.

Bipolar-to-radial transitions in LC droplets can also be quantified using a standard lab flow cytometer equipped with side and forward light-scattering detectors. This method permits rapid characterization of large populations of LC droplets (e.g., 10000 or more droplets).[27] This analytical approach exploits differences in the ways that light is scattered by bipolar and radial LC droplets, again owing to differences in their internal configurations. These differences give rise to distinct scattering profiles when the intensity of side scattering (SSC) is plotted against that of forward scattering (FSC).[27] Light scattering profiles arising from samples of bipolar droplets and radial droplets produced by the addition of 3-oxo-C12-AHL are shown in Figure S1 and are consistent with past studies on the characterization of surfactant-treated LC droplets.[27,30] Past studies have also established that FSC histograms can be used to quantify the percentage of radial LC droplets in samples that contain mixtures of both bipolar and radial droplets.[27] Accordingly, we used flow cytometry to characterize and quantify changes in the ordering of LC droplets upon exposure to 3-oxo-C12-AHL at concentrations ranging from 2 to 50 $\mu$M, which is in the range of AHL concentrations found in laboratory cultures of planktonic *P. aeruginosa*.[22]

Figure 3A shows results for each concentration of 3-oxo-C12-AHL tested expressed as the percentage of droplets present in the radial state, i.e., the percentage of droplets in a sample observed to have undergone a bipolar-to-radial transition, after treatment with AHL (see SI for details of this analysis). Inspection of these results reveals a clear dependence of the ordering of LC droplets on the concentration of 3-oxo-C12-AHL. We observed >90% of LC droplets to be in the radial state at concentrations of AHL at or above 15 $\mu$M. The percentage of radial droplets dropped to ~60% at 8 $\mu$M and ~10% at 4 $\mu$M; we observed no meaningful change in droplet configuration at 2 $\mu$M. This concentration dependence is similar to those observed in LC droplet transitions promoted by conventional surfactants, which have been reported to occur through a mechanism that involves the adsorption of amphiphiles at levels nearing droplet surface saturation coverage to promote the transition to radial droplets.[34] Conventional one- and two-tailed surfactants typically trigger these transitions at concentrations on the order of 10 $\mu$g/mL; other many-tailed amphiphiles trigger these transitions through defect-mediated mechanisms that occur at concentrations 5 orders of magnitude lower.[28−30]

To characterize structure/function relationships that could govern the triggering of bipolar-to-radial transitions by nonionic AHLs, we conducted additional concentration-dependence experiments using the other AHLs and derivatives shown in Figure 1 in the presence of LC droplets. The full set of concentration-dependence profiles using these additional compounds is shown in Figure S2. Table 1 summarizes key results and shows the minimum concentration of each AHL required to induce a change from the bipolar to the radial state in at least 50% of the LC droplets in a given sample, a value we hereon refer to as the $BR_{50}$ (BR = bipolar-to-radial; these values were obtained from sigmoidal regressions of the data plotted in Figures 3 and S2; see Figure S3). These results



https://dx.doi.org/10.1021/acsami.0c05792
ACS Appl. Mater. Interfaces 2020, 12, 29056−29065

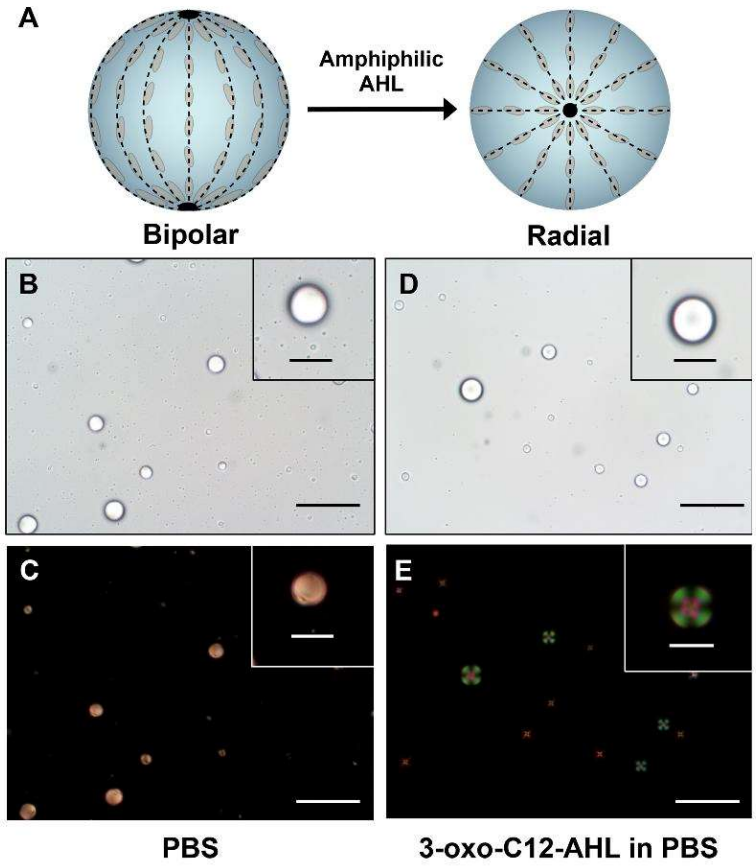


**Figure 2.** (A) Schematic of the LC director profiles (dotted lines) for spherical LC droplets in the bipolar (left) and radial (right) states. Black points represent characteristic defects associated with each state. B–E show bright-field (B, D) and polarized-light (C, E) micrographs of 5CB droplets in the bipolar (B, C) and radial (D, E) states. (B, C) Images of LC droplets dispersed in PBS. (D, E) Images of LC droplets dispersed in PBS after the addition of 3-oxo-C12 AHL (50 $\mu$M). Droplets in C and E were imaged using crossed polarizers oriented parallel to the 30 $\mu$m scale bars in the main image (scale bars = 10 $\mu$m for insets).

reveal the longer-tailed AHLs, namely 3-oxo-C12-AHL, 3-OH-C12-AHL, and the ring-opened AHL derivative 3-oxo-C12-HS, to have $BR_{50}$ values ranging from 7 to 20 $\mu$M. The small, but significant, difference between the $BR_{50}$ value for 3-oxo-C12-AHL (7.1 $\mu$M) and the values for 3-oxo-C12-HS and 3-OH-C12-AHL (20 and 16 $\mu$M) could arise from structural features that influence the interfacial density of these species through headgroup/headgroup interactions, as demonstrated in studies on surfactant-induced ordering transitions at LC-aqueous interfaces.[43,44] For example, the carboxylic acid moiety in the headgroup of 3-oxo-C12-HS has a reported $pK_a$ value of ~3, calculated from molecular structure studies,[11] suggesting that, in the conditions used here, it should be substantially ionized, leading to repulsive headgroup/headgroup interactions that could lead to a lower interfacial areal density.

Decreasing the length of the acyl tail by two carbons leads to a 4-fold increase in the $BR_{50}$ value from 20 and 16 $\mu$M for 3-oxo-C12-HS and 3-OH-C12-AHL, respectively, to >72 $\mu$M for C10-AHL (Figures S2 and S3; Table 1). This trend was also observed when moving from C10-AHL to C8-AHL, which exhibited a $BR_{50}$ value of >360 $\mu$M. We note here, however, that the extent of the bipolar-to-radial transition promoted by C8-AHL did not continue to increase at higher concentrations, as was observed for all longer-tailed AHLs; this shorter-tailed AHL did not promote transformations above ~60% at concentrations up to at least 500 $\mu$M (Figure S2D). Finally, AHLs with shorter acyl tails (C6-AHL and C4-AHL) failed to trigger distinguishable levels of bipolar-to-radial transitions in LC droplets even at concentrations as high as 1 mM (Figures 3B, S2E, and S2F; Table 1). These structure–function trends are consistent with those of past studies demonstrating that longer aliphatic tail groups and high areal densities of adsorbed surfactant are generally needed to promote robust changes in LC anchoring.[43,45–47]



https://dx.doi.org/10.1021/acsami.0c05792
ACS Appl. Mater. Interfaces 2020, 12, 29056–29065

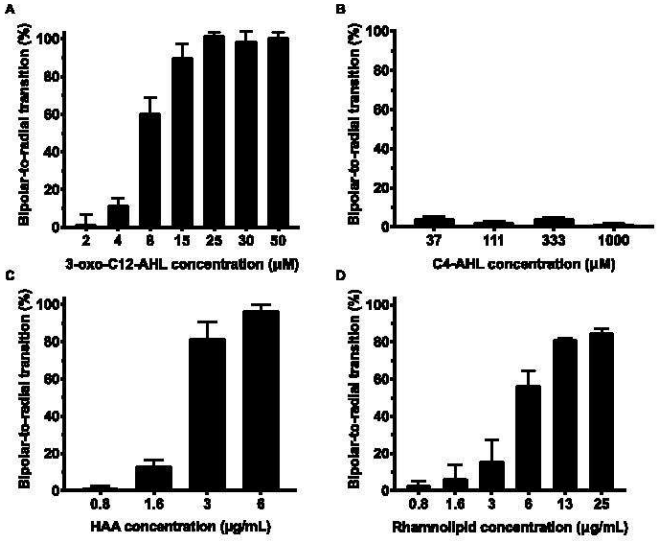


**Figure 3.** (A−C) Plots showing the percentage of LC droplets transformed from bipolar to radial as a function of the concentration of (A) 3-oxo-C12-AHL, (B) C4-AHL, and (C) HAA in PBS containing 1% v/v DMSO. (D) Plot showing the percentage of LC droplets transformed as a function of the rhamnolipid concentration. Data represent the mean ± SEM (standard error of the mean) ($n$ = 4).

We also subjected rhamnolipid and its biosynthetic precursor HAA to these same droplet screening experiments (Figure 3C and 3D; Table 1). These experiments were conducted at biologically relevant concentrations of these amphiphiles ranging from 0.8 to 25 $\mu$g/mL. Our results reveal that rhamnolipids promote bipolar-to-radial transformations in LC droplets at $BR_{50}$ values as low as ∼6 $\mu$g/mL. We estimate this value to be in the range of about 7 to 20 $\mu$M (see SI for details describing the estimation of this range). HAA triggered threshold levels at a $BR_{50}$ value of 2.3 $\mu$g/mL (∼8 $\mu$M). Overall, this range of threshold concentrations is similar to that determined for the three C12-AHL species and derivatives described above, suggesting that these different compounds promote changes in LC droplet configurations through a similar mechanism.

**LC Droplets Respond to AHLs and Rhamnolipid Produced in Growing Bacterial Cultures.** We next performed experiments to determine whether droplets of 5CB could respond to and report on the presence of AHLs and rhamnolipid produced by growing cultures of bacteria. For these experiments, we devised an experimental set up in which LC emulsions were enclosed in a laboratory dialysis cassette that could be placed directly into a bacterial culture flask (Figure 4A). This enabled us to expose small volumes and high concentrations of LC droplets to bacterial products produced in larger volumes of culture medium without diluting them or complicating analysis by microscopy or flow cytometry. For these proof-of-concept studies, we selected dialysis cassettes that allowed AHLs and rhamnolipid to diffuse over a period of 90 min and that permitted the extraction of LC emulsion samples by use of a syringe for the analysis. This approach also prevented the possibility of direct contact between the LC droplets and cells, which has also been reported to lead to bipolar-to-radial transitions in past studies.[26]

In a first series of experiments, we used cultures of the PAO1 wild-type strain of *P. aeruginosa*. Cultures were grown in LB medium with shaking at 37 °C, and dialysis cassettes were added at predetermined time points during growth and stationary phases to characterize changes in the responses of the LC droplets. We note that the nematic−isotropic transition temperature ($T_{N,I}$) for 5CB is 35 °C, i.e., at a temperature above 35 °C, 5CB undergoes a phase transition from the nematic LC phase to an isotropic oil that does not exhibit the optical birefringence necessary for detection.[48] Cultures were therefore cooled to ambient temperature (∼25 °C) prior to adding the LC droplet-containing dialysis cassettes; the cassettes were incubated with cultures for 90 min, removed, and sampled for analysis by flow cytometry. As an aside, we note that LCs with $T_{N,I}$ > 35 °C have also been demonstrated to form LC droplets that undergo bipolar-to-radial transformations.[27,36] Those additional LC formulations could also be used to further optimize experimental and analytical workflows.

Columns I and II of Figure 4B show the responses of LC droplets placed in flasks containing (I) LB medium or (II) cultures of the PAO1 strain of *P. aeruginosa* in LB medium at 6 h (white bars), 12 h (black bars), or 24 h (gray bars) after inoculation. These results reveal that cultures of PAO1 induce bipolar-to-radial transitions in the LC droplets and that the percentage of radial droplets increases monotonically over 24 h from ∼15% at 6 h of incubation to >90% at 24 h. In contrast, incubation with LB medium resulted in only ∼5% of radial droplets at 24 h. These results are consistent with the production of AHLs by these bacterial communities and/or the production of rhamnolipid and HAA, but they do not rule out responses that could be triggered by other products produced during bacterial growth.



https://dx.doi.org/10.1021/acsami.0c05792
ACS Appl. Mater. Interfaces 2020, 12, 29056−29065

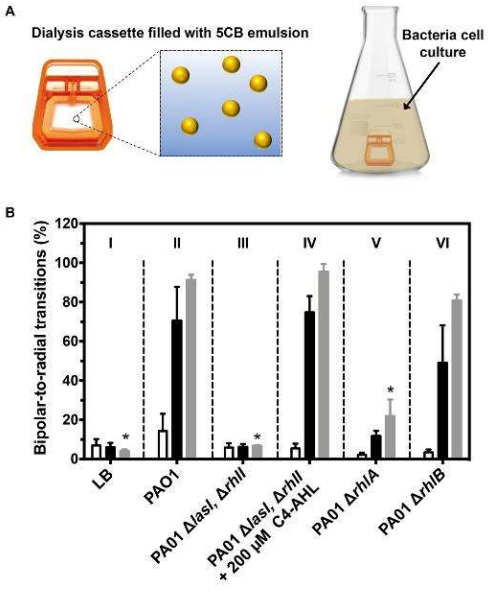


**Figure 4.** (A) Schematic showing experimental set up used to incubate LC emulsions with bacterial cultures using dialysis cassettes. (B) Plot showing percentage of LC droplets transformed from bipolar to radial after 90 min of incubation with cultures grown at 37 °C for 6 h (white bars), 12 h (black bars), and 24 h (gray bars). Columns I−VI show results of using an LB medium control (I) or using the indicated bacterial strains and conditions. Results are the average of 3 independent experiments; error bars represent SEM. Asterisk (*) indicates $p < 0.05$ for multiple comparisons of each group against group II (PAO1) at the 24 h time point.

To further investigate the factors that lead to droplet response under these conditions, we performed otherwise identical experiments using three mutant strains of *P. aeruginosa* lacking genes critical to either QS or rhamnolipid biosynthesis (see Table S1 for strain information). Strain PAO1 Δ*lasI*, Δ*rhlI* is unable to produce either of its native AHL signals, 3-oxo-C12-AHL or C4-AHL. This strain is thus unable to produce QS-associated virulence factors, including rhamnolipid (a detailed schematic of the QS regulatory pathway in *P. aeruginosa* is shown in Figure S4).[49] Strain PAO1 Δ*rhlB* is unable to produce the rhamnosyltransferase enzyme required to synthesize rhamnolipids,[50] and strain PAO1 Δ*rhlA* is unable to produce the rhamnolipid precursor HAA (and, as result, cannot produce any downstream rhamnolipids).[51] The results of experiments using these three knockout strains are included in Figure 4.

Inspection of the results shown in column III of Figure 4B reveals cultures of the PAO1 Δ*lasI*, Δ*rhlI* QS-knockout strain to promote bipolar-to-radial transitions at very low levels that are similar to that of the LB medium alone (the percentage of radial droplets was <7% at all points tested). This result suggests that the response of the LC droplets to the wild-type strain (Figure 4B, column II) was the result of either a QS signal or a factor regulated by bacterial QS, and not a metabolite, component of cellular debris or another factor resulting from bacterial growth or death. Experiments using the PAO1 Δ*rhlA* strain (Figure 4B, column V) showed a substantial (∼70%) decrease in the percentage of droplets present in the radial state. This strain is able to produce both C4-AHL, which did not trigger bipolar-to-radial transitions in the experiments reported above, and 3-oxo-C12-AHL, which did induce bipolar-to-radial transformations, to regulate QS, but it is unable to produce either HAA or rhamnolipid. We therefore interpret the response of the LC droplets to this strain to result from levels of 3-oxo-C12-AHL (and, likely, its hydrolyzed, ring-opened derivative product 3-oxo-C12-HS) that accumulate in the culture medium as the bacterial population density increases. The addition of exogenous C4-AHL (200 μM) to cultures of the PAO1 Δ*lasI*, Δ*rhlI* strain, which has been shown to promote the production of rhamnolipid, yielded a substantial increase in LC droplet response.[49] The percentage of radial droplets under these conditions (Figure 4B; column IV) was similar (>90%) to that observed in the wild-type strain (column II) and substantially higher than that observed in that strain in the absence of exogenous C4-AHL (∼6%; see column III). Because this strain does not produce 3-oxo-C12-AHL and because the exogenously added C4-AHL itself does not promote radial transitions at this concentration, this result suggests that the production of rhamnolipid is also sufficient to produce a robust LC droplet response. Lastly, column VI of Figure 4B shows the results of experiments using the PAO1 Δ*rhlB* strain, which can produce both 3-oxo-C12-AHL and HAA but not rhamnolipid. The extents of radial transitions observed using this strain (>80% at 24 h) in comparison to those using the PAO1 Δ*rhlA* strain suggest that the production of HAA alone can also promote robust LC droplet responses. We note that cell densities in all of these experiments were virtually identical across all strains at all time points tested (Figure S5) and that 5CB emulsions did not exhibit substantial toxicity to PAO1 cells (Figure S6), further supporting the view that transitions observed here were the result of excreted compounds associated with QS and not differences in metabolite concentration or other factors associated with cell growth.

We conclude on the basis of these results that (i) the LC droplets used in these experiments can respond to and report on concentrations of long-chain AHLs present in bacterial communities as well as rhamnolipid or amphiphilic rhamnolipid precursors that are produced once a quorum is reached, and (ii) the majority of the LC droplet response observed in the wild-type strain at 12 or 24 h is the result of rhamnolipid or HAA production (a comparison of columns II and IV of Figure 4 reveals >85% of the response observed for the wild-type strain at 24 h to arise from the production of rhamnolipid; only a small part of this response (∼15%) arises from the accumulation of 3-oxo-C12-AHL or its hydrolysis product). Notably, because rhamnolipid is a virulence factor that is only produced once a quorum is reached, these results suggest that these LC emulsions can be used to monitor bacterial cultures and distinguish between quorate and subquorate populations.

Finally, we performed additional analytical experiments to determine the concentrations of 3-oxo-C12-AHL and rhamnolipid produced by cultures of each of the *P. aeruginosa* strains used above and compare them to the values observed to promote bipolar-to-radial transformations in defined buffers. The results of those experiments are summarized in Figure S7 (see SI for an additional detailed discussion of findings and implications arising from those studies). Overall, the results of



https://dx.doi.org/10.1021/acsami.0c05792
ACS Appl. Mater. Interfaces 2020, 12, 29056−29065

those experiments are consistent with those shown in Figure 4 and provide additional support for the view that 3-oxo-C12-AHL, 3-oxo-C12-HS, and rhamnolipid produced in cultures of *P. aeruginosa* are responsible, either alone or in combination, for promoting ordering transitions in LC droplets.

## ■ CONCLUSIONS

QS signals are markers of not only the presence of bacteria but also their population densities. Approaches to detect these markers could thus provide a novel means by which to monitor the growth and behaviors of bacterial communities. We have demonstrated that LC emulsions can respond to amphiphilic AHL signals that control QS in Gram-negative bacteria. We have also demonstrated that LC droplets undergo bipolar-to-radial transitions upon exposure to products generated specifically by quorate populations of bacteria. The concentration of AHLs required to promote these transitions decreases with increasing carbon number in the acyl tail, reaching a $BR_{50}$ value of 8 $\mu$M for 3-oxo-C12-AHL, a native QS signal in *P. aeruginosa*. This concentration range is within that observed in quorate populations of *P. aeruginosa*. Our results also reveal these droplets to respond to biologically relevant concentrations of rhamnolipid, an amphiphile produced by *P. aeruginosa* under the control of QS.

These LC droplets remain configurationally stable in bacterial culture media, permitting them to be used to detect the presence of AHL and rhamnolipid in bacterial supernatants or be deployed *in situ* to report the presence of these products in growing bacterial cultures. Systematic studies using mutant *P. aeruginosa* strains, with certain aspects of their QS system rendered nonfunctional, support the conclusion that these LC droplets respond selectively to the production of rhamnolipid and other amphiphiles involved in the regulation of QS and not to other products produced by bacteria at lower subquorate densities. The proof-of-concept studies reported here provide new methods for the detection and monitoring of bacterial QS and the production of QS-associated goods using free-floating LC droplets that can be readily applied in aqueous environments. These methods could also be combined with approaches for the encapsulation and immobilization of LC droplets on surfaces to design sensor arrays or flexible test strips that could facilitate the rapid and *in situ* monitoring of bacterial communities in practical settings.

## ■ MATERIALS AND METHODS

**Materials.** The nematic thermotropic LC 4′-pentyl-cyanobiphenyl (5CB) was purchased from HCCH Jiangsu Hecheng Display Technology Co., Ltd. (Jiangsu, China). Disposable culture tubes (12 × 75 mm) were purchased from VWR (West Chester, PA). Phosphate-buffered saline (PBS) concentrate (137 mM NaCl, 2.7 mM KCl, and 10 mM phosphate) was obtained from Omnipur (EM Science, Gibbstown, NJ). Electrophoresis-grade sodium dodecyl sulfate (SDS) was purchased from Fisher Scientific (Pittsburgh, PA). Rhamnolipids, 90% pure (commercial mixture of glycolipids isolated from *P. aeruginosa*; see additional notes below) were purchased from AGAE Technologies (Corvallis, OR). Dialysis cassettes (10k MWCO, gamma irradiated, 0.5 mL) were purchased from ThermoFisher Scientific (Rockford, IL). Luria−Bertani medium, Lennox formulation (LB) was purchased from EMD Millipore (Burlington, MA). The native AHLs *N*-butanoyl-L-homoserine lactone (C4-AHL) and *N*-(3-oxo-dodecanoyl)-L-homoserine lactone (3-oxo-C12-AHL) were purchased from Cayman Chemical (Ann Arbor, MI) and Sigma-Aldrich (St. Louis, MO), respectively. The other AHLs and AHL derivatives examined in this study were synthesized according to our previously reported methods.[52,53] A detailed description of the synthesis and characterization of 3-(3-hydroxyalkanoyloxy)alkanoic acid (HAA) is included in the Supporting Information.

**General Considerations.** All absorbance measurements were made using 200 $\mu$L of solution in a clear 96-well microtiter plate (Costar 3370) using a Biotek Synergy 2 plate reader running Gen 5 software (version 1.05). Bacterial growth was monitored by measuring the culture density via absorbance at 600 nm ($OD_{600}$). Bright-field and polarized-light microscopy images were acquired using an Olympus IX71 inverted microscope (Waltham, MA) equipped with cross-polarizers (Olympus analyzer slider IX2-AN and condenser attachment IX-LWPO) and a binocular tube built-in Bertrand lens (Olympus U-BI90CT). Fields of view were recorded using an OPTO-EDU (Beijing, China) eyepiece camera model A59.2211 connected to a computer and controlled through ImageView imaging software version A30.2201. The percentage of 5CB droplets in the radial state within an emulsion sample was determined by flow cytometry measurements performed at room temperature using a BD FACSCalibur instrument. Assay data were analyzed using Microsoft Excel for Mac 2016, cytometry data were analyzed using FlowJo (v10), and graphs were created using GraphPad Prism (GraphPad Software version 7, San Diego, CA). Characterization of the emulsion droplet density was performed at room temperature using a BD Accuri C6 flow cytometer. The HPLC-MS/MS data analysis was performed using the MAVEN software (open-source)[54] and Thermo Xcalibur software packages (Waltham, MA). Unless otherwise noted, all AHL solutions were prepared by first dissolving AHL in DMSO and then diluting further to the desired concentration at 1% v/v DMSO.

We note that the commercially obtained rhamnolipids used in this study were isolated from *P. aeruginosa* as a mixture of congeners with different numbers of rhamnose sugar moieties (mono- and di-) linked to one or two molecules of hydroxy acid that differ in their aliphatic chain length. We also note that the composition of this mixture has been found to depend on various environmental factors, including the nutrient source and growth conditions.[55−57] Several studies have found that the most abundant species are mono- and dirhamnolipids containing one or two 8−10 $\alpha$-hydroxy fatty acids.[57] However, in cases where estimates of molar concentrations of rhamnolipid were calculated from diluted stocks of commercial rhamnolipid provided in units of $\mu$g/mL, we opted to establish a boundary range of molar concentrations by assuming two hypothetical uniform compositions consisting entirely of either the lowest or the highest molecular weight rhamnolipid congeners found in rhamnolipid mixtures. The actual molar concentration of rhamnolipid prepared from the commercial mixtures used here would then lie somewhere within that calculated range.

**Preparation of LC Emulsions and Characterization of LC Droplet Configuration.** LC-in-water emulsions were prepared using a procedure similar to that previously reported by Carter et al.[30] Briefly, 6 $\mu$L of 5CB was added to a glass test tube containing 3 mL of a 10 $\mu$M SDS solution in PBS. The mixture was vortexed for 30 s at ∼3000 rpm to yield a milky white emulsion and allowed to settle for 1 h. The emulsion was divided into aliquots of 50 $\mu$L that were subsequently diluted into 500 $\mu$L of aqueous solutions of either AHL or rhamnolipid, prepared at predetermined concentrations, to obtain final LC droplet densities of ∼10800 ± 900 droplets/$\mu$L. These mixtures were allowed to sit for at least 1 h before characterizing the LC droplets using polarized-light microscopy or flow cytometry. For flow cytometry experiments, forward light scattering (FSC) was measured at a detection angle of 0° ± 15° for a minimum of 10000 droplets pumped through the flow cytometer at a flow rate of 12 $\mu$L/min. Quantitative analyses of scattering plots to determine the percentage of droplets in the bipolar or radial configurations were performed using a previously reported procedure.[30,58]

**$BR_{50}$ Calculation.** $BR_{50}$ values, representing the minimum concentration of each analyte required to induce a change from the bipolar to the radial state in at least a 50% of the LC droplets in a given sample, were calculated by performing a sigmoidal regression fit



https://dx.doi.org/10.1021/acsami.0c05792
ACS Appl. Mater. Interfaces 2020, 12, 29056−29065

with a Hill slope ≠1 to plots of the percentage of droplets transitioned from bipolar-to-radial versus the analyte concentration. Fits were calculated using GraphPad Prism (GraphPad Software Version 7.0, San Diego, CA) and the built-in nonlinear regression model for dose−response curves with a variable Hill slope using the following equation:

$$Y = 100 \cdot \frac{X^{\text{Hillslope}}}{BR_{50}^{\text{Hillslope}} + X^{\text{Hillslope}}}$$

**Bacterial Strains and Growth Conditions.** The *P. aeruginosa* strains used in this study include the following: PAO1 (wild-type; isolated by B. Holloway from a human wound),[59] PW6886 (Δ*rhlA*) (PAO1 *rhlA-E08::ISphoA/hah*; tetracycline resistant),[51] PAO1 (Δ*rhlB*) (PAO1 containing an unmarked, in-frame *rhlB* deletion),[50] and PAO-SC4 (Δ*lasI*, Δ*rhlI*) (PAO1 containing unmarked, in-frame *rhlI* and *lasI* deletions; a generous gift from E. P. Greenberg). Bacteria were cultured in LB broth at 37 °C with shaking at 200 rpm unless otherwise noted. Freezer stocks for the bacterial strains were stored at −80 °C in LB with 25% glycerol. Spent media was collected at varying time points by centrifugation (3500 × *g*, 15 min) and stored at −80 °C until use.

**Incubation of Bacteria with LC Droplets.** A 2 mL overnight culture of each *P. aeruginosa* strain was grown for 20 h in a sterile borosilicate glass test tube. A subculture was prepared by directly diluting overnight culture 1:100 in 75 mL of fresh LB medium. For the induction of rhamnolipid production in PAO-SC4 (Δ*rhlI* Δ*lasI*), 150 μL of 100 mM C4-AHL stock solution was added to yield a final concentration of 200 μM; DMSO alone (150 μL; 0.2% DMSO) was added to all other strains. Subcultures were grown for 6, 12, or 24 h. Cultures were then briefly chilled on ice. Prior to use, dialysis cassettes were equilibrated in LB medium according to the manufacturer's instructions. LC suspension (600 μL) was then added to the cassette, and the cassette was added to the chilled culture. Cultures were incubated at 20 °C with shaking for 1.5 h. Cassettes were then removed from culture, and the LCs were collected for analysis by flow cytometry.

**Quantification of Rhamnolipid.** Rhamnolipid was quantified using the orcinol assay method described by Welsh et al. with the following modifications.[60] At time points of interest, 2 mL of culture was removed from the 75 mL subculture, and the cells were pelleted at 3500 × *g* for 15 min. A 1 mL aliquot of supernatant was removed, extracted, and characterized using the reported orcinol assay. The remaining supernatant was saved for the quantification of AHL, as discussed below. Samples were background-corrected using an LB negative control. Rhamnolipids were quantified using a rhamnose standard curve based on the assumption described by Pearson et al. that 1 g of rhamnose equals 2.5 g of rhamnolipid mixture.[49]

**Characterization of Cell Viability.** LC-in-water emulsions were prepared as described above. Droplet density was estimated based on a calibration curve obtained from correlations between event counts/μL detected using a BD Accuri C6 flow cytometer and dilutions from stock LC-in-water emulsions (of at least three different dilutions). A sample with a droplet density of 20000 events/μL was prepared from stock LC emulsion based on the estimated droplet density. Serial dilutions were performed from this LC emulsion. A 2 mL overnight culture of wild-type *P. aeruginosa* PAO1 was grown for 20 h and plated in a 1:1 dilution with varying dilutions of LC droplets in a 96-well microtiter plate. Plates were incubated under static conditions for 1.5 h at either 37 °C or room temperature. Cell viability was quantified using BacTiter-Glo microbial cell viability assay (Promega Corporation) and normalized using a no-LC control.

**Characterization of AHL Concentrations Using HPLC-MS/MS.** Cell-free supernatant was collected from each sample at 6, 12, and 24 h prior to the addition of the dialysis cassette and stored at −80 °C until use. After thawing, the samples were diluted 1:10 in 10:90 methanol:water with 5 mM ammonium formate and 0.1% formic acid (any samples doped with C4-AHL, including C4-AHL standards, were diluted 1:100 in the same solvent). AHL concentrations were measured using external calibration curves. AHL standards were prepared in PBS immediately before use. Ring-opened (i.e., hydrolyzed lactone) AHL standards were prepared by incubating AHLs in 1 M NaOH for 12 h at room temperature.

The method for HPLC-MS/MS analysis was adapted from that of Patel et al.[20] Aliquots totaling 2.5 μL of diluted supernatant samples were subjected to a HPLC-MS/MS analysis. HPLC was performed on a Vanquish μHPLC system (Thermo Scientific) using a C18 reversed-phase column (1.7 μm particle size, 2.1 × 50 mm; Acquity UPLC BEH). Solvent A consisted of 10:90 methanol:water with 5 mM ammonium formate and 0.1% formic acid, and solvent B was 100% methanol. The gradient profile for chromatography was as follows: 100% solvent A for 1 min, linear increase in solvent B to 90% over 4 min, isocratic 90% solvent B for 5.5 min, and then equilibration with 100% solvent A for 2 min. The flow rate was constant at 0.2 mL/min. Compounds separated by HPLC were detected by heated electrospray ionization coupled to high-resolution mass spectroscopy (HESI-MS) (QExactive; Thermo Scientific). The analysis was performed in the positive ionization mode. Settings for the ion source were as follows: 10 aux gas flow rate, 35 sheath gas flow rate, 1 sweep gas flow rate, 4 μA spray current, 4 kV spray voltage, 320 °C capillary temperature, 300 °C heater temperature, and 50 S-lens RF level. Nitrogen was used as the nebulizing gas by the ion trap source. The MS/MS method was designed to perform a MS1 full-scan (100 to 510 *m*/*z*, no fragmentation) together with a series of MS/MS scans (all-ion fragmentation) that divided the *m*/*z* range into partially overlapping windows of 40 *m*/*z* each. The MS1 full-scan provided data on $[M + H]^+$ pseudomolecular ions, while the MS/MS scans provided corresponding (matched by retention time) fragmentation spectra, all obtained within a single chromatographic run. MS/MS scans (all-ion fragmentation) were centered at 160, 210, 245, 280, 315, 350, 385, 420, 455, and 490 *m*/*z* using an isolation width of 40.0 *m*/*z*. Fragmentations were performed at 17.5, 35, and 52.5 NCE (normalized-collision energy). The mass resolution was set at 35000, the AGC target was 1E6, and the injection time was 40 ms.

**Statistical Information.** All statistical tests and sigmoidal regression fits were performed using GraphPad Prism (GraphPad Software Version 7.0, San Diego, CA). Statistical comparisons were evaluated using a two-way analysis of variance (ANOVA) using Dunnett's *post hoc* test for multiple comparisons. The criterion used to accept statistical significance was a *p* value of less than 0.05. Data were generated by at least three independent experiments. Separate biological replicates were the result of three technical replicates.

## ■ ASSOCIATED CONTENT

### Supporting Information

The Supporting Information is available free of charge at https://pubs.acs.org/doi/10.1021/acsami.0c05792.

Additional information on bacterial strains, characterization of LC droplets and culture supernatants, and synthesis of HAA (PDF)

## ■ AUTHOR INFORMATION


### Corresponding Authors

**Helen E. Blackwell** − *Department of Chemistry, University of Wisconsin−Madison, Madison, Wisconsin 53706, United States*; orcid.org/0000-0003-4261-8194; Email: blackwell@chem.wisc.edu

**David M. Lynn** − *Department of Chemical and Biological Engineering and Department of Chemistry, University of Wisconsin−Madison, Madison, Wisconsin 53706, United States*; orcid.org/0000-0002-3140-8637; Email: dlynn@engr.wisc.edu

### Authors

**Benjamín J. Ortiz** − *Department of Chemical and Biological Engineering, University of Wisconsin−Madison, Madison, Wisconsin 53706, United States*




https://dx.doi.org/10.1021/acsami.0c05792
ACS Appl. Mater. Interfaces 2020, 12, 29056−29065

**Michelle E. Boursier** − *Department of Chemistry, University of Wisconsin−Madison, Madison, Wisconsin 53706, United States*
**Kelsey L. Barrett** − *Department of Bacteriology, University of Wisconsin−Madison, Madison, Wisconsin 53706, United States*
**Daniel E. Manson** − *Department of Chemistry, University of Wisconsin−Madison, Madison, Wisconsin 53706, United States*
**Daniel Amador-Noguez** − *Department of Bacteriology, University of Wisconsin−Madison, Madison, Wisconsin 53706, United States*
**Nicholas L. Abbott** − *Department of Chemical and Biological Engineering, University of Wisconsin−Madison, Madison, Wisconsin 53706, United States;* orcid.org/0000-0002-9653-0326

Complete contact information is available at: https://pubs.acs.org/10.1021/acsami.0c05792

### Notes

The authors declare no competing financial interest.

## ■ ACKNOWLEDGMENTS

Financial support was provided by the NSF through a grant to the UW−Madison MRSEC (DMR-1720415) and the ONR (N00014-07-1-0255). We acknowledge the use of instrumentation supported by the NSF through the UW MRSEC. B.J.O. was supported by the Graduate Research Scholars program at UW−Madison and the NIH Chemistry-Biology Interface Training Grant (T32 GM008505).

## ■ REFERENCES

(1) Whiteley, M.; Diggle, S. P.; Greenberg, E. P. Progress in and Promise of Bacterial Quorum Sensing Research. *Nature* **2017**, *551*, 313−320.
(2) Rutherford, S. T.; Bassler, B. L. Bacterial Quorum Sensing: Its Role in Virulence and Possibilities for Its Control. *Cold Spring Harbor Perspect. Med.* **2012**, *2*, a012427.
(3) Daniels, R.; Vanderleyden, J.; Michiels, J. Quorum Sensing and Swarming Migration in Bacteria. *FEMS Microbiol. Rev.* **2004**, *28*, 261−289.
(4) Dickschat, J. S. Quorum Sensing and Bacterial Biofilms. *Nat. Prod. Rep.* **2010**, *27*, 343−369.
(5) Zhou, J.; Yao, D.; Qian, Z.; Hou, S.; Li, L.; Jenkins, A. T. A.; Fan, Y. Bacteria-Responsive Intelligent Wound Dressing: Simultaneous *in Situ* Detection and Inhibition of Bacterial Infection for Accelerated Wound Healing. *Biomaterials* **2018**, *161*, 11−23.
(6) Alatraktchi, F. A. A.; Noori, J. S.; Tanev, G. P.; Mortensen, J.; Dimaki, M.; Johansen, H. K.; Madsen, J.; Molin, S.; Svendsen, W. E. Paper-Based Sensors for Rapid Detection of Virulence Factor Produced by *Pseudomonas aeruginosa*. *PLoS One* **2018**, *13*, No. e0194157.
(7) Kim, M. K.; Zhao, A.; Wang, A.; Brown, Z. Z.; Muir, T. W.; Stone, H. A.; Bassler, B. L. Surface-Attached Molecules Control *Staphylococcus aureus* Quorum Sensing and Biofilm Development. *Nat. Microbiol.* **2017**, *2*, 17080.
(8) Broderick, A. H.; Breitbach, A. S.; Frei, R.; Blackwell, H. E.; Lynn, D. M. Surface-Mediated Release of a Small-Molecule Modulator of Bacterial Biofilm Formation: A Non-Bactericidal Approach to Inhibiting Biofilm Formation in *Pseudomonas aeruginosa*. *Adv. Healthcare Mater.* **2013**, *2*, 993−1000.
(9) Kratochvil, M. J.; Welsh, M. A.; Manna, U.; Ortiz, B. J.; Blackwell, H. E.; Lynn, D. M. Slippery Liquid-Infused Porous Surfaces That Prevent Bacterial Surface Fouling and Inhibit Virulence Phenotypes in Surrounding Planktonic Cells. *ACS Infect. Dis.* **2016**, *2*, 509−517.
(10) Laabei, M.; Jamieson, W. D.; Massey, R. C.; Jenkins, A. T. A. *Staphylococcus aureus* Interaction with Phospholipid Vesicles−a New Method to Accurately Determine Accessory Gene Regulator (Agr) Activity. *PLoS One* **2014**, *9*, No. e87270.
(11) Davis, B.; Richens, J.; O'Shea, P. Label-Free Critical Micelle Concentration Determination of Bacterial Quorum Sensing Molecules. *Biophys. J.* **2011**, *101*, 245−254.
(12) Daniels, R.; Reynaert, S.; Hoekstra, H.; Verreth, C.; Janssens, J.; Braeken, K.; Fauvart, M.; Beullens, S.; Heusdens, C.; Lambrichts, I.; De Vos, D. E.; Vanderleyden, J.; Vermant, J.; Michiels, J. Quorum Signal Molecules as Biosurfactants Affecting Swarming in *Rhizobium etli*. *Proc. Natl. Acad. Sci. U. S. A.* **2006**, *103*, 14965−14970.
(13) Fuqua, C.; Greenberg, E. P. Listening in on Bacteria: Acyl-Homoserine Lactone Signalling. *Nat. Rev. Mol. Cell Biol.* **2002**, *3*, 685−695.
(14) Schuster, M.; Lostroh, C. P.; Ogi, T.; Greenberg, E. P. Identification, Timing, and Signal Specificity of *Pseudomonas aeruginosa* Quorum-Controlled Genes: A Transcriptome Analysis. *J. Bacteriol.* **2003**, *185*, 2066−2079.
(15) Jiang, D.; Liu, Y.; Jiang, H.; Rao, S.; Fang, W.; Wu, M.; Yuan, L.; Fang, W. A Novel Screen-Printed Mast Cell-Based Electrochemical Sensor for Detecting Spoilage Bacterial Quorum Signaling Molecules (*N*-Acyl-Homoserine-Lactones) in Freshwater Fish. *Biosens. Bioelectron.* **2018**, *102*, 396−402.
(16) Das, S.; Sarkar, H. S.; Uddin, M. R.; Mandal, S.; Sahoo, P. A Chemosensor to Recognize *N*-Acyl Homoserine Lactone in Bacterial Biofilm. *Sens. Actuators, B* **2018**, *259*, 332−338.
(17) Baldrich, E.; Munoz, F. X.; García-Aljaro, C. Electrochemical Detection of Quorum Sensing Signaling Molecules by Dual Signal Confirmation at Microelectrode Arrays. *Anal. Chem.* **2011**, *83*, 2097−2103.
(18) Habimana, J. d. D.; Ji, J.; Pi, F.; Karangwa, E.; Sun, J.; Guo, W.; Cui, F.; Shao, J.; Ntakirutimana, C.; Sun, X. A Class-Specific Artificial Receptor-Based on Molecularly Imprinted Polymer-Coated Quantum Dot Centers for the Detection of Signaling Molecules, *N*-Acyl-Homoserine Lactones Present in Gram-Negative Bacteria. *Anal. Chim. Acta* **2018**, *1031*, 134−144.
(19) O'Connor, G.; Knecht, L. D.; Salgado, N.; Strobel, S.; Pasini, P.; Daunert, S., Whole-Cell Biosensors as Tools for the Detection of Quorum-Sensing Molecules: Uses in Diagnostics and the Investigation of the Quorum-Sensing Mechanism. In *Bioluminescence: Fundamentals and Applications in Biotechnology*; Springer, 2015; Vol. 3, pp 181−200.
(20) Patel, N. M.; Moore, J. D.; Blackwell, H. E.; Amador-Noguez, D. Identification of Unanticipated and Novel *N*-Acyl L-Homoserine Lactones (AHLs) Using a Sensitive Non-Targeted LC-MS/MS Method. *PLoS One* **2016**, *11*, No. e0163469.
(21) May, A. L.; Eisenhauer, M. E.; Coulston, K. S.; Campagna, S. R. Detection and Quantitation of Bacterial Acylhomoserine Lactone Quorum Sensing Molecules via Liquid Chromatography−Isotope Dilution Tandem Mass Spectrometry. *Anal. Chem.* **2012**, *84*, 1243−1252.
(22) Charlton, T. S.; De Nys, R.; Netting, A.; Kumar, N.; Hentzer, M.; Givskov, M.; Kjelleberg, S. A Novel and Sensitive Method for the Quantification of *N*-3-Oxoacyl Homoserine Lactones Using Gas Chromatography−Mass Spectrometry: Application to a Model Bacterial Biofilm. *Environ. Microbiol.* **2000**, *2*, 530−541.
(23) Barth, C.; Jakubczyk, D.; Kubas, A.; Anastassacos, F.; Brenner-Weiss, G.; Fink, K.; Schepers, U.; Bräse, S.; Koelsch, P. Interkingdom Signaling: Integration, Conformation, and Orientation of *N*-Acyl-L-Homoserine Lactones in Supported Lipid Bilayers. *Langmuir* **2012**, *28*, 8456−8462.
(24) Toyofuku, M.; Morinaga, K.; Hashimoto, Y.; Uhl, J.; Shimamura, H.; Inaba, H.; Schmitt-Kopplin, P.; Eberl, L.; Nomura, N. Membrane Vesicle-Mediated Bacterial Communication. *ISME J.* **2017**, *11*, 1504−1509.
(25) Davis, B. M.; Jensen, R.; Williams, P.; O'Shea, P. The Interaction of *N*-Acylhomoserine Lactone Quorum Sensing Signaling Molecules with Biological Membranes: Implications for Inter-Kingdom Signaling. *PLoS One* **2010**, *5*, No. e13522.

(26) Sivakumar, S.; Wark, K. L.; Gupta, J. K.; Abbott, N. L.; Caruso, F. Liquid Crystal Emulsions as the Basis of Biological Sensors for the Optical Detection of Bacteria and Viruses. *Adv. Funct. Mater.* **2009**, *19*, 2260−2265.
(27) Miller, D. S.; Wang, X.; Buchen, J.; Lavrentovich, O. D.; Abbott, N. L. Analysis of the Internal Configurations of Droplets of Liquid Crystal Using Flow Cytometry. *Anal. Chem.* **2013**, *85*, 10296−10303.
(28) Lin, I.-H.; Miller, D. S.; Bertics, P. J.; Murphy, C. J.; de Pablo, J. J.; Abbott, N. L. Endotoxin-Induced Structural Transformations in Liquid Crystalline Droplets. *Science* **2011**, *332*, 1297−1300.
(29) Miller, D. S.; Abbott, N. L. Influence of Droplet Size, pH and Ionic Strength on Endotoxin-Triggered Ordering Transitions in Liquid Crystalline Droplets. *Soft Matter* **2013**, *9*, 374−382.
(30) Carter, M. C.; Miller, D. S.; Jennings, J.; Wang, X.; Mahanthappa, M. K.; Abbott, N. L.; Lynn, D. M. Synthetic Mimics of Bacterial Lipid a Trigger Optical Transitions in Liquid Crystal Microdroplets at Ultralow Picogram-Per-Milliliter Concentrations. *Langmuir* **2015**, *31*, 12850−12855.
(31) Carlton, R. J.; Zayas-Gonzalez, Y. M.; Manna, U.; Lynn, D. M.; Abbott, N. L. Surfactant-Induced Ordering and Wetting Transitions of Droplets of Thermotropic Liquid Crystals "Caged" inside Partially Filled Polymeric Capsules. *Langmuir* **2014**, *30*, 14944−14953.
(32) Chang, C.-Y.; Chen, C.-H. Oligopeptide-Decorated Liquid Crystal Droplets for Detecting Proteases. *Chem. Commun.* **2014**, *50*, 12162−12165.
(33) Alino, V. J.; Pang, J.; Yang, K.-L. Liquid Crystal Droplets as a Hosting and Sensing Platform for Developing Immunoassays. *Langmuir* **2011**, *27*, 11784−11789.
(34) Gupta, J. K.; Sivakumar, S.; Caruso, F.; Abbott, N. L. Size-Dependent Ordering of Liquid Crystals Observed in Polymeric Capsules with Micrometer and Smaller Diameters. *Angew. Chem., Int. Ed.* **2009**, *48*, 1652−1655.
(35) Kinsinger, M. I.; Buck, M. E.; Abbott, N. L.; Lynn, D. M. Immobilization of Polymer-Decorated Liquid Crystal Droplets on Chemically Tailored Surfaces. *Langmuir* **2010**, *26*, 10234−10242.
(36) Guo, X.; Manna, U.; Abbott, N. L.; Lynn, D. M. Covalent Immobilization of Caged Liquid Crystal Microdroplets on Surfaces. *ACS Appl. Mater. Interfaces* **2015**, *7*, 26892−26903.
(37) Sivakumar, S.; Gupta, J. K.; Abbott, N. L.; Caruso, F. Monodisperse Emulsions through Templating Polyelectrolyte Multilayer Capsules. *Chem. Mater.* **2008**, *20*, 2063−2065.
(38) Miller, M. B.; Bassler, B. L. Quorum Sensing in Bacteria. *Annu. Rev. Microbiol.* **2001**, *55*, 165−199.
(39) Churchill, M. E.; Chen, L. Structural Basis of Acyl-Homoserine Lactone-Dependent Signaling. *Chem. Rev.* **2011**, *111*, 68−85.
(40) Yates, E. A.; Philipp, B.; Buckley, C.; Atkinson, S.; Chhabra, S. R.; Sockett, R. E.; Goldner, M.; Dessaux, Y.; Camara, M.; Smith, H.; Williams, P. *N*-Acylhomoserine Lactones Undergo Lactonolysis in a pH-, Temperature-, and Acyl Chain Length-Dependent Manner During Growth of *Yersinia pseudotuberculosis* and *Pseudomonas aeruginosa*. *Infect. Immun.* **2002**, *70*, 5635−5646.
(41) Deziel, E.; Lepine, F.; Milot, S.; Villemur, R. RhlA is Required for the Production of a Novel Biosurfactant Promoting Swarming Motility in *Pseudomonas aeruginosa*: 3-(3-Hydroxyalkanoyloxy) Alkanoic Acids (HAAs), the Precursors of Rhamnolipids. *Microbiology* **2003**, *149*, 2005−2013.
(42) Miller, D. S.; Carlton, R. J.; Mushenheim, P. C.; Abbott, N. L. Introduction to Optical Methods for Characterizing Liquid Crystals at Interfaces. *Langmuir* **2013**, *29*, 3154−3169.
(43) Lockwood, N. A.; Abbott, N. L. Self-Assembly of Surfactants and Phospholipids at Interfaces between Aqueous Phases and Thermotropic Liquid Crystals. *Curr. Opin. Colloid Interface Sci.* **2005**, *10*, 111−120.
(44) Uline, M. J.; Meng, S.; Szleifer, I. Surfactant Driven Surface Anchoring Transitions in Liquid Crystal Thin Films. *Soft Matter* **2010**, *6*, 5482−5490.
(45) Zhong, S.; Jang, C.-H. pH-Driven Adsorption and Desorption of Fatty Acid at the Liquid Crystal−Water Interface. *Liq. Cryst.* **2015**, *43* (3), 361−368.
(46) Brake, J. M.; Mezera, A. D.; Abbott, N. L. Effect of Surfactant Structure on the Orientation of Liquid Crystals at Aqueous− Liquid Crystal Interfaces. *Langmuir* **2003**, *19*, 6436−6442.
(47) Tan, L. N.; Carlton, R.; Cleaver, K.; Abbott, N. L. Liquid Crystal-Based Sensors for Rapid Analysis of Fatty Acid Contamination in Biodiesel. *Mol. Cryst. Liq. Cryst.* **2014**, *594*, 42−54.
(48) Porter, D.; Savage, J. R.; Cohen, I.; Spicer, P.; Caggioni, M. Temperature Dependence of Droplet Breakup in 8CB and 5CB Liquid Crystals. *Phys. Rev. E* **2012**, *85*, No. 041701.
(49) Pearson, J. P.; Pesci, E. C.; Iglewski, B. H. Roles of *Pseudomonas aeruginosa* Las and Rhl Quorum-Sensing Systems in Control of Elastase and Rhamnolipid Biosynthesis Genes. *J. Bacteriol.* **1997**, *179*, 5756−5767.
(50) Smalley, N. E.; An, D.; Parsek, M. R.; Chandler, J. R.; Dandekar, A. A. Quorum Sensing Protects *Pseudomonas aeruginosa* against Cheating by Other Species in a Laboratory Coculture Model. *J. Bacteriol.* **2015**, *197*, 3154−3159.
(51) Jacobs, M. A.; Alwood, A.; Thaipisuttikul, I.; Spencer, D.; Haugen, E.; Ernst, S.; Will, O.; Kaul, R.; Raymond, C.; Levy, R.; Chun-Rong, L.; Guenthner, D.; Bovee, D.; Olson, M. V.; Manoil, C. Comprehensive Transposon Mutant Library of *Pseudomonas aeruginosa*. *Proc. Natl. Acad. Sci. U. S. A.* **2003**, *100* (24), 14339−14344.
(52) Geske, G. D.; O'Neill, J. C.; Miller, D. M.; Mattmann, M. E.; Blackwell, H. E. Modulation of Bacterial Quorum Sensing with Synthetic Ligands: Systematic Evaluation of *N*-Acylated Homoserine Lactones in Multiple Species and New Insights into Their Mechanisms of Action. *J. Am. Chem. Soc.* **2007**, *129*, 13613−13625.
(53) Moore, J. D.; Rossi, F. M.; Welsh, M. A.; Nyffeler, K. E.; Blackwell, H. E. A Comparative Analysis of Synthetic Quorum Sensing Modulators in *Pseudomonas aeruginosa*: New Insights into Mechanism, Active Efflux Susceptibility, Phenotypic Response, and Next-Generation Ligand Design. *J. Am. Chem. Soc.* **2015**, *137*, 14626−14639.
(54) Clasquin, M. F.; Melamud, E.; Rabinowitz, J. D. LC-MS Data Processing with Maven: A Metabolomic Analysis and Visualization Engine. In *Current Protocols in Bioinformatics*; Baxevanis, A. D., Petsko, G. A., Stein, L. D., Stormo, G. D., Eds.; John Wiley & Sons, Inc., 2012; Vol. 37, pp 14.11.1−14.11.23.
(55) Mata-Sandoval, J. C.; Karns, J.; Torrents, A. Effect of Nutritional and Environmental Conditions on the Production and Composition of Rhamnolipids by *P. aeruginosa* UG2. *Microbiol. Res.* **2001**, *155*, 249−256.
(56) Zhao, F.; Shi, R.; Ma, F.; Han, S.; Zhang, Y. Oxygen Effects on Rhamnolipids Production by *Pseudomonas aeruginosa*. *Microb. Cell Fact.* **2018**, *17*, 39.
(57) Abdel-Mawgoud, A. M.; Lépine, F.; Déziel, E. Rhamnolipids: Diversity of Structures, Microbial Origins and Roles. *Appl. Microbiol. Biotechnol.* **2010**, *86*, 1323−1336.
(58) Miller, D. S.; Wang, X.; Buchen, J.; Lavrentovich, O. D.; Abbott, N. L. Analysis of the Internal Configurations of Droplets of Liquid Crystal Using Flow Cytometry. *Anal. Chem.* **2013**, *85*, 10296−10303.
(59) Holloway, B. Genetic Recombination in *Pseudomonas aeruginosa*. *Microbiology* **1955**, *13*, 572−581.
(60) Welsh, M. A.; Eibergen, N. R.; Moore, J. D.; Blackwell, H. E. Small Molecule Disruption of Quorum Sensing Cross-Regulation in *Pseudomonas aeruginosa* Causes Major and Unexpected Alterations to Virulence Phenotypes. *J. Am. Chem. Soc.* **2015**, *137*, 1510−1519.



https://dx.doi.org/10.1021/acsami.0c05792
*ACS Appl. Mater. Interfaces* 2020, 12, 29056−29065